



European Conference on Surface Science

www.ecoss2015.org

Barcelona 31 Aug - 4 Sept 2015

ecoss
Book of Abstracts
31



Index

Committees	Pg. 3
Acknowledgements	Pg. 4
Sponsors and exhibitors	Pg. 4
Plenary lectures	Pg. 8
Oral presentations	Pg. 14
Posters	Pg. 342
Index of authors	Pg. 609

Committees

International Advisory Committee

A. Berkó, Hungary
U. Diebold, Austria
P. Feibelman, USA
E. Meyer, Switzerland
M. McCoustra, UK
A. Michaelides, UK
E. Molinari, Italy
K. Morgenstern, Germany
C. Mottet, France

A. Nilsson, Sweden
C. Noguera (ECOS board), France
J.I.Pascual, Spain
J. Osterwalder, Switzerland
P. Rudolf (ECOS board), Netherlands
C. Stampfl, Australia
S. Suzer, Turkey
P. Thiel, USA
J. Fraxedas (Chair)

Program Committee

M. Altman, China
C. Ambrosch-Draxl, Germany
H. Bluhm, USA
A. Ciszewski (ECOS board), Poland
C. Di Valentin, Italy
R. Felici, France
S. Ferrer, Spain
E. G. Michel, Spain
G. Held (ECOS board), UK
L. Hornekaer, Denmark

N. Lorente, Spain
J. A. Martín-Gago, Spain
E. Ortega, Spain
K. Pussi, Finland
S. Stepanov, Switzerland
A. Taleb, France
K. von Bergmann, Germany
J. Zegenhagen, UK
J. Fraxedas (Chair)

Local Organizing Committee

A. Clotet
J. Llorca
A. Mugarza
C. Ocal
V. Pérez
J. Fraxedas (Chair)

Technical Secretariat



Pl. Europa 17-19, 1st floor
E-08908 L'Hospitalet de Llobregat, Barcelona, Spain
T +34 938 823 878
ecoss2015@barcelocongresos.com

Acknowledgements



Sponsors

Updated list as per 21 July 2015

Silver sponsor

SPÉCSTM

Other sponsors



Exhibitors

Updated list as per 21 July 2015

Stand 8



Stand 9



Stand 10



Stand 11



Stand 12



Stand 13



Stand 14



Stand 15



Stand 16



Stand 17



Stand 18



Stand 19



Stand 20



Stand 21



Stand 24



Stand 25



Stand 26



Stand 27



Stand 28



Stand 29



Stand 30



Stand 31



NAP-XPS Solutions

NEAR AMBIENT PRESSURE IN SITU SURFACE
ANALYSIS SYSTEMS

KEY FEATURES

- In Situ Analysis up to 100 mbar
- Backfilling or Reaction Cell
- PHOIBOS 150 NAP Electron Analyser
- NAP Laboratory X-ray and UV Sources
- Windowless Synchrotron Beam Entrance Stage



SPECS Surface Nano Analysis GmbH

T: +49 30 46 78 24-0
E: info@specs.com
H: www.specs.com

SPECSTM

ecoss 32**28 Aug. - 2 Sept. 2016
Grenoble, France****EUROPEAN CONFERENCE ON SURFACE SCIENCE**www.ecoss2016.org

Welcome of the Chair

On behalf of the Organizing Committee, it is my pleasure to announce the **32nd European Conference on Surface Science (ECOSS-32)**. ECOSS is a traditional annual meeting organized jointly by the Surface Science Division of IUVSTA and the Surface and Interface Section of the European Physical Society. After 10 years it is back in France.

The conference provides the occasion for European scientists to meet and discuss the latest advances, either experimental or theoretical, in surface physics and chemistry. The most recent technical developments are also presented.

Grenoble, capital of the French Alps, is the ideal place for this meeting. It is the location of the largest synchrotron radiation and neutron facilities in Europe as well as one of the most important areas for semiconductor research and industry.

Roberto Felici
Chair of ECOSS 32

Local Organising Committee (LOC)

Roberto Felici - ESRF, Grenoble
Chair

Aude Bailly - UGA/CNRS, Institut Néel, Grenoble

Eric De Vito - UGA/LITEN, CEA-Grenoble

Elisabeth Djurado - UGA, Grenoble INP

Giovanna Fragneto - ILL, Grenoble

Anouk Galtayries - SFV-ENSCP, Paris

Gweltaz Hirel - SFV, Paris

Laurence Magaud - UGA/CNRS, Institut Néel, Grenoble

Gilles Renaud - UGA/INAC, CEA Grenoble

Olivier Renault - UGA/LETI, CEA Grenoble

Hubert Renevier - UGA, Grenoble INP

Conference Secretary

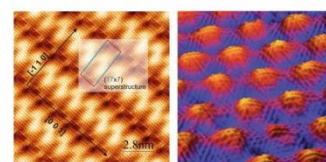
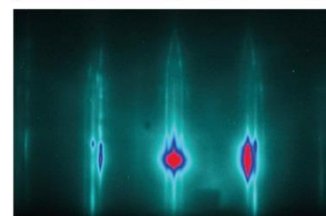
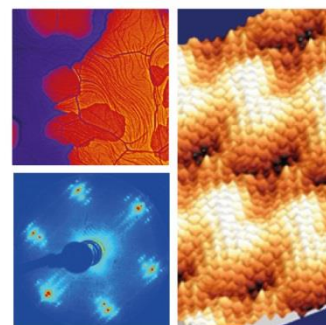


Société Française du vide

19 rue du Renard F-75004 Paris, France

Phone: +33 (0)1 53 01 90 30 - Fax: +33 (0)1 42 78 63 20

E-mail: sfv@vide.org - www.vide.org

ecoss 32**28 Aug. - 2 Sept. 2016
Grenoble, France**

Plenary lectures

PL1	Miquel Salmerón	Pg. 9
PL2	Alec M. Wodtke	Pg. 10
PL3	Cynthia Friend	Pg. 11
PL4	Qi-Kun Xue	Pg. 12
PL5	Fernando Flores	Pg. 13

PL1

Surface Science in the 21st century: dense, wet and fastMiquel Salmeron

Materials Science Division, Lawrence Berkeley National Laboratory and
Materials Science and Engineering, University of California, Berkeley, USA

Over the past century the science of surfaces has undergone an enormous progress. The atomic and electronic structure, reactivity, and dynamics of many material surfaces have been uncovered. Several Nobel prizes have marked the great accomplishments of our predecessors, from I. Langmuir in 1932 to G. Ertl in 2007. This progress has been fostered and propelled by the continuous development of powerful techniques that have provided atomic and molecular level details of surfaces, adsorption and desorption phenomena, vibration and electronic spectra, electron diffraction and real space imaging by the Scanning Tunneling Microscope. The nature of many techniques has constrained Surface Science to ultra-high vacuum environments. And yet practical surfaces are surrounded by gases and liquids at ambient conditions of pressure and temperature. Under these conditions the surfaces are covered with dense layers of adsorbed molecules. The last two decades have witnessed an acceleration in the development of new surface science techniques that can operate under ambient conditions, providing similar spatial and spectroscopic resolution as in vacuum. This new observation window has revealed previously unknown phenomena arising from the adsorption of molecules with weak surface interactions that are present on the surface in high concentration, but only when in equilibrium with the gas phase. At relevant ambient temperatures many kinetic processes that are frozen at the low temperatures required in vacuum environments are unlocked. In this lecture I will review the physics and chemistry of surfaces with dense layers of adsorbates and new phenomena that derive from this, including hydrogen dissociation reactions on Pd and Ru, dense CO layers and their effect on the structure of Pt and Cu surfaces. Prospects for similar studies of the solid-liquid interface, a new frontier in the field, and their impact in environmental science, electrochemistry and energy storage will be discussed. Finally I will discuss the potential of ultrafast techniques to study dynamic processes with the hope of determining elusive reaction transitions states.

PL2

The dynamics of molecular interactions and chemical reactions at metal surfaces: Testing the foundations of theory

Alec Wodtke

Institute for Physical Chemistry, Georg-August University and Department of Dynamics at Surfaces Max Planck Institute for Biophysical Chemistry, Göttingen, Germany

One of our most fundamental scientific challenges is to develop predictive theories of chemistry rigorously grounded in the laws of physics. In 1929, Dirac identified the problem famously in a comment about the importance of quantum mechanics to chemistry... “The underlying physical laws necessary for the mathematical theory of... the whole of chemistry are thus completely known, and the difficulty is only that the exact application of these laws leads to equations much too complicated to be soluble.” Despite electrifying advances in computational power, Dirac is still right. The theory of chemistry requires approximate methods for practical computations.

For the theory of surface chemistry, four central approximations are made, involving the use of: 1) classical mechanics for describing nuclear motion, 2) density functionals for calculating electronic states, 3) reduced dimensionality approximations and 4) the Born-Oppenheimer approximation to separate electronic and nuclear degrees of freedom. The growing importance of computational surface chemistry motivates us to design rigorous experimental tests of these assumptions.

Using modern molecular beams methods in state-to-state scattering experiments, we obtain a wealth of observational data characterizing the interactions of molecules with metal surfaces. Emphasizing quantitative comparison to first principles theories, we find that energy conversion can occur by unexpected mechanisms, where the electronically adiabatic approximation separating the time scales of electronic and nuclear motion no longer holds. The simplicity of the systems under study provides opportunities for developing new theories that go beyond the Born-Oppenheimer approximation, providing an atomic scale view of surface chemistry grounded in first principles.

PL3

Surface Chemistry and Catalysis of Gold: Spanning materials complexity and pressure

Cynthia M. Friend

Harvard University, Dept. of Chemistry and Chemical Biology and School of Engineering and Applied Sciences, Cambridge MA, USA

Fundamental surface science experiments in conjunction with atomistic theory are used to develop a molecular-scale mechanism for bonding and reactivity on Au(111) and (110) and on nanoporous Au (npAu), an alloy with ~3% Ag. The key for bond activation on gold is adsorption of oxygen atoms that lead to selective reaction on all surfaces investigated. Key factors that control bonding and reactivity include weak (van der Waals) interactions between molecular species and the surface, surface reconstruction, and the relatively weak bonding of molecules to Au. The binding and reactivity of key oxygen-containing molecules, e.g. alcohols and organic acids, were studied. For example, methanol is selectively coupled to methyl formate on both Au(111) and Au(110) that are pre-covered by adsorbed O. The selectivity for methyl formate production depends on the initial coverage of oxygen. Similar reactivity is also observed for npAu both under ultrahigh vacuum conditions and in a flow reactor at atmospheric pressure. A combination of spectroscopy (XPS, HREELS), imaging (STM, SEM and TEM) and temperature programmed reaction studies were used to establish reaction mechanism; density functional theory (DFT) was used to probe bonding and the nature of transition states. The case of methanol selective coupling will be used to illustrate the application of theory to this class of reactions. These studies establish a bridge between ultrahigh vacuum surface studies on well-defined surfaces and complex materials, e.g npAu, that function as robust working catalysts at atmospheric pressure. The work described provides a road map for relating fundamental studies to catalytic behavior that can be broadly applied.

PL4

Atomic-Level Control of Two Dimensional Material Growth: From Quantized Anomalous Hall Effect to Interface- Enhanced High T_c Superconductivity

Qi-Kun Xue

Department of Physics, Tsinghua University, Beijing, China

Molecular beam epitaxy (MBE) has been well-known as a powerful technique for preparing semiconductors and heterostructures. Combining MBE with two surface sensitive tools--scanning tunneling microscopy (STM) and angle resolved photoemission spectroscopy (ARPES), can even push its power to an unprecedented level in material quality control. We apply MBE-STP-ARPES to topological insulators and high T_c superconductors, which have recently attracted extensive attention. We show how quantized anomalous Hall effect could be achieved by atomic-level control of band-engineered and magnetically doped topological insulators with MBE-STP-ARPES. We then show the discovery of interface enhanced high temperature superconductivity in single unit-cell FeSe films on SrTiO₃ using the same approach. Implications on exploring other exotic quantum phenomena such as Majorana fermions in topological insulators and on searching for new high temperature superconductors will be discussed.

The author acknowledges the financial supports from National Science Foundation of China, and Ministry of Science and Technology and Ministry of Education of China.

PL5

Reversible phase transitions on semiconductor surfaces and dynamical fluctuations: soft modes, electron correlation effects and molecular diffusion

F. Flores¹ (EPS Invited Speaker), A. Tejeda² and J. Ortega¹

¹ Dept. de Física Teórica de la Materia Condensada and Condensed Matter Physics Center (IFIMAC), Universidad Autónoma de Madrid, Spain

² Laboratoire de Physique des Solides, Université Paris-Sud, CNRS, UMR 8502, Orsay, France

The enhancement of quasi-particle interactions in low dimensional systems gives rise to fascinating phase transitions like low-dimensional superconductivity, magnetic ordering or metal-insulator transitions. In particular, metallic overlayers on semiconductor surfaces are prone to creating temperature induced reversible phase-transitions, very often associated with dynamical fluctuations of surface atoms and /or with the many-body electronic properties of the system. In this talk, first of all a review of those systems will be presented discussing some properties of well-known dynamical fluctuations phase transitions. α -Sn/Ge(111) is a paradigmatic case [1] that changes its symmetry from $\sqrt{3}\times\sqrt{3}$ to 3×3 around 200 K, with a soft-phonon mode [2] identified as the driving mechanism of the transition [3]. However, another competing mechanism associated with electron correlation effects gives rise in this system, at very low temperature (≈ 50 K), to a $\sqrt{3}\times\sqrt{3}$ - Mott insulating phase [4]. The competing mechanisms of those phases will be discussed as well as the properties of another similar system: K/Si(111):B [5]. In-linear chains on Si(111) show a reversible $4\times 1 \rightarrow 8\times 2$ phase transition that is accompanied by a metal-insulator one. The 8×2 -structure is also associated with a soft phonon mode, corresponding to the shear motion of the In zigzag rows, and with the dimerization of the chain outer In-atoms [6]. In this system, the 4×1 -phase appears as the result of the local dynamical fluctuations associated with the 8×2 -degenerate ground states. Finally, experimental and theoretical evidence of a new $\sqrt{3}\times\sqrt{3} \rightarrow 2\sqrt{3}\times 2\sqrt{3}$ reversible phase transition for Sn/Si(111):B will be presented [7]. The transition appears at 520 K and the system has 6 Sn-atoms per a $2\sqrt{3}\times 2\sqrt{3}$ unit cell. LEED and STM-images, as well as photoemission experiments, will be shown. All these results are explained by means of a microscopic diffusive mechanism whereby a Sn-tetramer diffuses on the surface among 24 equivalent ground states, giving rise to the $\sqrt{3}\times\sqrt{3}$ symmetry. This is reminiscent of the In/Si(111) $4\times 1 \rightarrow 8\times 2$ phase transition, but it includes as an essential new ingredient the diffusion of tetramers along the surface. Results for the geometry of this surface and the diffusive Sn-tetramer processes will be shown as calculated using an appropriate DFT-molecular dynamics approach.

[1] J.M. Carpinelli et al, Nature (London) 381, 398 (1996)

[2] R. Pérez, J.Ortega and F.Flores, Phys Rev Lett.86, 4891 (2001)

[3] J. Avila et al, Phys Rev Lett 82, 442 (1999)

[4] R. Cortés et al, Phys Rev Lett 96, 126103 (2006)

[5] L.A. Cardenas et al, Phys Rev Lett 103, 046804 (1999); HH Weitering et al, Phys Rev Lett 78 1331 (1997)

[6] C Gonzalez et al, Phys Rev Lett 96, 136101 (2006)

[7] W. Srouf et al, Phys Rev Lett (2015), in press

Oral presentations

Session		From	To
Oral sessions, Monday 31 August			Pg. 16
S01	Surface magnetism	Mo-A1+2	Mo-A6
S02	Oxide surfaces and thin/ultra-thin oxide films	Mo-B1	Mo-B6
S03	Molecules at surfaces	Mo-C3+4	Mo-C6
S04	Electronic properties of surfaces	Mo-D1	Mo-D5+6
S05	Catalysis under ideal and real conditions	Mo-E1+2	Mo-E6
S06	Surface magnetism	Mo-A7	Mo-A11+12
S07	Oxide surfaces and thin/ultra-thin oxide films	Mo-B7	Mo-B12
S08	Molecules at surfaces	Mo-C7	Mo-C12
S09	Electronic properties of surfaces	Mo-D7+8	Mo-D12
S10	Catalysis under ideal and real conditions	Mo-E7	Mo-E12
S11	Superconductivity in 2D materials	Mo-A13	Mo-A17
S12	Oxide surfaces and thin/ultra-thin oxide films	Mo-B13+14	Mo-B18
S13	Molecules at surfaces	Mo-C13	Mo-C16
S14	Electronic properties of surfaces / Optoelectronic excitations / Strong correlations at surf.	Mo-D13	Mo-D16
S15	Catalysis under ideal and real conditions	Mo-E13	Mo-E16
Oral sessions, Tuesday 1 September			Pg. 88
S16	Graphene and carbon-based nanomaterials	Tu-A1+2	Tu-A8
S17	Oxide surfaces and thin/ultra-thin oxide films	Tu-B1	Tu-B7
S18	Molecules at surfaces	Tu-C1	Tu-C7+8
S19	Surface diffusion and growth	Tu-D1	Tu-D7
S20	Surface chemical reactions, kinetics and heterogeneous catalysis	Tu-E3+4	Tu-E8
S21	Graphene and carbon-based nanomaterials	Tu-A9	Tu-A13
S22	Oxide surfaces and thin/ultra-thin oxide films	Tu-B9+10	Tu-B14
S23	Molecules at surfaces	Tu-C9	Tu-C14
S24	Liquid/solid and liquid/liquid interfaces / Colloids and interfaces	Tu-D9	Tu-D12+13
S25	Surface chemical reactions, kinetics and heterogeneous catalysis	Tu-E9	Tu-E14
S26	Graphene and carbon-based nanomaterials	Tu-A15+16	Tu-A20
S27	Oxide surfaces and thin/ultra-thin oxide films	Tu-B15	Tu-B20
S28	Molecules at surfaces	Tu-C15	Tu-C19
S29	Liquid/solid and liquid/liquid interfaces / Colloids and interfaces	Tu-D15	Tu-D20
S30	Surface chemical reactions, kinetics and heterogeneous catalysis	Tu-E15	Tu-E19

Session		From	To
S31	Graphene and carbon-based nanomaterials	Tu-A21+22	Tu-A26
S32	Oxide surfaces and thin/ultra-thin oxide films	Tu-B21	Tu-B23
S33	Self-assembly at surfaces	Tu-C21	Tu-C25+26
S34	Liquid/solid and liquid/liquid interfaces / Colloids and interfaces	Tu-D21	Tu-D25
S35	Surface chemical reactions, kinetics and heterogeneous catalysis	Tu-E21	Tu-E25

Oral sessions, Wednesday 2 September

Pg. 196

S36	Surface magnetism	We-A1	We-A5+6
S37	Materials for energy: photovoltaics, solar and fuel cells, etc.	We-B1+2	We-B6
S38	Self-assembly at surfaces	We-C3+4	We-C6
S39	Surface structure	We-D1	We-D5
S40	Real-time processes at surfaces / Surface dynamics	We-E1	We-E5+6
S41	Surface magnetism	We-A7	We-A9
S42	Materials for energy: photovoltaics, solar and fuel cells, etc. / Metal, alloy and quasicrystal	We-B7	We-B12
S43	Self-assembly at surfaces	We-C7	We-C12
S44	Surface structure / Surface phases and phase transitions	We-D7	We-D11
S45	Tribology and mechanical properties at the atomic scale	We-E7	We-E11

Oral sessions, Thursday 3 September

Pg. 243

S46	Graphene and carbon-based nanomaterials	Th-A1	Th-A7+8
S47	Piezo and ferroelectricity at surfaces	Th-B1+2	Th-B7
S48	Polymer surfaces and interfaces	Th-C1	Th-C7
S49	Semiconductor surfaces	Th-D1+2	Th-D7
S50	Electrochemistry at surfaces	Th-E4+5	Th-E8
S51	Graphene and carbon-based nanomaterials	Th-A9	Th-A13+14
S52	Novel and advancement of experimental and computational methods	Th-B11	Th-B14
S53	Self-assembly at surfaces	Th-C9	Th-C14
S54	Band structure of surfaces	Th-D9+10	Th-D14
S55	Electrochemistry at surfaces / Corrosion at the atomic scale	Th-E9	Th-E14
S56	Graphene and carbon-based nanomaterials	Th-A15	Th-A23+24
S57	Novel and advancement of experimental and computational methods	Th-B15	Th-B24
S58	Self-assembly at surfaces	Th-C15	Th-C22
S59	Band structure of surfaces / Topological insulators	Th-D15+16	Th-D23
S60	Adsorption and desorption	Th-E15	Th-E24

Mo-A01+02

Magnetism on the magnetite (001) surface

Juan de la Figuera¹¹Instituto de Química Física "Rocasolano", CSIC, Madrid, Spain

Magnetite is arguably one of the oldest multifunctional materials. In addition to its role as a catalyst in several reactions, it is a soft ferrimagnet with a high Curie temperature, a half-metal conductor, and a multiferroic at low temperatures. Upon lowering the temperature it undergoes the grandfather of the metal-insulator transitions, the Verwey transition.

Among its most compact surfaces, the (001) surface has been the subject of many surface science studies. It presents a well defined and reproducible reconstruction whose detailed atomic structure has been recently solved [1] and that undergoes an order-disorder transition at 730 K [2]. The reconstruction is responsible for some of the differences in the surface magnetic moment relative to the bulk [3]. The Verwey transition has been observed in real space on this same surface [4], through the long-range roof-like distortion due to the formation of monoclinic twins.

We will focus on the evolution of the magnetic domains on the (001) surface observed by surface electron microscopies, and in particular, spin-polarized low-energy electron microscopy. Near room temperature complex magnetic domains arise from the competition of the magnetocrystalline anisotropy and the shape anisotropy [5]. The details of those magnetic domains are strongly temperature dependent, and present a reversible behavior in a range of temperatures. We will provide further insight into their evolution through micromagnetic simulations together with the known evolution of the magnetocrystalline anisotropy with temperature [6].

[1] Bliem, R. et al. Science 346, 1215 (2014).

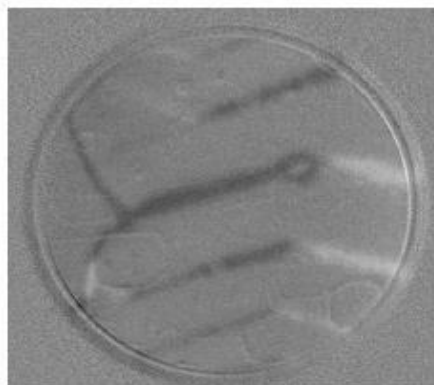
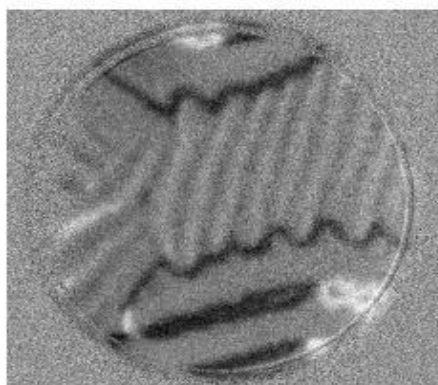
[2] Bartelt, N. C. et al. Phys. Rev. B 88, 235436 (2013).

[3] Martín-García, L. et al. Phys. Rev. B 91, 020408 (2015).

[4] de la Figuera, J. et al. Phys. Rev. B 88, 161410 (2013).

[5] de la Figuera, J. et al. Ultramicroscopy 130, 77 (2013).

[6] Řezníček, R., et al. J. Phys. Cond. Matt. 24, 055501 (2012).



Mo-A03

Cobalt doping of magnetite (100)- $\sqrt{2} \times \sqrt{2}$ R45°

Lucia Aballe¹, Raquel Gargallo-Caballero², Ms. Laura Martín-García², Adrián Quesada³, Cecilia Granados⁴, Michael Foerster¹, Juan de la Figuera²

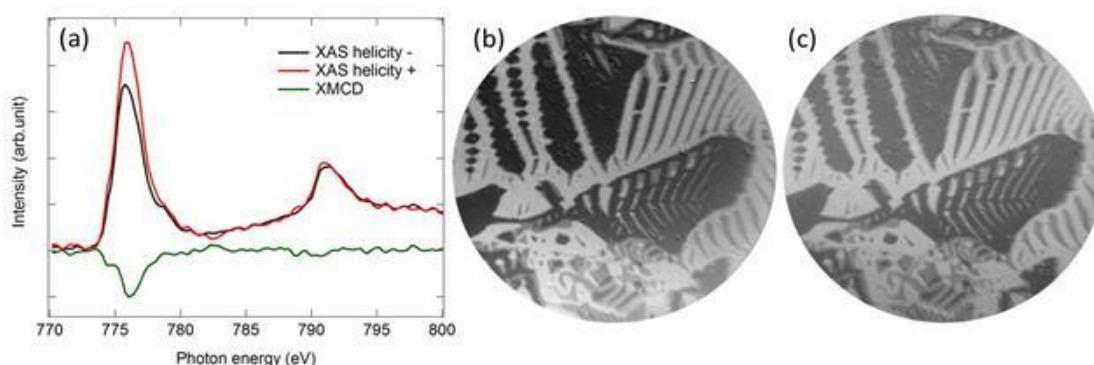
¹ALBA Synchrotron Light Facility, Cerdanyola del Valles, Spain, ²Instituto de Química Física "Rocasolano" (CSIC), Madrid, Spain, ³Instituto de Cerámica y Vidrio (CSIC), Madrid, Spain, ⁴Center for Materials Crystallography, Department of Chemistry and iNano, Aarhus, Denmark

The widely varying magnetic and electrical properties of spinel ferrites make them promising materials for spintronics. In particular, Fe_3O_4 (magnetite) is electrically conducting with $\langle 111 \rangle$ easy axis, while stoichiometric CoFe_2O_4 (cobalt ferrite) is insulating and ferrimagnet with high magnetocrystalline anisotropy and $\langle 100 \rangle$ easy axis [1]. By modifying the Co:Fe ratio and the preparation method, the magnetic and electrical properties can be tuned between those of magnetite and those of cobalt ferrite [2]. However, the detailed magnetic properties are difficult to predict because of the many degrees of freedom involved, such as the inversion level and the flexible cation distribution. Additional mechanisms might enter into play when cobalt ferrites are reduced to nanometer thickness. In this work, we focus on the study of the magnetic properties of the Co-doped magnetite surface. Co was deposited at room temperature on a well-characterized magnetite surface, prepared by sputtering/annealing cycles. The surface was characterized by X-ray Photoelectron Spectroscopy, X-ray absorption and X-ray Magnetic Circular Dichroism in Photoemission Electron Microscopy (Fig. 1a shows the absorption spectra for 0.5 ML Co) in order to obtain the composition, the magnetic domains distribution, and the near-surface orbital and spin magnetic moment of the individual cations [3]. The sample was subsequently annealed to increasing temperatures in order to promote the Co adatoms diffusion into the crystal lattice. The results suggest preferential incorporation as Co^{2+} , in good agreement with the results reported in the literature, while the surface magnetic domain distribution is not affected by the doping (Fig. 1b and 1c are 50 μm XMCD images on CoL_3 and FeL_3 absorption edges, respectively).

[1] V. A.M. Brabers in Handbook of Magnetism, Ed. Kronmuler and S. S. Parkin.

[2] J. A. Moyer et al., Phys. Rev. B 83, 035121 (2011).

[3] L. Martín-García et al, Phys. Rev. B 91, 020408 (2015).



Mo-A04

Sherman mapping of passivated Fe(001): A possible target for a multichannel spin polarimeter

Christian Thiede¹, Christian Langenkämper¹, Kaito Shirai², Anke B. Schmidt¹,
Stephan Borek³, Apl. Jürgen Braun³, Jan Minár³, Assistant Taichi Okuda⁴,
Hubert Ebert³, Markus Donath¹

¹Westfälische Wilhelms-Universität, Münster, Germany, ²Graduate School of Science, Hiroshima University, Hiroshima, Japan, ³Ludwig-Maximilians-Universität, München, Germany, ⁴HiSoR, Hiroshima University, Hiroshima, Japan

We propose the ferromagnetic Fe(001)-p(1×1)O surface as a spin-polarizing electron mirror with long-term stability for a multichannel spin polarimeter. Low-energy electron reflection measurements as a function of energy and angle are used to extract maps of the reflectivity, the Sherman function and the figure of merit for two transversal spin polarization directions, parallel and perpendicular to the scattering plane. In both scattering geometries, we find a maximum figure of merit of about 3×10^{-2} for a particular combination of energy and angle (≈ 2.6 eV, 58°). For the spin polarization perpendicular to the scattering plane, the contribution of spin-orbit coupling to the Sherman function is found to be one order of magnitude smaller than that of exchange interaction. We performed theoretical calculations by means of the SPKKR layer code which are in good agreement with our experimental results.

Mo-A05

XMCD Study on Co/Ni Multilayer on W(110)

Tsuneo Yasue¹, Masahiko Suzuki¹, Takeshi Nakagawa², Kouta Takagi³,
Toshihiko Yokoyama³, Takanori Koshikawa¹

¹Osaka Electro-Communication University, Osaka, Japan, ²Kyusyu University, Fukuoka, Japan, ³Institute for Molecular Science, Okazaki, Japan

Co/Ni multilayers are known to show perpendicular magnetic anisotropy (PMA). We have investigated the dynamic behavior of emerging PMA during the Co/Ni multilayer growth process on W(110) by a high-brightness and highly spin polarized LEEM [1]. In the beginning of the growth, the perpendicular magnetization appears during Ni deposition, while the magnetization becomes in-plane by Co deposition. After several repetition of Co/Ni stacking, PMA becomes stable even after Co deposition. In order to understand the magnetic origin of such behavior, XMCD measurements were performed in the present work. XMCD spectra of Ni and Co were taken with applying the external high magnetic field enough to saturate the magnetization. The magnetic field was parallel to the X-ray direction. The spin magnetic moments and the orbital magnetic moments of Ni and Co were derived from the measured XMCD spectra using the sum rules. The parallel and perpendicular components are separated for the orbital moment. The white line intensities of Ni and Co L-edge absorption spectra were almost constant over different multilayer repetitions examined. This indicates that the charge transfer between Ni, Co and the substrate W could be negligible. XMCD spectra of Ni strongly depend on the multilayer repetition. This indicates that the spin and orbital moments of Ni vary in the multilayer stacking sequence. Both spin and orbital moments increase with coverage up to 3 Co/Ni pairs and reach to the constant value above 4 pairs. The perpendicular orbital moment of Ni becomes more dominant with increasing coverage. On the contrary spin and orbital moments of Co do not show clear coverage dependence. Therefore it is concluded that PMA of the Co/Ni multilayer is mainly induced by the perpendicular orbital moment of Ni.

[1] M. Suzuki et al. J. Phys.: Condens. Matter 25, 406001 (2013).

Mo-A06

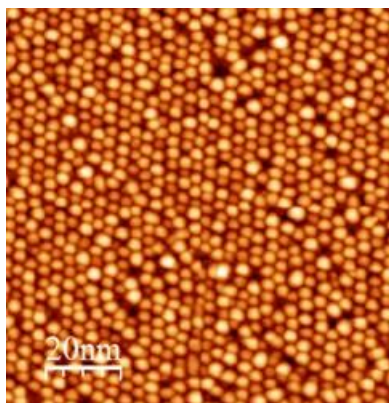
Magnetic properties of Cobalt nanodot arrays on rare-earth-Au² surface compounds

Frederik Schiller¹, Laura Fernández², Maxim Ilyn¹, Ana Magaña³, Enrique Ortega³

¹CSIC, San Sebastian, Spain, ²Philipps Universität Marburg, Marburg, Germany, ³University of the Basque Country UPV-EHU, San Sebastian, Spain

Cobalt deposition on prepatterned rare-earth (RE)Au₂/Au(111) substrates leads to self-organization into very dense hexagonal structures of Co nanodots (see Fig. 1). Depending on the substrate surface RE material one can achieve different interactions that determine the magnetic properties of the dots. In order to investigate in detail such effects, a combined study involving X-ray Circular Magnetic Dichroism and Scanning Tunneling Microscopy will be presented. Several substrates will be analyzed (SmAu₂, GdAu₂, and YbAu₂) that have the same RE-Au₂ surface structure and lattice but reveal ferromagnetic, anti-ferromagnetic [1], and non-magnetic interaction with the Co nanodot array, respectively. These interactions not only determine the magnetic properties below the Curie temperature of the substrate but also far above it and lead to enhancements of the magnetic anisotropy and blocking temperature of the Co nanodot array.

[1] L.Fernandez et al., Nano Letters 14, 2977 (2014).



Mo-B01

Atomic scale view of the early stages of a metal oxidation: Scanning Tunneling Microscopy and Spectroscopy study of the oxidation of Co ultrathin films.

Andrea Picone¹, Michele Riva¹, Dario Giannotti¹, Alberto Brambilla¹, Lamberto Duò¹, Franco Ciccacci¹, Marco Finazzi¹

¹Dipartimento di Fisica, Politecnico di Milano, Milano, Italy

Oxidation of metallic surfaces plays a fundamental role in many fields of modern nanotechnology, spanning from heterogeneous (nano) catalysis [1], corrosion protection [2], and metal/oxide layered structures [3,4]. From a more fundamental point of view, a detailed understanding of the atomistic mechanisms driving the transition from the metallic to the oxide phase is far from being conclusively achieved. Does the oxide nucleation occur over the atomically flat terraces or starts from surface defects sites? Which is the evolution of the surface electronic structure during the early stages of oxygen exposure? If compared to other surface science spatial averaging techniques, the number of Scanning Tunneling Microscopy (STM) and Spectroscopy (STS) studies investigating the early stages of metals oxidation is still scarce. Indeed, the oxidation process often induces the development of rough surfaces or even amorphous structures, rendering their investigation by means of STM a challenging task. In this contribution it will be shown that the oxidation of nanometer-thick Co films deposited on Fe(001) can be followed step by step, from the early stages of subsurface oxygen penetration, until a closed oxide overlayer is fully developed. Highly resolved STM images allow to resolve the atomic details of the oxide wetting layer, while STS and constant current topographic images acquired at variable tunneling conditions reveal the band gap opening since the early stages of oxide nucleation.

[1] S. Surnev, A. Fortunelli, F.P. Netzer, *Chem. Rev.* 113 (2013) 4314.

[2] F. H. Stott, *Rep. Prog. Phys.* 50 (1987) 861-913.

[3] S. Valeri and G. Pacchioni, eds., *Oxide Ultrathin Films* (Wiley-VCH Verlag, Weinheim, 2011).

[4] M. Finazzi, L. Duò, F. Ciccacci, *Surf. Sci. Rep.* 64 (2009) 139.

Mo-B02

Study the formation of surface oxide on Al(111) and Al(100) surfaces using synchrotron based X-ray photoemission spectroscopy and scanning tunneling microscopy.

Milad Ghadami Yazdi¹, Markus Soldemo¹, Jonas Evertsson², Lisa Rullik², Florian Bertram², Sareh Ahmadi¹, Jonas Weissenrieder¹, Edvin Lundgren², Mats Göthelid¹

¹ KTH Royal Institute of Technology, ICT, Material Physics, Stockholm, Sweden, ²Division of Synchrotron Radiation Research, Lund University, Lund, Sweden

Thin aluminum oxide films have significant importance in fields such as microelectronics, as these films are employed as dielectric, diffusion and tunneling barrier due to their high dielectric constant and large barrier height for electron tunneling [1]. Hence, the thickness, structure and chemical composition play an important role in understanding and tuning of such properties; yet, the fundamental knowledge of initial stages of oxidation on aluminum surface and its correlation toward resulting properties is poorly understood [2]. In our work, thermal oxidation of Al(111) and Al(100) was studied using photoelectron spectroscopy (PES), scanning tunneling microscopy (STM) and density functional theory (DFT). Exposures were performed in ultra-high vacuum (UHV) at oxygen doses up to 2000 L from room temperature (RT) up to 400°C. Measurements were done at beamline I311 at MAXlab synchrotron radiation facility, Lund, Sweden, and in Matslab, KTH. On both surfaces, a surface oxide is formed with an atomic structure different from the bulk oxide. Initial oxidation at RT is faster on (100), but the final oxide thicknesses are similar. The interface oxide remains between the metal and the growing amorphous bulk oxide in agreement with recently published work [3]. High resolution Al2p spectra reveal a 2-3 atomic layer thick oxide with aluminum atoms in gradually increasing oxidation states. The atomic structure shares similarities to Al₂O₃ films on NiAl [4], but the exact structure on Al(111) and Al(100) are different in terms of thickness, detailed atomic arrangements and thermal stability.

- [1] L.P.H. Jeurgens, W.G. Sloof, F.D. Tichelaar, E.J. Mittemeijer, *Surf. Sci.* 506 (2002) 313.
- [2] Z. Zhukov, I. Popova, J.T. Yates, *J. Vac. Sci. Technol. A* 17 (1999) 1727
- [3] D. Flötotto, Z.M. Wang, E.J. Mittemeijer, *Surf. Sci.* 633 (2015) 1.
- [4] A. Stierle, F. Renner, R. Streitl, H. Dosch, W. Drube, B.C. Cowie, *Science* 303 (2004) 1652.

Mo-B03

DFT study of 3D AFM - STM metal oxide imaging modes:
towards atomic species identification

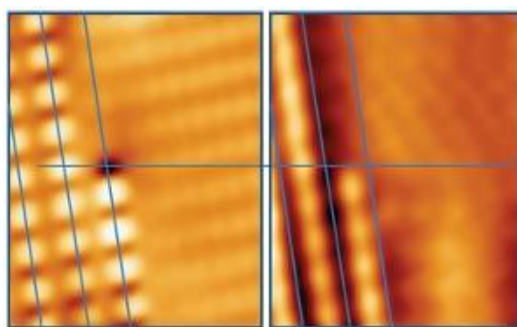
Diego Rodríguez Hermoso¹, Milica Todorovic¹, Harry Mönig³, S. Schüer³,
Gernot Langewisch³, Óscar Díaz Arado³, Alexander Timmer³, Harald Fuchs³,
Rubén Pérez^{1,2}

¹Theoretical Condensed Matter Physics Department, Universidad Autónoma de Madrid, Madrid, Spain, ²Condensed Matter Physics Center (IFIMAC), Universidad Autónoma de Madrid, Madrid, Spain, ³Institute of Physics and Center for Nanotechnology (CeNTech), University of Münster, Münster, Germany

Metal oxides have many diverse technological applications in fields ranging from catalysis to electronics. Scanning probe microscopes have proven their extraordinary capacity in studying surface properties at the atomic scale which govern the chemical and electrical response of metal oxides.

We present a joint theoretical and experimental study on the Cu(110)-(2x1)O surface. The oxide features added rows (ARs) of alternate Cu and O atoms atop the metal surface. These ARs are challenging for species identification as the atoms in them are separated by a very small distance. Atomic force microscopy (AFM) images show stripes with bright and dark spots while scanning tunneling microscopy (STM) show a bright line in the space between these stripes (Fig. 1). The information provided by the experiments is not sufficient for the identification. Hence, we made use of density functional theory (DFT) calculations. Simulations were performed with two atomically sharp Cu tips terminating in a Cu and an O atom. The strength of the interaction of the tip with the added row was measured following a previously reported protocol for the simulation of the force spectroscopy. We could determine that the bright spots in the AFM image corresponded to Cu atoms in the AR. Examining the contrast formation mechanisms of both candidates we could clearly identify the O terminated tip as the one responsible for this image formation. The calculation of 2D tunneling current maps, helped us understand the contrast differences observed between AFM and STM images. Also, we conducted simulations to determine the nature of the defect (darkest spot in the AFM image terminating one of the ARs).

Matching the images with the theoretical results, we were able to fully characterize the metal oxide surface and to determine how the tip termination influences the contrast formation. These results are a promising advance towards a generalized methodology for atomic species identification.



Mo-B04

The impact of thermal motion on ceria(100): revealing surface dynamics of lattice atoms

Marçal Capdevila-Cortada¹, N. López¹¹Institute of Chemical Research of Catalonia, Tarragona, Spain

The {100} facet of cerium oxide remains a rather unexplored termination. It presents macroscopic polarization along the surface normal, which causes a surface instability that has to be somehow compensated (most commonly by an intrinsic modification on the surface stoichiometry or on the surface electronic structure). The ceria {100} facet, despite being substantially less stable than other ceria termination planes, appears to be the only exposed facet of well-defined ceria nanocubes. This nanoshape has been shown to present marked differential reactivity than other ceria nanoparticles. STM and HREM images of ceria nanocubes revealed separated regions of either cerium or oxygen terminated surface. DFT studies are usually based on the c(2x2) reconstruction where half of an oxygen monolayer is transferred from the surface to the bottom of the slab. This termination would account for the experimentally resolved images exhibiting oxygen termination. An alternative reconstruction composed by CeO₄ pyramids exposing Ce atoms has also been recently suggested. This termination is slightly more stable (0.003 eV Å⁻²) than the oxygen terminated and would account for the cerium-terminated regions. In this work, Born-Oppenheimer Molecular Dynamics (BOMD) simulations have been carried out on the two aforementioned reconstructions of the (100) surface slab, as well as on the thoroughly studied (111) surface. The simulations, performed at several temperatures ranging from 400 to 800 K, are based on DFT+U calculations using the PBE functional. The common picture of static lattice atoms ready to interact with a given adsorbate appears to be questioned by the BOMD simulations. Instead, the lattice oxygen atoms exhibit high mobility and may even present diffusion at T ≥ 700 K.

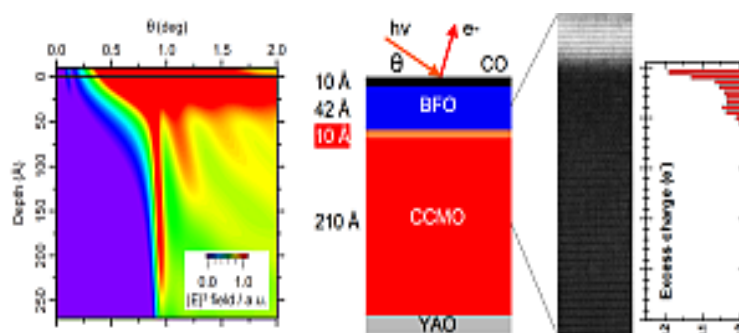
Mo-B05

Near-total reflection hard x-ray photo-emission spectroscopy for depth-resolved investigation of functional oxide interfaces

Julien Rault¹, Maya Marinova², Alexandre Gloter², Slavomir Nemsak⁴, Gunnar Karl Pallson⁴, Jean-Pascal Rueff¹, Charles Fadley⁴, Cécile Carrétéro³, Hiroyuki Yamada³, Katia March², Vincent Garcia³, Stéphane Fusil³, Agnès Barthélémy³, Odile Stephan², Christian Colliex², Manuel Bibes³

¹Synchrotron SOLEIL, Gif-Sur-Yvette, France, ²Laboratoire de Physique du Solide, CNRS UMR 8502, Université Paris Sud XI, Orsay, France, ³Unité Mixte de Physique CNRS/Thales, Palaiseau, France, ⁴Materials Sciences Division, Lawrence Berkeley National Laboratory, Berkeley, United States

The electric field control of functional properties is crucial in oxide-based electronics. Non-volatile switching between different resistivity or magnetic states in an oxide channel can be achieved through charge accumulation or depletion from an adjacent ferroelectric. However, how charge distributes near the interface between the ferroelectric and the oxide remains poorly known limiting our understanding of such switching effects. Here, we use a first-of-a-kind combination of near-total-reflection hard X-ray photoemission spectroscopy, scanning transmission electron microscopy with electron energy loss spectroscopy and ab-initio theory to address this issue. The element-specific chemical and electronic profile at a single $\text{Ca}_{1-x}\text{Ce}_x\text{MnO}_3/\text{BiFeO}_3$ interface in a bilayer sample has been investigated by standing-wave (SW) hard X-ray photoemission spectroscopy (HAXPES), in which depth profiling of buried layers and interfaces is achieved in grazing incidence or in near total reflection (NTR) conditions. In previous studies, the SW-HAXPES technique has been successfully shown to provide depth-resolved chemical state and electronic structure for samples grown either as or on top of a superlattice multilayer mirror. Here, we show that the multilayer mirror is not necessary, by using X-ray wave interference effects, including SW effects, in NTR conditions for a bilayer system. We achieve a direct, quantitative, atomic-scale characterization of the polarization-induced charge density changes at the interface between the ferroelectric and the doped Mott insulator. An excess of electron occurs over 1 nm, in agreement with the expected screening length of the CCMO electrode for downward BFO polarization. Our results furthermore agree with measurements of peak shifts in Mn L-edge TEM-EELS data. These observations explain well the macroscopic, polarization-dependent transport behaviour of this heterostructure. By using DFT calculations, we also provide insight on how interface-engineering can be used to tune such screening effects NTR HAXPES measurements are thus a promising new probe of buried interfaces chemical and electronic structure.



Mo-B06

Oxidation of FeO(111) Grown on Pt(111): Spectroscopic Evidence for Hydroxylation

Niclas Johansson¹, Lindsay R Merte^{1,2}, Elin Grånäs¹, Stefan Wendt², Jesper N Andersen^{1,3}, Joachim Schnadt¹, Jan Knudsen^{1,3}

¹Division of Synchrotron Radiation Research, Department of Physics, Lund University, Lund, Sweden, ²Interdisciplinary Nanoscience Center (iNANO) and Department of Physics and Astronomy, Aarhus University, Aarhus, Denmark, ³MAX-IV Laboratory, Lund University, Lund, Sweden

FeO(111) grown on Pt(111) is one of the most studied ultra-thin metal oxide films and both its reduction/adsorption[1-3] and catalytic properties [4] are well studied. During one of the catalysis studies [4] it was found that bilayer FeO(111) transforms into an oxygen-rich FeO₂ trilayer phase under reaction conditions for the CO oxidation reaction. This FeO₂ phase was then thoroughly characterized mainly with STM and DFT [5], but it has never been characterized in detail with spectroscopic techniques.

Here we present a spectroscopic investigation of the FeO(111) and FeO₂ film using High Resolution and Ambient Pressure Photoelectron Spectroscopy (HRPES/APPEs). We demonstrate that the FeO₂ trilayer films are extremely active for water dissociation as they immediately become hydroxylated upon their formation. Since we always observed hydroxylation of our freshly prepared FeO₂ films both when they are formed by oxidation of FeO(111) by O₂ in the mbar regime or by NO₂ in the UHV regime we suggest that catalytically highly active FeO₂ trilayer films are generally hydroxylated.

[1] Huang W, Ranke W (2006) Surf Sci. 600:793

[2] Knudsen J, Merte LR, Grabow LC, Eichhorn FM, Porsgaard S, Zeuthen H, Vang RT, Laegsgaard E, Mavrikakis M, Besenbacher F (2010) Surf Sci 604:11

[3] Merte LR, Knudsen J, Eichhorn FM, Porsgaard S, Zeuthen H, Grabow LC, Laegsgaard E, Bluhm H, Salmeron M, Mavrikakis M, Besenbacher F (2011) Jour Amer Chem Soc 133:10692

[4] Sun YN, Qin ZH, Lewandowski M, Carrasco E, Sterrer M, Shaikhutdinov S, Freund H (2009) Jour Cat 266:359

[5] Giordano L, Lewandowski M, Groot IMN, Sun YN, Goniakowski J, Noguera C, Shaikhutdinov S, Pacchioni G, Freund HJ (2010) J Phys Chem C 114:21504

Mo-C03+04

Donor/acceptor monolayer blends on noble metal surfaces

Patrizia Borghetti¹, Elizabeth Goiri², Afaf El-Sayed³, Celia Rogero⁴, Enrique Ortega^{2,4,5}, Dimas de Oteyza²

¹Institut des Nanosciences de Paris, Paris, France, ²Donostia International Physics Center, San Sebastian, Spain, ³Al-Azhar University, Nasr City, Egypt, ⁴Materials Physics Center, San Sebastian, Spain, ⁵Universidad del País Vasco, San Sebastian, Spain

In novel organic optoelectronic applications, the device efficiency depends crucially on the energy barrier that controls charge carrier injection at molecule/electrode interfaces. These processes are determined by the chemical interaction between the deposited species and the inorganic surface, as well as on morphological aspects. One possible strategy to further steer the structural and electronic properties at interfaces is to use molecular mixtures such as donor-acceptor molecular pairs, since the introduction of the supramolecular interaction may influence the molecule-substrate interaction. The accurate understanding of the intermolecular and molecule-substrate interactions, as well as of the interplay among them, is therefore a fundamental step for designing the functionality of the self-assembled system.

Within this framework, we use a powerful combination of surface sensitive techniques to determine the structure, the energy level alignment and interfacial charge transfer of two-dimensional donor-acceptor monolayers in direct contact with noble metal (111) surfaces. We show that the formation of an ordered mixed layer with a maximized donor-acceptor contact area leads to a characteristic energy level alignment at the molecule/metal interface regardless of the particular molecules and substrate [1]. We also provide evidence that the deposition of two different molecular species modifies the molecule's adsorption height, with relevant effects on the interfacial energy barrier as well on the chemical bonding with the metal surface [2]. Finally, we demonstrate that, by appropriate design of the supramolecular environment, charge transfer into empty molecular levels can be triggered across the metal-organic interface without the need to intercalate substrate-functionalizing buffer layers [3].

[1] A. El-Sayed, P. Borghetti, E. Ortega, D. de Oteyza, et al. ACS Nano, 7 (2013) 6914

[2] E. Goiri, P. Borghetti, D. de Oteyza, et al. Phys. Rev. Lett., 112 (2014) 117602

[3] P. Borghetti, A. El-Sayed, E. Ortega, and D. de Oteyza, et al. ACS Nano, 8 (2014) 12786

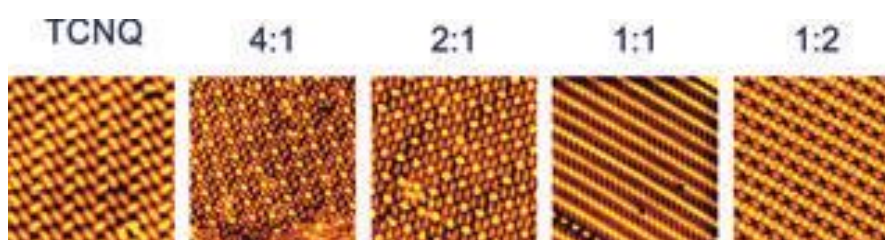
Mo-C05

Stoichiometry and Electronic Structure of Bidimensional Donor/Acceptor Superlattices on Metal Surfaces

Roberto Otero^{1,2}, Jonathan Rodríguez-Fernández¹, Alberto Martín-Jiménez², Maitreyi Robledo¹, Sergio Díaz-Tendero¹, José María Gallego^{2,3}, Fernando Martín^{1,2}, Rodolfo Miranda^{1,2}

¹Universidad Autónoma de Madrid, Madrid, Spain, ²IMDEA-Nanociencia, Madrid, Spain, ³ICMM-CSIC, Spain

Materials consisting of mixtures of strong organic acceptors (A) and donors (D) show a fascinating diversity of physical properties. The first purely organic metals were actually 1:1 mixtures of tetracyanoquinodimethane (TCNQ), a strong organic acceptor, and tetrathiafulvalene (TTF), a strong organic donor. After that, a large number of works have found a plethora of electronic behaviors such as Mott and Peierls insulators, charge- and spin-density wave states and organic superconductors. Whether one particular D:A mixture realizes one or the other of these states depend on their band filling which, in turn, depends on the D:A stoichiometry. Hitherto, however, the stoichiometry of D:A mixtures has been considered to be determined by the chemical nature of the donor and acceptor molecules, so that the only way to modify the D:A ratio in a controlled way would be the chemical functionalization of the molecular backbones. Here we show that the electronic flexibility offered by metal surfaces opens the possibility to choose the stoichiometry of 2D D:A mixtures supported on them from 2:1 to 1:4, as revealed by our STM investigations (see Figure). XPS and NEXAFS measurements together with DFT calculations demonstrate that the possibility of changing the stoichiometry is related to the variable doping of the 2D D:A layer with electrons arising from the substrate. This approach might thus open the possibility to synthesize 2D organic materials with a wide range of tunable properties that can be exploited to fabricate new electronic devices and sensors.



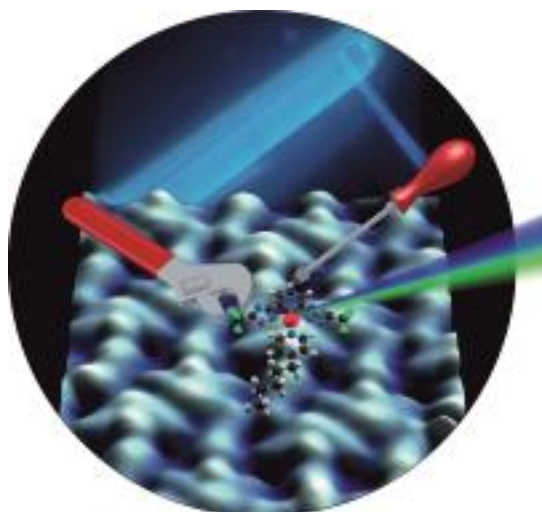
Mo-C06

Tunability of the Frontier Orbitals of Triplet Emitters studied by STM and STS

Pascal Raphael Ewen^{1,2}, Jan Sanning², Cristian A. Strassert², Alexander A. Khajetoorians¹, Daniel Wegner¹

¹Radboud Universiteit, Nijmegen, The Netherlands, ²Westfälische-Wilhelms Universität, Münster, Germany

State of the art organic light emitting diodes (OLEDs) are still under intense investigation both in fundamental research as well as development as challenges e.g. efficient deep blue emitters are still unsolved. Moreover, the physical and electronic behaviour on the nanoscale after thermal sublimation at the molecule-substrate interface is often unknown but can drastically determine the device performance. By using low temperature scanning tunnelling microscopy (STM) and spectroscopy (STS) we study the adsorption and electronic structure of recently synthesized Pt(II) complexes on Au(111). These molecules exhibit photoluminescent quantum yields up to 65 % and are used in prototype devices. By determining energies and spatial distribution of frontier orbitals of systematically changed organometallic complexes we are able to evaluate and control the impact of the ligands on the HOMO-LUMO gap which basically determines the emission and gives access to a wide range of wavelengths. Our findings provide a strategy to characterise and tailor organometallic molecules with targeted properties.



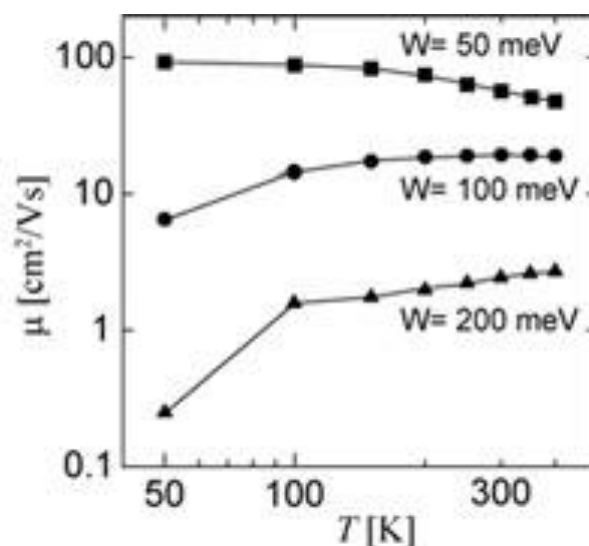
Mo-D01

Transport calculations of charge carrier coupled with molecular vibrations of organic semiconductors

Hiroyuki Ishii^{1,2}, Nobuhiko Kobayashi¹, Kenji Hirose³¹University of Tsukuba, Tsukuba, Japan, ²JST-PRESTO, Kawaguchi, Japan, ³NEC, Tsukuba, Japan

Organic semiconductors are expected as flexible, printable, lightweight device materials. Many chemists have synthesized various kinds of new organic semiconductors to improve the carrier mobility. Since the design and synthesis of new organic molecules require much time and labour, computational prediction of the device properties of the materials is very important for rapid progress of the present organic electronics. Therefore, we have developed a large-scale calculation methodology, which enables us to discuss the electron transport properties of various molecular crystals from an atomistic viewpoint. [1] We can evaluate the electron (hole) mobility by the Kubo formula based on the quantum wave-packet dynamics combined with the molecular dynamics simulations. Using the Chebyshev polynomial expansion for the time-evolution operator for the electron wave-packet motion, we treat the transport properties of huge systems with high-speed calculations. We can study the electron transport properties of materials from atomistic viewpoints up to 80 million molecules at various temperatures. We applied our method to some organic semiconductors and clarified the origin of transition from the low-mobility hopping-transport mechanism to the high-mobility band-like transport mechanism. Furthermore, we applied our method to the Hall effect analysis of organic semiconductors, which can reveal the intrinsic transport mechanism. These results will be a useful information when new organic semiconductors are designed. In my presentation, we will talk about the calculation method and the calculated results in detail. This work was supported by JST-PRESTO Molecular technology and creation of new functions.

[1] H. Ishii, et al., Phys. Rev. B 82, 085435 (2010); Phys. Rev. B 85, 245206 (2012); Phys. Rev. B 90, 155458 (2014).



Mo-D02

Organic radicals as electro- and magnetic-active units grafted on surface for molecular electronics and spintronics

Núria Crivillers¹, Yuan Li², Carlos Franco¹, Gonca Seber¹, Alexander Rudnev³, Marta Mas-Torrent¹, Concepció Rovira¹, Christian Nijhuis², Jaume Veciana¹

¹Institut de Ciència de Materials de Barcelona (ICMAB-CSIC), Campus de la Universitat Autònoma de Barcelona, Bellaterra, Spain ²National University of Singapore, Centre for Advanced 2D Materials and Graphene Research Centre, Department of Chemistry, Singapore, Singapore, ³Department of Chemistry and Biochemistry, University of Bern, Bern, Switzerland

For the preparation of functional organic materials designed to act as active components in molecular electronic devices, we employ the molecular bottom up approach. The ultimate goal of this approach is to employ functional building blocks to construct nanometer scale devices addressed to specific applications. For this, we have chosen the preparation of self-assembled monolayers (SAMs) as strategy to immobilize our target molecules on a suitable surface. In particular, our interest relies on the exploitation of stable organic radicals, with magnetic and electro-active properties, covalently linked to the substrate. These species have been grafted on gold and indium-tin oxide and it has been demonstrated that the redox and paramagnetic character measured in solution is preserved upon its adsorption on the surface. We have shown that they can perform as robust and non-volatile molecular memory devices [1] and that they are very promising for spintronics.[2] In this regard, in order to study the charge transport across SAMs based on these open-shell derivatives and to elucidate the transport mechanism, a family of molecules of different length consisting of a radical functional unit, a spacer with repeating methylene units and a thiol group as anchoring group has been synthesized. These molecules have been self-assembled on ultra-smooth template-stripped Au bottom electrodes, and softly contacted with GaO_x/EGaIn top-electrodes. The results obtained from these experiments are supported by temperature-depended measurements. Moreover, the electrical characteristics of these junctions have been correlated with the electronic structure based on the characterization done by UPS and NEXAFS.

[1] C. Simão, M. Mas-Torrent, N. Crivillers, V. Lloveras, J. M. Artés, P. Gorostiza, J. Veciana, C. Rovira. *Nat. Chem.* 2011, 3, 359.

[2] N. Crivillers, C. Munuera, M. Mas-Torrent, C. Simão, S. T. Bromley, C. Ocal, C. Rovira, J. Veciana. *Adv. Mater.* 2009, 21,1177.

Mo-D03

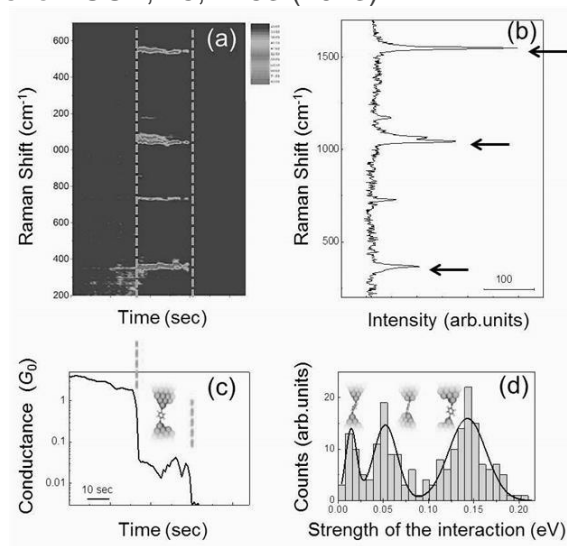
Electron transport and surface enhanced Raman scattering at structurally well-defined single 1,4-benzenedithiole

Satoshi Kaneko¹, Daigo Murai¹, Yuki Komoto¹, Kazuhito Tsukagoshi², Manabu Kiguchi¹¹Department of Chemistry, Tokyo Institute of Technology, Tokyo, Japan,²International Center for Materials Nanoarchitectonics, National Institute for Material Science, Tsukuba, Japan

Single molecular junctions (SMJs) have attracted wide interest due to their potential application to molecular electronic devices [1,2]. Since the structure of SMJs drastically affect on their electric structure, it is necessary to define their structure during conductance measurements. Surface enhanced Raman scattering (SERS) is one of the most promising technique to investigate the structure of single molecule. Although there are many efforts to measure SERS, there are few studies to measure SERS of SMJs, and quite few study revealed the electron transport of the SMJs in addition to SERS. In present study, we aim to reveal the electron transport of SMJs by measuring current-voltage characteristic property and SERS spectra simultaneously. We choose gold/1,4-benzenedithiole (BDT) system as a model system of SMJs. We fabricated SMJs by breaking gold nano contacts covered with BDT molecules. We simultaneously measured current-voltage characteristics and SERS spectra of a BDT-SMJ formed in breaking process at room temperature. We plotted time variation of the intensity of Raman bands and the conductance of nano contacts during breaking process (Figure 1 b,d). It revealed that SERS signal was drastically enhanced only when a SMJ was formed. The observed Raman bands were assigned to ring deformation mode coupled to CS stretching mode (360 cm^{-1}), ring breathing mode (1065 cm^{-1}), and CC stretching (1560 cm^{-1}). From the current-voltage characteristic measurement, we've found three different states which deferent in the strength of the interaction between BDT and gold (Figure 1d). The structure where BDT molecule adsorbed at atop site has the strongest interaction. It is revealed SERS signal drastically enhanced only when BDT adsorbed at atop sites. Strong interaction increases the charge transfer between BDT and gold, which enhance the resonant effect leading to the SERS signal.

[1] S.Kaneko, et al., Nanotechnology, 24 (2013) 315102.

[2] M.Kiguchi, S.Kaneko PCCP, 15, 2253 (2013).



Mo-D04

Unusually high electrical conductivity of a Pb monolayer on Ge(111)

Tetsuya Aruga¹, Shinichiro Hatta¹, Hiroshi Okuyama¹¹Kyoto University, Kyoto, Japan

Metal-covered semiconductor surfaces have long been serving as important subjects of surface science. Among them, the Pb/Ge(111) surface has been studied intensively with respect, for instance, to 2D melting transition and charge-density-wave (CDW) transition. The $\beta(\sqrt{3} \times \sqrt{3})$ phase of Pb/Ge(111) has a Pb coverage of $4/3$, which corresponds to an atomic number density of 9.62 nm^{-2} , 2% larger than that of Pb(111). The ARPES and DFT results [1,2] indicated that the $\beta(\sqrt{3} \times \sqrt{3})$ -Pb monolayer is well approximated by a 2D metal with nearly-free electrons (NFE). The NFE band is spin-split due to the Rashba spin-orbit interaction. The spin splitting amounts to 200 meV at EF. In order to study the physics related to the 2D NFE electrons in the $\beta(\sqrt{3} \times \sqrt{3})$ -Pb monolayer, we have measured the macro-scale electrical conductivity at $T = 10 - 330 \text{ K}$ [3]. The surface exhibits a high electrical conductivity, 10 mS/sq. , which is more than an order of magnitude larger than those reported previously for metal monolayers, such as In and Ag, on Si(111). An analysis indicates that the conductivity is dominated by the 2D NFE band in the $\beta(\sqrt{3} \times \sqrt{3})$ -Pb monolayer. Since the macro-scale surface conductivity is believed to be limited by the surface steps, we determined the step conductivity on this surface by comparing the conductivities on flat and vicinal substrates. The step conductivity determined on this surface was found to be two orders of magnitude larger than those in other metal monolayers on Si. In order to understand the origin of high step conductivity, the atomic and electronic structure of monatomic steps are discussed.

[1] K. Yaji, et al., Nat. Commun. 1, 17 (2010).

[2] K. Yaji, et al., Phys. Rev. B 86, 235317 (2012).

[3] S. Hatta et al., Phys. Rev. B 90, 245407 (2014).

Mo-D05+06

Charge re-distribution at organic interfaces to reach electronic equilibrium

Norbert Koch^{1,2}

¹Humboldt-Universität zu Berlin, Berlin, Germany, ²Helmholtz-Zentrum Berlin für Materialien und Energie, Berlin, Germany

Forming a contact between materials (metals and semiconductors or semiconductor heterojunctions) with different chemical potential of electrons requires a charge density redistribution to establish electronic equilibrium throughout the combined system. Depending on the electronic coupling strength at the interface, the charge redistribution can be highly localized in the form of a covalent bond or in the limit of negligible coupling by the transfer of integer charges, which leads to energy level bending in a semiconductor. Both cases can, however, be described by one electrostatic-based model, provided that the coupling-induced density of states is known. This will be discussed for a few prototypical examples, and the term "interface (-induced) doping" will emerge. Regarding interface doping, Fermi-level pinning at the frontier energy levels of the organic semiconductor determines the sign and magnitude of charge accumulation in the semiconductor and the associated energy level bending. Noteworthy, Fermi-level pinning – often induced by the presence of a remote electrode – is the reason for localized interface dipoles at organic heterojunctions, whereas un-pinned junctions are characterized by interface doping of only one constituent, while an electrostatic potential drop occurs in the other. These phenomena are exemplified with interfaces designed to exhibit Fermi-level pinning induced interface doping. Further complexity of such systems is introduced by contact-induced molecular orientation changes, which further alters the interface density of states. Only when all possible effects are accurately rationalized it is possible to derive reliable design rules for interfaces with organic semiconductors in opto-electronic devices.

Mo-E01+02

Hydrogen production from water by thermal and photo-excited methods

Hicham Idriss^{1,2}, Hamdan Al Ghamdi¹, Adnan Khan¹, Amtiaz Nadeem¹, Yahya Al-Salik¹

¹SABIC, Thuwal, Saudi Arabia, ²UCL, London, UK

Hydrogen production from water is at the essence of the energy system needed for a sustainable economy. Many methods for making hydrogen from water are pursued. Among the most promising of them are thermal- [1] and photo-reactions [2]. In thermal reactions, the main challenge is making reducible materials at temperatures low enough warranting applications while in photoreactions the main challenge is in the developments of photocatalysts with charge carriers' life time long enough affording high rates of electron transfers to and from the valence and conduction bands of the semiconductor [3]. In this work we are discussing our recent progress on both fronts. For thermal reactions a case study of the effect of doping CeO₂ with metal cations on its reducibility and therefore activity based on experimental and computational results is presented. The incorporation of iso-valent metal cations of similar size to Ce (+4 cations) can enhance the reduction of CeO₂ due to charge transfer and not to size effect. We correlate the extent of reduction of CeO₂ to its redox/activity for hydrogen production using core level spectroscopy and thermal gravimetric analyses. For photo-catalytic reactions we focus in particular on the effect of metal particle size and dispersion (Au and Pd) on the reaction rate. We have found for example a finite range for metal coverages affecting the rate of reaction by over an order of magnitude. These may be linked to charge transfer properties increasing/decreasing the charge carriers' lifetime and therefore the rate of reaction.

[1] W.C. Chueh, C. Falter, M. Abbott, D. Scipio, P. Furler, S.M. Haile, A. Steinfeld, *Science* 330 (2010) 1797.

[2] S. Bashir, A.K. Wahab, H. Idriss, *Catalysis Today* 240 (2015) 242.

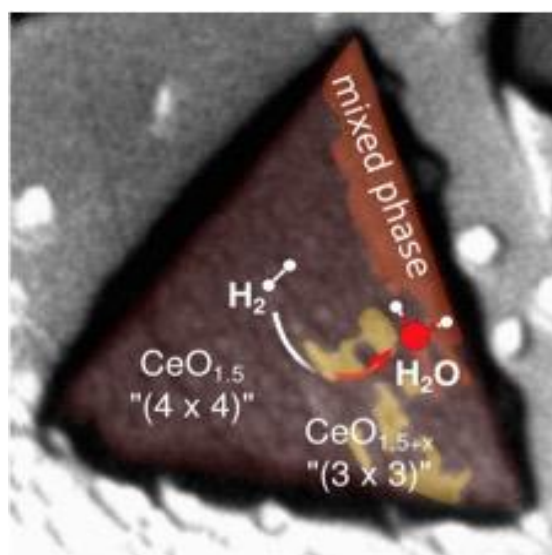
[3] M. Xu, Y. Gao, E.M. Moreno, M. Kunst, M. Muhler, Y. Wang, H. Idriss, C. Woll, *Phys. Rev. Lett.* 106 (2011) 138302.

Mo-E03

In situ microscopy of ceria inverse model catalysts using slow electrons

Jens Falta¹, Jan Ingo Flege¹¹University of Bremen, Bremen, Germany

Static characterization of model systems in heterogeneous catalysis has brought essential understanding in terms of the fundamental chemistry of the catalyst's surface. A deeper understanding of many crucial processes, however, requires dynamic information, in order to illuminate the development of reaction conditions. These often involve a substantial reorganization of the catalyst's structure and morphology. In situ probing promises a way out and may deliver unprecedented insights into their real-time evolution in a reactive environment. When combined with a spectro-microscopic approach, more complex situations can be addressed in which the catalyst contains an intrinsic heterogeneity or is comprised of multiple components on the nanoscale as, e.g., represented in conventional and inverse model catalyst architectures. Consequently, characterizing these geometries with a local, in situ probe facilitates an individual assessment of the component-specific structure and activity, and it provides a direct handle to the investigation of transient phenomena and cooperative effects. In this presentation, we show results from low-energy electron microscopy (LEEM) the preparation of ceria-containing model catalysts as well as their functionality under reaction conditions. Measuring the energy-dependent reflectivity of slow electrons, i.e. intensity-voltage $I(V)$ curves, delivers a powerful fingerprint of the local atomic structure and effectively bridges the gap between atomic, nanoscale, and mesoscale structures. For the inverse model system of ceria/Ru, we demonstrate the possibility of distinguishing between different oxygen-induced surface reconstructions and ceria oxide phases on the one hand and oxidation states, Ce^{+3} vs. Ce^{+4} , on the other hand, both with nanometer resolution. This allows following their structural transformations during redox reactions. Furthermore, the transferability of the approach to other transition metal surfaces and oxide systems will be addressed.



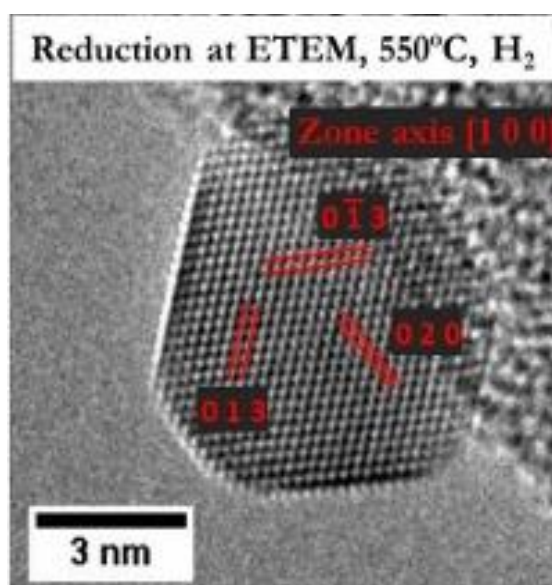
Mo-E04

In situ characterization of intermetallic Pd₂Ga/SiO₂ nanoparticles for low pressure CO₂ hydrogenation to methanol

Elisabetta Maria Fiordaliso¹

¹Center for Electron Nanoscopy, Technical Univ. of Denmark, Lyngby, Denmark

A nanodispersed intermetallic Pd₂Ga/SiO₂ catalyst is prepared by simple impregnation of industrially relevant high surface area SiO₂ with Pd and Ga nitrates, followed by drying, calcination and reduction in hydrogen. The catalyst is tested for CO₂ hydrogenation to methanol at ambient pressure, revealing that the intrinsic activity of the Pd₂Ga/SiO₂ is higher than that of the conventional Cu/ZnO/Al₂O₃, while the production of the undesired CO is lower. A combination of complementary in situ and ex situ techniques are used to investigate the Pd₂Ga/SiO₂ catalyst. In situ X-ray Diffraction (XRD) and in situ Extended X-ray Absorption Fine Structure Spectroscopy (EXAFS) show that the Pd₂Ga intermetallic phase is formed upon activation of the catalyst via reduction and remains stable during CO₂ hydrogenation. Identical Locations - Transmission Electron Microscopy (IL-TEM) images acquired ex situ, i.e. micrographs of exactly the same catalyst area recorded at the different steps of activation/reaction procedure show that nanoparticle size and dispersion are defined upon calcination with no significant changes observed after reduction and methanol synthesis. Similar conclusions can be drawn from electron diffraction patterns and images acquired at the Environmental TEM (ETEM) at 4 mbar, indicating that ETEM results are representative for the catalyst treated at ambient pressure. The chemical composition and the crystalline structure of the nanoparticles were identified by Scanning TEM Energy Dispersive X-Ray spectroscopy (STEM/EDX), Selected Area Electron Diffraction (SAED) patterns and atomically resolved TEM images.



Mo-E05

Revealing the important role of the catalytic support via in operando XPS measurements using the Near Ambient Pressure Photoemission (NAPP) endstation at the ALBA synchrotron

Carlos Escudero¹, Núria Jiménez Divins², Inma Angurell³, Jordi Llorca², Eric Pellegrin¹, Lucía Aballe¹, Josep Nicolas¹, Salvador Ferrer¹, Virginia Pérez-Dieste¹

¹ALBA synchrotron, Cerdanyola del Vallès, Spain, ²Institute of Energy Technologies and Centre for Research in NanoEngineering, Technical University of Catalonia-BarcelonaTECH, Barcelona, Spain, ³Department of Inorganic Chemistry, University of Barcelona, Barcelona, Spain

NAPP emerged in the last decade as a powerful tool to investigate surface chemical processes under conditions that are closer to the practical operation of catalysts compared to the traditional UHV-based spectroscopy techniques. At the Alba light source, a XPS setup operating from UHV to 20 mbar is in routine operation. Here we describe the first results concerning catalytic studies on the Ethanol Steam Reforming (ESR) reaction. [1] ESR is an interesting reaction for in situ hydrogen production, one of the future possibilities for cleaner energy applications. Determining the chemical surface composition of the catalyst during its operation is essential to understand how the catalyst works. In practice, the metallic catalysts are sitting on a support which is often a stable oxide. Here we report on the results obtained by comparing the surface composition of supported and unsupported bimetallic nanoparticles, as catalysts, under operating conditions. The unsupported model catalysts were nanoparticles of $\text{Rh}_{0.5}\text{Pd}_{0.5}$ deposited on a W foil and the supported real catalysts consisted of $\text{Rh}_{0.5}\text{Pd}_{0.5}$ nanoparticles on CeO_2 . By comparing photoemission data from Rh and Pd core levels at different photon energies, it was concluded that during the activation of the catalyst (by hydrogen reduction) Pd segregated toward the surface in both cases. However, under reaction conditions, the interaction with CeO_2 prevents the migration of Rh toward the outer shells in the real catalyst as compared to the model system and the surface of supported nanoparticles contains a large proportion of Pd and Rh oxides (Fig. 1) due to the capability of the CeO_2 support to activate water and donate oxygen atoms.

[1] N. J. Divins, I. Angurell, C. Escudero, V. Pérez-Dieste, J. Llorca, *Science* (2014), vol 346, issue 6209, p. 620-623

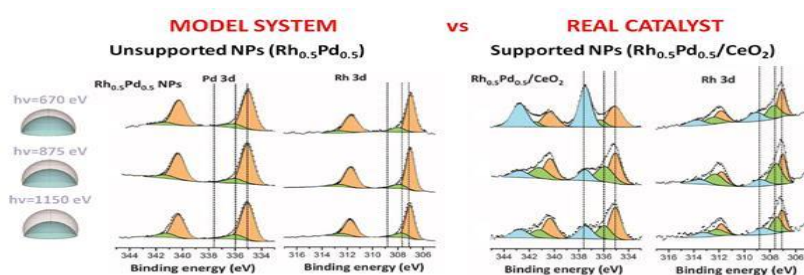


Fig. 1. XPS spectra of unsupported NPs (model system) and NPs supported on ceria (real catalyst) acquired at three different photon energies under ESR conditions at 823 K and 0.05 mbar. The peaks in orange correspond to the metallic species, the green ones to the Pd and Rh metal oxides (MO_x) and the blue peaks correspond to different oxidized Pd and Rh species arising by the interaction with the CeO_2 support.

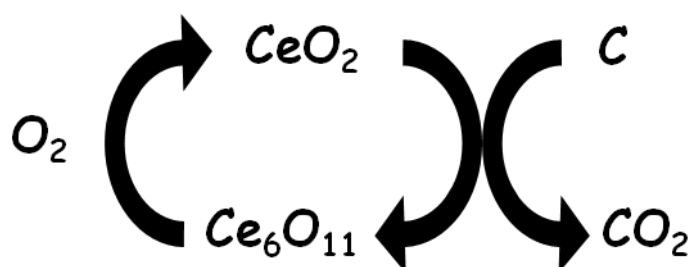
Mo-E06

How is soot oxidised over CeO_2 ? A combined AP-XPS and HRTEM study

Jordi Llorca¹, Albert Casanovas¹, Lluís Soler¹, Alessandro Trovarelli², Carlos Escudero³, Virginia Pérez-Dieste³

¹Institute of Energy Technologies, Univ. Politècnica de Catalunya, Barcelona, Spain, ²Dipartimento di Chimica, Fisica e Ambiente. Università di Udine, Udine, Italy, ³ALBA synchrotron light source, Cerdanyola del Vallès, Spain

The ability of ceria in promoting oxygen storage/redox behaviour is at the basis of its application as catalyst for combustion of soot particulate under conditions typical of diesel car exhaust. The use of CeO_2 and ceria-based materials has received increased attention in the last decade due to the low soot oxidation temperatures displayed by ceria and related materials, which is associated with the availability of surface active oxygen combined with good surface reducibility. Here we study the oxidation of soot over cerium dioxide under AP-XPS operando conditions at ALBA synchrotron. The experiments are performed over polycrystalline ceria (blank) and ceria mixed with soot at 1 mbar from room temperature up to 823 K under (i) inert atmosphere (the only oxygen available is in the ceria lattice), and (ii) oxygen atmosphere. These results, together with a detailed ex situ HRTEM characterization, have allowed us to propose a mechanism for the soot oxidation reaction. Our results unambiguously show that soot is oxidized by the oxygen atoms in the CeO_2 lattice –not by oxygen present in the gas phase– which transforms in an ordered phase, Ce_6O_{11} , and later on it reoxidizes to CeO_2 by abstracting oxygen from the gaseous environment. This is crucial information for the design of new catalysts for soot abatement in environmental applications.



Mo-A07

Achieving long range magnetic order on a monolayer of TCNQ adsorbed on graphene / Ru(0001)

Amadeo Vázquez De Parga¹, Manuela Garnica¹, Sara Barja¹, Daniele Stradi¹, Fabian Calleja¹, Cristina Diaz¹, Manuel Alcamí¹, Nazario Martín¹, Fernando Martín¹, Rodolfo Miranda¹

¹Universidad Autonoma de Madrid and IMDEA Nanoscience, Madrid, Spain

Epitaxial graphene grown on Ru(0001) is spontaneously nanostructured forming a hexagonal array of 100 pm high nanodomains with a periodicity of 3 nm and localized electronic states. Low Temperature Scanning Tunnelling Microscopy and Spectroscopy (LT-STM/STS) and Density Functional Theory (DFT) simulations show that isolated TCNQ molecules deposited on gr/Ru(0001) acquire charge from the substrate and develop a sizeable magnetic moment, which is revealed by a prominent Kondo resonance [1]. The magnetic moment is preserved upon dimer and monolayer formation. The self-assembled molecular monolayer develops spatially extended spin-split electronic bands with only the majority band filled, thus becoming a 2D organic magnet whose predicted spin alignment in the ground state is visualized by spin-polarized STM at 4.6 K [2]. The long range magnetic order is originated by the charge transfer from graphene to TCNQ (which creates the magnetic moments) plus the self-assembly of the molecular adlayer on the periodically corrugated graphene layer (which creates spin-polarized intermolecular bands where the added electrons delocalize). Examples will be shown where the adsorbed molecules accept charge and develop magnetic moments, but do not form bands and, accordingly, no long-range order appears (F4-TCNQ on graphene/Ru(0001)), or where molecules do form similar bands, but they are not populated because there is no charge transfer to the molecules (TCNQ on gr/Ir(111)). No long range magnetic order develops in these cases.

[1] M. Garnica et al. Nano Letters 14, 4560 (2014)

[2] M. Garnica et al. Nature Physics 9, 368 (2013)

Mo-A08

Intermolecular magnetic interactions in phthalocyanine sandwiches

Barbara Brena¹, Heike Herper¹, Johann Lüder¹, Rocío Sánchez de Armas¹, Olle Eriksson¹, Biplab Sanyal¹

¹Uppsala University, Uppsala, Sweden

Organic molecules like phthalocyanines and porphyrins containing divalent 3d transition metals, are among the most promising candidates for applications in molecular electronics and spintronics. It has been proved that the electronic structure and the spin of these compounds can be affected by factors such as ligands and adsorption configurations. In search of a practically feasible magnetic switching mechanism, we have previously studied how the molecular spin in porphyrins and phthalocyanines is affected by the interaction with magnetic substrates [1-3] as well as by the adsorption of gases.[4] As a new step, in view to study the magnetic behavior in novel supra-molecular architectures, we have analysed the magnetic coupling and moment in molecular sandwiches of various types of transition metal phthalocyanines, like FePc and MnPc. We have performed ab initio and hybrid Density Functional Theory (DFT) studies of metal phthalocyanine sandwiches in gas phase as well as adsorbed on metallic surfaces, with the GGA+U method including van der Waals dispersion forces. We find generally weak ferromagnetic couplings between the molecules, apart from the case of sandwiches of MnPc. We find also that the coaxial adsorption of gases like CO and NO has a strong effect on the spin, reducing the magnetic moments of the molecule on which they are adsorbed. The spin reduction effect depends on the gas and amounts to some μ_B .

[1] S. Bhandary, et al. Rev B, 88. (2013) 024401.

[2] D. Klar, et al. Phys. Rev. B 88. (2013) 224424.

[3] H. C. Herper, et al. Phys. Rev. B 89 (2014) 085411.

[4] H. Herper, B. Brena, published online. DOI: 10.1063/1.4917242

Mo-A09

Magnetic properties of tetra-phenyl-porphyrins adsorbed on metal surfaces

Mirco Panighel^{1,2,4}, Marco Caputo³, Giovanni Di Santo⁴, Andrea Goldoni⁴

¹Institut Català de Nanociència i Nanotecnologia, Campus de la UAB, Bellaterra, Barcelona, Spain, ²Università degli Studi di Trieste, Trieste, Italy,

³Laboratoire de Physique des Solides, Université Paris Sud, Orsay Cedex, France, ⁴Elettra Sincrotrone-Trieste, Basovizza, Trieste, Italy

Within the next few years the traditional semiconductor technology will reach its essential size limit. The use of organic molecules as single functional units in metal-organic based devices could overcome this limitation. However, the success of this approach strongly depends on the understanding of the interaction of the molecules with metallic substrates which determines the electronic and magnetic properties of these interfaces. Organic molecules such as porphyrins can be deposited in the sub-monolayer regime on single crystal surfaces in ultra high vacuum and geometrically ordered structures can be obtained from this procedure [1]. Taking advantage of the flexibility in choosing their molecular substituents, in combination with the presence of active sites of interactions with metals [2-4], this kind of molecules can be used to fabricate two-dimensional arrays of metallic centres with nanometric spacing, making them promising candidates for applications in emerging fields like spintronics and molecular electronics. By means of XPS, NEXAFS and XMCD techniques we studied the self-assembly, metalation and magnetic properties of tetra-phenyl-porphyrins (TPP) on metal substrates. Focusing on the magnetic coupling of two layers of molecules with a ferromagnetic thin film, we will show that, in the case of a MnTPP layer on FeTPP/Fe(110), the magnetic coupling extends to the second molecular layer, and its magnetization is opposite with respect to the substrate [5].

[1] G. Di Santo et al., Chem. Eur. J. 18 (2012) 12619

[2] M. Panighel et al., J. Phys. Conf. Ser. 470 (2013) 012012

[3] G. Di Santo et al., J. Phys. Chem. C 115 (2011) 4155

[4] A. Goldoni et al., ACS Nano 6 (2012) 10800

[5] M. Panighel et al., Oral. Comm., SINFO II, 25-27 June 2014, Trieste

Mo-A10

Tuning the magnetocrystalline anisotropy of single molecules

Benjamin W. Heinrich¹, Lukas Braun¹, Jose I. Pascual^{2,3}, Katharina J. Franke¹

¹Freie Universität Berlin, Berlin, Germany, ²CIC nanoGUNE, Donostia-San Sebastian, Spain, ³Ikerbasque, Basque Foundation for Science, Bilbao, Spain

Magnetism in single atoms and molecules is governed by the atomic-scale surrounding, which determines the ligand field splitting of the d states and the magnetic anisotropy [1]. Here, we determine the magnetocrystalline anisotropy of Fe-octaethyl-porphyrin and Fe-octaethyl-porphyrin-chloride molecules adsorbed on Pb(111) by inelastic scanning tunnelling spectroscopy. We observe that the axial anisotropy of the chlorinated species shows a monotonous increase as the tip of the scanning tunneling microscope approaches towards the Fe center [2], whereas it decreases on the dechlorinated species. We ascribe these changes to a deformation of the molecules in the presence of the attractive force of the tip, which leads to a change in d level alignment and consequently the magnetocrystalline anisotropy [3].

[1] D. Gatteschi, Molecular Nanomagnets, Oxford University Press: Oxford (2006).

[2] B.W.Heinrich et al., Nat. Phys. 9, 765 (2013).

[3] B.W.Heinrich et al., Nano Lett. (2015), DOI: 10.1021/acs.nanolett.5b00987.

Mo-A11+12

Exploring magnetic interaction strengths of metal-organic molecules on a superconductor

Katharina Franke¹¹Freie Universität Berlin, Berlin, Germany

The magnetic properties of atoms and molecules are significantly affected by their adsorption on a surface. Hybridization of the adsorbate's electronic states with the electronic states of the substrate may change or even quench the spin state. Scanning tunneling spectroscopy is an ideal tool to resolve these effects on the atomic scale. Here, we use a superconducting Pb crystal as a substrate for different paramagnetic metal-organic molecules. The two Bardeen-Cooper-Schrieffer (BCS) energy gaps around the Fermi level arise due to electron-phonon coupling on the s-p- and d-like bands of the Pb Fermi surface [1]. We show that the energy gap is ideally suited to study magnetism of paramagnetic adsorbates in the limit of weak coupling, i.e., without detectable magnetic interaction, and with sizeable magnetic interactions, which lead to the formation of Shiba states inside the superconducting energy gap. Fe-Octaethylporphyrin-Chloride (FeOEP-Cl) is a prime example of weak magnetic interaction. We show that the lifetime of excited spin states in this molecule is orders of magnitude longer on a superconductor than on a normal metal. We ascribe this increase in spin relaxation time to the superconducting energy gap at the Fermi level, which prohibits efficient pathways of energy quenching into the substrate [2]. Mn-Phthalocyanine, on the other hand, exhibits a triplet of Shiba states inside the superconducting energy gap as a fingerprint of magnetic interaction. The bound state energy varies with the adsorption site. We explain the splitting of the Shiba states as a result of magnetic anisotropy, which has been theoretically predicted [3].

[1] M. Ruby, B. W. Heinrich, J. I. Pascual, K. J. Franke, Phys. Rev. Lett. 114, 157001 (2015)

[2] B. W. Heinrich, L. Braun, J. I. Pascual, K. J. Franke, Nature Physics 9, 765 (2013)

[3] R. Zitko, O. Bodensiek, T. Pruschke, Phys. Rev. B 83, 054512 (2011)

Mo-B07

Surface-interface exploration of ultra-thin MgO oxide films grown onto metallic and semiconductor substrates

Brice Sarpi¹, Rachid Daineche¹, Christophe Girardeaux¹, Maxime Bertoglio¹, Frederic Derivaux¹, Jean-Paul Biberian², Anne Hemeryck³, Sebastien Vizzini¹

¹Aix Marseille Université-IM2NP, Marseille, France, ²Aix Marseille Université-CINaM CNRS, marseille, France, ³Université de Toulouse-CNRS,LAAS, Toulouse, France

For relevant applications in microelectronics and semiconductor-based spintronic, the main issue is to find new routes to process well controlled homogenous oxide layers onto semiconductor surfaces known for their high reactivity to oxygen species, and more precisely on how to reach a high-quality interface between the deposit and the silicon substrate. Some recent studies explore an innovating growth method, in which the oxidation is performed at room temperature (RT) on a metallic monolayer (ML) previously deposited on silver or silicon substrates, resulting in a high homogenous oxide layer with sharp interfaces and preventing interfacial silicon oxide formation. We will report in this talk our results concerning the RT growth and oxidation of Mg deposited onto Si(100)-2x1 and Ag(111) surfaces. Coverages from 0.05 ML to 3 ML were investigated using scanning tunneling microscopy (VT-STM), Auger electron spectroscopy (AES) and low energy electron diffraction (LEED), in a specific UHV experimental setup dedicated to in situ elaboration and characterization of ultrathin oxide films. The RT growth mode for magnesium onto Si(100) was identified as a two steps process. At very low coverage, there is formation of an amorphous ultrathin silicide layer with a band gap of 0.74 eV, followed by a layer-by-layer growth of metallic Mg on top of this silicide layer. Topographic images reveal that each metallic Mg layer is formed by 2D islands coalescence process on top of the silicide interfacial layer. Associated preliminary results were recently published in Applied Physics Letters 106, 021604 (2015). During RT oxidation of the Mg ML, the interfacial silicide layer acts as diffusion barrier for the oxygen atoms with a decomposition of the silicide film to a magnesium oxide as a function of molecular oxygen exposure.

Mo-B08

In situ growth and redox study of ultrathin cerium oxide films on Au(111) and Pt(111)

Marc Sauerbrey¹, Gabriele Gasperi^{2,3}, Jens Falta¹, Paola Luches³, Sergio Valeri^{2,3}, Jan Ingo Flege¹

¹Institute of Solid State Physics, University of Bremen, Bremen, Germany,

²Dipartimento FIM, Università di Modena e Reggio Emilia, Modena, Italy, ³S3, Istituto Nanoscienze - CNR, Modena, Italy

Cerium oxide (ceria) is well-known for its enhancing effect on the catalytical activity of noble metal surfaces. For example, deposition of ceria turns the usually inert Au(111) surface into a highly active water-gas-shift catalyst. However, little is known about the fundamental growth and interaction mechanisms. In this contribution, a comparative Low-Energy Electron Microscopy (LEEM)-based growth and redox study of the inverse model catalysts ceria on Au(111) and ceria on Pt(111) is presented. For this purpose, ceria was grown by reactive molecular beam epitaxy (rMBE) as well as by post-oxidation of MBE deposited metallic cerium in the temperature range between 100°C and 770°C. In order to gain insight into the dynamic morphological and structural changes occurring during growth and oxidation/reduction, processes were followed in-situ in real-space (LEEM) as well as in reciprocal space (LEED). The oxidation state of the ceria films was determined by probing the local unoccupied bandstructure using Intensity-Voltage LEEM (I(V)-LEEM). Fully oxidized ceria islands were obtained on both substrates. LEED reveals a preferential collinear azimuthal alignment of the ceria lattice with the substrate. During reduction and (re)oxidation, significant morphological inhomogeneities can be observed in real space accompanied by the appearance of a variety of superstructures in reciprocal space. Their occurrence and evolution dynamics strongly depend on the ceria film thickness. Also the shape and morphology of the ceria islands exhibit a strong dependence on the deposition temperature as well as on the substrate. Since the catalytical properties of surfaces are heavily affected by their structure, morphology, and oxidation state, our results will help to find ways of preparing tailor-made catalysts of devised functionality.

Mo-B09

In-situ atomic-scale control of the pulsed-laser growth of a polar perovskite oxide

Michele Riva¹, Stefan Gerhold¹, Michael Schmid¹, Ulrike Diebold¹¹Institute of Applied Physics, TU-Wien, Wien, Austria

Pulsed-laser deposition (PLD) provides the best control and reproducibility of the chemical and structural properties of complex, multicomponent transition metal oxides. Despite the widespread use of PLD in the preparation of thin films and heterostructures, the complexity of the grown materials and the poor preparation of substrate surfaces largely prevented the investigation of growth with atomic-scale resolution [1]. On the other hand, a detailed understanding of such mechanisms is of paramount relevance to allow tuning the entangled chemical, structural, electronic, magnetic and catalytic properties of these materials. By combining PLD, high-pressure RHEED, in-situ STM, XPS, and LEIS, we investigate the growth of perovskite oxides on the polar SrTiO₃(110) surface. To compensate for the net bulk dipole moment, an overlayer of either tetrahedrally- or octahedrally-coordinated Ti atoms develops on the surface, resulting in a variety of surface structures [2]. Fine-tuning between such structures can be achieved by control of the Sr/Ti stoichiometry, allowing the investigation of the dependence of the growth kinetics on the substrate surface structure. We follow the homoepitaxial growth on the SrTiO₃(110)-(4×1) [3] surface, consisting of ordered rings of TiO₄ tetrahedra, and on octahedrally-terminated (2×4)/(2×5) SrTiO₃(110) [4]. Anisotropic diffusion is observed for the adspecies, whose preferential direction is determined by the surface structure. Moreover, kinetic barriers limit mobility across boundaries separating different surface structures. By tuning growth parameters, such as laser intensity, fluency and frequency, background oxygen pressure, and substrate temperature we can achieve either layer-by-layer or step-flow growth, with the TiO_x structures of the topmost layer continuously floating to the surface of the film.

[1] R. Shimizu, et al., Cryst. Growth Des. 14, 1555 (2014).

[2] Z. Wang, et al., Phys. Rev. B 83, 155453 (2011).

[3] Z. Wang, et al., Phys. Rev. Lett. 111, 056101 (2013).

[4] Z. Wang, et al., submitted

Mo-B10

Ultra-thin stepped iron oxide films on high index Pt surfaces

Elin Grånäs^{1,2}, Niclas Johansson², Mohammad A. Arman², Jacek Osiecki³,
Karina Schulte³, Jesper N. Andersen^{2,3}, Joachim Schnadt², Jan Knudsen^{2,3}

¹NanoLab, Deutsches Elektronen-Synchrotron (DESY), Hamburg, Germany,

²Division of Synchrotron Radiation Research, Lund University, Lund, Sweden,

³MAX IV Laboratory, Lund University, Lund, Sweden

Iron oxide islands grown on metal surfaces show high catalytic activity for reactions such as CO oxidation and the water-gas shift. It has been suggested that the high activity is due to under-coordinated Fe atoms at the edge of the FeO islands.[1] On such FeO islands the active edge sites are few and heterogeneous, making it difficult to characterize the active sites with chemically sensitive averaging techniques like X-ray photoelectron spectroscopy (XPS). Further, whether the metal substrate is essential for the activity of the edge sites remain an open question. Here we present FeO films grown on Pt(322), producing stepped films with a very high density of homogenous FeO-FeO edge sites, making it well suited for adsorption studies using techniques like XPS. Using scanning tunneling microscopy we show that approximately 20 % of the sites are edge sites.

Water adsorption studies on the stepped FeO film reveal an enhanced ability to split water compared to planar FeO, which is known to only interact weakly with water at UHV conditions.[2] As the Pt(322) substrate is fully covered by stepped FeO we assign the high water splitting ability to the pure FeO-FeO step sites.

[1] L. Xu, Z. Wu et al., J. Phys. Chem. C 115, 14290 (2011)

[2] F. Ringleb, Y. Fujimori, H.-F. Wang et al., J. Phys. Chem. C 115, 19328–19335 (2011)

Mo-B11

Structure and chemical properties of ultra-thin FeO films on Ag(100)

Lindsay R. Merte¹, Christopher J. Heard³, Feng Zhang², Mikhail Shipilin¹, Sara Ataran¹, Juhee Choi², Sara Blomberg¹, Chu Zhang¹, Anders Mikkelsen¹, Johan Gustafson¹, Jason F. Weaver², Henrik Grönbeck³, Edwin Lundgren¹

¹Lund University, Lund, Sweden, ²University of Florida, Gainesville, USA,

³Chalmers University of Technology, Göteborg, Sweden

Monolayer-thick iron oxide films have received significant attention recently owing to their novel chemical and catalytic properties. FeO(111) films on Pt(111) in particular have been studied in detail, and have been found to exhibit higher catalytic activity than the Pt(111) surface, attributed to formation of a reactive O-Fe-O trilayer structure [1]. Because the oxide film is only a monolayer thick, the underlying Pt surface plays an important role in determining the film's chemical properties, providing/accepting charge to/from adsorbates and inducing formation of a moiré superstructure. It is therefore expected that the chemical and catalytic properties of monolayer FeO can be modulated by growing it on different metal substrates. To test this, we have studied the growth of ultra-thin iron oxide films on Ag(100) and compared their structural and chemical properties with those studied previously on Pt(111). Depending on the deposition conditions, we observe formation of monolayer FeO(111), an FeO(111)-like multilayer phase, or FeO(100). The FeO(111) monolayer is similar to that grown on Pt(111), but we find that it exhibits an expanded in-plane lattice parameter suggestive of a flattening of the film due to the weaker interaction with the Ag substrate [2]. TPD and RAIRS measurements show that unlike FeO/Pt(111) [3], NO chemisorbs easily and strongly onto the Ag-supported FeO film at 90 K. DFT+U calculations confirm the flattening of the FeO film and indicate that the strong effect of the substrate on reactivity is due primarily to steric effects linked to the subtle differences in structure, the Fe ions in the Ag-supported film being more accessible to impinging gas molecules.

[1] Sun, Y.-N. et al. *Angew. Chem. Int. Ed.* 49, 4418–4421 (2010).

[2] Merte, L. R. et al. *J. Phys. Chem. C* 119, 2572–2582 (2015).

[3] Lei, Y. et al. *ChemCatChem* 3, 671–674 (2011).

Mo-B12

Fe₃O₄(001) thin film growth on Pt(100): Tuning of surface termination with an Fe buffer layer

Earl Matthew Davis¹, Ke Zhang¹, Yi Cui¹, Helmut Kuhlbeck¹, Shamil Shaikhutdinov¹, Hans-Joachim Freund¹

¹Fritz-Haber Institute of the Max-Planck Society, Berlin, Germany

Investigations on the structures of iron oxides have primarily focused on close-packed surfaces such as Fe₃O₄(111) and Fe₂O₃(0001). Recently, more work has been directed toward the Fe₃O₄(001) surface following expectations of a large difference in reactivity when compared to the (111) surface [1]. We have studied the preparation of well-ordered thin Fe₃O₄(001) films on a metallic substrate, Pt(100), using LEED and STM. The results show that film growth either by Fe reactive deposition in oxygen or by deposition–oxidation cycles onto pure Pt(100) results primarily in (111)-oriented surfaces. The growth of Fe₃O₄(001) films requires the preparation to include the deposition of an Fe buffer layer as previously suggested for the growth of Fe₃O₄(001) on MgO(001) [2]. Two stable (so called “dimer”- and B-layer) surface terminations were observed, both exhibiting a ($\sqrt{2}\times\sqrt{2}$)R45° reconstruction. Several intermediate, Fe-rich terminations were observed during the annealing process of an initially dimer-type surface structure. The process critically depends on the thickness of the buffer layer, which can be used as a tuning parameter for the surface structure.

[1] Kendelewicz et al. Surf. Sci. 453 (2000) 32

[2] Spiridis et al. Phys. Rev. B 74 (2006) 155423

Mo-C07

Energy alignment and electron dynamics at the porphyrin/silver interface

Silvia Tognolini¹, Stefano Ponzoni¹, Francesco Sedona², Mauro Sambi²,
Stefania Pagliara¹

¹Università Cattolica Del Sacro Cuore Di Brescia, Brescia, Italy, ²Università degli studi di Padova, Padova, Italy

In the last decades we have witnessed to a growing interest in the field of electronic and opto-electronic devices based on organic materials, like OFETs, OLEDs and photovoltaic cells; these new devices rely on the use of organic conjugated molecules and polymers as active components in multilayer device applications [1]. Among these organic molecules, porphyrins and related compounds have been widely investigated due to the wide variety of important biological processes in which these molecules are involved and due to their catalytic properties. Moreover, porphyrins in a donor–acceptor system can harvest light efficiently and, once photoexcited, act as an electron donor for an acceptor moiety [2]. In this framework, the control of the electron dynamics, such as charge transfer and recombination processes, at the organic/metal interface is of paramount importance to improve the performance of many optoelectronic organic devices. In this work, we have tracked the energy level alignment of the HOMO and of the excited states with respect to metal Fermi level at the porphyrin/Ag(100) and porphyrin/Ag(111) interfaces by growing different layers thick film of tetraphenylporphyrin (TPP) and by subsequently collecting both linear and non-linear photoemission spectra. Moreover, by using time-resolved photoemission (in the pump-probe setup) snapshots of the charge carrier injection from the metal to TPP have been collected.

[1] F. Flores, J. Ortega and H. Vázquez, *Phys. Chem. Chem. Phys.* 11 (2009) , 8658–8675.

[2] M.R. Wasielewski, *J. Org. Chem.* 71 (2006), 5051.

Mo-C08

Hydrogen-bonding bimolecular networks on metal surfaces:
Hierarchical and charge separation effects

Christian Steiner¹, Maximilian Ammon¹, Tim Sander¹, Zechao Yang¹, Ute Meinhardt², Bettina Gliemann², Martin Gurrath^{2,3}, Bernd Meyer^{2,3}, Milan Kivala², Sabine Maier¹

¹Department of Physics, University of Erlangen-Nürnberg, Erlangen, Germany,

²Department of Chemistry and Pharmacy, Universität Erlangen-Nürnberg, Germany, Erlangen, Germany, ³Computer-Chemie-Centrum, University Erlangen-Nürnberg, Erlangen, Germany

Understanding and controlling the formation of multi-component molecular self-assemblies is important for the design of donor-acceptor networks which are an integral part of organic optoelectronic devices.[1-2] Here, we present a low-temperature scanning tunneling microscopy and spectroscopy study of homomolecular and bimolecular networks assembled from dimethylmethylen-bridged triphenylamines. The molecules have an identical central scaffold, and differ only in their functional groups that are carboxylic and diaminotriazine groups, respectively. First we discuss the subtle balance of molecule-surface and molecule-molecule interactions of the triphenylamines on Au(111) and Cu(111). On Cu(111) both molecules form compact self-assemblies owing to the strong molecule-surface interaction. The strong molecule-surface interaction is manifested in the partial deprotonation of the carboxylic groups and the preferential adsorption site of the amino moieties on Cu, respectively. In contrast, both triphenylamines adsorb intact on Au(111) and arrange in large porous hydrogen-bonded networks adopting the energetically most favorable bonding-motifs, indicating a predominant molecule-molecule interaction. Upon co-adsorption on Au(111), the molecules form perfectly ordered bimolecular honeycomb networks stabilized by hydrogen bonds between the carboxylic and the diaminotriazine groups. Density functional theory (DFT) calculations show no remarkable difference in the binding strength between the homo and bimolecular networks indicating that mainly geometrical aspects lead to the perfect intermixing. The HOMO-LUMO gap in the mixed network is defined by the two types of molecules, which is typical for an electron donor-acceptor scheme. We will discuss charge separation effects in the donor-acceptor network based on the shifts of the molecular orbitals measured in scanning tunneling spectroscopy and complementary DFT calculations.

[1] Barth et al., Nature, 2005, 437, 671-679

[2] El-Sayed et al., ACS Nano, 2013, Vol.7, No.8, 6914-6920

Mo-C09

On-surface preparation of self-terminating molecular chains

Emil Sierda^{1,2}, Maciej Bazarnik^{1,2}, M.Sc. Bernhard Bugenhagen³, Marc Heinrich Prosenc³, Wojciech Koczorowski¹, Roland Wiesendanger²

¹Institute of Physics, Poznan University of Technology, Poznan, Poland,

²Institute of Applied Physics, University of Hamburg, Hamburg, Germany,

³Institute of Inorganic and Applied Chemistry, University of Hamburg, Hamburg, Germany

Molecular spintronics employs organic molecules and metal-organic complexes as carriers of spin information. Considering the construction of an all-spin logical device, it is obvious that for each electronic component a spintronic counterpart is needed. The components typically encountered include conductors and junctions. In order to construct such devices a “bottom-up” approach is much more effective than the traditional “top-down” approach used for semiconductor electronics. It can be achieved by a precise control of self-organized growth of molecular systems, i.e. either by a clever design of molecules [1] or modifications of physico-chemical properties of the substrate (e.g. changing the Moiré pattern of intercalated graphene systems in order to shape the surface potential landscape and in effect control the molecules’ preferred adsorption sites [2]). In this work we show a solution to engineer short well defined molecular chains, built from cobaltosalophen molecules with bromide substitution of hydrogen on 5 and 5’ positions. Such molecules can form chains by utilizing an on-surface Ullmann reaction [3]. A molecule with only one bromide substitution acts as a terminator of the chain. Accurate control of the proportion of both types of molecules on the surface allows changing the preferred length of the molecular chains obtained. The structures may be used as wires in spintronic devices due to an antiferromagnetic coupling of spins localized on adjacent metallic molecular centers [3].

We gratefully acknowledge financial support from the DFG via SFB668 and in part from the Polish budget for education in the years 2014-2017 as a research project under the program known as “Diamond Grant” under number 0084/DIA/2014/43.

[1]. Grill L. et al. Nature Nanotechnology 2007, 2, 687-691.

[2]. Bazarnik M. et al. ACS Nano 2013, 7, 11341–11349.

[3]. DiLullo A. et al. Nano Letters 2012, 12, 3174-3179.



Mo-C10

On-surface polymerization on semiconductor surfaces

Marek Kolmer¹, Rafal Zuzak¹, Piotr Olszowski¹, Bartłomiej Zapotoczny¹, Jakub S. Prauzner-Bechcicki¹, Szymon Godlewski¹, Marek Szymonski¹

¹Centre for Nanometer-Scale Science and Advanced Materials, NANOSAM, Faculty of Physics, Astronomy and Applied Computer Science, Jagiellonian University, Krakow, Poland

On-surface chemistry has recently developed into a rapidly burgeoning field with the prospect of interfacing well-defined crystalline inorganic substrates with the in-situ custom-synthesized organic polymer layers. Although various reactions and monomer building blocks have been extensively studied on metal substrates [1], such polymerization processes are still only rudimentary developed on semiconductors. For the sake of practical applications of the on-surface covalent coupling, the semiconductor surfaces clearly represent much more attractive platforms. In this context we would like to report on strategies leading to an efficient oligomer formation on semiconductor surfaces with the emphasis on: (1) properly designed precursor molecules and (2) a proper surface functionalization. In particular, the surfaces of rutile TiO₂, the model representative of the whole class of transition metal oxides, will be discussed [2]. In this case, we will show that the presence of surface hydroxyl groups on TiO₂ is crucial for the polymerization reaction. Moreover, we will demonstrate that reaction efficiency could be steered by varying the density of surface hydroxyls. These results are in agreement with the recently proposed C-C coupling mechanism, which involves proton transfer from a surface hydroxyl group to the precursor molecule [2]. Finally, we will describe our attempts to initiate the polymerization reaction on hydrogenated semiconductors, i.e. Ge(001):H and Si(001):H. These substrates are of particular interest in the context of potential applications of covalently linked molecular structures in monomolecular electronic devices [3].

This research was supported by the 7th Framework Programme of the European Union Collaborative Project PAMS (contract no.610446).

- [1] G. Franc, A. Gourdon, *Physical Chemistry Chemical Physics* 2011, 13 (32), 14283
- [2] M. Kolmer, A. A. A. Zebari, J. S. Prauzner-Bechcicki, W. Piskorz, F. Zasada, S. Godlewski, B. Such, Z. Sojka, M. Szymonski, *Angewandte Chemie - International Edition* 2013, 52, 10300
- [3] J.S. Prauzner-Bechcicki, S. Godlewski, M. Szymonski, *Physica Status Solidi A* 2012, 209(4), 603–613.

Mo-C11

Solvation and thermodynamic calculations of small organic molecules on calcite

Akin Budi¹, Martin P Andersson¹, Susan L S Stipp¹¹University of Copenhagen, Copenhagen, Denmark

The understanding of how organic molecules interact with mineral surfaces is of major interest and relevance to a wide range of fields, including biomineralisation and enhanced oil recovery, and can bring with it significant environmental impact and economic benefits. Molecular modelling techniques, such as density functional theory (DFT), provide a powerful means to complement experimental techniques and gain insight into the fundamental bonding mechanism between organic molecules and mineral surfaces. However, these DFT calculations are generally performed in vacuum at 0 K, which can limit their applicability when compared with experiments performed, for example, in solution at ambient temperature. In this project, we aimed to incorporate thermodynamics and solvation effects into the description of small organic molecule adsorption on mineral surfaces, specifically, calcite. The thermodynamic results were obtained from explicit DFT calculations while the solvation effects were obtained using the COSMO-RS implicit solvent method. We also developed a description of model oil to serve as a basis for probing the solvation effects on the adsorption of the small organic molecules on calcite. This combined approach provided information about the adsorption behaviour of these small organic molecules on calcite at a variety of temperatures in different solutions. The results indicate that the combination of solvation and thermodynamics affects the adsorption of the molecules on calcite significantly, with only a handful still stable on the calcite surface in solution at 25 °C. Furthermore, most of these molecules are less stable in the water phase than in the oil phase of our model oil.

Mo-C12

Direct measurement of the molecular dynamics of rupture and reformation of confined liquid layers

Josep Relat-Goberna¹, Sergi Garcia-Manyes¹¹King's College London, School of Natural and Mathematical Sciences, London, United Kingdom

Understanding the structural properties of liquids at the solid interface is fundamental to many applications in the fields of nanotribology, wetting or molecular biophysics. When confined between two flat surfaces separated by a few nanometers, liquids organize in well-defined solid-like solvation layers, giving rise to oscillatory forces with a periodicity of about one molecular diameter. Confined layers have been studied over the last two decades using Surface Force Apparatus and Atomic Force Microscopy, which have revealed invaluable information about the molecular packing properties of a variety of chemically distinct liquids, all exhibiting a priori similar force-induced rupture mechanisms. This progress notwithstanding, the reverse process encompassing the reversible reformation of each individual layer remained completely elusive. Here, we make use of force-clamp spectroscopy AFM to directly capture the forced-induced rupture and reformation of each of the individual solid-like ordered layers populating the 1-undecanol-HOPG and the Ethylammonium Nitrate (EAN)-mica interfaces. These observations enabled us to map out the complete energy landscape of a confined liquid and to determine the number of bonds (or interactions), N , that withstand force. Our results for 1-undecanol indicate that a unique interaction ($N=1$) needs to be broken to induce the formation of a pore in the solid-like liquid layer. We speculate that the pore created in the structure of the confined liquid induces the lateral shift of a whole row of molecules. By contrast, for the ionic liquid EAN we measure a value of $N=2$, suggesting that two interactions, probably involving an individual ion-pair, have to be broken in tandem to induce the force-induced breakthrough and reformation of the individual solvation layer. Altogether, our experiments directly capture the molecular motions involved in the rupturing and self-assembly processes of individual solid-like liquid layers and highlight their single-molecule nature when confined in the nanometre realm.

Mo-D07+08

Polar discontinuities at grain boundaries in 2D materials

Miguel Pruneda¹¹Institut Catala de Nanociencia i Nanotecnologia, Bellaterra, Spain

Inversion domain boundaries have been observed in a number of ionic monolayers deposited on metallic and insulating substrates. Examples include hexagonal boron nitride on Ni(111), ultrathin EuO films on Ir(111), or transition metal dichalcogenides monolayers on HOPG [1-3]. These grain boundaries are visible as sharp bright lines in scanning tunneling microscopy (STM) images, and have been related to the presence of vacancy lines in the monolayers. However, inversion domains in 2D materials can also result in polar discontinuities, similar to those observed at interfaces of bulk oxides. The polar discontinuity gives rise to a bound polarization charge localized at the 1D interface, and under certain circumstances can give rise to new electronic states with metallic characteristics, explaining the experimental observation of a sharp bright peak in STM. So far, these effects had only been discussed theoretically [4-5], but their experimental verification might not be that distant. Ab initio DFT calculations will be presented to illustrate the electronic structure of inversion domain grain boundaries in 2D materials, and the screening effect of a metallic substrate discussed.

- [1] W. Auwarter et. al. Surf. Science 454 (2003) L735-L740
- [2] S. Schumacher et. al. Phys. Rev. B 89 (2014), 115410.
- [3] H. Liu et. al. Phys. Rev. Lett. 113 (2014), 066105.
- [4] N. C. Bristowe et. al. Phys. Rev. B 88 (2013) 161411R.
- [5] M. Gibertini et. al. Nat. Comm. 5 (2014) 5157.

Mo-D09

Lateral heterojunctions on GdAg₂ surface alloy

Lucia Vitali^{1,2}, Alexander Correa^{1,3}, Bin Xu^{4,5,6}, Matthieu Verstraete^{4,5}

¹Ikerbasque Foundation for Science, Bilbao, Spain, ²Departamento de física de materiales, Universidad del País Vasco EHU/UPV, San Sebastian, Spain, ³Donostia International Physics Center (DIPC), San Sebastian, Spain, ⁴Département de Physique, Université de Liège, Sart Tilman, Belgium, ⁵European Theoretical Spectroscopy Facility (<http://www.etsf.eu>), San Sebastian, Spain, ⁶ Department of Physics and Institute for Nanoscience and Engineering, University of Arkansas, Fayetteville, Arkansas, USA

A two dimensional GdAg₂ surface alloy layer is formed exposing the surface of Ag(111) to gadolinium atoms. Due to lattice mismatch with the supporting substrate this alloy forms moiré patterns with different periodicities. These result from minute relative reorientations of the alloy layer with respect to the Ag(111) surface and possibly of different in-layer strain [1, 2]. Although these patterns are formed by the same chemical structure and composition, they show surprisingly distinct electronic properties. Combining scanning tunneling microscopy and spectroscopy, we will explain the relation between the electronic properties and the layer structure. Density functional theory calculations have been performed to predict the electronic properties of this alloy as the band structure, work functions and spin-orbit coupling strengths. The reason for the striking difference in the electronic properties will be explained in terms of in-layer coupling strength of the Gd atoms in the alloy and their coupling with the underlying Ag substrate. A comparison with the GdAu₂ alloy grown on Au(111) surface [3], whose electronic and consequently magnetic structure show almost no dependence with the more periodicity, will be presented.

[1] K.Hermann J.Phys. 24, 314210 (2012)

[2] Lucia Vitali, M.Ramsey, F P.Netzer, Surf.Sci.452, L281 (2000)

[3] L.Fernandez, M.Blanco-Rey, M. Ilyn, Lucia Vitali, A. Magana, A. Correa, P.Ohresser, J.E.Ortega, A.Ayuela, F. Schiller, Nano letters, 14, 2977 (2014)

Mo-D10

Identifying distinctive electronic features of terminal and bridging hydroxyl groups of dissociated H₂O on TiO₂(110).Annapaola Migani¹¹Institut Català de Nanociència i Nanotecnologia, Bellaterra, Spain

In 1972 Fujishima and Honda demonstrated the photocatalytic splitting of H₂O into H₂ and O₂ on TiO₂ electrodes. Since this discovery, tremendous research efforts have gone into understanding the interaction of H₂O with quasi-stoichiometric and defective TiO₂ surfaces. Ultraviolet photoelectron spectroscopy (UPS) and scanning tunneling microscopy (STM) measurements have shown H₂O thermal dissociation occurs at bridging oxygen (O_{br}) vacancies of defective TiO₂(110), giving two bridging O_{br}H hydroxyl groups.¹ STM and two-photon photoemission (2PP) experiments have shown H₂O adsorbed at coordinately unsaturated (cus) Ti sites can be photochemically dissociated.¹ In this dissociation, both bridging as well as terminal hydroxyl O_tH groups lying atop cus Ti atoms are generated.¹ Recently, UPS measurements have shown O_tH groups are also formed via the interaction of O₂ with O_{br}H on TiO₂(110) with interstitial Ti defects.² Both O_{br}H and O_tH groups are important photocatalytic active species. It is therefore very important to identify the experimental fingerprints of these species. Here, we show that many-body quasiparticle GW techniques, namely G₀W₀, based on density functional calculations with PBE or hybrid HSE exchange-correlation functionals provide a quantitative assignment of UPS and 2PP experiments of H₂O on quasi-stoichiometric and defective TiO₂(110).³ Our G₀W₀ calculations: (i) reproduce the changes in the UPS spectra associated with thermal H₂O dissociation; (ii) permit to discern between the O_tH and O_{br}H features in UPS spectra; (iii) provide an accurate alignment relative to the Fermi level of the reduced Ti³⁺ levels of TiO₂(110) with O_{br}H groups, and finally (iv) provide a quantitative assignment of the so-called “wet-electron state” resonance of 2PP spectra.

[1] Friend, C.M. Perspectives on Heterogeneous Photochemistry. Chemical record (New York, N.Y.) 2014.

[2] Gabriele Tocci, PhD thesis.

[3] Migani, A.; Mowbray, D. J.; Zhao, J.; Petek, H. Quasiparticle interfacial level alignment of highly hybridized frontier levels: H₂O on TiO₂(110) J. Chem. Theory Comput. 2015, 11, 239–251.

Mo-D12

Momentum resolved electron-phonon coupling analysis for inelastic tunneling and photoemission

Ryuichi Arafune¹, Emi Minamitani², Noriyuki Tsukahara³, Satoshi Watanabe²,
Maki Kawai³, Noriaki Takagi³

¹International Center for Materials Nanoarchitectonics, National Institute for Materials Sciences, Tsukuba, Japan, ²Department of Materials Engineering, the University of Tokyo, Tokyo, Japan, ³Department of Advanced Materials Science, the University of Tokyo, Japan, Chiba, Japan

Electron phonon coupling (EPC) plays a crucial role in determining the range of the electrical thermal diffusion for femtosecond laser pulse excitation, forming the charge density waves, cooper-pair creation in superconductivity, etc. The EPC has been mostly analyzed through the momentum-averaged description such as the Eliashberg function. While such rather simplified description has successfully served a basis for intuitive understanding the above phenomena, it is often not sufficient to analyze the low-dimensional system and high-resolved experimental data. In this study, we have found that calculating the momentum resolved EPC is requisite for analysis of both the inelastic tunneling spectroscopy with STM (STM-IETS) [1] and inelastic photoemission spectroscopy (IEPES) [2]. The spectrum of the STM-IETS experiments for the Cu(110) surfaces shows a peak at 6 meV, while that of the IEPES for the same surface shows a step structure at 14.7 meV. The above characteristic energy does not appear in the phonon density of states straightforwardly. We have demonstrated that these energies agree with the peak energy of the spectra for the momentum resolved EPC which faithfully describes the matrix element of the interband transition of the electron with transferring the energy and momentum to the phonon. The density functional perturbation theory calculations show the strong peak at around 6.2 meV in the EPC spectrum for the electron near the Fermi level at the Γ point and at 14.5 meV for the electron just above the vacuum level at the Y point. Although the elementary processes of the inelastic tunneling and photoemission are different, the momentum resolved EPC calculations effectively describes the selectivity of the phonon excitation from among many possible phonon modes in both inelastic processes.

[1] R. Arafune et al., in preparation.

[2] E. Minamitani et al., Phys. Rev. B 88, 224301 (2013).

Mo-E07

Novel Solutions for Ambient Pressure and In-Situ Photoelectron Spectro-Microscopy

Hikmet Sezen¹, Matteo Amati¹, Luca Gregoratti¹¹Elettra Sincrotrone Trieste, Trieste, Italy

A technique based on photoelectron spectroscopy (PES) providing simultaneously spectroscopy and microscopy capabilities and being compatible with ambient pressure conditions is still missing. Ambient pressure PES (APPES) offers an optimal spectroscopic solution to overcome pressure barrier for surface related studies. Unfortunately, APPES has very limited spatial resolution. On the other hand, a better than 100 nm spatial resolution scanning photoelectron microscopes (SPEMs) is available in few synchrotrons. A direct adaptation of the APPES approach to SPEM technique is not possible because of geometric constraints, stabilities and sustainability of x-ray optics and the photoelectron detection system under near ambient pressures and severe pumping conditions. In this presentation we will introduce two novel solutions for near-ambient pressure SPEM with ~100nm spatial resolution and compatible with in-situ/operando conditions operated at ESCA microscopy beamline at Elettra synchrotron. Dynamic high pressure is the one of our near-ambient pressure SPEM solution. The technique is based on generating high pressure pulsed gas packets directed to the sample. Under influence of gas pulses the sample falls a few mbar pressure in a burst instant, then gas packets dilute into the SPEM chamber to yield a 1×10^{-5} mbar background pressure. From the test results a 10^{-3} - 10^{-2} mbar equivalent static pressure was felt by Si and Rh samples during in-situ oxidation reaction.

Effusive cell is another solution for near-ambient pressure SPEM. The sample is encapsulated with a vacuum sealed cell and located just 30-50 μm behind of a 200 μm diameter size pinhole. The focused x-ray beam are scanning the sample through the pinhole to generate photoelectrons. We can achieve ca. a $200 \times 100 \mu\text{m}^2$ aerial point of view on the sample. The pressure inside the cell can be raised up to mbar while the pressure in the main chamber kept around 1×10^{-5} mbar which is the safety limit for SPEM system. Heating and biasing of sample, and thermocouple connections are available.

Mo-E08

In-situ UV-vis and mass spectroscopy studies of syngas conversion model catalysts

Hans Fredriksson¹, Hans Niemantsverdriet¹, Kees-Jan Weststrate¹¹Eindhoven University of Technology, Eindhoven, Netherlands

Methanol and Fischer-Tropsch synthesis are well-established, commercially used catalytic processes. Yet, our understanding of the catalysts and in particular their de-activation mechanisms is incomplete. The reasons for this are the complexity of the reaction itself and of the catalysts, containing promoter and support materials as well as three-dimensional, random distributions of the catalyst materials in pores. In contrast, on flat model systems, catalyst properties as well as gas composition and temperature can be precisely controlled and measured. Therefore, changes in catalyst oxidation state, stability towards sintering and contact between the various catalyst components can be accurately studied. We demonstrate the fabrication of model catalysts using physical vapour deposition and wet-chemical approaches. These catalysts have been extensively characterized and tested using XPS, TEM. We also demonstrate catalyst testing in a newly developed micro reactor, equipped with in-situ UV-vis and mass spectroscopy. The strength of this approach is demonstrated in several experiments, including in-situ catalyst oxidation/reduction and sintering of syngas conversion catalysts. We also demonstrate that the micro reactor is sensitive enough to measure catalytic activity from model catalyst with surface areas less than one cm² thus allowing us to correlate catalyst performance with fundamental properties, in real time.

Mo-E09

Novel surface oxide on Pt(111) as the active phase for NO and CO oxidation studied with the ReactorSTM

Matthijs Van Spronsen¹, Joost Frenken¹, Irene Groot¹¹Huygens-Kamerlingh Onnes Laboratory, Leiden University, Leiden, Netherlands

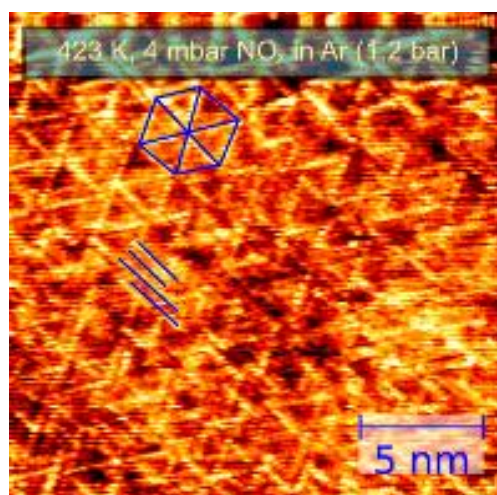
Although automotive catalysis has been extensively investigated, questions still exist. Under oxygen-rich reaction conditions, it is uncertain what the active phase is. This is even true for the Pt(111) surface, which is the facet lowest in energy. An early operando Scanning Tunneling Microscopy (STM) study [1] showed a stepwise increase in CO oxidation activity at oxygen-rich conditions. This increase concurred with a dramatic and instantaneous morphology change. From the STM images, the atomic structure could not be resolved. Under similar conditions, Surface X-ray Diffraction found a thin, bulk-like α -PtO₂ [2]. Surprisingly, a theoretical study concluded that this oxide is inert to CO oxidation [3]. With the high-pressure, high-temperature ReactorSTM [4], we studied the oxidation of Pt(111) both by exposing to pure O₂ and to NO oxidation conditions. Upon oxidation with O₂ (1.0 bar, 423-523 K), we found a structure consisting of triangles assembled in a 'spoked-wheel' superstructure. In addition, we found a lifted-row pattern. The two were coexisting on different regions on the surface. The lifted-row structure became more predominant at higher O₂ pressure. We propose that both structures share the same building block, which are expanded Pt-oxide rows. This results in a one-layer thick surface oxide. These surface oxides were not vacuum stable. Furthermore, the combination of high temperature and pressures was needed to form nicely-ordered structures. Exposure of Pt(111) to NO and O₂ or exposure to NO₂ resulted in the formation of a mixture of small domains of both the spoked-wheel and the lifted-row oxides. Although these surface oxides were not directly observed in CO oxidation, identical roughness development indicates a similar surface structure.

[1] Bobaru, PhD thesis, Leiden University, 2006

[2] Ackermann, PhD thesis, Leiden University, 2007

[3] Li & Hammer, Chem. Phys. Lett., 409, (2005), 1

[4] Herbschleb, et al., Rev. Sci. Instrum., 85, (2014), 083703



Mo-E10

Local surface reaction kinetics "just by imaging"

Yuri Suchorski¹, Martin Datler, Ivan Bepalov, Johannes Zeininger, Günther Rupprechter

¹Vienna University of Technology, Vienna, Austria

Many of the catalytic surface reactions can be visualized in situ by PEEM. For the reactions which follow the Langmuir-Hinshelwood mechanism, obtained real time images reflect the correlation between the local catalytic activity of particular surface regions and the local photoemission yield [1]. Both quantities depend on the surface coverage of reacting adsorbates, which in turn governs the local work function and thus the yield of emitted photoelectrons, i.e. the intensity of the PEEM image. Such correlation is scalable down to the nm-scale and allows in principle to obtain the laterally-resolved kinetic information with the resolution of the corresponding device. Such "reaction kinetics by imaging" approach has been realised using the digital analysis of the video-PEEM sequences recorded during the ongoing CO oxidation and was applied first to the individual μm -sized Pt and Pd grains of polycrystalline foils and supported Pd powders [1-3]. In present contribution we apply this approach for the first time to study the local kinetics of H_2 oxidation on individual Rh(hkl) domains of polycrystalline Rh foil and on the Rh powder supported by ZrO_2 .

[1] Y. Suchorski, C. Spiel, D. Vogel, W. Drachsel, R. Schlögl, G. Rupprechter, Chem. Phys. Chem. 11 (2010) 3231.

[2] D. Vogel, Ch. Spiel, A. Suchorski, A. Trinchero, R. Schlögl, H. Grönbeck and G. Rupprechter, Angew. Chem. Int. Ed. 51 (2012) 10041

[3] D. Vogel, C. Spiel, M. Schmid, M. Stöger-Pollach, R. Schlögl, Y. Suchorski, G. Rupprechter, J. Phys. Chem. C, 117 (2013)

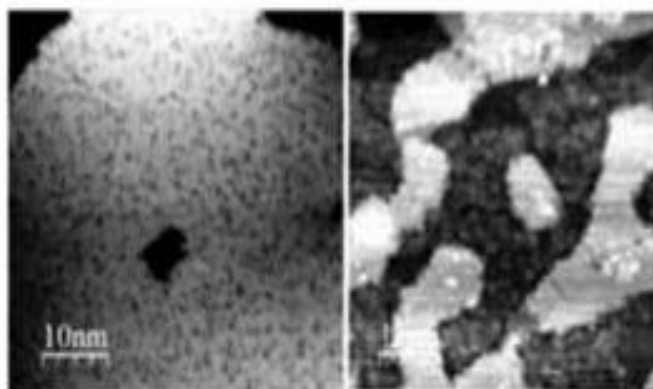
Mo-E11

Surface science studies of iron molybdate catalysts for the selective oxidation of methanol.

Michael Bowker¹, Ms Catherine Brookes¹, Chanut Bamroongwongdee¹

¹Cardiff Catalysis Institute, Cardiff University, Cardiff, United Kingdom

Methanol is oxidised in a selective manner to formaldehyde via the methoxy surface intermediate, but is combusted via the non-selective surface intermediate, the formate. I will report on the stability, formation, structure and active sites for this reaction on Cu(110), determined using a molecular beam reactor, TPD and STM. Only very particular sites are able to selectively oxidise methanol, and these are the three-fold coordinate oxygen sites, while the majority are four-coordinate. Copper is actually a relatively poor catalyst for methanol oxidation, and oxides have become commercialised for the reaction. The basics learned from surface science apply also to the reaction on the best of these oxides, iron molybdate ($\text{Fe}_2(\text{MoO}_4)_3$), with methoxy and formate intermediates shown to be involved. I will describe our understanding of this reaction on the high area catalyst oxide surfaces, using surface science methods on both oxide single crystals, and on real catalysts on which we deposit only one monolayer of the active phase on the surface. This can then be probed by XAS, Raman and a variety of other techniques to give us insight into the nature of the surface of such important materials.



Atomically resolved STM images of the clean $\text{Fe}_2\text{O}_3(111)$ crystal showing the expected Fe termination (left) and with 1.5 ML of MoO_3 on the surface (right), showing doubled periodicity of the Mo oxide overlayer.

Mo-E12

Square pyramidal structure of oxo vanadium (V) and (IV) species over low coverage VO_x/TiO₂ (101) and (001) anatase catalysts and modified Brønsted acidity via metal substitutions

Logi Arnarson¹, Søren B. Rasmussen², Hanne Falsig², Jeppe V. Lauritsen¹, Poul Georg Moses²

¹iNANO, Aarhus University, Aarhus, Denmark, ²Haldor Topsøe A/S, Copenhagen, Denmark

Catalysts based on vanadium oxide supported on titanium oxide are known to be good catalysts for reducing nitrogen oxides by selective catalytic reduction (SCR) and for the oxidation of o-xylene to ophthalmic anhydride. Further improvement of the performance of these catalysts requires that the nature of the active sites is known. Nonetheless, the molecular structure of the active sites is still debated. We present how the molecular structure of hydrated, low coverage vanadium sites depends on the surface facet of the TiO₂(anatase) support based on density functional theory (DFT) calculations and electron paramagnetic resonance spectroscopy (EPR). The TiO₂(anatase) support does in addition to dispersing the active phase also influence its shape and ultimately its reactivity. We find that hydrated VO_x species where V is present in oxidation state +5 are present in distorted tetrahedral configuration on the most stable TiO₂(101) surface whereas on the less stable TiO₂(001) surface are present in distorted octahedral configurations. Furthermore we find the reduced states of same species where V is present in oxidation state +4 also exhibit the same local coordination independent of degree of hydration. These new structural information can be of great value when considering e.g. the SCR reaction which is known to be a redox process where the reduced state is a part of the catalytic mechanism. Additionally we investigate the influence of modified Brønsted acidity of the surface on the SCR reaction by studying different Metal \leftrightarrow Ti substitutions in form of ammonium formation energies. It turns out that these can be used as a descriptor for the SCR reaction when working in excess of O₂ as the ammonium formation energies are linearly correlated with the energy of the transition state of the rate determining part of the reaction.

Mo-A13

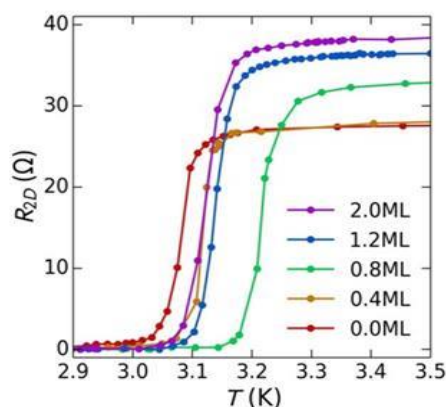
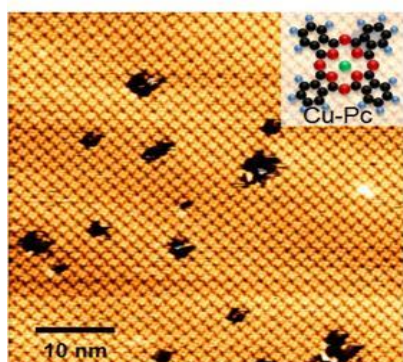
Tuning of the Surface Superconductor Si(111)-($\sqrt{7}\times\sqrt{3}$)-In with Self-assembled Magnetic Molecules

Takashi Uchihashi¹, Shunsuke Yoshizawa¹, Saranyan Vijayaraghavan¹,
Tomonobu Nakayama¹, Howon Kim², Yukio Hasegawa², Yasumasa Takagi³,
Toshihiko Yokoyama³

¹National Institute for Materials Science, Tsukuba, Japan, ²The Institute for Solid State Physics, The University of Tokyo, Kashiwa, Japan, ³Institute for Molecular Science, Okazaki, Japan

Recently, superconductivity was discovered for metal-induced silicon surface reconstructions by scanning tunneling microscopy (STM) and electron transport measurement [1-6]. One of unique features of these surface materials compared to bulk counterparts is that the electronic properties of the whole system can be modified by molecule adsorption. This opens a way to tune the macroscopic superconducting properties through charge and spin doping from organic molecules. We have found that phthalocyanines with Cu, Mn, and Fe atoms coordinated at the center (CuPc, MnPc, FePc) can be self-assembled on the Si(111)-($\sqrt{7}\times\sqrt{3}$)-In surface reconstruction, which becomes superconducting around 3 K. The fact that the underlining In layer on the silicon surface remains intact is clearly shown by the superconducting transition of the system after molecule adsorption and assembly. The dependence of superconducting transition temperature (T_c) on the molecule coverage is strikingly different among the three phthalocyanines. For CuPc, T_c first slightly increases and then decreases as the coverage is increased from 1 to 2 ML (see Fig.1). MnPc has a strong effect of suppressing T_c , while FePc has an intermediate tendency of the above two. For MnPc, temperature-dependent transport measurement reveals a resistance minimum, suggesting the occurrence of the Kondo effect. The results are discussed in terms of charge transfer and the spin states of molecules, which were investigated by STM and X-ray magnetic circular dichroism.

- [1] T. Zhang et al., Nat. Phys. 6, 104 (2010).
- [2] T. Uchihashi et al., Phys. Rev. Lett. 107, 207001 (2011)
- [3] T. Uchihashi et al., Nanoscale Res. Lett. 8, 167 (2013).
- [4] M. Yamada et al., Phys. Rev. Lett. 110, 237001 (2013).
- [5] S. Yoshizawa and T. Uchihashi: J. Phys. Soc. Jap. 83, 065001 (2014).
- [6] S. Yoshizawa et al., Phys. Rev. Lett. 113, 247004(1-5) (2014)



Mo-A14

Remarkable interaction of superconductivity with defects in 2D materials

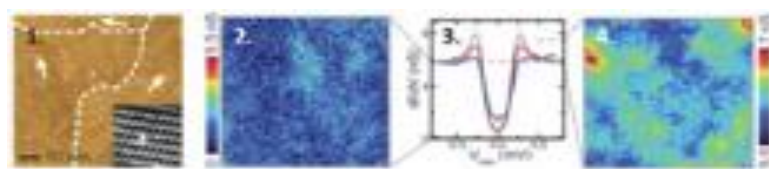
Stéphane Pons^{1,2}, Christophe Brun², Tristan Cren², Gerbold Menard², Vladimir Cherkez², François Debontridder², L. B. Loffe^{3,4}, B. L. Altshuler⁵, D. Fokin², M. C. Tringides⁶, S. Bozhko⁷, Dimitri Roditchev^{1,2}

¹Laboratoire de Physique et d'Etude des Matériaux (LPEM) CNRS - ESPCI-ParisTech - UPMC, Paris, France, ²Institut des Nanosciences de Paris (INSP), CNRS, UPMC, Paris, France, ³Laboratoire de Physique Théorique et Hautes Énergies (LPTHE), CNRS, UPMC, Paris, France, ⁴Department of Physics and Astronomy, Rutgers University, Piscataway, USA, ⁵Physics Department, Columbia University, New York, USA, ⁶Ames Laboratory-US Department of Energy, and Department of Physics and Astronomy, Iowa State University, Ames, USA, ⁷Institute for Solid State Physics, Chernogolovka, Russia

The remarkable phenomenon of superconductivity, evidenced in 2010 in single layers of Pb/Si(111) [1], was completely unexpected from the theoretical and experimental points of view. These samples show two-dimensional (2D) interfacial states and represent a unique opportunity to study superconductivity in real 2D materials. Our scanning tunneling microscopy/spectroscopy (STM/STS) experiments [2] performed at 300mK and under UHV and high magnetic field show that the superconductivity develops at the very interface of Pb and Si and is not directly related to the superconducting nature of Pb bulk material. We discovered that the $\sqrt{7}\times\sqrt{3}$ reconstructed single layer of Pb (topography image Fig 1.1) exhibits a strong pair-breaking effect (gap filling, Fig 1.2) and a modulation of the superconducting quasiparticle peak (Fig. 1.4) at shorter scale than the coherence length. These effects are extremely unusual for conventional superconductivity and were never revealed before. However, they can be understood considering the interaction of non-magnetic defects with superconductivity in a two-dimensional material and taking into account an additional spin-triplet component of the superconducting order parameter.

[1] T. Zhang et al., Nature Phys. 6, 104 (2010).

[2] C. Brun et al., Nature Phys., 10, 444–450 (2014).



Mo-A15

Superconductivity in the 2D limit: T_c enhancement in 2H-TaS₂ few-layers

Samuel Mañas Valero¹, Eugenio Coronado¹, Efrén Navarro Moratalla¹, Joshua Island², Andrés Castellanos-Gómez², Herre Van der Zant², Luca Chirulli³, Francisco Guinea³

¹University of Valencia, Paterna, Valencia, Spain, ²Delft University of Technology, Kavli Institute of Nanoscience, Delft, The Netherlands, ³Instituto de Ciencia de Materiales de Madrid (CSIC), Madrid, Spain

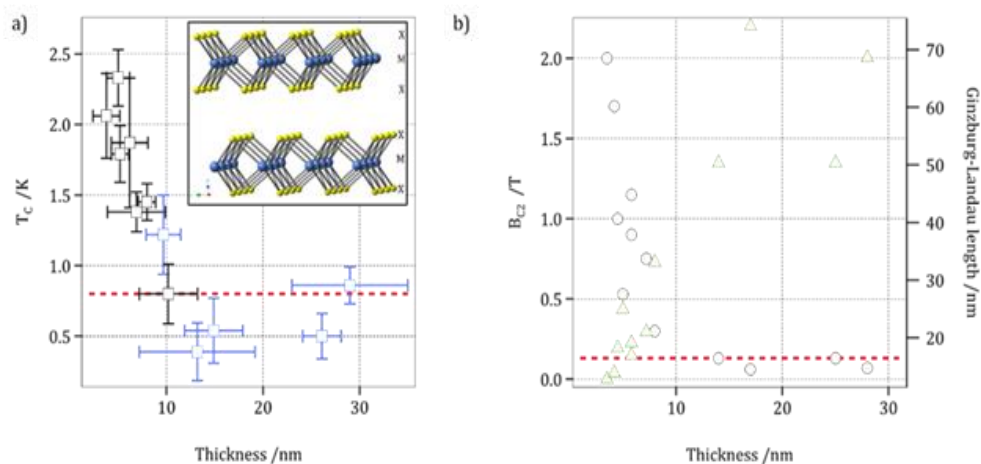
Graphene [1] is one of the most studied materials due to its unique properties such as hardness or high electric and thermal conductivity. However, probably the best quality of graphene is that it is opening the field to many other 2D crystals [2] as superconductors or topological insulators. In this work we show 2D superconductivity in 2H-TaS₂ thin-layers, as revealed by the Ginzburg-Landau coherence length. We explore the synthesis and characterization of 2H-TaS₂ from bulk to few-layers system. Interestingly, a T_c enhancement (Figure 1) is observed from bulk (0.8 K) to the thinnest layer investigated (ca. 2K), in contrast with the suppression of superconductivity reported in other superconductor 2D crystals [3]. This result can be interpreted on the basis of a simple band model and on optical phonons localized in each plane; it shows that the tunneling between the bands decreases the effectiveness of the pairing interaction that in turn is mediated by in-plane phonons. This result brings superconductivity into the flatland and opens the door for their future use in magnetic sensors or low energy applications.

[1] K.S. Novoselov, et al., Science 2004, 306, 666.

[2] L. Britnell, et al. Science 2013, 340, 1311.

[3] M.S. El-Bana, et al. Superconductor Science and Technology 2013, 26, 1.

Figure 1.- a) Variation of the T_c (from four-probe transport measurements) as a function of the thickness of the TaS₂ layers. Devices exhibiting non-zero RRR are plotted in blue. Inset: Stack of two layers of 2H-TaS₂ made out of sulfur (X) and tantalum (M). b) Variation of B_{c2} (circles) and G-L length values (triangles) as a function of thickness. A dashed red line has been placed at the T_c and B_{c2} values found for bulk flakes (thick layer limit).



Mo-A16

Scanning Tunneling Microscopy of Superconducting Vortices Trapped at Atomic Steps of Si(111)-($\sqrt{7}\times\sqrt{3}$)-In

Shunsuke Yoshizawa¹, Howon Kim², Takuto Kawakami¹, Yuki Nagai³,
Tomonobu Nakayama¹, Xiao Hu¹, Yukio Hasegawa², Takashi Uchihashi¹

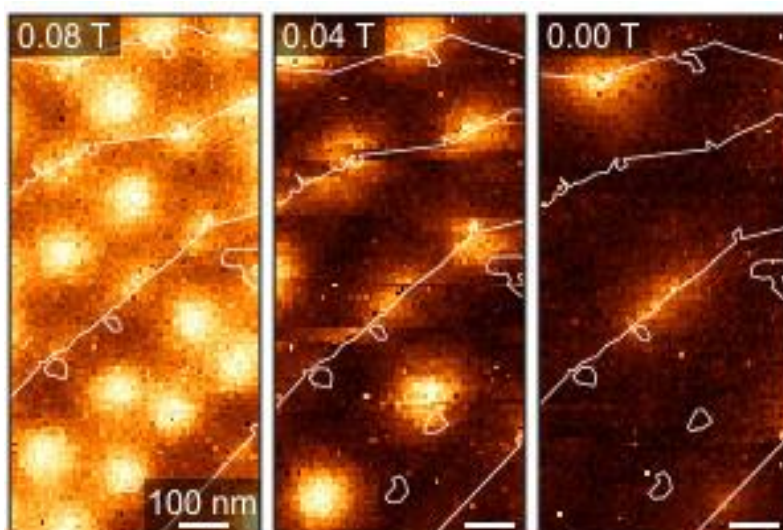
¹International Center for Materials Nanoarchitectonics, National Institute for Materials Science, Tsukuba, Japan, ²Institute for Solid State Physics, The University of Tokyo, Kashiwa, Japan, ³CCSE, Japan Atomic Energy Agency, Kashiwa, Japan

Si(111)-($\sqrt{7}\times\sqrt{3}$)-In undergoes a superconducting phase transition at $T_c = 3$ K [1]. As the conducting layer is atomically thin, various surface defects including atomic steps can affect the superconducting properties. Previous transport measurements have suggested that the atomic steps work as Josephson junctions and limit the macroscopic critical current [2]. However, there were no direct information on the influence of atomic steps on the flow of superconducting currents. To address this issue, we performed low-temperature scanning tunneling microscopy on Si(111)-($\sqrt{7}\times\sqrt{3}$)-In in magnetic fields [3]. Superconducting vortices were imaged by mapping zero-bias conductance measured at each point over a field of view containing several atomic steps, as shown in the figure. Vortices in the terrace regions have a round-shaped core and superconducting gap is completely suppressed at the center. In contrast, vortices trapped at atomic steps have an anisotropic core elongated along the steps and the superconductivity is only weakly suppressed inside. These properties can be understood as those of Josephson vortices, indicating that the atomic steps allow superconducting currents to travel at a limited rate. Detailed analyses show that the critical current density at each step depends on the quality of film growth at the step.

[1] T. Zhang et al.: Nature Physics 6, 104 (2010).

[2] T. Uchihashi et al.: Phys. Rev. Lett. 107, 207001 (2011).

[3] S. Yoshizawa et al.: Phys. Rev. Lett. 113, 247004 (2014).



Mo-A17

Tunneling processes into localized subgap states in superconductors

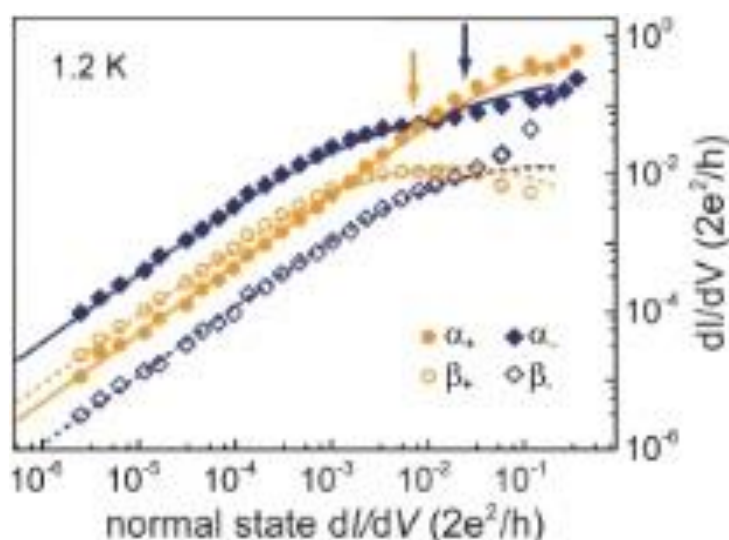
Michael Ruby¹, Falko Pientka^{1,2}, Yang Peng^{1,2}, Benjamin W. Heinrich¹, Felix v. Oppen^{1,2}, Katharina J. Franke¹

¹Institut für Experimentalphysik, Freie Universität Berlin, Berlin, Germany

²Dahlem Center for Complex Quantum Systems, Freie Universität Berlin, Berlin, Germany

The Yu-Shiba-Rusinov states bound by magnetic impurities in conventional s-wave superconductors are a simple model system for probing the competition between superconducting and magnetic correlations. Shiba states can be observed in scanning tunneling spectroscopy (STS) as a pair of resonances at positive and negative bias voltages in the superconducting gap. These resonances have been interpreted in terms of single-electron tunneling into the localized sub-gap states [1-3]. This requires relaxation mechanisms that depopulate the state after an initial tunneling event. Recently, theory suggested that the current can also be carried by Andreev processes which resonantly transfer a Cooper pair into the superconductor [4]. We performed high-resolution STS experiments on single adatom Shiba states on the superconductor Pb. Figure 1 shows the evolution of the STS peak intensities at positive and negative bias (α_{\pm} , β_{\pm}) as a function of the normal state conductance at a temperature of 1.2 K. The deviation from linear to sublinear behavior (indicated by the arrows in Fig. 1) provides evidence for the existence of two transport regimes, and matches well with the theoretical analysis (solid and dashed lines). Single-electron tunneling dominates at large tip-sample distances and small currents, whereas Andreev processes become important at stronger tunneling [5].

- [1] A.V. Balatsky, I. Vekhter, and J.-X. Zhu, Rev. Mod. Phys. 78, 373 (2006)
- [2] M.E. Flatté, J.M. Byers, Phys. Rev. Lett. 78, 3761 (1997)
- [3] M.I. Salkola, A.V. Balatsky, and J.R. Schrieffer, Phys. Rev. B 55, 12648 (1997)
- [4] I. Martin and D. Mozyrsky, Phys. Rev. B 90, 100508 (2014)
- [5] M. Ruby et al., arXiv:1502.05048



Mo-B13+14

Oxygen defects, surface chemistry and catalysis of ceria-based systems: Theoretical and experimental model catalysts

Maria Veronica Ganduglia-Pirovano¹¹Institute of Catalysis and Petrochemistry-CSIC, Spain

Ceria (CeO₂) is the most significant of the oxides of rare-earth elements in industrial catalysis with its reducibility being essential to its functionality in catalytic applications. The complexity of real (powder) catalysts hinders the fundamental understanding of how they work. Specifically, the role of ceria in the catalytic activity of ceria-based systems is still not fully understood. To elucidate it, well-defined ceria-based model catalysts are prepared experimentally or created theoretically and studied. In this talk, the emphasis is put on theoretical studies and special attention is given to the reduction of ceria surfaces [1] and the effects of ceria on the activity and selectivity of CeO₂(111) [2] and Ni/CeO₂(111) [3] as model catalysts for partial alkyne hydrogenation and hydrogen production in the water-gas shift reaction, respectively.

- [1] M. V. Ganduglia-Pirovano, J. L. F. Da Silva, and J. Sauer, *Phys. Rev. Lett.* 102, 026101 (2009); J.-F. Jerratsch, X. Shao, N. Nilius, H.-J. Freund, C. Popa, M. V. Ganduglia-Pirovano, A. M. Burow, and J. Sauer, *Phys. Rev. Lett.* 106, 246801 (2011); G. E. Murgida and M. V. Ganduglia-Pirovano, *Phys. Rev. Lett.* 110, 246101 (2013).
- [2] J. Carrasco, G. Vilé, D. Fernández-Torre, R. Pérez, J. Pérez-Ramírez, and M. V. Ganduglia-Pirovano, *J. Phys. Chem. C* 118, 5352 (2014); D. Fernández-Torre, J. Carrasco, M. V. Ganduglia-Pirovano, and R. Pérez, *J. Chem. Phys.* 141, 014703 (2014).
- [3] J. Carrasco, L. Barrio, P. Liu, J. A. Rodriguez, and M. V. Ganduglia-Pirovano, *J. Phys. Chem. C* 117, 8241 (2013); J. Carrasco, D. López-Durán, Z. Liu, T. Duchoň, J. Evans, S. D. Senanayake, E. J. Crumlin, V. Matolín, J. A. Rodríguez, M. V. Ganduglia-Pirovano, *Angew. Chem. Int. Ed.* 54, 3917–3921 (2015).

Mo-B16

High chemical activity of a perovskite surface: adsorption of CO on $\text{Sr}_3\text{Ru}_2\text{O}_7$ and $\text{Ca}_3\text{Ru}_2\text{O}_7$

Florian Mittendorfer¹, Daniel Halwidl¹, Bernhard Stöger¹, Wernfried Mayr-Schmölzer¹, Josef Redinger¹, Michael Schmid¹, Ulrike Diebold¹

¹Vienna University of Technology, Vienna, Austria

In the recent years, complex transition metal oxide surfaces have received enormous attention, both due to the fundamental properties as well as their potential for applications in the field of energy storage and conversion. Yet only little is known about the chemistry of these materials. On the basis of density functional theory (DFT) calculations, I will present a theoretical study on the surface chemistry of $\text{Sr}_3\text{Ru}_2\text{O}_7$ and $\text{Ca}_3\text{Ru}_2\text{O}_7$, supported by experimental STM measurements. Surprisingly, the STM study shows a high chemical activity of the $\text{Sr}_3\text{Ru}_2\text{O}_7$ surface [1]. We conclude that these observations are related to the facile adsorption of carbon monoxide (CO), which can easily be converted to a carboxylate-like COO species at the surface. With an adsorption energy of -2.2 eV, the latter structure shows a high chemical stability. We predict a similar adsorption mechanism for the adsorption of CO on $\text{Ca}_3\text{Ru}_2\text{O}_7$, although the additional tilting of the perovskite octahedra changes the appearance in the STM measurements drastically.

[1] B. Stoegeer et al., Phys. Rev. Lett. 113 (2014) 116101

Mo-B17

The structure and reactivity of Rh layers supported and covered by atomically thin molybdenum oxides

László Deák¹, Imre Szenti², Zoltán Kónya^{1,2}

¹Hungarian Academy of Sciences, MTA-SZTE Reaction Kinetics and Surface Chemistry Research Group, Szeged, Hungary, ²University of Szeged, Department of Applied and Environmental Chemistry, Szeged, Hungary

The aim of the study was to reveal the effect of molybdenum oxide supports and overlayers on the structural and chemical properties of rhodium nanoparticles. The behaviour of rhodium layers deposited on oxidized, 0.15-20.0 ML thick Mo films formed on a nearly stoichiometric TiO₂(110) single crystal was characterized by AES, TPD and work function (WF) measurements. The oxidation of 0.15-2.7 ML thick Mo deposits was performed via the redox reaction with the titania support at 1000 K. Molybdenum oxide supports of MoO₃ and MoO₂ surface composition were formed by the oxidation of 20 ML thick Mo multilayers by O₂ at 650 K and 1000 K, respectively. Rh grows in a layer-by-layer fashion on a mixed titanium-molybdenum oxide produced in the reaction between titania and 0.15 ML Mo, corresponding to a considerably enhanced dispersion of rhodium as compared with that on the clean TiO₂(110). The surface reactivity of Rh layers supported by molybdenum oxides as a function of pre-annealing temperature was followed by carbon monoxide adsorption-desorption cycles. The molecular CO desorption (T_p=560 K) from a 0.4 ML thick Rh film formed on the MoO₃ support was strongly suppressed at 300 K, indicating the encapsulation of rhodium with MoO_x species of low surface free energy. The release of CO from rhodium particles supported by both MoO₃ and MoO₂ layers was eliminated due to pre-annealing at 600 K, related to the extended decoration of metal particles by MoO_x moiety. The encapsulation of the rhodium films proceeded above 600 K on both supports, and annealing to 1000 K resulted in nearly equal WF values, indicating the formation of MoO_x overlayers of similar surface composition close to MoO₂. AES depth profiles revealed that the 0.4 ML thick Rh deposits covered by MoO_x at 1000 K preserved their island structure.

Mo-B18

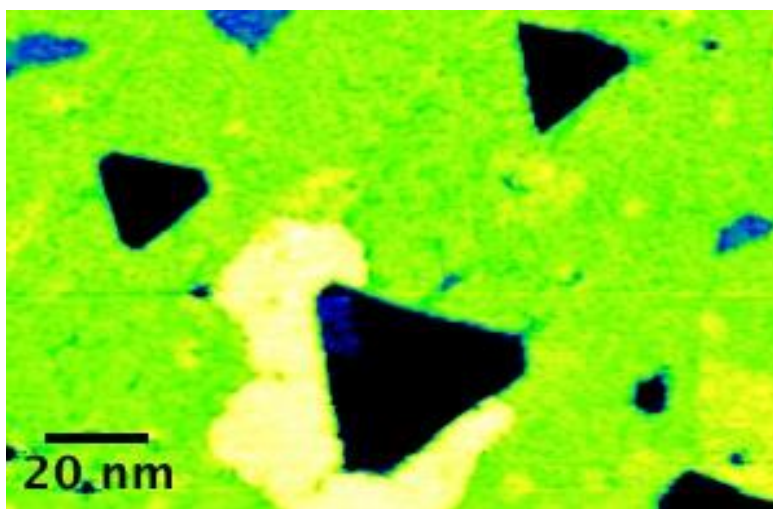
Metal/zirconia and zirconia/metal (inverse) model catalysts:
Growth and SMSI effectJoong Il Jake Choi¹, Ulrike Diebold¹, Michael Schmid¹¹Institute of Applied Physics, TU Wien, Vienna, Austria

Zirconia (ZrO_2) is a catalyst support and solid-state electrolyte for gas sensors and solid-oxide fuel cells. Understanding the ZrO_2 -metal interaction is essential for these applications. ZrO_2 is an electronic insulator up to high temperatures, which prevents surface-science studies by many methods involving charged particles such as scanning tunnelling microscopy (STM). To overcome this limitation, we have created ultra-thin ZrO_2 films by oxidation of suitable alloys [1-3] and studied growth of various metals on them. We find an increasingly strong metal-oxide interaction in the sequence Ag-(Au, Pd)-(Fe, Ni). With the exception of (electronegative) Au, this can be explained by increasing oxygen affinity of the metals. Cluster densities are higher than on alumina, which can be explained by the structure of the oxide. We have also studied inverse systems, ZrO_2 grown on Pt(111) and Rh(111). On both substrates, we observe dewetting at elevated temperature. Interestingly, the Pt(111) surface remains covered by an ultrathin zirconia film under reducing conditions (UHV), while the bare metal is exposed when annealing in $5\text{E-}7$ mbar oxygen. This behavior is known as strong metal-support interaction (SMSI), a phenomenon usually considered only for reducible oxides. The driving force for the SMSI effect and implications concerning reducibility of ultrathin zirconia films are discussed. The image shows a $\text{ZrO}_2/\text{Rh}(111)$ film in the initial stages of dewetting, with outflow of material from an 1.8 nm deep pit.

[1] Antlanger et al., Phys. Rev. B 86, 035451 (2012).

[2] Choi et al., J. Phys.: Condens. Matter 26, 225003 (2014).

[3] Li et al., J. Phys. Chem. C 119, 2462 (2015).



Mo-C13

Adsorption of Thiophene-Based Molecules at Passivated Silicon Surfaces

Mark Gallagher¹, Renjie Liu¹, Chaoying Fu², Dmitrii Perepichka²

¹Lakehead University, Thunder Bay, Canada, ²McGill University, Montreal, Canada

Molecular self-assembly of 2-d organic layers at surfaces is a powerful method to achieve the design and fabrication of nanostructures. The self-assembly of supramolecular networks at silicon surfaces is a particular challenge due to the large number of dangling bonds which can suppress the diffusivity of adsorbed molecules and even break the molecules apart via the formation of Si-C bonds. We have studied the adsorption of brominated π -conjugated tetrathienoanthracene (TBTTA) molecules onto the Si(111) $\sqrt{3}\times\sqrt{3}$ -Ag and Si(111) $\sqrt{3}\times\sqrt{3}$ -B surfaces at room temperature. Both $\sqrt{3}$ surfaces are devoid of Si dangling bonds and therefore should provide a high mobility surface for TBTTA adsorption. Thiophene based molecules like TBTTA are of considerable interest in organic semiconductor research due to their efficient conjugation and chemical stability [1].

Scanning Tunneling Microscopy images reveal that TBTTA molecules adsorbed onto the $\sqrt{3}$ -Ag surface readily migrate to step edges and defects. With increasing coverage the molecules eventually form compact supramolecular structures defined by an oblique unit cell of dimensions 17 Å x 11 Å. The spatial extent of these structures is often limited by defects in the underlying $\sqrt{3}$ layer. Our results suggest the supramolecular features on the $\sqrt{3}$ -Ag surface are held together by weak intermolecular forces. In addition to results on the $\sqrt{3}$ -Ag surface, we will discuss our more recent experiments on the boron passivated surface.

[1] R. Gutzler et al., *Nanoscale* 6, 2660-2668 (2014).

Mo-C14

Reversible Formation of Chemical Bonds between Organic Molecules and Single Atoms on Hydrogenated Semiconductors

Szymon Godlewski¹, Marek Kolmer¹, Mads Englund², Hiroyo Kawai³, Rafal Zuzak¹, Aran Garcia-Lekue⁴, Bartosz Such¹, Jakub Lis¹, Antonio Echavarren⁵, Christian Joachim⁶, Daniel Sanchez-Portal^{2,4}, Mark Saeys⁷, Marek Szymonski¹

¹Jagiellonian University, Kraków, Poland, ²Centro de Fisica de Materiales CSIC-UPV/EHU, Donostia-San Sebastian, Spain, ³Institute of Materials Research and Engineering, Singapore, Singapore, ⁴Donostia International Physics Center, Donostia-San Sebastian, Spain, ⁵Institute of Chemical Research of Catalonia (ICIQ), Tarragona, Spain, ⁶Nanosciences Group & MANA Satellite, CEMES-CNRS, Toulouse, France, ⁷Ghent University, Gent, Belgium

The interaction of organic molecules with single atoms attracts recently growing attention inspired by both the potential applications in the construction of nanoscale machines, rotors or electronic circuitries, light harvesting, heterogeneous catalysis as well as by the interest in the fundamental knowledge of elementary processes occurring between the molecules and atoms. Among several concepts in electronic technology the idea of single organic molecules utilized as active parts of nanoscale electronic devices has gained growing attention and several prototypical single molecule electronic circuits have been demonstrated. It is expected that the problem of strong coupling of the electronic structure of the molecule with the metallic substrate could be resolved by application of passivated surfaces. Detailed characterization could be achieved by application of a scanning tunneling microscope providing amazing and unprecedented precision of measurements. In the presentation we will characterize behavior of trinaphthylene molecules on the hydrogenated Ge(001):H substrate with the application of low temperature scanning tunneling microscopy/spectroscopy (STM/STS) supported by the advanced theoretical modeling. We will demonstrate that with the application of the STM tip sophisticated surface nanostructures may be fabricated and the chemical bonds between the molecules and unsaturated surface defects could be reversibly formed and broken. Moreover, we will demonstrate that the balance between chemisorbed and physisorbed conformations allows for switching with the STM. For the first time we will discuss the performance of the tip induced manipulation of single atoms and molecules on hydrogenated surfaces and present the dynamical effects induced by tunneling electrons. Finally we will introduce prospects for utilization of the control over connecting individual molecules with surface single atoms.

This research was supported by the Polish Ministry for Science and Higher Education (contract no. 0322/IP3/2013/72) and the 7th Framework Programme of the European Union Collaborative Project PAMS (contract no.610446).

Mo-C15

Mechanistic Insight into CO₂ Dissociation on Copper Surfaces

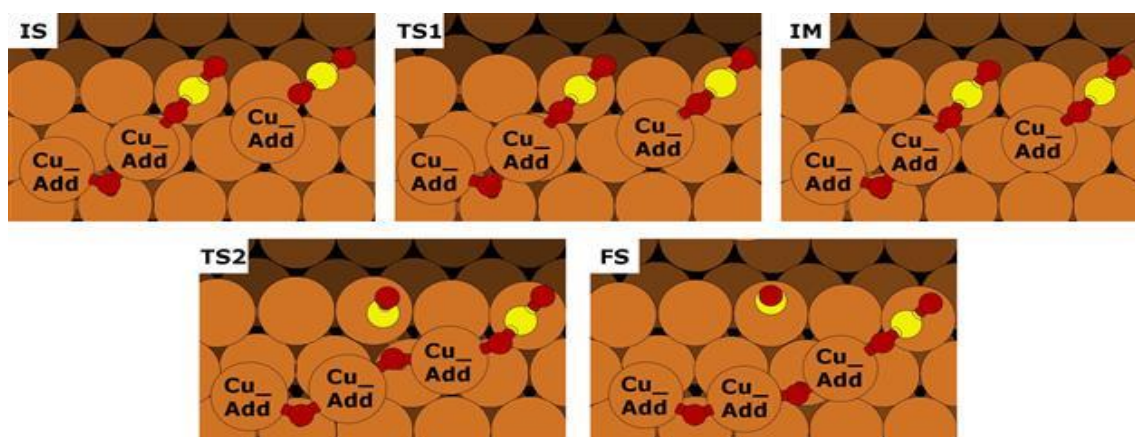
Fahdzi Muttqaqien¹, Yuji Hamamoto¹, Hidetoshi Kizaki¹, Kouji Inagaki¹, Yoshitada Morikawa¹

¹Department of Precision Science and Technology, Osaka University, Osaka, Japan

Adsorption and reaction of CO₂ on metal surfaces are fundamentally important in surface chemistry and other related fields. Koitaya and co-workers showed that CO₂ dissociation takes place on the stepped Cu(997) surface rather than on flat Cu(111) surface at 83 K by using infrared reflection absorption spectroscopy (IRAS).¹ However, it has not been reported theoretically that CO₂ dissociation takes place on Cu surfaces at low temperature. Thus, we studied the dissociative adsorption of CO₂ on the Cu(111), Cu(221), Cu(211), and Cu(11 5 9) surfaces by using state-of-the-art density functional theory (DFT).² We obtained that the barrier energy for CO₂ dissociation on the flat Cu(111) surface is 1.33 eV. While, the barrier energies of CO₂ dissociation on Cu(221), Cu(211), and Cu(11 5 9) surfaces are 1.06 eV, 0.67 eV, and 1.02 eV, respectively. Even though the activation energy is 0.66 eV lower on the stepped Cu(211) surface than on the flat Cu(111) surface, we concluded that CO₂ does not dissociate on ideal flat, stepped or kinked Cu surfaces at low temperature. We also studied the effect of Cu adatoms and water molecules in the CO₂ dissociation processes. We propose that the CO₂ dissociation is followed by the Cu-O-Cu chain formation (Fig. 1) with 0.46 eV barrier energy. By introducing water molecule impurity, CO₂ dissociation takes place via hydrocarboxyl (COOH) intermediate with 0.48 eV barrier energy. According to these results, additional factors on the Cu surface such as adatoms and/or gas phase impurity, which can be found in “real” experiment condition, are important to enhance CO₂ dissociation.

[1].T. Koitaya, Y. Shiozawa, K. Mukai, S. Yoshimoto, and J. Yoshinobu, 14th International Conference on Vibrations at Surfaces, 2012.

[2].F. Muttqaqien, Y. Hamamoto, K. Inagaki, and Y. Morikawa, J. Chem. Phys. 141, 034702 (2014).



Mo-C16

Hole-induced nonlocal desorption of chlorobenzene from Si(111)-7x7 in the STM

Scott Holmes¹, Tianluo Pan², Richard E Palmer¹¹University of Birmingham, Birmingham, United Kingdom , ²Ruhr-Universität Bochum, Bochum, Germany

The scanning tunneling microscope (STM) tip is a low energy, low current, and highly localized electron source which enables us to investigate electron-mediated processes on surfaces. We have investigated the nonlocal desorption of chlorobenzene molecules via injection of holes (rather than electrons) on the Si(111)-7x7 surface at a range of different temperatures between 77K and 260K. Desorption occurs at locations remote from the STM tip, which we attribute to the capture of holes by the molecules after their propagation from the tip across the surface [1]. Both the desorption yield resulting from hole injection at 2.0eV and the effective range of the injected holes are found to increase with increasing temperature. The molecular cross-section for desorption is found to be thermally activated with an activation energy comparable to molecular vibrational modes and surface phonon energies, with small variations depending on the exact bonding location within the unit cell. At higher temperature (around room temperature), previous non-local electron-stimulated desorption experiments [2,3] identified a much higher activation energy associated with the physisorbed precursor state of the chlorobenzene molecule. Our interpretation of the low temperature behaviour focuses instead on the coupling of the molecule to surface electronic states, and the role played by vibrational modes in enhancing this process.

[1] P. A. Sloan, S. Sakulsermsuk and R. E. Palmer, Phys. Rev. Lett. 105, 048301 (2010). See also Electron 'submarines' help push atoms around, E.S. Reich, New Scientist, 31 July 2010, p. 11.

[2] S. Sakulsermsuk, P. A. Sloan and R. E. Palmer, ACS Nano 4, 7344 (2010).

[3] T. L. Pan, P. A. Sloan, and R. E. Palmer, J. Phys. Chem. Lett. 5, 3551 (2014).

Mo-D13

Measuring the efficiency of plasmon excitation by tunnelling currents

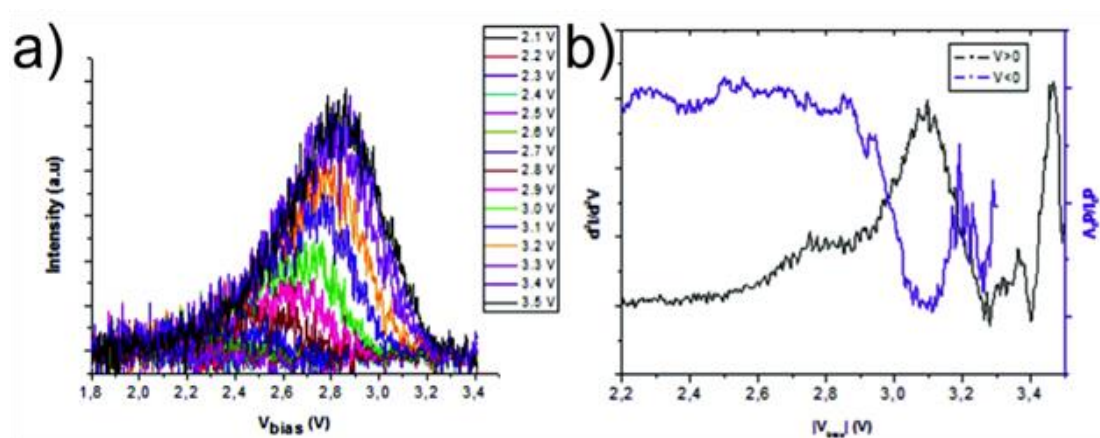
Alberto Martin-Jimenez¹, David Ecija¹, Daniel Granados¹, Jose María Gallego²,
Rodolfo Miranda^{1,3}, Roberto Otero^{1,3}

¹IMDEA-Nanoscience, Madrid, Spain, ²ICMM-CSIC, Madrid, Spain, ³Dep. de Física de la Materia Condensada, Univ. Autónoma de Madrid, Madrid, Spain

The fact that light is emitted when a current is injected through a tunnel junction was first found in the 70's by Lambert and McCarthy [1], and is currently exploited to analyze the light arising from the local junctions created between the tip and the sample in Scanning Tunneling Microscopes (Scanning Tunneling Luminescence, STL) [2]. It was long understood that the origin of the light is the radiative decay of Localized Surface Plasmon Resonances (LSPRs) which are excited by electrons tunneling inelastically between the electrodes. However, the relatively large energies of LSPR modes hindered any experiment aimed at measuring the inelastic signal in $I(V)$ curves recorded while tunneling (Scanning Tunneling Spectroscopy, STS). In this contribution we show STS measurements displaying a clear inelastic signal in the same energy range as the light recorded in STL experiments with the same tip. Our experiments allow for a quantification of the plasmon excitation efficiency by tunneling electrons which might become essential to extract information from STL spectra.

[1] J. Lambert, S. L. McCarthy, Phys. Rev. Lett. 57, 923 (1976).

[2] F. Rossel, M. Pivetta, W.-D. Schneider, Surf. Sci. Rep. 65, 129 (2010)



Mo-D14

Coupling an electrical circuit to surface plasmons with a single molecule.

Michael Chong¹, Gael Reeht¹, Hervé Bolou¹, Alex Boeglin¹, Fabrice Mathevet², Fabrice Scheurer¹, Guillaume Schull¹

¹Institut de Physique et Chimie des Matériaux de Strasbourg - CNRS, Strasbourg, France, ²Laboratoire de Chimie des Polymères - CNRS - Université Pierre et Marie Curie, Paris, France

Electroluminescence of a single molecule can be induced by means of scanning tunnelling microscopy (STM). It has been shown that when a molecule is placed in between two metallic electrodes it is necessary to use an insulating layer to decouple the molecule from the electrodes. This allows measuring the fluorescence of a single molecule [1]. However, if we envision any kind of electronic circuit configuration, direct contact of the molecule with the electrodes (tip and substrate) is required, which leads to a broadening [2] or quenching [3] of the fluorescence peaks. We propose here a bottom-up approach to introduce a chromophore in a π -conjugated molecular chain through on-surface copolymerisation. The STM tip is then used to lift the wire and to decouple the chromophore from the electrodes while keeping a circuit-like configuration.

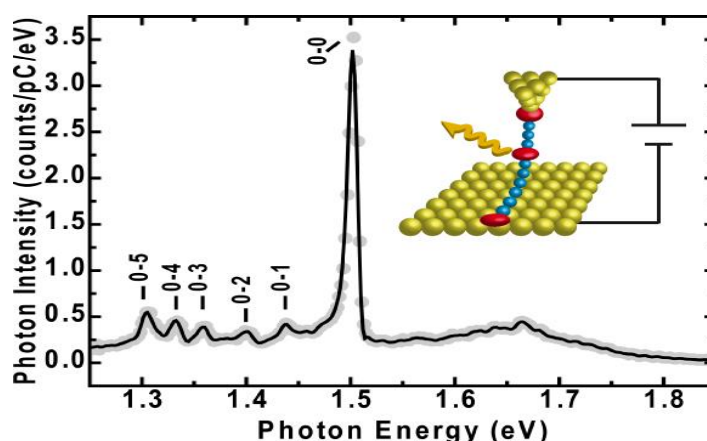
Tunneling current generated by applying a bias between the electrodes, allows to excite the chromophore molecule which exhibits a narrow emission line (FWHM < 2 meV) [4]. The plasmonic environment created by the metallic nanocavity (tip and substrate) plays a major role in the whole STM induced electroluminescence process. Here we report some insights on a mechanism, unreported at the molecular scale, implying excitation and de-excitation via interaction with the localised plasmons. We demonstrate that this configuration allows to control the lifetime of the single molecule excited state (i.e. the coherence of the emitted light) over two orders of magnitude. Our system might open the way to the realisation of controlled molecular transducers between electronic and plasmonic signals.

[1] X. H. Qiu, et al. Science 299, 542 (2003)

[2] G. Reeht, et al. Phys. Rev. Lett 112, 047403 (2014)

[3] N. L. Schneider, et al. Phys. Rev. Lett. 109, 186601 (2012)

[4] M. Chong, et al. submitted for publication



Mo-D15

In(4x1)/Si(111): Interwire coupling probed by local surface transport

Ilio Miccoli¹, M.Sc. Frederik Edler¹, M.Sc. Stephanie Demuth¹, Herbert Pfnür^{1,2}, Stefan Wippermann³, M. Sc. Andreas Lücke⁴, Wolf Gero Schmidt⁴, Christoph Tegenkamp^{1,2}

¹Institut für Festkörperphysik, Leibniz Universität Hannover, Hannover, Germany, ²Laboratory of Nano and Quantum Engineering (LNQE), Hannover, Germany, ³Interface Chemistry and Surface Engineering Department, Max-Planck-Institute for Iron Research GmbH, Düsseldorf, Germany, ⁴Lehrstuhl für Theoretische Physik, Universität Paderborn, Paderborn, Germany

Atomic chain ensembles are prototype 1D systems with peculiar electronic properties. The In(4x1)/Si(111) reconstruction shows strong anisotropic transport properties and a temperature driven metal-insulator transition (MIT). Despite comprehensive studies over the last decade the effect of defects induced by adsorption (eg. oxygen) and the inherent change of transport findings such as the transition temperature are still under current debate. A better understanding of the influence of atomic sized imperfections and a correlation with transport measurements can be achieved by a spatial constriction of the electron path. According to literature [1] spatial restriction can increase the sensitivity. In our case the spatial restriction was performed by using a standard Si approach (optical ex-situ lithography with reactive ion etching). We are showing a systematic investigation of finite size effects in anisotropic systems demonstrating the transition from quasi infinite to confined case and the increase of the sensitivity towards imperfections of almost one order of magnitude. Here, our measurements were performed by means of a 4-tip STM/SEM system. The combination of SEM and STM allowed the precise positioning of feedback controlled STM tips, enabling gently contacting without inducing significant strain to the surface and therefore transport measurements which avoids the need of additional sample processing that could potentially alter the surface/induce defects. Moreover, additional oxygen adsorption dependent transport studies by us show not only an expected reduction of conductivity along the direction of atomic chains but also a decrease in the direction perpendicular to the chains. This has not been reported before and clearly reveals an effective interwire coupling between the chains which is in agreement with recent DFT calculations [2].

[1] I. Miccoli, F. Edler, H. Pfnür, C. Tegenkamp, JPCM 2015 (in press).

[2] F. Edler, I. Miccoli, S. Demuth, H. Pfnür, S. Wippermann, A. Lücke, W.G. Schmidt, C. Tegenkamp (in preparation).

Mo-D16

Triangular Atom Lattice with Strong Coulomb Correlations:
Epitaxy of Sn on a SiC(0001) Substrate

Joerg Schaefer¹, Stefan Glass¹, Gang Li¹, Florian Adler¹, Julian Aulbach¹,
Andrzej Fleszar¹, Ronny Thomale¹, Werner Hanke¹, Ralph Claessen¹

¹Department of Physics, University of Wuerzburg, Wuerzburg, Germany

Here we report a novel realization of a two-dimensional electron system, supported on the wide-band gap substrate SiC(0001). For the first time, an artificial high-Z atom lattice on SiC is achieved by Sn atoms. Using gas phase hydrogen etching, well-ordered SiC surfaces are prepared, and by subsequent Sn evaporation a triangular lattice in ($\sqrt{3}\times\sqrt{3}$) reconstruction at low coverage (1/3 monolayer) is grown. Based on a combination of scanning tunneling microscopy and density-functional theory, we derive a structural model for this system, with Sn adatoms at T4 sites. While simple electron counting results in a half-filled metallic band, photoemission data show a clear lack of spectral weight at the Fermi level, with a full gap of ~ 2 eV. This indicates pronounced Coulomb correlations and a Mott-insulating scenario [1]. Interestingly, the system is isostructural to the likewise correlated ($\sqrt{3}\times\sqrt{3}$) Sn on Si(111) [2], yet with a 20% smaller lattice constant. However, unexpectedly, the chemically inert behavior of the wide-gap SiC substrate plays the key role in the present case: the hopping is decreased, and in addition, the reduced screening boosts the on-site Coulomb interaction. Together this leads to unusually strong electron correlations. Our calculations moreover show that the spin-orbit coupling is enhanced, and indicate that the system is susceptible to antiferromagnetic superstructures. Such artificial lattices on SiC(0001) thus offer a novel platform for coexisting Coulomb correlations and spin-orbit coupling, with bearing for unusual magnetic phases and proposed topological quantum states of matter.

[1] S. Glass et al, arXiv:1501.04602v1 (2015).

[2] G. Li et al., Nature Commun. 4, 1620 (2013).

Mo-E13

Catalytic Reactivity at High Coverage, a Theoretical Approach: Butadiene Hydrogenation on Pt(111) and Sn/Pt(111)

Sarah Gautier¹, Philippe Sautet¹

¹École Normale Supérieure of Lyon, Lyon, France

Theoretical hydrogenation studies are usually carried out at low coverage of hydrogen to compare with UHV experiments. However, industrial production of alkenes implies to work under pressure of hydrogen of about 1 to 10 bar. Butadiene hydrogenation into 1-butene is one reaction involved in the production of linear low-density polyethylene (LLDPE) and requires a hydrogen pressure of about 5 bar. This implies to treat the problem considering a high coverage of hydrogen on the surface. In this work, we first studied the coadsorption of butadiene and hydrogen on two well known surface catalysts that are Pt(111) and Pt/Sn-Pt(111). To understand the effects of the polarizability of butadiene on its reactivity, we compared the results obtained with two types of functionals: PBE and the optPBE van der Waals functional. A thermodynamic model was coupled to the DFT calculations carried out with the VASP code. The hydrogenation mechanism considered in those cases is the Langmuir-Hinshelwood mechanism involving transition states very similar to those obtained at low coverage. However, we also studied the weak adsorption of butadiene on the surface fully covered by hydrogen. For this, another reaction mechanism needs to be considered, the so-called Eley-Rideal mechanism, where butadiene comes from the gas phase to physisorb on the surface precovered with hydrogen. In this case, the dispersion forces have a quite large component in the total energy which justifies the use of optPBE. We found new types of transition states which opened new routes with lower barriers. We also show that the competition between the two mechanisms is very tight and implies the need of a deep study of both the thermodynamics and the kinetics of the system to understand the weight of each mechanism in this reaction.

Mo-E14

Surface chemistry of small amino acids on bare and oxygen-covered Ni model catalyst surfaces

Georg Held^{1,2}, Jacopo Ardini^{1,2}, Richard E. J. Nicklin¹, Silvia Baldanza¹, Alix L. Cornish¹, Rachel A. Price¹, Chanan Euaruksakul^{1,2}

¹University of Reading, Reading, United Kingdom, ²Diamond Light Source, Harwell, United Kingdom

Heterogeneous enantioselective catalysis is potentially superior to homogeneous processes in many respects. One of the most studied examples of enantioselective heterogeneous catalysis is the asymmetric hydrogenation of β -ketoesters over Ni based catalysts which are modified by chiral molecules, such as tartaric acid or alanine [1]. For a mechanistic picture we need to understand the surface chemistry of modifier molecules on the low-surface-energy terminations, {111}, {100} and {110}, which dominate Ni nanoparticles used as heterogeneous catalysts. Compared to the vast literature about amino acids on Cu surfaces there is very little information on Ni surfaces.

Here we present an extended study of the adsorption behaviour and decomposition pathways of glycine and alanine on bare and oxygen covered Ni{111}, Ni{100}, and Ni{110} using photoelectron spectroscopy (XPS), X-ray absorption (NEXAFS), and temperature-programmed desorption (TPD) experiments. Both amino acids adsorb predominantly in their anionic form with bonds to the surface through the O and N atoms. Upon annealing glycine and alanine show very similar decomposition path ways, whereby the molecules appear to be less stable the more close packed the surfaces are, i.e. the stability increases in the order {110} > {100} > {111}. The adsorption on oxygen-covered Ni surfaces results in a significant loss of oxygen, which is attributed to the production and desorption of water, and an increase in decomposition temperature. A scenario where surface hydrogen facilitates the dissociation of the amino acid backbone bond could explain both the higher stability in the presence of oxygen, which removes surface hydrogen, and the higher stability on open surfaces, where hydrogen atoms are more strongly bound and hence less likely to react with the amino acid.

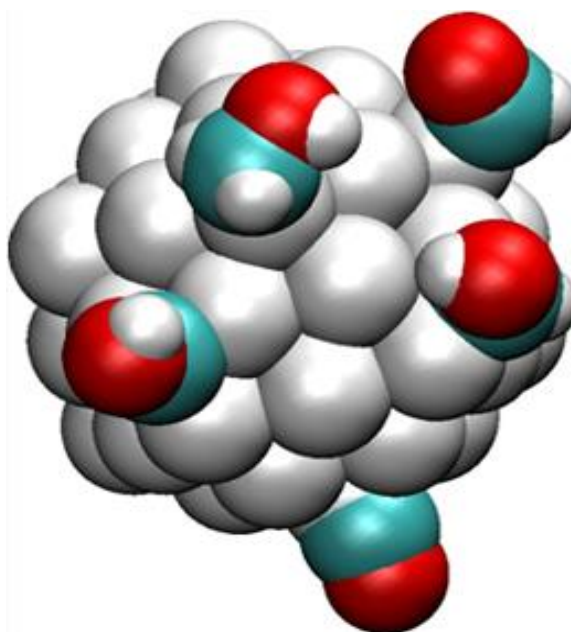
[1] E. Klabunovskii, G. V. Smith, and A. Zsigmond, "Heterogeneous Enantioselective Catalysis", Springer, 2006

Mo-E15

DFT study of methanol decomposition on Pt nanoparticles

Sergey Dobrin¹¹University of Toronto, Toronto, Canada

Catalytic reactions on transition metal surfaces are of great importance for many applications. While reactions on single-crystal surfaces were extensively studied for a long time, reactions on surfaces of metal nanoparticles, which is a common form of industrial catalysts, are studied in a much less degree. To understand the mechanisms of catalytic reactions on nanoparticles it is necessary to know to what extent a surface of the nanoparticle or nanocluster resembles the single-crystal surface. This work is devoted to the Density Functional Theory study of methanol decomposition on the surface of one-nanometer and larger platinum nanoparticles of various shapes, which is important for direct fuel cells. Atomic structures of various reaction intermediates were calculated on different adsorption sites of the nanoparticles. Transition states and activation energies of elementary steps of methanol decomposition on (111) and (100) facets, as well as on the low-coordinated Pt-atoms at the edge and corner sites were found. Obtained results allow one to compare alternative pathways of methanol decomposition and to suggest the most probable pathway on nanoparticles.



Mo-E16

Methane oxidation over palladium oxide from first-principles based micro-kinetic modelling

Henrik Grönbeck¹, Maxime Van den Bossche¹¹Chalmers University of Technology, Göteborg, Sweden

A major challenge within heterogeneous catalysis is to determine the active phase during operating conditions. This is valid, in particular, for structurally ill-defined catalysts that are realized as metal particles dispersed on porous oxides. Nevertheless, it is structural information at the atomic scale that allow for catalyst development beyond trial-and-error approaches. One long standing puzzle is the active phase of palladium during oxidation reactions where the metallic state competes with oxide phases. High-pressure X-ray photoelectron spectroscopy, mass spectrometry and density functional theory calculations have recently shown that PdO(101) films are highly active for methane oxidation [1]. In this contribution [2], we investigate the catalytic oxidation of methane to carbon dioxide and water over PdO(101) with first-principles based micro-kinetic modelling. Extensive exploration of the reaction landscape allows for determination of preferred pathways at different reaction conditions. The predicted kinetic behaviour is in good agreement with a range of experimental findings including reaction orders in methane, water and oxygen as well as apparent activation energies. The dissociative adsorption of methane is determined to be the rate-determining step over a wide range of reaction conditions. This is despite the fact that the enthalpy barrier for the first C-H dissociation is lower than for some of the subsequent reactions. Interestingly, the oxidation steps are generally taking place through a Mars van Krevelen mechanism where oxygen vacancies are formed in the surface. The vacancies are healed by O₂ adsorption. At low temperatures, the reaction is limited by H₂O adsorption.

The study demonstrate the predictive power of first-principles based kinetic modelling for oxide surfaces when hybrid functionals are applied and kinetic models that go beyond the mean-field approximation is used.

[1] N.M. Martin, M. Van den Bossche, et al. ACS Catalysis, 4, 3330 (2014).

[2] M. Van den Bossche and H. Grönbeck (Submitted).

Tu-A01+02

Understanding Charge and Spin Transport in Graphene-based Materials: From Concepts to Applications

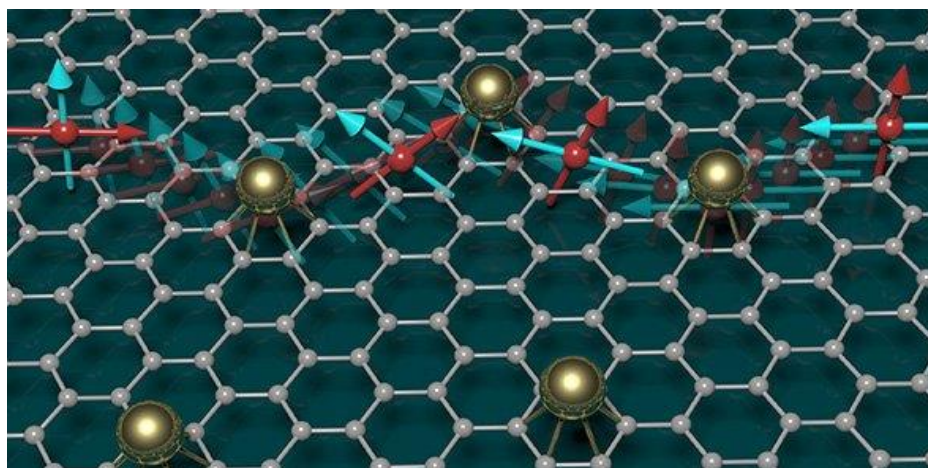
Stephan Roche²

¹Institut Català de Nanociència i Nanotecnologia (ICN2), Bellaterra, Spain,

²ICREA, Institució Catalana de Recerca i Estudis Avançats, Barcelona, Spain

In this talk, I will discuss charge and spin transport in complex forms of graphene (chemically reduced, polycrystalline graphene, chemically functionalized) of relevance for current and future applications in flexible electronics, energy harvesting and spintronics. The crucial contribution of multiscale simulation will be illustrated, demonstrating an achieved high level of predictive capability for very large system sizes (with up to 1 billion atoms), reaching the experimental and technology scales. One illustration will be the quantitative analysis on the transport properties of structural imperfections produced during the wafer-scale production of graphene through chemical growth (CVD), or the mechanical/chemical exfoliation and chemical transfer to versatile substrates, followed by the device fabrication. Fundamental properties of charge mobilities in polycrystalline graphene, accounting the variability in average grain sizes and chemical reactivity of grain boundaries as observed in real samples grown by CVD will be presented, together with their relevance for device optimization and diversification of applied functionalities such as chemical sensing.

In a second part, I will focus on spin transport in graphene functionalized by ad-atom deposits (gold, thallium) and ultraclean graphene in presence of electron-hole puddles and vanishingly small spin-orbit interaction. Unique spin dynamics phenomena in graphene, such as the formation of the Quantum Spin Hall state and a crossover to the Spin Hall effect under ad-atom segregation will be shown, as well as the role of spin-pseudospin entanglement in driving the spin relaxation mechanism in the ultraclean graphene limit (graphene on BN substrate), or the manifestation of Dyakonov-Perel mechanism for graphene on SiO₂. These results clarify current controversies and open unprecedented perspectives for achieving proofs of concepts of spin manipulation, contributing to the progress towards non-charge based revolutionary information processing and computing.



Tu-A03

Spatial variation of a giant spin-orbit coupling effect induces electron confinement in graphene on Pb islands

Juan Jesús Navarro¹, Fabian Calleja¹, Héctor Ochoa², Manuela Garnica^{1,3}, Sara Barja^{1,3}, Andrés Black^{1,3}, Mikhail M. Otrokov^{4,5}, Evgueni V. Chulkov^{4,6}, Andrés Arnau^{4,6}, Amadeo L. Vázquez de Parga^{1,3}, Francisco Guinea¹, Rodolfo Miranda^{1,3}

¹Instituto Madrileño de Estudios Avanzados en Nanociencia, Madrid, Spain,

²Instituto de Ciencia de Materiales de Madrid, Consejo Superior de Investigaciones Científicas, Madrid, Spain, ³Departamento de Física de la Materia Condensada and IFIMAC, Madrid, Spain, ⁴Donostia International Physics Centre (DIPC), San Sebastian, Spain, ⁵Tomsk State University, Tomsk, Russia, ⁶Departamento de Física de Materiales UPV/EHU and Centro de Física de Materiales (CFM), San Sebastian, Spain

The electronic band structure of a material can acquire interesting topological properties in the presence of a magnetic field or due to the spin-orbit coupling. By means of LT-STM/STS we study graphene grown on Ir(111) with Pb monolayer islands intercalated between the graphene sheet and the Ir surface [1]. The intercalated Pb atoms form a rectangular lattice which corresponds to a c(4x2) superstructure commensurate with Ir and, therefore, incommensurate with graphene. While the graphene layer is structurally unaffected by the presence of the Pb islands, its electronic properties change dramatically and regularly spaced resonances appear in the scanning tunnelling spectroscopic data acquired in ultra high vacuum conditions and at 4.2K. With the help of DFT simulations and phenomenological Hamiltonian we interpret these resonances as the effect of a strong and spatially modulated spin-orbit coupling, induced in graphene by the Pb monolayer. These results demonstrate the possibility of spatial spin orbit coupling engineering in epitaxial graphene and pave the way for practical applications of graphene in spintronics.

[1] F. Calleja, et al., "Spatial variation of a giant spin-orbit effect induces electron confinement in graphene on Pb islands", *Nature Phys.* 11, 43 (2015)

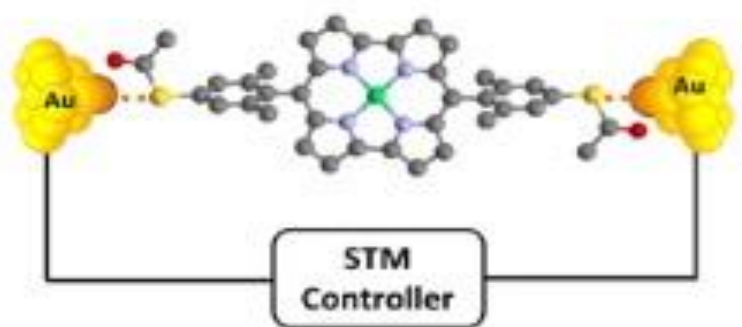
Tu-A04

An anti-aromatic approach to enhanced molecular charge-transport

Santiago Marqués-González¹, Shintaro Fujii¹, Manabu Kiguchi¹, Ji-Young Shin², Hiroshi Shinokubo²

¹Department of Chemistry, Graduate School of Science and Engineering, Tokyo Institute of Technology, Tokyo, Japan, ²Department of Applied Chemistry, Graduate School of Engineering, Nagoya University, Nagoya, Japan

Here we present the first single-molecule conductance study of an anti-aromatic molecular wire. As one of the most fundamental concepts in chemistry, aromaticity has been a core guideline in the design of molecular candidates for charge-transfer applications. Early studies showing enhanced electrical performance for π -conjugated aromatic systems quickly led to the nowadays ubiquitous use of aromatic systems for charge transfer applications. However, recent studies have shown that the aromatic stabilization energy can negatively affect the charge transfer capabilities of a molecular junction. This counterintuitive fact arises from a misalignment of the molecular frontier orbitals with respect to the electrode Fermi level, as a result of a large aromatic stabilization. Based on these findings, we tested a novel approach to enhance molecular charge transport i.e. anti-aromaticity. According to Huckel's rule, planar cyclic conjugated system with $4n$ π -electrons undergo an anti-aromatic destabilization. As a result, anti-aromatic compounds feature a small HOMO-LUMO gap, while maintaining an extended π -conjugated system. We employed the scanning tunnelling microscope break-junction (STM-BJ) technique, to test the conductance of a novel anti-aromatic norcorrol complex [Ni(Nor)]. The results were benchmarked against a porphyrin-based aromatic [Ni(Porph)] analogue. Over 5000 current/distance traces were collected for each molecule and statistically analysed. The conductance of the novel anti-aromatic complex [Ni(Nor)] ($5 \times 10^{-4} G_0$) was found to be an order of magnitude higher than that of its aromatic counterpart [Ni(Porph)]. These results prove the enhanced charge-transfer capabilities of anti-aromatic compounds, and provide relevant synthetic guidelines for the next generation of molecular systems in molecular electronics and related research fields (DSSCs, OLEDs, and energy storage).



Tu-A05

Graphene monovacancies: electronic and mechanical properties from large scale ab initio simulations

Lucía Rodrigo¹, Pablo Pou^{1,2}, Rubén Pérez^{1,2}

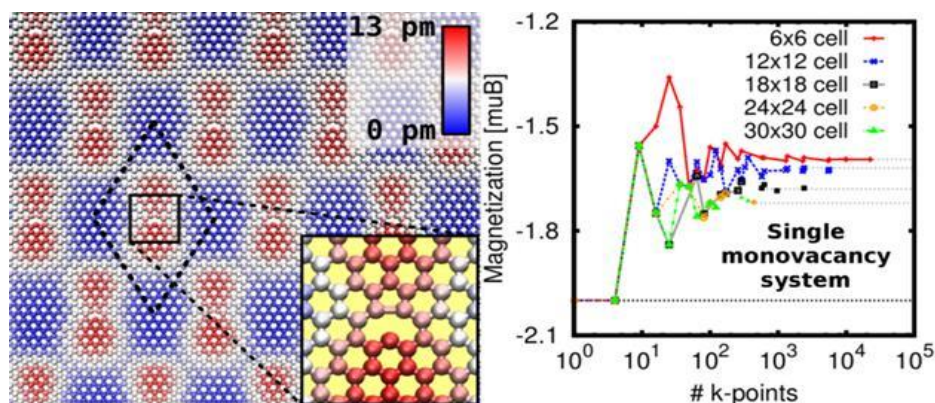
¹Departamento de Física Teórica de la Materia Condensada, Universidad Autónoma de Madrid, Madrid, Spain, ²Condensed Matter Physics Center (IFIMAC), Universidad Autónoma de Madrid, Madrid, Spain

The inclusion of graphene in new devices requires the study of its properties in real conditions, including defects that strongly modify its basic properties. Of particular interest are point vacancies, which are very common in non-ideal samples. They have been reported to be responsible of both the origin of local magnetic moments [1] –although there is some controversy about this [2]– and an enhancement of the stiffness of the layer [3]. We have carried out a complete set of DFT simulations to characterize the magnetic and mechanical properties of graphene as a function of the monovacancy concentration. The slow convergence of the magnetic moments with the system size and the k-points mesh makes it a challenging computational problem. Our simulations on systems with up to a G(30x30) cell size and several thousand k-points meshes show a clear tendency to converge the local magnetic moment of diluted monovacancies to 2 μ_B . Moreover, the vacancy reconstructs in the well-known 1+2 configuration (see figure) and induces a corrugation of 13 pm. We have also studied mechanical properties and tensile-strain-induced changes in the local magnetism of monovacancies on graphene. Due to the convergence difficulties present in the single vacancy case, we have used two vacancies in opposite sublattices in a G(12x12) cell (antiferromagnetically coupled), whose convergence is much faster. We obtain that the local magnetization increases upon stretching (x1.5 at 5%) and decreases upon compression (x0.7 at -2%). We have not found a stiffness enhancement comparable to the experimental information, which shows that thermal fluctuations –absent in our simulations– could be ruling the changes in the mechanical properties of tailored graphene layers.

[1] Ugeda et al., PRL 104, 096804 (2010)

[2] Palacios et al., PRB 85 (24) (2012)

[3] López-Polín et al., Nat. Phys. 11, 26–31 (2015)



Tu-A06

Probing excitonic effects in chevron-like graphene nanoribbons

Valentina De Renzi^{1,2}, Alberto Lodi Rizzini^{1,2}, Deborah Prezzi², Alice Ruini^{1,2}, Andrea Ferretti², Roberto Biagi^{1,2}, Valdis Corradini², Andrea Candini², Marco Affronte^{1,2}, Umberto del Pennino^{1,2}, Elisa Molinari^{1,2}, Richard Denk³, Michael Hohage³, Peter Zeppenfeld³, Jinming Cai⁴, Roman Fasel^{4,5}, Pascal Ruffieux⁴, Zongping Chen⁶, Akimitsu Narita⁶, Xinliang Feng, Klaus Mueller⁶

¹Department of Physics, Informatics and Mathematics, University of Modena and Reggio Emilia, Modena, Italy, ²CNR-Nanoscience Institute, S3 Center, Modena, Italy, ³Institute of Experimental Physics, Johannes Kepler University, Linz, Austria, ⁴Empa, Swiss Federal Laboratories for Materials Science and Technology, Duebendorf, Switzerland, ⁵Department of Chemistry and Biochemistry, University of Bern, Bern, Switzerland, ⁶Max Planck Institute for Polymer Research, Mainz, Germany

Graphene nanoribbons (GNRs) are raising great interest as they exhibit width-tunable band-gaps, while maintaining the outstanding properties of graphene. Covalent self-assembly of suitable molecular precursors [1] is a powerful approach to obtain atomical control on GNRs width, shape and chemical composition, opening the way to a precise tuning of their properties. Recently, we demonstrated the importance of excitons in determining the optical properties of armchair-GNRs[2]. For chevron-GNRs (chGNRs), which have less pronounced 1D character, the role of excitons is not yet established. In fact, Bronner et al. [3] explained the dominant feature observed in their EELS spectrum in terms of HOMO-LUMO gap. The absence of any excitonic feature is indeed puzzling, as they should be present in EEL-spectra, in particular for confined molecular systems [4]. In this work, we combine ab-initio DFT calculations with optical (RDS) and electronic (EELS) measurements, to obtain a full description of chGNR properties in terms of differential (RDS) and averaged (EELS) adsorbate dielectric function ϵ_{ads} . For EELS, we find it crucial to optimize the experimental conditions in order to maximize the weight of the adsorbate contribution relative to that of the gold surface plasmon [5]. Both, optical and electronic spectra were analyzed applying the three-phase dielectric model. We modeled ϵ_{ads} with four damped harmonic oscillator located at 2.2 eV (2.3 for HREELS), 2.8 eV, 3.4 eV and 4.4 eV. The experimental ϵ_{ads} is in good agreement with theoretical results, demonstrating the fundamental role played by excitons in determining the optical and electronic properties of chGNRs.

[1] J. Cai et al., Nat. 466, 470 (2010)

[2] R. Denk et al. , Nat. Comm. 5, 4253 (2014)

[3] C. Bronner et al. Angew. Chem. 125, 4518 (2013)

[4] B-Y. Han et al. Phys. Rev. B 51, 7179 (1995)

[5] M. Smieri et al. Phys. Rev. Lett. 113, 186804 (2014)

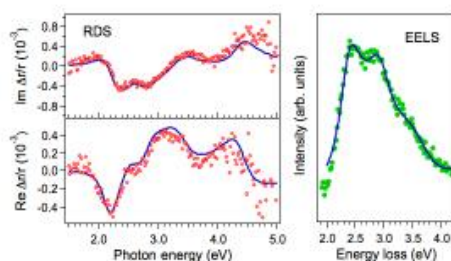


Fig. 1 RDS (left panels) and EELS (right panel) measurements of chevron-type GNRs grown on the Au(788) and Au(111) surfaces, respectively. The three-phase model fitting curves are shown as solid lines

Tu-A07

Terahertz optical modes of supported graphene bilayer

Alberto Lodi Rizzini^{1,2}, Valentina De Renzi^{1,2}, Roberto Biagi^{1,2}, Valdis Corradini²,
Daniela Pacilè³, Antonio Politano³, Umberto Del Pennino^{1,2}

¹Dipartimento FIM - Università di Modena e Reggio Emilia, Modena, Italy,

²CNR-Nanoscience Institute, S3 Center, Modena, Italy, ³Dipartimento di Fisica, Università della Calabria, Cosenza, Italy

The thermal properties of graphene are strongly influenced by interactions with the substrate, presence of defects and lattice distortions. At low temperature, thermal capacity and conduction are mainly related to the properties of the acoustic modes. The ability to tune these modes can therefore open the way to a fine control on the thermal properties of graphene-based systems [1]. Moreover, ultra-low frequency vibrations could have interesting applications in the THz range [2]. In this work, we investigate by HREELS the vibrational properties of a graphene bilayer, grown on the Ru(1000) surface (BLG@Ru) [3], unraveling the details of low-frequency phonon dispersions. A typical HREEL spectrum is built by several peaks, observed in both loss and gain sides (see Inset). Fig.1 presents the dispersion curves of the BLG@Ru, together with the theoretical dispersion of the freestanding bilayer of graphene (BLG) [4]. In the BLG case, the ZA branch gives origin to one optical mode ZO', i.e. a breathing mode of the two layers [4,5]. Instead, we observed two such modes at 12.5 and 8.2 meV, due to the presence of the substrate. A possible role of the Moiré-derived corrugation is also envisaged. Indeed, also the higher-energy ZO mode is splitted (107 and 88 meV). Another non-dispersing mode is observed at 4.7 meV and tentatively attributed to an interlayer shear mode, originated from TA/LA [6,7]. The possible origin of its localized nature will be discussed.

[1] E. Pop et al., MRS Bulletin, 37 1273 (2012)

[2] J.S. Bunch et al., Science, 315, 490 (2007)

[3] P.W. Sutter et al., Nat. Mater. 7, 406 (2008)

[4] J.-A. Yan et al, Phys. Rev B, 77, 125401 (2008)

[5] P.T. Araujo et al., Sci. Rep. 2, 1017 (2012)

[6] P.H. Tan, et al., Nat. Mater., 11, 294 (2012)

[7] C. Cong et al., Nat. Comm., 5, 4709 (2014)

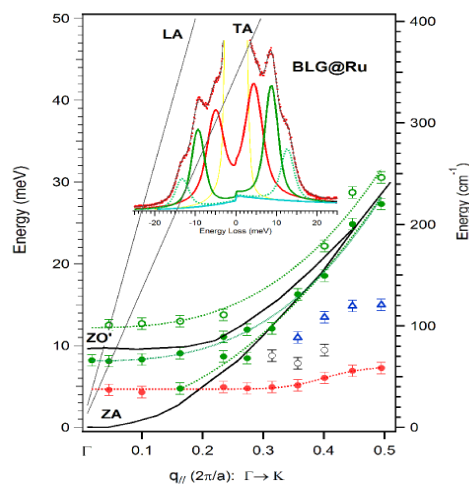


Fig. 1: Phonon dispersion curves of BLG@Ru (opened and filled symbols). The solid-line black curves represent the free BLG dispersions [4].

Tu-A08

Coherent phonons of Cs-intercalated graphene on Ir(111)

Kazuha Watanabe¹, Marin Petrović², Marko Kralj², Predrag Lazić³, Toshiki Sugimoto¹, Yoshiyasu Matsumoto¹

¹Kyoto University, Kyoto, Japan, ²Institut za fiziku, Zagreb, Croatia, ³Ruđer Bošković Institute, Zagreb, Croatia

Epitaxial growth of graphene on transition metal surfaces has been known as a conventional method to obtain macroscopic high quality graphene sheet. On Ir(111), graphene can be prepared with an exceptionally high structural quality by a conventional chemical vapor deposition. Chemical doping by alkali atom intercalation between graphene and Ir substrate induces large shift of the Dirac point. While their electronic structures have been extensively investigated [1], their dynamical responses have been less explored. In this contribution, we focus on Cs-intercalated graphene / Ir(111) and describe its peculiar optical response and ultrafast electron-phonon couplings revealed by steady state as well as femtosecond time-resolved reflectivity measurements. Experiments were carried out by slightly modifying the pump-probe setup with an UHV chamber developed by some of the authors [2]. The Cs intercalation brings about a strong resonance feature in the optical reflectance spectra with a maximum reflectance change more than 10 % in visible region (2.1-2.2 eV). This giant response is possibly ascribed to a surface plasmon resonance of the Cs-intercalated graphene activated by a moiré type periodic modulation of the graphene structure. In contrast to recent intensive researches on graphene plasmonics which mainly focus on far-infrared region, this indicates a possible strategy for pushing the resonance photon energy to visible region. In the pump-probe reflectivity measurement, a femtosecond laser pulse tuned to the resonance band induces time-domain oscillatory modulations of the resonance band. With a help of theoretical calculations, those oscillations are ascribed to coherent nuclear motions of intercalated Cs and graphene, and ultrafast couplings between the plasmonic excitation and surface nuclear motions are revealed.

[1] M. Petrović et al. Nat. Commun. 4, 2772 (2013).

[2] K. Watanabe et al. J. Phys. Chem. A, 115, 9528 (2011).

Tu-B01

Adsorption of CO and CO₂ onto Co₃O₄(111) and CoO(111) films grown on Ir(100)

Mohammad Alif Arman¹, Pascal Ferstl², Johan Gustafson¹, Karina Schulte³, M. Alexander Schneider², Lutz Hammer², Edvin Lundgren¹, Jan Knudsen^{1,3}

¹Division of Synchrotron Radiation Research at Lund University, Sweden, Lund, Sweden, ²Solid State Physics, University Erlangen-Nürnberg, Germany, Erlangen-Nürnberg, Germany, ³MAX IV Laboratory, Lund University, Sweden

Cobalt oxide nanomaterials are active for CO oxidation at temperatures as low as 220 K [1, 2]. On the Ir(100) surface a large number of ultrathin Co oxide film structures can be grown [3, 4], which are well characterized at the atomic level by scanning tunneling microscopy (STM) and low energy electron diffraction (LEED) [3, 4]. This wealth of Co oxide structures gives us a unique tool to vary the stoichiometry, surface termination etc. and study their impact on the adsorption of probe molecules. Here, we studied the adsorption of CO and CO₂ at 100 K onto well-ordered spinel-type Co₃O₄(111) and rocksalt-type CoO(111) thin films on Ir(100) mainly using high-resolution X-ray photoelectron spectroscopy (HR-XPS). In all cases we observe co-existing species both in C 1s and O 1s spectra. Using temperature programmed XPS we assign the different components to weakly adsorbed CO/CO₂ species and carbonate. We find that much more CO/CO₂ is adsorbed on the Co₃O₄(111) compared to the CoO(111) surface and we relate that different behavior mainly with Co ions terminating only the Co₃O₄(111) surface.

[1] D. A. H. Cunningham et al., Catal. Lett. 25, 257 (1994)

[2] J. Jansson et al., J. Catal. 211, 387 (2002)

[3] K. Biedermann et al., J. Phys. Cond. Matt. 21, 185003 (2009)

[4] K. Heinz and L. Hammer, J. Phys. Cond. Matt. 25, 173001 (2013)

Tu-B02

Water adsorption on ferroelectric oxide surfaces: A synchrotron Near Ambient Pressure X-ray Photoelectron Spectroscopy (XPS) study.

Albert Verdaguer^{1,2}, Laura Rodríguez^{1,2}, Maria José Esplandiu^{1,2}, Kumara Cordero¹, Carlos Escudero³, Virginia Pérez³, Annalisa Calò¹, Neus Domingo¹

¹ICN2 - Institut Català de Nanociència i Nanotecnologia, Campus UAB, Bellaterra, Spain, ²CSIC - Consejo Superior de Investigaciones Científicas, ICN2 Building, Bellaterra, Spain, ³ALBA Synchrotron Light Source, Barcelona, Spain

Under ambient conditions all surfaces are covered by a thin film of water, ranging in thickness from a fraction of a monolayer to a macroscopic film. Even the thinnest film can profoundly affect the physical and chemical properties of the substrate. The nature of the substrate determines the interaction with the water molecules, and the interplay of water–substrate and water–water interactions can induce myriad different structures. It has been shown that the presence and orientation of electrical dipoles on surfaces determines how the surface interacts with water molecules of the environment. For example, ferroelectric surfaces with opposite polarity have different properties for adsorbing molecules, which screen the strong electric fields at the surface of such materials. In these materials, understanding the interplay between ferroelectric phase stability, screening and atomistic processes at the surface is a key to control low-dimensional ferroelectricity. Near-ambient X-ray photoelectron spectroscopy (XPS) has proved its power to study water films on oxide surfaces in the past. Using this technique, we studied water adsorption and desorption on ferroelectric oxide crystals and thin films at the line CIRCE in ALBA. In this contribution we will show our results on water adsorption on different materials ($\text{Pb}(\text{Zr,Ti})\text{O}_3$, LiNbO_3 and BiFeO_3) as a function of surface polarization. We were able to identify the presence of molecularly absorbed water and OH groups on the surface exposed to pressures ranging from high vacuum conditions to 5 mbar of water vapor. We observed that water stays on most of the polarized surfaces for temperatures above 200°C, even in high vacuum conditions. We also observed that water always adsorbs preferentially on surfaces showing the same polarization, independently of the material used or if the material is a crystal or a thin film. This suggests that our findings can be considered as a general property for ferroelectric oxide materials.

Tu-B03

Mechanism of Water Dissociation on CoO_x nanoislands on Au(111)Jakob Fester¹, Alexander Walton¹, Jeppe V Lauritsen¹¹Interdisciplinary Nanoscience Center, Aarhus University, Aarhus, Denmark

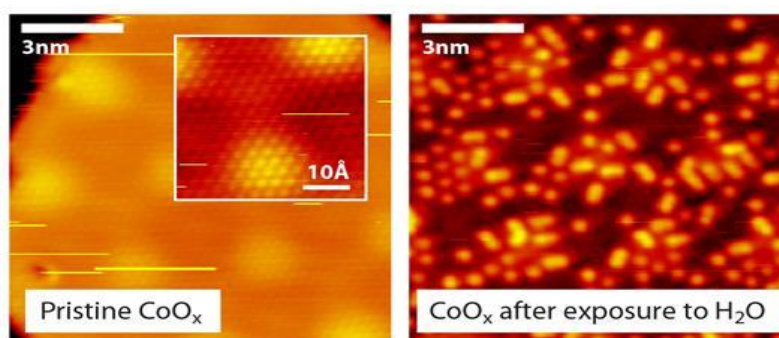
Cobalt oxides are among the best performers as future alternative electrocatalysts for the water splitting reaction with attractive properties in terms of stability, efficiency, abundance and low-cost [1]. However, fundamental understanding of the catalytic properties of cobalt oxides is still limited. To elucidate the fundamental structure, composition and surface chemistry of CoO_x based catalysts, we characterize the surface of CoO_x nanoislands under ultra-high vacuum conditions by high-resolution Scanning Tunneling Microscopy (STM) and X-Ray Photoelectron and Absorption Spectroscopies (XPS and XAS). The Au(111) surface is used as a growth template and the effects of varying synthesis conditions on the resulting CoO_x nanostructures are explored [2]. This allows for atomic-scale investigations of adsorption of water, water dissociation, potential studies of promotional effects by metal substitution with Ni, Mn and Fe [3] and synergistic effects with the Au(111) substrate [4]. We find that the oxygen pressure has a profound effect on the CoO_x structure and cobalt oxidation states. The structure at low pressure is a rocksalt Co-O bilayer exposing the (111) plane with cobalt in the 2+ oxidation state. However, an additional layer of oxygen can be intercalated into the island/gold interface, changing the cobalt oxidation state to 3+. Both structures exhibit a strong activity towards water dissociation at room temperature, leading to hydroxylation of up to 50% of the island basal plane oxygen atoms as observed both in STM experiments and by analysis of the hydroxyl component in the O1s core-level XPS spectrum. The reactivity towards water dissociation is measured as function of island edge concentration, revealing the edges to host the active sites.

[1] ACS Catalysis, 2014. 4(10): p. 3701-3714.

[2] ACS Nano, 2015. 9(3): p. 2445-2453.

[3] Journal of the American Chemical Society, 2012. 134(41): p. 17253-17261.

[4] Journal of the American Chemical Society, 2011. 133(14): p. 5587-5593.



Tu-B04

Wet chemically prepared titanium dioxide surfaces: Substrates for studies under non-UHV conditions

Rob Lindsay¹, Mahmoud Ahmed¹, Francis Lydiatt¹, Jon Treacy¹, Dimitri Chekulaev¹, Andrew Thomas¹, Paul Wincott¹, David Vaughan¹, Xavier Torrelles², Chris Nicklin³, Joon Jang⁴, Steve Baldelli⁴, Geoff Thornton⁵

¹University of Manchester, Manchester, UK, ²Institut de Ciència de Materials de Barcelona, Bellaterra, Spain, ³Diamond Light Source, Didcot, UK, ⁴University of Houston, Houston, USA, ⁵University College London, London, UK

Researchers in surface science are becoming increasingly concerned with more complex systems and conditions. Focusing on the latter area, greater complexity largely involves a move away from UHV work to studies in more technologically pertinent environments, i.e. measurements performed with samples immersed in fluids. An issue of interest associated with such effort is preparation of well-defined substrate surfaces. One route is simply to prepare the sample under UHV conditions, and then introduce the fluid. Alternatively, a non-UHV recipe may be adopted. This second option is attractive as it potentially eliminates the requirement for UHV facilities, although substrate characterisation is still required to adhere to a rigorous surface science approach. Here, we contribute to this topic through presenting a non-UHV recipe for rutile-TiO₂ surfaces. Several non-UHV approaches for preparation of single-crystal TiO₂ surfaces have been already implemented. Despite varying in detail, almost all of these recipes can be labelled as so called wet-chemical procedures, involving high temperature annealing and chemical cleaning. In this presentation, a somewhat modified wet-chemical recipe for the preparation of TiO₂(110) and TiO₂(011) will be described. For both surfaces characterization with AFM, LEED, AES, and VSFS indicate that flat, well-ordered, carbon-free surfaces can be generated. Notably, in contrast to the (2x1) surface unit cell found for TiO₂(011) prepared in UHV, wet chemical preparation results in a (4x1) termination; wet chemically prepared TiO₂(110) displays a (1x1) surface. Further characterisation of the wet-chemically prepared TiO₂(110)(1x1) surface has been achieved with SXRD; measurements were undertaken in a helium atmosphere, i.e. a non-UHV environment. Analysis of these diffraction data demonstrate that the substrate termination is similar to that found in UHV, i.e. topmost layer exhibits fivefold Ti atoms, as well as in-plane and bridging O atoms. Additionally, the surface is decorated with a significant concentration of adsorbed hydroxyl species.

Tu-B05

Surface Science studies of submonolayer Vanadium supported on TiO₂-anatase (101)

Stig Koust¹, Jeppe Vang Lauritsen¹, Stefan Wendt¹

¹Aarhus University, Aarhus C, Denmark

Tighter regulations concerning nitrogen oxides (NO_x) and an increased public concern, highlighted recently by a study from ICCT [1], demonstrating that new diesel cars emit more than seven times the allowed NO_x levels, gives rise to a requirement for developing more effective catalysts for NO_x removal. The Selective Catalytic Reduction (SCR) is widely used to reduce NO_x levels into N₂ and H₂O in flue and exhaust gasses and the reactions is best catalysed using a TiO₂-anatase supported sub-monolayer VO_x-based catalyst promoted with W or Mo. Unfortunately, the reaction mechanism(s) is still debated, and the nature of the active site is uncertain [2]. To tackle these issues, the preparation and characterization of good model catalyst model systems may provide new fundamental insights. Here we present atomically resolved STM images of submonolayer vanadium supported on TiO₂-anatase (101). Specifically, we observed vanadium embedding into the near-surface region. Vanadium deposited at liquid nitrogen temperature are seen to embed the surface upon annealing to room temperature. This conclusion is further supported by a shift in binding energy of the V2p XPS feature. Finally, our DFT calculations suggest a substitution of vanadium with surface titanium atoms.

[1] <http://www.theicct.org/real-world-exhaust-emissions-modern-diesel-cars>

[2] G.Busca et al. App. Catalysis B (1998)

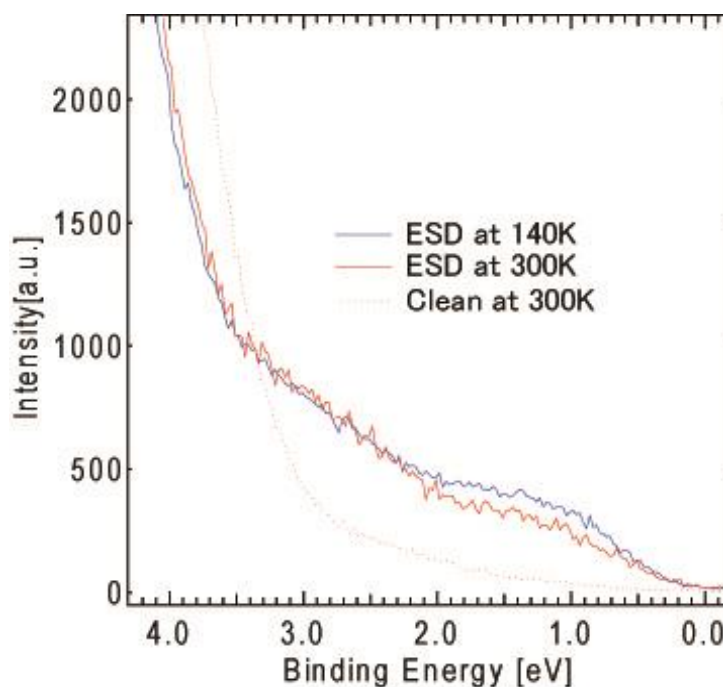
Tu-B06

In-gap states induced by electron irradiation at anatase TiO₂ (101) surfaces

Naoki Nagatsuka¹, Kanta Asakawa¹, Kotaro Takeyasu¹, Shohei Ogura¹, Katsuyuki Fukutani¹

¹Institute of Industrial Science, The University of Tokyo, Shibuya, Japan

Titanium dioxide (TiO₂) is a typical material for photocatalysis, and its anatase phase shows a higher reactivity than the rutile phase, of which the reason is yet to be elucidated. The TiO₂ surfaces are readily reduced forming oxygen vacancies (Vo's), and it is known that Vo's migrate to the subsurface site at the anatase TiO₂ (101) surface while Vo's dominantly remain on the surface of rutile TiO₂ (110). In aimed at clarifying the relationship of surface and subsurface Vo's with the electronic states, we have investigated the surface electronic states of anatase TiO₂ (101) at various temperatures with ultraviolet photoemission spectroscopy (UPS) and low energy electron diffraction (LEED). Vo's were created by means of electron-stimulated desorption (ESD) with energies of 50 and 500 eV at sample temperatures of 140 and 300 K. Figure 1 shows the UPS spectra near the Fermi level taken for the clean surface at 300 K, and surfaces after ESD at 300 and 140 K. The spectrum of the ESD surface at 300 K shows in-gap states at 1.2 and 2.3 eV below the Fermi level. While the peak at 1.2eV initially appeared at a low electron dose, the broad peak at 2.3 eV grew after saturation of the former peak. The spectrum of ESD at 140 K also revealed similar two peaks at 1.2 and 2.3 eV. When the 140 K-ESD surface was annealed to 300 K, on the other hand, the in-gap state at 1.2 eV was found to be reduced in intensity, whereas the intensity of the other in-gap state remained the same. On the basis of these results, we discuss that the two in-gap states have different origins of oxygen vacancies and Ti interstitials.



Tu-B07

Charging of small metal clusters on titania - The effect of doping

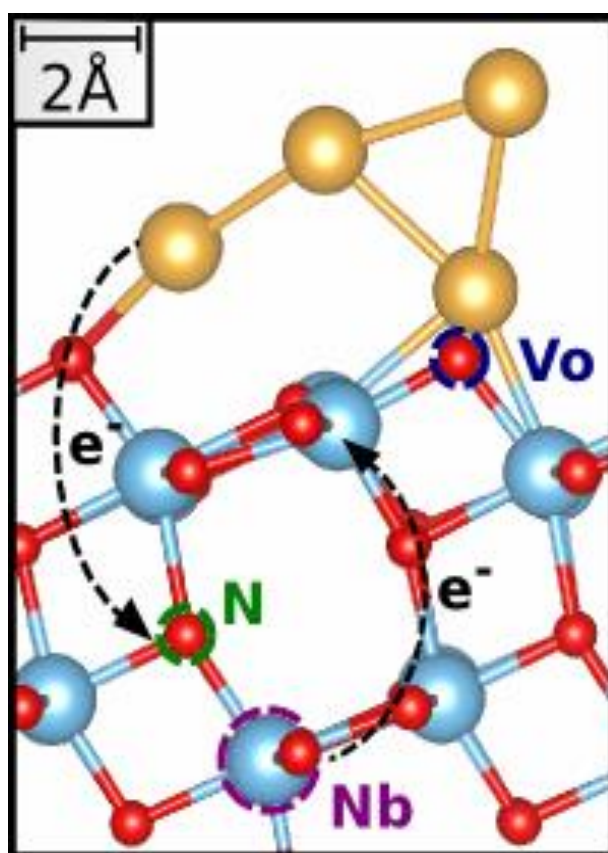
Philomena Schlexer¹, Gianfranco Pacchioni¹

¹University of Milano-Bicocca, Milan, Italy

Small metal clusters deposited on titania show promising catalytic activity for a variety of reactions, such as CO oxidation, photo-catalytic degradation and propene oxidation [1,2]. The metal-support interaction plays thereby a fundamental role. In our study, we investigated the effect of intrinsic and extrinsic defects of titania on the metal-support interaction using DFT. The effect of oxygen vacancies, N- and Nb- doping on the binding nature of small metal clusters (Ag_n and Au_n , $n=1,4,5$) on titania anatase was studied. Defects and dopants create new states in the band gap of titania. These new states often give rise to charge transfer between defect, support and/or metal cluster. We found that the occurrence and the direction of charge transfer strongly depend on defect-type, adsorbate and adsorption site. Introducing dopants, it is possible to tune the charge state of small metal clusters, consequently affecting their aggregation behaviour and reactivity.

[1] B. R. Cuenya, F. Behafarid, Surface Science Reports 70 (2015) 135-187

[2] G. Pacchioni, Phys. Chem. Chem. Phys. 15 (2013) 1737-1757



Tu-C01

Probing the site-dependent Kondo response of nanostructured graphene with organic molecules

Fabian Calleja¹, Manuela Garnica, Daniele Stradi, Sara Barja, Cristina Diaz, Manuel Alcamí, Andres Arnau, Amadeo Lopez Vazquez de Parga, Fernando Martin, Rodolfo Miranda

¹Universidad Autónoma De Madrid, IMDEA Nanociencia, Madrid, Spain

Epitaxial graphene grown on Ru(0001) is spontaneously nanostructured forming a hexagonal array of 100 pm high nanodomains with a periodicity of 3 nm due to the difference in lattice parameter between the graphene overlayer and the Ru(0001) substrate [1]. This difference produces a modulation in the interaction between the graphene overlayer and the Ru substrate and in turn modulates the density of states with localized electronic states in some areas of the moiré pattern [2]. TCNQ molecules adsorbed on this surface acquire an extra electron by charge transfer from the substrate and develop a sizeable magnetic moment as demonstrated by means of Low Temperature Scanning Tunneling Microscopy and Spectroscopy (LT-STM/STS) and Density Functional Theory (DFT) simulations. The singly charged TCNQ molecules are used as a sensitive probe for the Kondo response of the electron gas of a nanostructured graphene grown on Ru(0001). As mentioned before all adsorbed molecules acquired an extra electron by charge transfer from the substrate, but only those adsorbed in the FCC-Top areas of the moiré show magnetic moment and Kondo resonance in the STS spectra. DFT calculations trace back this behavior to the existence of a surface resonance in the low areas of the graphene moiré, whose amplitude and penetration into the bulk strongly depends on the stacking sequence between graphene and Ru(0001), quenches the magnetic moment of the electron acceptor molecules adsorbed on the HCP-Top areas of the moiré [3].

[1] S. Marchini et al. Phys. Rev. B 76, 075429 (2007)

[2] A.L. Vázquez de Parga et al. Phys. Rev. Lett. 100, 056807 (2008)

[3] M. Garnica et al. Nano Letters 14, 4560 (2014)

Tu-C02

Interaction of delocalized spins engineered by doping a molecular layer with single atoms

Taner Esat^{1,2}, Thorsten Deilmann³, Benedikt Lechtenberg⁴, Christian Wagner^{1,2}, Peter Krüger³, Ruslan Temirov^{1,2}, Frithjof Anders⁴, Michael Rohlfing³, Stefan Tautz^{1,2}

¹Peter Grünberg Institute (PGI-3), Forschungszentrum Jülich, Jülich, Germany,

²Jülich Aachen Research Alliance (JARA), Fundamentals of Future Information Technology, Jülich, Germany, ³Institut für Festkörpertheorie, Westfälische

Wilhelms-Universität Münster, Münster, Germany, ⁴Lehrstuhl für Theoretische Physik II, Technische Universität Dortmund, Dortmund, Germany

The utilization of molecular self-assembly offers the opportunity to create tailored arrays of single spins and therefore a promising platform for spintronics. In this context, the engineering and switching of the interactions between single spins is crucial for future applications. In this work we transfer a single spin into an extended π -orbital of a PTCDA molecule physisorbed on a Au(111) surface by doping with single Au atoms [1]. Unlike common molecules with an unpaired spin, which usually resides in a d- or f-orbital of a metal ion, we look at a complex where the spin is carried by a π -orbital. The delocalized character of π -orbitals makes this Au-PTCDA complex an interesting system in the study of spin phenomena and interaction. By means of LT-STM and STS we have investigated the interaction of the Au-PTCDA complexes with each other and observed a short ranged coupling between two neighbouring complexes. In two neighbouring Au-PTCDA complexes the hybridization between the spin-moment carrying orbitals and the direct Hund's rule type exchange interaction are causing two competing ground states: for a dominating hybridization, a chemical bond between the two π -orbitals with a spin singlet ground state is formed, while a strong exchange interaction would cause the spins to align in a spin-triplet state allowing for a Kondo-effect at low temperatures once coupled to the substrate. We will show that the presented system of two neighbouring Au-PTCDA complexes on a Au(111) surface is indeed located very close to a quantum phase transition so that both phases are realised depending on the precise engineering of the Au atom positions on the two PTCDA molecules.

[1] T. Esat et al., Phys. Rev. B 91, 144415 (2015)

Tu-C03

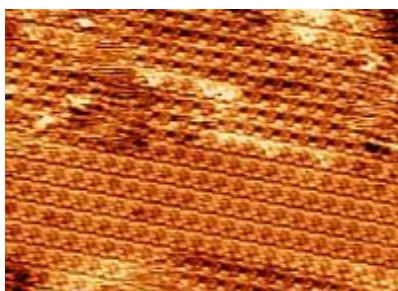
Adsorption of homochiral organic molecules on metal surfaces: Structure and enantiospecific photoelectron spin polarization

Juan José de Miguel¹, Miguel Angel Niño², Rogger Palacios³, Francisco Jesus Luque¹, Iwona Agnieszka Kowalik⁴, Sonia Matencio³, Esther Barrena³, Dimitri Arvanitis⁵, Carmen Ocal³

¹Department of Condensed Matter Physics, University Autonoma Madrid, Madrid, Spain, ²IMDEA-Nanoscience Madrid, Madrid, Spain, ³Institute of Materials Science, ICMAB-CSIC, Barcelona, Spain, ⁴Institute of Physics, Polish Academy of Sciences, Warsaw, Poland, ⁵Dept. Physics and Astronomy, Uppsala University, Uppsala, Sweden

We report on a study of films of purely organic chiral molecules adsorbed on two types of metal surfaces: paramagnetic Cu(100) and an epitaxial, ferromagnetic Co(100) film. Two different but structurally similar chiral molecules have been used: 1,2-diphenyl-1,2-ethanediol (DPED) and 1,2-diphenylethylenediamine (DPEDA). Both of them possess two chiral centres located at the two carbon atoms of the ethane (ethylene) chain and present two chiral enantiomers which are designated according to their conformation and optical activity as (R,R)-(+ and (S,S)-(-). The molecular layers were adsorbed in ultra-high vacuum on the metal surfaces and studied with a variety of surface-sensitive techniques. Spin-polarised, angle-resolved valence band photoemission has shown that the photoelectrons emitted through the adsorbed layers of both enantiomers of DPED display a clear spin polarization at room temperature, independent of their binding energy. Furthermore, when adsorbed on a ferromagnetic Co surface the spins of the photoemitted electrons point along different directions in space: in-plane for (R,R)-(+)-DPED and out-of-plane for (S,S)-(-)-DPED. These findings make the chiral molecules attractive candidates for spin filtering. The enantioselective response observed has been tentatively ascribed to different adsorption geometries of the molecules on the corresponding surfaces. To clarify this point, a detailed structural characterization has been undertaken combining X ray absorption and diffraction and also scanning tunnelling microscopy (STM). This latter allows us to visualize the various ordered structures formed by the adsorbed molecules on the different surfaces under study. These findings may create opportunities for applications not only in organic-based molecular spintronics but also in other fields such as asymmetric chemical synthesis, as well as provide some insight into the origins of the chiral asymmetries found in Nature.

M. Á. Niño et al., Adv. Mater. 26, 7474 (2014).



Tu-C04

Ideal metal-molecule chemical linkers for single molecule transport studied through first principles simulations in and out of equilibrium

Hector Vazquez¹¹Inst. of Phys., Acad. Sci. Czech Republic, Prague, Czech Republic

Single molecule circuits are ideal systems for studying a range of quantum phenomena. Molecular conductance depends delicately on the nature of the molecular chemical linker groups that bind the molecule to the electrodes [1]. In this talk I will present a comprehensive first-principles study of the conducting properties of single molecules having different linker groups in and out of equilibrium. The study was carried out through first-principles transport calculations based on DFT-NEGF. I will first present results for zero-bias calculations of alkanes bound to Au through different linkers, including highly-conducting direct Au-C links between the metal and the molecular backbone. These were shown to result in conductance values higher than with any other linker [2,3]. Through the comparison of different metal-molecule contacts, I will address the question of the “ideality” of metal-molecule linkers. I will then analyze the conducting properties of these systems under an applied bias, where the junction electronic structure out of equilibrium was calculated self-consistently. I will discuss the potential drop across the molecule and relate it to the screening ability of the different metal-molecule linkers.

[1] J.C. Cuevas and E. Scheer, ‘Molecular Electronics: An Introduction to Theory and Experiment’, (World Scientific Series in Nanotechnology and Nanoscience 2010).

[2] Z-L Cheng, R. Skouta, H. Vázquez, J. Widawsky, S. Schneebeli, M.S. Hybertsen, R. Breslow and L. Venkataraman, ‘In situ formation of highly conducting covalent Au–C contacts for single-molecule junctions’, Nat. Nanotechnol. 6 353 (2011).

[3] W. Chen, J.R. Widawsky, H. Vázquez, S. Schneebeli, M.S. Hybertsen, R. Breslow and L. Venkataraman, ‘Highly Conducting pi-Conjugated Molecular Junctions Covalently Bonded to Gold Electrodes’, J. Am. Chem. Soc. 133 17160 (2011).

Tu-C05

Interactions between benzene derivatives on noble metal surfaces

Sergey Filimonov¹, Larisa Nikitina², Mikhail Pidchenko¹¹National Research Tomsk State University, Tomsk, Russian Federation,²National Research Tomsk Polytechnic University, Tomsk, Russian Federation

Adsorption of small aromatic molecules on metal and semiconductor surfaces is currently attracting great attention due to prospects of their use as the building blocks of new types of nanoelectronic devices based on single adsorbed molecules and thin molecular films. The key factors affecting electronic and optical properties of the adsorbed molecules are the nature and strength of the molecule-substrate and intermolecular interactions. As has been recently shown, fine tuning of the molecule-substrate interactions might be achieved by changing the molecule constitution or/and the metal substrate [1,2]. In the present work we employ first-principles density functional theory calculations to systematically explore the mechanism of intermolecular interactions for benzene derivatives adsorbed on noble metal surfaces. Calculations have been performed with the FHI-aims all-electron code [3] using the PBE+vdW^{surf} method [4] to account for the van der Waals interactions and collective substrate response effects. The effect of the substitution of hydrogen by halogen atoms on the optimal molecule-molecule distance and on the strength of the intermolecular bonds is analyzed. The role of dispersive forces and the influence of the substrate on the intermolecular interactions are discussed. This work was supported by the Russian Science Foundation (grant #14-12-00813).

[1] W. Liu, et al., Nat. Commun. 4:2569 (2013, doi: 10.1038/ncomms3569).

[2] R. Peköz et al., J. Phys. Chem. C 118, 6235 (2014).

[3] V. Blum et al. Comp. Phys. Comm. 180, 2175 (2009).

[4] V.G. Ruizet al. Phys. Rev. Lett. 108, 146103 (2012).

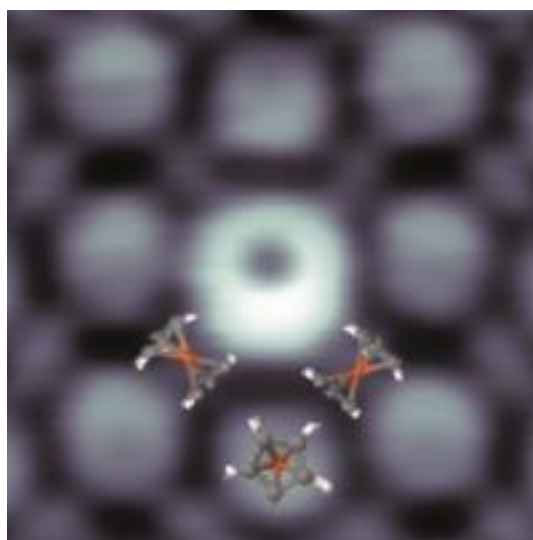
Tu-C06

On-surface engineering of upstanding ferrocene-based molecules

Nicolas Bachellier¹, Maider Ormaza¹, Paula Abufager², Roberto Robles², Martin Vérot⁴, Tanguy Le Bahers⁴, Marie-Laure Bocquet³, Nicolas Lorente², Laurent Limot¹

¹IPCMS, Strasbourg, France, ²ICN2, Barcelona, Spain, ³ENS Paris, Paris, France, ⁴ENS Lyon, Lyon, France

The ability to manipulate the magnetic properties and the spin-polarized current through single molecules is at the basis of molecular spintronics. Many experimental investigations have reported on the possibility of manipulating the molecular spin by metallizing or altering the chemical environment of molecules such as porphyrin-based or phthalocyanine-based molecules adsorbed on metallic surfaces. However, experimental data on metallocenes (MCp₂ where Cp is a cyclopentadienyl and M = Fe, Co, Ni etc.), or more generally metallocene-based wires, remain scarce, despite the wealth of predictions concerning their half-metallicity and ideal spin filtering efficiency. Here, we present the first controlled formation of novel magnetic cobalt-ferrocene molecules (Co-Cp-Fe-Cp, CoFc hereafter) on a metallic surface. After the co-deposition of cobalt atoms and of ferrocene molecules onto a Cu(111) surface, we are able to build with atomic control a single upstanding CoFc molecule by using the tip of a low-temperature scanning tunneling microscope (STM). In an effort to generalize the CoFc formation and bypass STM manipulation, we also demonstrate that the same molecule can be self-assembled by exposing a Fc layer to single Co atoms. Through a combined STM and density functional theory (DFT) study, we then show that unlike Fc, CoFc exhibits a magnetic moment revealing a change on the spin state of Fc. This result can be generalized to other metallocene molecules and other atom, as we have already checked, opening up the tantalizing prospect of tailoring molecules with the desired chemical composition, hence with the desired spintronic behavior.



Tu-C07+08

Single-ion magnets on metal and oxide surfaces

Pietro Gambardella¹¹ETH Zurich, Switzerland

Metal atoms in low coordination environments can develop extremely large magnetic moments and anisotropy properties leading, in some case, to slow relaxation of the magnetization. In this talk I will discuss different strategies to enhance the magnetic response of atoms and molecules on surfaces based on axial coordination, charge transfer, and coupling to ferromagnetic or antiferromagnetic films. I will present experiments on 3d as well as 4f ions on MgO, Pt, and graphene surfaces.

Tu-D01

GIFAD inside MBE, a most valuable combination

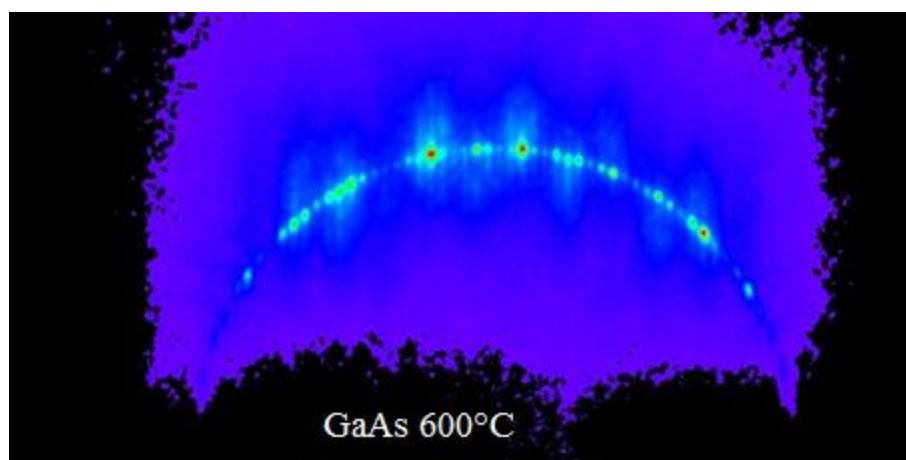
Philippe Roncin¹, Paola Atkinson², Asier Zugarramurdi¹, Maxime Debiossac¹, Andrei Guenadievich Borisov¹, Hocine Khemliche¹, Maxime Mulier¹, Boubekeur Lalmi¹, Anouchah Momeni¹, Mahmoud Eddrief², Fabio Finnochi², Victor Etgens²

¹ISMO, CNRS Université Paris Saclay, Univ. Paris sud, Orsay, France, ²INSP, CNRS-Universités Paris Sorbonnes, UPMC, Paris, France

Grazing incidence Fast Atom Diffraction is similar to RHEED in terms of geometry and the diffraction images look somewhat similar, however, the use of helium atoms as projectiles provides properties closer to HAS; absence of subsurface penetration and high sensitivity to the shape of the surface electronic density profile. We have installed a GIFAD setup inside a MBE Chamber to evaluate its performance in growth conditions. Investigating the homo-epitaxy of GaAs, we have been able to record up to ten diffraction images per second. The intensity oscillations with successive layers, similar to those observed in RHEED display a high contrast ratio. More important, the position of the oscillations maxima is shown to be independent of the beam energy and incidence angle providing an absolute reference of layer termination [1]. In static conditions i.e. before or after the growth process, GIFAD can be used in a high resolution mode to get extremely detailed information on the surface topology and electronic density profile. Sensitivity in the range of ten picometers on the electronic density profile is demonstrated [2] challenging state of the art DFT calculation. The effective interaction energy can be tuned between few meV up to hundred meV useful to disentangle the contribution of the Van der Waals forces from that of the pure topology of the electron density making GIFAD a very flexible tool. Semi-classical interpretations are supported by quantum diffraction approach.

[1] Atkinson et al. Appl. Phys. Lett. 105, 021602 (2014)

[2] Debiossac et al. Phys. Rev. B 90, 155308 (2014)



Tu-D02

Pushing and moving along the steps: correlated motion measurements of strongly-repulsive Na atoms on a stepped (115) copper surface

Gil Alexandrowicz¹, Oded Godsi¹, Gefen Corem¹, Tatayan Kravchuk¹, Andrew Peter Jardine², Holly Hedgeland², William Allison², John Ellis², Cord Bertram³, Karina Morgenstern³

¹Technion - Israel Institute of Technology, Haifa, Israel, ²Cavendish Laboratory, Cambridge, UK, ³Ruhr-Universität Bochum, Bochum, Germany

Single atomic steps are a dominant surface defect which can modify the diffusion of adsorbed atoms and molecules. Studying motions on vicinal surfaces supplies a controlled environment to study the role steps play in various aspects of adsorbate structure and dynamics. In this talk we will present measurements of Na atoms diffusing on the 115 surface of copper. The system we chose to study offers a good opportunity to quantify the effect of the steps, as the motion of Na atoms on the flat copper surface has been extensively studied in the past, both when moving in isolation and at higher coverage where collective effects govern the motion [1,2]. Using the helium spin echo technique [3], we followed the collective atomic-scale motion of the Na atoms within a range of pico to nano-seconds. Using analytical considerations supported by molecular dynamics simulations we quantify the rate for the motion parallel and perpendicular to the atomic steps direction, provide estimates for the different diffusion barriers and also evaluate the inter-atomic interactions between the adsorbed Na atoms. The interpretation also allows us to rule out motion within the terraces in a direction perpendicular to the steps, which excludes the possibility of more than one equivalent adsorption site within the terrace width, i.e. the dynamics we measure serve as a method for assessing the adsorption geometry in a disordered and highly dynamic surface system.

[1] A. P. Graham et al. Phys. Rev. Lett. 78, 3900 (1997).

[2] G. Alexandrowicz et al. Phys. Rev. Lett., 97, 156103 (2006).

[3] A. P. Jardine et al. Phys. Chem. Chem. Phys., 11,3355 (2009).

Tu-D03

Atomic scale view of the surfactant action in the epitaxial growth of a metastable phase: oxygen assisted growth of Co on Fe(001)

Dario Giannotti¹, Andrea Picone¹, Michele Riva¹, Guido Fratesi², Alberto Brambilla¹, Lamberto Duò¹, Franco Ciccacci¹, Marco Finazzi¹

¹Dipartimento di Fisica, Politecnico di Milano, Milan, Italy, ²Dipartimento di Fisica, Università degli Studi di Milano, Milan, Italy

The desire to achieve a full control of thin-film growth on solid surfaces stimulates intense experimental and theoretical research, the goal of which is the development of nanomaterials with tailored physical properties [1]. In this framework, the use of small quantities of foreign atoms (termed surfactants), adsorbed on the substrate prior the film deposition, has been demonstrated to be a successful strategy in order to change the growth mode of the overlayer and its physical and chemical properties [2]. Here, the effects induced by an ordered oxygen overlayer on the growth of metastable body centered tetragonal (bct) Co films on the Fe(001) surface are investigated by means of Auger spectroscopy and atomically resolved Scanning Tunneling Microscopy images. The oxygen overlayer efficiently floats on top of the growing film, influencing both the film nucleation and the transition from the bct phase to the thermodynamically stable hexagonal close packed (hcp) structure. Co deposited on the oxygen-free surface grows in a layer-by-layer mode and is characterized by a dramatic decrease of the island saturation density for increasing film thickness [3]. On the other hand, when the growth is performed on the oxygen passivated surface, the maximum number of islands per unit area remains constant as the number of layers is increased. The bct/hcp phase transition of Co on pristine Fe(001) occurs at about 10 atomic layers and is accompanied by the development of a three-dimensional morphology (Stransky Krastanov growth), while on the oxygen passivated sample continuous surface distortions are observed. These surface undulations arrange in an highly ordered pattern, due to a dislocations network generated at the Co/Fe buried interface.

[1] M. Einax et. al., Rev. Mod. Phys. 85, 921 (2013).

[2] A. Picone et. al., Phys. Rev. Lett. 113, 046102 (2014).

[3] Camarero et. al., Phys. Rev. Lett. 81, 850 (1998).

Tu-D04

Growth of near-surface Co nanoclusters

Oleg Kurnosikov¹, Timothy Siahaan¹, Henk Swagten¹, Bert Koopmans¹

¹Eindhoven University of Technology, Eindhoven, Netherlands

A direct subsurface growth of Co nanoclusters by depositing Co atoms on the Cu(001) surface in a single stage at elevated temperature is reported. At the temperature range close to 650K Co is able to diffuse easily a few atomic layers below the Cu surface whereas a remarkable diffusion in the bulk is still not activated. Co accumulates near the surface and forms the subsurface clusters while Co on the surface or embedded in the surface is presented insignificantly. Although the formed nanoclusters are hidden below the copper surface they can still be detected using STM/STS by the analysis of the sub-atomic deformation of the Cu(001) surface as well as via local variations of surface electron density of copper above the clusters. It is possible to deduce the shape of subsurface Co nanoclusters: they are typically 5-10 nm in lateral size but only 2 to 3 ML in thickness. The kinetics of growth indicates a dead nucleation time. A simple model is implemented to describe the growth kinetics. The results in this study reveal that intense processes of diffusion, nucleation, and growth take place down to 1 nm below the surface, thus defining the near-surface region.

Tu-D05

Stabilizing Phthalocyanines on Ag(100)

Grażyna Antczak¹, Wojciech Kamiński¹, mgr Agata Sabik¹, Christopher Zaum²,
Karina Morgenstern³

¹Institute of Experimental Physics University of Wrocław, Wrocław, Poland,
²Leibniz University Hannover, Hannover, Germany, ³Ruhr-Universität Bochum,
Bochum, Germany

Phthalocyanine (Pc) molecules are model molecules that are, among others, investigated with respect to optoelectronics [1], sensors [2], and quantum computing [3]. That is why it is important to know the conditions under which those molecules form stable structures on surfaces. Using the scanning tunneling microscopy and density functional theory calculations we investigated a stabilizing role of Ag adatoms for phthalocyanines superstructures and explored the diffusion characteristic of Pc molecules on Ag(100). We show that Ag atom is able to link four or three CuPc molecules in a CuPc-Ag coordination network [4]. We also will report the activation energies and the prefactor for diffusivity of quasi-isolated CoPc molecules on Ag(100) and discuss the mechanism of its mobility, based on the potential energy surface of the CoPc-Ag(100) system.

- [1] M. Neghabi M. Zadsar, S. Mohammad, B. Ghorashi, Mater. Sci. Semicond. Process 17 (2014) 13.
- [2] A. M. Paoletti G. Pennesi, G. Rossi, A. Generosi, B. Paci, V. R. Albertini Sensors 9 (2009) 5277.
- [3] M. Warner, S. Din, I. S. Tupitsyn, G. W. Morley, A. M. Stoneham, J. A. Gardener, Z. Wu, A. J. Fisher, S. Heutz, Ch. W. M. Kay, G. Aeppli Nature 503 (2013) 504.
- [4] G. Antczak, W. Kamiński, K. Morgenstern J. Phys. Chem. C. 119 (2015) 1442

Tu-D06

Long-range ordered graphene on epitaxial Iridium (111) thin film deposited on (0001) Sapphire: a non-expensive support for the synthesis of nanocluster superlattice

Arti Dangwal Pandey¹, Dirk Franz^{1,2}, Roman Shayduk¹, Vedran Vonk¹, Patrick Mueller^{1,2}, Thomas F. Keller^{1,2}, Heshmat Noei¹, Andreas Stierle^{1,2}

¹Deutsches Elektronen-Synchrotron (DESY), Hamburg, Germany, ²Fachbereich Physik, Universität Hamburg, Hamburg, Germany

Graphene moirés on noble metal surfaces are very useful support to grow metal nanocluster superlattices, which form a model system to study heterogeneous catalysis, magnetism etc. [1] Large-area epitaxial graphene has been deposited successfully by chemical vapor deposition on 4d and 5d transition metal single crystals. These substrates are of high quality, but very expensive; which drives the search for alternatives to using cheaper substrates. Iridium has low carbon solubility and does not support multilayer formation of graphene, which makes it attractive as a substrate for large-area single-layer Graphene growth. It has been reported recently that epitaxial graphene can be synthesized on epitaxial Ir films, which was deposited by pulsed laser deposition [2]. Here we report on the deposition of epitaxial Ir (111) films on (0001) sapphire substrate by means of e-beam evaporation under ultrahigh vacuum, which is used to synthesize long-range ordered crystalline Graphene on top. Ethylene is used as a carbon source for depositing graphene by CVD. The crystallinity of the Ir film has been investigated using grazing incidence X-ray diffraction and low energy electron diffraction (LEED), while XPS measurements confirmed the high purity of Ir films. The influence of the growth parameters (flux, substrate temperature, film thickness) on the quality of the Ir films is studied systematically, and their effects on the properties of synthesized Graphene, as observed by means of x-ray diffraction, LEED and secondary electron microscopy, will be discussed in detail.

[1] Dirk Franz et al. Phys. Rev. Lett. 110, 065503 (2013).

[2] Chi Vo-Van et al. App. Phys. Lett. 98,181903 (2011).

Tu-D07

Faceting of Equilibrium and Metastable Nano- and Micro-structures: A Phase-Field Model of Surface Diffusion Tackling Realistic Shapes

Marco Salvalaglio¹, Roberto Bergamaschini¹, Rainer Backofen², Marco Albani¹, Fabrizio Rovaris¹, Francesco Montalenti¹, Axel Voigt², Leo Miglio¹

¹L-NESS and Dipartimento di Scienza dei Materiali, Università degli Studi di Milano-Bicocca, Milano, Italy, ²Institut für Wissenschaftliches Rechnen, Technische Universität Dresden, Dresden, Germany

Fine tuning of crystal morphology is nowadays an important step for a large variety of applications, such as the performance improvement in cutting-edge electronic devices. However, full control over the different, sometimes competing phenomena, is far from trivial and has yet to be reached. Numerical simulations are precious in limiting the parameter space to be sampled in actual experiments when searching for the desired system morphology, and also in the design of future, innovative structures. Here, we present a phase-field (PF) model of surface diffusion [1], able to describe the morphological evolution by means of a real kinetic pathway, driven by the minimization of the surface energy. A convenient and general description of surface-energy anisotropy, allowing us to simulate faceting also in the “strong anisotropy” regime, is introduced [2] and several illustrative applications to semiconductor structures are described. Complex phenomena, involving even topological changes, can be readily tackled in the PF framework, and their occurrence in the processing of technology-relevant microstructures [3] is also shown as an example, demonstrating the predicting power of our approach.

Finally, we discuss preliminary but encouraging results, revealing the possibility to extend our model including further key phenomena such as misfit-strain relaxation, anisotropic fluxes, and orientation-dependent growth velocity.

[1] B. Li, J. Lowengrub, A. Rätz and A. Voigt. Commun. Comput. Phys. 6, 433 (2009).

[2] M. Salvalaglio, R. Backofen, R. Bergamaschini, F. Montalenti and A. Voigt, Accepted, Cryst. Growth Des. (2015). DOI:10.1021/acs.cgd.5b00165

[3] C. V. Falub, H. von Känel, F. Isa, R. Bergamaschini, A. Marzegalli, D. Chrastina, G. Isella, E. Müller, P. Niedermann and L. Miglio. Science 335, 1330 (2012).



Tu-E03+04

Supported metallic and bimetallic nanocatalysts

Francesca Baletto¹¹Physics Department, King's College London, London, United Kingdom

Metal clusters are small nanoscale objects consisting of a countable number of atoms of metal elements, with novel properties distinct from both the molecular and bulk regimes that could be exploited in a wide range of technological applications from catalysis to biomedicine [1]. The range of possibilities increases enormously if bimetallic cases are considered [2]. Here, we propose a numerical study where a density function (DF) and empirical potential (EP) are combined in order to address how shape, size are affected by external factors, such as temperature and the presence of a support. In the latter case, both zeolite and oxide interfaces have been considered. From a methodological point of view, we used a new metadynamics approach developed for metallic and bimetallic nanoparticles [3].

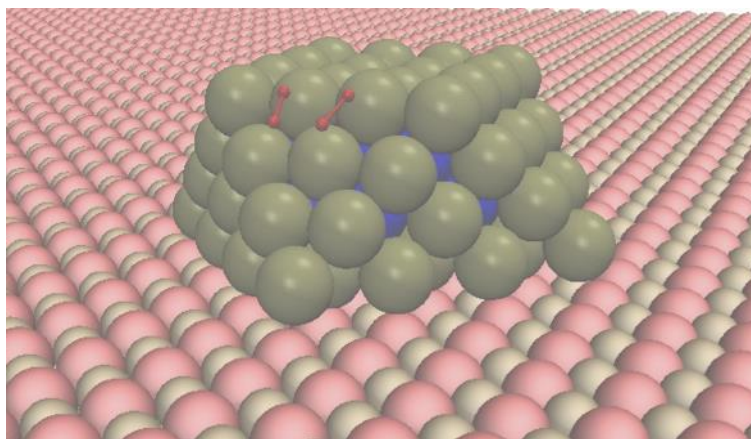
Finally, catalytic properties of nano-systems have been then discussed at DF level. As a paradigmatic example, we discuss the catalytic properties of Pt-based nanoalloys in the gas-phase or supported upon MgO [4].

[1] F. Baletto and R. Ferrando, Rev. Mod. Phys. 2005

[2] R. Ferrando, J. Jellinek and R.L. Johnston, Chem Rev 2008

[3] L.Pavan, C. DiPaola and F. Baletto, EPJD 2013; L. Pavan, K. Rossi and F. Baletto in preparation

[4] C. DiPaola and F. Baletto, PCCP 2011; O. Paz-Borbon, GG. Asara and F. Baletto in preparation.



Tu-E05

Modeling Elementary Heterogeneous Atmospheric (Photo)chemical Processes on Ice and their Dynamics using Amorphous Solid Water

Patrick Ayotte¹, Jonathan Vermette¹, Pierre-Alexandre Turgeon¹, Sarah Delage¹, François Masse¹

¹Université de Sherbrooke, Sherbrooke, Canada

A thermodynamically reversible path was suggested to exist linking the low density forms of amorphous ice (LDA) and deeply supercooled liquid water (LDL), through the so-called no man's land and finally onto normal liquid water. Furthermore, at temperatures below its calorimetric glass transition temperature ($T_g \sim 136\text{K}$), transport kinetics are exceedingly slow in amorphous solid water (ASW). Therefore, it might provide a convenient model system to study elementary heterogeneous atmospheric chemistry processes that occur on the quasi-liquid layer (QLL) that forms at the air-ice interface in the atmosphere at $T > 180\text{K}$. We will discuss how studying interfacial dynamics at cryogenic temperatures enables the decoupling of processes occurring onto the surface of ASW from those that take place within the bulk by strongly inhibiting the diffusive uptake kinetics. Using this strategy, we will show that ionic dissociation of simple acids (i.e., HF, [2] HCl, [3] HNO_3 [4]) remain facile down to temperatures as low as 20K at the surface of ASW. We will also demonstrate that heterogeneous nitrates photolysis can be enhanced up to 3-fold at the ASW surface hinting at a significant contribution from heterogeneous (photo)chemistry to the photochemical NO_x fluxes that emanate from the sunlit snowpack to polar boundary layer.[5]

[1] O. Mishima and H.E. Stanley, *Nature* 396, 329–335 (1998).

[2] P. Ayotte, M. Hébert, and P. Marchand, *JCP* 123, 184501 (2005); R. Iftimie, et al, *JACS* 130, 5901 (2008); P. Ayotte, S. Plessis and P. Marchand, *PCCP* 10, 4785 (2008); P. Ayotte, Z. Rafiei, F. Porzio, and P. Marchand, *JCP* 131, 124517 (2009); G. Marcotte and P. Ayotte, *JCP* 134, 114522 (2011).

[3] P. Ayotte, et al, *JPCA* 115, 6002 (2011).

[4] P. Marchand, G. Marcotte, and P. Ayotte, *JPCA* 116, 12112 (2012); G. Marcotte, et al., *JPCL* 4, 2643 (2013).

[5] G. Marcotte, et al, *JPCA* 119, 1996 (2015).

Tu-E06

Fundamentally understanding Fischer-Tropsch synthesis on cobalt: how experimental surface science can help

CJ Weststrate^{1,2}, JW (Hans) Niemantsverdriet^{1,2}¹Syngaschem BV, Eindhoven, Netherlands, ²Laboratory for Physical Chemistry of Surfaces, Eindhoven, Netherlands

The molecular details of the Fischer-Tropsch synthesis reaction, in which synthesis gas is converted into a mixture of long-chain hydrocarbons on catalysts such as Fe, Co and Ru have intrigued researchers in the field of heterogeneous catalysis for decades. The advent of computational modeling and its application in understanding of the Fischer-Tropsch mechanisms has given a new dimension to the level of understanding that can be reached.

Experimental surface science has been around for several decades. In the 1990's several papers appeared in which single crystals were employed to get insight into Co FTS catalysts. Other than that, there are relatively few surface science studies in which cobalt single crystal surfaces were studied in the context of FTS. In my contribution I will show how 'classical' surface science using advanced tools such as synchrotron XPS, STM and in-situ work function measurements in addition to thermal desorption experiments and low energy electron diffraction can provide new insights into the FTS chain growth mechanism on cobalt catalysts, catalyst deactivation by carbon and elementary reaction steps such as C-O bond scission and oxygen reduction.

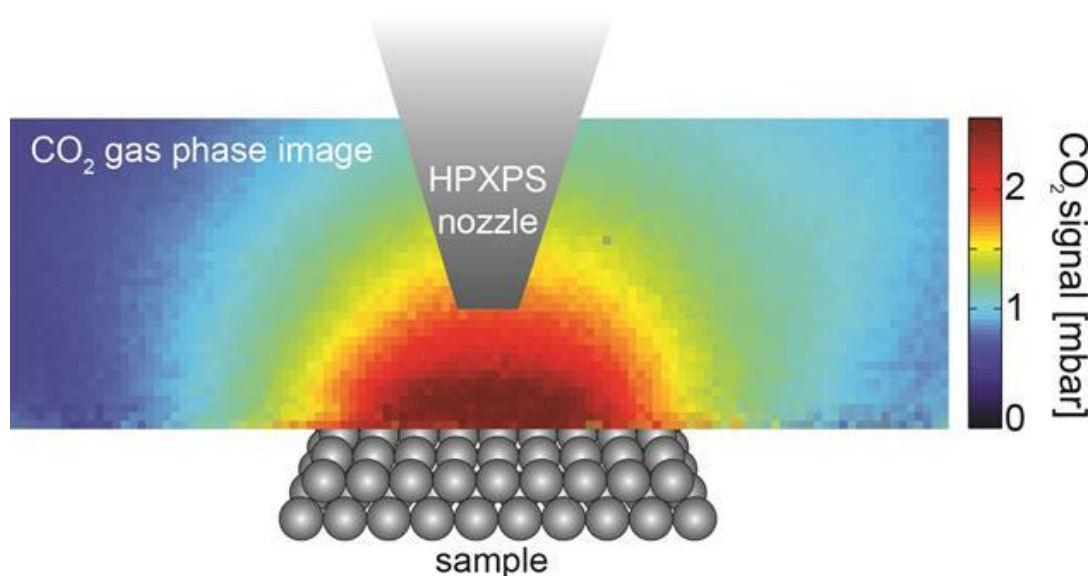
Tu-E07

Combined HP-XPS measurements and gas phase imaging during CO oxidation over Pd single crystals

Sara Blomberg¹, Johan Zetterberg¹, Johan Gustafson¹, Jianfeng Zhou¹,
Christian Brackmann¹, Edvin Lundgren¹

¹Lund University, Lund, Sweden

The CO oxidation over model catalysts has been studied intensively for many decades and has resulted in great knowledge of the active phase of the catalyst under ultra-high vacuum (UHV) conditions. Less is known about the reaction mechanism under more realistic operating conditions for the catalyst and many surface studies have therefore recently been focused on experiments carried out at higher pressures, in order to bridge the pressure gap. High pressure X-ray photoelectron spectroscopy (HPXPS) is has been developed to operate at higher pressures (<1 mbar) and is often used to investigate the surface structure of a catalyst. The possibility to follow the surface reconstruction in situ during the reaction has shown that transition metals reach the highly active phase for CO oxidation immediately after the ignition, simultaneously as a reconstruction of the surface is observed. Great attention has been directed to the surface structure of this highly active phase of the catalyst but not so much to the gas phase. HPXPS provides information about the gas phase but in order to interpret the spectra, a more complete picture of the gas phase has been needed. We have therefore imaged the gas phase close to the sample surface during CO oxidation using Planar laser-induced fluorescence, which shows that a boundary layer of gases builds up around the surface when the catalyst reaches the highly active phase. Within this boundary layer the gas composition is completely different as compared to the rest of the chamber, which also affect the surface structure of the catalyst. By comparing the information gained from the two techniques an extended knowledge about the gas molecules interacting with the surface in the highly active regime during CO oxidation is achieved, which has resulted in an improvement of the interpretation of the gas phase spectra achieved by HPXPS.



Tu-E08

Nano-effects in MoS₂ nanoparticles: dynamic phenomena and stabilization of metastable phases through interaction with a metallic support

Albert Bruix¹, Jeppe V. Lauritsen¹, Bjørk Hammer¹, Henrik G. Füchtbauer¹

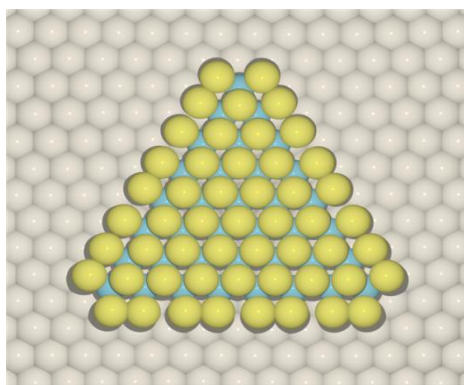
¹Aarhus University iNANO and Department of Physics and Astronomy, Aarhus, Denmark

Nanomaterials based on MoS₂ are very versatile; MoS₂ nanoparticles are proven catalysts for processes such as hydrodesulphurization and the hydrogen evolution reaction, and transition metal dichalcogenides in general have recently emerged as novel 2D components for nanoscale electronics and optoelectronics. The properties of such materials are intimately related to their structure and dimensionality. For example, only the edges exposed by MoS₂ nanoparticles are catalytically active [1] and extended MoS₂ systems show different character (direct or indirect gap semiconducting, or metallic) depending on their thickness and crystallographic phase.[2] In addition, the interaction with a support can also have a significant effect on both structure and properties of nanostructured MoS₂. Understanding such effects is thus crucial for rationally designing materials based on MoS₂. By means DFT-based calculations, we have optimized the structure of computational models of MoS₂ nanoparticles supported on the Au(111) surface. We address how particle size, composition, structure, and the interaction with the support affect the stability of MoS₂ nanostructures. Our analysis shows that the interaction with Au drastically changes the relative stability of the different nanoparticle types. In particular, nanoparticle terminations and crystallographic phases that are metastable when unsupported become greatly stabilized upon interaction with the Au surface. These results also explain remarkable dynamic phenomena observed via Scanning Tunnelling Microscopy of model systems in UHV conditions, where complex nano-effects give rise to reversible phase transitions.[3]

[1] Jaramillo TF, Jørgensen KP, Bonde J, Nielsen JH, Horch S, Chorkendorff I., *Science*, 317: 100-102, 2007.

[2] Zhao, W., Ribeiro, R. M., & Eda, G., *Accounts of Chemical Research*, 48(1), 91–9, 2015.

[3] “Nanoeffects in supported MoS₂ nanoparticles: dynamic phenomena and stabilization of metastable phases.” Albert Bruix, Signe Sørensen, Henrik G. Füchtbauer, Jeppe Vang Lauritsen, Bjørk Hammer, in preparation.



Tu-A09

Hybrid {magnetic/free-standing Graphene} structures: fabrication and advanced x-ray characterization by XMCD and XMCD-PEEM

Manuel Valvidares¹, Pierluigi Gargiani¹, Carlos Quirós², Cristina Blanco², Maria Vélez², Anthony Young³, Andreas Scholl³

¹Experiments Division, ALBA Synchrotron Light Facility, Cerdanyola del Valles, Spain, ²Departamento de Física, Universidad de Oviedo, Oviedo, Spain,

³Advanced Light Source, Lawrence Berkeley National Laboratory, Berkeley, United States

We will present recent results on the fabrication and characterization of some Magnetic/Graphene hybrid structures which seem not to have been realized or studied in detail to date. Whereas an increasing number of detailed studies is devoted to the study of magnetic materials deposited on top of Graphene, most studies focused on systems that can be obtained by evaporation of magnetic materials on top of CVD grown Graphene on high quality single crystal surfaces. The CVD approach together with related intercalation procedures, allows a significant range of materials to be done and substrates to be used, but still sets some limits to the type of systems that can be fabricated and therefore investigated. In contrast, a much smaller number of studies report on the properties of magnetic materials fabricated on free-standing Graphene, an otherwise very important substrate platform in term of its light weight, and its flexible and optically transparent nature. We will describe a simple and effective approach for the realization and characterization of some magnetic heterostructures and nanostructures of interest which avoids technical difficulties at the fabrication and characterization stages. Detailed results on the investigation of some of the structures fundamental properties and aspects using a combination of x-ray absorption spectroscopy and micro-spectroscopy, will be discussed.

Tu-A10

Exchange coupled metal films mediated by a single layer graphene sheet

Pierluigi Gargiani¹, Hari Babu Vasili¹, Manuel Valvidares¹

¹ALBA Synchrotron Light Facility, Cerdanyola del Valles, Spain

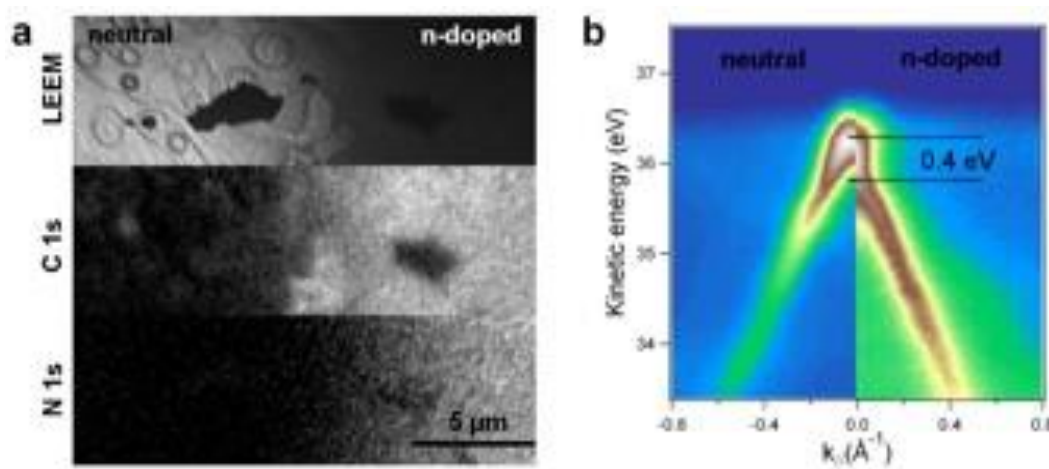
Graphene, due to its peculiar electronic and transport properties is considered one of the most promising elements in the development of novel electronic devices. Being formed by a light element such as carbon, graphene is appealing as a material for spintronic application showing large spin diffusion length in spin-transport devices when coupled to suitable magnetic electrodes. We present a soft X-Ray Absorption (XAS) and X-Ray Magnetic Circular Dichroism (XMCD) study of the exchange coupling between magnetic metallic layers with strong out-of-plane anisotropy mediated by a graphene single layer grown in-situ by CVD. The inter-layer coupling has been investigated in a range of different temperatures and growth conditions revealing surprising robustness and tunability. Moreover the magnetic field dependence of the interlayer coupling reveal a rather unexpected strong character when compared to similar multilayered systems. The nature of the coupling may have strong interest in the development of novel nanostructured spin devices.

Tu-A11

n-doped micropatterns in graphene by low energy nitrogen-ion irradiation

Alessandro Sala¹, Giovanni Zamborlini¹, Tevfik Onur Menteş¹, Andrea Locatelli¹¹Elettra Sincrotrone Trieste, Trieste, Italy

The reduced dimensionality of graphene determines unique electronic and transport properties, promising new architectures for a plethora of devices. However, the exploitation of graphene in the next generation electronics depends crucially on the capability of preserving and tailoring such properties. Chemical doping via substitutional implantation of exo-species into the C lattice mesh, B or N in particular, is an appealing method most frequently obtained during growth, for example by carrying out chemical vapor deposition (CVD). As an alternative approach to these methods, ion irradiation is recently emerging as a powerful means to functionalize both carbon nanotubes and graphene. Due to its intrinsic lithographic capabilities, the development of such technique is most desirable, since most devices require the fabrication of a heterojunction between a semiconducting active material and a metallic electrode. In this presentation, we report a proof of principle experiment demonstrating that low-energy (100 eV) ion irradiation can be used to achieve local control on the doping in graphene. In particular, we tackle the fabrication of a sharp junction between n-doped and free-standing single-layer graphene on Ir(111), grown via CVD of ethylene at elevated sample temperature, exhibiting metallic or semimetal-like density of states, characterizing the transition region between the two areas. LEEM and XPEEM images of the C 1s and N 1s core level emission (Fig. 1a) show the junction quality achievable with such method. μ -ARPES measurements of the doped and non-doped area (Fig. 1b) confirm the local shift of the Dirac cone by 0.4 eV. The full characterization of the micropatterned n-doped graphene, as well as the possibility to miniaturize the process towards nanometer scale and preserve the system in normal atmospheric conditions, will be discussed.



Tu-A12

Destructive interference towards chemical discrimination of N and B dopants in the B,N co-doped graphene/SiC(0001)

Mykola Telychko¹, Pablo Merino², Pingo Mutombo¹, Francois Bocquet^{3,4}, Jessica Sforzini^{3,4}, Martin Ondráček¹, Prokop Hapala¹, Pavel Jelínek¹, Martin Švec¹

¹Institute of Physics ASCR, Prague, Czech Republic, ²Max Planck Institute for Solid State Research, Stuttgart, Germany, ³Jülich-Aachen Research Alliance (JARA); Fundamentals of Future Information Technology, Jülich, Germany, ⁴Peter Grünberg Institut (PGI-3), Forschungszentrum Jülich, Jülich, Germany

We will present tunable method for substitutional co-doping of epitaxial graphene grown on the SiC(0001) substrate by single boron and nitrogen atoms. Nitrogen doping was achieved using direct nitrogen ion implantation into the graphene lattice and subsequent thermal stabilization [1]. Whereas boron doping was produced by introducing an additional source of boron atoms during growth process of the graphene/SiC(0001). We carried out simultaneous STM/AFM, XPS, NEXAFS and DFT studies to analyze the structural and electronic properties of the B, N co-doped graphene.

Atomically-resolved low-temperature STM measurements of single substitutional nitrogen and boron dopants reveal that the nitrogen dopants in graphene lattice feature a strong quantum interference effect, tunable by changing the tip-sample separation. The current dependence on the tip position is successfully modelled by STM simulations for the both types of dopants. Absence of the destructive interference over the boron dopants allows clear chemical discrimination between the N and B atoms. Moreover, AFM measurements point out different reactivity over of N and B sites with respect to bare graphene.

[1] M. Telychko, et al, ACS Nano, 8(7):7318–7324, 2014.

Tu-A13

In situ dynamic transmission electron microscopy observation of graphene formation process in nanoscale

Masaki Tanemura¹, Mohamad Saufi Rosmi¹, Mohd Zamri Bin Mohd Yusop², Yazid Bin Yaakob³, Golap Kalita¹, Chisato Takahashi⁴

¹Nagoya Institute of Technology, Nagoya, Japan, ²Universiti Teknologi Malaysia, UTM Skudai, Malaysia, ³Universiti Putra Malaysia, Selangor Darul Ehsan, Malaysia, ⁴Aichi Gakuin University, Kusumoto-cho, Chikusa-ku, Nagoya, Japan

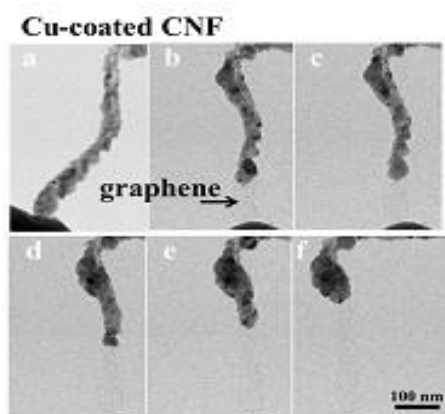
To realize the variety of applications of graphene, larger scale synthesis of high quality graphene of larger domain size, and also the growth area (position) control of graphene nano-ribbons should be achieved. To control their growth, their growth process should be well understood in atomic scale. In this talk, in situ dynamic transmission electron microscopy (TEM) observation of the graphene synthesis by solid phase reaction will be dealt with.

For this purpose, metal-included and pristine (metal free) amorphous carbon nanofibers (CNFs) were fabricated on an edge of a graphite foil by Ar ion irradiation with and without a supply of metals at room temperature, respectively. Cu-coated pristine CNFs were also prepared. The current-voltage characteristics of the CNF samples thus prepared were measured in direct current (DC) and field emission (FE) modes in TEM equipped with a piezo-controlled nanoprobe electrode. For metal-included CNFs, metal nanoparticles were dispersed in amorphous CNF matrix, and depending on the included metal element in the CNFs, different types of nanocarbons, such as ring-shaped graphene and carbon nanotubes, were formed during the electron current flow [1, 2]. For Ag-included CNFs, for instance, during FE amorphous carbon around the Ag nanoparticles were transformed to graphene-like structure and the Ag nanoparticles evaporated gradually from the apex to base of the CNF owing to Joule heating induced by FE current, leaving ring-shaped graphene in the CNF [2]. By contrast, graphene sheet formed during the DC current flow for Cu-coated pristine CNFs (fig. 1) [3]. It is believed that the graphene formation by solid phase reaction is essential also for the growth area (position) control of graphene nano-ribbon.

[1] M. Zamri Yusop, et al., ACS Nano 6 (2012) 9567.

[2] Y. Yaakob, et al., RSC Advances, 5 (2015) 5647.

[3] M. Rosmi, et al., Scientific Reports, 4 (2014) 7563.



Tu-B09+10

Ionic conductivity in oxide thin films: the role of interface defects

Carmela Aruta¹, Nan Yang^{1,2}, Vittorio Foglietti¹, Antonello Tebano^{1,3}, Giuseppe Balestrino^{1,3}, Claudia Cantoni⁴, Alex Belianinov⁴, Evgheni Strelcov⁴, Stephen Jesse⁴, Sergei Kalinin⁴, Christoph Schlueter⁵, Tien-Lin Lee⁵, Angelo Bongiorno⁶

¹National Research Council, CNR-SPIN, Rome, Italy, ²University Niccolò Cusano, Rome, Italy, ³University of Tor Vergata, Rome, Italy, ⁴Oak Ridge National Laboratory, USA, ⁵Diamond Light Source, Didcot, United Kingdom, ⁶Georgia Institute of Technology, Atlanta, USA

Functional properties caused by mobile ions are of great importance for next-generation electrochemical energy storage/conversion systems, such as solid oxide fuel cells (SOFCs). To improve performance and broaden the applications of this important technology, new materials and solutions are needed to abate costs, enhance durability and efficiency, and to reduce the temperatures at which SOFCs operate. Current SOFC technology is based on oxygen-ion conducting electrolytes. However, the activation energies for proton mobility is significantly lower than that of oxygen-ion conducting electrolytes, making proton-ion conductors, such as barium-based perovskite oxides, a valid alternative as electrolyte materials in SOFCs. Reducing the dimensions of the electrolyte material to the nanoscale is an increasingly common strategy to improve ion conductivity. Space-charge effects, epitaxial strain, and atomic reconstruction at the interface between two different materials were proposed to account for the observed conductivity enhancement. In this presentation, I will mainly concentrate on the results obtained on yttrium doped barium zirconate (BZY) thin films which have recently shown high values of conductivity, increasing as the sample thickness decreases.[1] This demonstrates that the relevant physical phenomena are occurring predominantly at the interface between film and substrate. Such interfaces were investigated with local techniques: namely, cross-sectional electrochemical strain microscopy, to directly visualize the interface reactivity, and scanning transmission electron microscopy to obtain information on the structural and chemical defects at the interface.[2] These studies were complemented by bulk sensitive hard x-ray photoemission spectroscopy measurements which, together with Density Functional Theory calculations, show that Y and, to some extent, also Zr ions, substitute for Ba near the interface with the substrate. This suggests that interface defects could be at the origin of the enhanced ionic conductivity observed experimentally.

[1] V. Foglietti et al. Appl. Phys. Lett. 104, 081612 (2014)

[2] N. Yang et al. Nano Lett. 15, 2343 (2015)

Tu-B11

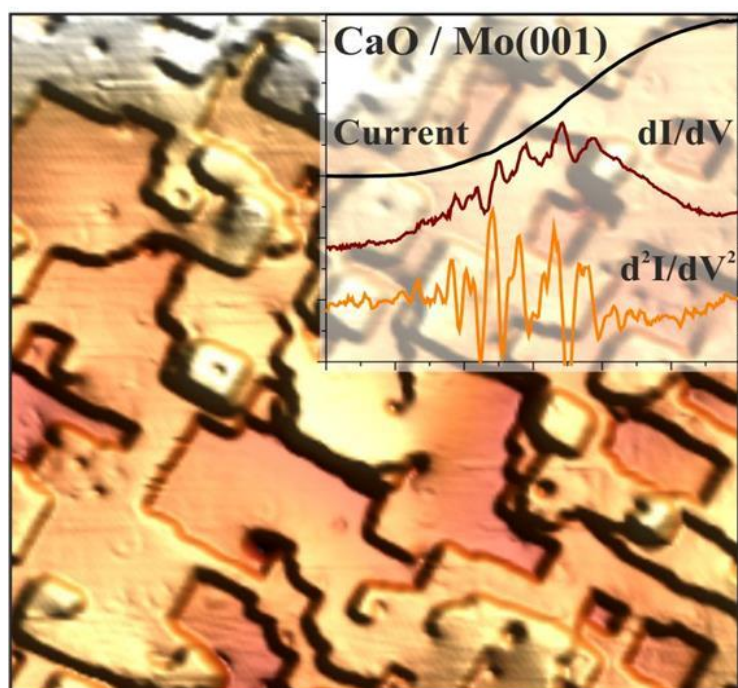
Phonon-Mediated Electron Transport through CaO Thin Films

Niklas Nilius¹, Yi Cui², Hans-Joachim Freund²

¹Carl von Ossietzky University, Oldenburg, Germany, ²Fritz-Haber-Institute, Berlin, Germany

Scanning tunneling microscopy (STM) has developed into a powerful tool for the characterization of conductive surfaces, for which the overlap of tip and sample wave functions determines the image contrast. On insulating layers, direct overlap between initial and final states is not possible anymore and electrons are transported via hopping through the conduction-band states of the dielectric material. In this case, charge transport is accompanied by strong phonon excitations that can be probed with STM conductance spectroscopy at the local scale.

In my presentation, electron transport through wide-gap CaO films of 40-60 ML thickness grown on Mo(001) is discussed. STM spectra taken across the oxide band onsets reveal a characteristic oscillatory behavior in the conductance that can be associated with an inelastic transport mode excited upon electron injection. The mode energy of roughly 80 meV is compatible with phonon excitations in the CaO lattice, altered by polaronic contributions. On top of surface defects, e.g. oxide dislocation lines, a slight reduction of the characteristic energy is observed, indicative for a local softening of the vibrational excitations. Our study provides insight into the kind of STM experiments that can be performed on samples, for which electron motion is governed by hopping transport.



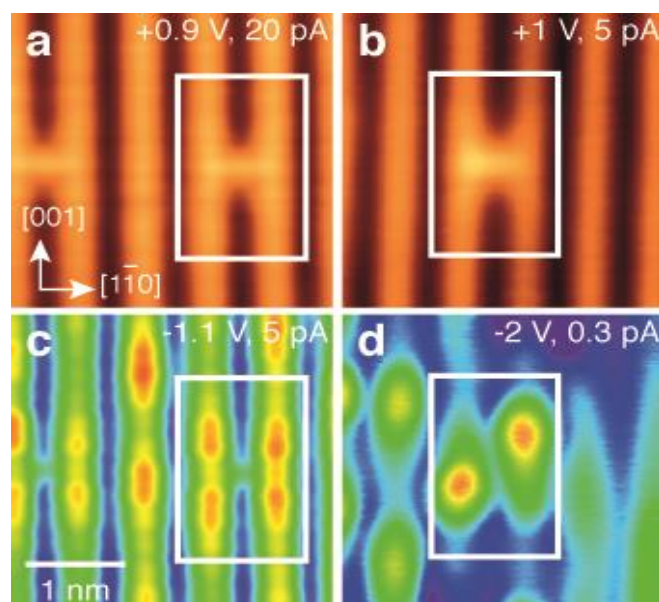
Tu-B12

Engineering polarons at a metal oxide surface

Chi Ming Yim¹, Matthew B Watkins², Chi Lun Pang¹, Matthew J Wolf³, Kersti Hermansson³, Geoff Thornton¹

¹Department of Chemistry and London Centre for Nanotechnology, University College London, London, United Kingdom ²Department of Physics and Astronomy and London Centre for Nanotechnology, University College London, London, United Kingdom ³Department of Chemistry, Ångström, Uppsala University, Uppsala, Sweden

Polarons in metal oxides are important in processes such as catalysis, high temperature superconductivity, and dielectric breakdown in nanoscale electronics. Here, we study the behaviour of oxygen vacancy-induced electron polarons in rutile $\text{TiO}_2(110)$ with a combination of scanning tunnelling microscopy and theoretical calculations. The electrons are symmetrically distributed around the vacancy at 78 K but as the temperature is reduced, this distribution becomes increasingly asymmetric. Thus we directly visualize the temperature dependence of polaron hopping. A series of multimer vacancy complexes were created by manipulating the lateral positions of individual vacancies; their associated excess electrons are also polaronic. Thus, we demonstrate that the configurations of polarons can be engineered, paving the way for the construction of conductive pathways germane to resistive switching devices.



Tu-B13

Surface Phonons and Ferroelectric Coupling in ultrathin Perovskite Oxides

Wolf Widdra^{1,2}, Florian Schumann¹, Maik Christl¹, Klaus Meinel¹, Stefan Förster¹, Andreas Trützschler¹

¹Uni Halle-Wittenberg, Halle, Germany, ²Max-Planck-Institute für Mikrostrukturphysik, Halle, Germany

Phonons and their softening are key elements for the understanding of the long-range coupling in ferroelectric and multiferroic materials, which causes, e.g., the paraelectric to ferroelectric phase transition. In thin films, these ferroelectric properties are often controlled by strain from the underlying substrate or heterostructures. Here we study ferroelectric properties and surface phonons of BaTiO₃(001) ultrathin films grown pseudomorphically on Pt(001) and Au(001), which corresponds to 2% lateral compression and 2% expansion in the BaTiO₃(001) film, respectively. By high-resolution electron energy loss spectroscopy (HREELS), all thin film spectra are characterized by three well-developed energy loss peaks. These excitations are identified as surface phonon polaritons by comparison with theory. They show a thickness dependent red shift in the thin films due to a coupling to the metallic substrate. Using piezo-response atomic force microscopy (PFM) in combination with scanning tunneling microscopy and spectroscopy (STM, STS), we are able to resolve the ferroelectric coupling in films as thin as 0.8 nm. Intrinsic ferroelectric nanodomains are formed in these films, which can be remanently polarized by PFM as well as STM.

Tu-B14

Inducing electric polarization in ultrathin insulating layers.

José Martínez-Castro^{1,2,3}, Marten Piantek³, Mats Persson⁴, David Serrate³,
Cyrus Hirjibehedin^{1,2,5}

¹London Centre For Nanotechnology, University College London (UCL), London, UK, ²Department of Physics and Astronomy, UCL, London, UK,

³Instituto de Nanociencia de Aragón and Laboratorio de Microscopías Avanzadas, Universidad de Zaragoza, Zaragoza, Spain, ⁴SSRC, University of Liverpool, Liverpool, UK, ⁵Department of Chemistry, UCL, London, UK

Studies of ultrathin polar oxide films have attracted the interest of researchers for a long time due to their different properties compared to bulk materials. However they present several challenges such as the difficulty in the stabilization of the polar surfaces and the limited success in tailoring their properties. Moreover, recently developed Van der Waals materials have shown that the stacking of 2D-layers trigger new collective states thanks to the interaction between layers. Similarly, interface phenomena emerge in polar oxides, like induced ferroelectricity or high temperature superconductivity. This represents a promising way for the creation of new materials with customized properties that differ from those of the isolated layers. Here we present a new approach for the fabrication and study of atomically thin insulating films. We show that the properties of insulating polar layers of sodium chloride (NaCl) can be engineered when they are placed on top of a charge modulated template of copper nitride (Cu₂N). STM studies carried out in ultra-high vacuum and at low temperatures over NaCl/Cu₂N/Cu(001) show that we are able to build up and stabilize interfaces of polar surface at the limit of one atomic layer. In combination with density functional theory calculations, we observe that the lattice constant of the NaCl film is compressed by 8% compared to the free-standing structure due to the electrostatic interaction with the underlying polar Cu₂N layer. Out-of-plane buckling of the NaCl induces an out of plane dipole moment that enhances the one that exists in the underlying Cu₂N layer. In addition, we examine the electronic structure of the overlayers to explore new electronic states to the fore at the new formed interaction of the ultrathin insulators. This new approach opens the door to engineered polar surfaces on rock-salt structures as well as on polar oxides.

Tu-C09

Role of orbital structure in high-resolution STM images of molecules on surface

Ondrej Krejci^{1,2}, Prokop Hapala¹, Martin Ondracek¹, Pavel Jelinek¹¹Institute of Physics of the Czech Academy of Sciences, Prague, Czech Republic, ²Charles University in Prague, Faculty of Mathematics and Physics, Prague, Czech Republic

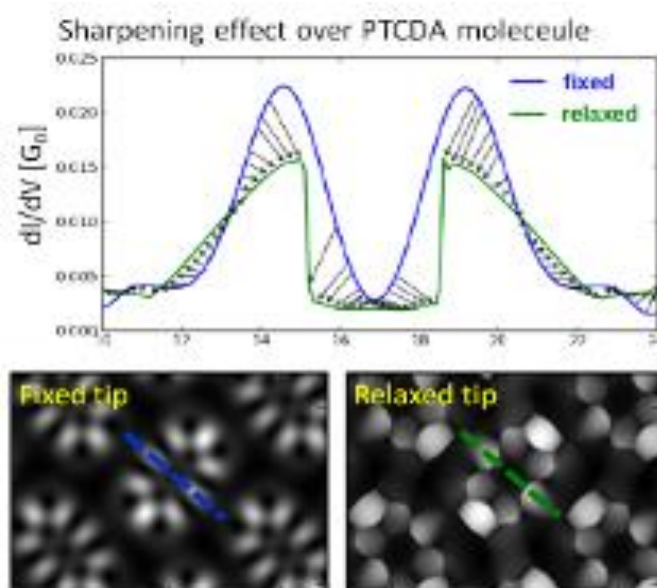
High-resolution STM [1] and AFM [2] images of molecules with sub-molecular contrast open new horizons in surface science. While the mechanism for AFM imaging fairly is well understood [3,4], the correct interpretation of STM images is still challenge. Recently, we demonstrated that most features visible in high-resolution AFM images of molecules can be explained by simple mechanical model [4] considering relaxation of a probe particle attached to the tip. On top of this, we introduced a simple model for calculating STM current considering only inter-atomic hoppings between tip, relaxed probe particle and molecule [4]. The simple model is able to reproduce the main characteristics of high-resolution STM maps in close distance regime where the probe particle relaxation effects prevail. But since it completely neglects an electronic structure of the scanned sample, it fails at far distances where the electronic structure is dominating in the STM current. In this work, we present a new efficient method for simulation of the high-resolution STM images considering the molecular electronic structure and the probe particle relaxation as well. The method is able to reproduce observed contrast in both the close distance and the far distance regimes, including the gradual transition between them. It gives solid theoretical background for better understanding of high-resolution STM experiments.

[1] R. Temirov et al, New. J. Phys. 10, 053012 (2008).

[2] L. Gross et al, Science 325, 1110 (2009).

[3] N. Moll et al, New. J. Phys. 12, 125020 (2010).

[4] P. Hapala et al., Phys. Rev. B 90, 085421 (2014).



Tu-C10

Direct Observation of Photoinduced Intramolecular Hydrogen Transfer within a Single Porphycene Molecule on a Cu(111) Surface

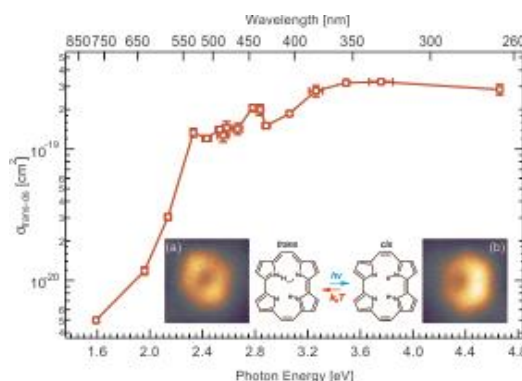
Hannes Boeckmann¹, Sylwester Gawinkowski², Jacek Waluk², Leonhard Grill^{1,3}, Martin Wolf¹, Takashi Kumagai¹

¹Department of Physical Chemistry, Fritz-Haber Institute of the Max-Planck Society, Berlin, Germany, ²Institute of Physical Chemistry, Polish Academy of Sciences, Warsaw, Poland, ³Department of Physical Chemistry, University of Graz, Graz, Austria

Photoinduced hydrogen transfer is of vital importance in several chemical reactions and elementary steps of biological processes [1]. In order to examine the underlying mechanism, the intramolecular hydrogen transfer reaction (tautomerization) can serve as a fundamental model system and can furthermore be employed in switching devices for nanoscale molecular electronics. Hence, the tautomerization of individual molecules received considerable attention and was previously observed in a porphycene molecule by our group in low-temperature STM studies [2]. Here we report the direct observation of photoinduced tautomerization within a single porphycene molecule on a Cu(111) surface using a combination of low-temperature STM and laser excitation, ranging from the UV to the NIR spectral region. Porphycene molecules adsorb on the surface as monomers (without aggregating to clusters at low coverage), and the trans tautomer is observed as the thermodynamically stable state (Fig. 1a). However, laser irradiation can convert the trans tautomer to the metastable cis state unidirectionally (Fig. 1b), while heating the substrate transitions the molecule back to the trans tautomer. We quantified the tautomerization cross-section $\sigma(\text{trans-cis})$ in this process to be $\sim 1\text{E-}19\text{ cm}^2$ for visible and UV wavelengths, which makes porphycene a highly efficient photoswitch even on a metallic substrate. Furthermore, the spectral dependence reveals a strong increase of the cross-section from IR to visible frequencies (Fig. 1). We will discuss the mechanism underlying the observed spectral features with regard to a surface mediated excitation of the molecule. Our approach provides a novel insight into photoinduced adsorbate reactions at the single molecule level.

[1] J. T. Hynes et al., Hydrogen-Transfer Reactions (Wiley-VCH, Weinheim, 2007).

[2] T. Kumagai et al. PRL 111, 246101 (2013); T. Kumagai et al. Nature Chem. 6. 41 (2014).



Tu-C11

Submolecular resolution in 3D

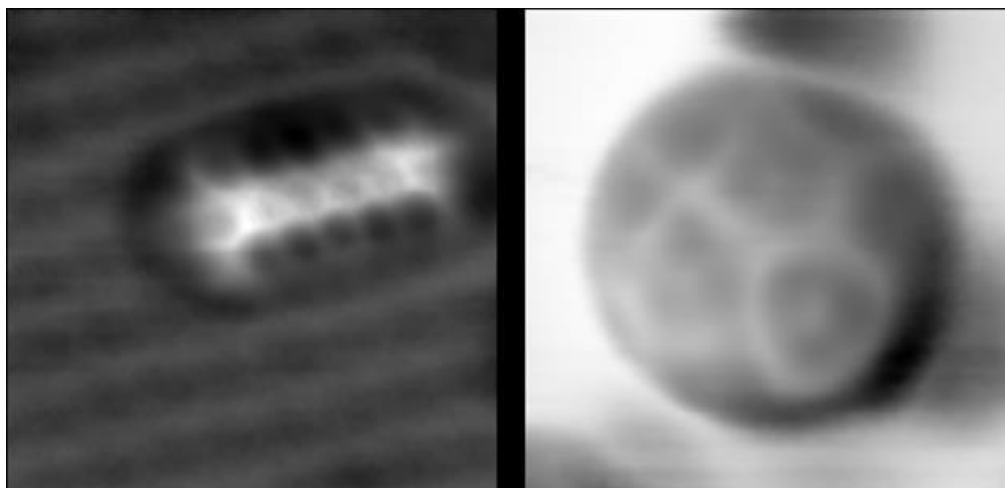
Cesar Moreno¹, Oleksan Stetsovych², Tomoko K. Shimizu³, Oscar Custance³

¹Catalan Institute of Nanoscience and Nanotechnology (ICN2), Bellaterra, Spain, ²Institute of Physics, Academy of Sciences of the Czech Republic, Cukrovarnicka 10, Prague, Czech Republic, ³National Institute for Materials Science (NIMS), Tsukuba, Japan

Submolecular resolution accomplished by atomic force microscopy (AFM) has recently attracted considerable attention [1,2] because its potential to unveil the chemical structure of unknown molecules [3], characterise charge distributions [4] and bond ordering [5] within molecules, as well as to study chemical transformations [6,7] and intermolecular interactions [8,9]. So far, most of these achievements make use of planar molecules because high-resolution imaging of three-dimensional (3D) surface structures with AFM remains challenging.

Here we present a general method for submolecular imaging of non-planar molecules and the study of 3D surface systems with atomic resolution using a cantilever-based AFM [10]. We demonstrate this method by characterising the step-edges of a TiO₂(101) anatase surface at atomic scale[11], by simultaneously visualising the chemical structure of a pentacene molecule together with the atomic positions of the substrate [Fig.1 left] , and by resolving the chemical structure of a C₆₀ molecule [Fig. 1 right] with intra-molecular resolution.

- [1] L. Gross et al., Nature Chemistry 3, (2011) 273 .
- [2] L. Gross et al., Science 325, (2009) 1110 .
- [3] L. Gross et al., Nature Chemistry 2, (2010) 821 .
- [4] F. Mohn et al., Nature Nanotechnology 2, (2010) 821 .
- [5] L. Gross et al., Science 337, (2012) 1326 .
- [6] D.G. de Oteyza et al., Science 340, (2012) 1434 .
- [7] F. Albrecht et al., J. Am. Chem. Soc. 135, (2013) 9200 .
- [8] S. Kawai et al., ACS Nano 7, (2013) 9098 .
- [9] J. Zhang et al., Science 342, (2012) 611 .
- [10] C. Moreno et al., Nano Lett.,15, (2015) 4, pp 2257–2262
- [11] O. Stetsovych et al., Nat. Comm. Accepted



Tu-C12

Low Temperature Photoemission Study of PTCDA on Sn/Si(111)- $\sqrt{3}\times\sqrt{3}$

Hanmin Zhang¹, Lars Johansson¹

¹Karlstad University, Karlstad, Sweden

The 3,4,9,10-perylene tetracarboxylic dianhydride (PTCDA) is a model compound in studies of organic films on various substrates. Flat lying molecules can be formed on physically interacting surfaces such as Ag/Si(111)- $\sqrt{3}\times\sqrt{3}$ [1]. Another example is Sn/Si(111)- $\sqrt{3}\times\sqrt{3}$ (Sn- $\sqrt{3}$), where at room temperature (RT) the surface chemically interacts with PTCDA so that molecules stand up [2]. However, as showed in this study, at low temperature (LT) the molecules show a very different behavior. The Sn- $\sqrt{3}$ surface is interesting since it electronically adapts a 3×3 structure. As shown in Fig. 1, the clean Sn 4d core-level contains two components, located at binding energies of 24.0 and 24.4 eV. After PTCDA depositions at LT, the Sn 4d spectra show a new component, which is located around 25.0 eV. Surprisingly it is the large component at 24.4 eV that loses intensity; while the small one seems unchanged. From the earlier studies, the outer Sn atom (small component) in a 3×3 cell receives charge from the two inner Sn atoms (large component), forming a fully-occupied band. Thus it is the inner Sn atoms with charge deficit (large component) that transfer charge to PTCDA. Though this sounds like a surprise, it actually could be explained by the valence band structure. There are two valence bands near the Fermi level for the clean surface. The one associated with the small component forms a fully occupied band, located at a higher binding energy; while the upper one associated with the large component forms a metallic band. Our experimental data show that the metallic band donates charge to the carboxylic C so that the molecules lie down to the surface.

[1] J. B. Gustafsson, et al, Phys. Rev. B 75, 155414 (2007).

[2] H. M. Zhang, et al, Phys. Rev. B 84, 205420 (2011).

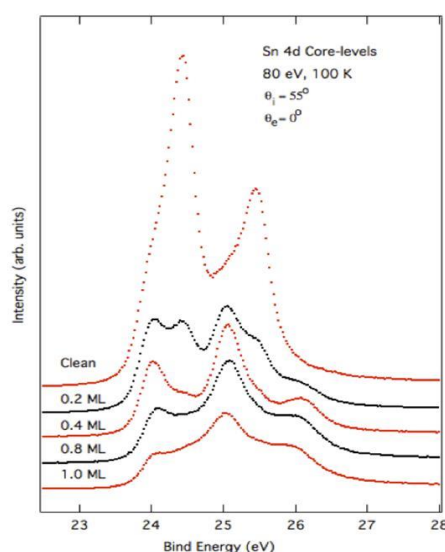


Figure 1 Sn 4d core-level spectra with different PTCDA coverages on Sn- $\sqrt{3}$ surface at 100 K.

Tu-C13

Measuring the orbitals of adsorbed organic molecules in 3D

Sergey Subach¹, Simon Weiß¹, Daniel Lüftner², Thomas Ules², Eva Maria Reinisch², Hendrik Kaser³, Alexander Gottwald³, Mathias Richter³, Georg Koller², Michael Ramsey², Peter Puschnig², Stefan Tautz¹

¹Forschungszentrum Jülich, Jülich, Germany, ²University of Graz, Graz, Austria,

³Physikalisch-Technische Bundesanstalt, Berlin, Germany

The conventional basis for a quantum-mechanical description of matter is electron wave functions. For atoms and molecules, their spatial distributions and phases are known as “orbitals”. Although molecular orbitals are very powerful concepts to describe molecular properties, experimentally only the electron densities and electron energy levels are directly observable. Recently an ARPES-based technique, called orbital tomography, emerged which enables deconvolution of photoemission spectra into individual orbital contributions and orbital-by-orbital characterisation of large adsorbate systems. In particular, it has been utilized to study the hybridization of molecular states with the substrate, explore intermolecular band dispersions, shed light on the role of intermolecular versus molecular-substrate interactions, determine molecular orientations, reveal the nature of doping-induced states etc. Moreover, ARPES-based imaging of molecular orbitals in reciprocal space opens the way to their complete reconstruction in 3D retrieving also the phase distribution which is commonly meant to be lost in photoemission experiment. To this end, a series of photon energy dependent ARPES measurements on PTCDA/Ag(110) monolayer was conducted using specifically calibrated light source. We find that the overall dependence of the photocurrent on the photon energy can be well accounted for by assuming a plane wave for the final state. However, the experimental data, both for the highest occupied and the lowest unoccupied molecular orbital of PTCDA, exhibits an additional feature attributed to a final state resonance. Taking into account these effects beyond a plane wave final state, we are able to reconstruct a fully 3D image of the highest occupied and the lowest unoccupied molecular orbital of PTCDA from the experimental ARPES data.

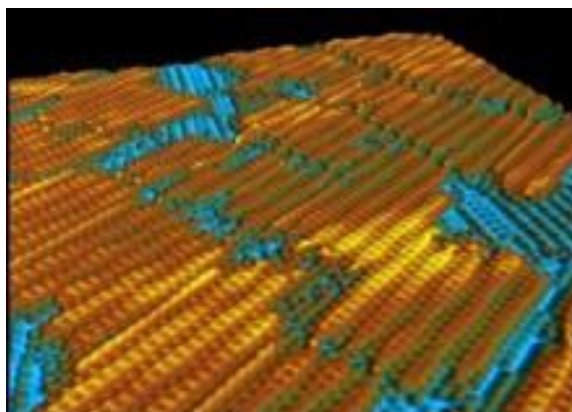
Tu-C14

Quasi One-Dimensional Metallic Band Dispersion In long Range Ordered Polymeric wires

Guillaume Vasseur^{1,2}, Pr. Yannick Fagot-Revurat², Muriel Sicot², Pr. Bertrand Kierren², M. Luc Moreau², Pr. Daniel Malterre², M. Gianluca Galeotti³, Luis Cardenas³, Josh Lipton-Duffin³, Pr. Frederico Rosei³, M. Marco Di Giovannantonio⁴, Gorgio Contini⁴, Patrick Lefevre⁵, Francois Bertrand⁵, Vincent Meunier⁶, Dmitrii Perepichka⁷

¹Centro De Fisica De Materiales, Donostia-San Sebastián, Spain, ²Institut Jean Lamour, Nancy, France, ³Institut National de la Recherche Scientifique, Varennes, Canada, ⁴Istituto di Struttura della Materia, Rome, Italy, ⁵Synchrotron SOLEIL, Gif sur Yvette, France, ⁶Rensselaer Polytechnic Institute, New York, United States, ⁷McGill University, Montreal, Canada

Graphene-like 2D organic materials can be grown and confined onto suitable surfaces depositing and activating selected molecules with different strategies in order to be employed as active media in organic electronics devices. In this respect, the surface-confined polymerization is a very promising bottom-up approach that allows the creation of layers with desired architectures and tunable optical or electronic properties [1-3]. In this work, using Angle Resolved Photoemission (ARPES) and Scanning Tunneling Spectroscopy (STS), we mapped the electronic structure of an ordered array of poly-para-phenylene (PPP) synthesized via the surface-catalyzed dehalogenative polymerization of (1,4)-dibromobenzene on copper (110) (figure 1). These chains are equivalent to hydrogen passivated three atoms armchair graphene nanoribbons (3-AGNR). By STS, the quantization of LUMO states is measured as a function of oligomer length. In the longest chains, these states cross the Fermi energy conferring to the polymer a metallic character. ARPES also reveals a quasi one-dimensional graphene-like HOMO-derived band as well as a HOMO-LUMO gap of 1.15 eV, since LUMO states are partially occupied through adsorption on the surface. Investigation of the dispersion in the perpendicular direction allows us to evidence a weak inter-chain interaction. Tight-binding modeling and ab initio calculations lead to a full description of the organic bandstructure, including the dispersion, the ARPES spectral weight, the gap size and charge transfer mechanisms which drive the system into metallic behavior. Figure 1 : 3D STM picture of the PPP chains grown on the Cu(110) surface. [1] L. Grill et al., Nature Nanotech. 2, 687-691 (2012); [2] J. Cai et al., Nature 466, 470-473 (2010) ; [3] M. Di Giovannantonio et al., ACS Nano 7, 8190 (2013).



Tu-D09

Recent progress in high pressure analyser and experimental method development applied to liquid/solid interface studies

Julia Maibach², Chao Xu², Susanna K. Eriksson², John Åhlund¹, Torbjörn Gustafsson², Hans Siegbahn³, Håkan Rensmo³, Kristina Edström¹, Maria Hahlin³

¹VG Scienta, Uppsala, Sweden, ²Department of Chemistry–Ångström Laboratory, Uppsala, Sweden, ³Department of Physics and Astronomy, Uppsala, Sweden

High-pressure Photoelectron Spectroscopy (HP-PES) is a rapidly developing technique with applications in a wide range of scientific fields, e.g. solar cell, catalysis, and battery research. Here we present measurements on a solid/liquid interface using a HP-PES setup equipped with a I K α X-ray source [1] [2]. In electrochemical systems, the conversion between electrical and chemical energy occurs through redox reactions in the interface region. Improvements of such systems when it comes to efficiency, long term stability, etc., require in-depth knowledge of the composition, formation, and chemical processes occurring at these interfaces under operating conditions.

HP-PES is a perfect tool to study these type of systems. Here we investigate a liquid electrolyte on a silicon electrode in propylene carbonate [3]. The system is sensitive to both air and vacuum, since the material will react with oxygen and evaporate in vacuum. To overcome these problems a new method for transferring samples without contact with air or vacuum below the vapor pressure of the liquid has been developed. With this method it is possible to characterize the liquid and solid/liquid interface using HP-PES and extending the approach towards operando solid/liquid interface studies using liquid electrolytes seems now feasible.

[1] Susanna K. Eriksson, et al., Review of Scientific Instruments 85, 075119 (2014)

[2] Mårten O. M. Edwards, et al., Nuclear Instruments and Methods in Physics Research A, 785, 191 (2015)

[3] Julia Maibach, et al., Review of Scientific Instruments 86, 044101 (2015)

Tu-D10

Soft X-ray Photoelectron Spectroscopy at the graphene-liquid interface

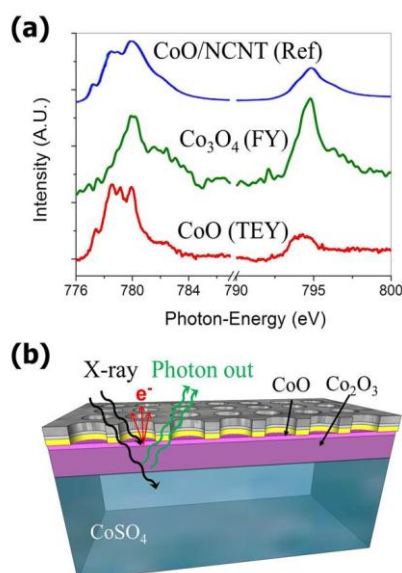
Juan-Jesus Velasco-Velez^{1,2}, Verena Pfeifer¹, Michael Hävecker^{1,3}, Robert Weatherup^{4,6}, Rosa Arrigo¹, Cheng-Hao Chuang⁵, Miquel Salmeron⁶, Robert Schlögl^{1,2}, Axel Knop-Gericke¹

¹FHI of the MPI, Berlin, Germany, ²MPI for CEC, Mülheim, Germany,

³Helmholtz-Center Berlin for Materials and Energy, BESSY II, Berlin, Germany,

⁴Engineering Department, University of Cambridge, Cambridge, United Kingdom, ⁵Department of Physics, Tamkang Univ., Tamsui, Taiwan, ⁶Materials Science Division, Lawrence Berkeley National Laboratory, Berkeley, USA

One of the main goals in electrochemistry is the characterization of electrode-electrolyte interfaces under operating conditions, to capture their electronic structure and chemical composition when in contact with the electrolyte and in the presence of applied electrical bias. However, the lack of surface sensitive techniques able to monitor the electronic structure under reaction conditions in aqueous environment hinders the total understanding of such processes. We have overcoming this issue thanks to the development of a new electrochemical setup based in a bi-layer of graphene which makes possible electron spectroscopy in situ, i.e during electrochemical reactions (see Fig.1a). Using this approach, we have investigated the local electronic structure of electrodeposited cobalt and its interaction with graphene. We have found that the covalent bonding established between graphene and cobalt reduces Co+3 species to Co+2 revealing that the anchorage between cobalt and graphene prompts the reduction from Co₃O₄ to CoO (see Fig.1b). In addition to providing a direct insight into the Cobalt-graphene reaction by means of x-ray photoelectron spectroscopy, our method opens the way for studies of virtually any solid-liquid interface, which was not possible with techniques such as x-ray absorption in fluorescence mode used until now. This includes electrode batteries, photocatalysis, atmospheric phenomena and biological processes as photosynthesis and nitrogen fixation that occur under aqueous conditions and are essential for life.



Tu-D11

Quantitatively interpreting MD simulation profiles for X-ray photoelectron spectroscopy using SESSA

Giorgia Olivieri¹, Matthew Brown¹

¹Laboratory for Surface Science and Technology, Department of Materials, ETH Zürich, Zurich, Switzerland

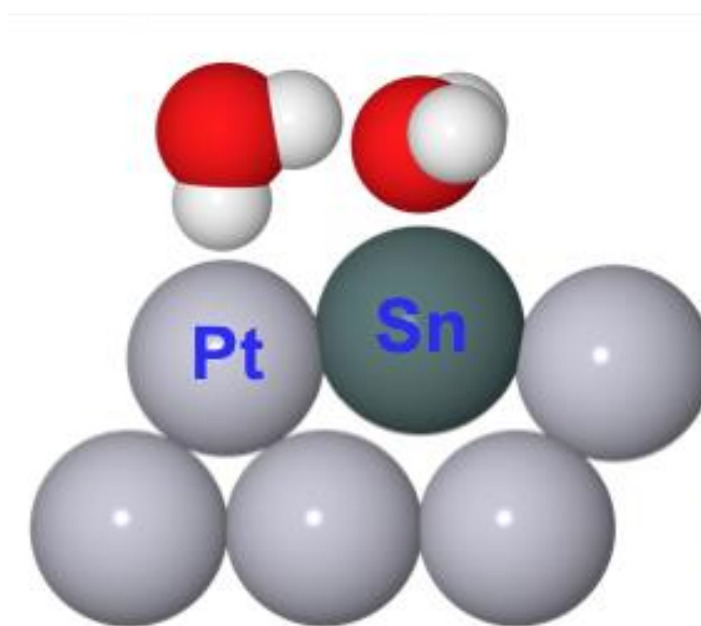
Over the last decade near ambient pressure photoemission (NAPP) has been used extensively to investigate the air/aqueous interface of electrolyte solutions. X-ray photoemission spectroscopy (XPS) measurements from saturated salt solutions have revealed (on multiple occasions) a segregation of the ions to the water/air interface, measured as an enhancement of the anion/cation ratio by as much as 400 %, which contradicts the classical view of ion depletion at an interface. Molecular dynamics (MD) simulations have for the most part provided qualitative support to these findings. In this study we use a combination of theory and experiment to show that the anion/cation enhancement at the water surface is no more than 20% of its bulk value and that indeed, in agreement with the thermodynamic interpretation of surface tension, both the anion and cation are depleted at the air/water interface relative to the bulk concentration. We use SESSA software, developed by the National Institute of Standard and Technology (NIST) and based on a Monte Carlo calculation of electron trajectories, to quantitatively calculate XP spectra from MD simulation profiles. Contrary to most publications, SESSA simulations predict that the energy dependent XPS measurements should show a depletion of both the anion and cation at the air/water interface. Our simulations are complemented by liquid microjet photoemission experiments that are shown to be in good agreement for both concentration dependent effects (NaI) and specific ion effects (NaI, NaBr and NaCl). We hypothesize as to the potential origin of our results in comparison to previous studies.

Tu-D12+13

Water structures and the wetting of metals and nano-structured interfaces

Andrew Hodgson¹¹The University of Liverpool, Liverpool, United Kingdom

Water–metal interfaces are important in fields as diverse as corrosion, heterogeneous catalysis and electrocatalysis, but models for the water–solid interaction remain relatively crude, and often little is known about the species present at the surface or the hydrogen bonding structures formed. Water structures are delicate, held together by weak water–metal and water–water hydrogen bonds, and small changes to the surface can introduce dramatic changes to the local water structure and macroscopic properties, such as wetting. Key issues to understand include how water wets different surfaces, how the presence of hydroxyl changes the first layer structure and how the molecular structure of the first water layer influences the overall properties of the water–solid interface. This talk will focus on how the hydrogen bonding structure of water depends on the symmetry and reactivity of some simple metal surfaces, particularly how water adsorption and wetting is modified by the presence of hydroxyl or by creation of a 2D nano-structured surface, for example an ordered surface alloy or a nano-structured polar organic adsorbate array. Examples will include the wetting of Cu(110), the effect of changing the lattice parameter on the wetting of the $(\sqrt{3}\times\sqrt{3})R30^\circ$ Sn M(111) surface alloys and the wetting and hydration of a nano-structured bitartrate layer on Cu(110). These experiments reveal a much richer, more complex picture of adsorption than originally anticipated, but some simple general considerations persist and provide insight into the structure of water at solid surfaces, allowing us to anticipate and rationalise the adsorption behaviour of more complex surfaces, such as the organic nano-structured bitartrate surface.



Tu-E09

Single-Molecule and Single-Active-Site Studies of Stereocontrol by Chemisorbed Chiral Molecules

Peter McBreen¹, Yi Dong¹, Jean-Christian Lemay¹

¹Laval University, Québec, Canada

Isolated adsorbed chiral molecules can stereodirect prochiral co-adsorbates on reactive metal surfaces and the application of this phenomenon underpins a method to perform asymmetric heterogeneous catalytic reactions. Typically, the stereochemical action is attributed to intermolecular interactions in complexes formed by docking the prochiral substrate in a chiral pocket created by the chemisorbed chiral molecule. We will present results from combined variable temperature STM and optB88-vdW DFT studies of individual bimolecular docking complexes formed by enantiopure 1-(1-naphthyl)ethylamine and selected prochiral molecules on Pt(111). The experiments reveal sub-molecularly resolved and time-resolved site-specific and stereospecific data. The results show that a single chemisorbed enantiomer simultaneously presents several chiral pockets, each displaying a specific prochiral ratio for a given substrate molecule. A hierarchy of metal-molecule and molecule-molecule interactions is found to control prochiral selection at each site. Time-lapsed STM measurements of individual substrate molecules sampling a set of chiral pockets provide new insight on the dynamics of stereocontrol.

Tu-E10

Competitive displacement reactions on single crystal gold surfaces: role of weak interactions

Robert Madix¹, Juan Carlos Rodriguez-Reyes², Cassandra Siler¹, Wei Liu³, Alexandre Tkatchenko³, Cynthia Friend¹

¹Harvard University, Cambridge, United States, ²Universidad de Ingenieria y Tecnologia, Lima, Peru, ³Fritz Haber Institute, Berlin, Germany

To achieve high selectivity for catalytic reactions between two or more reactants on a heterogeneous catalyst, the relative concentrations of the adsorbed reactive intermediates must be optimized. If species compete for binding sites, their concentrations depend on their relative surface binding strengths. Here we describe a general framework for predicting the relative stability of adsorbed organic intermediates (Bads) involved in oxygen-assisted reactions on metallic gold with broad relevance to catalysis by metals. Combining theory and experiment (in both UHV and catalytic conditions), we establish that van der Waals interactions with the surface, determine relative stabilities and dictate the conditions for optimum selectivity. Overall, the stabilities trend with the gas phase acidities of the parent molecule (BH), but inconsistencies with this correlation are explained by theoretical computation of the surface binding energies of the intermediates (Bads). Two types of experiments were performed on Au(111) to determine the relative adsorption strengths of different species: (1) displacement reactions and (2) competitive adsorption reactions. Common to both, the surface was first prepared with 0.05 ± 0.01 ML of adsorbed O. For displacement reactions BH was then adsorbed at 140 K and ~ 0.1 ML Bads isolated by mild heating. A second species, B'H, was then dosed at 140 – 200 K onto the surface to test for displacement. Alternatively, competitive adsorption was studied by dosing a mixture of BH and B'H onto the surface in excess of the pre-adsorbed 0.05 ML O/Au at ~ 140 . The relative amounts of Bads and B'ads were distinguished in both cases by TPRS on the basis of their signature products or by HREELS.

The principles have broad applicability for determining the stability of intermediates on the surfaces of metals and specifically demonstrate the critical role of weak interactions in determining reaction selectivity among reactions of complex molecules

Tu-E11

Using In-situ Infrared Spectroscopy Wisely in Catalysis— One Spectrum to Include both the Surface Species and the Change of Catalyst Itself under the Realistic Reaction Condition

Mingshu Chen¹, Xuefei Weng¹, Ding Ding¹, Huilin Wan¹

¹Xiamen University, Xiamen, China

Fundamental understanding of catalysts and how they function under the reaction conditions is the foundation for design and preparation of new and improved catalysts and catalytic conversion processes. Such understanding can be achieved only by characterization of catalysts in the presence of reacting mixtures at the temperatures and pressures of practical operation because catalyst structures and the mechanisms of catalytic reactions depend on the reaction environment. Raman spectroscopy is one of the few instrumental methods that in a single measurement can provide information about both solid catalysts and the molecules reacting on them. However, its sensitivity for the submonolayer surface species and the surface change under catalytic reaction is limited. Infrared spectroscopy is also a wide spectral range (6000-50 cm⁻¹) technique that enables examination of the nature of molecular species, identification of solid phases. Unfortunately, most of the heterogeneous catalysts consist of oxides as the active components or as the supports, which strong IR adsorption (below 1200 cm⁻¹) limits the in situ IR to measure only the surface species (4000~900 cm⁻¹). In this presentation, we will present our new developments of in-situ infrared spectroscopies with a spectral range of 4000~400 cm⁻¹, for both the reflection adsorption infrared spectroscopy (IRAS) and transparent infrared spectroscopy (FTIR, unpublished data), that are capable of measuring both the surface species and changes specific to the surface.

Tu-E12

Determination of the Potential Energy Curve of Diethyl Ether on Si(001) - A Combined Optical Second-Harmonic Generation and Molecular Beam Study

Marcel Reutzel¹, Michael Dürr^{1,2}, Ulrich Höfer¹

¹Philipps-Universität, Marburg, Germany, ²Justus-Liebig-Universität, Giessen, Germany

The functionalization of semiconductor surfaces with organic molecules has attracted much interest with respect to the challenges arising from the miniaturization in semiconductor device physics. Adsorption studies of many organic molecules show that the adsorption mechanism typically proceeds via an intermediate state. For organic molecules containing a heteroatom such as nitrogen or oxygen, this intermediate state involves lone-pair electrons of the heteroatom and, in the case of Si(001), the empty dangling bond of the lower silicon atom. Most recently, we have shown for ether molecules that this datively bonded intermediate can be isolated at low temperatures; at elevated temperatures cleavage of the O-C bond of the otherwise inert ether group was observed [1,2]. Despite the importance of these intermediate states, only very little information is available on the respective potential energy curves. Here we show that, using optical second-harmonic generation, we can follow in situ the conversion of diethyl ether from the intermediate to the final adsorption configuration. Measuring the kinetics as a function of surface temperature thus allows us to determine the conversion barrier ϵ_a . Complementary information is obtained from sticking probabilities measured by means of molecular beam experiments. The dependence of the initial sticking probability on surface temperature reveals the difference $\epsilon_d - \epsilon_a$ between the desorption and the conversion barrier. Combining both techniques, most important parameters of the potential energy curve of diethyl ether on Si(001) are determined: The binding energy ϵ_d of the datively bonded intermediate state and the barrier ϵ_a for conversion into the final state. Together with our results on the adsorption mechanism [2], we present a comprehensive picture of an adsorption process via a datively bonded intermediate state on Si(001).

[1] G. Mette et al., ChemPhysChem 15, 3725 (2014).

[2] M. Reutzel et al., J. Phys. Chem. C 119, 6018 (2015).

Tu-E13

In Situ Study of the Reactivity of Graphene-Supported Nanocluster Arrays

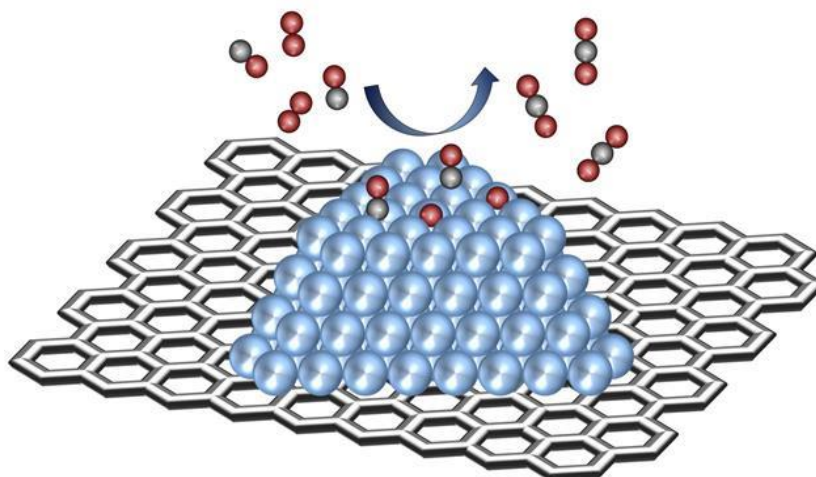
Christian Papp¹, Karin Gotterbarm, Florian Späth, Hans-Peter Steinrück¹Universität Erlangen-Nürnberg, Erlangen, Germany

Nanocluster arrays on graphene are intriguing model systems for catalysis. We studied the adsorption and oxidation of CO and the chemistry of SO₂ on Pt/Gr/Rh(111) with high-resolution X-ray photoelectron spectroscopy. For the first time it was possible to obtain quantitative and site-resolved information of adsorbates on nanoclusters. On the nanoclusters, CO is found to adsorb at three different sites: namely, on-top, bridge, and step. The C 1s spectra exhibit remarkable similarities to those on Pt(355). Similar to the case for stepped Pt surfaces, a clear preference for the adsorption on step sites is found, while the preference for the adsorption on on-top sites over bridge sites on the terraces is less pronounced in comparison to that on single crystals. Temperature programmed XPS revealed an enhanced binding energy for the cluster step sites, similar to the situation on stepped Pt surfaces. The oxidation of CO on graphene-supported Pt nanoclusters follows a pseudo-first-order rate law. Applying an Arrhenius analysis, we found an activation energy of 13±4 kJ/mol, which is much smaller than that on Pt(111), due to the more reactive step and kink sites on the nanoclusters.

Atomic sulfur and its oxides are catalyst poisons and interesting research subjects. SO₂ adsorbs in two geometries – perpendicular and parallel to the surface – on cluster facets and steps. Further insight is gained from the comparison of our results to data on the adsorption of SO₂ on flat and stepped platinum surfaces. We find a remarkable similarity to the adsorption on Pt(322). However, thermal evolution experiments revealed several similarities to both Pt(322) and Pt(355), showing that the Pt nanoclusters exhibit of (100) and (111) steps. The reactivity of the nanoclusters is strongly increased as compared to the single crystals.

SFB 953 is acknowledged for funding.

[1] K. Gotterbarm, et al. ACS Catalysis, 5 (2015) 2397.



Tu-E14

Spectators Control Selectivity in Surface Chemistry for Acrolein Partial Hydrogenation reaction over Pd model surfaces

Francisco Ivars Barceló¹, Karl-Heinz Dostert¹, Casey P. O'Brien¹, Svetlana Schauermann¹, Hans-Joachim Freund¹

¹Fritz-Haber-Institut Der Max-Planck-Gesellschaft, Berlin, Germany

A mechanistic study on the selective hydrogenation of acrolein over model Pd surfaces (single crystal Pd(111) and Pd nanoparticles supported on a model oxide support) will be presented. We show that Pd(111) surface is modified with an overlayer of oxopropyl spectator species that are formed from acrolein during the initial stages of the reaction. Thus, metal surface becomes nearly 100% selective to unsaturated alcohol formation. The chemical nature of the surface spectator and the reactive intermediate (propenoxy species) were identified by pulsed multi-molecular beam experiments and in-situ infrared reflection-absorption spectroscopy. Moreover, the simultaneous evolution of the reactive intermediate on the surface and the formation of the reaction product in the gas phase were experimentally followed.

Tu-A15+16

Graphene/metal Moirés: Unveiling structural and electronic modulations with STM and DFT simulations

Ruben Perez¹¹Universidad Autonoma de Madrid, Madrid, Spain

The local modulations in the structure, charge density and electronic properties of graphene induced by the interaction with metal surfaces can be exploited to tune the transport properties in graphene-based electronic devices. We have combined high-resolution STM experiments by different groups and our DFT/STM calculations to characterize the moire patterns formed on both weakly (Pt, Cu) and strongly interacting (Rh) cases. G/Pt shows the dramatic effect of the defects in the strength of the interaction [1] and unveils the atomic structure of the boundary between a graphene zigzag edge and a Pt(111) step [2].

In G/Cu, we have demonstrated that STM can selectively visualize either the graphene layer, the substrate underneath or even both at the same time and exploited this tunable transparency to provide a comprehensive picture of the G-metal coupling with atomic precision and high energy resolution [3], with important implications for the accurate description of van der Waals interactions. Our calculations explain the tunable transparency in terms of the short out-of-plane extension of the graphene electronic states, suggesting that it should apply to a good number of graphene/substrate systems. Our study of G/Rh(111) challenges some of established ideas for strongly interacting G-metal systems. The experiments conclusively prove the formation of different moiré structures with a wide distribution of surface periodicities. A proper simulation of the current beyond the standard Tersoff-Hamman approach is needed to reproduce quantitatively the trends observed in the STM apparent corrugation. Based on this agreement, we discuss the relative contribution of strain, corrugation and G-metal binding to stabilize the observed moires [4].

[1] M. M. Ugeda, et al. Phys Rev Lett. 107, 116803 (2011).

[2] P. Merino et al., ACS Nano 8, 3590–3596 (2014).

[3] H. Gonzalez-Herrero et al. Nature Comm., under review (2015).

[4] A. Martin-Recio et al. Nanoscale, DOI: 10.1039/C5NR00825E (2015).

Tu-A17

Long range corrugation of monolayer graphene on 6H-SiC(0001) characterized by Grazing Incidence Fast Atom Diffraction

Hocine Khemliche¹, Asier Zugarramurdi¹, Maxime Debiossac¹, Petru Lunca-Popa¹, Andrew Mayne¹, Anouchah Momeni^{1,2}, Andrei Borisov¹, Zhao Mu¹,
Philippe Roncin¹

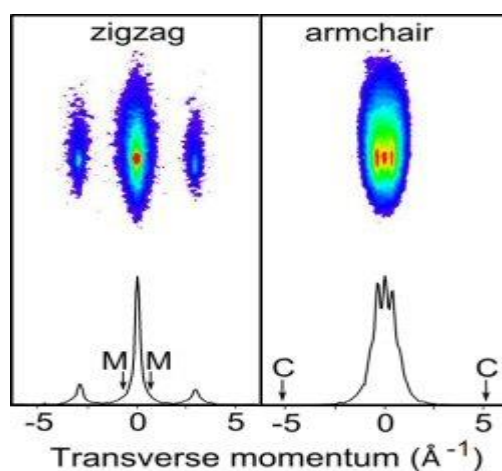
¹ISMO, CNRS-UnivParis-Sud, Orsay, France, ²Universite de Cergy-Pontoise, Cergy, France

Properties of supported graphene can be seriously degraded due to interaction with the underlying support. In the case of CVD graphene grown on crystalline metals or epitaxial graphene on SiC, a long range topographic corrugation appears as a signature of the coupling with the substrate. This Moiré-like corrugation is difficult to identify with accuracy by standard surface science techniques. We present a Grazing Incidence Fast Atom Diffraction (GIFAD) study of monolayer graphene on 6H-SiC(0001). This system shows a Moiré-like 13x13 superlattice above the reconstructed carbon buffer layer; the intrinsic electronic corrugation of pristine graphene is modulated by these geometric structures. Due to the averaging property of GIFAD [1], these two contributions to the corrugation can be separated (see figure). Along the zigzag direction, the diffraction pattern is that expected from a perfect honeycomb structure. Using a simple C-He binary potential, the calculated diffraction pattern is in good agreement with the observed intensities; in other words the graphene appears as perfectly flat. At variance, the diffraction pattern observed along the armchair direction shows the 16 Å spacing characteristic of the 13x13 superlattice. An analysis of the peak intensity distribution provides a quasi Gaussian corrugation of 0.27 Å height. This shape is compatible with the ab-initio prediction by Varchon et al. [2] but with an amplitude almost 30% weaker. All experimental results are well reproduced by a quantum diffraction calculations [3] where the graphene layer topography can be described by any particular pattern.

[1] A. Zugarramurdi et al.; App. Phys. Lett. 106, 101902 (2015)

[2] F. Varchon et al.; Phys. Rev. B 77, 235412 (2008).

[3] A. Zugarramurdi and A. Borisov; Phys. Rev. A 86, 062903 (2012)



Tu-A18

Comparative atomic-scale scanning probe microscopy study of graphene and boron nitride on noble metal surfaces

Manuela Garnica¹, Jacob Ducke¹, Martin Schwarz¹, Yuanqin He^{1,2}, Felix Bischoff¹, Daniele Stradi³, Mads Brandbyge³, Johannes V. Barth¹, Willi Auwärter¹

¹Physik Department E20, Technische Universität München, Germany, ²Institute for Advanced Study, Technische Universität München, Germany, ³Department of Micro- and Nanotechnology, Center for Nanostructured Graphene, Technical University of Denmark, Denmark

In recent years, the research of graphene and other 2D materials has spurred tremendous expectations from the fundamental point of view as well as for potential technological applications. As initial step, the synthesis and characterization of these layers on substrates become crucial. For highly reactive metals the chemical vapour deposition (CVD) technique has been shown to be an effective method to grow large areas of graphene and hexagonal boron nitride (h-BN). However, the low reactivity of noble metals makes the synthesis of 2D materials using the standard CVD techniques cumbersome [2]. In this work, we explore different growth methods of graphene and h-BN layers on Ag(111) and Cu(111) substrates. We combine novel and well-established protocols like CVD, e-beam evaporation, intercalation or ion gun assisted deposition. The characterization of the structural properties of these layers was achieved by atomic-scale scanning probe microscopy (STM/AFM). Furthermore, we explore the influence of the 2D layers on the surface potential and occupation of the surface state of the metals by means of scanning tunneling spectroscopy and first principles calculations. In particular, the analysis of the binding energy shift of the Shockley-state is used to shed light on the relative strength of the interaction between the epitaxial layer and the metallic substrate [3].

[1] M. Batzill, Surf. Sci. Rep. 67 (2012) p83.

[2] B. Kiraly et al. Nat. Commun. 4 (2013) p2804; F. Müller et al. Phys. Rev. B 82 (2010) p113406; Martinez-Galera et al, Nano Lett 11 (2011) p3576.

[3] J. Ziroff et al. Surf. Sci. 603 (2009) p354.

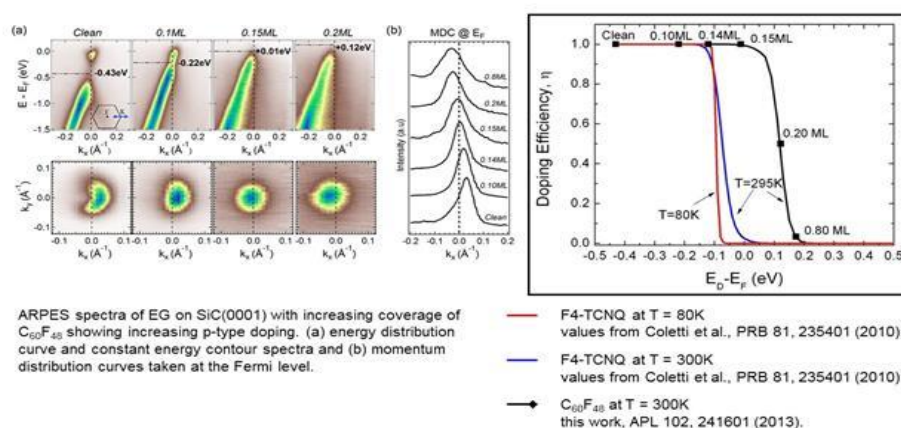
Tu-A19

Surface Charge Transfer of Epitaxial Graphene on SiC(0001) by Fluorinated Fullerenes

Martina Wanke¹, Anton Tadich², Mark Edmonds³, Felix Fromm¹, Christian Raidel¹, Christian Heidrich¹, Yaou Smets⁴, Lothar Ley⁵, Zoran Mazej⁶, Chris Pakes⁴, Thomas Seyller¹

¹TU Chemnitz, Institut für Physik, Chemnitz, Germany, ²Australian Synchrotron, Soft-X-ray-Beamline, Clayton, Australia, ³Monash University, Clayton, Australia, ⁴La Trobe University, School of Physics, Bundoora, Australia, ⁵FAU Erlangen-Nürnberg, Erlangen, Germany, ⁶Josef Stefan Institute, Ljubljana, Slovenia

The monocrystalline graphene epitaxial grown on SiC(0001) promises highest structural quality in wafer-size [2] in combination with an insulating substrate so that no transfer is necessary. Epitaxial graphene (EG) on SiC(0001) is intrinsically n-type doped due to the strong influence of the substrate interface [2, 3]. To control the type of charge carriers and their density it is necessary to overcome this n-type doping and tune the carriers in a specified direction. While intercalation modifies the graphene/substrate interface, substitutional doping changes the honeycomb lattice of the graphene itself. Adsorbate doping uses the surface charge transfer effect to dope the graphene leaving its lattice structure and the substrate interface intact. Adsorbed molecules on top of the graphene/substrate interface dope by collecting or donating electrons. Various molecules have been investigated while only a few show a stronger doping effect. Surface charge transfer doping, e.g. by F₄-TCNQ, has achieved charge neutrality by various groups [4], and thereby increasing the carrier mobility as well [4]. The F₄-TCNQ molecular layer is found not very stable. In our investigations C₆₀F₄₈ was successfully used for doping EG on SiC(0001). These C₆₀F₄₈ have a sufficiently high electron affinity to dope graphene by surface charge transfer [5]. This charge transfer mechanism using C₆₀F₄₈, is well understood on other surfaces as for the case of diamond [6]. Molecular doping of EG using C₆₀F₄₈ yields not only in doping the graphene up to charge neutrality for a coverage of only 0.15ML of C₆₀F₄₈, but the charge carriers were tuned from electron to hole for higher coverages [7]. A charge transfer model will be presented explaining the different doping efficiencies for different molecules to graphene. The model explains why only charge neutrality can be obtained with F₄-TCNQ, while net p-type doping is possible with C₆₀F₄₈ [7].



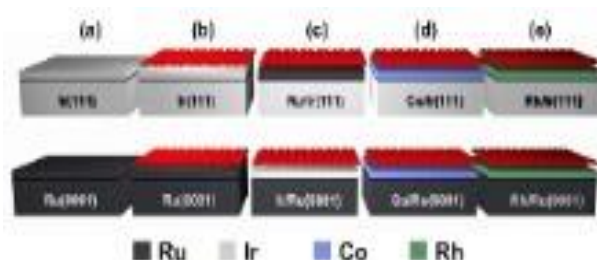
Tu-A20

Unravelling the roles of surface chemical composition and geometry for the graphene-metal interaction through C1s core-level spectroscopy

Francesco Presel¹, Naila Jabeen^{1,2,3}, Monica Pozzo⁴, Davide Curcio¹, Luca Omiciuolo¹, Paolo Lacovig⁵, Silvano Lizzit⁵, Dario Alfè^{4,6}, Alessandro Baraldi^{1,5,7}

¹Physics Department, University of Trieste, Trieste, Italy, ²International Centre for Theoretical Physics, Trieste, Italy, ³Nanosciences & Catalysis Division, National Centre for Physics, Islamabad, Pakistan, ⁴Department of Earth Sciences, Department of Physics and Astronomy, Thomas Young Centre@UCL, London Centre for Nanotechnology, University College London, London, United Kingdom, ⁵Elettra - Sincrotrone Trieste S.C.p.A., Trieste, Italy, ⁶IOM-CNR, DEMOCRITOS National Simulation Centre c/o SISSA, Trieste, Italy, ⁷IOM-CNR, Laboratorio TASC, Trieste, Italy

The coupling of graphene with metallic surfaces is an important topic in contemporary materials science, due to its potential impact on a number of high-performance electronic applications. In particular, such applications require graphene to be efficiently coupled to metallic contacts. This can be achieved by growing it directly on top of metallic surfaces via Chemical Vapour Deposition. The interaction of graphene with metal surfaces, however, causes modifications to the electronic properties of the former: a good understanding of the interactions occurring at interfaces between graphene and metals is therefore required to create and tailor the properties of high-performance graphene-based nanoelectronic devices. In the present work [F. Presel et al., Carbon, accepted for publication] we have shown that by using a combined experimental and theoretical approach it is possible to separate the contributions to the interaction strength between epitaxial graphene and transition metal surfaces arising from the geometrical and chemical properties of the supporting surfaces. This has been achieved by performing photoelectron measurements and numerical simulations of the C1s core level spectral distribution for a large number of graphene-metal systems, which have been obtained by systematic intercalation of different metals (Co, Rh, Ir and Ru) at the graphene-Ir(111) and graphene-Ru(0001) interfaces. We have demonstrated that the chemical species of the substrate's topmost layer plays a major role in determining the coupling between graphene and its substrate. Moreover, we have showed that both the experimental and the theoretical C1s spectral centres of mass are in linear relationship with the d-band centre of the transition metal substrate, which is considered a reliable descriptor of the graphene-substrate interaction strength. Our results provide a simple method to determine and tailor the properties of graphene-metal contacts.



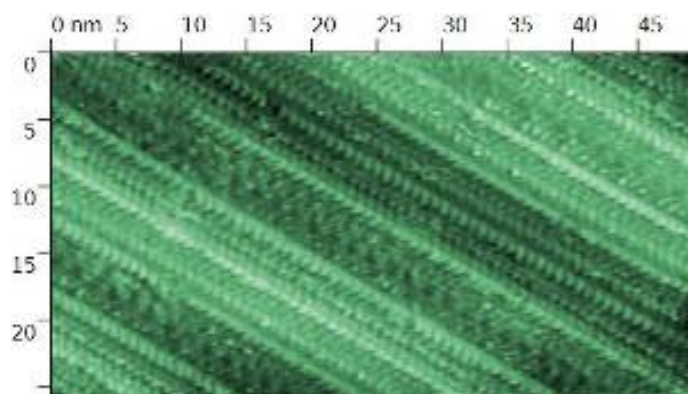
Tu-B15

Tungsten Oxide One-Dimensional Nanostructures

Romana Sediva¹, Karel Mašek¹, Carolina Pistonesi², María Estela Pronsoato²,
Tomáš Duchoň¹, Marie Aulická¹, Vitalii Stetsovych¹, Vladimír Matolín¹

¹Department of Surface and Plasma Science, Faculty of Mathematics and Physics, Charles University in Prague, Prague 8, Czech Republic, ²Department of Physics, Universidad Nacional del Sur, Bahía Blanca, Argentina

Tungsten oxide is a reducible oxide and it serves as an important material in the fields of heterogeneous catalysis and gas sensing. Particularly one-dimensional nanostructures with high surface to volume ratio can have unique physicochemical properties compared to their bulk counterparts. However the real systems are not suitable for fundamental research due to their complex structure. We present study of the tungsten oxide thin films in a form of highly ordered one-dimensional nanostructures prepared on the Cu(110) single crystal surface under UHV conditions. Electron diffraction methods (RHEED – Reflection High Energy Electron Diffraction, LEED – Low Energy Electron Diffraction) and STM (Scanning Tunneling Microscopy) were used for investigation of the system's structure and morphology. Chemical properties were studied by the means of photoelectron spectroscopy (XPS - X-ray Photoelectron Spectroscopy, ARPES - Angle Resolved Photoelectron Spectroscopy). According to the diffraction patterns we observed formation of self-organized one-dimensional structures along Cu[1-10] crystallographic direction. Oxidation state of the layers was deduced from the shape of W 4f emission line in XPS spectrum. The STM images clearly showed tungsten oxide nanorods on the substrate surface (Figure 1). Momentum-dependent modulation of the valence band electron structure shown by ARPES measurement also reflected one-dimensionality of the system. The structure was studied further by Density Functional Theory calculations using the generalized-gradient approximation (GGA) with the Perdew-Burke-Ernzerhof (PBE) functional. We modelled the wires formed by one and two lines of tungsten oxide developing the one-dimensional structures. Average W-W distances for both models were found similar to the lattice parameter of tungsten oxide in pseudo-cubic phase. Presented studies have shown that the one-dimensional tungsten oxide nanostructures can be prepared on the Cu(110) surface representing a well-defined and stable model system which could prove itself useful for investigation of the tungsten oxide's reactivity as well as for other applications.



Tu-B16

One-dimensional metal-oxide hybrid structures formed on the Ir(100) surface: Crystallographic analysis and properties

Pascal Ferstl¹, Florian Mittendorfer², Mathias Gubo¹, Klaus Heinz¹, Josef Redinger², Lutz Hammer¹, Alexander Schneider¹

¹Solid State Physics, Univ. Erlangen-Nürnberg, Erlangen, Germany, ²Institute of Applied Physics and Center for Computational Materials Science, TU Wien, Vienna, Austria

We present the self-organized growth of one-dimensional cobalt oxide nanowires on the Ir(100) surface. These metal-oxide hybrid structures grow as large (3x1) domains on plain Ir(100) terraces thereby circumventing the need for templated growth on vicinal surfaces as employed previously [1,2]. As a consequence a high areal density and high degree of order of the nanostructures is achieved. Depending on the oxidizing agent (O₂ or NO₂) nanowires of either CoO₂ or CoO₃ stoichiometry can be formed. Evenmore, both oxidic wires can be completely reduced by hydrogen to give a purely metallic ordered Ir₂Co surface alloy. Hence, the system can be switched reversibly between different Co oxidation states. We determine the atomic structure of all observed phases by means of full-dynamical LEED I(E)-analyses using the Erlangen Tensor-LEED code [3]. The final fit structures yield an excellent agreement between experimental and calculated spectra expressed by Pendry R-factors between 0.090 and 0.116. Furthermore, the accuracy of the structural results is impressively demonstrated by an agreement in the picometer range between structural parameters derived from LEED and those from DFT total-energy calculations of the respective model structures. From the structural point of view all phases consists of a homogeneous 3x1-periodic arrangement of monoatomic Co wires. In case of the ordered surface alloy these Co wires are embedded in the outermost Ir layer, whereas in the oxidized state the cobalt chains are completely decoupled from the substrate and linked only via the oxygen atoms at both sides.

[1] F. Li et al., Langmuir, 26 (2010) 16474

[2] S. Surnev et al., Chem. Phys. Chem. 11 (2010) 2506

[3] V. Blum, and K. Heinz, Comp. Phys. Comm. 134 (2001) 392

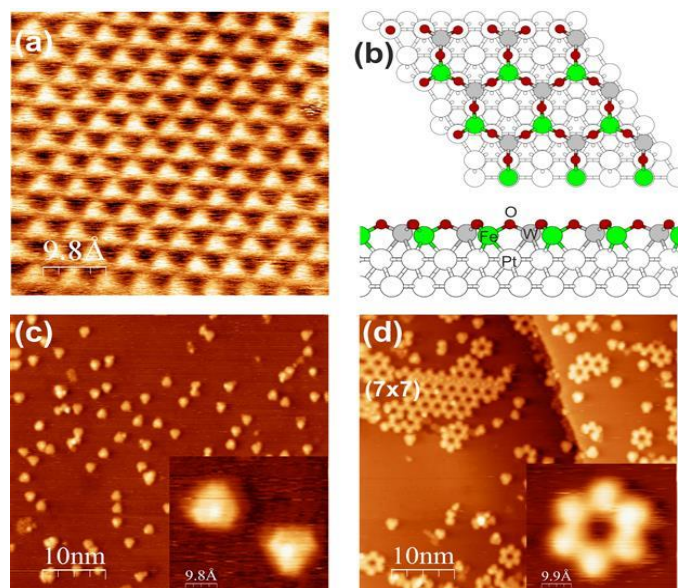
Tu-B17

Two-dimensional condensation of ternary oxide FeWO_x nanostructures on a $\text{Pt}(111)$ surface

David Kuhness¹, Sascha Pomp¹, Luca Sementa², Giovanni Barcaro², Venu Mankad¹, Alessandro Fortunelli², Falko P. Netzer¹, Svetlozar Surnev¹

¹Institute of Physics, University of Graz, Graz, Austria, ²CNR-ICCOM and IPCF, Consiglio Nazionale delle Ricerche, Pisa, Italy

Iron tungstate (FeWO_4) is a promising material for applications in the catalysis, photoluminescence, microwave technology and gas sensing. These materials have been synthesized mostly in a bulk form, but with the advance of nanotechnologies there is a growing interest in preparing FeWO_4 structures at the nanoscale, whose physical and chemical properties are unexplored yet. We have investigated the growth of two-dimensional (2-D) iron tungstate nanostructures on $\text{Pt}(111)$ by STM, LEED, XPS, and DFT calculations. A well-ordered epitaxial (2×2) FeWO_x monolayer phase (Fig. 1a) has been fabricated by a 2-D solid-state reaction of $(\text{WO}_3)_3$ clusters with a $\text{FeO}(111)$ bilayer on the $\text{Pt}(111)$ surface. The XPS analysis reveals that this reaction is accompanied by a diffusion of Fe atoms from the FeO layer in the Pt subsurface region, which is driven by the strong tendency for a Pt-Fe alloy formation. The DFT-derived structure model for the (2×2) phase (Fig. 1b) comprises a mixed layer of Fe and W atoms located in fcc and hcp positions on the $\text{Pt}(111)$ surface and arranged in a (2×2) honeycomb lattice. Each Fe and W atom is terminated by 3 O atoms, which yields a formal FeWO_3 stoichiometry of this novel 2-D tungstate phase. Co-deposition of low coverage of Fe atoms and $(\text{WO}_3)_3$ clusters onto clean $\text{Pt}(111)$, followed by oxidation at elevated temperatures, results in the formation of other FeWO_x nanostructures. At 400°C triangular-shaped clusters form (Fig. 1c), which transform with increasing the oxidation temperature to 500°C into some hexagram clusters and small nano-porous 2-D islands, exhibiting a (7×7) kagomé lattice (Fig. 1d). Eventually, after the oxidation at 600°C the $\text{Pt}(111)$ surface is covered by larger islands with the (7×7) structure. This phase transformation has been envisioned as a reductive condensation of triangular FeWO_x clusters into larger ternary oxide nanostructures.



Tu-B18

Formation of Anti-phase domain boundaries in two-dimensional silica via transformative recrystallization

Shashank Mathur^{1,2,3}, Sergio Vlaic^{1,2,4}, Eduardo Machado-Charry¹, Emmanuel Hadji^{1,3}, Pascal Pochet^{1,3}, Johann Coraux^{1,2}

¹Université Grenoble Alpes, Grenoble, France, ²CNRS- Institute NEEL, Grenoble, France, ³CEA-INAC-SP2M, Grenoble, France, ⁴ESPCI-Paris, Paris, France

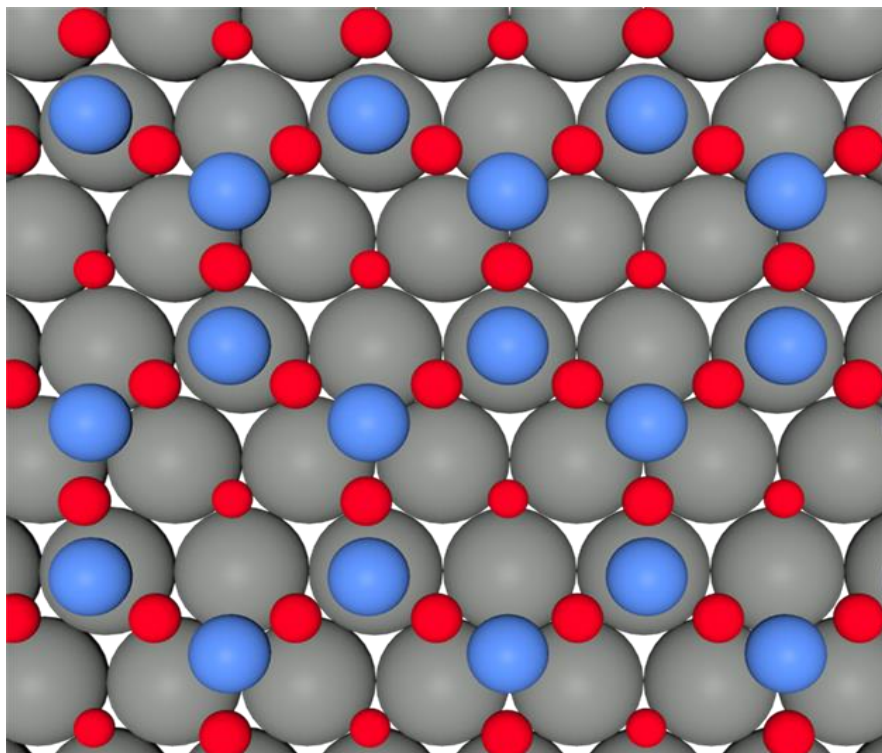
The two-dimensional phase of silica [1] grown on metal surfaces is characterized by a high density of anti-phase domains [2]. The formation of the latter domains has never been explained in the literature. By means of scanning tunneling microscopy and in operando reflection high energy electron diffraction we rationalize the formation of the anti-phase domains in terms of a transformative recrystallization of the reconstructed Ru(0001) surface [3]. This mechanism leads to the formation of anti-phase domain boundaries comprising of 7- and 5- sided rings of silica on Ru(0001) surface. The latter boundaries are different from those observed on other metal surfaces. Finally, the atomic-scale registry of the monolayer silica system is explained based on the STM analysis of the silica reconstructed surface of Ru(0001) and their DFT counterparts.

[1] Huang, P. et al. Nano Lett. 12, 1081(2012).

[2] Yang, B. et al. Nano Lett. 13, 4422 (2013).

[3] Mathur, S. et al., submitted.

[4] Weissenrieder, J. et al. Phys. Rev. Lett. 95, 076103 (2005)



Tu-B19

Identification of structure and electronic states of $\text{La}_{0.75}\text{Ca}_{0.25}\text{MnO}_3$ surface by density functional theory

Yasunobu Ando¹, Shunya Nakamura¹, Emi Minamitani¹, Ryota Shimizu²,
Katsuya Iwaya³, Takeo Ohsawa⁴, Taro Hitosugi^{2,5}, Satoshi Watanabe¹

¹The University of Tokyo, Tokyo, Japan, ²Tohoku University, Sendai, Japan,
³RIKEN, Japan, ⁴NIMS, Japan, ⁵JST-PRESTO, Japan

Perovskite oxides (perovskites) are promising candidates for oxidation catalysis in solid-state fuel cells because of their high chemical activity on the surface and variety in composition. However, direct observation of their surface structures and properties has been difficult due to the lack of easy-cleavage plane. Recently, some of the co-authors of this presentation have succeeded in epitaxial growth of $\text{La}_{0.75}\text{Ca}_{0.25}\text{MnO}_3$ (LCMO) thin films and their scanning tunnelling microscope (STM) observation at low temperature (see Fig. 1). They found that the LCMO surface is reconstructed and shows a zigzag pattern with $\sqrt{2} \times \sqrt{2}$ periodicity. They also revealed via scanning tunneling spectroscopy that the surface is insulating. In order to identify its atomic structure and mechanism of its insulating nature, we have carried out first-principle simulations with the LCMO slab models. We use the Vienna ab-initio simulation package (VASP) with local spin density approximation (LSDA) + U method. We adopted several doping models of the $\text{La}_{0.75}\text{Ca}_{0.25}\text{MnO}_3$ four-layered slab. STM images were simulated using the local density of states (LDOS) at 1.5 eV below the Fermi level and at 2 Å from the surface. Simulated STM image for the most stable model (See Fig. 2) shows the same zigzag tendency as the experimental ones. This trend can be understood by the reconstruction of the coordinated O atoms around Mn. Some of the unstable doping models do not show the zigzag tendency because of large surface distortion due to the Ca dopant near the surface. The stable doping model also reproduces the insulating nature of surface. On the other hand, layer projected density of states show no band gap for the inner layers of the slabs. Structural analysis together with the charge analysis suggests that this difference is led by the surface reconstruction around the Mn atoms.

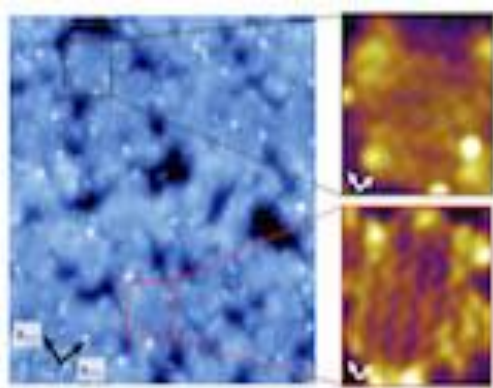


Fig. 1 Observed STM images of $\text{La}_{0.75}\text{Ca}_{0.25}\text{MnO}_3$.

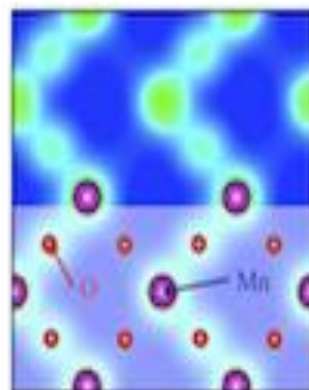


Fig. 2 Simulated STM image of the most-stable model.

Tu-B20

Direction of magnetization of Fe₃O₄ (111) surface

Kanta Asakawa¹, Taizo Kawauchi¹, Xiao Wei Zhang², Katsuyuki Fukutani¹

¹Institute of Industrial Science, The University of Tokyo, Tokyo, Japan, ²Institute of Material Structure Science, High Energy Accelerator Research Organization (KEK), Tsukuba, Ibaraki, Japan

Magnetite (Fe₃O₄) is a ferromagnetic material with the inverse spinel structure, and has attracted interest due to its fascinating characters such as catalytic activity, predicted half-metallicity, and metal-to-insulator transition at 120 K called the Verwey transition. Its unit cell includes two kinds of Fe sites; tetrahedrally coordinated Fe(A) sites and octahedrally coordinated Fe(B) sites. The Fe(B) sites consist of Fe²⁺ and Fe³⁺ ions, which play an important role in the Verwey transition and the appearance of the half-metallicity. It is believed that the origin of the Verwey transition is freezing of electron hopping between the Fe(B) sites. Under the Verwey transition, the magnetic easy axis in the bulk also changes from <111> to <100> axes. In this study, we investigated the magnetization of the Fe₃O₄(111) surface at 300 K by conversion electron Mössbauer spectroscopy (CEMS) and nuclear resonant X-ray scattering (NRS). In order to achieve the surface sensitivity, ⁵⁷Fe₃O₄ layer of 2 nm was deposited on the surface at 550 K with oxygen partial pressure of 8*10⁻⁴ Pa, and the NRS experiment was performed in a grazing-incidence condition. The time spectrum of NRS showed clear quantum beats reflecting the internal magnetic field. By analysing the NRS and the CEMS spectra, we found that the surface magnetization is parallel to the three <111> axes and the perpendicularly magnetized domains are missing. This indicates that the surface is occupied by closure domains. By comparing the CEMS spectra before and after the ⁵⁷Fe₃O₄ deposition, the magnetization was found to rotate away from the <111> axes towards the surface parallel direction due to the magnetostatic effect.

Tu-C15

PEARL - A New User Laboratory for Surface Structure Studies

Matthias Muntwiler¹, Jun Zhang¹, Roland Stania^{1,2}, Thomas Greber², Roman Fasel³, Philipp Aebi⁴, Thomas Jung^{1,5}, Thilo Glatzel⁵, Ernst Meyer⁵

¹Paul Scherrer Institut, Villigen PSI, Switzerland, ²Universität Zürich, Zürich, Switzerland, ³EMPA, Dübendorf, Switzerland, ⁴Université de Fribourg, Fribourg, Switzerland, ⁵Universität Basel, Basel, Switzerland

The Photo-Emission and Atomic Resolution Laboratory (PEARL) is a new soft X-ray beamline and surface science laboratory at the Swiss Light Source (SLS). PEARL is dedicated to the structural characterization of local bonding geometry of molecular adsorbates on metal or semiconductor surfaces, of nanostructured surfaces, and of surfaces of complex materials. The main techniques for structural characterization are X-ray photoelectron diffraction (XPD/PhD) and scanning tunneling microscopy (STM). XPD in angle-scanned mode measures bonding angles and the orientation of small molecules with respect to the substrate, while in energy scanned mode it measures the distance between neighbouring atoms, for example, between adsorbate and substrate. STM provides complementary, real space information, and is also useful for comparing sample quality with reference measurements at the home lab. The X-ray spectrum of the beamline covers the energy range from 60 eV to 2000 eV, and delivers a maximum photon flux of 10^{11} photons/s/0.1%BW at 800 eV. Flux can be traded for resolution (up to $E/\Delta E \approx 7000$) where chemical states or spin multiplets need to be resolved. The spot size on the sample can be switched between 180 x 60 microns (focused) and 1 x 1 mm (unfocused). While the main photon polarization mode of the bending magnet beamline is linear, the beamline can also be operated in partially circular polarization mode. In this contribution, the key features and measured performance data of the beamline and of the experimental station are presented. In addition, first XPD and STM results from test samples demonstrate the capabilities of the new laboratory. The beamline is now partially open for external users.

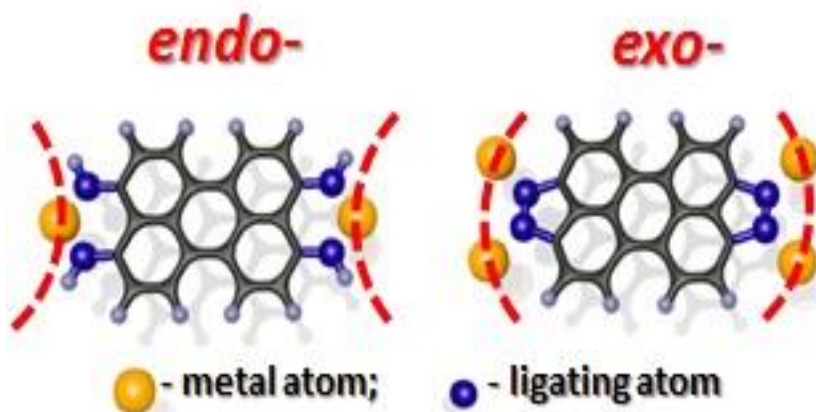
Tu-C16

Programming the dimensionality of on-surface polymers by endo-/exo-ligation

Olha Popova¹, Aneliia Wäckerlin, Christian Wäckerlin, Jan Nowakowski, Sylwia Nowakowska, Jonas Björk, Shadi Fatayer, Jan Girovsky, Thomas Nijs, Susanne Martins, Armin Kleibert, Nirmalya Ballav, Meike Stöhr, Lutz H. Gade, Thomas A. Jung

¹University of Basel, Basel, Switzerland

Coordination between organic molecular ligands and metal adatoms has been established to form stable, well-ordered and here chemically tunable endo or exo-ligands and corresponding polymers. By combining Scanning Tunneling microscopy (STM), X-ray Photoelectron Spectroscopy (XPS), Near Edge X-Ray Absorption Fine Structure (NEXAFS) and Density Functional Theory (DFT), we demonstrate that the amino-functionalized perylene derivative, 4,9-diaminoperylene quinone-3,10-diimine (DPDI), undergoes specific levels of dehydrogenation (-1 H_2 or -3 H_2) depending on the nature of the present adatoms (Fe, Co, Ni or Cu) [1]. In this way, the molecule is forming a coordination complex exhibiting a concave or convex arrangement of ligating atoms, which is decisive for the formation of either 1D or 2D coordination polymers. Moreover, the Cu-coordinated 3deh-DPDI network which is created after the deposition of DPDI on Cu(111) and subsequent annealing [2] confines the Shockley surface state into well-defined quantum boxes. [3]



Tu-C17

Origin and modification of the Confined State in a 2D molecular nanoporous network

Ignacio Piquero-Zulaica¹, Sylwia Nowakowska², Lutz H. Gade³, Thomas A. Jung⁴, J. Enrique Ortega^{1,5,6}, Jorge Lobo-Checa¹

¹Centro de Física de Materiales (CFM), San Sebastian, Spain, ²Department of Physics, University of Basel, Basel, Switzerland, ³Anorganisch-Chemisches Institut, Universität Heidelberg, Heidelberg, Germany, ⁴Laboratory for Micro- and Nanotechnology, Paul Scherrer Institute, Villigen, Switzerland, ⁵Dep. Física Aplicada I, Universidad del País Vasco, San Sebastian, Spain, ⁶Donostia International Physics Center, San Sebastian, Spain

Surface electrons are scattered by ad-atoms, ad-molecules and steps and can therefore be confined within nanostructures if the characteristic dimensions are smaller than the electron coherence length. Stable networks can be formed on surfaces from sublimed molecular building blocks by ad-atom coordination, which unambiguously show such confining capabilities. The nanoporous coordination network generated by a Perylene derivative (DPDI) on Cu(111), in particular, has been reported to trap surface electrons and to give rise to a new band structure [1, 2]. However, open questions remain regarding the nature and the origin of the confined state and its possible modification by guest entities. In the present work we use angle-resolved photoemission (ARPES) to tackle these questions. To address the origin of the confined state, we study its temperature dependence in comparison to the surface state of the pristine surface. We observe that both states simultaneously shift to higher binding energies when decreasing the sample temperature [3]. This result evidences that the reported confined state originates from the Shockley state. In addition, we modify the confined state by the physisorption of Xe atoms on the DPDI/Cu(111) network pores. We observe a tiny shift of the confined state minimum by only 30meV towards the Fermi level, which is surprisingly small compared to the 143meV shift reported for Xe/Cu(111) [4]. We explain this result in terms of a modification of the surface potential on the atomic scale.

[1] S. Nowakowska et al., Nat. Commun. 6, 6071 (2015).

[2] J. Lobo-Checa, et al. . Science 325, 300 (2009).

[3] R. Paniago et al., Surface science, 336(1-2), 113 (1995).

[4] F. Forster, et al. J. Phys. Chem. B. 108, 14692 (2004).

Tu-C18

The growth of organic thin films studied by photoelectron emission and optical reflectance spectroscopy

Ebrahim Ghanbari¹, Andrea Navarro-Quezada¹, Markus Aiglinger¹, Thorsten Wagner¹, Peter Zeppenfeld¹

¹Johannes Kepler University Linz, Linz, Austria

The optical and electronic properties of π -conjugated organic materials have been an issue of considerable interest due to their fundamental and technological importance. Various experimental studies in past decades have addressed the interaction between organic molecules and metallic surfaces. Despite the significant improvement in performance of prototype devices, precise understanding and control of thin film growth on metallic surfaces is still a matter of debate. In this work, we show that photoelectron emission microscopy (PEEM) and differential reflectance spectroscopy (DRS) can be applied simultaneously during the growth of organic nanostructures to obtain complementary information during a single deposition experiment. In particular, we focus on the growth of perfluoro-pentacene (PFP) molecules on a Ag(110) surface. Our experimental setup allows the synchronous acquisition of PEEM images and DRS data during deposition of the organic material. In particular, PEEM and DRS use the same light source, namely a Xe lamp. The PEEM utilizes the local variation of the photoelectron emission yield to generate the image contrast. Therefore PEEM is perfectly suited to study the film morphology on the μm scale in real-time. On the other hand, DRS can be employed to investigate the temporal evolution of the (global) optical properties during deposition of the organic thin films. Both, photoelectron emission and the optical reflectance of the surface, depend on the (linear) polarization state of the incident light. Substrate and adsorbate layer are crystalline and therefore exhibit an inherent anisotropy of the reflectance as well as of the photoelectron emission. It will be shown, that the polarization dependence of both techniques can be used to obtain additional information on the geometric structure of the surface, e.g. about the orientation of the molecules on the surface.

Tu-C19

Synthesis of Polyphenylene wires by Ullmann polymerization on a copper-oxide surface

Gianluca Galeotti¹, Marco Di Giovannantonio², Nicola Angelo Rana³, Maryam Ebrahimi¹, Josh Lipton-Duffin^{1,4}, Dmitrii F. Perepichka⁵, Giorgio Contini², Federico Rosei^{1,5}

¹Centre Énergie, Matériaux et Télécommunications, INRS, Varennes, Canada, ²Istituto di Struttura della Materia, CNR, Rome, Italy, ³Physics department, University of Roma Tor Vergata, Rome, Italy, ⁴CARF, Institute for Future Environments, Queensland University of Technology, Brisbane, Australia, ⁵Department of Chemistry and Center for Self-Assembled Chemical Structures, McGill University, Montreal, Canada

We present the results of a study of the surface-confined Ullmann coupling of 1,4-diiodobenzene (dIB) and 1,4-dibromobenzene (dBB) on Cu(110)-(2x1)O, to produce polyphenylene wires on an oxide surface. While Ullmann coupling is an established route for obtaining conjugated polymers on transition metals, [1] the presence of the host substrate is an obstacle to the integration of these polymers into devices. Oxygen passivation is a known method to modify the catalytic activity of the surface [2], and may be used to tune the electronic properties of the molecular layer. The (2x1)O superstructure on Cu(110) is simply obtained and provides an ideal testbed for exploring the possibility of decoupling the polymer from the catalyst. Scanning tunneling microscopy (STM) and X-ray photoelectron spectroscopy (XPS) show that polymers can be formed via Ullmann coupling on Cu(110)-(2x1)O. A comparison of the reaction on both the bare Cu(110), and the passivated Cu(110)-(2x1)O surfaces will be shown.

[1] M. Xi and B. E. Bent, JACS 1993, 115, 7426-7433; J. Lipton Duffin et al., Small 2009, 5, 592–597; L. Lafferentz et al., Nature Chemistry 2012, 4, 215–220

[2] M. El Garah et al., Chem. Asian J. 2013, 8, 1–6.

Tu-D15

Interfacial Properties of Colloidal Nanoparticles Studied In-Situ by Second Harmonic Scattering

Grazia Gonella¹¹Max Planck Institute for Polymer Research, Mainz, Germany

The field of nano-bio interactions, investigates how nanomaterials interact with biological systems. This is an important issue because, in order to be able to engineer nanostructures capable of traveling in the body and interacting with cells, we need to develop an understanding of how the physico-chemical properties of nanoparticles (NPs) affect the way these objects interact with biological systems. For instance, when considering a cancer nanomedicine different parameters have to be taken into consideration [1]. An understanding of how the NP size, shape, composition, structure, charge and surface chemistry influence transport to the tumor site [2] can help to maximize the efficiency of delivery of the drugs or contrast agents for imaging as well as the effectiveness of photothermal therapy [3]. Second harmonic scattering (SHS) is a coherent second-order optical technique that is specifically surface sensitive and can be performed in-situ [4]. It has been recently shown to be sensitive to size, shape and composition of metallic and dielectric NPs with or without adsorbed molecular monolayers. In this presentation, specific examples relative to the information from SHS experiments on the structure of, and kinetics at, the interface of nano-objects will be given [5].

[1] A. Albanese, et al.. Annu. Rev. Biomed. Eng. 2012, 14, 1.

[2] M. Ferrari. Trends Biotechnol. 2010, 28, 181.

[3] R. Bardhan, et al.. Adv. Func. Mater. (2009) 19, 3901.

[4] S. Roke and G. Gonella. Annu. Rev. Phys. Chem. 2012, 63, 353.

[5] S.-H. Jen, et al., J. Phys. Chem. A 2009, 113, 4758; S.-H. Jen, et al., J. Phys. Chem. C 2010, 114, 4302; W. Gan et al. J. Chem. Phys. 2011, 134, 041104; G.Gonella and H.-L. Dai, Phys. Rev. B 2011, 84, 121402; G.Gonella, et al., J. Phys. Chem. Lett. 2012, 3, 2877. G. Gonella and H.-L. Dai, Langmuir 2014, 30, 2588. B. Xu, et al., J. Phys. Chem. B 2015, 119, 5454

Tu-D16

The Calcite {10.4}/Alcohol Interface: A Simple Model System for Studying Rock-Oil Interfaces

Sepideh Sadat Hakim¹, Henning O. Sørensen¹, Nicolas Bovet¹, Jakob Bohr², Robert Feidenhans'l³, Susan L. S. Stipp¹

¹Department of Chemistry, University of Copenhagen, Copenhagen, Denmark,

²DTU NanoTech, Technical University of Denmark, Kgs. Lyngby, Denmark,

³Niels Bohr Institute, University of Copenhagen, Copenhagen, Denmark

Determination of structure and interactions at the interfaces between mineral surfaces and various organic compounds is of particular interest for a number of industrial and environmental applications. Chalk, a rock almost exclusively composed of submicrometer sized calcite crystals, is the host of most Danish natural resources, e.g. drinking water aquifers and oil reservoirs. Crystallization of calcite plays a crucial role in functioning of many organisms, where crystal growth, in biomineralization process is controlled by the presence of biological macromolecules. Furthermore, interaction of calcite surface with organic compounds provides a simple model system to study wetting behavior and flow properties of rocks in oil recovery and contamination remediation. It is possible to compare the results obtained on the calcite {10.4} surface with rock salt samples, because the cleaved {10.4} surface of the rhombohedral crystal system has the structure of a distorted rock salt surface. Previous studies using atomic force microscopy (AFM), X-ray photoelectron spectroscopy (XPS), X-ray reflectivity (XRR) and molecular dynamic (MD) simulations have shown that ethanol forms semi-ordered layers on calcite surfaces with a different density from the bulk liquid. In the present study, we use XRR to study the calcite {10.4} surfaces cleaved in two other alcohols; isopropanol and methanol. XRR is the technique particularly well suited for investigating the characteristics of thin layers on flat surfaces. The main aim in this project is to investigate the density profile and the thickness of the ordered layers of the alcohols that are adsorbed on calcite {10.4} surface, which allows us to develop a surface model that explains this ordering behavior on the calcite surface. The experiments have been performed at I811 beamline at the MAX-IV Laboratory, Lund, Sweden.

Tu-D17+18

Collective behavior at electrochemical interfaces

David Limmer¹¹Princeton University, Princeton, United States

Solvated interfaces are of fundamental importance to the development of renewable energy resources and energy storage devices. The properties of such interfaces are traditionally rationalized within a mean-field or continuum limit, which renders their behavior as a simple combination of the known bulk properties of electrode and solution. Increasingly, surface-sensitive measurements and molecular simulation are providing a much richer picture of these interfaces. In my talk, I will describe systems that exhibit important spatiotemporal correlations and result in a variety of emergent behaviors.

Tu-D19

Effects of pH and ionic strength on the surface charge density of self assembled monolayers (SAM)

Mats H.M. Olsson¹, Jesper Matthiesen¹, Søren Dobberschütz¹, Martin P. Andersson¹, Nina R. Pedersen¹, Tue Hassenkam¹, Lijuan Shi¹, Susan L.S. Stipp¹

¹Nano-Science Center, Department of Chemistry, Copenhagen University, Copenhagen, Denmark

The properties of a surface depend very much on its surface charge density and polarity. Charged or highly polar surfaces are usually hydrophilic and interact strongly with polar molecules. In some cases, such surface-organic affinities enhance organic compound adsorption. Surface charge density is therefore also important in making our society more sustainable through, for example, designing new material properties, filtering drinking water, ensuring safe CO₂ storage and enhancing oil recovery. In this study, we have used ionizable COOH-terminated self assembled monolayers (SAM) to investigate the effect of solvent pH and ionic strength on surface charge density. We set up different models for the effective charge-charge interaction between neighboring COO⁻ groups and calculated the fraction of deprotonated SAMs for various ionic strengths. The effective pK_a value for the SAM is substantially higher than the monomer value at low salinity because of the increased charge-charge interaction between neighbors. As ionic strength decreases, the titration curves become flatter and deviate significantly from the standard Henderson-Hasselbalch expression. The result we obtain from our models are nicely consistent with data from chemical force microscopy. We have also investigated how homogenization of ionisable surface groups affects its properties, i.e. 1) how clustering vs. homogeneously dispersed functional groups affect surface charge density at various pH and ionic strength values and 2) how the in plane interactions between surface ionizable groups interact, compared with standard, simplified Coulomb interactions. The homogenization works well for randomly distributed ionizable sites when the surface charge density is low, whereas the homogenized surface charge density deviates significantly when surface sites are clustered or when the surface charge density is high. This suggests that models using a homogeneous, equispaced surface charge distribution give an idealized and sometimes over simplified view about surface properties.

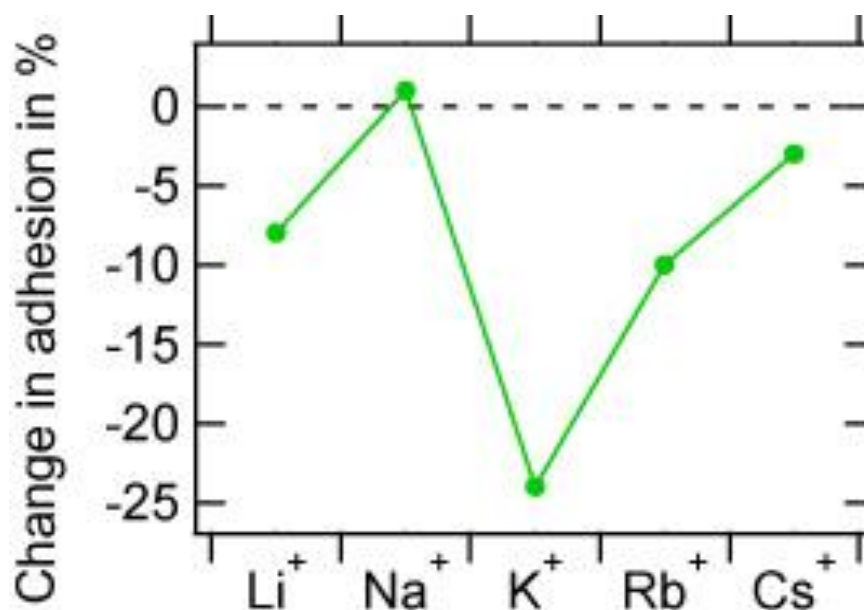
Tu-D20

Interaction of alkali and alkali earth metal ions with benzene self-assembled monolayers

Jesper Matthiesen¹, Morten Rikken¹, Martin P. Andersson¹, Nico Bovet¹, Tue Hassenkam¹, Susan L. S. Stipp¹

¹Nano-Science Center, Dept. of Chemistry, University of Copenhagen, Copenhagen, Denmark

We have explored the interaction of alkali (Li^+ , Na^+ , K^+ , Rb^+ , Cs^+) and alkaline earth (Mg^{2+} , Ca^{2+} , Sr^{2+} , Ba^{2+}) metal ions with surfaces functionalized with benzene terminated molecules because such interactions are found throughout nature and specifically are important for the so-called low salinity enhanced oil recovery. We used a flat, gold coated substrate and a gold coated atomic force microscopy (AFM) tip, that were both functionalized with 11-phenoxyundecane-1-thiol. We measured the adhesion between tip and substrate in solutions of the chloride salts of the nine metal ions. Additional information regarding the binding of metal ions to the benzene terminated layers was obtained using X-ray photoelectron spectroscopy (XPS) and density functional theory (DFT) calculations. The alkali metal ions Na^+ and Cs^+ affected the adhesion very little, whereas Li^+ , K^+ and Rb^+ all lead to a significant decrease in adhesion compared with the adhesion in pure water (Figure). The adhesion decrease correlates well with the calculated binding energies of these ions to benzene from DFT. This suggests that the adhesion decrease is caused by charging of the benzene coated surfaces. For the alkaline earth metal ions, the adhesion trend, as atomic number increases from Mg^{2+} to Ba^{2+} , is similar to the trend for the alkali ions. Adhesion is highest for Ca^{2+} . The behaviour of the monovalent and the divalent series of ions underlines the importance of both charge and size for determining interactions even with a nonpolar molecule, such as benzene.



Tu-E15

Surface-assisted Dehydrogenative Homo-coupling of Porphyrin Molecules

Alissa Wiengarten¹, Knud Seufert^{1,2}, Wilhelm Auwärter¹, David Écija^{1,3}, Katharina Diller^{1,4}, Francesco Allegretti¹, Felix Bischoff¹, Sybille Fischer¹, David A. Duncan^{1,5}, Anthoula C. Papageorgiou¹, habil. Florian Klappenberger¹, Robert G. Acres⁶, Yuanqin He¹, Jacob Dücke¹, Manuela Garnica Alonso¹, Johannes V. Barth¹

¹Physik Department E20, Technische Universität München, Munich, Germany,

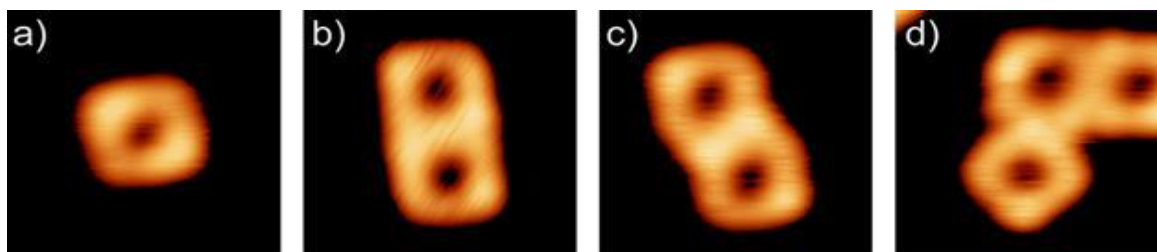
²Karl-Franzens-Universität Graz, Graz, Austria, ³IMDEA NANOSCIENCE, Madrid, Spain, ⁴École polytechnique fédérale de Lausanne, Lausanne, Switzerland, ⁵Diamond Light Source, Didcot, United Kingdom, ⁶Elettra-Sincrotrone Trieste, Trieste, Italy

The templated synthesis of porphyrin dimers, oligomers, and tapes has recently attracted considerable interest due to their potential application in molecular electronics and their tunable optical properties.[1] Here, the temperature-induced covalent dehydrogenative coupling between metal-free and Co-porphine units is discussed. On a heated Ag(111) support dimers, trimers and larger oligomers are formed under ultra-high-vacuum conditions,[2] reminiscent of porphyrin tapes in solution.[3] Our multi-technique approach including scanning tunneling microscopy, high resolution atomic force microscopy, near-edge X-ray absorption fine structure and photoelectron spectroscopy complemented by theoretical modeling allows a comprehensive characterization of the resulting nanostructures. For both molecules distinct coupling motifs are identified, however their occurrence and thus the structure of the oligomers is different for the metalated and the metal-free porphine. The attachment of substituents introduces additional coupling configurations. As reported for porphyrin tapes in solution, we observe a decrease of the electronic gap and a modification of the frontier orbitals directly associated with the formation of triply-fused dimeric species. This on-surface reaction mechanism offers prospects for model systems addressable with sub-molecular resolution, and opens pathways to extended oligomers with tailored chemical and physical properties.

[1] S. Mohnani and D. Bonifazi *Coord. Chem. Rev.* 254, 2342 (2010); W. Auwärter et al. *Nat. Chem.* 7, 105 (2015)

[2] A. Wiengarten et al. *J. Am. Chem. Soc.* 136, 9346 (2014)

[3] A. Tsuda and A. Osuka *Science* 293, 79 (2001)



Tu-E16

Revisiting the CO chemisorption on stepped Pt(111) with a curved crystal surface: imaging step-density dependent properties

Enrique Ortega^{1,2,3}, Andrew Walter^{3,4}, Jorge Lobo-Checa², Frederik Schiller², Martina Corso², D. Antón Brion³, Pepa Cabrera-San Félix³, Daniel Sánchez-Portal², Florian Bertram⁵, Johan Gustafson⁵, Lindsay Merte⁵, Edvin Lundgren⁵

¹Universidad del País Vasco, San Sebastian, Spain, ²Centro de Física de Materiales Centro Mixto CSIC-UPV/EHU, San Sebastian, Spain, ³Donostia International Physics Center DIPC, San Sebastian, Spain, ⁴Brookhaven National Laboratory, Upton, USA, ⁵Lund University, Lund, Sweden

Stepped surfaces featuring arrays of atomic steps of lattice constant d are known to strongly influence relevant surface phenomena, such as chemical reactions. Using surfaces with curved shape one can smoothly vary the step-density $1/d$ on a single sample, allowing a rational assessment of the influence of steps on surface chemical reactions. Here we utilize a curved Pt(111) surface to revisit the chemisorption of CO on stepped Pt(111). We demonstrate the enormous potential of the curved surface approach, not only to study molecule/surface chemistry problems, but also to reveal subtle $1/d$ properties of stepped surfaces, which straightforwardly arise by scanning the curved surface with spectroscopic and microscopic probes. Our systematic STM analysis is focused on the statistical distribution of the steps. Such study allows the striking, direct observation of the universal transition from entropic repulsion to energetically-interacting steps. The entropic regime applies in sparse step lattices ($1/d \ll 1$), whereas at higher $1/d$ values the elastic strain field of contiguous steps overlaps, effectively leading to a mutual repulsive interaction. Such increasing strain in surface atoms is evidenced in the $1/d$ -dependent shift of the Pt 4f surface core-level, imaged by a direct XPS scan on the curved surface. For the CO/Pt(111) problem the curved surface allows the straightforward determination of the known hierarchy in surface adsorption sites, namely, step preference versus terrace, and on-top chemisorption for B-type steps versus on-top and bridge for A type. At low doses, the $1/d$ C1s scan of the curved surface reflects a rapid $1/d$ -dependent transition from CO-covered to CO-free terraces, which is explained as due to CO migration and attachment to step edges. At CO saturation we discover a characteristic C 1s core-level shift that mirrors the variable strain of the underlying Pt substrate.

Tu-E17

Model Systems for Co Fischer-Tropsch catalysts: STM investigations of alkali metal on Co single crystal surfaces

Marie Strømsheim¹, Ingeborg-Helene Svenum², Anne Borg³, Hilde Johnsen Venvik¹

¹Department of Chemical Engineering, Norwegian University of Science and Technology (NTNU), Trondheim, Norway, ²SINTEF Materials and Chemistry, Trondheim, Norway, ³Department of Physics, Norwegian University of Science and Technology (NTNU), Trondheim, Norway

In Fischer-Tropsch synthesis (FTS) [1] natural gas, biomass or coal are converted to liquid fuels via synthesis gas. Alkali metals (AM) strongly inhibit the FTS activity [2] of Co-based catalysts. However, FTS experiments over 20wt%Co/0.5wt%Re/ γ -Al₂O₃-supported catalysts with AM impurity loadings up to 1000 ppm found that while the catalytic activity decreased, the H₂ chemisorption properties [2] and the H₂ and CO differential heats of adsorption [3] remained unaffected. In the present work, we study AM deposited on Co single crystal surfaces, and their influence on synthesis gas adsorption to elucidate this inhibition effect. Alkali metal adsorption sites at submonolayer coverage on the Co(11-20) surface and subsequent CO adsorption behavior have been investigated by Scanning Tunneling Microscopy (STM). Complementary Density Functional Theory (DFT) calculations have been carried out using the Vienna Ab initio Simulation Package (VASP) [4], which utilizes pseudo-potentials and plane wave basis sets. Figure 1 shows the atomic structure (a) and typical step edges (b) of the clean Co(11-20) surface. Step edges after deposition of submonolayer amounts of K are displayed in (c). From the changes observed at the step edges after K deposition, it is conjectured that K may be decorating the step edges of the Co(11-20) surface, as was observed for adsorption of K on the Ni(100)(2×2)p4g-N surface [5]. Results from adsorption experiments on alkali-precovered Co will be presented and discussed along with relevant comparison to modelling investigations.

- [1] F. Fischer Tropsch, H., Brennstoff-Chem. 4 (1923).
- [2] C. Balonek et al., Catal. Letters 138 (2010) 8.
- [3] E. Patanou et al., Ind. Eng. Chem. Res. 53 (2014) 1787.
- [4] G. Kresse, J. Hafner, Phys. Rev. B 47 (1993) 558.
- [5] A.G. Norris et al., Surf. Sci. 424 (1999) 74.

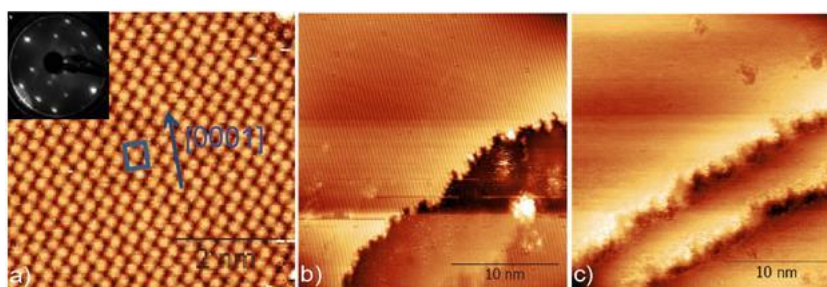


Figure 1: a) and b) STM images of clean Co(11-20), and c) after submonolayer deposition of K. The unit cell, and [0001]-direction for the clean structure is indicated, along with the corresponding LEED pattern.

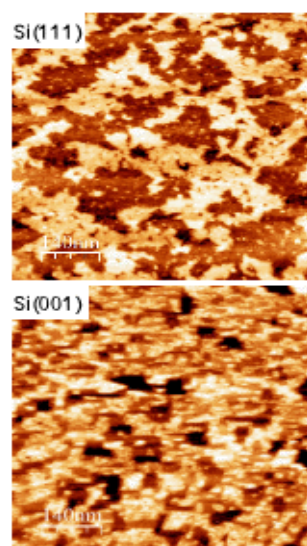
Tu-E18

Strain-induced oxide decomposition at SiO₂/Si(001) and SiO₂/Si(111) interfaces studied by X-ray photoelectron spectroscopy and scanning tunnelling microscopy

Jiayi Tang¹, Shuichi Ogawa¹, Akitaka Yoshigoe², Yuden Teraoka², Yuji Takakuwa¹

¹Tohoku University, Sendai, Japan, ²Japan Atomic Energy Agency, Sayo, Japan

Thermal decomposition of SiO₂ layers formed on Si substrate is well known to proceed via the inhomogeneous void nucleation and subsequent 2D enlargement. As reported previously, Si adatom migrating within the clean void area is associated with the 2D void enlargement. However, the void nucleation mechanism, that is, what is a driving force for the void nucleation, is still not clear yet. In this study, the thermal decomposition kinetics of SiO₂/Si(001) and SiO₂/Si(111) substrates were observed in real time by X-ray photoelectron spectroscopy using synchrotron radiation at SPring-8 to obtain simultaneously information on the interfacial strained Si atom as well as the oxide thickness and oxidation states. Si(001) and Si(111) surfaces were oxidized at 100°C, 300°C, and 500°C at a O₂ pressure of 4.6×10⁻⁵ Pa and then annealed at 650°C during decomposition. Si 2p components of dimer Si atoms were used as an indicator of void appearance. It was found that Si 2p components of Si^α and Si^β, which indicate the compressive and tensile strain of Si atoms at the interface, respectively, increased corresponding to the decrease of oxide until the voids appeared. After the void appearance, the amount of Si^α and Si^β remained unchanged regardless of the 2D void enlargement. In order to interpret the relation of the interfacial strain and oxide decomposition during the void nucleation, we propose a reaction model that the oxidation-induced strain causes a point defect generation at the interface and the resultant emitted Si atom is responsible for the decomposition species of SiO. In addition, the inhomogeneous point defect generation is assumed to accumulate the interfacial strain, resulting in the acceleration of oxide decomposition and eventually the appearance of void. We examine this model for the different amount of Si^α and Si^β before decomposition prepared by the different oxidation temperature on Si(001) and Si(111).



Tu-E19

Carbon dioxide activation on model Fe₃O₄ (111) thin films

Francesca Mirabella¹, Francisco Ivars¹, Petr Dementyev¹, Svetlana Schauermann¹, Hans-Joachim Freund¹

¹Fritz-Haber-Institut der Max-Planck-Gesellschaft, Berlin, Germany

The activation of small molecules on oxide surfaces is an important elementary step in many catalytic reactions. Of particular interest is the use of CO₂ as sustainable and readily available feedstock. Efficient and inexpensive conversion of CO₂ by partial hydrogenation into valuable chemicals (e.g. methanol) holds great potential to contribute to reducing CO₂ emission into the atmosphere. Activation and splitting of CO₂ are the most important and challenging steps in this process because of the difficulties associated with the chemical inertness of this molecule. In this study, the adsorption and chemical transformations of CO₂ on Fe₃O₄ (111) thin films grown on Pt (111) single crystal substrates were investigated by isothermal molecular beam, infrared reflection-absorption spectroscopy (IRAS) and temperature-programmed desorption (TPD) experiments under ultra-high vacuum conditions. Our primary goal was elucidation of the atomistic details of these processes finding direct correlations between the surface structure of iron oxide and CO₂ activation. Particularly, adsorption and transformations of CO₂ were investigated as a function of surface temperature and CO₂ surface coverage. Different chemical behavior was observed at different surface temperatures: in particular pronounced chemical transformations were spectroscopically detected between 140 K and 160 K. These changes in the spectroscopic signatures can be clearly related to strong interaction and activation of CO₂ on Fe₃O₄ (111). In order to assign the IRAS vibrational bands related to these newly formed chemical species, experiments with isotopically labelled ¹³CO₂ and C¹⁸O₂ as well as CO₂ adsorption on labelled (¹⁸O) iron oxide were carried out. Additionally, CO₂ co-adsorption with water, which is known to dissociate on iron oxide forming OH groups, was investigated to explore the possibility to hydrogenate CO₂ using water as a cheap ecological stock. Clear changes in CO₂ chemical transformations were detected that can be related to CO₂ interaction with the co-adsorbed OH species.

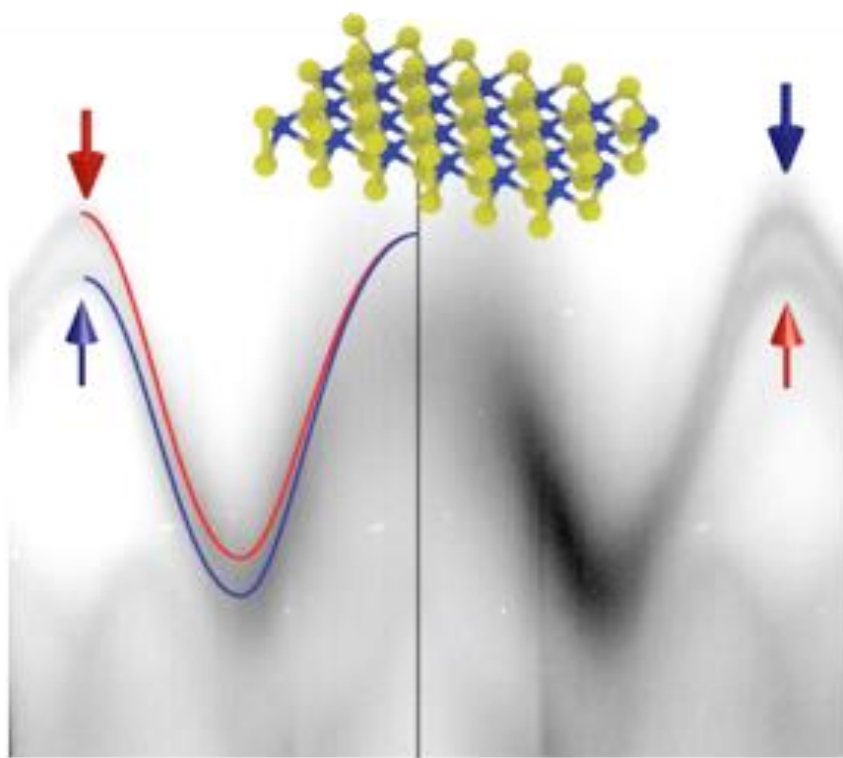
Tu-A21+22

Electronic Structure and Electron Dynamics in Two-Dimensional Materials

Philip Hofmann¹

¹Aarhus Universitet, Denmark

Changing the dimensionality of a material results in significant modifications of its electronic properties. This is even the case if the parent material already has a layered structure with little interaction between the layers, as in the case of graphene, and the layered transition metal chalcogenides. This talk discusses the possibility to epitaxially grow high-quality two-dimensional materials on single crystal surface, such that they can be used for electronic structure investigations by time- and angle-resolved photoemission spectroscopy. Results of such studies are presented for graphene, bilayer graphene and single-layer MoS₂.



Tu-A23

Mini-gaps in the electronic structure of graphene on Pt vicinal surface

Arlensiú Eréndira Celis Retana^{1,2}, Maya Narayanan Nair³, Amina Taleb-Ibrahimi³, Antonio Tejeda Gala^{1,2}

¹Laboratoire de Physique des Solides - Université Paris Sud, CNRS UMR 8502, Orsay, France, ²Synchrotron SOLEIL, L'Orme des Merisiers, Saint Aubin, Gif-sur-Yvette, France, ³UR1 CNRS/Synchrotron SOLEIL, L'Orme des Merisiers, Saint Aubin, Gif-sur-Yvette, France

From a technological point of view it is desired to tailor the electronic states of a system, which can be done by producing nanostructures and controlling their size. Fundamental studies have been performed for instance on noble metal surfaces where the Shockley surface state feels a superperiodic potential giving rise to electronic confinement [1, 2]. Here graphene grown on vicinal Pt presents a band-gap opening that we associate to the superperiodicity of graphene on the surface. Graphene is grown by Chemical Vapor Deposition (CVD) of ethylene on a metallic curved Pt substrate. Since Pt is a catalytic metal, the CVD technique allows the decomposition of ethylene at the hot substrate surface to form a continuous graphene layer. The curvature of the substrate allows to access at the same time the (111) surface, as well as different vicinal surfaces. The Gr/Pt system was then characterized by Scanning Tunneling Microscopy (STM) and Angle Resolved Photoemission (ARPES) in order to correlate its atomic and electronic structure as a function of the vicinality. STM measurements show that graphene is continuous across the steps, while we observe a bandgap opening on the graphene electronic bands related to the vicinal periodicity of the underlying Pt surface.

[1] Didiot, C., Tejeda, A., Fagot-Revurat, Y., Repain, V., Kierren, B., Rousset, S. and Malterre, D. Interacting quantum box superlattice by self-organized Co nanodots on Au(788). *Physical Review B* 76, 081404(R) (2007).

[2] Mugarza, A., Mascaraque, A., Pérez-Dieste, V., Repain, V., Rousset, S., Garcia de Abajo, F. J. and Ortega, J. E. Electron Confinement in Surface States on a Stepped Gold Surface Revealed by Angle-Resolved Photoemission. *Physical Review Letters* 87, 107601 (2001).

Tu-A24

Tuneable band gap opening in graphene by high-temperature hydrogenation

Jakob Jørgensen¹, Richard Balog^{1,2}, Antonija Grubisic Cabo¹, Line Kyhl Hansen¹, Liv Hornekær¹

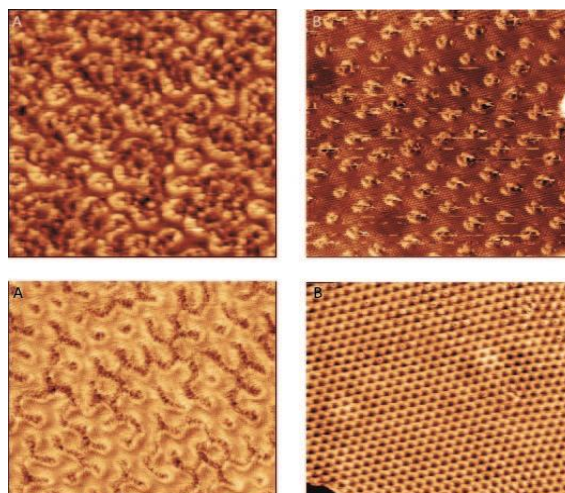
¹Aarhus University, Aarhus C, Denmark, ²Nanogune, San Sebastian, Spain

Functionalization of graphene on Ir(111) with hydrogen represents a possible route towards a band gap opening in the otherwise semimetallic material.[1] XPS data on hydrogenated graphene on Ir(111) have shown that hydrogen binds to the carbon atoms of graphene with different energies depending on the carbon position in the Moiré superstructure[2]. Here we present a combined Scanning Tunnelling Microscopy (STM) and angle resolved photoemission spectroscopy (ARPES) study of hydrogen structures and the corresponding band gaps obtained following exposure of a hot graphene coated Ir(111) surface to atomic hydrogen. The hot surface favours the binding of hydrogen only in the most stable positions yielding a well organized hexagonal pattern of hydrogen clusters. Images suggest that the clusters are confined to the FCC sites of the Moiré [3] pattern contrary to room temperature deposition where extended clusters are observed. ARPES measurements reveal a highly tunable band gap depending on the sample temperature during hydrogenation with values ranging from 450 meV at room temperature, 281 meV at 645K to 148 meV at 675K. We are thus able to tune the gap merely by adjusting the sample temperature. These findings are of interest for attempts to control graphene electronic properties. The size of the bandgap can be fine tuned by controlling the degree of hydrogenation. Furthermore, the hydrogen pattern can act as a template for second step functionalization opening the possibility for patterned functionalizing of graphene with larger molecules.

[1] Balog, R., et al., Bandgap opening in graphene induced by patterned hydrogen adsorption. *Nature Materials*, 2010. 9(4): p. 315-319.

[2] Balog, R., et al., Controlling Hydrogenation of Graphene on Ir(111). *ACS Nano*, 2013. 7(5): p. 3823-3832.

[3] N'Diaye, A.T., et al., Structure of epitaxial graphene on Ir(111). *New Journal of Physics*, 2008. 10: p. 16.



Tu-A25

Confinement effects in epitaxial graphene nanoflakes

Julia Tesch¹, Philipp Leicht¹, Felix Blumenschein¹, Anders Bergvall², Tomas Löfwander², Luca Gagnaniello¹, Mikhail Fonin¹

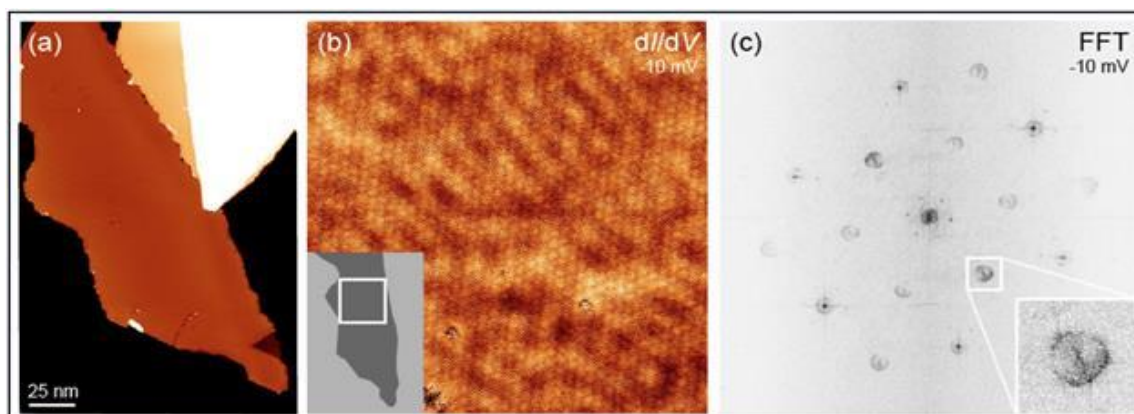
¹Universität Konstanz, Konstanz, Germany, ²Chalmers University of Technology, Gothenburg, Sweden

Graphene nanostructures represent an exciting topic for research, as a strong spatial confinement together with the edge structure impose new electronic properties, making them promising candidates for future nanoscale electronic units. By means of low-temperature scanning tunnelling microscopy and spectroscopy we investigate the electronic properties of elongated quasi-freestanding epitaxial graphene nanoflakes (GNFs) on Ag(111) and Au(111). Samples are prepared by temperature programmed growth of graphene flakes on Ir(111) and subsequent intercalation of noble metals. This procedure allows the fabrication of predominantly zigzag GNFs with single hydrogen termination and no substantial edge bonding towards the substrate [1]. We implement local density of states (LDOS) mapping to analyze standing wave patterns arising from elastic scattering processes within single GNFs [2]. Fourier analysis of the obtained LDOS maps shows that the characteristic ringlike features due to the intervalley and intravalley scattering observed for large graphene sheets are also visible on the GNFs with lateral sizes down to 20nm. For GNFs, additional features appear inside the ringlike structures, which can be related to the transverse confinement in a nanoflake [3]. Our experimental results are supported by tight-binding calculations of realistic flakes, which very well reproduce the experimentally observed fingerprints of confinement in the Fourier transform of the standing wave patterns and confirm the strong influence of edge type as well as confinement direction and dimensions on the scattering in GNFs.

[1] P. Leicht et al., ACS Nano, 8, 3735, (2014)

[2] G.M. Rutter et al., Science, 317, 219, (2007)

[3] A. Bergvall et al., Phys. Rev. B, 87, 205431, (2013)



Tu-A26

A structural and electronic characterisation of new C-C bond formation at the graphene basal plane.

Andrew Cassidy¹, Mikkel Kongsfelt², Jakob Jørgensen³, Steen Pederson², Kim Daasbjerg², Liv Hornekær¹

¹Aarhus University, Dep of Physics, Aarhus, Denmark, ²Aarhus University, Dep of Chemistry, Aarhus, Denmark, ³Aarhus University, iNano, Aarhus, Denmark

Creating sp^3 defect sites in an otherwise perfect sp^2 graphene lattice, in a controlled manner, has been shown to introduce a band gap in the electronic structure of graphene. Here, we exploit the Moire lattice which emerges following the epitaxial growth of graphene on an Ir(111) surface to create sp^3 defect sites, in patterned formation, on the graphene basal plane. Uniquely, these sp^3 defects are created by forming new C-C bonds to the graphene lattice, introducing new chemical functional groups to the graphene surface. The aromatic sp^2 C- bonds in the graphene lattice are thermodynamically stable and it requires highly reactive species to break the aromatic system and form new C-C bonds. This has directed research efforts towards the generation of reactive radical species in the vicinity of the graphene layer. Typically, therefore, reaction pathways rely on electron transfer between the graphene sheet and the reactant molecule to generate radicals, with reactions taking place in conducting solvents. The uneven distribution of electron-hole puddles in graphene has been shown to have a large effect on the success of many of these reactions, in particular reactions involving diazonium salts. We have used the thermal decomposition of triazene moieties, adsorbed as a molecular monolayer on a graphene sheet under ultra-high vacuum conditions, to produce aryl-radicals which subsequently react with and bind to the underlying graphene sheet. This clean, surface science approach to functionalizing the graphene basal plane allows us to follow this reaction with cryo-scanning tunnelling microscopy, x-ray photoelectron spectroscopy and angle-resolved photoemission spectroscopy. The results provide a detailed spatial and electronic profile of the chemically functionalised graphene sheet. X-ray photoemission spectroscopy confirms that new C-C bonds are formed while scanning tunnelling microscopy data shows that C-C bonds are selectively formed at preferred sites on the Moire pattern.

Tu-B21

Unique possibility of dual-use of Al₂O₃ layers in the functional nanostructures

Elena Filatova¹, Aleksei Konashuk¹, Marina Konyushenko¹, Sergei Sakhonenkov¹, Andrey Selivanov¹, Andrey Sokolov^{1,2}

¹St-Petersburg State University, St-Petersburg, Russian Federation,

²Helmholtz-Zentrum Berlin für Materialien und Energie GmbH, Berlin, Germany

Aluminum oxide is an important dielectric, ceramic and catalyst. Due to its wide band gap, low leakage current and modest value of dielectric constant Al₂O₃ is considered as a suitable insulator for various electronic applications ranging from gate dielectric in metal-oxide-semiconductor (MOS) transistors to trapping or blocking insulator in charge trapping non-volatile memory cells. Al₂O₃ is a unique material, which can be used both as oxygen scavenging and buffer layer depending on the material with which it contacts. In the current work we demonstrate the dual nature of the Al₂O₃ layers using x-ray spectroscopy. We discuss the different functionality of Al₂O₃ layers depending on its thickness and contact with metal or dielectric with reference to the functional nanostructures. It will be shown that oxygen scavenging provoked from Al₂O₃ layers in contact with metal can lead to the formation of polarized layer at the interface Al₂O₃/metal, which direct impact on the functionality of the devices. The inserting a thin (0.5 -3 nm) Al₂O₃ layer between dielectric/metal effectively prevents intermixing the adjacent layers. As an example, the inserting a thin layer of Al₂O₃ prevents intermixing of HfO₂ and TiN and results in essential decrease in the interlayer thickness in the system HfO₂/Al₂O₃/TiN/Si. The effect of ultra-thin Al₂O₃ layer (capping TiO₂ surface or inserting at the interface TiO₂/ITO or both cases) on the resistive switching process in TiO₂/ITO/metal (glass) assemblies depending on the thickness of active TiO₂ layer and material of the substrate are in the focus of this work and promote deeper understanding the resistive switching process. In the current work the joint electro-physical and spectroscopic researches (near edge x-ray absorption fine structure (NEXAFS) and hard x-ray photoelectron spectroscopy (HAXPES)) carried in the same point of the sample are discussed.

This work was supported by SPbSU grant 11.37.656.2013.

Tu-B22

Ab initio study of ways to improve adhesion at zinc/alumina interfaces

Ha-Linh Thi LE^{1,2,3}, Jacek Goniakowski^{1,2}, Claudine Noguera^{1,2}, Alexey Koltsov³, Jean-Michel Mataigne³

¹CNRS, UMR7588, Institut des Nanosciences de Paris, Paris, France,

²Sorbonne Universités, UPMC Univ Paris 06, UMR7588, INSP, Paris, France,

³ArcelorMittal Maizières Research, voie Romaine, Maizières lès Metz, France

Adhesion at zinc/alumina interfaces is one of the key issues in steel manufacturing industries, where galvanization is the most efficient way to protect steel against corrosion. Indeed, while enrichment in elements, such as Al, improves the strength of new steel grades, the selective oxidation of aluminum may lead to the formation of a quasi-continuous alumina film at the steel surface, which dramatically reduces zinc adhesion strength. In this context, we present an ab initio study of the role of interfacial buffer layers to improve the adhesion at alumina/zinc interface. We show that, while interaction of Zn with α -Al₂O₃(0001) is weak [1, 2], the introduction of a thin Cr or Ni layer at the interface, substantially strengthens the adhesion. Moreover, since metallic buffers are likely oxidized under realistic conditions, we have extended the study as to take into account the formation of interface oxides (CrO_x or NiO_x). We show that an excess of oxygen may reduce considerably the favorable effect of the metal buffer. We rationalize the calculated separation energies with a bond analysis including the number and strength of interfacial metal-oxygen and metal-zinc bonds. Our study clearly shows that, under controlled conditions, Cr or Ni buffers can be used to improve the adhesion of anticorrosive zinc coatings in the case of Al-enriched steel grades.

[1] R. Cavallotti, J. Goniakowski, R. Lazzari, J. Jupille, A. Koltsov, and D. Loison, *J. Phys. Chem. C*, 2014, 118, 13578-13589.

[2] R. Cavallotti, PhD thesis, UPMC, Sorbonne Universités, 2014.

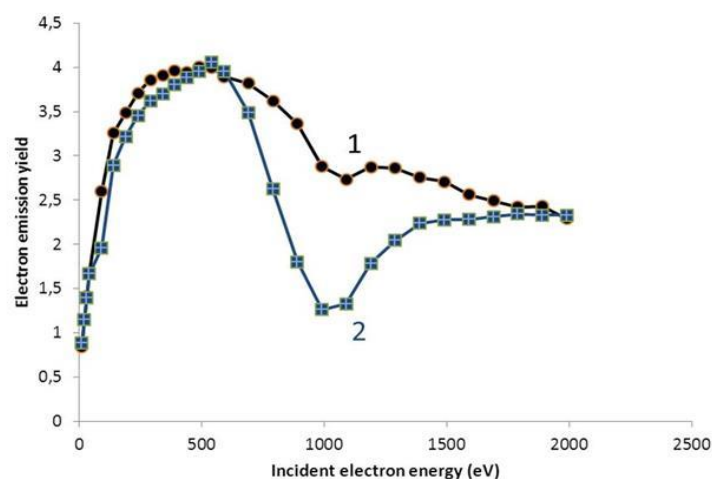
Tu-B23

Dielectric/metal structure: effect of the dielectric thickness on the secondary electron emission

Mohamed Belhaj¹, K. Makasheva², G. Teyssedre²¹ONERA - The French Aerospace Lab., Toulouse, France, ²LAPLACE - Lab. Plasma et Conversion d'Énergie, Université de Toulouse; CNRS, UPS, INPT, Toulouse, France

Secondary and backscattered electron emission from solids submitted to electron-irradiation is of considerable interest in many fields of science and technology: electron beam analyse techniques, electron lithography, study of the behaviour of satellites charging processes in orbit submitted to irradiation, field emission display technologies, Hall effect thrusters. Regardless the specific area of interest, the knowledge of the electron emission yield (EEY) is highly requested. The EEY is the number of emitted electrons (secondary and backscattered) with respect to the incident electrons number. In some applications, low EEY is needed (rf components, spacecraft materials) in others conversely a high yield is needed (electron amplifiers). One interesting approach that could be used to tune the EEY is to coat the material by very thin dielectric layer. Two different techniques were applied for the sample elaboration: (1) thermal growth and (2) plasma deposition process. Very thin SiO₂ layers (up to 100 nm) were thermally grown on highly doped Si-substrates at 1100°C under slightly oxidizing atmosphere using N₂-O₂ gas mixture with 1% O₂. Plasma SiO₂ layers were deposited in the plasma of radiofrequency capacitively coupled discharge sustained at low pressure in a mixture of argon-hexamethyldisiloxane-oxygen (Ar-HMDSO-O₂). The layer thicknesses were measured by spectroscopic ellipsometry. In this work, we show that the thickness of the dielectric layer as well as its microstructure affect significantly the electron emission processes (see Fig 1). Based on our experimental results, we show that this result is mainly due to the sensitivity of the transport of the secondary electron undergoing emission on both the dielectric microstructure and the inner electric field. Practical consequences and potential applications of the presented results will be discussed during the conference.

Figure 1: EEY of SiO₂/Si as function of the incident electron energy at normal incidence and room temperature. Curve 1: 10 nm of thermal SiO₂ and curve 2: 90 nm of thermal SiO₂.



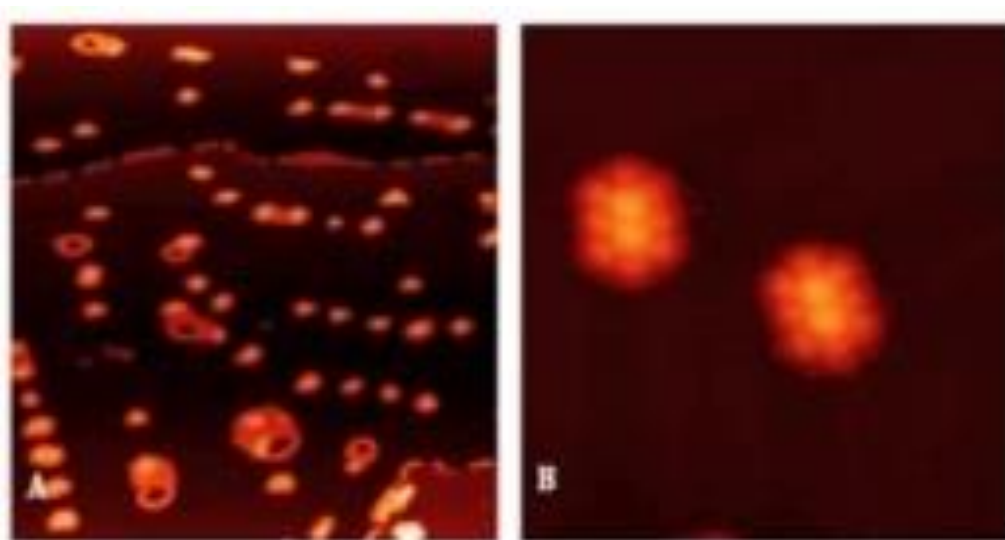
Tu-C21

Investigating the size distribution of $(C_{60})_m-Au_n$ clusters on Au (111) with a VT-STMMahroo Rokni Fard¹, Dogan Kaya¹, Quanmin Guo¹¹Nanoscale Physics Research Laboratory, School of Physics and Astronomy, University of Birmingham, Birmingham, United Kingdom

Self-assembly of organic molecules such as C_{60} has been intensely investigated, due to their potential in nano-scale molecular devices. Recently our group reported the formation of $(C_{60})_m-Au_n$ clusters with regular shapes and sizes. These clusters are formed by sequential deposition of Au and C_{60} on a clean Au (111) sample at 110 K under UHV conditions. Temperature of the sample was then slowly increased to room temperature that resulted in the formation of thermally stable structures [1]. Here we report improvements on size selection of stable clusters by varying the amount of Au and C_{60} . We find that the $(C_{60})_m-Au_n$ Cluster shift to larger sizes when we increase the material deposited.

[1] Y.C.Xie, L.Tang and Q.Guo, Phys. Rev. Lett. 111, 186101 (2013).

A) Stable structures formed at RT. 90 nm × 90 nm $V = -1.61$ V, $I = 0.05$ nA. B) $(C_{60})_{10}$ Clusters.



Tu-C22

Synthesis of Core Shell Heterogeneous Nanowires with Strong Raman Enhancement

Isabel Pita^{1,3}, Shalini Singh^{2,3}, Christophe Silien^{1,3}, Kevin Ryan^{2,3}, Ning Liu^{1,3}

¹Department of Physics and Energy, University of Limerick, Limerick, Ireland,

²Department of Chemical and Environmental Science, University of Limerick, Limerick, Ireland, ³Materials and Surface Science Institute, University of Limerick, Limerick, Ireland

A method has been developed for the wet synthesis of core shell heterogeneous nanowires which demonstrate strong Raman enhancement, and are suitable for probe tip incorporation. In this synthesis silver nanowires were grown, using soft solution phase synthesis, to act as the metallic core of the nanowire. A thin 5-10 nm thick insulating layer of silica was then grown around the nanowires using a modification of the well documented Stöber method. Heteroaggregation was used to attach an outer semiconductor layer to the nanowires, as this method allowed for close packing of nanoparticles on the surface. This was achieved by dispersing the nanowires into Toluene solutions containing Cadmium Selenide (CdSe) nanoparticles (NPs). Coverage of the NPs on the nanowire surface improved with increasing nanoparticle size, something which we have attributed to Van der Waals interactions between the NPs and wire surface which overcomes the steric repulsion. The Raman and photoluminescence properties of the completed nanowires were obtained using a 532 nm 1 mW laser. The results indicated a fluorescence peak at 650 nm and Raman bands at 210 cm^{-1} and 410 cm^{-1} , corresponding to the LO and its overtone of CdSe. The intensities of these properties varied depending on the thickness of the silica, due to interactions between the metal and semiconductor layers, resulting in strong Raman enhancement in the bands of the nanowires when compared to a CdSe monolayer. The nanowire's unique shape and enhanced Raman spectra, through propagating surface plasmons, gives them an advantage over plain CdSe or metal tips for signal detection, and makes their potential for sensor tip incorporation apparent.

Tu-C23

Lead nanoribbons on the Si(553) and Si(110) surfaces

Marek Kopciuszynski¹, Ryszard Zdyb¹, Paweł Dyniec¹, Mariusz Krawiec¹,
Mieczysław Jałochowski¹

¹Maria Curie-Skłodowska University, Lublin, Poland

Silicon vicinal surfaces are composed of flat terraces separated by atomic steps. The tilt angle in respect to a low index plane defines the separation between steps and therefore width of structures that may be formed on each terrace. The Si(553) and Si(110) surfaces have similar symmetry and may serve as templates for the formation of one-dimensional structures with high atomic number elements like Au, Bi and Pb through a self-organization [1-4]. Those systems may be also good candidates for the investigation of the Rashba effect in one-dimensional metallic structures. In this contribution we report the crystallographic and electronic properties of the Si(553)-Pb and Si(110)-Pb surfaces investigated with the reflection high energy electron diffraction (RHEED), scanning tunnelling microscopy (STM), spin and angle resolved photoelectron spectroscopy (SARPES) techniques. Deposition of 1.4 monolayers Pb with subsequent annealing at 260°C results in the formation of quasi one dimensional ribbons. The width of the structures obtained on the Si(553) and Si(110) substrates are surprisingly similar 1.46 nm and 1.63 nm, respectively. The Pb ribbons are parallel to the [1-10]. The electronic structure shows highly anisotropic metallic bands with parabolic dispersion in the [1-10] direction.

This work was partially supported by the National Science Centre under Grant 2013/11/B/ST3/04003.

- [1] J. N. Crain et. al, Phys. Rev. B 69, 125401 (2004)
- [2] P. Nita et. al, Phys. Rev. B 84, 085453 (2011)
- [3] M. Kopciuszynski et. al, Phys. Rev. B 88, 155431 (2013)
- [4] M. Kopciuszynski et. al, Appl. Surf. Sci. 305, 139 (2014)

Tu-C24

Annealing temperature induced self-organization of thin Au layer deposited on Ge(001) reconstructed surface studied by high-resolution electron microscopy

Benedykt R. Jany¹, Marek Nikiel¹, Konrad Szajna¹, Dominik Wrana¹, Nicolas Gauquelin², Johan Verbeeck², Franciszek Krok¹

¹Marian Smoluchowski Institute of Physics, Jagiellonian University Krakow, Krakow, Poland, ²EMAT University of Antwerp, Antwerp, Belgium

The self-organized gold nanostructures on Ge(001) surface are currently of special interest due to their applications for mono-molecular electronic devices. The understanding of electrical as well as physical properties of the system is of great importance. In the presentation, we report on studies concerning post-annealing induced nanostructures formation after room temperature deposition of thin film of Au on Ge(001) in UHV. Deposition of 6 ML of Au by MBE resulted in the formation of a continuous Au overlayer as checked by RHEED to be crystalline. Just after deposition, the samples were post-annealed in UHV to temperatures ranging from 473 K to 773 K. The self-organized structures, in form of atomic chains and Au nanoislands, were characterized by HR-SEM and HR-STEM methods.

It has been found that there exists preferred island's orientation along crystallographic direction of the substrate surface. For an annealing temperature close to the eutectic temperature of Au/Ge system (640 K), change in size and shape of Au nanoislands is observed, indicating eutectic melting of the system. The crystallographic orientation of single Au nanoislands was determined by EBSD. A (011) orientation of the Au islands with respect to Ge surface was discovered, independently of the annealing temperature. TEM measurements of Au/Ge(001) sample cross sections revealed that the nanoislands created upon annealing at $T < 640$ K are on top of the Ge(001) surface, while for $T > 640$ K part of the island is buried beneath the substrate surface, which confirms the eutectic AuGe melting. The crystallographic structure of the Au islands and the Au/Ge interface was studied by quantitative atomically resolved HAADF-STEM and supports the preferred (011) nanoisland orientation. The chemical composition of the Au/Ge atomic chains was uncovered using a combination of HAADF and EELS measurements and might indicate that the atomic chains have core/shell structure.

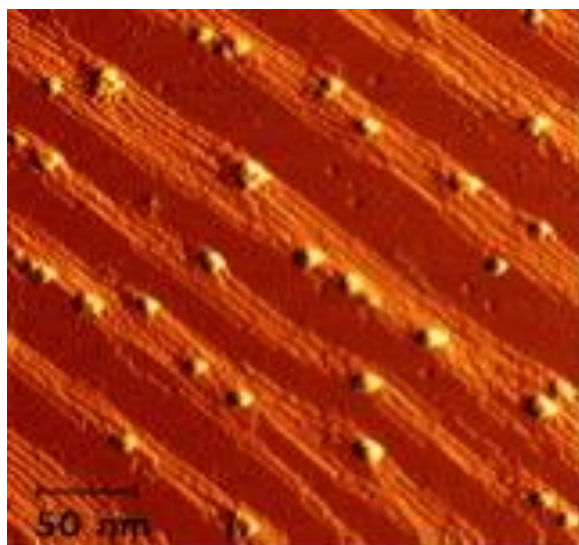
Tu-C25+26

Self-Organised Growth of Epitaxial Silicide Nanoislands

Ilan Goldfarb, Rachel Levy¹, Federico Cesura¹, Matan Dascalu¹, Yotam Camus¹, Jitendra Tripathi², Gil Markovich¹, Rajesh Chalasani¹, Amit Kohn¹

¹Tel Aviv University, Ramat Aviv, Tel Aviv, Israel, ²Purdue University, West Lafayette, USA

Many transition metal and rare earth silicides have been intensely studied in basic and applied science due to their good lattice match with silicon and interesting electronic, optical, and magnetic properties. However, such studies have been primarily focused on silicides in the form of thin films, such as intimate low-resistance contacts in traditional microelectronic architectures. Less is known about size-effects in silicide nanostructures, namely variation of the silicide properties in discrete nanometric islands rather than thin continuous films. The goal of this work has been two-fold: (a) to gain understanding of controlled self-assembled growth of silicide nanoislands, and of the (b) resulting size-effects. Self-organized mesoscopic ordering in several Me-Si (Me=Ti, Co, Fe, Ni, Er) nanometric systems on vicinal Si(111) and Si(001) surfaces will be demonstrated, along with their size/shape/order-dependent electronic and magnetic properties.



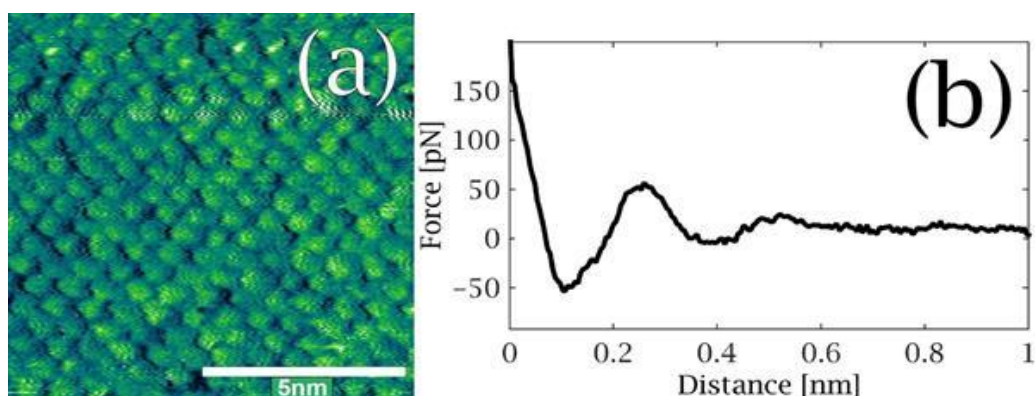
Tu-D21

An Ultra-Low Noise, Liquid Environment Atomic Force Microscope

Uri Sivan¹, Itai Schlesinger¹, Kfir Kuchuk¹

¹Dep. of Physics, Technion, Israel Institute of Technology, Haifa, Israel

The design considerations and eventual performance of a new, ultra-low noise FM-AFM, are presented. The microscope, designed specifically for the study of hydration layers and ion organization next to solid surfaces and biomolecules displays consistently total integrated noise levels well below 10 picometers. The sensitivity of the optical beam deflection sensor (OBD), operating at frequencies up to 9MHz is 10fm/Sqrt(Hz), allowing for the utilization of high frequency cantilevers of low thermal noise, as well as high harmonics imaging. A superior signal stability is achieved by replacing the commonly used laser diode with a Helium-Neon laser. Despite the long coherence length the microscope proves to be free of any speckle noise. Photothermal excitation of the cantilever by a second laser produces pure harmonic oscillations, minimizing the generation of deleterious sound waves characterizing the commonly used cantilever excitation by a piezoelectric crystal. To simplify construction, the OBD was designed to fit on top of a commercial Multimode® piezo tube and accommodate the latter's commercial liquid cell. The corresponding compact design results in extraordinarily low levels of mechanical noise. The performance of the new AFM is demonstrated by high quality atomic resolution imaging and 3D force spectroscopy of mica and HOPG surfaces under aqueous solution. An example of such unfiltered high-resolution image and force vs. distance curve over mica surface is shown in Figure 1.



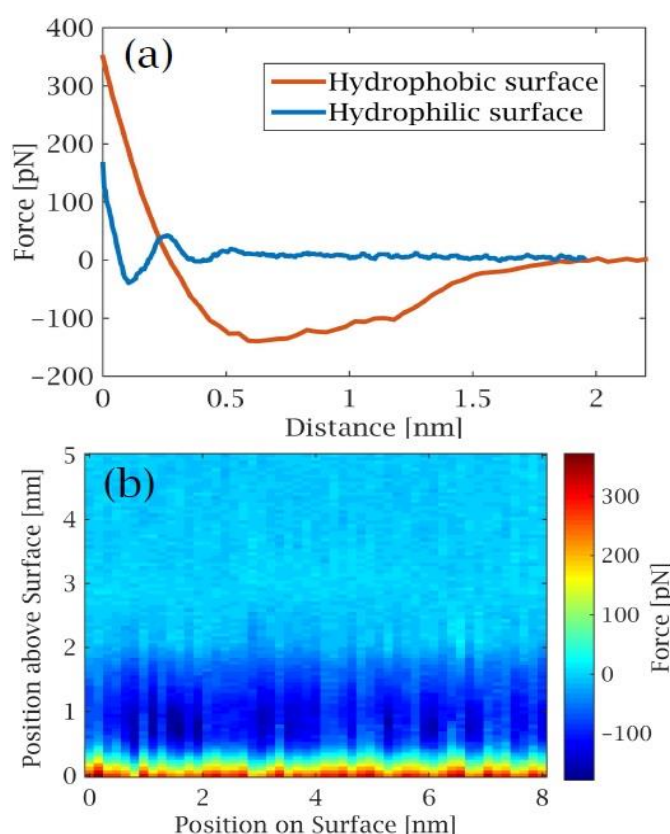
Tu-D22

The hydrophobic interaction probed by high resolution 3d force spectroscopy in water

Itai Schlesinger¹, Uri Sivan¹

¹Technion, Israel Institute of Technology, Haifa, Israel

After two centuries of research, the origin of hydrophobic interactions in aqueous solution remains elusive largely due to the absence of experimental tools capable of probing the short-range physics at high enough resolution. Early attempts to probe this interaction using surface force apparatus and colloidal AFM have led to conflicting results which were eventually traced to sample inhomogeneity or instabilities associated with bubble formation. At any rate, those attempts lacked the 3D atomic resolution needed for the construction of a microscopic, fundamental theory for such a short-range phenomenon and particularly for answering the long standing question of water density next to a hydrophobic surface. In the present contribution we take these studies a significant step forward by applying atomic resolution liquid FM-AFM to study water ordering near several hydrophobic and hydrophilic surfaces and cantilever tips. The forces acting between hydrophilic mica and hydrophobic HOPG surfaces and a hydrophilic SiO₂ tip are depicted in Figure 1(a). In accordance with previous reports we attribute the exponentially growing oscillatory force in the hydrophilic surface case to the removal of water layers when the two surfaces approach each other. The force acting between a hydrophobic surface and a hydrophilic tip is profoundly different showing long range (~1.8nm) attraction and no sign of oscillations. Three dimensional force maps were collected above the surfaces to retrieve information about the spatial dependence of the force. Figure 1(b) shows a section cut from a larger 3D force map above an HOPG surface. The data sets constraints on possible models to be discussed at the conference.



Tu-D23

Force reconstruction from dynamic AFM on differently terminated thiol SAMs

Annalisa Calò¹, María José Esplandiu², Sergio Santos³, Albert Verdaguer²

¹nanoGUNE, San Sebastian-Donostia, Spain, ²ICN2, Bellaterra, Spain, ³iEnergy Masdar Institute of Science and Technology, Abu Dhabi, United Arab Emirates

Dynamic AFM modes have been proven to be a powerful tool to characterize inorganic surfaces and to study water/solid interfaces in ambient conditions and complex phenomena as nanoscale wetting [1, 2]. Static force curves and maps collected in DC mode suffer the jump-to-contact instability where information in a range of distances before mechanical contact is lost, especially when experiments are performed in air. The use of dynamic modes enhances the vertical resolution in force spectroscopy experiments, as a proper choice of the operational parameters allows recovering the full tip-sample interaction force without discontinuities [3]. Furthermore, a main advantage of dynamic modes over DC modes relies on the capacity to simultaneously probe conservative and dissipative forces during tip approach and scanning [4]. In previous studies we demonstrated that the force reconstruction method from amplitude modulation AFM allows recognizing nanoscale capillary interactions acting between adsorbed water layers on top of the tip and the surface on wet inorganic crystals [2,5]. In this work we applied the same method to characterize the surface of thiol self-assembled monolayers (SAMs) in dry conditions. Highly crystalline, flat gold surfaces containing methyl- and carboxy-terminated ordered SAMs monolayers were prepared that are topographically undistinguishable. Force, dissipated energy and phase difference profiles vs. distance were compared, especially in the non-contact region, where the main differences between the two surfaces are expected due to the different surface chemistry. Experimental data were compared with theoretical predictions [6].

- [1] V. Barcons et al., J. Phys. Chem. C 2012, 116, 7757.
- [2] A. Calò et al., J. Phys. Chem. C 2015, 119, 8258.
- [3] S. Santos et al., J. Phys. Chem. C 2013, 117, 10615.
- [4] J. P. Cleveland et al., Appl. Phys. Lett. 1998, 72, 2613.
- [5] A. Calò et al., Beilstein J. Nanotechnol. 2015, 6, 809.
- [6] K. R. Gadelrab et al., J. Phys. D: Appl. Phys. 2012, 45, 012002.

Tu-D24

How nanobubbles nucleate at a hydrophobic/water interface

Ing-Shouh Hwang¹, Chung-Kai Fang¹, Hsien-Chen Ko¹, Chih-Wen Yang¹,
Yi-Hsien Lu¹

¹Academia Sinica, Taipei, Taiwan

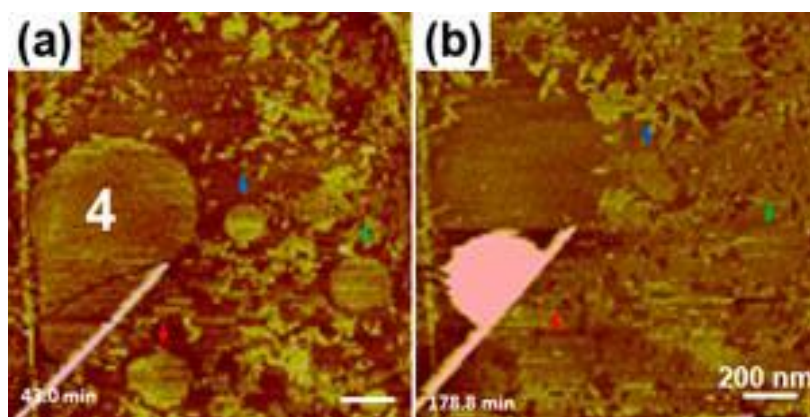
Nanobubbles at solid/water interface, often called surface nanobubbles or interfacial nanobubbles (INBs), have attracted much attention because of their great fundamental and applied interest [1,2]. Most studies so far focus on why INBs exhibit a high stability and their rather flat morphology; however, there is no consensus yet. In addition, the nature of INBs remains highly debated. Here we employ advanced atomic force microscopy techniques, frequency-modulation and PeakForce modes, to image the initial evolution of various gas-containing structures at a graphite/water interface using air-supersaturated water. Two competing processes are observed. A fluid phase first appears as a circular wetting layer of approximately 0.3 nm thick within minutes of water deposition. It grows laterally but is confined at a later time. At a certain point, there is a transition from the fluid layer to a three-dimensional (3D) cap-shaped structure, or an INB (Fig. 1). The detailed transformation process varies with the lateral dimension of the confined fluid region. In addition, we observe nucleation and slow growth of small gas-containing ordered domains [3,4]. They appear outside or at the perimeter of the fluid structures, which eventually confine the fluid regions in the lateral dimension and limit the growth of the fluid structures only in the vertical direction. Scenarios are proposed to explain the evolution of the interfacial structures of gases. This study provides important clues about the microscopic interactions among gas molecules, water, and hydrophobic solids and may better understanding various phenomena of gas at hydrophobic/water interfaces.

[1] J.R.T. Seddon and D. Lohse, *J. Phys.: Condens. Matter* 23, 133001 (2011).

[2] V.S.J. Craig, *Soft Matter* 7, 40 (2011).

[3] Y.-H. Lu, C.-W. Yang, and I.-S. Hwang, *Langmuir* 28, 12691 (2012).

[4] Y.-H. Lu, C.-W. Yang, C.-K. Fang, H.-C. Ko, I.-S. Hwang, *Scientific Reports* 4, 7189 (2014).



Tu-D25

Friction Reduction for Nanobubble at Water-HOPG Interface

Chih-Wen Yang¹, Hsien-Chen Ko¹, Ren-Feng Ding¹, Ing-Shouh Hwang¹

¹Institute of Physics, Academia Sinica, Taipei, Taiwan

Presence of nanobubbles at the interfaces between water and hydrophobic solids was first proposed in 1994. Many studies using atomic force microscopy (AFM) have confirmed existence of these interfacial nanobubbles. Those studies also show that nanobubbles are soft and deformable nanostructures (height of 1.5-100 nm and diameter of 40-2000 nm). Previous AFM studies measure the out-of-plane mechanical properties of nanobubbles at water/solid interface. In this work, we present lateral force imaging on nanobubbles at the HOPG/water interface based on contact mode operation. We have obtained the mapping of both the height and lateral force (Figures 1a-1c). Figures 1 (d) and (e) show the height profile and the corresponding trace and retrace lateral forces measured at a nanobubble near the bottom. A large hysteresis loop in the trace and retrace lateral forces is clearly seen for most parts of the interface, but, surprisingly, the hysteresis gap almost disappears when the tip scans over the nanobubble. This indicates strong friction-reduction when the tip scans over a nanobubble. In addition to nanobubbles, a certain degree of friction reduction is seen when the tip scans over a micropancake, as indicated by a black-arrow in Figure 1(e). The friction reduction on nanobubbles is most dramatic and we have seen zero hysteresis gap on nanobubbles occasionally, indicating that nanobubbles are the nearly friction-free regions for the tip to scan over the solid/water interface. Our force-displacement measurement indicates a snap-in followed by a constant compliance region when the tip gets in contact with a nanobubble. The lateral force recorded simultaneously indicates a twisting behavior of the cantilever very similar to its normal deflection. The measurements suggest occurrence of contact line pinning when the tip touches a nanobubble. The new finding reported in this work may better understanding of nanobubbles at liquid-solid interfaces.

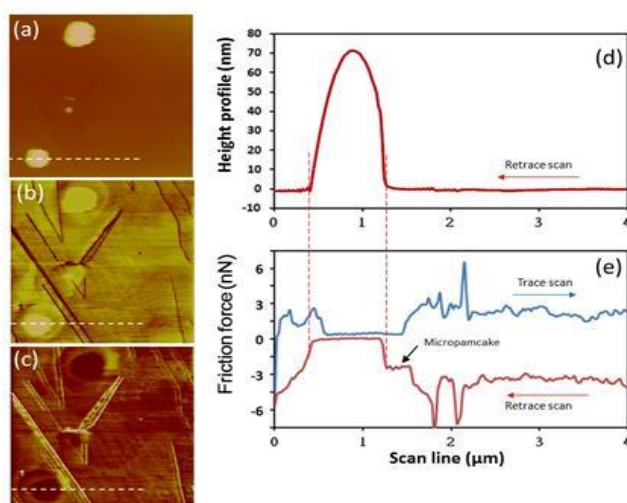


Figure 1. Height image (a) and retrace lateral force image (b) and trace lateral force image (c) of a water-HOPG interface taken with the contact mode. Height (d) and lateral force profiles (e) are measured along the dash lines shown in (a), (b) and (c), respectively. The scan rate is 5 Hz/line; normal setpoint force ~ -50 pN, $k_s \sim 0.08$ N/m.

Tu-E21

Strong metal-support interaction between Pt and Fe₃O₄: The support effects.

Ke Zhang¹, Shamil Shaikhutdinov¹, Hans-Joachim Freund¹

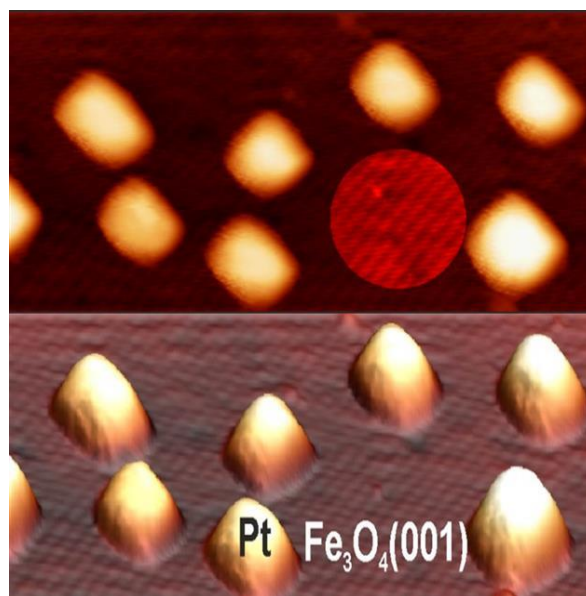
¹Fritz Haber Institute of the Max Planck Society, Berlin, Germany

We studied nucleation, growth and thermal stability of Pt deposited on the ($\sqrt{2}\times\sqrt{2}$)R45° reconstructed surface of Fe₃O₄(001) thin films grown on Pt(100). At low coverages, Pt preferentially adsorbs monoatomically on the so-called “narrow” sites, i.e. in the same manner as previously reported for Ag[1], Pd[2] and Au[3] ad-atoms supported on a Fe₃O₄(001) single crystal. At higher coverages, UHV annealing above 700 K leads to Pt sintering and concomitantly to re-shaping (at ~1000 K) into cuboid Pt nanoparticles, with edges oriented along the crystallographic directions of the Fe₃O₄(001) surface. In addition, high-temperature annealing suppresses CO adsorption on Pt, thus manifesting a strong metal-support interaction (SMSI) via Pt encapsulation by the oxide support. Combined LEED, STM and TPD results provide strong evidences for encapsulating overlayer to be identified as FeO(111). The results are compared with the Pt/Fe₃O₄(111) system, also showing the encapsulation of (111)-oriented, hemispherical Pt nanoparticles by the FeO(111) layer. The comparison of two systems suggests that the SMSI effect via encapsulation is rather insensitive to the surface structure of oxide, although the latter strongly affects the particle morphology.

[1] a)Z. Novotný, G. Argentero, Z. Wang, M. Schmid, U. Diebold, G. S. Parkinson, Phys. Rev. Lett. 2012, 108, 216103; b)N. Spiridis, E. Madej, J. Korecki, J. Phys. Chem. C 2014, 118, 2011-2017; c)K. Jordan, S. Murphy, I. V. Shvets, Surf. Sci. 2006, 600, 5150-5157.

[2] G. S. Parkinson, Z. Novotny, G. Argentero, M. Schmid, J. Pavelec, R. Kosak, P. Blaha, U. Diebold, Nat. Mater. 2013, 12, 724-728.

[3] R. Bliem, R. Kosak, L. Perneczky, Z. Novotny, O. Gamba, D. Fobes, Z. Mao, M. Schmid, P. Blaha, U. Diebold, G. S. Parkinson, ACS Nano 2014, 8, 7531-7537.



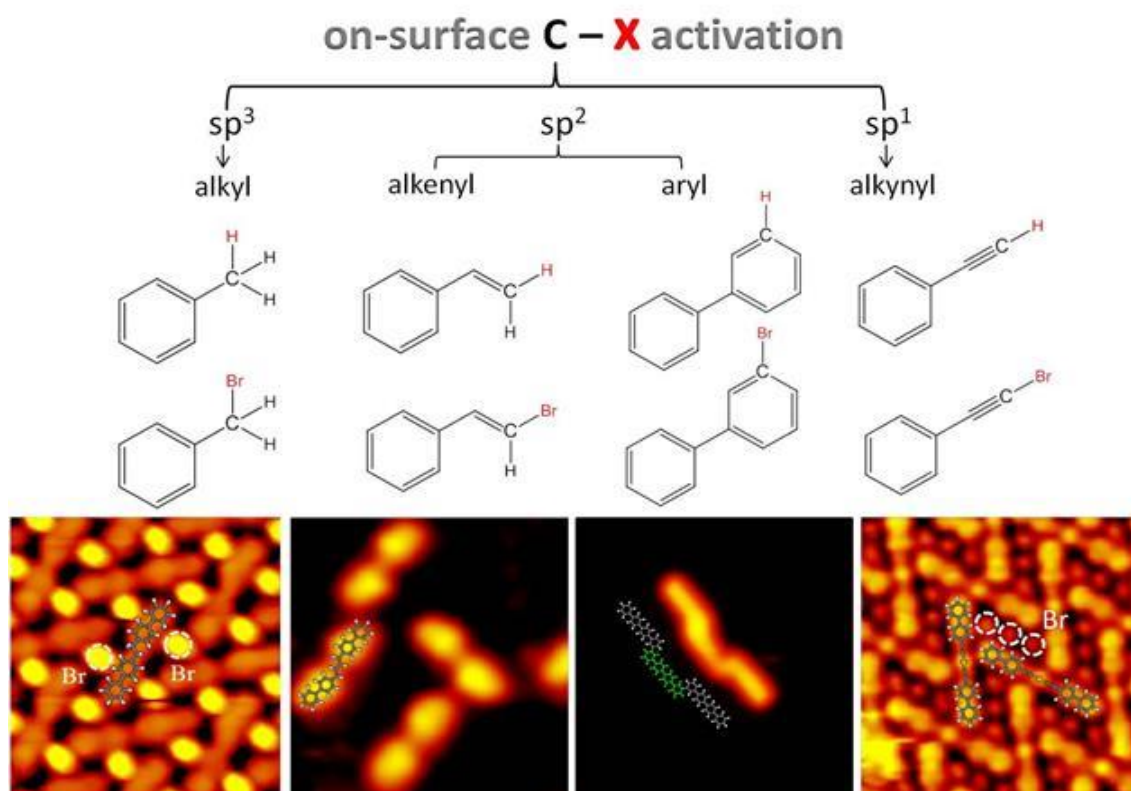
Tu-E22

Atomic-insight into the on-surface C-X bond activation

Qiang Sun¹, Wei Xu¹Tongji University, Shanghai, China

Recently, on-surface chemistry involving hydrocarbons has aroused great attention due to its fascinating potential in constructing novel carbon nanostructures. In particular, C-C coupling between reactants by cleaving the pre-defined C-X groups (X stands for hydrogen and halogens) followed by forming new carbon-carbon bonds, represents one of the best choices.

Here, by real space direct visualization at submolecular scale in combination with density functional theory calculations, we have shown a comprehensive picture of the on-surfaces C-X bond activations and their different C-C coupling scenarios on surfaces, which involve: (1) different carbon species including alkynyl (sp^1), alkenyl (sp^2) alkyl (sp^3) and aryl (sp^2) groups. (2) dehydrogenation or dehalogenation. These findings have given us a general understanding of the different chemical properties between different C-X bonds on metal surfaces, and provided fruitful strategies for synthesis of novel complexes and construction of advanced carbon nanostructures on surfaces.



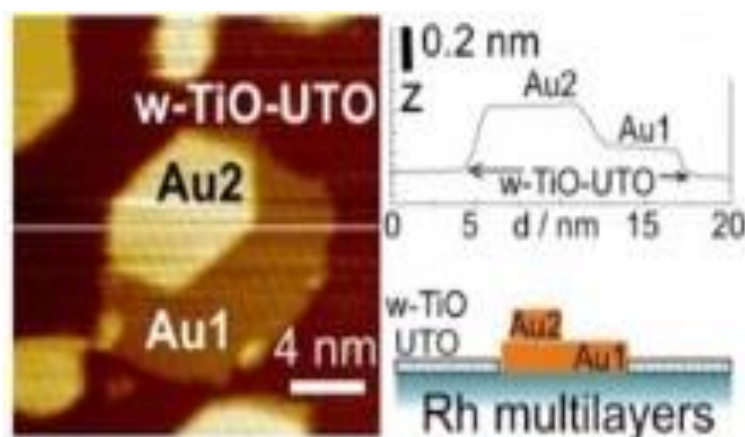
Tu-E23

STM-visualization of site selective adsorption of CO and O₂ around the 1D interface formed between mono-(bi-)layer Au and w-TiO-UTO films supported on Rh(111)András Berkó¹, Richárd Gubó², Zoltán Kónya^{1,2}¹MTA-SZTE Reaction Kinetics and Surface Chemistry Research Group, Szeged, Hungary, ²SZTE TTK Department of Applied and Environmental Chemistry, Szeged, Hungary

Formation of CO₂ through low temperature CO+O₂ reaction proceeds with high efficiency over Au/TiO₂ catalysts. It was previously revealed by kinetic measurements that the metal/oxide interface, more precisely, the 1D perimeter line of the supported Au nanoparticles is probably active for the dissociation of O₂, while the low coordinated metal atoms of Au nanoparticles show high activity for CO adsorption [1]. In a recent paper we presented a special model system in which a 1D interface is formed between quasi-monoatomic Au and wheel-like ultrathin TiO_x oxide (w-TiO-UTO) layers supported on Rh(111) [2]. This system shown in Figure 1 was exposed to CO or O₂ in a wide pressure range of 10⁻⁵-10¹ Pa at room temperature. Following the different gas exposures STM images were recorded at 300 K in UHV. A clear difference was detected between the cases of CO and O₂ treatments. As an effect of CO, the step atoms of the second layer of Au particles (Au₂) were reactive resulting in a complete disruption of this layer, while only a slight morphological change was observed on the w-TiO-UTO film or at the Au₁/w-TiO-UTO interface. In contrast to this behaviour, the exposure to O₂ resulted in an intensive structural modification of the Au₁/w-TiO-UTO interface regions. The presented STM images strongly support the above assumptions deduced from the kinetic measurements and provide a clear visualization of the site selective adsorption of CO and O₂.

[1] M. M. Schubert et al., J. Catal. 197 (2001) 113.

[2] R. Gubó et al., Langmuir 30 (2014) 14545.



Tu-E24

Eley-Rideal Type Mechanism of Formate Synthesis from Carbon Dioxide on Cu Surfaces

Takahiro Kondo¹, Jiamei Quan¹, Tetsuya Ogawa¹, Guichang Wang², Junji Nakamura¹

¹University of Tsukuba, Tsukuba, Japan, ²Nankai University, Tianjin, China

Formate synthesis on Cu surface ($\text{CO}_2 + \text{H(a)} \rightarrow \text{COOH(a)}$) is an initial step of the methanol synthesis reaction which is one of the most promising conversion methods of CO_2 into a useful chemical feedstock. Our previous kinetic analysis of formate synthesis suggests that the mechanism of the reaction can be an Eley-Rideal type, in which gaseous CO_2 directly reacts with hydrogen atoms on Cu surfaces [1]. In this work, to prove the mechanism of formate synthesis on Cu surface directly, we have examined the effect of the translational and vibrational energies of CO_2 molecules on the formate synthesis by using supersonic molecular beam technique. Firstly, hydrogen atoms were pre-adsorbed on Cu single crystals (Cu(111) or Cu(110)) with hot tungsten filament. Then CO_2 molecular beam seeded in He ($\text{CO}_2:\text{He} = 1:9$) was irradiated to the surface at 170 K (or 250 K). The relationship between the incident energy of CO_2 molecules and the amount of formate formation was investigated by TPD. It has been found that the formate was formed when we irradiated CO_2 beam ($3.3 \times 10^5 \text{ L}$) at the nozzle temperature over 950 K. This indicates that translational and/or vibrational energies of CO_2 are used for the formate synthesis, while surface temperature is irrespective to the formate synthesis. Our DFT calculations also suggests that the formate synthesis proceeds via Eley-Rideal type mechanism, where CO_2 directly reacts with H on Cu without adsorption process on Cu surface. The part of the activation barrier is found to be composed by the Pauli repulsion between CO_2 and H/Cu surface and OCO angle is found to bend just before the transition state. These results are consistent with our experimental results and suggest that both translational and vibrational energies are used for formate synthesis.

[1] H.Nakano, I.Nakamura, T.Fujitani, J.Nakamura, J. Phys. Chem. B 2001, 105, 1355.

Tu-E25

Photocatalytic and Photoelectrochemical Properties of Lanthanide-doped-Aurivillius Phase Layered Perovskites

Ceren Yılmaz¹, Uğur Ünal^{1,2,3}¹Chemistry Department, Koc University, Sarıyer/İstanbul, Turkey, ²Graduate School of Science and Engineering, Koc University, Sarıyer/İstanbul, Turkey,³Koc University Surface Science and Technology Center (KUYTAM), Sarıyer/İstanbul, Turkey

Photocatalysis is an attractive and promising future technology for renewable and sustainable energy challenge which includes clean energy production (H_2 production from water splitting), decrease in the CO_2 emission levels (by CO_2 reduction) and elimination of hazardous organic pollutants under solar light or other illuminating light source. Bi_2WO_6 has been evaluated as a new kind of photocatalyst. Although, $Bi_2W_2O_9$ has been reported to display photocatalytic activity over ten times higher than Bi_2WO_6 for H_2 evolution and O_2 evolution under UV radiation, [1] there are few reports on $Bi_2W_2O_9$ as a photocatalyst. In this work, we studied photocatalytic and photoelectrochemical properties of lanthanide-doped $Bi_2W_2O_9$ powders. Visible-light harvesting $Bi_2W_2O_9$ photocatalysts doped with Pr(III), Nd(III), Tm(III), Ho(III) and Ce(IV) were prepared by solid-state synthesis. The obtained products were characterized by SEM, EDX, XRD, XPS and DRS technologies. The photocatalytic activities of the photocatalysts were evaluated by the decolorization of rhodamineB (RhB) in aqueous solution under visible light (>420 nm) and stimulated sunlight (AM1.5 air filter, 100 mW/cm^2) irradiation. Photoelectrochemical behavior of the powders in correlation with photocatalytic activity was also investigated. The effect of dopant identity and concentration on optical and photoelectrochemical properties of the lanthanide-doped- $Bi_2W_2O_9$ powders will be discussed.

We would like to acknowledge TUBITAK for funding through project 114Z452 (Synthesis of two dimensional luminescent perovskite nanosheets).

[1] Kudo A., Hiji S., Chem. Lett. 28 (1999) 1103–1104

We-A01

Non-collinear magnetic order in artificial mono-atomic wires driven by competing exchange interactions

María Moro-Lagares^{1,2}, M. Carmen Martínez-Velarte^{1,2}, Luis Morellón^{1,2},
Ricardo Ibarra^{1,2}, David Serrate^{1,2}

¹INA-LMA, University of Zaragoza, Zaragoza, Spain, ²Dept. Física de la Materia Condensada, University of Zaragoza, Zaragoza, Spain

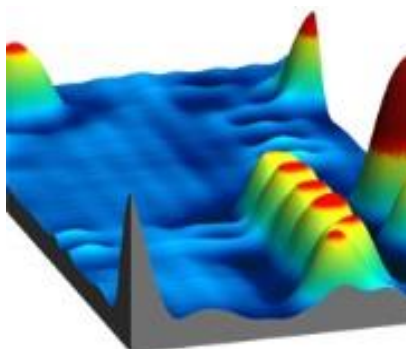
The spin degree of freedom in one-dimensional (1-D) structures of transition metal atoms is at the frontiers of spintronic research. Compared to larger structures, 1-D magnetic objects exhibit low coordination number, quantum confinement effects and enhanced magnetocrystalline anisotropy, which provide unexplored functionalities towards controlling the flow and storage of information. Owing to the complexity of fabricating and probing 1-D atomic wires, few experimental works are available to back the theoretical progress. Successful approaches to this challenge have been the formation of free standing monoatomic wires in break junctions [1] or the self-assembly of quasi 1-D structures over reconstructed surfaces [2]. In this work, we make use of the often praised ability of a scanning tunnelling microscope (STM) to engineer nanostructures atom-by-atom. We have built Co atomic wires over the non-collinear Mn/W(110) magnetic template[3]. In this way, the spin alignment imposed by the substrate can be tuned by choosing the wire construction direction. Instead of investigating the wire's ground state through the magnetic excitation spectra, as in the case of Mn chains on Cu₂N[4], we obtain direct evidence of each atom's spin state by means of spin-polarized STM. The competition between the Co spin coupling to the magnetic substrate and the direct Co-Co exchange interaction allows us to infer that the direct interatomic exchange interaction is antiferromagnetic in nature. When both interactions are of different sign, the wire ground state is found to be non-collinear.

[1] M.R. Calvo et al., Nature 458, 1150 (2009) // F. Strigl et al., Nature Commun. 6, 6182 (2015)

[2] P. Gambardella et al., Nature 416, 301 (2002) // M. Menzel et al., Phys. Rev. Lett. 108, 197204 (2012)

[3] M. Bode et al., Nature 447, 190 (2007)

[4] C.F. Hirjibehedin et al., Science 312, 1021 (2006)



We-A02

Fingerprints of Degenerate and Non-Degenerate Spin Centers in Transport and Force Measurements by STM/AFM

Peter Jacobson¹, Matthias Muenks¹, Gennadii Laskin¹, Tobias Herden¹, Oleg Brovko², Valeri Stepanyuk², Markus Ternes¹, Klaus Kern^{1,3}

¹Max Planck Institute for Solid State Research, Stuttgart, Germany, ²Max Planck Institute of Microstructure Physics, Halle, Germany, ³Institute de Physique de la Matière Condensée, École Polytechnique Fédérale de Lausanne, Lausanne, Switzerland

To engineer the magnetism of quantum devices, it is necessary to quantify how the structural and chemical environment of the junction influences the spin. Metrics such as coordination number or symmetry provide a simple method to quantify the local environment, but neglect the many-body interactions of an impurity spin when coupled to contacts. We have utilized the highly corrugated hexagonal boron nitride (h-BN) monolayer to mediate the coupling between a cobalt spin in CoH_x (x=1,2) complexes and the metal contact. While the number of hydrogen controls the total effective spin, the corrugation is found to smoothly tune the Kondo exchange interaction between the spin and the underlying metal. Using scanning tunneling microscopy and spectroscopy together with numerical simulations, we quantitatively demonstrate how the Kondo exchange interaction mimics chemical tailoring and changes the magnetic anisotropy.

These results are complemented by atomic force microscopy measurements on CoH_x spin centers at 1 K. Frequency Shift-Distance measurements show distinct behavior for spin 1/2 and spin 1 complexes. Converting the frequency shift to force using the Sader-Jarvis algorithm we are able to determine and compare how the short range forces decay for these dissimilar spins systems. Interestingly, the force decay constant for the two spin species differs by a factor of 2. The behavior of the decay constant will be discussed in terms of quantum degeneracy between the tip and surface adatom. These results set the stage for purely force-based measurements of single spin centers in the absence of inelastic electron tunneling processes.

We-A03

Spin Interface of Organic-Ferromagnetic Heterojunction

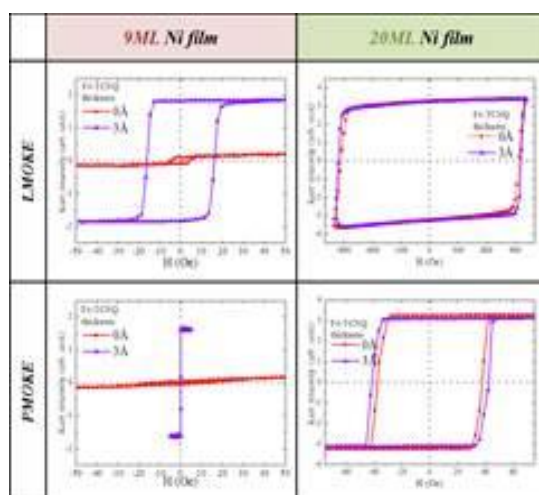
Yao-Jane Hsu^{1,5}, Po-Hung Chen², Yu-Ling Lai¹, Ming-Wei Lin¹, Tu-Ngoc Lam³, Der-Hsin Wei¹, Hong-Ji Lin¹, Jeng-Han Wang⁴

¹National Synchrotron Radiation Research Center, Hsinchu, Taiwan ,

²Department of Engineering and System Science, National Tsing Hua University, Hsinchu, Taiwan , ³Institute of Nanotechnology, National Chiao Tung University, Hsinchu, Taiwan, ⁴Department of Chemistry, National Taiwan Normal University, Taipei, Taiwan, ⁵Institute of Electro-Optical Science and Engineering, National Cheng Kung University, Tainan, Taiwan

Organic spintronics with organic tailored functionality and enduring spin coherence have attracted growing interest. However, the interplay between ferromagnetic electrodes and organic layers critically affects the efficiency of spin filtering in the devices. A fundamental understanding on the hybridized properties at organic-ferromagnetic heterostructure is hence important. We investigated the spin interface in terms of electronic structure and magnetic coupling of tetrafluorotetracyanoquinodimethane (F₄-TCNQ)-tailored nickel (Cu(100)/Ni) surface. Surface magnetic anisotropy performed by the magneto-optical Kerr effect (MOKE) displays magnetic hardening upon F₄-TCNQ adsorption. The magnetic domains inspected by photoelectron-emission microscope (PEEM) measurements also exhibits improved magnetic ordering with larger domain sizes and less domain boundary. To elucidate the origin of enhanced magnetic ordering after molecular tailoring, surface-sensitive and element specific X-ray Magnetic Circular Dichroism (XMCD) were employed. The XMCD reveals the orbital and spin moment of in-plane Ni is significantly increased, while that keep almost unaltered at out-of-plane. Through the strong superexchange coupling at in-plane, the nonmagnetic F₄-TCNQ is spin polarized. Our results suggest the enhanced magnetic ordering of such organic-ferromagnetic interface is an effective spin filtering for constructing high efficient organic spintronics.

- [1] Yao-Jane Hsu, et al., Phys. Rev. B. 91, 041204(R) (2015).
- [2] Yao-Jane Hsu, et al., J. Phys. Chem. Lett., 4, 310 (2013)
- [3] Yuet-Loy Chan, et al., Phys. Rev. Lett. 104, 177204 (2010).



We-A04

Magneto chemical interactions at the (CrTPP(Cl))/Co(001) interface

Fotini Ravani¹, Miloš Baljžović¹, Jan Girovsky¹, Kartick Tarafder^{2,3}, Christian Wäckerlin¹, Jan Nowakowski¹, Dorota Siewert⁴, Tatjana Hählen¹, Aneliia Shchyrba⁴, Armin Kleibert⁵, Nirmalya Ballav⁶, Thomas Jung¹, Peter Oppeneer²

¹Paul Scherrer Institut/Laboratory for Micro- and Nanotechnology, Villigen, Switzerland,

²Department of Physics and Astronomy, Uppsala, Sweden,

³Department of Physics, BITS-Pilani Hyderabad Campus, Shameerpet, India,

⁴Department of Physics, University of Basel, Basel, Switzerland, ⁵Swiss Light Source, Paul Scherrer Institute, Villigen, Switzerland, ⁶Department of Chemistry, Indian Institute of Science Education and Research, Pune, India

Fundamental insight into the origin of the physicochemical properties at interfaces, down to the level of the single electron/spin and molecule, is essential to understand the macroscopic behavior of spintronic interfaces and their implementation in future devices [1,2]. Among various systems screened, Cr-tetraphenylporphyrin chloride (CrTPP(Cl)) at the (CrTPP(Cl))/Co(001) interface, is magnetized by antiferromagnetic (AFM) exchange coupling up to room temperature and higher [3]. This unusual behavior is here investigated by element-specific x-ray absorption and x-ray magnetic circular dichroism spectroscopy, XAS and XMCD respectively, while the chemical state of the CrTPP(Cl) molecules is further probed by X-ray photoelectron spectroscopy (XPS). The discovered AFM coupling is assigned to interaction of the less than half-filled d shell of the high spin Cr ion in the Cr(II)TPP molecules with the substrate. In addition scanning tunneling microscopy (STM) provides information on the orientation and the shape of the CrTPP molecules on Co thick film. A statistical analysis of the adsorption sites of the molecules and their binding to chlorine is also addressed. The experimental results are analyzed and discussed in comparison to DFT+U calculations.

[1] A. Scheybal et al, Chem. Phys.Lett, 411, 214 (2005)

[2] H. Wende et al, Nat. Mater. 6, 516 (2007)

[3] J. Girovsky et al, Physical Review B 90, 220404(R) 2014

We-A05+06

Chiral magnetic textures stabilized by interfaces: from domain walls to skyrmions

Stanislas Rohart¹

¹Université Paris-Sud, Orsay, France

The lack of inversion symmetry at interfaces, combined with spin-orbit interaction is at the origin of an additional magnetic coupling called Dzyaloshinskii-Moriya interaction (DMI). Predicted by A. Fert in 1990, it promotes non collinear magnetism and chirality. It is thus in competition with conventional magnetic coupling and may give rise to spin modulation on length scales given by the usual exchange to DMI ratio. It has been proved to be relevant in ultrathin ferromagnetic films in contact with large spin-orbit non magnetic layers, giving rise to spin modulations (spin spirals, skyrmion arrays) with a unique sense of rotation. As DMI promotes non collinear magnetic ordering, its main consequence is to lower the energy of magnetic textures such as domain walls and increase their stability. One of the most fascinating manifestations of DMI is the observation of skyrmions, kind of nano bubbles corresponding to a non trivial topological state (in the same manner as a knot on a rope, they cannot be transformed continuously toward the collinear state). Beyond their fundamental aspect, they open new path of spintronic devices based on the motion of magnetic textures (either domain walls or skyrmions), where they could support information with a ultrahigh density. In this talk, I will review the consequences of DMI on the magnetic ordering in ultrathin films in contact with a high spin-orbit layer, and their associated dynamics, in the light of the recent progresses in spintronics.

We-B01+02

Looking at the structure of organic-organic interfaces in solar cells

Esther Barrena¹, Mahdiah Aghamohammadi¹, Felix Buss², Wilhelm Schabel²,
Carmen Ocal¹

¹Instituto de Ciencia de Materiales de Barcelona (ICMAB CSIC), Cerdanyola del Valles, España, ²Karlsruhe Institute of Technology (KIT), Karlsruhe, Germany

The interface between donor and acceptor molecules is the fundamental element of organic photovoltaic devices for efficient photogeneration of free charges. Still many conceptual aspects are not well understood in regard to the specific structural and electronic properties of D/A heterointerfaces and their effect on the device performance.

In the first part of this talk, we address the impact of the nanomorphology in solution-processed solar cells. The fundamental concept of solution-processed solar cells resides in the nano-phase separation developing in a binary blend formed by a polymer (donor) and a fullerene derivative (acceptor) when the solvent evaporates, the so-called bulk-heterojunction (BHJ). The performance of such solar cells critically depends on the crystallinity and length-scale of the spatial organization of the donor and acceptor materials. We employ real-time grazing incidence wide angle x-ray scattering (GIWAXS) combined with optical interference to gain detailed insight into the evolution of the microstructure during film formation and about the role of additives to control the nanomorphology [1-3]. In the second part, we assess the impact of the relative orientation between donor (D) and acceptor (A) molecules at the heterojunction on the exciton dissociation. Our strategy is to grow nanoscale D/A heterojunctions, which exemplify two model interfaces with the π -stacking direction either perpendicular or parallel to the heterointerface. Scanning probe methods, photoluminescence and ultraviolet photoelectron spectroscopy (UPS) are employed to investigate the structural, optical and electronic properties of the heterojunctions. We successfully provide a clear identification of molecular orientation as one of the factors governing recombination through interface states [4].

[1] M. Sanyal et al. *Advanced Energy Materials* (2011) 1, 362

[2] B. Schmidt-Hansberg et al. *ACS Nano* (2011) 5, 8579

[3] B. Schmidt-Hansberg et al. *Macromolecules* (2012) 45, 7948

[4] M. Aghamohammadi et al. *J. Phys. Chem. C* (2014) 118, 14833

We-B03

Dye-based solar cells via titania: Basic physics to applications, what we learn from first-principle calculations

Ersen Mete¹, Hatice Ünal¹, Deniz Gunceler², Oğuz Gülseren³, Şinasi Ellialtıoğlu⁴

¹Department of Physics, Balıkesir University, Balıkesir, Turkey, ²Department of Physics, Cornell University, Ithaca, USA, ³Department of Physics, Bilkent University, Ankara, Turkey, ⁴Basic Sciences, TED University, Ankara, Turkey

Electronic and optical properties of anatase nanowires sensitized by various organic dye molecules have been investigated using the standard and the screened-Coulomb hybrid density functional theory calculations. Moreover, non-linear polarizable continuum model is utilized in order to study the solute effect on the dye-nanowire system. Adsorption of coumarin, C2-1, cyanidin-3-O glucoside, and TA-St-CA molecules are considered on (001) and (101) facets of anatase nanowires. Local density of states, charge density distributions, and optical absorption spectra are obtained to interpret for the effective light harvesting, electron-hole generation, and electron injection.

Titania has received great attention in the dye sensitized solar cell applications due to its electrochemical and charge transport properties. Grätzel type solar cells can be described as a process in which the dye molecules harvesting the visible light and the excited electron is injected into the conduction band of the oxide. The anchoring groups of the adsorbed molecules, their bonding nature, the positions of HOMO and LUMO levels relative to titania band-gap edges, morphology of titania surfaces, and various other conditions are considered in the construction of dye-nanowire system. The anatase polymorph is preferred as nanowire due to its most stable and catalytically most active surface, and high surface-to-volume ratio. Coumarin, cyanidin-3-O glucoside, π -conjugated electron-donor-acceptor (D- π -A) type tetrahydroquinoline based C2-1, and oligophenylenevinylene based TA-St-CA molecules, when adsorbed on (001) and (101) facets, cause changes on the structural, electronic, and optical properties. The mechanisms and reasons of these changes are investigated by the screened Coulomb hybrid DFT. With this aim, local density of states, charge density distributions, and optical absorption spectra are compared. Dye-nanowire system in solutes (water and chloroform) is seen to have weakened bonds, especially for simple coumarin, as expected. Among the four dye molecules considered in this work, bidentate TA-St-CA is found to be the most successful one.

This work is supported by TÜBİTAK (Grant number 110T394).

We-B04

The role of (de)localized defects for Charge carrier separation at photoactive interfaces

Martin Rohrmüller¹, Uwe Gerstmann¹, Eva Rauls¹, Wolf Gero Schmidt¹,
Mohammad Waseem Akhtar², Alexander Schnegg², Klaus Lips²

¹University of Paderborn, Paderborn, Germany, ²Helmholtz-Zentrum, Berlin, Germany

To develop novel materials for photovoltaic or photocatalytic application a detailed atomistic understanding of charge carrier separation and the corresponding recombination processes is crucial. In this work we show how microscopic modeling of the involved defect states helps to analyze the data obtained from magneto-optical experiments. It will also be demonstrated that theory can give valuable information about the charge carrier separation, which give some hints for further improvement of the materials, even if this kind of information is not directly accessible by experiment. This is shown using the interface of hydrogenated amorphous silicon and crystalline silicon (a-Si:H/c-Si) in heterojunction solar cells as a prototype example [1]. Combining orientation dependent electrically detected magnetic resonance (EDMR) and density functional theory (DFT) we analyze the spin-dependent recombination in miniature solar cells. By this we find that (i) the interface exhibits microscopic roughness, (ii) the localized interface defects mimic the famous Pb-centers at the Si/SiO₂ Interface, (iii) we identify the microscopic origin of the conduction and valence band tail states, and (iv) we discuss how charge carrier separation can be supported by conduction band tail states.

[1] A. B. M. George, J. Behrends, A. Schnegg, T. F. Schulze, M. Fehr, L. Korte, B. Rech, K. Lips, M. Rohrmüller, E. Rauls, W. G. Schmidt, and U. Gerstmann, Phys. Rev. Lett. 110, 136803 (2013).

We-B05

Modification of hematite electronic properties with trimethyl aluminum to enhance the efficiency of photoelectrodes

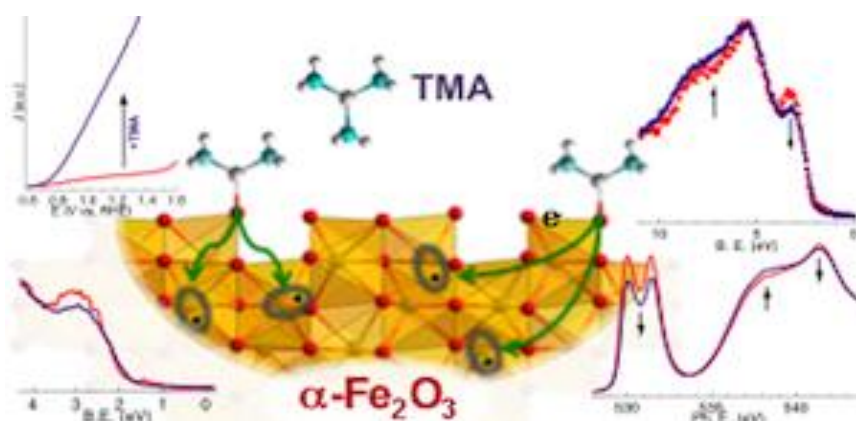
Massimo Tallarida¹, Chittaranjan Das², Dejan Cibrev³, Kaupo Kukli^{4,5}, Aile Tamm⁵, Mikko Ritala⁴, Teresa Lana-Villareal³, Roberto Gómez³, Markku Leskelä⁴, Dieter Schmeisser²

¹ALBA Synchrotron Light Source, Cerdanyola del Vallès, Spain, ²Brandenburg University of Technology, Cottbus, Germany, ³Universitat d'Alacant, Alicante, Spain, ⁴University of Helsinki, Helsinki, Finland, ⁵University of Tartu, Tartu, Estonia

We show how very thin films of Al₂O₃, prepared by atomic layer deposition (ALD), influence the photoresponse of hematite photoanodes. With our investigations we were able to establish, for the first time, that the reactions of the Al-precursor (trimethyl-Al, TMA) with hematite modify their electronic properties and improve the charge transfer mechanism [1]. We proposed that electrons are transferred from TMA to hematite as a consequence of the removal of one methyl group when TMA is chemisorbed on it.

We used two powerful spectroscopic methods, synchrotron radiation photoemission and X-ray absorption spectroscopy, to demonstrate that both the valence and conduction bands are modified already after one TMA pulse. With the photoelectrochemical characterization we observed that TMA induces a photoresponse enhancement by a factor around 8. We investigated three different hematite photoanodes to discern between the general effects of TMA/Fe₂O₃ reactions and other processes that might be dependent on the quality of hematite, e.g. morphology. In particular we found that in multifaceted hematite samples, a stronger Fe(III) to Fe(II) reduction occurred after the TMA pulses. However, we verified that this reduction does not further improve the photoanode efficiency. In this contribution we will also show results of resonant photoemission (ResPES) experiments that give a further proof of our thesis, confirming the change of hybridization in the O2p-Fe3d and O2p-Fe4s4p states. Thus, we offer a detailed investigation of the TMA/Fe₂O₃ system but we find that the mechanism causing the photoresponse enhancement in this system is general and explains similar results with other hematite modifications.

[1] M. Tallarida et al. J. Phys. Chem. Lett. 2014, 5, 3582–3587, DOI: 10.1021/jz501751w



We-B06

Two steps processes fabrication of large scale CZTS thin film absorber for sustainable photovoltaics

Mac Mugumaoderha¹, Stéphane Lucas¹, Jean-Jacques Pireaux¹

¹PMR, University of Namur, Namur, Belgium

Photovoltaic (PV) energy is obviously a stakeholder in the coming energy revolution. Inorganic thin-film PV technologies have interesting potential when it comes to the module's power output and the cost of Wp products. To meet the nowadays rising energy needs, these technologies have to overcome the limited availability of the raw materials (indium and tellurium) that are required. $\text{Cu}_2\text{ZnSnS}_4$ or copper zinc tin sulfide (CZTS) has been identified as a material with great potential in PVs and for which large amounts of natural resources are available. Unlike other PV thin-film based technologies, the CZTS active layer has the advantage of using only non-toxic materials, providing a totally sustainable technology. The main challenge is to improve the efficiency of both cell and module. This requires optimizing the processes at laboratory and industrial scale. This work aims at two steps fabrication of CZTS active layer. For this, additional sulfur is thermally incorporated ex-situ in a precursor film deposited by magnetron sputtering (of ZnS, Cu and Sn successive layers) or co-evaporation (of ZnS, Cu_2S and SnS) on $\sim 25 \text{ cm}^2$ glass/Mo substrate. The relatively large substrate size allows for multiple cells fabrication, for good statistics and fits well with basic industrial constrains. CZTS phase formation is known to compete with other multiple phases [1,2]. By combining different techniques: X-ray photoemission spectroscopy, X-ray diffraction spectroscopy, cross section scanning electron microscopy, UV-Vis spectroscopy, we demonstrated the formation of the kesterite CZTS. Our founding is systematically corroborated by independent Raman spectroscopy measurements.

[1] S. Siebentritt, Thin Solid Films 535 (2013) 1

[2] Siebentritt and Schorr, Prog Photovolt Res Appl (2012)

We-C03+04

The role of functional groups for (supra)molecular assemblies on surfaces

Meike Stöhr¹

¹Zernike Institute for Advanced Materials, University of Groningen, Groningen, Netherlands

The interest in studying organic nanostructures on surfaces emerges from their prospective applications in nanoscale electronic or optoelectronic devices, in which the spatially addressable functional units are to be assembled on the molecular level. By making use of molecular recognition processes based on non-covalent interactions, well-ordered 1D and 2D molecular structures can be formed on surfaces. The understanding of the interplay of the underlying intermolecular and molecule substrate interactions is highly important since the resulting molecular structures are based upon these two interactions.

Over the last years, cyano-functionalized molecules have gained increasing interest for the construction of on-surface molecular assemblies. The asymmetric charge distribution of cyano ligands leads to the formation of an intrinsic dipole, which can be involved in intermolecular dipolar coupling, hydrogen bonding or metal-ligand interactions and thus, can be used to effectively steer the structure formation. For different cyano-functionalized molecules, the adsorption on Au(111) will be discussed. In addition, the effect of post deposition annealing as well as the change of the substrate has been investigated. The findings will be compared to another to identify similarities / differences, also with respect to the guiding role of the cyano group.

We-C05

STM study of adsorption and supramolecular assembly of diarylethene

Tomoko Shimizu^{1,2,3}, Jaehoon Jung³, Hiroshi Imada³, Yousoo Kim³

¹National Institute for Materials Science, Tsukuba, Japan, ²JST PRESTO, Kawaguchi, Japan, ³RIKEN, Wako, Japan

In the exploration for organic molecules for device applications, it is crucial to understand molecular adsorption properties on electrode metals and dielectric insulators. In particular, it is important to find a way to fabricate desired structures on surfaces such as well-ordered 2D films and 1D chains. Here we report on a combined study of scanning tunneling microscopy (STM) and density functional theory (DFT) calculation of a diarylethene derivative adsorbed on Cu(111). We have successfully formed a homogeneous monolayer film consisting of closed-form isomer of diarylethene by coadsorption of NaCl and thermal annealing. Comparison between experimental observations and theoretical calculations indicates that a row structure within the film is formed as a result of interactions between the Na cations and diarylethene molecular dipoles, which dramatically changes the adsorption configuration from that without Na cations.

We-C06

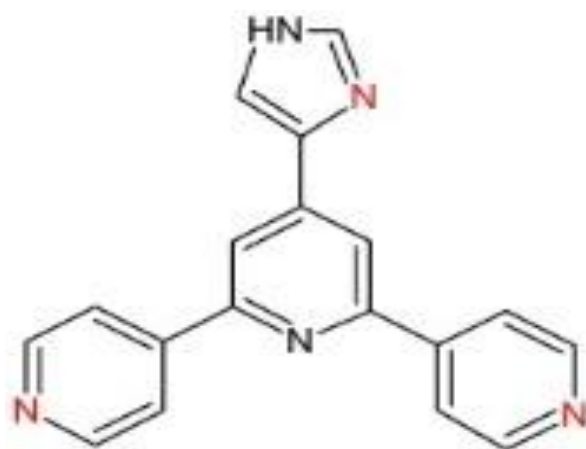
Controlled assembly of 4,2':6',4''-terpyridine derivatives into different porous on-surface networks

Thomas Nijs¹, Frederik J. Malzner², Shadi Fatayer¹, Aneliia Wäckerlin¹, Sylwia Nowakowska¹, Catherine E. Housecroft², Edwin C. Constable², Thomas A. Jung^{1,3}

¹Department of Physics, University of Basel, Basel, Switzerland, ²Department of Chemistry, University of Basel, Switzerland, ³Laboratory for Micro- and Nanotechnology, PSI, Villingen, Switzerland

Surface metal organic frameworks (SurfMOFs) are used as artificial supramolecular building blocks to form functionalised surfaces. These highly functional architectures allow performing biochemical processes such as light harvesting or site and shape selective chemical reactions. Here we present a study on the self-organization of a 4,2':6',4''-terpyridine derivative, namely 4'-(1H-imidazol-4-yl)-4, 2':6', 4''-terpyridine¹ on Au(111) single crystal. In contrast to the well-established chelating 2,2':6',2''-terpyridines, this molecule includes inherent design features to facilitate metal-coordination through N atoms (Fig. 1) in dependence of controllable parameters. By combining Scanning Tunneling Microscopy (STM) and X-ray Photoelectron Spectroscopy (XPS) we are able to analyse the transition of the inter-molecular bond from hydrogen-bonding to Cu-coordination. After deposition on Au(111), two asymmetric molecules form a dimer which compensates the irregular symmetry of the building blocks and enables the formation of a chiral 6-fold nanoporous hydrogen-bonded network. By supply of Cu adatoms to this assembly, the intermolecular binding motive changes from hydrogen bonded to metal-coordinated. Due to the increased substrate-absorbate interaction, the molecules were found to assemble into chains of linked heterocyclic macrocycles, which generally follow the fcc domains of the Au(111)(22x√3) reconstruction.²

Fig. 1: Imidazole-functionalized ligand



We-D01

Using van der Waals DFT functionals to study diffractive scattering of noble gases from metal surfaces

Cristina Díaz¹, Marcos del Cueto¹, Alberto S. Muzas¹, Gernot Fuechsel²,
Fernando Martín^{1,3}

¹Universidad Autónoma de Madrid, Madrid, Spain, ²University of Leiden, Leiden, The Netherlands, ³Instituto Madrileño de Estudios Avanzados en Nanociencia (IMDEA-Nanoscience), Madrid, Spain

For long time, accurate theoretical studies, by means of DFT, of periodic or semi-periodic systems, in which van der Waals (vdW) interaction forces are called to play an important role, have been largely prevented, due to the intrinsic shortcomings of the method. However, the development of new DFT functionals that, in one way or another, take into account dispersion forces (see [1] for a review) opens the possibility of performing such studies. For example, the approach taken by Grimme [2,] had been found to give reasonable results for organic molecules and layer adsorption on metal surfaces [3,4]. However, diffraction of noble gases atoms presents a higher challenge, because diffraction patterns are very sensible to the subtle characteristics of the underlying potential energy surface (PES).

Here we have studied the diffractive scattering of He and Ne atoms from Ru(0001), by means of classical and quantum dynamics calculations, using several PESs built by interpolation of DFT data, which have been computed with different functionals. Our results show, by comparison with available experimental results [5], that: (1) vdW interaction forces have to be taken into account to describe these kind of systems; (2) to properly describe these systems one have to go beyond the Grimme correction. We will show that PESs based on vdW functionals, which include the non-local correction in the exchange-correlation energy [6], are the only ones able to describe accurately the interaction between noble gases and metal surfaces.

[1] Prates-Ramalho et al RSC Adv. 3, 13085 (2013)

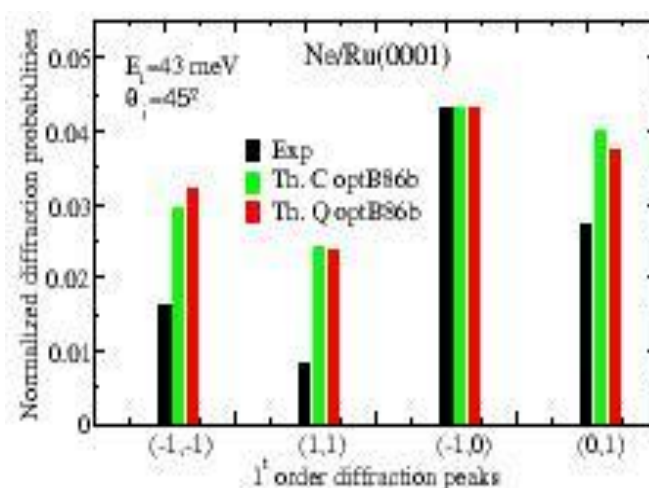
[2] S. Grimme et al J. Comput. Chem. 27, 1787 (2006)

[3] D. Stradi et al Phys. Rev. Lett. 106, 186102 (2011)

[4] D. Stradi et al Nanoscale DOI: 10.1039/c4nr02917h

[5] M. Minniti et al J. Phys.: Condens. Matter 24, 354002 (2012)

[6] M. Dion et al. Phys. Rev. Lett. 92, 246401 (2004)



We-D03

Faceting of Rh(553) during CO oxidation

Chu Zhang¹, Edvin Lundgren¹, Per-Anders Carlsson², Olivier Balmes³, Lindsay Merte¹, Mikhail Shipilin¹, Johan Gustafson¹

¹Div. of Synchrotron Radiation Research, Lund University, Sweden,

²Competence Centre for Catalysis, Chalmers University of Technology, Sweden, ³MAX IV laboratory, Lund University, Sweden

We have investigated faceting of Rh(553) during catalytic CO oxidation using Surface X-ray Diffraction (SXR). The surface was exposed to a flow with different ratios of CO and O₂ in the 0.1-100 mbar range at 250°C. We find significant rearrangements of the surface, which might have implications for the fundamental understanding of the catalytic reaction. Our results are summarized in Fig 1, with an overview model in (A), mass spec signal in (B) and SXR mesh plots in (C). Starting with panel II, close to stoichiometric reaction conditions results in exposure of the overall (553) surface orientation. Under CO rich conditions (I) the steps get closer in (110) facets coexisting with larger (111) areas. Under O₂ rich conditions (III) the surface forms coexisting (331) and (111) oriented areas, while at even more oxygen rich conditions (IV) a surface oxide forms on the (111) facets, and the signal from the (331) facets decreases, probably in favour for surface oxide covered (11-1) facets.

For the O₂ rich conditions, similar faceting has been seen before. At intermediate O₂ pressures (about 10⁻⁵ mbar) the surface faceted into of (331) and larger (111) facets, while (111) and equivalent (11-1) facets formed together with the surface oxide at about 10⁻³ mbar. The results found in CO excess are to our knowledge new. At these pressures, we may expect that it is thermodynamically favourable to maximize the coverage. On the other hand, CO is known to prefer adsorption at step edges prior to the flat areas. Hence we speculate that the surface facets into a structure that can accommodate as much CO as possible without removing any step adsorption sites. This leads to the steps being bunched together in (110) facets, while large non-interrupted (111) areas are available to adsorb large quantities of CO.

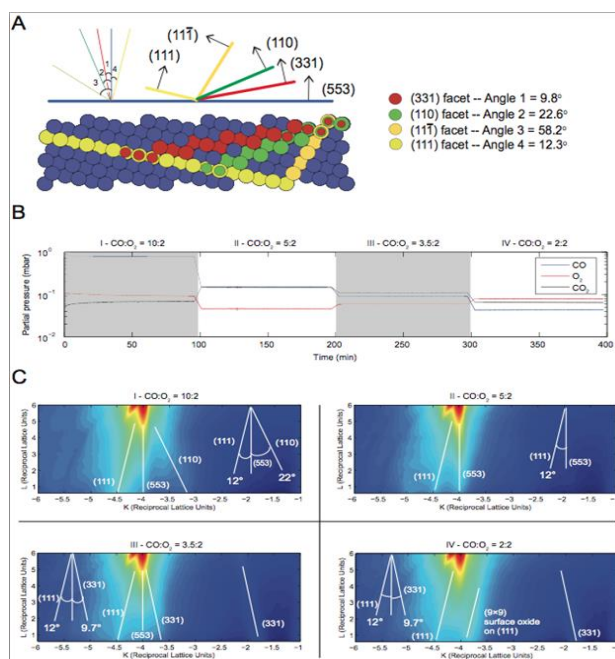


Figure 1. (A) Model of the Rh(553) surface with the different gas-induced facets. (B) Mass spectrometry signal of gas compositions for each measurement. (C) SXR meshplots for different gas mixtures.

We-D04

Surface roughening and interface effects during Co intercalation under Graphene on Ir(111)

Ilaria Carlomagno^{1,2,3}, Jakub Drnec¹, Sergio Vlaic⁴, Nicolas Rougemaille⁴, Johann Couraux⁴, Juliana Gonzalez⁴, Roberto Felici¹

¹ESRF, Grenoble, France, ²Università di Roma Tre, Roma, Italy, ³Université Grenoble Alpes, Grenoble, France, ⁴CNRS Institut Néel, Grenoble, France

Magnetic hybrid systems are interesting for the development of new magnetic memories. In particular, thin Cobalt (Co) films below 10nm, deposited on Iridium (Ir) substrates show perpendicular magnetic anisotropy (PMA), crucial for the development of new ultra-high density memory devices [1].

When dealing with such thin films, the oxidation of the magnetic layer can compromise the magnetic behavior of the whole system. A graphene (Gr) capping layer can be used to lower the Co chemical reactivity and prevent its oxidation.

Gr/Co/Ir(111) systems can be obtained by deposition of Cobalt onto Gr/Ir followed by annealing promoted Co intercalation through the Gr layer deposited on the Ir substrate. This procedure results also into an enhanced PMA [2].

The intercalation process is relatively straightforward but the high temperatures (500K) required to drive it, can affect the Co/substrate interface and its magnetic behavior. A detailed characterization of structure and morphology is then mandatory to reliably understand the structural evolution upon the intercalation and its effects on the magnetic response.

Here we report a deep investigation of Gr/Co/Ir(111) and Co/Ir(111) systems. From the comparison of the two systems one can distinguish the graphene-induced modifications in the magnetic response.

Complementary probes were employed in order to investigate the magnetic properties (MOKE) and structural features (Surface x-ray diffraction, LEED, XPS, and STM).

Our results prove that the magnetic properties of the thin Co films depend on atomic scale modifications which can be induced by thermal treatments: even subtle changes to the preparation conditions of Gr/Co/Ir can cause severe modifications to the magnetic response of the final device.

[1] J.Couraux et al., J. Phys. Chem. Lett. 3 (2012) 2059

[2] N. Rougemaille et al., Appl. Phys. Lett. 101 (2012) 142403

We-D05

Structure determination of graphene on metal substrate using total-reflection high-energy positron diffraction

Yuki Fukaya¹, Shiro Entani¹, Seiji Sakai¹, Izumi Mochizuki², Ken Wada², Toshio Hyodo², Shin-ichi Shamoto¹

¹Advanced Science Research Center, Japan Atomic Energy Agency, Tokai, Naka, Japan, ²Institute of Materials Structure Science, High Energy Accelerator Research Organization (KEK), Tsukuba, Ibaraki, Japan

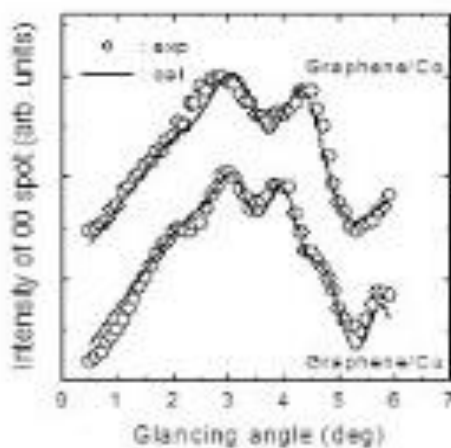
Graphene has attracted increasing attention because of its high electron mobility and many other promising futures. Recently, the synthesis of graphene is successfully performed on various metal surfaces. The theoretical calculations demonstrate that the spacing between the graphene and the substrate is dependent on the substrate and modulates the shape of the Dirac cone of the energy dispersion [1]. Therefore, the graphene height is the important factor in understanding its electronic properties. However, the substrate dependence of the graphene height is not confirmed experimentally. In this study, we determined the structures of graphenes on the Cu(111) and Co(0001) substrates using total reflection high-energy positron diffraction (TRHEPD).

TRHEPD is a surface-sensitive tool owing to the positive charge of positrons. Since the crystal potential energy for positrons is positive, opposite to that for electrons, the positron beam at grazing incidence is totally reflected at the surface. The penetration depth of the positron beam under the total reflection region is less than a few Å, which corresponds to the thickness of 1-2 atomic layers. Thus, the TRHEPD method is suitable for structure determinations of graphene suspended on the substrate.

The TRHEPD rocking curves from the graphenes on the Cu(111) and Co(0001) substrates clearly show the different shapes. From the structure analysis based on the dynamical diffraction theory, the graphene heights for the Cu(111) and Co(0001) were determined to be 3.32 Å and 2.24 Å, respectively. The former value is close to the layer distance in graphite. Thus, the graphene on the noble metal weakly interacts with the substrate as compared with that on the transition metal. We will also discuss the structure difference with silicene on the Ag(111) [2].

[1] G. Giovannetti et al., Phys. Rev. Lett. 101, 026803 (2008).

[2] Y. Fukaya et al., Phys. Rev. B 88, 205413 (2013).



We-E01

An In-situ GISAXS investigation of the growth of Permalloy thin films on nano-rippled Si templates

Sarathlal Koyiloth Vayalil¹, Gonzalo Santoro^{1,2}, Stephan V Roth¹, Peng Zhang¹,
Ajay Gupta³

¹Photon Science, DESY, Hamburg, Germany, ²Instituto de Ciencia de Materiales de Madrid, Madrid, Spain, ³Amity Center for Spintronic Materials, Amity University, Noida, India

Nanostructured magnetic thin films have gained significant relevance due to its applications in magnetic storage and recording media. Self-organized arrays of nanoparticles and nanowires can be produced by depositing metal thin films on nano-rippled substrates. The substrate topography strongly affects the film growth giving rise to anisotropic properties (optical, magnetic, electronic transport). Ion-beam erosion (IBE) method can provide large area patterned substrates with the valuable possibility to widely modify pattern length scale by simply acting on ion beam parameters (i.e. energy, ions, geometry, etc.)

In this work, investigation of the growth mechanism of magnetic thin films of Permalloy thin films on nano-rippled Si (100) substrates using in-situ μ GI-SAXS measurements have been done. We have performed in-situ real time GISAXS at the P03/MiNaXS beamline of PETRA III storage ring during the sputter deposition of thin films. Nanorippled Si substrates prepared by low energy ion beam sputtering with average wavelength of 40 nm and depth of 3 nm have been used as a template. The thickness of the thin films has been calibrated by ex-situ x-ray reflectivity measurements. In the very low thickness regime, the film replicates the morphology, rather an increase in the thickness lead to growth of nanowires in an orientation nearly 55° from the surface. It has been found that, growth is highly anisotropic along and normal to the ripple wave vectors in both the cases. The annealing followed by the deposition generates large range ordered nanowires. Detailed results of simulation using FitGISAXS will be addressed.

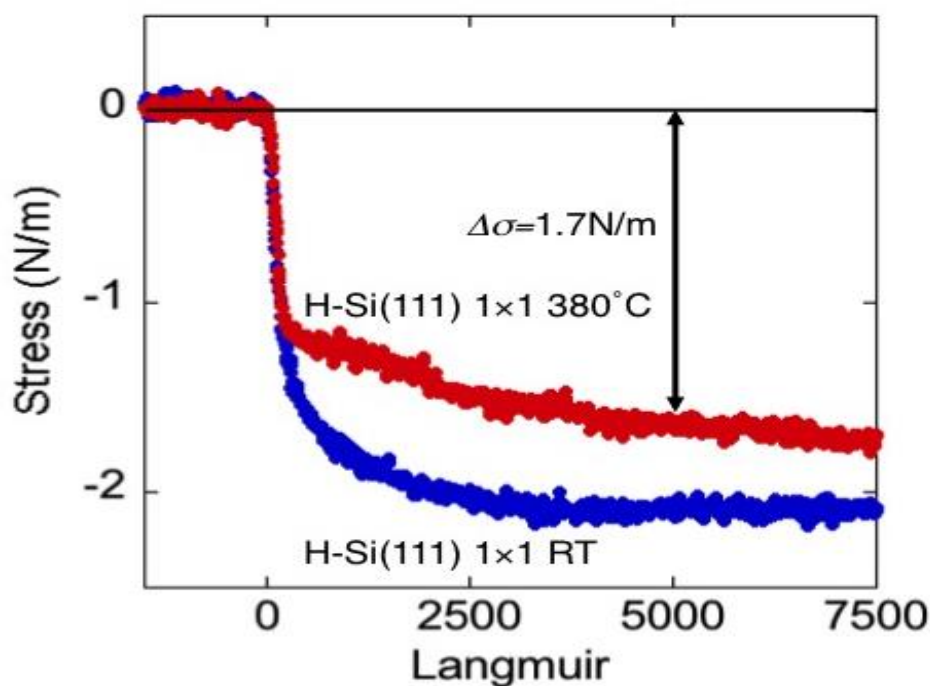
We-E02

Real-time stress measurement during Si surface reconstruction and Ge nanodot growth on Si

Hidehito Asaoka¹, Yuki Uozumi¹¹Advanced Science Research Center, Japan Atomic Energy Agency, Tokai, Japan

In the long history of thin-film-growth physics, it has been long recognized that the stress and the morphology of the film have a strong relationship. Although the Si(111) 7×7 reconstructed surface largely reduces the electronic surface energy by reducing the number of surface dangling bonds, the surface reconstruction increases the surface stress and the surface energy as well. Despite the importance of the surface energy of Si, the experimental knowledge on the impacts of reconstruction on the Si surface has been quite limited.

We have succeeded in measurements of the surface stress in Si(111) as a function of 7×7 reconstruction by comparison with the H-terminated Si(111) 1×1 surface and a detail stress evolution during initial nanodot growth stage of Ge growth on Si(111). The stress evolutions are observed by measuring the curvature of free-standing substrates which allows ideally unconstrained bending. As a result, we find the Si(111) 1×1 surface releases 1.7 N/m (=J/m²), or (1.4 eV/(1×1 unit cell)), of the surface energy from the strong tensile Si(111) 7×7 reconstruction (Fig.1). Moreover, a stress evolution has been found to exist in the early stage of the nanodot formation, which is concurrent with onset of the surface roughening of the wetting layer and of the dislocations in the Ge nanodots.



We-E03

Determination of the Sb(111)-phonon dispersion relation using inelastic HAS measurements

Florian Apolloner¹, Patrick Kraus¹, Christian Gösweiner¹, Giorgio Benedek^{2,3}, Wolfgang E. Ernst¹

¹Institute of Experimental Physics, Graz University of Technology, Graz, Austria, ²Dipartimento di Scienza dei Materiali, Università di Milano-Bicocca, Milano, Italy, ³Donostia International Physics Centre (DIPC), University of the Basque Country (EHU-UPV), San Sebastián, Spain

The semimetal antimony (Sb) is one of the building blocks for topological insulators [1] and also an interesting candidate for spintronic applications, yet there is little known about its surface dynamics. While simulations based on the density functional perturbation theory (DFPT) for the phonon dispersion of the Sb(111) surface exist, measurements to complement those theoretical models have been missing up to now [2]. Using helium atom scattering (HAS) it is possible to obtain information about surface structure, electronic corrugation, phonon dispersion and the surface-helium interaction potential [3,4,5].

We have measured the phonon dispersion relation for an antimony sample at 160 K and 300 K in two high symmetry directions using inelastic HAS and analyzing the time of flight data. The resulting phonon dispersion shows acoustic modes up to 10 meV and optical modes between 15 and 20 meV. Additional modes in the acoustic region are visible due to a strong electron-phonon coupling, which allows for charge density oscillations of the surface electron cloud induced by the movement of atoms in the bulk. The dispersion relation also reveals a new mode below the Rayleigh mode, resulting in an upshift of the latter by roughly 0.5 meV compared to the simulations.

[1] H. Zhang et al., Nature Physics 5 (2009) 438-442

[2] D. Campi et al., Phys. Rev. B. 86 (2012) 075446

[3] M. Mayrhofer-Reinhartshuber et al., J. Phys. Condens. Matter 25 (2013) 395002

[4] A. Tamtögl et al., Surface Science 617 (2013) 255-228

[5] M. Mayrhofer-Reinhartshuber et al., Phys. Rev. B 88 (2013) 205425

We-E04

A surface spin-echo study of hydrogen diffusion on Cu(111)

Peter Townsend¹, Anton Tamtogi¹, David Ward¹, William Allison¹, John Ellis¹

¹University of Cambridge, Cambridge, UK

Understanding the interaction of hydrogen with metal surfaces is relevant for a range of hydrogen technologies. As the lightest atom, hydrogen is prone to diffusing by quantum mechanical tunnelling when confined on a surface. An accurate description of the associated quantum-classical crossover in the rate, and in particular the isotope effect, is an ongoing challenge for theory [1].

We present surface spin-echo [2] measurements of the structure and dynamics of the two stable isotopes of hydrogen on the Cu(111) surface between 100 K and 250 K at sub-monolayer coverage. The observations are broadly consistent with independent hydrogen atoms diffusing by single jumps over two surface sub-lattices. The structural and dynamical data taken together imply that this diffusion occurs between ordered islands that grow upon cooling. The data at the higher temperatures are consistent with a semiclassical interpretation. We discuss the quantum mechanical influence on the jump rate at the lower temperatures in terms of both the tunnelling process itself and of the coupling to the substrate heat bath.

[1] E.M. McIntosh, K.T. Wikfeldt, J. Ellis, A. Michaelides, and W. Allison. Quantum effects in the diffusion of hydrogen on Ru(0001). *The Journal of Physical Chemistry Letters*, 4(9):1565–1569, 2013.

[2] A.P. Jardine, H. Hedgeland, G. Alexandrowicz, W. Allison, and J. Ellis. Helium-3 spin-echo: Principles and application to dynamics at surfaces. *Progress in Surface Science*, 84(11-12):323-379, 2009.

We-E05+06

Ultrafast surface chemistry and catalysis probed with optical and x-ray lasers

Henrik Öström¹

¹Stockholm University, Stockholm, Sweden

Heterogeneous catalysis and surface chemistry form the backbone of the chemical industry and one of the great challenges in chemical physics is to capture the transition states and ultrafast dynamics of catalytic surface reactions. We use a combination of optical and x-ray laser techniques to study dynamics and microscopic mechanisms of catalysis. Using pump-probe soft x-ray spectroscopy we selectively probe the adsorbate electronic structure in both transient intermediates and the transition state region during catalytic surface reactions. With femtosecond optical laser mass spectrometry techniques we probe the ultrafast dynamics and reaction mechanisms specifically in the reaction coordinate. This combination of experiments provides a high level of understanding of the microscopic processes that govern catalytic surface reactions.

We-A07

Detecting Spin Excitations and Correlations in Scanning Tunneling Spectroscopy

Markus Ternes¹

¹Max-Planck Institute for Solid State Research, Stuttgart, Germany

In recent years inelastic spin-flip spectroscopy using a low-temperature scanning tunneling microscope has been a very successful tool for studying not only individual spins but also complex coupled systems. When these systems interact with the electrons of the supporting substrate correlated many-particle states can emerge, making them ideal prototypical quantum systems. In this presentation I will show that experiments in conjunction with model Hamiltonians which takes the coupling to the environment into account enables to achieve a profound understanding of the underlying mechanism which influences the magnetic anisotropy and leads to the emergence of correlations and entanglement.

We-A08

Radio Frequency Scanning Tunneling Spectroscopy for Single-Spin Resonance

Stefan Müllegger¹, Stefano Tebi¹, Giulia Serrano¹, Stefan Wiespointner-Baumgarthuber¹, Reinhold Koch¹

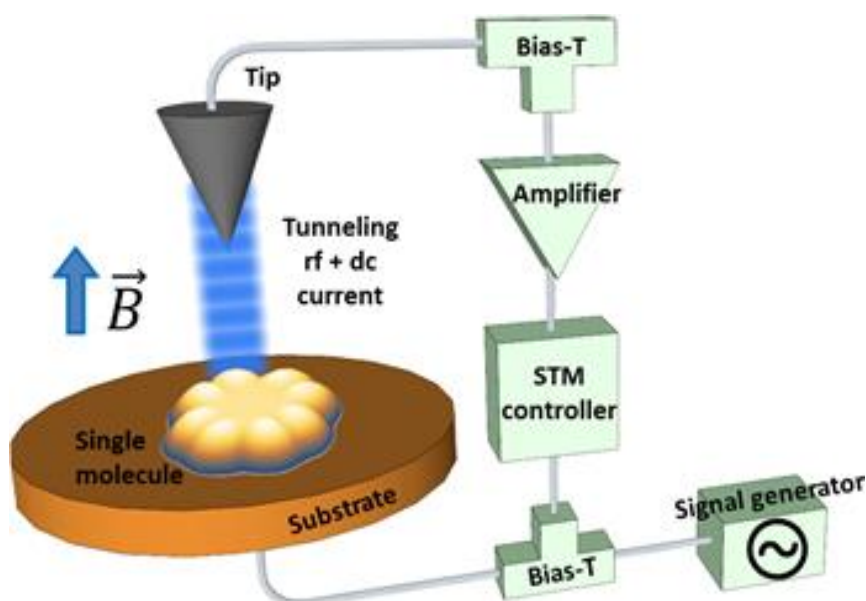
¹Institute of Semiconductor and Solid State Physics, Johannes Kepler University Linz, Linz, Austria

In the second half of the 20th century two investigation techniques emerged that both revolutionized science and technology in their fields: electron/nuclear magnetic resonance (MR) exhibiting a superior energy resolution and scanning tunneling microscopy (STM) providing spatial resolution at the atomic length scale. In order to benefit from both, the superior spatial resolution of the STM and the exceptional energy resolution of resonance techniques, we developed a radio frequency (rf) STM based on a commercial low-temperature STM upgraded by a home-built rf spectroscopic system [1,2]. Here, we report the excitation of electron, nuclear and combined electron/nuclear spin transitions by resonant rf tunneling in single molecular quantum dots [3]. Our novel technique enables resonant spin spectroscopy of single quantum spins unbound from electromagnetic dipole selection rules. Thus, we reveal by experiment the complete manifold of nuclear (I) and electronic (J) spin transitions of single quantum spins of up to $\Delta I_z = \pm 3$ and $\Delta J_z = \pm 12$ with sub-nanometer spatial resolution. The molecular quantum dots are formed by molecules of the single-molecule magnet bis-phthalocyanato terbium (III) on Au(111) at 5 K.

[1] S. Müllegger, M. Rashidi, K. Mayr, M. Fattinger, A. Ney, and R. Koch, Phys. Rev. Lett. 112, 117201 (2014).

[2] S. Müllegger, A.K. Das, K. Mayr, and R. Koch, Nanotechn. 25, 135705 (2014).

[3] S. Müllegger, S. Tebi, A. K. Das, W. Schöfberger, F. Faschinger, and R. Koch, Phys. Rev. Lett. 113, 133001 (2014).



We-A09

Magnetic properties of ultra-thin Cr layers on Fe(100): surfactant effect of oxygen for the formation of a sharp interface

Giulia Berti¹, Alberto Brambilla¹, Alberto Calloni¹, Andrea Picone¹, Michele Riva^{1,2}, Gianlorenzo Bussetti¹, Marco Finazzi¹, Lamberto Duò¹, Franco Ciccacci¹

¹Physics Department, Politecnico di Milano, Milan, Italy, ²Institute of Applied Physics, Vienna University of Technology, Vienna, Austria

Antiferromagnetic (AF)/ferromagnetic (F) interfaces have attracted much attention during last years, thanks to a variety of effects they show, mainly due to reduced dimensionality and magnetic couplings. The Fe/Cr system is one of the most studied since it is considered as a model F/AF heterostructure and because of its importance for the GMR effect and in spintronic devices. The magnetic properties of this system can be affected by the interplay of several parameters, such as interface mixing, strain and defects. If the growth of ultra-thin layers is performed on iron substrates kept at high temperature, chemical mixing prevents the formation of a well-defined interface, while low-temperature deposition leads to three-dimensional growth, both issues being detrimental for the study of ultra-thin Cr films on Fe(100). We found [1] that a sharp Cr/Fe interface can be obtained even at relatively high deposition temperatures by depositing Cr on the oxygen passivated Fe-p(1x1)O substrate: oxygen floats on the growing film acting as a surfactant and promoting a layer-by-layer growth, so for sub-monolayer coverages a Cr oxide is formed. For thicker films, the Cr oxide layer is confined at the surface. We report on the magnetic behavior of such thin Cr films: we investigate the coupling between the Fe substrate and the Cr overlayer, and demonstrate the effectiveness of our growth recipe in promoting the formation of a layer-wise AF structure in the Cr film, starting right from the interface. The magnetic characterization is performed by means of X-ray magnetic circular dichroism [2], and spin-resolved photoemission spectroscopy [3]. Experimental results are in nice agreement with theoretical calculations [1].

[1] A. Picone et al., Phys. Rev. B 87, 085403 (2013).

[2] A. Brambilla, G. Berti, et al., J. Appl. Phys. 114, 123905 (2013).

[3] G. Berti et al., Appl. Phys. Lett. 106, 162408 (2015).

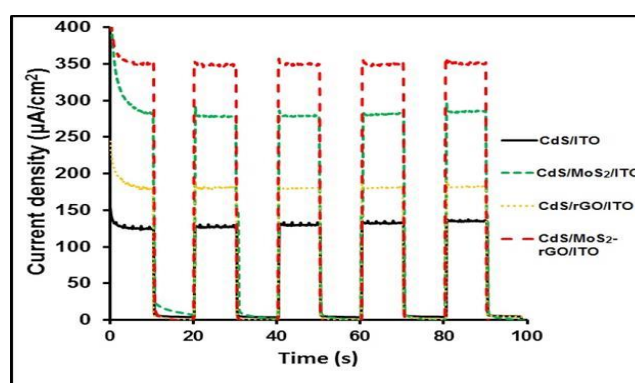
We-B07

Synergetic Effect of MoS₂ - Graphene Nanosheets in Improving Photoelectrochemical Performance of CdS Nanoparticles

Alireza Z. Moshfegh^{1,2}, Mohammad Zirak¹, Omran Moradlou³, Morasa Samadi¹, Navid Sarikhani⁴, Hao-Li Zhang⁵

¹Department of Physics, Sharif Univ. of Technology, Tehran, Iran, ²Institute of Nanoscience and Nanotechnology, Sharif University of Technology, Tehran, Iran, ³Department of Chemistry, Alzahra University, Tehran, Iran, ⁴Department of Mechanical Engineering, Sharif University of Technology, Tehran, Iran, ⁵State Key Laboratory of Applied Organic Chemistry, Lanzhou University, Lanzhou, P.R. China

Preparation of visible active and stable photoelectrode is an important subject for solar energy applications. CdS is a promising photoactive material but suffers from photocorrosion. Herein, we have used a simple and effective method to combine reduced-graphene oxide (rGO) and exfoliated few-layer MoS₂ nanoflakes with CdS nanoparticles deposited on Indium tin oxide (ITO) substrate with remarkable photo-stability. The rGO nanosheets were prepared by modified Hummers' method. MoS₂ nanoflakes were prepared via additive-free sonication-exfoliation method in a mixed water-ethanol solvent. The rGO sheets and MoS₂ nanoflakes were deposited on ITO substrate via electrophoretic method ($V=8V$, $t=1min$). Then CdS nanoparticles were deposited by successive ion layer adsorption and reaction (SILAR) method. The bare rGO/ITO, MoS₂/ITO and CdS/ITO thin films were also prepared with the same procedure for comparison. Atomic force microscopy (AFM) analysis revealed that MoS₂ nanosheets have the average thickness and lateral dimensions of ~5 and ~60 nm, respectively. These parameters were determined at ~2 nm and ~1.5 μm for rGO sheets, respectively. High resolution transmission electron microscopy (HRTEM) analysis verified formation of the atomic junction between MoS₂, rGO and CdS (with average particle size of ~8 nm). Surface chemical composition of the samples was determined by X-ray photoelectron spectroscopy (XPS) and Raman spectroscopy indicating stoichiometric formation of MoS₂ and CdS. Photoelectrochemical performance of the combined systems was examined in a three-electrode electrochemical cell under 500 W Xenon lamp in a 50 mM Na₂S aqueous solution. The bare CdS/ITO showed a photo-current density of ~125 $\mu A/cm^2$. Incorporation of rGO and MoS₂ nanosheets caused a synergetic effect resulted in increasing of photo-current density of the CdS/rGO-MoS₂/ITO electrode ~3 times as compared with the CdS/ITO electrode (Fig 1). A significant photo-stability was also observed for this ternary system. A possible mechanism was proposed for the stability and enhancement of this hybrid electrode.



We-B08

A Synchrotron Radiation X-ray Photoelectron Spectroscopy Study of PbS/CdS core/shell Colloidal Quantum Dots

Philippa Clark¹, Atip Pengpad¹, Hanna Radtke¹, Andrew Williamson¹, Simon Fairclough², Darren Neo³, Andrew Watt³, Karsten Handrup⁴, Karina Schulte⁴, Jacek Osiecki⁴, Federica Bondino⁵, Igor Pis⁵, Silvia Nappini⁵, Elena Magnano⁵, Fausto Sirotti⁶, Mathieu Silly⁶, Wendy Flavell¹

¹School of Physics and Astronomy and the Photon Science Institute, The University of Manchester, Manchester, United Kingdom, ²Department of Physics, Kings College London, London, United Kingdom, ³Department of Chemistry, The University of Oxford, Oxford, United Kingdom, ⁴Lund Universitet, MAX-lab, Lund, Sweden, ⁵IOM CNR, Laboratorio Nazionale TASC, Area Science Park, Basovizza, Italy, ⁶Synchrotron SOLEIL, Saint-Aubin, France

Lead sulfide quantum dots (QDs) are promising candidates for next generation solar cells, but improvements in efficiency and stability are needed before they can be made commercial. The main factor limiting their efficiency is their low open circuit voltage VOC, due to a large number of surface defect states. Through cation exchange methods, PbS quantum dots have been passivated with CdS leading to an improvement in VOC, due to a reduction in recombination, giving a power conversion efficiency of 5.6%¹. The CdS has been assumed to form a shell around the QD, which if too thick reduces the short circuit current in a simple solar cell design¹.

SR-excited depth profiling XPS is one of very few techniques which allow the core-shell composition of such QDs to be probed^{2 3}. Here we apply it to study PbS/CdS QDs, and demonstrate that Cd is concentrated at the outer surfaces of the QDs, underneath a layer of ligands. We compare these results with those for unpassivated PbS QDs, and show that the extent of surface oxidation to produce surface sulfate is reduced by the addition of Cd. Nevertheless, the valence band photoemission (in particular the position of the valence band maximum) remains characteristic of PbS. We present calculations of the CdS shell thickness for different PbS core sizes, which provide insight into the effectiveness of the passivation for different preparative routes.

¹Darren C J. Neo et al. Chemistry of Materials, 26, 4004-4013 (2014).

²Samantha J. O. Hardman et al., Phys. Chem. Chem. Phys.13, 20275-20283 (2012)

³Robert C Page et al. Small, 11, 1548-1554 (2015).

We-B09

Type II Colloidal Quantum Dots - Depth-profiling XPS study of the effects of Oxidation and Halide Passivation on the Shell Structure

Atip Pengpad¹, Andrew Williamson¹, Hanna Radkte¹, Robert Page², Karina Schulte³, Jacek Osiecki³, David Binks¹, Wendy Flavell¹

¹School of Physics and Astronomy and Photon Science Institute, The University of Manchester, Manchester, United Kingdom, ²School of Chemistry, The University of Manchester, Manchester, United Kingdom, ³Lund Universitet, MAX-lab, Lund, Sweden

Type II colloidal semiconductor quantum dots (QDs) are nanoparticles with a 'core-shell' structure which on photoexcitation results in spatially separated carriers. This reduces the recombination rate for these carriers, which can be used in many applications such as solar cells. However, colloidal QDs do not necessarily have the target composition, or have complete atomically-abrupt interfaces between the core and the shell. Moreover, significant surface degradation of colloidal QDs has been observed [1, 2], and this influences the bandgap structure within the QDs. Here, we use synchrotron-excited depth-profiling XPS to investigate how oxidation affects the structure of type II quantum dots at the interface between the core and shell, and at the surface. We also explore the effect of a recently demonstrated passivation route involving halide ions on the surface composition and electronic properties [3]. In this work, we performed depth-profiling XPS on CdTe (core)/CdSe (shell)/butylamine (ligand) QDs. The results confirm that selenium is present at the surface of the QDs as we expect for a CdSe shell. However, tellurium is found throughout the QDs which suggests the alloying of the core and the shell. Tellurium oxide is observed after the sample was aged in air. The valence band spectra show a characteristic valence band maximum (VBM) of a CdTe system. Following surface passivation with chloride anions, we show that Cl is present at the surfaces of the QDs. Valence band photoemission shows that the Cl anions bond to the QD surfaces by donating electrons into otherwise partially-filled surface trap states. This has the effect of significantly increasing the carrier recombination time, and (in the case of CdTe QDs) results in near-unity quantum yields [3].

- [1] S. Hardman, et al., Phys. Chem. Chem. Phys. 13(2011), 20275.
- [2] S. Fairclough, et al., J. Phys. Chem. C 116(2012), 26898.
- [3] R. Page, et al., Small 11(2015), 1548.

We-B10

Structure, morphology and chemical ordering in nanoalloys:
a theoretical studyChristine Mottet¹, Jérôme Creuze², Hazar Guesmi³, Beien Zhu⁴, Bernard Legrand⁵¹CINaM - CNRS / AMU, Marseille, France, ²ICMMO/SP2M, Pars-Sud University, Orsay, France, ³ICGM / MACS, Montpellier, France, ⁴Shanghai Institute Of Applied Physics, Shanghai, China, ⁵SRMP-DMN, CEA Saclay, Gif-sur-Yvette, France

Metallic nanoparticles made of more than one element (i.e. nanoalloys) are developed because beside the size reduction effect, they can present synergy effects which are particularly interesting to enhance a wide range of properties in catalysis, magnetism or optics. These properties are linked to the structure and the chemical arrangement of the different atom types inside the particles, which must be controlled during the synthesis steps, and that we can predict by numerical simulations.

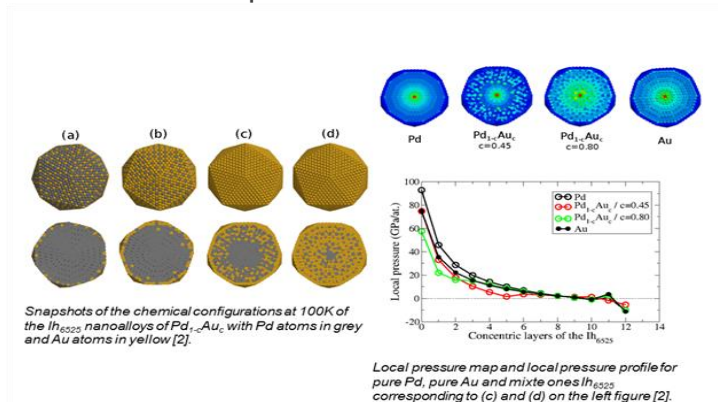
Knowing size-dependence of their structure (symmetry, morphology), we studied the equilibrium structure and morphology of Pd-Au nanoalloys by comparing different motifs among the most probable ones i.e. the icosahedron (Ih), the decahedron (Dh) and the truncated octahedron (TOh).

We performed Monte Carlo and quenched molecular dynamics simulations using a tight binding semi-empirical potential fitted to ab initio calculations in order to compare the steady state energy of the different motifs. The smaller sizes (less than 300 atoms) have been also calculated within the DFT method, starting from the configurations optimized with the semi-empirical potential.

Whereas the TOh motif is stabilized as soon as the sizes of 2 to 3 nm and above in the CoPt system with a strong tendency to chemical ordering [1], we find that the Ih is stable in a large range of size in Pd₃Au and PdAu nanoalloys [2]. This can be explained regarding the core stress in the Ih structure, as illustrated on the figure below, which can be released by replacing large atoms (Au) by smaller ones (Pd).

1. P. Andréazza, C. Mottet, C. Andréazza-Vignolle, J. Penuelas, et al., Phys. Rev. B 82, 155453 (2010).

2. B. Zhu, H. Guesmi, J. Creuze, B. Legrand, C. Mottet, Phys. Chem. Chem. Phys. (2015) DOI : 10.1039/c5cp00491h



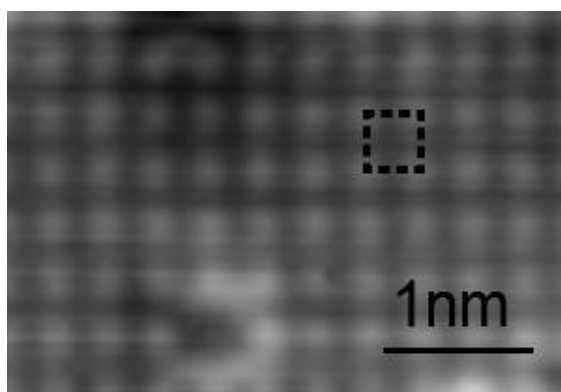
We-B11

STM study of initial silicidation on Ni(001)

Tsuneo FUKUDA¹¹Osaka City University, Osaka, Japan

Silicides, known as compounds between metals and silicon, are indispensable materials for advanced electronic devices. Ni and Co silicides are known to form epitaxial films on Si substrates with atomically flat surfaces and interfaces, and studies on these materials have been an issue central to surface science for decades. Silicides on metal surfaces, on the other hand, have been less attracted and virtually no studies have been conducted so far.

Here we address initial silicide formation on Ni(001) studied by scanning tunnelling microscopy (STM) in an UHV. By depositing Si onto Ni(001) at 373-573 K, impinged Si displaces substrate Ni, and Si is embedded into the top surface layer. As a result atomic-size dark sites due to the embedded Si were seen in the STM images. These dark sites tend to align in the $\langle 1 \ -1 \ 0 \rangle$ directions, forming one-dimensional troughs on the surface. Increasing Si deposition to 0.5 ML induces an uniform $\sqrt{2} \times \sqrt{2}$ R45 degree reconstruction (a checkerboard structure, see attached figure. An unit cell is indicated by a broken square), which consists of alternating Si and Ni in $\langle 1 \ 0 \ 0 \rangle$ directions. The stability of the checkerboard structure originates from the invariant bond lengths between Ni-Ni and Ni-Si and it is also confirmed by the first-principles total energy calculation. Further Si deposition does not replace the substrate Ni, but the second silicide layer was formed. In addition to ordinary silicide islands, one-dimensional atomic-size clusters connected each other are stabilized between 373-473 K. We will discuss the checkerboard structure relevant to the bulk counterpart and compare Si/Ni(001) to Si/Ni(111) and Si/Ni(110) silicides.



We-B12

Single and binary films of immiscible Sn and Pb metals on Ru(0001)

Rafal Topolnicki¹, Robert Kucharczyk¹¹Surface Theory Group, Institute of Experimental Physics, University of Wrocław, Poland

Motivated by recent LEED, AES and STM measurements [1-3], we investigated the structural and electronic properties of submonolayer-thick single-metal Sn and Pb films as well as their binary alloys on Ru(0001) by first-principles DFT calculations. Since experimental data on the arrangement of deposited Sn are inconsistent, we computed the surface phase diagram for Sn/Ru(0001) and determined the long-range ordered (1/2 ML)-c(2x8), (3/5 ML)-($\sqrt{7}\times\sqrt{3}$) and (2/3 ML)-($\sqrt{3}\times\sqrt{3}$)rect structures to be thermodynamically most stable for increasing Sn coverage [4]. For Pb/Ru(0001), the corresponding computations yielded (1/2 ML)-c(4x2) and (4/7 ML)-($\sqrt{7}\times\sqrt{7}$) phases, in agreement with experiment [3]. DFT-optimized adatom arrangements of single-metal Sn and Pb phases on Ru(0001) were favorably confronted with available STM images.

Next, we simulated co-adsorption of immiscible Sn and Pb metals to establish conditions for the existence of their two-dimensional ordered alloys on Ru(0001), recently revealed experimentally [2]. Several models of binary film formation, reflecting the experimental procedure of subsequent deposition of fixed doses of compositionally minor and major elements, were considered. We found an energetic preference towards mixing of Sn and Pb atoms within the wetting layer, and identified the favorable morphology of Sn-Pb surface alloys in terms of their stoichiometry, lateral symmetry and optimal adatom configuration. In particular, hexagonal-like ($\sqrt{7}\times\sqrt{7}$) alloy structure with the PbSn₃ composition was predicted to occur at nominal Sn and Pb coverages of around 0.40 ML and 0.15 ML, respectively, in accordance with [2]. The measured and simulated STM images coincide, confirming the proposed structural model of PbSn₃ alloy on Ru(0001).

[1] M.T. Paffett et al., J. Phys. Chem. 97 (1993) 690.

[2] J. Yuhara et al., Surf. Sci. 616 (2013) 131.

[3] M. Jurczyszyn et al., Appl. Surf. Sci. 311 (2014) 426.

[4] R. Topolnicki et al., Appl. Surf. Sci. 329 (2015) 376.

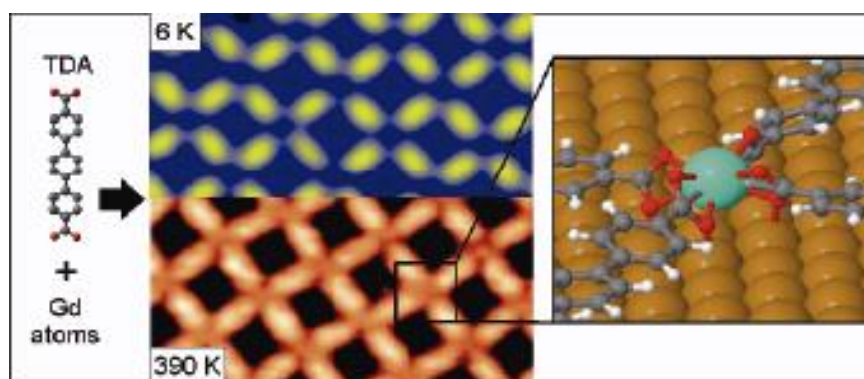
We-C07

Surface-Supported Robust Two-Dimensional Lanthanide-Carboxylate Coordination Networks

Borja Cirera¹, Jose Ignacio Urgel², Yan Wanf^{1,3}, Willy Auwärter², Roberto Otero^{1,4}, Jose Maria Gallego^{1,5}, Manuel Alcamí^{1,3}, Svetlana Klyatskaya⁶, Mario Ruben⁶, Fernando Martin^{1,3}, Rodolfo Miranda^{1,4}, David Eciija^{1,2}, Johannes Barth²

¹IMDEA Nanoscience, Madrid, Spain, ²Physik Department E20 Technische Universität München, Munich, Germany, ³Departamento de Química Módulo 13, Universidad Autónoma de Madrid, Madrid, Spain, ⁴Departamento Física de la Materia Condensada, Universidad Autónoma de Madrid, Madrid, Spain, ⁵Instituto de Ciencia de Materiales de Madrid CSIC, Madrid, Spain, ⁶Institute of Nanotechnology, Karlsruhe Institute of Technology, Eggenstein-Leopoldshafen, Germany

The lanthanide metals are of vital relevance in different fields such as photonics, magnetism, sensing, catalysis, materials science and medicine. In particular, they recently also emerged as important playground for coordination chemists to engineer novel functional molecules and materials, by exploiting their special characteristics and typically high coordination numbers. On the other hand, the exploration of functional surfaces and interfaces is rapidly advancing, whereby the interest is concomitantly driven by the need to advance the control of matter at the molecular scale and the discovery of novel procedures to produce self-assembled nanostructures at well-defined templates. However, despite its scientific interest and technological potential, interfacial coordination chemistry of lanthanides is still in its infancy and further advances are mandatory to fully exploit the potential of rare-earth elements in this respect. Here we present a multi-technique study, combining low- and variable-temperature scanning tunneling microscopy, x-ray photoelectron spectroscopy experiments and density functional theory simulations, demonstrating the gadolinium-directed assembly of interfacial 2D coordination networks on Cu(111) by exploiting metal-ligand interactions between ditopic carboxylate linkers and Gd centers. Our gives detailed, atomistic insights into the geometry and electronic nature of the lanthanide-carboxylate bond in a 2D environment, notably indicating chelating arrangements based on an unprecedented lateral coordination number of 8 for Gd vertexes. Furthermore, our observations and theoretical analysis indicates a coupling motif with ionic characteristics between the anionic carboxylate moieties and the positively charged Gd centers. Thanks to the high coordination number and appreciable bonding strength, the assemblies are thermally stable.



We-C08

Transition metal phthalocyanines adsorbed on Cu110: A massive surface reshaping mediated by metal-organic complexes

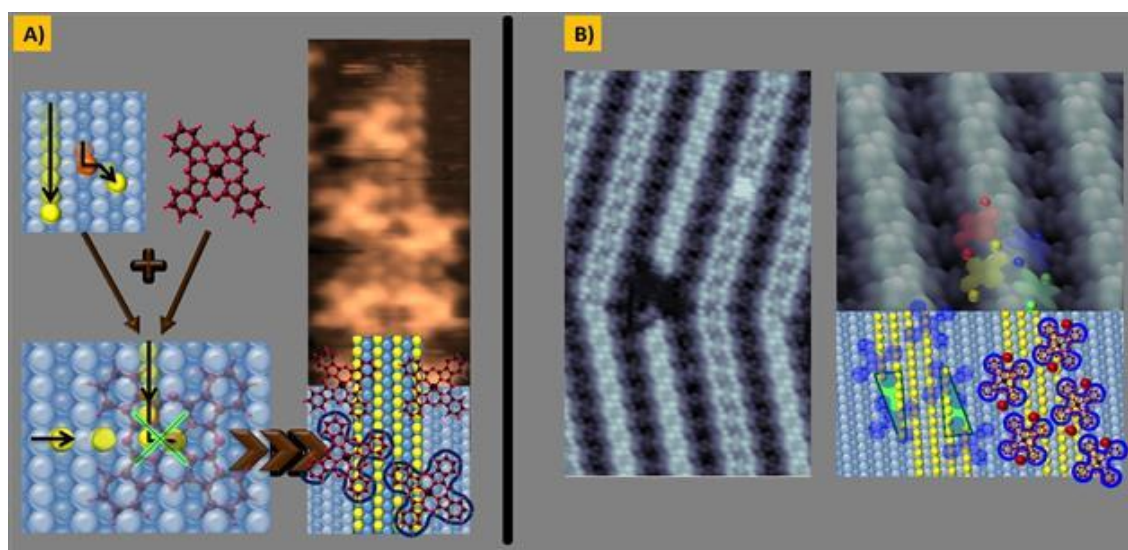
Mikel Abadia¹, Ruben González-Moreno¹, Ane Sarasola^{1,2}, Gonzalo Otero-Irureta³, Andrea Verdini⁴, Luca Floreano⁴, Aran Garcia-Lekue⁵, Celia Rogero¹

¹Material Physics Center (CSIC-UPV/EHU), San Sebastian, Spain,

²Departamento de Física Aplicada I UPV/EHU, Bilbao, Spain, ³Instituto de Ciencia de Materiales de Madrid (CSIC), Madrid, Spain, ⁴Istituto Officina dei Materiali (CNR-IOM), Laboratorio TASC, Trieste, Italy, ⁵Ikerbasque; Basque Foundation for Science, Bilbao, Spain

The actual demand of increasingly smaller devices drives the endeavors to explore new methods to miniaturize the designs. Thus, developments to produce ordered nanostructured surfaces are stimulating fields. In this context, a novel molecular/substrate interaction mechanism that derives in a unique adsorbate induced surface reconstruction is presented. In particular we show how metalated phthalocyanines can promote the formation of regular arrays of Cu nanoribbons on its (110) surface [1].

At variance with the conventional changes of metal reconstructions upon molecular adsorption observed so far, the presented faceting is found to involve a massive reorganization of Cu adatoms. The energy gain of the final system comes not only from the preferential adsorption position of phthalocyanines on the copper surface, but also from their interaction with the surrounded adatoms. By combining experimental (STM, XPS and NEXAFS) and theoretical surface science techniques, we demonstrate that indeed the mechanism behind the massive surface reshaping involves a molecular mediated uni-directional blocking of diffusing surface adatoms (Figure 1A). Optimizing the organometallic network involves the trapping of extra adatoms between the molecules (Figure 1B).



We-C09

Growth of Eu-Cyclooctatetraenide Nanowires on Graphene

Felix Huttmann¹, Nicolas Schleheck¹, Thomas Michely¹

¹II. Physikalisches Institut, Universität zu Köln, Germany

Organometallic nanowires made of alternating Eu atoms and ring-like cyclooctatetraene (Cot) molecules have been theoretically predicted to be ferromagnetic semiconductors and as such have potential for efficient spin filters [1]. Here, we have grown EuCot nanowires by molecular-beam epitaxy, and investigated the samples in situ using scanning tunneling microscopy. By varying the growth conditions, we find a rich spectrum of morphologies from a disordered, spaghetti-like growth to highly ordered, anisotropically shaped, two-dimensional crystallites made of wire bundles. The wires twist and turn, both as a mode of grain intergrowth as well as to avoid having open ends, which are electronically unsaturated and correspond to a polar termination of these quasi-one-dimensional, ionic crystals. In wire bundles, the wires are offset against their nearest neighbors to allow the wires to hook into each other, and where wire bundles bend, a characteristic bending angle is often observed to accommodate this. We furthermore find a remarkable temperature stability of the wires up to 600 K.

[1] Ke Xu et al., J. Chem. Phys. 131, 104704 (2009)

We-C10

Tailoring molecular self-assembly on nanostructured epitaxial graphene

Muriel Sicot¹, Bertrand Kierren¹, Yannick Fagot-Revurat¹, Daniel Malterre¹, Frédéric Chérioux², Frank Palmينو², Iann Gerber³, Damien Tristant³

¹Institut Jean Lamour, UMR 7198, CNRS Université de Lorraine, Vandoeuvre lès Nancy, France, ²Institut FEMTO-ST, Université de Franche-Comté, CNRS, ENSMM, Besançon, France, ³Université de Toulouse, INSA-CNRS-UPS, LPCNO, Toulouse, France

The bottom-up construction of molecular nanomaterials on surfaces is an active research area due to fundamental interests in self-assembly processes as well as potential applications in nanotechnology and molecular electronics. Epitaxial graphene on metal (Gr/M) has emerged as an appealing substrate as it offers a versatile testing ground for investigating the formation of 2D molecular networks [1]. Based on the fact that self-assembly at surfaces is governed by a subtle balance between intermolecular and molecule-substrate interactions, we exploit the idea to tailor molecular arrangements by varying the graphene-metal interaction. This can be realized by the intercalation of foreign atoms (X) leading to Gr/X/M interfaces. Moreover, intercalation offers the possibility to create nanostructured graphene [2] and therefore to investigate the influence of spatial constraints on self-assembly. In this framework, we have investigated the growth of 1,3,5-tri(4'-bromophenyl)benzene (TBB) on Gr/Ir(111) and Gr/Cu/Ir(111) by means of scanning tunneling microscopy and spectroscopy (STM/STS) at 77 K. A Density-Functional-Theory (DFT) study of TBB adsorbed on graphene taking into account the van der Waals interactions and simulated STM images have also been performed. Upon adsorption of TBB at room temperature on Gr/Ir, STM images reveal the formation of two kinds of 2D supramolecular arrangements composed of dimers chains. When adsorbed on Gr/Cu/Ir interfaces, TBB also forms 2D supramolecular networks but exhibit a third kind of arrangement which is confined at the surface of Cu intercalated nanoislands. Electronic properties at the molecular level measured by STS are discussed in the light of DFT calculations. In conclusion, we have shown that molecular self-assembly can be tailored by graphene interface engineering. This work opens new routes towards the realization of molecular architectures with novel properties.

[1] J. M. MacLeod and F. Rosei, *Small* 10 (2014) 1038

[2] M. Sicot et al., *Appl. Phys. Lett.* 105 (2014) 191603

We-C11

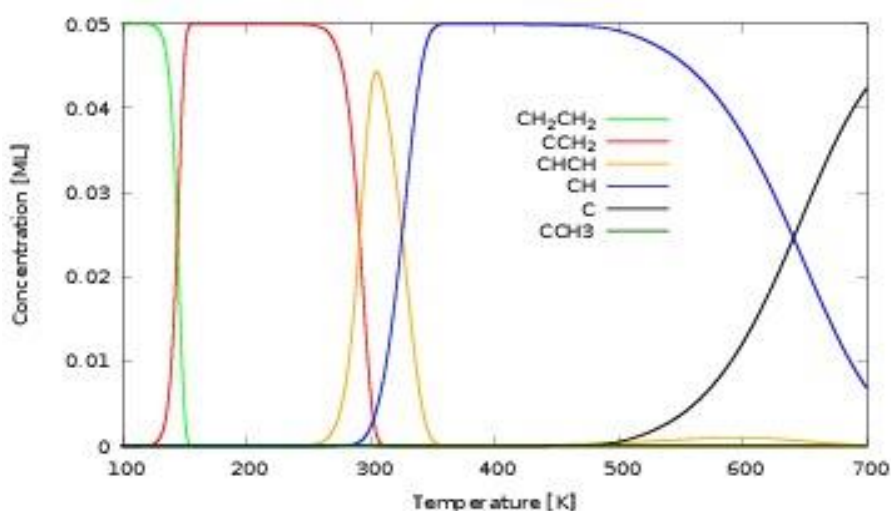
Ethylene decomposition on Ir(111): initial path towards graphene formation

H Tetlow¹, J Posthuma de Boer², D Curcio³, L Omicciolo³, D Lizzit³, D Vvendsky², I Ford⁴, A Baraldi³, L Kantorovich¹

¹King's College London, London, United Kingdom, ²Imperial College London, London, United Kingdom, ³University of Trieste, Trieste, Italy, ⁴University College London, London, United Kingdom

Graphene has attracted a large amount of interest due to its properties and potential applications. However, for this graphene needs to be produced in large quantities and with high quality. This may be possible using epitaxial growth. In particular one method of epitaxial graphene growth, temperature programmed growth (TPG), has successfully been used to grow graphene islands. In this method hydrocarbon molecules are deposited onto a transition metal surface at room temperature and then the temperature is increased in order to facilitate the thermal decomposition of the hydrocarbons and lead to the formation of graphene flakes.

We have examined the early stages of temperature programmed graphene growth starting from the decomposition of ethylene after it is deposited onto the Ir(111) surface, and then gradually heated to high temperatures. To investigate this we have combined a mixture of experimental and theoretical techniques in order to fully understand the decomposition mechanism. X-ray photoelectron spectroscopy (XPS) experiments have been used along with core level binding energy calculations to identify the evolution of species on the surface as the temperature is increased. Furthermore we have developed a complete reaction scheme where all possible reactions involved starting from the decomposition of the initial molecule to form adsorbed carbon are included. The energy barriers for each reaction have been calculated using the DFT based nudged elastic band method, and used to simulate the kinetics and determine the species evolution on the surface, under the same conditions as the experiments. By utilising both the experimental and theoretical results we are able to obtain a proper understanding of the decomposition process. Overall we find a good agreement between the experimental and theoretical results and conclude that a variety of reaction processes are important to the decomposition process.



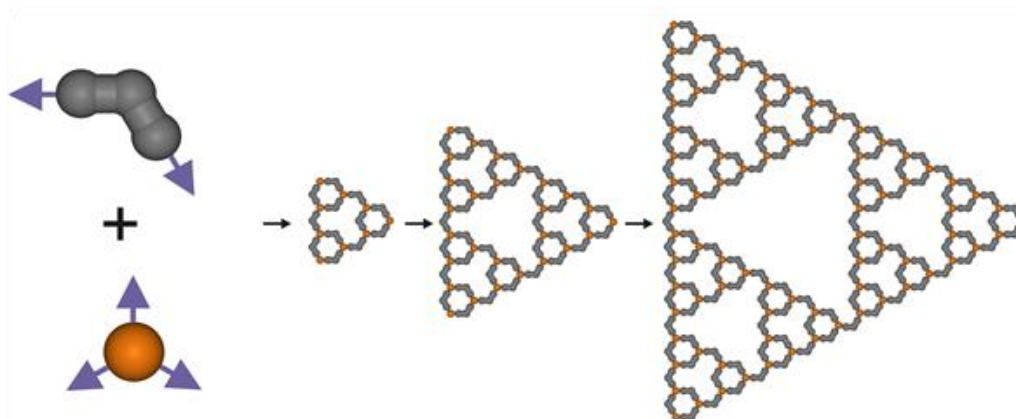
We-C12

Self-assembly of 2D molecular fractals: design rules from theoretical modeling

Paweł Szabelski¹, Damian Nieckarz¹¹Maria Curie-Skłodowska University, Lublin, Poland

Ordered fractal structures such as the Sierpiński triangle are one of most complex patterns which until recently have been viewed as purely theoretical constructs with no reference to real systems. The latest experiments on 2D self-assembly of molecular building blocks, including DNA tiles[1] and smaller functional organic molecules[2,3] have demonstrated the ability of these units to form aggregates resembling deterministic fractal sets. The key factor which directs the fractal self-assembly has been molecular shape and proper encoding of intermolecular interactions which sustain the resulting aggregates. In this contribution we show how theoretical modeling can be used to predict fractal structure formation in adsorbed systems comprising simple molecular tectons and metal coordination centers. To that end the lattice Monte Carlo model of surface-confined metal-organic self-assembly is presented [4,5] and its main results are discussed and linked with recent experimental findings. It is demonstrated that a suitable choice of molecular bricks combined with fine tuning of directional metal-linker interactions can largely facilitate the creation of extended patterns with the Sierpiński triangle architecture. The design rules deduced from the simulations are generalized and their potential use in construction of fractal molecular systems stabilized by other intermolecular interactions is outlined. The results from our theoretical investigations can be helpful in designing new supramolecular structures and synthesis of fractal macromolecules.

1. P. W. K. Rothmund, N. Papadakis, E. A. Winfree, PLOS Biol., 2004, 2, 2041
2. R. Sarkar, K. Guo, K., C.N. Moorefield, M. J. Saunders, C. Wesdemiotis, G. R. Newkome, Angew. Chem. Int. Ed., 2014, 53, 12182
3. J. Shang, Y. Wang, M. Chen, J. Dai, X. Zhou, J. Kuttner, G. Hilt, X. Shao, J. M. Gottfried, K. Wu, Nature Chem., 2015, 7, 389
4. D. Nieckarz, P. Szabelski, Chem. Comm., 2014, 50, 6843.
5. D. Nieckarz, P. Szabelski, J. Phys. Chem. C, 2013, 117, 11229.



We-D07

Formation of amorphous networks - finding order in chaos

Christin Büchner¹, Stefanie Stuckenholtz¹, Kristen Burson¹, Philomena Schlexer², Markus Heyde¹, Hans-Joachim Freund¹

¹Fritz-Haber-Institut der Max-Planck-Gesellschaft, Berlin, Germany, ²Università degli Studi di Milano-Bicocca, Italy

Recent advances in preparations of thin oxide films have enabled us to study the atomic structure of a 2D glass. A bilayer SiO₂-film on a Ru(0001) support can be investigated with a combined low temperature AFM and STM [1]. Images with atomic resolution reveal a continuous random network in accordance with Zachariasen's 1932 postulation for amorphous solids [2]. SiO₄ building blocks are connected at random angles, forming rings containing four to nine Si-atoms. While recurring structural motifs are observed, an unambiguous structural description, like the Miller indices for crystals, is lacking. We will present structure data on this system, compare them to other unordered structures and discuss how amorphous materials can be appropriately categorized. Studying pair correlation functions builds a bridge towards diffraction data and therefore relates our 2D system to 3D materials. However, investigating ring size distributions and ring neighborhoods is a more useful approach for materials that lack long-range order [3].

Fundamental understanding of amorphous materials and their formation principles will help to study the important relationship between composition, preparation and structure, which is a significant challenge in application-oriented research as well.

[1] L. Lichtenstein, et al., Angew. Chem., Int. Ed. 51, 404 (2012)

[2] W. H. Zachariasen, J. Am. Chem. Soc. 54, 3841 (1932)

[3] C. Büchner, et al., Z. Phys. Chem. 228, 587 (2014)

We-D08

Total-reflection high-energy positron diffraction (TRHEPD)
analysis of the Ge(001)-c(8×2)-Au surface structure

Izumi Mochizuki¹, Yuki Fukaya², Ken Wada¹, Tetsuo Shidara¹, Ayahiko Ichimiya¹, Toshio Hyodo¹

¹High Energy Accelerator Research Organization, KEK, Tsukuba, Japan,

²Japan Atomic Energy Agency, Tokai, Japan

Total-reflection high-energy positron diffraction (TRHEPD), which is the positron counterpart of reflection high-energy electron diffraction (RHEED), provides an ideal technique [1] for the determination of an atomic configuration of the topmost surface of a crystal. Recently we developed a new TRHEPD apparatus [2] on a beam line of a linac-based intense positron beam at the Slow Positron Facility, KEK, Japan. The intense beam enables us to install a brightness-enhancement section [3] for the observation of clear positron diffraction patterns [1, 3] from crystal surfaces.

Here we report an investigation of the atomic configuration of Au-induced nanowires formed on a Ge(001) surface, that is, the Ge(001)-c(8×2)-Au structure [4]. There has been a debate about the detailed structure of this surface; several models have been proposed based on scanning tunneling microscopy observations [4, 5], surface X-ray diffraction analysis [6], and first-principles calculations with density functional theory [7, 8]. We found that none of these previously proposed models [4-8] was consistent with the TRHEPD diffraction spot analysis based on a fully dynamical diffraction theory, or TRHEPD rocking-curve analysis.

We thus propose a new model for the atomic configuration of the Ge(001)-c(8×2)-Au structure.

[1] Y. Fukaya et al., Appl. Phys. Express 7, 056601, 2014.

[2] K. Wada, et al., Eur. Phys. J. D 66, 37, 2012; J. Phys.: Conf. Ser. 443, 012082, 2013.

[3] M. Maekawa et al., Eur. Phys. J. D 68, 165, 2014.

[4] J. Wang et al., Phys. Rev. B 70, 233312, 2004.

[5] J. Schäfer et al., Phys. Rev. Lett. 101, 236802, 2008.

[6] S. Meyer et al., Phys. Rev. B 85, 235439, 2012.

[7] S. Sauer et al., Phys. Rev. B 81, 075412, 2010.

[8] S. López-Moreno et al., Phys. Rev. B 81, 041415(R), 2010.

We-D09

Potassium adsorption on TiO₂(110): structural and electronic investigation

Celine Dupont¹, Sylvie Bourgeois¹, Jacques Jupille², Alberto Verdini³, L. Floreano³, A. Cossaro³, Peter Krüger¹, Bruno Domenichini¹

¹Institut Carnot de Bourgogne - University of Burgundy - CNRS, Dijon, France,

²Institut des NanoSciences de Paris, UPMC-CNRS, Paris, France, ³CNR-IOM, Laboratorio TASC, Trieste, Italy

Localizing electronic states induced by point defects and/or impurities at oxide surfaces is a crucial issue for understanding the surface reactivity involved in many applications such as gas sensing, photo and heterogeneous catalysis, etc. X-ray and UV photoelectron spectroscopies are among the most used tools to study oxide surface defects. In addition, photoelectron diffraction (PED) allows probing the crystallographic structure locally, around selected species. It is thus a powerful structural tool for localizing species in the topmost layers of a material. In the case of very low defect concentrations, the very weak features induced by defects in the valence band spectra can be enhanced through resonant photoemission process. Associating PED and resonance process allows then the determination of defect charge distribution in oxide top-most layers. Previously, we have illustrated the power of this new method called Resonant Photo Electron Diffraction (RPED) in the case of charge excesses induced in TiO₂(110) surface through simple non-stoichiometry (oxygen vacancies) or through reaction with sodium.

In this communication, we will present our investigation of the interaction between potassium and TiO₂(110). The experimental patterns, both for Ti3d and K2p, are interpreted through theoretical modelling based on DFT calculations. The plane-wave code VASP is used to model the structures, while diffraction patterns are calculated using EDAC [1]. These calculations allow to determine both the best position for potassium atoms and the optimal coverage that reproduce the experimental results. On Figure 1, we report both the recorded (left) and the modelled (right) patterns for Ti3d states after potassium adsorption on TiO₂(110). Once the material structure is known, the calculations allow a detailed interpretation at the electronic level. In particular, the localization of the charge excess is compared for the potassium adsorption, the sodium adsorption and defective TiO₂.

[1] Garcia de Abajo F. J., et al., Phys. Rev. B 63 (2001) 075404.

We-D10

Formation of hexagonal Fe-N atomic layer on Cu (001)

Koichiro Ienaga¹, Yukio Takahashi¹, Masamichi Yamada¹, Norikazu Kawamura², Toshio Miyamachi¹, Fumio Komori¹

¹The University of Tokyo, Chiba, Japan, ²NHK Science and Technology Research Laboratories, Tokyo, Japan

Iron nitrides have been known as ideal replacements for rare-earth magnets in terms of large magnetic moments and chemical stability. Fe-N system has various compositions in its phase diagram and the excellent magnetic properties are expected in those with low N concentration. Recently epitaxial growth of iron nitrides on a Cu (001) substrate has been studied for advance of magnetic data storage, and its magnetic properties have been clarified using synchrotron-radiation-based techniques [1,2]. However, in most cases, Fe₄N is preferentially formed on Cu (001) despite demands for improvement of magnetic properties through composition control. Previous fabrication [2] of iron nitride atomic layers on Cu (001) has been on this line, and monoatomic Fe₂N square lattice is formed as a component of fcc Fe₄N consisting of Fe layer and Fe₂N layer. To change N contents, we fabricate with a different way in ultra high vacuum. We first expose Cu (001) to N⁺ bombardment and subsequently deposit submonolayer Fe atoms. After annealing this sample up to 670 K, hexagonal-shape islands with a few stacking layers appear near step edges beside usual Fe₂N square lattices. By further annealing, the islands change to well ordered hexagonal atomic layers with stripe corrugations. The formation of these new iron-nitride atomic layers is attributed to excess N supply and strain relaxation.

[1] J. M. Gallego et al. Phys. Rev. Lett. 95, 136102 (2005).

[2] Y. Takagi et al. Phys. Rev. B 81, 035422 (2010).

We-D11

An NMR study of crystalline and amorphous phases of vapor deposited ice

Elina Lisitsin¹, Oren Ofer¹, Tatyana Kravchuk¹, Gil Alexandrowicz¹¹Schulich Faculty of Chemistry, Technion - Israel Institute of Technology, Haifa, Israel

Amorphous-Solid-Water (ASW) is the most abundant form of ice in the universe and extensive efforts are being invested in characterizing its properties, even so there is a great deal of uncertainty and controversy regarding its properties and the various phase transitions it undergoes [1]. The NMR technique is a sensitive tool for studying structure and dynamics of solid state matter. Nevertheless, due to technical difficulties very few NMR studies of water ice have been performed, focusing on crystalline phase (CI) and low and high density amorphous phases obtained by pressurizing CI. To the best of our knowledge NMR experiments have never been performed on vapor deposited ice, i.e ASW.

In this talk we will present recent NMR measurements which show that vapor deposited ice exhibits a unique spin-lattice relaxation behavior which is strikingly different from that seen for other forms of ice. Above 130K a simple exponential relaxation time takes place over a long time scale (hours). On the other hand, macroscopic ice samples grown at lower temperatures appear to be composed of two different populations with T1 spin-relaxation times which differ by up to four orders of magnitude. Another interesting observation is that annealing the ASW samples at elevated temperatures (200K) which are well above the ASW to CI transition, does not result in a transformation to the NMR relaxation profiles obtained when growing above 130K. The dependence of the relaxation profiles on the substrate interface, the temperature and the flux of the vapor deposition supplies clues to the origin of the complex relaxation profile. Finally, our future plans to measure NMR of ultra-thin ASW films and even sub-monolayer water films, which could be possible using our magnetically focused ortho-H₂O source [2] will be described briefly.

[1] C. A. Angell, Annu.Rev.Phys.Chem.55,559 (2004).

[2] T. Kravchuk et al. Science,331,319 (2011).

We-E07

Tribochemical Reactions of Diamond-like Carbon during Water Lubrication Process by Tight-Binding Quantum Chemical Molecular Dynamics Simulation

Shandan Bai¹, Jingxiang Xu², Yuji Higuchi², Nobuki Ozawa³, Koshi Adachi³, Shigeyuki Mori¹, Kazue Kurihara^{4,5}, Momoji Kubo²

¹New Industry Creation Hatchery Center, Tohoku Univ., Sendai, Japan,

²Institute for Materials Research, Tohoku Univ., Sendai, Japan, ³Graduate School of Engineering, Tohoku Univ., Sendai, Japan, ⁴Advanced Institute for Materials Research, Tohoku Univ., Sendai, Japan, ⁵Inst. of Multidisciplinary Research for Advanced Materials, Tohoku Univ., Sendai, Japan

Diamond-like carbon (DLC) is paid attention as the tribo-coating for industrial mechanical application due to its low friction and antiwear properties. Furthermore, DLC in water lubrication improves its friction properties and reduces the emission of CO₂ for an earth friendly environment. However, it is still unclear the relationship between the friction coefficient and contact pressure in details because the chemical reaction occurs at the interface. Our tight-binding quantum chemical molecular dynamics (TB-QCMD) method is very effective for clarifying chemical reactions at contact surfaces and tribological properties during friction process, because it enables large-scale long calculations on an electronic and atomic scale [1,2]. In this study, tribo-chemical reaction of DLC films in water lubrication is investigated by our TB-QCMD code. In Fig 1(a), we perform friction simulation of DLC in water, contact pressures of 1 and 7 GPa are applied on the top of upper substrate. In Fig. 1(b), we observe that the C-H and C-OH bonds are formed on the DLC surface during friction under a contact pressure of 1 GPa because of the chemical reactions of water molecules. On the other hand, it is interesting to see that not only the C-OH and C-H bonds but also C-O-C bond are formed on the DLC surface under a contact pressure of 7 GPa in Fig. 1(c). The friction coefficients are 0.15 and 0.07 for DLC in water under contact pressures of 1 and 7 GPa, respectively. The friction coefficient reduces with an increase in contact pressure on boundary lubrication. We suggest that the structure change caused by the C-O-C generation on the DLC surface leads to low friction properties of DLC in water even under a high contact pressure.

[1] S. Bai, M. Kubo et al., J. Phys. Chem. C, 116, 12559 (2012).

[2] S. Bai, M. Kubo et al., RSC Adv., 4, 33739 (2014).

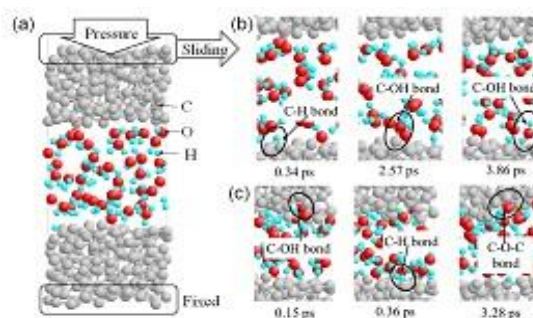


Fig. 1 (a) Friction simulation model of DLC in water lubrication. Snapshots of the friction interfaces in water lubrication under contact pressures of (b) 1 and (c) 7 GPa.

We-E08

Friction Property of Oxidized MoS₂ Layers by Tight-Binding Quantum Chemical Molecular Dynamics Simulation

Hiroki Murabayashi¹, Takeshi Tsuruda¹, Yang Wang¹, Shandan Bai², Takeshi Nishimatsu¹, Yuji Higuchi¹, Nobuki Ozawa³, Koshi Adachi³, Jean-Michel Martin⁴, Momoji Kubo¹

¹Institute for Materials Research, Tohoku University, Sendai, Japan, ²New Industry Creation Hatchery Center, Tohoku University, Sendai, Japan,

³Graduate School of Engineering, Tohoku University, Sendai, Japan,

⁴Laboratoire de Tribologie et Dynamique des Systemes, Ecole Centrale de Lyon, Lyon, France

Diamond-like carbon (DLC), which is composed of sp² and sp³ carbon atoms, is paid attention as a solid lubricant material for an automotive engine application because of its excellent friction properties. To enhance its low friction property, molybdenum dithiocarbamate (MoDTC) is used as additive on DLC coating. When MoS₂ is generated from MoDTC during the sliding, friction coefficient of DLC decreases. However, the oxidation of MoS₂ leads to a high friction of MoS₂, which means the degradation of MoS₂ friction property. To achieve stable low friction of DLC films lubricated with MoDTC, the understanding of influence of oxygen on friction property of MoS₂ is required. We develop our tight-binding quantum chemical molecular dynamics code which can handle chemical reaction and perform large scale calculation [1-2]. In this study, we perform friction simulation of MoS_{2-x}O_x using this code to clarify the effect of oxygen on friction property of MoS₂. In the simulation model of MoS_{2-x}O_x layers, sulfur atoms are replaced by oxygen atoms. When x in MoS_{2-x}O_x is smaller than 0.67, MoS_{2-x}O_x layers keep low friction. However, when x in MoS_{2-x}O_x is larger than 0.67, we observe an increase in friction coefficient. We investigate why O-rich MoS_{2-x}O_x layers increase friction coefficient. The snapshots of MoS_{0.2}O_{1.8} layers during sliding at 0 ps and 20 ps are shown in Fig. 1(a), (b). Fig. 1(a), (b) show that surface asperity is formed by sulfur atoms of MoS_{0.2}O_{1.8} layers. We analyze interlayer distance and friction coefficient of MoS_{0.2}O_{1.8} layers during the sliding (Fig. 1(c)). The interlayer distance and friction coefficient suddenly increase at 20 ps. Therefore, we found that O-rich MoS_{2-x}O_x layers take a larger friction coefficient because of forming surface asperity. The mechanism of forming surface asperity is discussed in this conference.

[1] K. Hayashi, M. Kubo, J. Phys. Chem. C, 115 (2011) 22981.

[2] K. Hayashi, M. Kubo, Faraday Discuss., 156 (2012) 137.

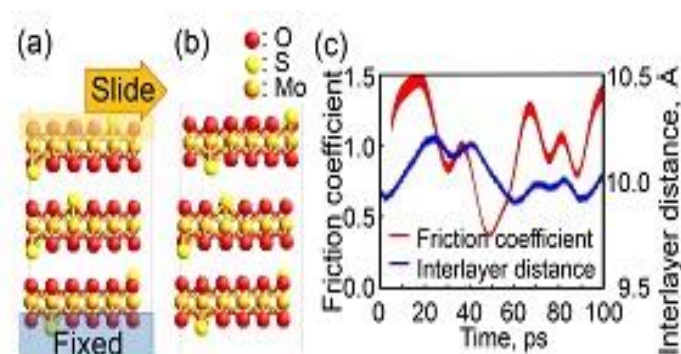


Fig. 1 Friction simulation of the MoS_{0.2}O_{1.8} layers at (a) 0 ps and (b) 20 ps. (c) Friction coefficient and interlayer distance of MoS_{0.2}O_{1.8} layers.

We-E09

Influence of DLC Film Structures on Its Friction Property by Quantum Chemical Molecular Dynamics Simulation

Takeshi Tsuruda¹, Hiroki Murabayashi¹, Yang Wang¹, Takuya Kuwahara¹, Shandan Bai², Takeshi Nishimatsu¹, Yuji Higuchi¹, Nobuki Ozawa³, Koshi Adachi³, Jean-Michel Martin⁴, Momoji Kubo¹

¹Institute for Materials Research, Tohoku University, Sendai, Japan, ²New Industry Creation Hatchery Center, Tohoku University, Sendai, Japan,

³Graduate School of Engineering, Tohoku University, Sendai, Japan,

⁴Laboratoire de Tribologie et Dynamique des Systemes, Ecole Centrale de Lyon, Lyon, France

Diamond-like carbon (DLC) films consisting of sp^2 carbon (Csp^2) and sp^3 carbon (Csp^3) have low friction property. DLC is expected to be used at aerospace instruments, micro-electro mechanical systems, and mechanical contact surfaces. It was suggested that the formation of a graphite like structure consisting of Csp^2 on the DLC surface decreases its friction. To achieve super-low friction property of the DLC films, we should clarify the relationship between Csp^2 and friction property at an atomic scale. We have already developed our tight-binding quantum chemical molecular dynamics (TB-QCMD) simulator which can reduce computation time and treat large scale model [1,2]. Moreover, our TB-QCMD simulator is capable of handling the chemical reactions, which can not be realized by classical MD method. In this study, to elucidate the effect of sp^2 structure on low friction property, we perform friction simulation for amorphous carbon (a-C) films by our TB-QCMD simulator. We use two a-C film models with different Csp^2 ratio. The snapshots of a-C film during friction are shown in Fig. 1. In Fig. 1(a), a-C film with high Csp^2 ratio shows smooth friction. On the other hand, in Fig. 1(b) a-C film with low Csp^2 ratio shows the generation of C-C bonds at the friction interface. Friction coefficients of a-C film are 0.09 and 0.93 for high and low Csp^2 ratio, respectively. We have already reported that friction coefficient increases to a large value by the generation of C-C bonds at the friction interface [2]. It indicates that a-C film with high Csp^2 ratio exhibits low friction coefficient because C-C bonds are not generated at the friction interface. Therefore, we propose that a-C film with high Csp^2 ratio shows lower friction property than that with low Csp^2 ratio.

[1] K. Hayashi, M. Kubo, Faraday Discuss., 156 (2012) 137.

[2] K. Hayashi, M. Kubo, J. Phys. Chem. C, 115, (2011) 22981.

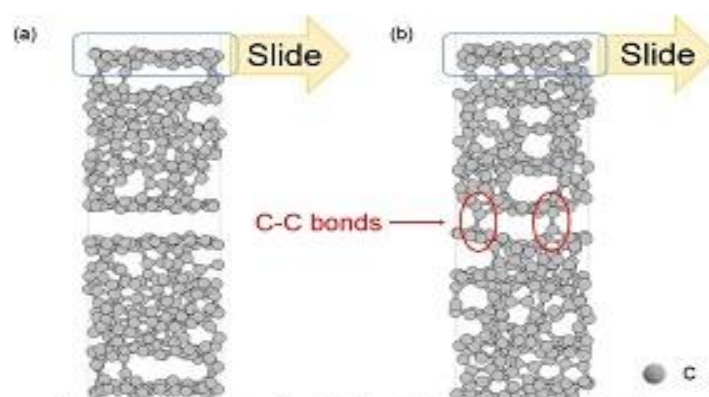


Fig. 1 Snapshots of a-C film with (a) high Csp^2 ratio and (b) low Csp^2 ratio during friction.

We-E10

Biomimicking Butterfly Wing Surface Texture for Improved Tribological Performance

Eui-Sung Yoon¹, Harpreet Singh Grewal¹, Hyogeun Shin¹, Il-Joo Cho¹

¹Centre for Biomicrosystems, Korea Institute of Science and Technology, Seoul, South Korea

Friction and wear becomes significantly important at micro and nano scales. They influence the performance and durability of several nano/micro electromechanical systems (NEMS/MEMS). Biomimicking the surface texture of different living organisms has helped to improve the tribological performance of these systems. In this study, we examined the friction and adhesion behavior of textured surfaces that were derived by mimicking the surface morphology of butterfly wing. Three kinds of mimicked structures of similar solid/air fraction but different contact perimeters were fabricated on Si wafer using photolithography and deep reactive ion-etching technique. These patterns were subsequently coated with polytetrafluoroethylene (PTFE), diamond-like carbon (DLC), and fluorine incorporated diamond-like carbon (F-DLC) thin layers using plasma-enhanced chemical vapor deposition (PECVD) technique. Atomic force microscope was used to investigate the friction and adhesion properties of the coated and un-coated samples under the various range of applied normal load. Wetting behavior of the textured and control surfaces was measured using sessile-drop method. Results showed a significant influence of the textured geometry on the wetting and tribological behavior. The increase in perimeter of textured geometry induced directional wettability and friction. The wetting was controlled by the contact-line pinning phenomenon modulated by the texture geometry. The effect of surface chemistry and texture geometry is explained by intermolecular forces and contact mechanics. High stiffness and mechanical integrity is responsible for the superior performance of the mimicked surface and PTFE and F-DLC coatings helped in reducing the coefficient of friction and adhesion. These results suggest that the mimicked textures with directional friction and wetting behavior may be used as a potential transport system which will be useful for different biological studies and nano-fluid based systems.

We-E11

New halogen-free room temperature ionic liquids as external lubricants for different tribo-materials

Noelia Saurín¹, Ichiro Minami², José Sanes¹, María Dolores Bermúdez¹

¹Universidad Politécnica de Cartagena, Cartagena, Spain, ²Luleå Technical University, Luleå, Sweden

Room temperature ionic liquids (RTILs) are advanced functional fluids for different scientific and technological fields. Generally, RTILs possess excellent thermal stability, non-volatility, non-flammability, high heat capacity, and electrical conductivity. They are composed of solely anion and cation, and exist as fluids without any solvents. In the previous works, we have shown good lubrication properties in terms of low friction and low wear using fluorinated RTILs, under severe tribological conditions. We also demonstrated that the tribological properties of thermosetting resins could be improved if RTILs were incorporated in resin matrix. Although fluorine-containing RTILs are beneficial for both boundary lubricity and hydrophobic properties, they have drawbacks regarding environmental friendless and corrosion to metals. In addition, fluorine-containing RTILs are costly compared to corresponding hydrocarbons.

In a series of our work on designing materials for tribological purposes, the present work aims at evaluating newly designed, hydrophobic fluorine-free RTILs as external lubricants. A reciprocating tribo-tester was employed with steel-ceramic and steel-thermosetting resin contact under boundary conditions. Four different halogen-free RTILs provided excellent tribological properties with friction coefficient of lower than 0.1 and almost non-detectable wear. Also they exhibited low corrosion to metals. The compatibility of material-lubricant will be discussed in the light of material design.

Th-A01

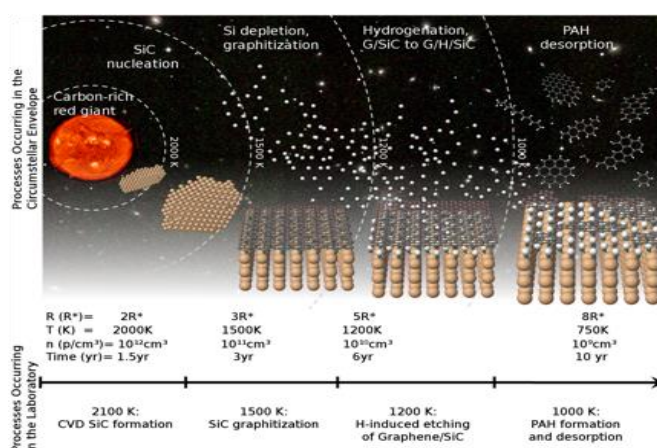
H-induced Graphene Etching as Origin of Polycyclic Aromatic Hydrocarbons Formation: From the Stars to the Laboratory

Jose I. Martinez¹, Jose Cernicharo¹, Jose A. Martin-Gago¹

¹Department of Surfaces, Coatings and Molecular Astrophysics, Institute of Material Science of Madrid (ICMM-CSIC), Madrid, Spain

A recent theory explains the origin of polyaromatic-hydrocarbon-molecules (PAHs) in the universe, where these molecules are formed by hydrogen-etching of the graphitic surface of the stardust particles. Measurements made using large radio-telescopes show the presence of large amounts of PAHs in the vicinity of some stars. The PAHs form in interstellar space via atomic hydrogen adsorption on graphite layers covering the surface of the particles of stardust, subsequent decomposition of graphene and final release of polyaromatic-molecules. Experiments were carried out using STM, studying the interaction of atomic hydrogen with the graphene grown on SiC in conditions similar to those in the interstellar medium (UHV and high temperature). A significant subsidization of graphene layer, accompanied by formation of graphene flakes passivated by hydrogen, was evinced, which was further supported by advanced first-principles calculations showing the decomposition of graphene with hydrogen at high temperatures.

Additionally, in order to get a deeper insight on the specific mechanisms leading to the formation of hydrocarbons from the hydrogen-induced graphene-etching, a step forward was given from the purely conceptual theory point of view in the attempt to design and elaborate a theoretical model explaining the quantitative point of view of such processes. On this basis, a novel mechanism explaining the formation of hydro(carbons/carbyls) from hydrogenated graphene/graphite has been recently proposed; hard C-C bonds are weakened and broken by the synergistic effect of chemisorbed hydrogen and high temperature vibrations. Total energies, optimized structures, and transition states are obtained from DFT-based simulations. These values have been used to determine the Boltzman probability for a thermal-fluctuation to overcome the kinetic-barriers, yielding the time-scale for an event to occur. This mechanism can be used to rationalize the possible routes for the creation of small hydro(carbons/carbyls) from etched graphene/graphite in both circumstellar regions and conventional Surface Science laboratories.



Th-A02

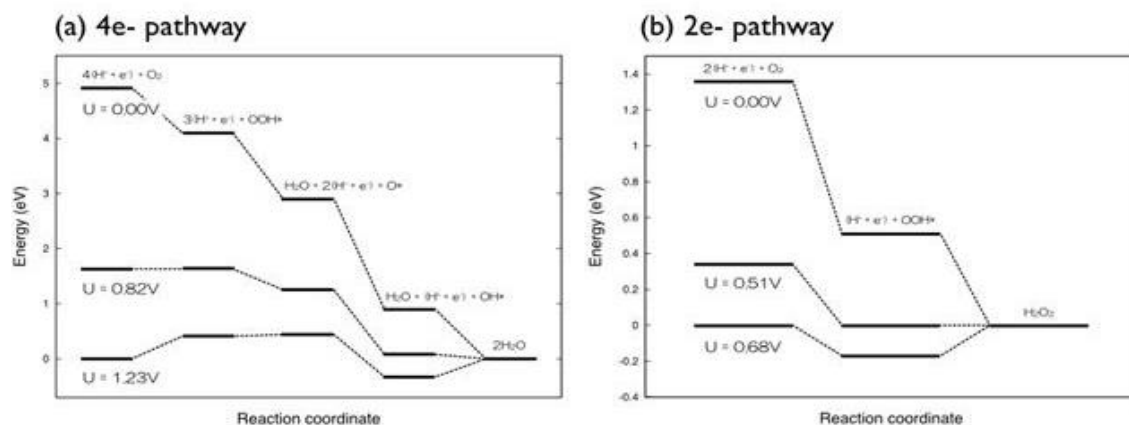
Oxygen reduction reaction on the basal plane of nitrogen-doped graphene

Jun Nakamura^{1,2}, Akihito Ichikawa^{1,2}, Haruyuki Matsuyama^{1,2}, Akira Akaishi^{1,2}¹The University of Electro-Communications (UEC-Tokyo), Tokyo, Japan, ²JST-CREST, Saitama, Japan

Recently, several groups have reported high oxygen reduction reaction (ORR) activities in nitrogen-doped carbon nanomaterials which are candidates of metal-free catalysts for ORR. Local atomic configurations of dopants in nitrogen-doped graphene are typically classified into three functional groups (pyrrole-like, pyridine-like, and graphite-like configurations). However, the mechanism of the ORR on the nitrogen-doped graphene and its correspondence to the local atomic configurations have not fully understood.

We examine the ORR on the nitrogen-doped graphene containing the graphitic N using first-principles calculations. In general, ORR occurs mainly two pathways: The two-electron pathway (2e-) that is reduced to hydrogen peroxide (H₂O₂), and the direct four-electron pathway (4e-) that reduces to water (H₂O). In case of the associative mechanism for the two- and four- electron reduction pathways, the electrocatalytic activity is governed by the stability of reaction intermediates like OOH*, OH*, and O* (where "*" refers to a surface site). Free energies of the reaction intermediates have been calculated based on the computational hydrogen electrode model. We have taken account of effects of electrode potential, pH of a solution, a local electric field in double layer, and water environment.

We have constructed energy diagrams at several electrode potentials on the basis of the first-principles calculations. It has been shown that the 2e- and 4e- reduction processes proceed at potentials up to about 0.5V and 0.8V, respectively. This means that we can control the reduction pathway for the nitrogen-doped graphene with the graphite-like N. Proton-electron transfer to OOH* (the 2e- pathway), and the formation of OOH* (the 4e- pathway) are confirmed to be the rate-limiting steps, respectively. Density dependence of N on the ORR activity will also be discussed in the presentation.



Th-A03

Nano-scale Observation of Graphene Oxide Using Scanning Tunneling Microscopy and Spectroscopy

Satoshi Katano¹, Tao Wei¹, Yoichi Uehara¹

¹Tohoku University, Sendai, Japan

Fluorescence and quenching of light from graphene oxide (GO) have been extensively investigated due not only to the basic interests but also to the technological applications, such as transparent conductors and biosensors. The unique optoelectronic properties of GO stem from the decoration with the oxygen-containing functional groups, resulting in a mixture of sp^2 - and sp^3 -hybridized carbon domains. In this paper, we present results for the nano-scale observation of GO on Au(111) covered with the octanethiolate (C8S) self-assembled monolayer (SAM) as a first step towards revealing the local electronic states of GO.

C8S-SAM/Au(111) was prepared by immersing the Au(111)/mica substrate in 1 mM octanethiol solution in ethanol, on which GO flakes were subsequently deposited by the spin coating method. STM and scanning tunneling spectroscopy (STS) measurements were carried out at room temperature in the ultrahigh vacuum chamber with the base pressure of 10^{-10} Torr.

In the STM image of GO/ C8S-SAM/Au(111), flat terraces and monatomic steps were clearly observed, indicating that an atomically-flat Au(111) was well prepared. In addition, the GO layer, having grains with a diameter of 8 to 10 nm, was simultaneously observed. The GO measures 0.8 nm in thickness, which is corresponding to the single layer of GO. We performed STS measurements in order to elucidate the electronic structure of GO. Although the C8S-SAM spectrum does not exhibit a distinct peak near the Fermi level, the characteristic peaks associated with the π and π^* states were observed in the GO spectrum. We found that the bandgap value varies depending on the location of the STS measurement, indicating the nano-scale heterogeneity of sp^2 domain in GO.

Th-A04

Tuning the Redox Properties of Cobalt Particles Supported on Metal-oxides by an in-between Graphene Layer

Wen Luo¹, Spiros Zafeiratos¹

¹Institut de Chimie et Procédés pour l'Energie, l'Environnement et la Santé (ICPEES), ECPM, UMR 7515 du CNRS, Univ. of Strasbourg, France

Recently we have demonstrated that the metal-support interaction between cobalt nanoparticles and a ZnO substrate is significantly modified by the insertion of an in-between graphene layer (interlayer) [J. Phys. Chem. Lett. 2014, 5, 1837]. Here we study the effect of the graphene interlayer to the reduction-oxidation (redox) properties of cobalt exposed to gas phase oxygen and hydrogen. Single-layer chemical vapor deposition (CVD)-grown graphene was transferred onto planar ZnO and SiO₂ substrates forming a large-area, low-defect density, protective layer. Cobalt was deposited on the substrates by electron beam evaporation under vacuum. Oxygen and hydrogen exposure was performed at low (5×10^{-7} mbar) and intermediate (10 mbar) pressure regimes, while X-ray photoelectron and Raman spectroscopies as well as atomic force microscopy, were used to analyze the samples before and after exposure to the gas phase. We show that oxidation of cobalt by O₂ takes place at similar temperatures with or without the presence of the graphene interlayer and does not depend on the substrate. On the contrary, in H₂ graphene interlayer has a dominant effect on the reduction temperature. In particular, in the presence of graphene, reduction of cobalt oxide takes place at considerably lower temperature (up to 400 degrees lower) as compared to the same oxide substrate not being covered by graphene. Raman spectroscopy indicates a relative increase of the graphene defect sites due to the gas exposure, but without major destruction of the graphene characteristics. This study shows that an atomic thick carbon layer could be used to manipulate the oxidation state of supported cobalt nanoparticles and can potentially affect the reaction pathways of cobalt-based catalysts or even limit deactivation of catalysts caused by undesired strong metal-support interaction.

Th-A05

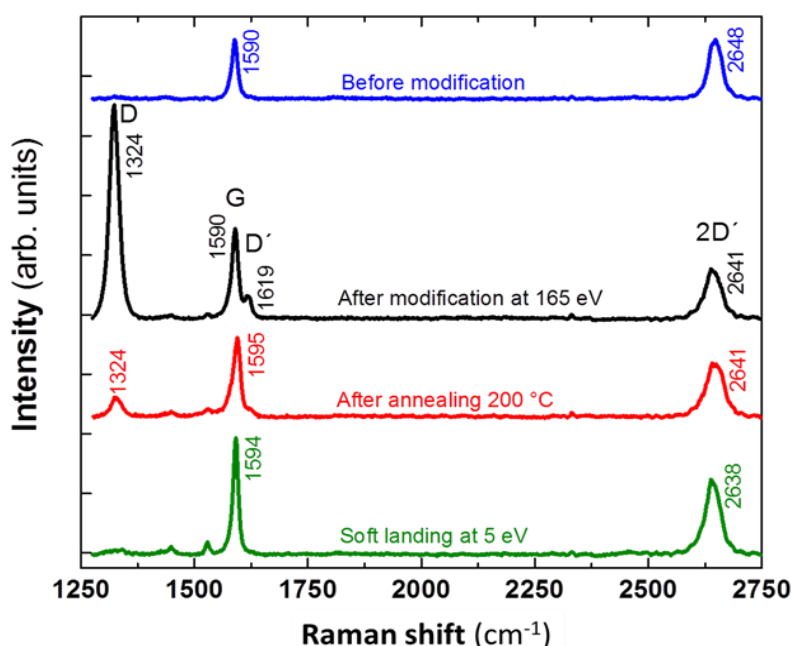
Chemical Functionalization of Graphene via Hyperthermal Molecular Ion-Surface Reaction

Stephan Rauschenbach¹, Girjesh Dubey¹, Roberto Urcuyo¹, Sabine Abb¹,
Gordon Rinke, Marko Burghard¹, Klaus Kern^{1,2}

¹Max-Planck-Institute for Solid State Research, Stuttgart, Germany, ²EPFL,
Institut de Physique de la Matière Condensée, Lausanne, Switzerland

Covalent functionalization represents a viable pathway for tailoring graphene's electronic properties, for instance to open a band-gap. It furthermore enables subsequent chemical coupling for applications in molecular diagnostics and molecular electronics. In this study, chemical vapor deposited (CVD) graphene is covalently functionalized through electrospray ion beam deposition (ES-IBD) of hyperthermal molecular cation beams of 4,4'-azobis(pyridine). The one-step, room temperature ion-surface reaction process takes place in high vacuum (10^{-7} mbar), and requires a threshold kinetic energy of 165 eV of the molecular ions. The covalent attachment of the molecules is proven by the effect of thermal annealing, which removes the intense D peak in the Raman spectrum of the functionalized graphene. Based upon X-ray photoelectron spectroscopy data, we conclude that the attached species are azopyridinium groups. A high functionalization degree of 3% of the carbon atoms of graphene is attained after 3-5 hours of ion exposure of 2×10^{14} azopyridinium/cm² of which 50% bind covalently.

G. Dubey et al.: J. Am. Chem. Soc. 136, 13482-13485 (2014)



Th-A06

Gold nanoparticles supported on carbon nanotubes for CO oxidation

Madjid Arab¹, Virginie Checallier¹

¹Toulon University, IM2NP UMR CNRS, La Garde, France

Nanocomposites made on carbon nanotubes present many advantages like hollow nanotubular structure and new properties. Nanocomposites based on carbon nanotubes (CNTs) offer promising applications in electrochemistry, catalysis, electronic conduction, gas storage, etc. They are also suitable materials as electrodes in double layer capacitors

Multi walled carbon nanotubes (MCNTs) supported gold nanoparticle catalysts were prepared for monoxide carbon CO transformation. MCNTs were prepared by assisted aerosol chemical vapor deposition and the gold nanoparticles were synthesized with two sizes by citrate method. After that, the composite were obtained by grafting the gold nanoparticles on the surface of oxidized nanotubes, in an aqueous medium.

The composite were characterized by X-ray diffraction, scanning and transmission electron microscope. The catalytic reactivity of the powder samples was analyzed using a homemade reactor coupled to a combined system of Fourier Transform Infrared spectrometer (FTIR) and Mass Spectrometer apparatus. The catalytic activities were performed under CO gas flows with different gas carriers (Air and Argon) as a function of time and temperature.

The oxidation kinetics of CO into CO₂, until the total transformation, was analyzed from the evolutions of FTIR absorption band intensities. As the gold nanoparticles size changes, the catalytic efficiency was strongly modified.

To understand this oxidation process, electrical studies were performed to characterize the charge transfer. Measurements have been carried out using these catalysts as sensitive layers on interdigitated microelectronic support. The samples revealed their abilities to detect CO at low temperature.

Th-A07+08

Chemistry above and below graphene

Jan Knudsen¹¹Lund University, Lund, Sweden

Graphene (Gr) supported arrays of well-ordered nanoparticles and graphene covered transition metal surfaces are attractive model systems for studies of nanoparticle chemistry and for studying confinement effects, respectively.

First, I will discuss how Pt-clusters binds to Gr grown on Ir(111) and how this is visible in X-ray Photoelectron spectroscopy spectra (XPS). Molecular adsorption of CO and cluster coalescence upon CO adsorption will also be discussed [1, 2].

Secondly, I will present an atomic scale picture of H₂-, O₂- and CO-structures formed under Gr [3, 4, 5]. I will demonstrate how the dosing conditions and Gr morphology can control the intercalation: Oxygen intercalates Gr flakes above 400 K while a closed film is stable until 700 K where etching sets in [3, 6], CO intercalates Gr in the mbar regime [4], and H₂ only intercalates Gr at temperatures close to 100 K [5]. Further, I will show that noble gas atoms can be trapped under Gr upon ion irradiation and remains stable to 1300 K [7, 8].

Finally, I will compare H₂ and CO titration of oxygen on clean Ir(111) and intercalated underneath Gr. Without Gr, both H₂ and CO react with oxygen and form H₂O and CO₂, respectively, which desorb. With Gr, the CO₂ formation is unaffected, while the water formation is significantly changed, leading to a trapped superdense phase of mixed H₂O and OH intercalating Gr [9].

[1] Knudsen et al., Phys. Rev. B, 85, 035407 (2012)

[2] Gerber et al., ACS nano, 7, 2020 (2013)

[3] Grånäs et al., ACS nano, 11, 9951 (2012)

[4] Grånäs et al., Journal of Physical Chemistry C, 117, 16438 (2013)

[5] Grånäs et al., Submitted

[6] Schröder et al., Submitted

[7] Herbig et al., ACS nano, accepted

[8] Herbig et al., Submitted

[9] Grånäs et al., Submitted

Th-B01+02

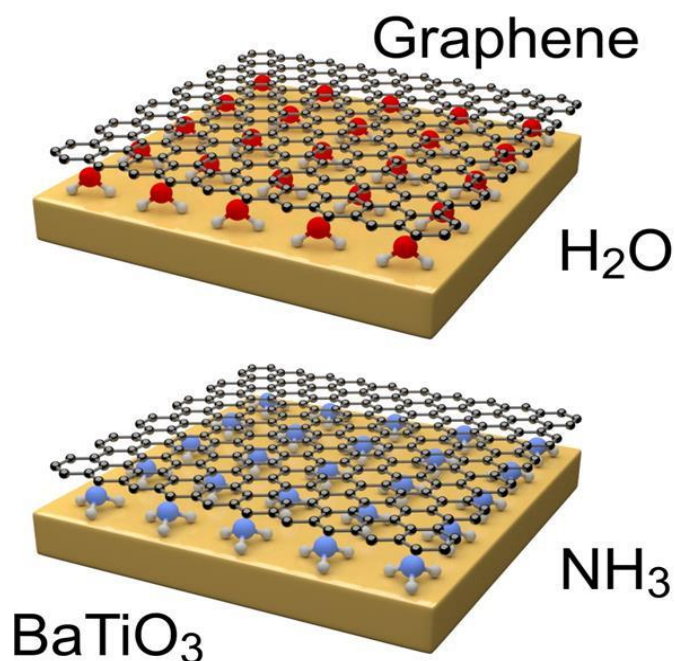
Polarization-enabled electronic properties of hybrid 2D-ferroelectric structures

Alexei Gruverman¹

¹University of Nebraska-Lincoln, Lincoln, United States

In recent years there has been an unprecedented interest in various two-dimensional (2D) materials that often possess unique physical and chemical properties that cannot be found in their three-dimensional counterparts. Due to their planar morphology they can be easily integrated with other 2D materials and functional films, resulting in multilayered structures with new properties. In particular, there was a considerable interest in a novel type of electronic devices, in which graphene, a 2D carbon material, was coupled with different ferroelectric (FE) materials. Electrically switchable ferroelectric polarization opens a possibility of electrical control of the functional properties of the adjacent graphene layer.

In this presentation, we discuss implementation of the hybrid electronic devices comprising 2D materials and FE thin films (2D-FE) that exhibit polarization-controlled non-volatile modulation of the electronic transport. While many 2D materials can be considered in conjunction with FE materials, this talk primarily focuses on the use of graphene and transition metal dichalcogenides. Specifically, we show how polarization reversal modulates (1) the in-plane transport of the interfacial conducting channel in the FE field effect devices, and (2) the perpendicular-to-plane tunneling conductance in the FE tunnel junction devices. We demonstrate that interface engineering is a critical component determining the functional properties of these devices. We use simple phenomenological modeling to predict how the interface chemistry affects the electronic and transport properties of the 2D-FE structures.



Th-B03

Skin layers on multiferroic and relaxor single crystals

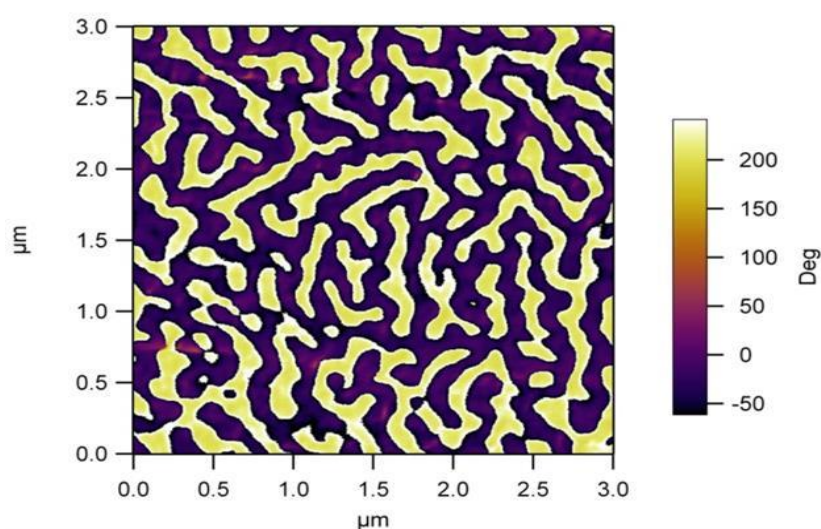
Neus Domingo Marimon¹, Núria Bagués^{1,2}, José Santiso^{1,2}, Gustau Catalan^{1,3}

¹ICN2, Bellaterra, Spain, ²CSIC, Bellaterra, Spain, ³ICREA, Barcelona, Spain

Skin effects are commonly observed in different types of single crystals: in regions close to the surface, structural and functional properties different from that of the bulk can be observed. Here, we will overview the main features that characterize skin layers observed in different types of ferroelectric single crystals, from multiferroic materials such as BiFeO₃ to different examples of relaxors such as PZN-PT.

Skin layer of BiFeO₃ has been analyzed with different techniques from surface impedance and grazing incidence X-ray diffraction to atomic force based techniques such as Piezoresponse Force Microscopy (PFM), showing a specific phase transition at $T^* = 275$ °C, below the bulk transition temperature, characteristic dielectric properties and a complex distribution of near-surface ferroelectric nanodomains that organize in a hierarchical metastructure on top of the existing bulk domains.

On the other hand, morphotropic phase boundary relaxors have been intensely studied for the last 15 years, on account of their giant electromechanical performance. For reasons that are as yet not understood, relaxor ferroelectrics display fairly thick surface layers (“skin layers”) with different symmetry compared to bulk. Thus, in morphotropic phase boundary materials such as PMN-PT, X-ray diffraction indicates that the symmetry of the surface layer is instead rhombohedral, and investigations by piezoresponse force microscopy show a labyrinthine 180 degree domain structure with out-of-plane polarization. In this presentation, we will show in closer detail the surface layer of these materials, and in particular the temperature dependence of its properties. Using a combination of temperature-dependent Piezoresponse force microscopy (PFM) and grazing incidence X-ray (XRD) we confirmed that the skin layer indeed has different symmetry and different domain structure as compared to the bulk, surviving to temperatures hundreds of degrees above the bulk, corroborating that skin layers have their own phase diagram quite independent from that of bulk.



Th-B04

Switchable mechanical properties on ferroelectric materials

Rohini Kumara Cordero Edwards¹, Amir Abdollahi¹, Jordi Sort², Neus Domingo¹, Gustau Catalán¹

¹Institut Català de Nanociència i Nanotecnologia (ICN2), Bellaterra, Spain,

²Universitat Autònoma de Barcelona, Bellaterra, Spain

The mechanical properties of materials are expected to be invariant with respect to space inversion. Our recent work, using the nano-indentation technique and PFM images, provide evidences that this spatial inversion symmetry is broken in ferroelectric materials. The nano-indentation technique allows us to simultaneously mobilize this effect by producing highly inhomogeneous strain field and measure the mechanical properties of the material. The measurements on a single crystal ferroelectric LiNbO₃ indicate that the plasticity index, stiffness, and fracture toughness are asymmetric with respect to the sign of the polarization. The PFM images of the nano-indented areas show that the flexoelectric effect induces domain switching in positively poled regions, resulting in different polarization patterns in 180 antiparallel domains. We show that this new physical phenomenon is enabled by the interplay between ferroelectricity and flexoelectricity (coupling between strain gradient and polarization). Aside from the fundamental importance of this new insight, the predicted asymmetry may also find uses in smart nano-devices and coatings with switchable mechanical properties.

Th-B05

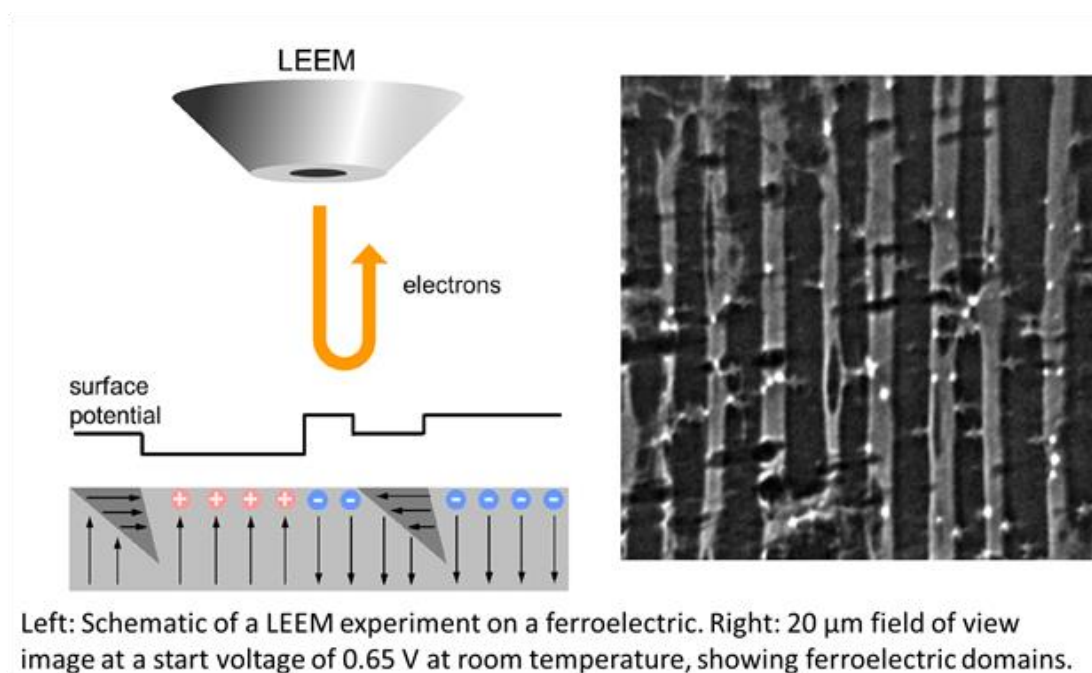
Evolution of surface charge through the ferroelectric-paraelectric phase transition in BaTiO₃(001)

Claire Mathieu¹, Jelle Dionot¹, Dominique Martinotti¹, Nick Barrett¹

¹CEA / IRAMIS / SPEC, Gif-Sur-Yvette, France

The perovskite BaTiO₃, which presents a tetragonal structure at room temperature, has its bulk polarization along the c-axis or the a-axes. For out-of-plane (perpendicular to the surface) polarized domains, the surface discontinuity leads to fixed polarization charge which in turn modifies the electrostatic surface potential. Charge-screening can alter the magnitude and sign of the surface potential. For example, unscreened and fully screened surfaces show opposite surface potential for the same underlying polarization. However at the surface, the atomic distortions associated with the ferroelectric (FE) state can be considerably altered. One recent report suggests that in BaTiO₃ the signature of surface domain ordering may persist well above the Curie temperature (T_C). The aim of the present study is to improve our understanding of how surface charge and polar adsorbates interact to influence domain order before, during and after the FE-PE phase transition.

We have used low energy electron microscopy to study the evolution of the surface charge and domain structure in BaTiO₃(001) during the ferroelectric-paraelectric phase transition. At room temperature, in- and out-of-plane polarized domains are observed with ferroelectric and ferroelastic domain walls. Strong adsorbate screening is present resulting in inversion of the electrostatic surface potential contrast. As temperature increases, desorption of screening charge takes place and domain walls become mobile. Transient ferroelastic domains appear momentarily at T_C to relieve elastic strain induced by the tetragonal to cubic phase transition. Persistence of domain-related surface charge above T_C may be due to a combination of atomic relaxation, residual adsorbates and oxygen vacancies near domain walls.



Th-B06

Contact-free surface pyroelectric measurements of organic crystals using CREM

Hagai Cohen¹, Elena Meirzadeh¹, David Ehre¹, Meir Lahav¹, Igor Lubomirsky¹

¹Weizmann Institute, Rehovot, Israel

Pyroelectricity is a property of polar materials, encountering surface charge under temperature changes. It is known to appear only in 10 polar out of 32 crystallographic classes. However, in contrast to the generally accepted symmetry restrictions, we found that non-polar crystals of amino acids exhibit surface pyroelectricity [1, 2] at specific crystal faces. This work focuses on pure and doped α -glycine crystals, in which we measured surface, bulk or both pyroelectric effects.

Conventional pyroelectric measurements are frequently challenging, due to the typically rapid charge compensation by adsorbed moieties, as well as various difficulties arising as a result of contacts introduction. In particular, surface pyroelectric measurements are extremely sensitive to the above difficulties and, therefore, they require complementary measuring techniques. Here we exploit the recent chemically resolved electrical measurements (CREM),[3] based on x-ray photoelectron spectroscopy (XPS), to measure in a non-contact mode and, importantly, under ultra high vacuum,[4] the bulk and surface pyroelectricity of pure (non-polar) and L-threonine doped (polar) α -glycine crystals.

Our CREM data successfully provides the total pyroelectric coefficient of these organic crystals, complemented by sample quality characterizations via the in-situ surface chemical analysis. Moreover, it distinguishes between the surface and bulk components, for which competing tendencies are observed. Minimization of the x-ray induced damage and other technical difficulties encountered in these experiments will be described.

1) S. Piperno, E. Meirzadeh, E. Mishuk, D. Ehre, S. Cohen, M. Eisenstein, M. Lahav, I. Lubomirsky, *Angew. Chem. Int. Edit.* 52, 6513 (2013).

2) E. Mishuk, I. Weissbuch, M. Lahav, I. Lubomirsky, *Cryst. Growth Des.* 14, 3839 (2014).

3) H. Cohen, *Appl. Phys. Lett.* 85, 1271 (2004).

4) D. Ehre, H. Cohen, *Appl. Phys. Lett.* 103, 052901 (2013).

Th-C01

Molecular Dynamics Study on Effects of Wettability of Surface on Proton Transport in Polymer Electrolyte Thin Films

Joji Aochi¹, Takuya Mabuchi¹, Takashi Tokumasu²

¹Graduate School of Engineering, Tohoku University, Sendai, Japan, ²Institute of Fluid Science, Tohoku University, Sendai, Japan

A cathode catalyst layer (CL) is one of the main components of membrane electrode assembly (MEA) in polymer electrolyte fuel cell (PEFC). The cathode CL consists of Pt-supported carbon covered with polymer electrolyte thin films. Nafion has been commonly used for this film. In atomic scale, Nafion thin films consist of hydrophobic polytetrafluoroethylene backbones and hydrophilic side chains attributed to sulfonate group, and water clusters which serve as a proton transport channel are formed around sulfonate group. Thus, proton transport properties depend on the structure of Nafion thin films and water clusters. It has been known that wettability of the carbon surface can be controlled by various materials and surface modification. In addition, the surface often gets a hydrophilic property caused by vacancy defects. Therefore, the structure of Nafion thin films and water clusters on the carbon surface could be affected by wettability of the carbon surface, leading to peculiar proton transport properties as compared to that in bulk system. In this study, we report proton transport properties in terms of diffusivity in Nafion thin films using molecular dynamics simulations, focusing on dependence of wettability of the surface. Our results show that proton diffusivity is similar to that in bulk system in case of the hydrophobic surface, due to a lack of water clusters on the surface. In contrast, the peculiar proton transport properties are shown in case of the hydrophilic surface. Our results could help designing optimum CL, leading to further development of PEFC technology.

Th-C02

Reversibly Photoswitchable Hydrophilic/Hydrophobic Surfaces

Dorothea Helmer¹, Nico Keller¹, Bastian E. Rapp¹

¹Karlsruhe Institute of Technology, Eggenstein-Leopoldshafen, Germany

Superhydrophobic surfaces can be fabricated by the attachment of hydrophobic molecules to surfaces that possess the appropriate nano- and microstructures. These structures enable the surface to hold a film of air on which a droplet of water can rest without wetting the surface itself (the so-called “salvinia effect”). Of special interest are surfaces with reversibly switchable superhydrophobicity since they possess many applications, e.g. for microfluidics and as smart membranes. It is well-known that azobenzene compounds can be switched between cis and trans conformation by irradiation with UV light. With the appropriate hydrophobic functional groups attached to an azobenzene compound bound to a structured surface, the surface can be reversibly switched between hydrophobic and hydrophilic properties. By attaching an azobenzene compound with a trifluoromethyl-group the surface energy of nanostructured glasses or polymers can be reduced so that the surface becomes superhydrophobic with the ability to switch back to superhydrophilic. We have created nano- to microstructured surfaces from glass by soot deposition and nanoimprinting of sol-gel layers and from polymers by phase separation polymerisation. Subsequent functionalization with a trifluoromethyl-azobenzene compound resulted in photoswitchable, partly transparent substrates. By using a maskless photolithography device built in our group we were able to create complex hydrophilic/hydrophobic patterns on the prepared glass and polymer surfaces. As opposed to previously reported employment of this technique on silicon wafers, using transparent substrates with sufficient transmission for UV light enables us to photoswitch the azobenzene compounds through the substrate, i.e. whilst water droplets are on the surface. This way we can switch the wettability inside microfluidic channels or use the hydrophobic/hydrophilic areas as barrier-free reaction cavities that can be switched to hydrophilic to retain a reaction mixture and back to hydrophobic to wash the mixture off.

Th-C03

Assessing the local nanomechanical properties of self-assembled block co-polymers thin films by Peak Force tapping

Matteo Lorenzoni¹, Laura Evangelio¹, Sophie Verhaeghe¹, Célia Nicolet²,
Christophe Navarro², Francesc Pérez-Murano¹

¹Instituto de Microelectrónica de Barcelona (IMB-CNM, CSIC), Bellaterra,
Barcelona, Spain

²Arkema France, Lacq, France

The mechanical properties of several types of block co-polymers (BCP) thin films have been investigated using PeakForce™ quantitative nanomechanical mapping. The samples consisted in polystyrene/polymethylmethacrylate based BCP thin films with different pitch both randomly oriented and self-assembled. The measured films have a critical thickness below 50 nm and present features to be resolved of less than 22 nm. Beyond measuring and discriminate surface elastic modulus and adhesion forces of the different phases we tune the Peak Force parameters in order to be reliably measure with those samples avoiding plastic deformation. The nanomechanical investigation is also capable of recognizing local stiffening due to the preferential growth of alumina deposited by atomic layer deposition on BCP samples.

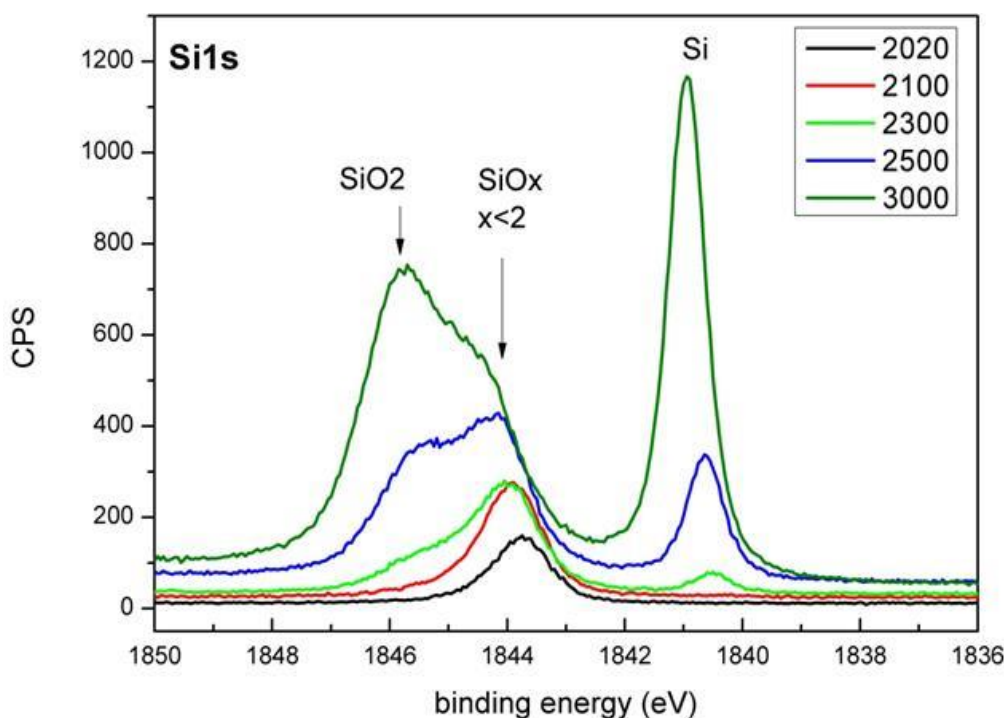
Th-C04

Characterization of buried interfaces of grafted polymer films using high kinetic energy photoemission

Laura Evangelio^{1,3}, Matteo Lorenzoni¹, Federico Gramazio³, Francisco Miguel Espinosa², Ricardo García², Francesc Pérez-Murano¹, Jordi Fraxedas³

¹Instituto de Microelectrónica de Barcelona (IMB-CNM, CSIC), Bellaterra, Barcelona, Spain, ²Instituto de Ciencia de Materiales de Madrid (ICMM, CSIC), Madrid, Spain, ³Institut Català de Nanociència i Nanotecnologia (ICN2), Bellaterra, Barcelona, Spain

We have characterized the buried interfaces of oxidized PS-OH layers grafted on native silicon oxide with high kinetic energy photoemission using synchrotron radiation at the HIKE endstation at the BESSY II photon source (Helmholtz-Zentrum Berlin für Materialien und Energie). 4.7 nm thick PS-OH layers have been prepared by spin-coating on silicon substrates and oxidized using gold-coated PDMS stamps, replicating DVD patterns, and formed by parallel hillocks 320 nm wide and spaced 740 nm with protrusions heights of 40 nm. The oxidation was achieved by applying a 35 - 40 V bias voltage at an elevated relative humidity (above 70%). Figure 1 shows the Si1s photoemission lines taken with photons in the 2020-3000 eV range. At 2020 eV (black continuous line) only the feature associated to sub-stoichiometric silicon oxide (SiO_x) is detected, which builds the interface with the grafted polymer. At increasingly higher photon energies, first the stoichiometric oxide (SiO₂) and then the silicon substrate are observed. The signal of the bare silicon can be used as internal energy reference. We thus observe that the PS-OH/SiO_x, SiO_x/SiO₂ and SiO₂/Si interfaces can be selectively approached by tuning the electron kinetic energies, which permits to modulate the required mean free path. Surprisingly, the PS-OH layer is not oxidized in this process as clearly observed from the C1s signal.



Th-C05

Experimental and theoretical model of a poly-epoxy surface:
formation and simulation of XPS spectra

Thomas Duquet, Andreas Gavrielides, Maëlen Aufray, Corinne Lacaze
Dufaure

¹CIRIMAT laboratory, CNRS, University of Toulouse, Toulouse, France

Our group is involved in the development of coatings for polymer composite parts in space applications. Whereas some success has been reached, our methods and methods available in the literature result from empirical studies. Hence, it is quite impossible to generalize this knowledge for a broader audience: a specific surface treatment is usually not applicable to a different system. Therefore, we need to improve our mechanistic understanding of the surface of polymers, regarding chemical reactivity, heterogeneous reactions during thin film deposition, nucleation and growth, and adhesion mechanisms. With this aim, we want to create a surface template for the study of further treatments at the molecular and nanoscale.

In this framework, we develop an experimental and theoretical methodology based on the DGEBA / ethylene diamine system. The choice of the two reactants is supported by the great representativity of DGEBA / amines systems and the reduced number of atoms for calculations. We synthesize samples of which surfaces are clean, chemically homogeneous, with a minimum of defects at the nanometer scale, and compare our characterization results with DFT calculations performed on a model macromolecule. The synthesis protocol is validated by bulk (DSC, FTIR), and surface (AFM, XPS) techniques, showing that roughness ($R_a < 1$ nm) and defects density (0.21 defect/ μm^2) are low, and that the surface is homogeneous. In parallel, DFT calculations are performed to simulate XPS spectra in the framework on the generalized transition-state theory with deMon 4.3 -that is taking into account the excitation occurring in the photoemission process.

After a presentation of the experimental results, we discuss the correlation between experimental XPS and simulated X-ray emission spectra.

Th-C06

Wrinkle as a chromaticity stabilizer and light out-coupler for OLED applications

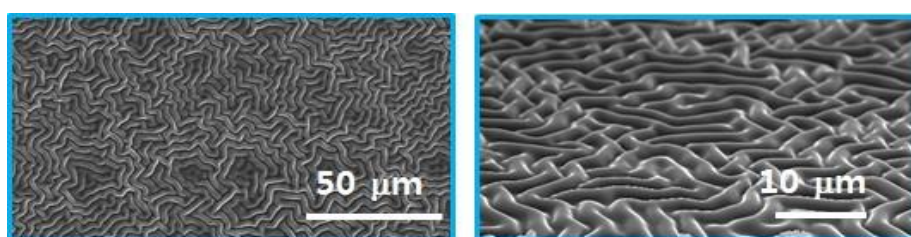
Jaehyun Moon¹, Keunsoo Lee¹, Seung Koo Park¹, Jonghee Lee¹, Chul Woong Joo¹, Jin-Wook Shin¹, Jun-Han Han¹, Doo-Hee Cho¹, Nam Sung Cho¹, Byoung-Gon Yu¹, Jeong-Ik Lee¹

¹Electronics and Telecommunications Research Inst. (ETRI), Daejeon, South Korea

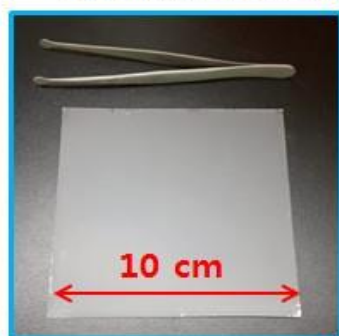
Wrinkles are observed ubiquitously in nature. Readily observable examples are human skin, dry fruit skin and soaked leather goods. Wrinkle formation may be described by the difference in Young moduli between the upper and lower parts. To be specific, there exists a driving force to form wrinkles when a hard film is placed on a soft foundation. In this work we present a synthesized liquid prepolymer which spontaneously forms randomly distributed wrinkles during the UV crosslinking. This single material approach is in contrast to existing two-material system wrinkle fabrication methods, in which the upper part is a thin hard material and the lower part a soft support. By adjusting processing conditions, we show that the wrinkle size, period and height, is controllable.

We applied our wrinkles to stabilize the chromaticity and enhance the light out coupling of organic light emitting diodes (OLEDs), both in monochromatic and white emissions. We demonstrate that our wrinkles can be readily applied not only to remove spectral distortion but also enhance the out-coupling efficiencies. Optical analyses reveal our wrinkles' capacity of deflecting the traveling path of the incident light.

Our wrinkle forming method does not require a two-layer structure, vacuum deposition or thermal annealing, offering a facile approach in fabricating wrinkles. Our wrinkle offers a new platform in which various light and photonic applications can be explored.



➤ SEM images of wrinkles, Plain view (left) and Tilt view (right)



➤ Large area wrinkle film



➤ Luminance enhancement using wrinkle film

Th-C07

Direct bonding of glass and polymer film by adhesive-free molecular joining

Yasunori Taga¹, Keisuke Nishimura¹, Yuri Hisamatsu¹¹Chubu University, Kasugai-shi, Japan

Without using adhesives, borosilicate glass and cycloolefin (COP) polymer film were directly bonded by molecular joining. Glass and COP surfaces were both exposed to mixture gas of silane and water vapor after plasma treatment and then laminated and annealed at about 100°C for several min for interface reaction. Joining force was evaluated by 180 degree peel test and durability was examined under the conditions of 60°C, 95%RH and Xenon lamp of 60 W/m². It was found that joining force was found to be controllable between 1-10N/25mm, which remained unchanged over 2000 hours even after exposure to the conditions of durability test. Thickness of joining layer was evaluated by the XPS to be at least 1~2 nm by taking inelastic mean free path of photoelectrons into consideration. The results can be explained in terms of changes in surface functional group by plasma treatment to form H-H hydrogen bonding and C-O-Si covalent bonds via silanols after interface chemical reaction. In conclusion, adhesive-free direct bonding of glass and polymer film was thus established and their performance and durability were investigated. As a result, ultimate thin layer joining without using adhesives was demonstrated by the formation of hydrogen and covalent bonds at the interface by low temperature interface reaction process.

Th-D01+02

Toward atom scale ultra low power electronic circuitry

Robert Wolkow¹¹University of Alberta, Edmonton, Canada

Decades of academic study of silicon with scanned probe and related techniques have made it possible to now envisage a silicon-based, atom-scale, ultra-low power circuitry that merges with and enhances CMOS electronics technology.

A key step was made in 2008 (patent initiated, then published (PRL 102, 046805 (2009)), patent issued recently) when single silicon dangling bonds on an otherwise H-terminated surface were shown to behave as the ultimate small quantum dots. Because all such dots are identical, and spacing between dots can be identical, and dots can be placed very closely to achieve strong interaction, and because many, many dots can be printed easily there appears to be prospects for interesting circuitry. The same dots can be deployed to make “passive” elements like wires and to make active elements of diverse kinds including quantum cellular automata with the prospect of room temperature operation, and single electron transistors (SETs) of extremely narrow device to device variation.

Among most recently published work I will describe single-electron, single-atom transport dynamics, PRL 112, 256801 (2014), and, PRL 112, 246802 (2014) which uses multi-probe STM to show surface conduction among collectives of DBs.

Soon to be published STM spectral studies of silicon atoms will be shown and the remarkable roles of controlled single atom charge state change and of near surface dopants will be identified. Very new QPlus results showing high resolution imaging and force curves over H-terminated Silicon will be shown (if manuscript is finished by talk date).

A robust, readily repairable, single atom tip and its varied applications to will be described also.

Th-D03

Scanning tunneling spectroscopy reveals a silicon dangling bond charge state transition

Hatem Labidi^{1,2}, Marco Taucer¹, Mohammad Rashidi^{1,2}, Mohammad Koleini^{1,2},
Lucian Livadaru², Jason Pitters², Martin Cloutier², Mark Salomons², Robert
Wolkow^{1,2}

¹Department of physics, University of Alberta, Canada, Edmonton, Canada,

²National Institute for Nanotechnology, National Research Council of Canada,
Edmonton, Canada

Silicon dangling bonds (DB) on the Si(100):H surface are increasingly attracting attention as they are emerging as promising building blocks for novel nanoelectronic circuits. In this presentation, we report prominent characteristics of single DBs that were never seen before. Using a low temperature STM, we show that the concentration of subsurface arsenic dopants can be tuned to influence the electronic conduction through single DBs. When a relatively large subsurface dopant depletion layer is formed, a single DB exhibits a sharp conduction step in its I(V) spectroscopy, i.e. a sharp peak in dI/dV, that is not due to a density of states effect but rather corresponds to a DB charge state transition, similarly to the characteristic charge transition peaks seen in I(V) curves of a single electron transistor. The voltage onset of this transition is perfectly correlated with bias dependent changes in STM images of the DB at different charge states. However, this onset voltage can be different from one DB to another even on the same sample. Through DFT calculations, we show that this could be partially explained by the influence of the non-uniformly distributed arsenic subsurface dopants on the DB state. Local surface defects can also play a role. Interestingly, neighboring DBs that can be precisely created by the STM tip can act as a local static gate to shift the charge transition voltage onset. This property was exploited to create new coupled DB structures. This work further demonstrates the pertinence of considering the DB as a single atom quantum dot and opens the door for further perspectives of DB based electronic devices.

Th-D04

Surface phonon dispersion of the hydrogen-terminated Si(110)-(1×1) surface: Experiment and theory

Shozo Suto¹, SY Matsushita¹, Chunping Hu², Erina Kawamoto¹, Hiroki Kato², Kazuyuki Watanabe²

¹Tohoku Univ., Sendai, Japan, ²Tokyo Univ. of Sci., Tokyo, Japan

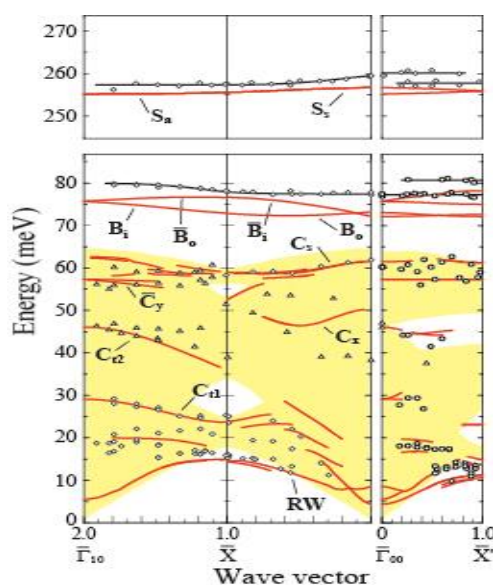
Recently, attention has been paid to the Si(110) surface due to the suitability of the substrate surface for the multi-gate field effect transistor(FET). We report here the surface phonon dispersion of the hydrogen-terminated Si(110)-(1×1) [H:Si(110)] surface calculated by the first-principle calculations within the framework of density functional theory (DFT), in comparison with experimental dispersion measured by the high-resolution electron energy loss spectroscopy (HREELS)[1]. H:Si(110) surface is the bulk terminated surface and has the highly anisotropic structure with a rectangular unit cell along Γ -X and Γ -X' directions. It is the good test bench to check the calculation method.

The calculations were performed by using program package ABINIT, which is a plane-wave pseudo-potential approach. To represent the H:Si(110) surface, a symmetric slab with 11 Si layers was used, which was fully covered with H atoms on both sides. The experiments were carried out using HREELS as reported in the ref. [1].

We plotted the first and second surface Brillouin zone due to the existence of glide planes along Γ -X. The vibrational modes around 260 meV and 75 meV are the stretching and bending modes of topmost H atoms, respectively. Below 65 meV, the surface phonon modes of Si atoms exist. The theoretical curves are in good agreement with the experimental data. In comparison with the calculation based on the semi-empirical total-energy scheme, we find that our DFT calculation explains the surface phonon modes quite well. In particular, the finite dispersion of the stretching mode, which did not exist in the result of semi-empirical calculation, explains the experiment.

We will discuss the detailed analysis and the recent progress on the surface phonon calculations based on the DFT, as manifested by the phonons on the H:Si(110) surface.

[1] S.Y. Matsushita et al., J. Chem. Phys. 140, 104709 (2014).



Th-D05

From surface energetics to local work-function measurements on Ag/Si(111)- $\sqrt{3}\times\sqrt{3}$ -R30° with Low-Energy Electron Microscopy

Fabien Cheynis¹, Stefano Curiotto¹, Frédéric Leroy¹, Pierre Müller¹

¹Centre Interdisciplinaire de Nanoscience de Marseille-CINaM, Marseille, France

Ag/Si(111) is probably one of the most widely-studied system in surface science. The main reasons are that it defines a model system for (i) metal-on-semiconductor interfaces as both materials are immiscible in the bulk and (ii) applications in micro- nanoelectronics and plasmonics [1]. Ag/Si(111)- $\sqrt{3}\times\sqrt{3}$ -R30° is obtained by depositing Ag on Si(111)-7x7 substrate in the 470-770K temperature range. Interestingly, this 2D material shows a charge transfer between the 2D adatom gas (2DAG) and a reconstruction-induced surface state when an additional sub-monolayer Ag layer is deposited as evidenced by transport and spectroscopic properties [2], thus forming a 2D electron gas (2DEG). This 2DEG has compelling properties including a deviation from a pure quadratic dispersion relationship at high doping [3] and a metal-to-insulator transition observed in temperature [5,6].

In this work, we show that a real-time monitoring of the Ag 2DAG concentration inferred from the surface reflectivity in Low-Energy Electron Microscopy (LEEM)[7] makes it possible to determine surface energetic quantities (e.g. Ag adatom surface diffusion energy) over a wide temperature range (210-500K) in quantitative agreement with previous results. LEEM also allows to measure the work-function of a surface [8]. A clear dependence of the surface work-function on the Ag adatom concentration is demonstrated. Unexpectedly, 2D maps of the work-function and real-time monitoring below room-temperature (≈ 210 K) reveal both spatial and temporal variation of the local work-function. Quantitative charge transfer determination will be attempted.

- [1] B.-H. Li et al. Nano Lett. 12, 6187 (2012)
- [2] Y. Nakajima et al. Phys. Rev. B 66, 6782 (1997)
- [3] J.N. Crain et al. Phys. Rev. B 72 (2005) 045312
- [5] I. Matsuda et al. Phys. Rev. Lett 99, 146805 (2007)
- [6] Y.-Y. Tang et al. Front. Phys. 8 (2013) 44
- [7] J. de la Figuera et al. Surf. Sci. 600 (2006) 4062
- [8] M. Babout et al. J. Phys. D 13 (1980) 1161

Th-D06

Visualization of intermediate surface structures during the growth of Ga on Ge(100) surface upon short temperature pulses

Cho-Ying Lin¹, Han-Te Cheng¹, Dengsung Lin¹¹National Tsing Hua University, Hsinchu, Taiwan

Scanning tunnelling microscopy and synchrotron radiation core-level photoemission have been employed to investigate the the adsorption and growth processes of Ga on the Ge(100) surface at various substrate temperatures and Ga coverages. At room temperature (RT), parallel Ga ad-dimers are the dominant species and a well ordered Ga terminated (2 x 2) surface is formed at 0.5 ML. Further deposition results in small Ga clusters at RT and (8 x n) reconstruction above 300°C. These observations are similar to the Ga/Si(100) growth system. However, a 60-s annealing or growth at $\geq 150^\circ\text{C}$ causes the Ga adatoms to diffuse into the subsurface layers and the surface roughens. By applying short temperature pulses between 150 and 200°C at sub-monolayer coverages, we are able to image the same surface area and compare the surface atomic structure before and after annealing. Ga adatoms at ends of parallel Ga ad-dimer rows are seen to in-diffuse with minimal diffusion. Perpendicular Ga dimers as predicted previously are observed at lower annealing temperature, meaning that they are stable intermediate structure. Some isolated mixed Ga-Ge dimers are also present on the terraces.

Th-D07

MBE growth, structural and optical properties of Ga(Bi,As) layers and nanowires

Janusz Sadowski^{1,2}, Slawomir Kret², Aloyzas Siusys², Tomasz Wojciechowski², Lukasz Gluba³, Oksana Yastrubchak³, Alexei Zakharov¹, Michal Szot², Jaroslaw Z. Domagala²

¹MAX-IV laboratory, Lund University, Lund, Sweden, ²Institute of Physics, Polish Academy of Sciences, Warszawa, Poland, ³Institute of Physics, Maria Curie-Skłodowska University, Lublin, Poland

Alloying GaAs with Bi results in a ternary alloy with interesting optical properties, due to the important band-gap reduction and enhancement of the spin-orbit splitting in Ga(Bi,As). The maximum Bi content in uniform Ga(Bi,As) compound reported so far reaches about 5 at%. Attempts to obtain higher composition of Ga(Bi,As) solid solution leads to Bi segregation either at the growth front or inside the volume of the growing crystal [1, 2]. We have investigated the molecular beam epitaxy (MBE) growth of Ga(Bi,As) nanowires (NWs), with the Bi content increased beyond the maximum value reported so far for epitaxial layers. The NWs have been grown on GaAs(111)B substrates using Au-catalysed vapor-liquid-solid (VLS) growth mode. Both the GaAs NWs uniformly doped with Bi, and the core-shell heterostructures with Ga(Bi,As) shells deposited on the {110} side-walls of the GaAs core NWs have been investigated. Together with the NWs the Ga(Bi,As) layers were grown simultaneously on planar GaAs(100) and GaAs(110) substrates. Structural properties of the NW samples have been characterized by FEI Titan 80-300 electron transmission microscope equipped with the image corrector operating at 300 kV. Optical properties were investigated by photoreflectivity and micro-photoluminescence techniques applied for NWs transferred from the growth substrate onto optically neutral support. The homogeneity of the Bi distribution in NWs and in the planar layers was probed by TEM and by the photoemission microscope (PEEM) setup connected to the soft-X-ray beamline at the MAX-II storage ring of the Swedish national synchrotron radiation facility (MAX-IV). The incorporation of Bi into GaAs will be compared for the two classes of samples, namely MBE layers and Au-catalysed nanowires grown at identical conditions.

[1] E. Sterzer, N. Knaub, P. Ludewig, R. Straubinger, A. Beyer, K. Volz, J. Crystal Growth, 408, 71 (2014).

[2] E. Luna, M. Wu, J. Puustinen, M. Guina, and A. Trampert, J. Appl. Phys. 117, 185302 (2015).

Th-E04+05

Operando XPS Studies of the Electrode Surface Stability in Electrochemical Energy Storage Systems

Daniil Itkis¹, Lada Yashina¹, Yang Shao-Horn², Axel Knop-Gericke³, Luca Gregoratti⁴, Virginia Pérez-Dieste⁵

¹Lomonosov Moscow State University, Moscow, Russian Federation,

²Massachusetts Institute of Technology, Boston, USA, ³Fritz Haber Institute of Max Planck Society, Berlin, Germany, ⁴ELETTRA Sincrotrone Trieste, Basovizza, Italy, ⁵ALBA Synchrotron, Barcelona, Spain

Electrochemical energy storage often plays a crucial role in overall performance of various devices. Electrochemical systems all deal with the electrode - electrolyte interfaces, where charge separation and chemical reactions occur. The evolution of the chemical composition and structure at the interfaces affects all the functional parameters of the device including power and long-term stability of its performance. That's why chemical processes including side reactions at the interface should be thoroughly analysed. Although it is of a great importance, the analytical techniques are still very limited, and in most cases electrochemists act blinded as they have no ability to accomplish the electrochemical data with direct experimental characterisation of the interface, which is buried under electrolyte and thus is inaccessible to the most common surface science tools.

The approaches to probe chemical reactions at electrified interfaces by X-ray photoelectron spectroscopy are discussed in the talk. Recent XPS observations of the electrochemical interfaces involving both solid and liquid electrolytes will serve as examples for illustration of the new possibilities delivered by synchrotron radiation induced photoemission. Carbonaceous and some binary inorganic electrode materials for Li-air batteries were investigated and found to be intrinsically unstable due to its reactivity towards electrochemical reaction intermediates, namely superoxide species.

Th-E06

The formation and stability of aluminum oxides

Edvin Lundgren¹, Florian Bertram¹, Lisa Rullik¹, Jonas Evertsson¹, Anders Mikkelsen¹, Jinshan Pan², Fan Zhang², Francesco Carla³

¹Lund University, Lund, Sweden, ²KTH, Stockholm, Sweden, ³ESRF, Grenoble, France

Aluminum and aluminum alloys are used in a broad range of everyday commercial products as well as of interest in future microelectronics. However, many applications for Al require increased corrosion protection for better durability. This can be obtained by increasing the thickness of the native protective oxide [1,2] by electrochemical means using anodization. Anodization is the electrochemical growth of an oxide by applying a potential to the aluminum in an electrolyte. Much less is known about the atomic scale structures and chemical processes occurring on Al surfaces under these conditions, since it is necessary to perform measurements during the electrochemical reaction and the process of forming a thick anodic oxide.

On the other hand, the protective alumina film is a challenge in important processing stages of aluminum products. For instance in the brazing process of aluminum, which is important for aluminum based heat exchangers, the oxide barrier is instead an obstacle. Therefore, to improve on the brazing of aluminum requires the detailed understanding on how the oxide breaks up/melts during heating as the liquid braze melt is formed in the process of generating solid metallic joints.

In this contribution, we will present recent results from in situ reflectivity measurements from aluminum single crystals and industrial aluminum polycrystalline alloys during anodization show that we can extract structural information while growing alumina film in the electrochemical cell [3]. We will also present a combined XPS/PEEM study while heating commercial aluminum alloys to study the segregation properties and ultimate oxide break-up/melting on the microscopic scale [4].

[1] N. Cabrera and N. F. Mott, Rep. Prog. Phys. 12 163 (1948).

[2] F. P. Fehlner and N. F. Mott. Oxid. Met. 2 59 (1970).

[3] F. Bertram et. al, J. Appl. Phys. 116 (2014) 034902.

[4] L. Rullik et. al, In preparation.

Th-E07

Direct correlations between XPS analyses and in-situ interfacial electrochemical responses of InP in liquid ammonia (-55°C)

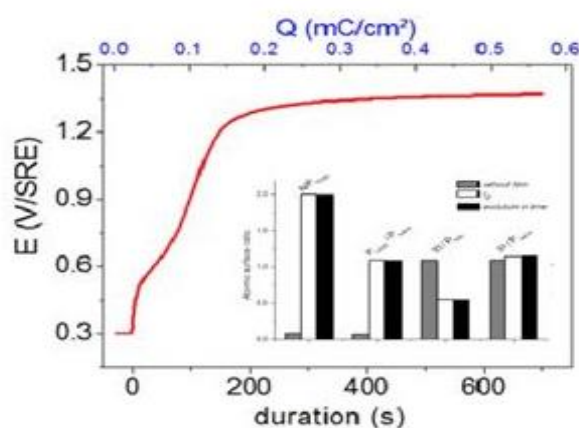
Anne-Marie Gonçalves¹, Christian Njel¹, Damien Aureau¹, Arnaud Etcheberry¹

¹University of Versailles, UMR 8180 Institut Lavoisier, Versailles, France

Reproducible electrochemical responses are obtained on InP in liquid ammonia (-55°C). An anodic wave, with a charge around 7mC/cm² is shown during the first scan by cyclic voltametry. A passivation is assumed due to the lack of an anodic wave during the second and subsequent scans. By chronoamperometry, InP electrode is kept at a constant potential whereas a specific shape of the current versus time is recorded at the interface with a charge around 20mC/cm²[1]. In contrast, the galvanostatic treatment requires keeping InP at a constant current density. Unlike other electrochemical methods, the galvanostatic treatment reaches low charges (0.03mC/cm²). A flat bands potential shift is also observed by in-situ capacitance measurements during the anodic treatments. Even if a surface modification is assumed from electrochemical responses, chemical analyses of the surface by XPS (X-ray Photoelectron Spectroscopy) are crucial. The challenge is huge since the semiconductor is at -55°C and thermal shocks could irreversible damage InP surface. An extraction from the solvent of InP sample is successfully performed through temperature steps from -55°C to ambient temperature. Thanks to XPS, a gradual chemical evolution of the surface is reached according to the anodic charge. This work presents step by step the process of InP nitridation. A reproducible polyphosphazene like film is then revealed ((H₂N) P=N)n [2]. The lowest charge is then compared to the density of surface atoms (10¹⁵ /cm²). Only some layers of InP are therefore involved. The high chemical stability of the modified surface is evidenced by XPS since no air ageing of the surface is observed and no effect of strong oxidants is observed on the surface. This tremendous stability is also in accordance with the high level of luminescence kept with time.

[1] C. Njel et al. Eletrochim. Acta 139 (2014) 152

[2] A-M. Gonçalves et al. Thin Solid Films 538 (2013) 21



Th-E08

Oxygen reduction reaction activities and electrochemical stabilities for Pt/Pt_xNi_{1-x}(111) model catalyst surfacesToshimasa Wadayama¹, Ryutaro Kawamura¹, Masato Asano¹, Naoto Todoroki¹¹Tohoku University, Sendai, Japan

Because atomic alignments and compositions of bimetallic alloy surfaces determine electro-catalysis, relation between the surface structures and oxygen reduction reaction (ORR) activities should give us crucial information for developments in new alloy catalysts for fuel cells. In this study, model alloy catalysts are prepared through Pt epitaxial growth on Pt_xNi_{1-x}(111) ordered single crystal substrate surfaces in UHV: ORR activity and electrochemical stability are evaluated after the sample-transfer from UHV to electrochemical (EC) environment without being exposed to air.

The UHV-EC apparatus is described elsewhere [1]. Pt was deposited onto clean Pt₅₀Ni₅₀(111) and Pt₂₅Ni₇₅(111) substrates by an electron-beam evaporator. After surface scientific analysis (LEED, STM, XPS, LEISS), cyclic voltammetry (CV) and linear sweep voltammetry (LSV) measurements were conducted in 0.1M HClO₄ by an EC apparatus set in a N₂-purged glove-box. To discuss EC stability, potential cycling between 0.6-1.0V was applied to the samples.

STM images for various monolayer-thick Pt on Pt₅₀Ni₅₀(111) and Pt₂₅Ni₇₅(111) substrates showed Moire-like height modulations (Fig. 1), suggesting surface strains of the Pt(111) epitaxial lattice induced by underlying substrates. CV curves for the Pt_{2ML}/Pt_xNi_{1-x}(111) (Fig. 1) exhibited that the regions of H_{ads} and OH_{ads} shifted to lower and higher potentials, respectively. The ORR activity enhancements for the Pt_xNi_{1-x}(111) are remarkable and, particularly, Pt_{2ML}/Pt₂₅Ni₇₅(111) showed 25-fold higher activity than Pt(111). On the basis of the surface scientific analysis, we deduce that shrinkage in electrochemical charges for H adsorption/desorption and positive shift in the onset potential of OH species are common features of CV for highly ORR-active Pt-M(111) surfaces and surface strains of topmost Pt(111) epitaxial lattice that induced by lattice mismatch between the underlying Pt-M(111) substrate determine ORR activity enhancement for the Pt-M(111) bimetallic surfaces.

[1] T.Wadayama et al. Electrochem. Commun. 12, 1112 (2010). N.Todoroki et al., PCCP, 15, 17771 (2013).

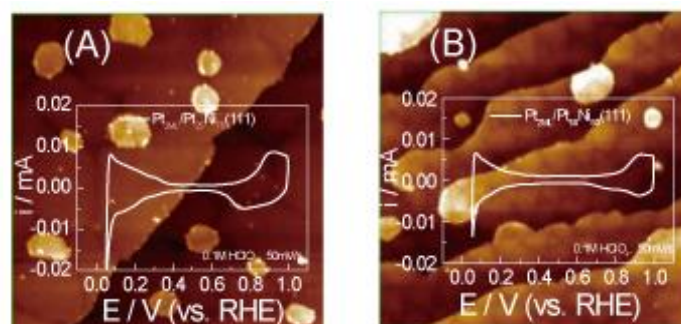


Fig.1 STM images & CVs for (A) Pt_{2ML}/Pt₅₀Ni₅₀(111) and (B) Pt_{2ML}/Pt₂₅Ni₇₅(111) (right)

Th-A09

Molecules–Oligomers–Nanowires–Graphene Nanoribbons: Stepwise On-Surface Covalent Synthesis Preserving Long-Range Order

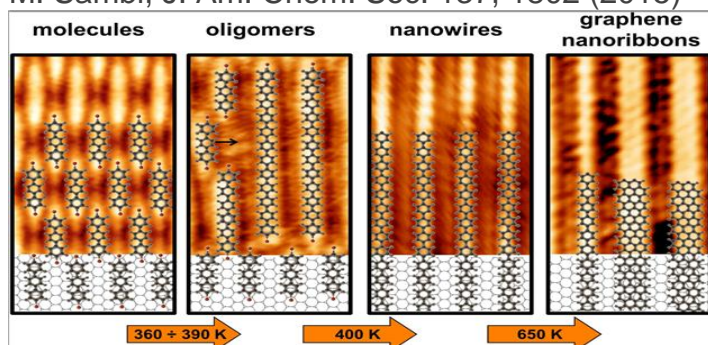
Francesco Sedona¹, Andrea Basagni¹, Louis Nicolas², Mattia Cattelan¹, Maurizio Casarin¹, Carlo A. Pignedoli³, Guillaume Vasseur^{4,5}, Jorge Lobo-Checa^{4,5}, Enrique Ortega^{4,5,6}, Dimas G. de Oteyza^{4,5}, Manuel Vilas-Varela⁷, Diego Peña Gil⁷, Mauro Sambi¹

¹Dipartimento Scienze Chimiche Università Degli Studi Di Padova, Padova, Italy, ²Ecole Normale Supérieure de Cachan, Cachan, France, ³NCCR MARVEL, Empa, Swiss Federal Laboratories for Materials Science and Technology, Dübendorf, Switzerland, ⁴Donostia International Physics Center, San Sebastian, Spain, ⁵Centro de Física de Materiales (CSIC-UPV/EHU), Spain, ⁶Departamento de Física Aplicada I, Universidad del País Vasco, Spain, ⁷Centro de Investigación en Química Biológica y Materiales Moleculares (CIQUS) Universidad de Santiago de Compostela, Spain

Synthesis of graphene nanoribbons (GNRs) with atomic precision was recently demonstrated using a bottom-up approach. Reactions at predefined locations between appropriately designed precursors were showed to end in atomically precise AGNRs with seven or thirteen carbon dimer lines across its width (7-13-AGNR) [1]. We report on an alternative stepwise on-surface polymerization reaction leading to oriented GNRs on Au(111) as the final product [2]. Starting from the precursor 4,4''-dibromo-p-terphenyl and using the Ullmann coupling reaction followed by dehydrogenation and C–C coupling, we have developed a fine-tuned, annealing triggered on-surface polymerization that allows us to obtain an oriented nanomesh of GNR via two well-defined intermediate products, namely, p-phenylene oligomers with reduced length dispersion and ordered submicrometric molecular wires of poly(p-phenylene). A fine balance involving gold catalytic activity in the Ullmann coupling, appropriate on-surface molecular mobility, and favorable topochemical conditions provided by the used precursor leads to a high degree of long-range order that characterizes each step of the synthesis and is rarely observed for surface organic frameworks obtained via Ullmann coupling. The same approach has been used also with stepped surfaces leading to a precise control of the width obtaining 6-AGNRs and with modified precursor molecules doped with nitrogen atoms obtaining a fine control of the band gap.

[1] Cai, J.; Ruffieux, P.; Jaafar, R.; Bieri, M.; Braun, T.; Blankenburg, S.; Muoth, M.; Seitsonen, A. P.; Saleh, M.; Feng, X.; Müllen, K.; Fasel, R. *Nature* 2010, 466, 470–473.

[2] A. Basagni, F. Sedona, C. A. Pignedoli, M. Cattelan, L. Nicolas, M. Casarin, M. Sambi, *J. Am. Chem. Soc.* 137, 1802 (2015)



Th-A10

From Armchair to Zigzag and Beyond: Recent Progress in the Bottom-up Fabrication of Atomically Precise Graphene Nanoribbons

Carlos Sánchez-Sánchez¹, Jia Liu¹, Shiyong Wang¹, Thomas Dienel¹, Leopold Talirz¹, Prashant Shinde¹, Carlo Pignedoli¹, Oliver Gröning¹, Bo Yang², Junzhi Liu², Xinliang Feng³, Klaus Müllen², Pascal Ruffieux¹, Roman Fasel¹

¹Swiss Federal Laboratories for Materials Science and Technology, EMPA, Duebendorf, Switzerland, ²Max-Planck Institut für Polymerforschung, Mainz, Germany, ³Center for Advancing Electronics Dresden (CFAED) & Department of Chemistry and Food Chemistry, Technische Universität Dresden, Dresden, Germany

Graphene nanoribbons (GNRs) are promising candidates to overcome the low on/off-behaviour of graphene – a zero band gap semiconductor – while still preserving the high charge carrier mobility that is essential for the fabrication of efficient field effect transistors. It has been shown that atomically precise GNRs can be fabricated by an on-surface bottom-up approach [1]. This versatile method has been successfully applied to the fabrication of armchair GNRs (AGNRs) of different widths [1-4] – and consequently different band gaps – as well as more complicated structures like chevron GNRs [1] or heterojunctions [5,6]. However, one of the most interesting types of GNRs has remained elusive: GNRs with zigzag edges (ZGNRs). ZGNRs are predicted to exhibit intriguing electronic properties like the existence of localized edge states with antiferromagnetic ordering across the ribbon width, thus giving rise to spin-polarized edges [7]. In this talk we will show how the on-surface synthesis approach can be extended to afford the fabrication of a new family of GNRs including atomically precise 6-ZGNRs, edge-modified variants thereof, as well as cove-edged GNRs. Spectroscopic evidence of the zigzag edge state is reported, with a significant energy splitting between occupied and unoccupied states that reflects the strong electron-electron interaction in these one-dimensional materials.

- [1] J. Cai et al. *Nature* 466, 470 (2010).
- [2] N. Abdurakhmanova et al. *Carbon* 77, 1187 (2014).
- [3] H. Zhang et al. *J. Am. Chem. Soc.*, 137, 4022 (2015).
- [4] Y.-C. Chen et al. *ACS Nano* 7, 6123 (2013).
- [5] Y.-C. Chen et al. *Nature Nanotech.* 10, 156 (2015).
- [6] J. Cai et al. *Nature Nanotechnology* 9, 896 (2014).
- [7] M. Fujita et al. *J. Phys. Soc. Jpn.* 65, 1920 (1996)

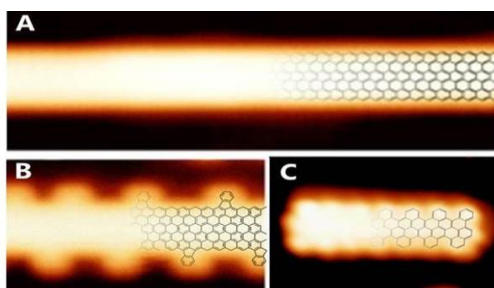


Figure 1. STM images with partially overlaid structural models of 6-ZGNR (A), edge-modified 6-ZGNR (B) and cove-edge 5-ZGNR (C) fabricated on a Au(111) surface.

Th-A11

Surface-Assisted Polymerization of Brominated Polyacenes on Cu(110) and Ag(110) Substrates

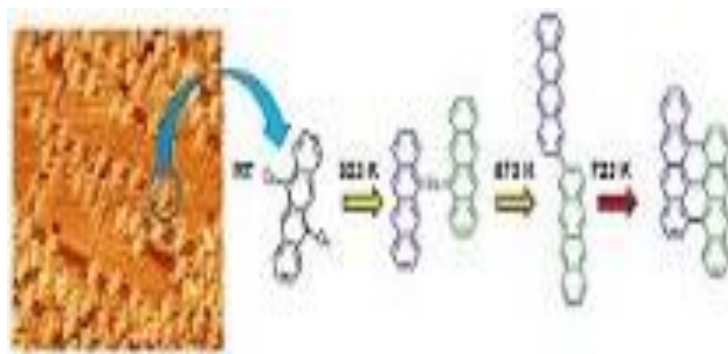
Igor Pis^{1,2}, Lara Ferrighi³, Thanh Hai Nguyen⁴, Mattia Cattelan⁴, Silvia Nappini², Andrea Basagni⁴, Matteo Parravicini³, Antonio Papagni³, Francesco Sedona⁴, Elena Magnano², Federica Bondino², Cristiana Di Valentin, Letizia Savio⁵, Marco Smerieri⁵, Stefano Agnoli⁴

¹Elettra-Sincrotrone Trieste, Basovizza, Italy, ²IOM CNR, Laboratorio TASC, Basovizza, Italy, ³Universita di Milano-Bicocca, Department of Materials Science, Milano, Italy, ⁴University of Padua, Department of Chemical Sciences, Padova, Italy, ⁵IMEM CNR, Genoa, Italy

The fundamental understanding of the organization of molecules on surfaces is the basis of the development of new devices in organic electronics and optoelectronics. Ultra-thin films made up of aromatic molecules can exhibit quite unique properties, which are connected not only to the specific chemical nature of the molecular units, but also to their connectivity. Controlling their growth in bottom-up fashion from molecular precursors with specific active sites has become a promising approach.

Adsorption and Ullmann coupling reaction of dibromotetracene and dibromopyrene on Cu(110) [1] and Ag(110) surfaces have been studied by synchrotron radiation X-ray photoelectron spectroscopy (XPS), near-edge X-ray absorption spectroscopy (NEXAFS), scanning tunnelling microscopy (STM), and density functional theory (DFT) calculations. After deposition at room temperature, the substrates were stepwise annealed up to 800K. At room temperature, molecules are transformed into organometallic complexes through debromination and carbon-radical binding to substrate adatoms. Organometallic oligomers and chains are present on the surface up to the temperature around 520K. Annealing to higher temperatures induces rapid C-C coupling and formation of covalent polymers along the closed-packed surface atomic rows. Further annealing starts massive dehydrogenation and formation of graphene nanostructures. The effect of substrate reactivity on the growth and structure of the surface covalent organic frameworks will be discussed.

[1] Ferrighi et al., Control of the Intermolecular Coupling of Dibromotetracene on Cu(110) by the Sequential Activation of C-Br and C-H bonds, Chem. Eur. J., 2015, 21, 5826-5835



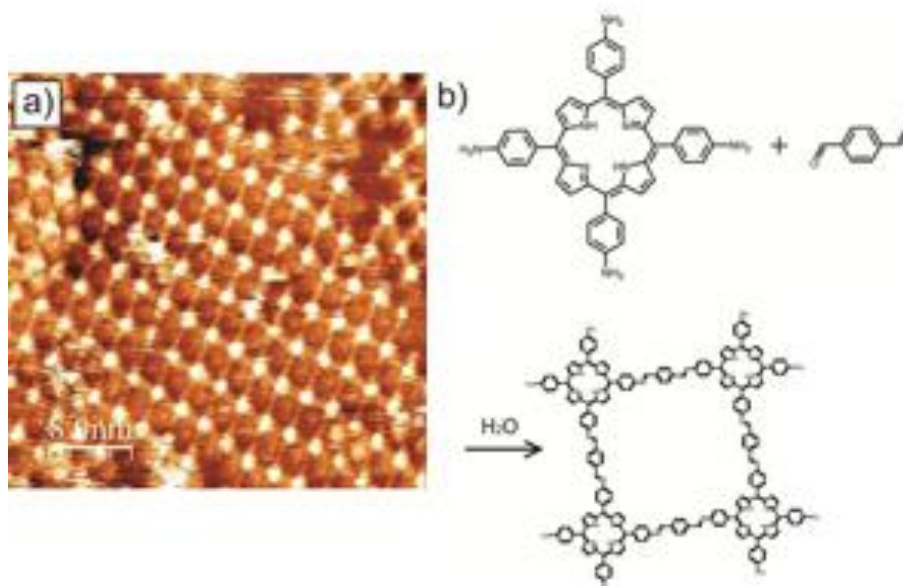
Th-A12

Two-dimensional covalent-organic frameworks (2D-COF) via Schiff-base condensation reactions between porphyrins

Ya Hu¹, Ying Chen¹, Hugo Bronstein¹, Matthew Blunt¹¹Department of Chemistry, University College London (UCL), London, United Kingdom

Since the successful isolation of individual graphene sheets in 2003 two-dimensional covalent materials have evolved in to one of the most widely studied areas of chemistry and physics. A particularly successful way of synthesizing new 2D covalent materials has been via a bottom-up approach in which suitably functionalised molecules are covalently linked together to form 2D covalent-organic frameworks (2D-COFs). This approach has been employed with a range of different reactions schemes and molecular building blocks [1]. An important step forward in this area was the use of reversible reactions that allowed the formation of the 2D-COF to take place under thermodynamic control [2-3], leading to the formation of highly ordered structures. In this work we present recent scanning tunneling microscopy (STM) results on the growth of 2D-COFs using free-base and metal-containing tetraphenyl amine porphyrin (TAPP) building blocks (fig1a). The TAPP molecules are linked together via a Schiff-base condensation reaction with benzene-1,4-dicarboxaldehyde (BDCA). This reaction forms imine linkages between the porphyrin components (fig1b). By controlling the synthesis conditions highly ordered and large scale (100's nm) 2D-COFs can be produced. In addition, by controlling the symmetry and chemical functionality of both the porphyrin and the linking aldehyde molecule 2D-COFs with more complex structures can be fabricated. Finally, investigations on the possibility of post synthesis functionalization of the resulting 2D-COF structures will be discussed.

- [1].J. W. Colson and W. R. Dichtel, Nat. Chem., 2013, 5, 453-465.
 [2].C. Z. Guan, D. Wang and L. J. Wan, Chem. Commun., 2012, 48, 2943–2945.
 [3].X. H. Liu, C. Z. Guan, S. Y. Ding, W. Wang, H. J. Yan, D. Wang, J. Am. Chem. Soc. 2013, 135, 10470–10474.



Th-A13+14

Bottom-up fabrication of graphene nanoribbons: From molecules to devices?

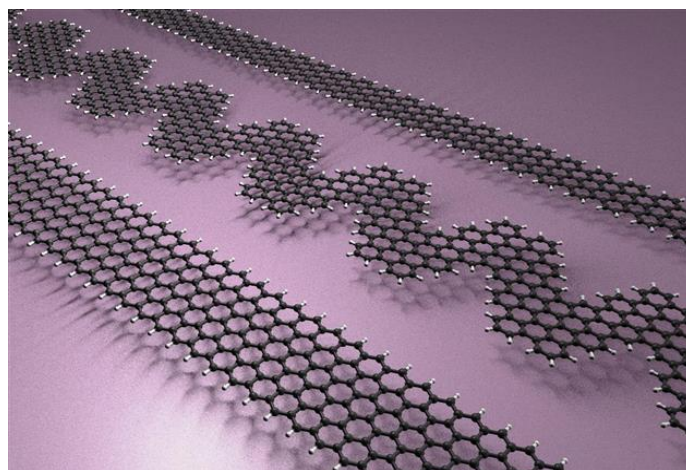
Roman Fasel¹

¹Empa, Swiss Federal Laboratories for Materials Science and Technology,
Duebendorf, Switzerland

Graphene nanoribbons (GNRs) – narrow stripes of graphene – have emerged as promising building blocks for nanoelectronic devices. The lateral confinement in GNRs opens a bandgap that sensitively depends on the ribbon width, allowing for the design of GNR-based structures with tunable properties. However, structuring with atomic precision is required to avoid detrimental effects induced by edge defects. Recently, we have introduced a versatile route for the bottom-up fabrication of GNRs [1], allowing for the atomically precise synthesis of ribbons with different shapes as well as heterostructures [2,3]. In this presentation, I will report on detailed experimental and computational investigations of the structural, electronic and optical properties of selected GNRs and heterojunctions [2-6].

For the case of armchair GNRs of width $N=7$, the electronic band gap and band dispersion have been determined with high precision [4,5]. Optical characterization has revealed important excitonic effects [6], which are in good agreement with ab initio calculations including many-body effects. For the case of heterojunctions between pristine (undoped) GNR segments and deterministically N-doped segments, we find a behavior similar to traditional p–n junctions. With a band shift of 0.5 eV and an electric field of 2×10^8 V/m at the heterojunction, these materials bear a high potential for applications in photovoltaics and electronics. First attempts at field effect transistor fabrication reveal, however, serious challenges in patterning and contact fabrication that are related to the nanoscale dimensions of individual AGNRs.

- [1] J. Cai, et. al Nature 466, 470 (2010).
- [2] S. Blankenburg, et al. ACS Nano 6, 2020 (2012).
- [3] J. Cai, et al. Nature Nanotech. 9, 896 (2014).
- [4] P. Ruffieux, et al. ACS Nano 6, 6930 (2012).
- [5] H. Soede, et al. Phys. Rev. B 91, 045429 (2015).
- [6] R. Denk, et al. Nat. Commun. 5, 4253 (2014).



Th-B11

New developments in small spot and imaging Near Ambient Pressure XPS

Andreas Thissen¹, Stephan Bahr¹, Thorsten Kampen¹, Oliver Schaff¹

¹SPECS Surface Nano Analysis GmbH, Berlin, Germany

Over the last 15 years, Near Ambient Pressure (NAP-) XPS has demonstrated its promising potential in a wide variety of applications. Starting from the Catalysis and Ice paradigm, the focus has shifted towards solid-liquid interfaces, liquid jets and in-situ electrochemistry. Initially, the experiments had to be carried out using advanced synchrotron sources to reach reasonable count rates. But now, the SPECS PHOIBOS 150 NAP offers optimized transmission for electrons, even at pressures up to and above 100mbar, so researchers can now use it with conventional X-ray and UV sources in their own laboratories. Because of the widened application fields, standard XPS is now also attainable when combined with easily adjustable monochromated X-ray sources that offer stable operation, small excitations spots, and high photon flux densities, even in Near Ambient Pressure conditions. The latest designs and results are presented showing small spot performance for spot sizes < 30 µm, while also showcasing the latest implementations of imaging NAP-XPS that uses a new concept allowing for lateral resolved measurements without a compromise in count rate and usability. Highlighting on how sample environments (in situ cells for gases and liquids, electrochemical cells, gas inlets) and integration are both absolutely essential to obtain relevant results from well-defined samples, the presentation will demonstrate the use of NAP-XPS systems for high throughput-XPS measurements, as well as a variety of applications.

Th-B12

The ALBA spectroscopic LEEM-PEEM experimental station

Michael Foerster¹, Lucia Aballe¹, Eric Pellegrin¹, Josep Nicolas¹, Salvador Ferrer¹

¹Cells-Alba, Cerdanyola del Vallès, Barcelona, Spain

The ALBA spectroscopic PhotoEmission Electron Microscope (PEEM) is a multi-technique instrument for the study of surfaces, thin films, and nanostructures [1]. It is based on a low energy electron microscope with energy analyser which, in combination with the variable polarization tunable x-rays of the CIRCE beamline, permits imaging with chemical, structural, and magnetic sensitivity down to a lateral resolution better than 20 nm.

This experimental station is well suited for surface science, with base pressure in the low 10^{-10} mbar range and flexible in situ preparation capabilities including ion sputtering, high temperature flashing, exposure to gases, and metal evaporation on quick exchange ports. In the microscope, surface annealing, low pressure ($< 10^{-6}$ mbar) gas treatments and thin film growth can be monitored in real time in either real or reciprocal space. It can be made available for in situ sample preparation previous to regular beamtimes granted on call for proposal basis.

The microscope's different working modes (imaging, diffraction and dispersive) will be presented, including recent examples from X-ray absorption (XAS), photoemission (XPS), spectromicroscopy, electron microdiffraction (μ -LEED), low energy electron microscopy (LEEM) including dark field imaging and I-V scans, angle resolved photoemission (ARPES) and X-ray circular magnetic dichroism (XMCD).

[1] The ALBA spectroscopic LEEM-PEEM experimental station: Layout and performance. L. Aballe, M. Foerster, E. Pellegrin, J. Nicolas, S. Ferrer, J. Synch. Rad. 22, 745 (2015)

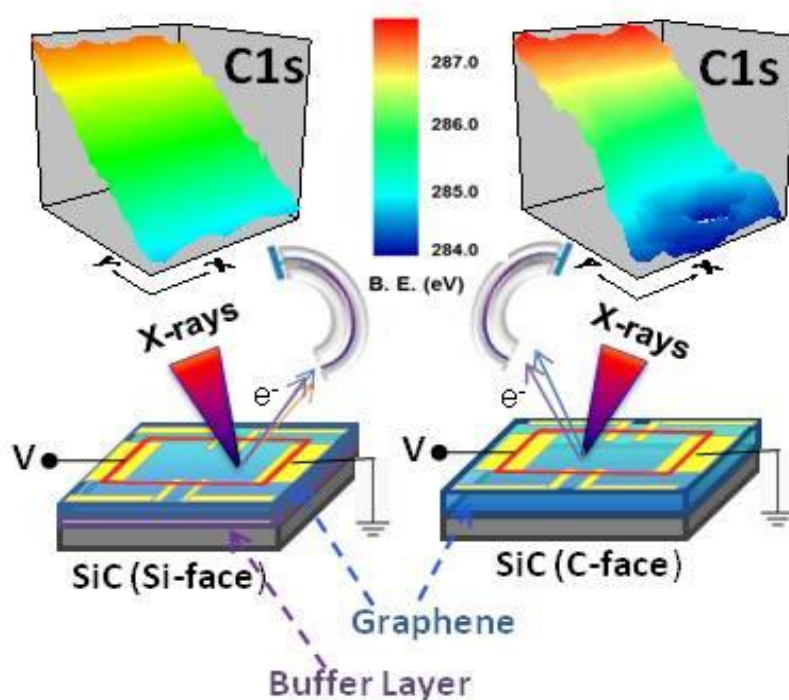
Th-B13

Chemical Characterization of Graphene Based Devices by XPS

Sefik Suzer¹

¹Bilkent University, Ankara, Turkey

Unlike common optical spectroscopic techniques, XPS is a charged particle based chemical analysis technique, extremely sensitive to the electrical potentials developed due to uncompensated charges. In the early days of XPS, charging was considered as a nuisance for characterization of insulating (electrets) materials. Hence elaborate compensation methods were developed using low energy electron and/or ions to minimize it. However, complete removal is only an ideal, and besides one can learn a lot by controlled use of the charging/discharging phenomena (a blessing). The generated photoelectrons' energy is influenced by the local electrical potential(s) (V_{loc}) resulting from charge accumulation, in addition to the chemical identity of the atoms, which is the mainstay of the technique. There are a myriad of chemical, physical, thermal, optical, mechanical phenomena contributing to charge accumulation on materials and/or surface structures, all amenable to charge sensitive XPS analysis. It is equally surprising that, although XPS has been utilized for more than 5 decades, this capability is almost completely left-out, untapped, and not utilized, except by few groups around the globe. We will describe its power by giving a variety of applications from our recent work, particularly related to characterization of graphene-based devices.



Th-B14

Initial and Final State Contributions to Core-Level Binding Energies: The Meaning and the Proper Use of Kohn-Sham Orbital Energies

Paul Bagus¹, Noelia Pueyo Bellafont², Francesc Illas²

¹Chemistry / University of North Texas, Denton, United States, ²Química Física, Universitat de Barcelona, Madrid, Spain

It is important to separate initial and final state contributions to the core-level binding energies, BE's, typically measured in X-Ray Photoelectron Spectroscopy, XPS. The initial state contributions directly reflect the charge state and physical and chemical environment of the ionized atom and are quantities of direct chemical and physical interest. On the other hand, the final state contributions arise from the relaxation, or response, of the "passive" electrons to the core-hole created and are of less interest for identifying the chemical and physical environment of the ionized atom. We present rigorous definitions, valid within both Hartree-Fock, HF, and Density Functional Theory, DFT, to separately determine these two contributions to the BE. In this connection, we examine the definition and the use of Kohn-Sham, KS, and HF orbital energies, ϵ 's. It is common to use the approximation $BE = -\epsilon$, commonly described as Koopmans' Theorem, KT. Indeed, often KS ϵ 's are used to determine initial state contributions to BE's. Previous work has shown, and we confirm, that this leads to negative relaxation energies, which would appear to cast doubt on the validity of using KS ϵ 's to determine initial state BE's. We give strong evidence that shows the shifts of KS ϵ 's very closely track the rigorous calculation of initial state contributions. This important result validates a large body of work where KS ϵ 's have been used, especially for solids and surfaces. Our conclusions are based on HF and DFT studies of a broad range of molecules using several density functionals. Provided that one examines trends or BE shifts, consistent results for the decomposition are obtained with HF and with DFT all functionals tested.

Th-C09

Steering the self-assembly of bridged triphenylamines on KBr(001)

Christian Steiner¹, Maximilian Ammon¹, Natalie Hammer², Ute Meinhardt², Bettina Gliemann², Martin Gurrath^{2,3}, Bernd Meyer^{2,3}, Milan Kivala², Sabine Maier¹

¹Department of Physics, University of Erlangen-Nürnberg, Erlangen, Germany,

²Department of Chemistry and Pharmacy, University of Erlangen-Nürnberg, Erlangen, Germany, ³Computer-Chemie Centrum and Interdisciplinary Center for Molecular Materials, University of Erlangen-Nürnberg, Erlangen, Germany

Molecules on insulating surfaces usually suffer from a weak unspecific molecule-surface interaction, which often leads to the growth of unordered structures. Through a careful design of the molecules functional groups, we were able to tune the self-assembly of bridged triphenylamines from porous and compact two-dimensional networks to nearly upright standing π - π stacked one-dimensional molecular aggregates on KBr(001).

Here, we present a systematic non-contact atomic force microscopy (nc-AFM) study in ultra-high vacuum on the adsorption and self-assembly of hydrogen-bonding and halogen functionalized triphenylamines on KBr(001). We show that triphenylamines bridged with bulky dimethylmethylene side groups adopt flat-lying adsorption geometries, which allow even the formation of porous networks. In contrast, the more compact carbonyl side groups favor intermolecular π - π interactions leading to nearly upright adsorption geometries of the molecules. The structure and orientation of both, the porous networks and the one-dimensional aggregates, are clearly influenced by the underlying KBr lattice. We discuss the role of the intermolecular and molecule-surface interactions based on molecularly resolved nc-AFM images and DFT calculations.

Th-C10

Following the condensation process of Xe in quantum boxes sequentially, atom-by-atom

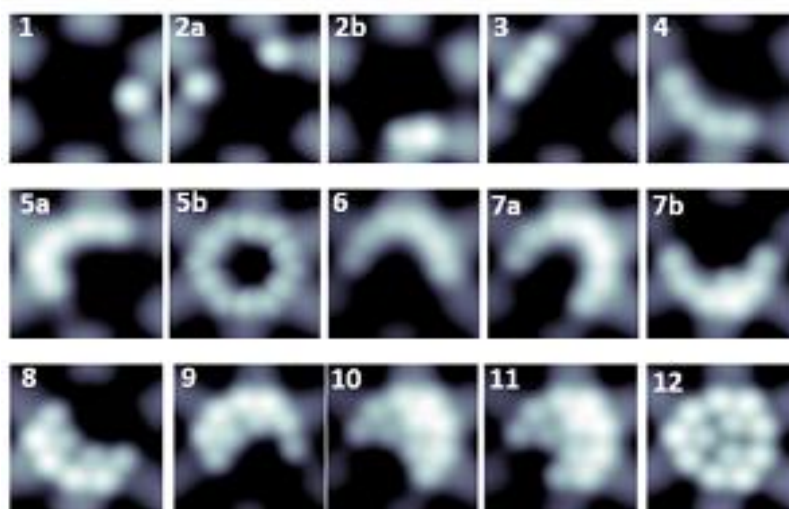
Sylwia Nowakowska¹, Aneliia Wäckerlin¹, Shigeki Kawai^{1,2}, Toni Ivas¹, Jan Nowakowski³, Shadi Fatayer^{1,4}, Christian Wäckerlin³, Thomas Nijs¹, Ernst Meyer¹, Jonas Björk⁵, Meike Stöhr⁶, Lutz H. Gade⁷, Thomas A. Jung³

¹University of Basel, Basel, Switzerland, ²PRESTO, Japan Science and Technology Agency, Honcho, Kawaguchi, Saitama, Japan, ³Paul Scherrer Institute, Villigen PSI, Switzerland, ⁴Universidade Estadual de Campinas, Campinas, Brazil, ⁵Linköping University, Linköping, Sweden, ⁶University of Groningen, The Netherlands, ⁷Universität Heidelberg, Germany

Condensation processes are of key importance in nature and play a fundamental role in the development of chemistry and physics. Due to size effects occurring for condensates with nanometer dimensions, it is conceptually desired to experimentally probe the structure of such condensates in dependence on the number of constituents one by one.

Here, we present an approach to study condensation process atom-by-atom with the scanning tunneling microscope, which provides a direct real-space access with atomic precision to the aggregates formed in atomically-defined 'quantum boxes'. Our analysis reveals the subtle interplay of competing directional and non-directional interactions in structure formation and provides unprecedented input for the structural comparison with quantum mechanical models. This approach focuses on - but is not limited to - the model case of xenon condensation and goes significantly beyond the well-established statistical size analysis of clusters in atomic or molecular beams by mass spectrometry.

S. Nowakowska et. al., Interplay of weak interactions in the atom-by-atom condensation of xenon within quantum boxes, *Nature Communications*, 6, 6071 (2015).



Th-C11

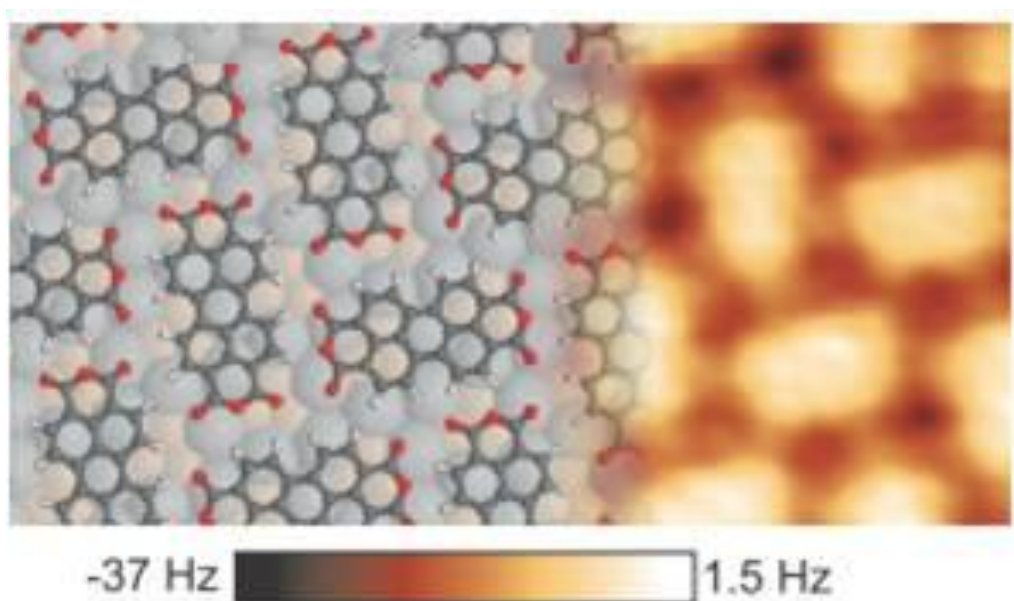
Intramolecular force contrast and dynamic current-distance measurements at room temperature

Sonia Matencio¹, Ferdinand Huber², Alfred John Weymouth², Carmen Ocal¹,
Esther Barrena¹, Franz Josef Giessibl²

¹Instituto de Ciencia de Materiales de Barcelona ICMAB-CSIC, Barcelona, Spain, ²Institute of Experimental and Applied Physics, University of Regensburg, Regensburg, Germany

Frequency-modulation atomic force microscopy (FM-AFM), in combination with scanning tunneling microscopy (STM), can be used to probe the internal atomic structure of flat organic molecules [1]. Intramolecular resolution requires an unreactive tip and has, until now, been demonstrated only at liquid helium and liquid nitrogen temperatures. In the presented work we demonstrate intramolecular and intermolecular force contrast at room temperature on 3,4,9,10-perylene tetracarboxylic dianhydride (PTCDA) molecules adsorbed on a Ag/Si(111)- $\sqrt{3}\times\sqrt{3}$ surface [2].

In addition the oscillating force sensor allows us to dynamically measure the vertical decay constant of the tunneling current, κ [3, 4]. The obtained κ maps show contrast between the two non equivalent PTCDA molecules giving evidence of a different tunneling barrier height.



Th-C12

Heteromolecular surface-based self-assembly of thymine functionalised porphyrins

Matthew Blunt¹, Ya Hu¹, Anna Slater², Lixu Yang³, Stephen Argent³, William Lewis³, Neil Champness³

¹Department of Chemistry, University College London, London, United Kingdom

²Department of Chemistry, University of Liverpool, Liverpool, United Kingdom

³School of Chemistry, University of Nottingham, Nottingham, United Kingdom

Understanding the complex hydrogen bonding behaviour of DNA nucleobases is an important step in directing two-dimensional (2D) molecular self-assembly on surfaces [1,2]. In this study, the surface-based self-assembly of a target molecule, tetra-(phenylthymine)porphyrin (tetra-TP) is investigated at the liquid-solid interface between highly oriented pyrolytic graphite (HOPG) and an organic solvent layer using scanning tunneling microscopy (STM) and molecular mechanics (MM) simulations. Through hydrogen bonding interactions between thymine groups, the tetratopic tectons form an extended square lattice network on an HOPG substrate (Figure.1). In addition, the investigation on the coadsorption of tetra-TP and an adenine derivative, 9-propyladenine reveals the formation of a self-assembled array bonded by adenine-adenine hydrogen bonding and Watson-Crick [3] thymine-adenine interactions, which have been indicated as a favourable hetero-intermolecular interaction in the solid state [4]. Moreover, the diversity of self-assembled tetra-TP structures is further explored by including melamine molecules which are found to act as both linkers and guests in the tetra-TP-melamine network. In the presentation, the overall concentration and molar ratio dependence of the molecular components in the binary networks will also be discussed. These studies demonstrate the possibility of making use of molecular recognition between DNA nucleobases to fabricate multicomponent self-assembled arrays on surfaces.

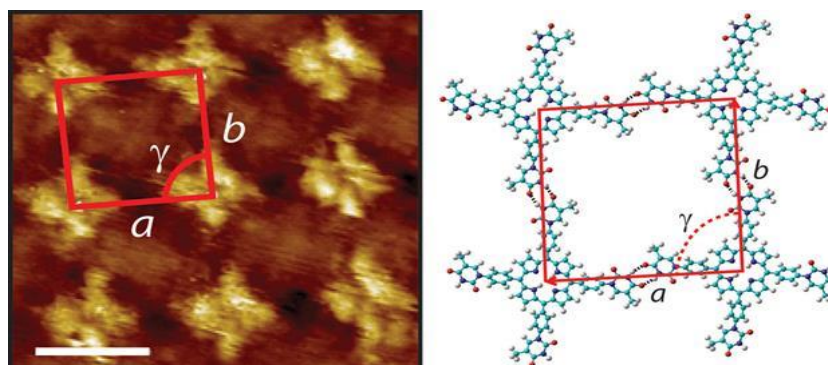
[1]. L. Liu, D. Xia, L. H. Klausen and M. Dong, *Int. J. Mol. Sci.*, 2014, 15, 1901-1914.

[2]. W. Mamdouh, M. Dong, S. Xu, E. Rauls and F. Besenbacher, *J. Am. Chem. Soc.*, 2006, 128, 13305-13311.

[3]. J. D. Watson and F. H. C. Crick, *Nature*, 1953, 171, 737-738.

[4]. A. Slater, Y. Hu, L. Yang, S. Argent, W. Lewis, M. O. Blunt and N. R. Champness, *Chem. Sci.*, 2015, 6, 1562-1569.

Figure 1: High resolution, drift corrected STM image and corresponding molecular model for the tetra-TP network. Scale bar = 2 nm.



Th-C13

Molecular self-assembled structures of biphenyl dicarboxylic acid: A comparison between Cu(111) and ultrathin CoO as substrate

Tobias Schmitt¹, Lutz Hammer¹, Alexander Schneider¹

¹Solid State Physics, University Erlangen-Nürnberg, Erlangen, Germany

Molecular self-assembly on surfaces is controlled by a complex balance between molecule-substrate and intermolecular interactions. We report on ordered phases of 4,4'-biphenyl-dicarboxylic acid (BDA) on Cu(111) and on CoO(111)/Ir(100) thin films using low temperature scanning tunneling microscopy in ultrahigh vacuum. Based on thermally activated deprotonation self-assembled structures with varying hydrogen content are found on the Cu surface. While non-deprotonated BDAs form linear H-bonded networks, deprotonated BDAs strongly bind to Cu atoms which results in a reduced molecular diffusivity and in the formation of chevron like structures. In a next step BDA molecules were adsorbed on thin CoO(111) films [1,2] to decouple them from the metal surface. While non-deprotonated BDAs form linear H-bonded chains equivalent to those on the Cu(111) surface, deprotonated molecules arrange themselves differently depending on the CoO(111) thickness. With increasing film thickness we observe a reduction of the influence of the surface corrugation and a dominance of molecule-molecule interaction promoting a parallel alignment of BDAs.

[1] C. Tröppner, et al., Phys. Rev. B 86, 235407 (2012)

[2] K. Biedermann, et al. J. Phys.: Condens. Matter 21, 185003 (2009)

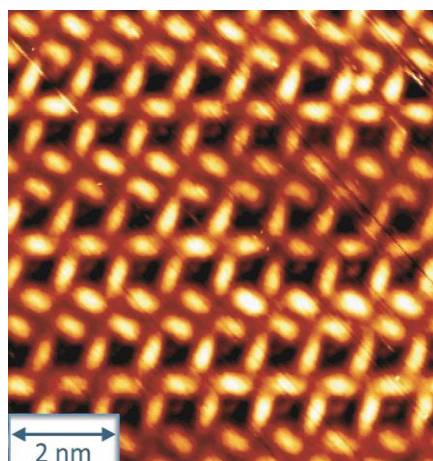
Th-C14

Self-assembly of functionalized indoles on Au(111) and Ag(111) surfaces

Fabrizio De Marchi¹, Maryam Ebrahimi¹, Josh Lipton-Duffin^{1,2}, Jennifer MacLeod^{1,3}, Federico Rosei^{1,4}

¹Centre Énergie, Matériaux et Télécommunications, Institut National de la Recherche Scientifique, Varennes, Canada, ²Central Analytical Research Facility (CARF), Institute for Future Environments, Queensland University of Technology, Brisbane, Australia, ³School of Chemistry, Physics, and Mechanical Engineering, Queensland University of Technology, Brisbane, Australia, ⁴Center for Self-Assembled Chemical Structures, McGill University, Montreal, Canada

The self-organization of small molecular building blocks leads to the formation of large and complex biological structures that are essential for the life of bigger organisms. By mimicking such type of self-assembly processes, it is, in principle, possible to design a particular motif by properly choosing an appropriate set of monomers. One of the most intriguing possibilities for the future manufacturing of self-assembled structures is to confine the self-assembly process to a surface, to be potentially used as the basic unit for organic thin film devices. However, predicting a priori how a molecule on a surface will interact with its neighboring molecules or with the substrate itself is challenging. Therefore, much more insights could be gained by the systematic study of small and simple molecules. We report here, our investigation on the self-assembly of two indole molecules, and how increased functionalization of the monomer opens the gate to new bonding motifs extending to different architectures. The first molecule, 2-carboxylic acid (I2CA) has a single carboxyl group whose interaction with its neighboring molecules leads to a simple ordered pattern, relatively independent of the substrate and the applied preparation conditions. Our second studied indole is 5,6-dihydroxyindole-2-carboxylic acid (DHICA) - one of the building blocks of eumelanin that is one of the pigments present in most organisms. Due to its additional hydroxyl groups, the self-assembled networks of DHICA presents a much wider range of features. A summary of the formed self-assembled architectures of the two indole molecules on Au(111) and Ag(111), imaged by Scanning Tunneling Microscopy, and the models based on Density Functional Theory calculations will be presented. We conclude that the substrate and the preparation conditions to form the organic molecular films are the determining factors to further engineer the structure of self-assembled molecular networks.



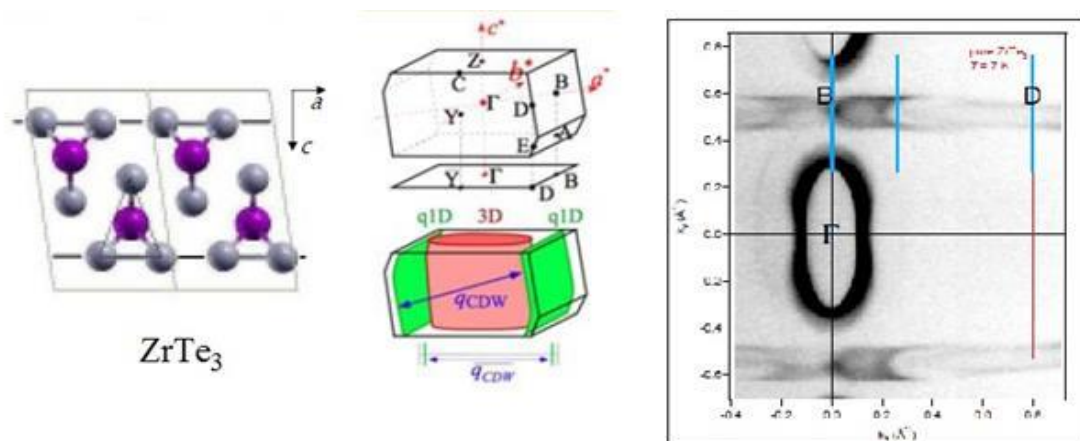
Th-D09+10

Angle-resolved photoemission from transition-metal tri-chalcogenides

Moritz Hoesch¹

¹Diamond Light Source, Didcot, United Kingdom

The quest to understanding the properties of the one-dimensional metallic state with its various manifestations of charge density waves, suppressed ordering and instability of the Fermi liquid state is best studied in compounds with parallel, but ideally non-interacting molecular or atomic chains. The uniaxial crystal ZrTe_3 is easily cleaved to expose atomically clean Te-terminated surfaces. On these we have studied the Fermi surface and charge density wave phenomena by angle-resolved photoemission. While the observations fall into the expected ball park compared to bulk properties, the surface electronic structure shows signs of further reduced dimensionality that are interpreted as due to surface relaxation. The family of $\text{M}_2\text{Mo}_6\text{Se}_6$, where M represents Tl, In, Cs, Rb, or lighter alkali metals forms such a quasi one-dimensional crystal structure with a host lattice of $(\text{M}_{36}\text{Se}_3)$ molecular chains that are weakly coupled by the M guest ions. These samples are experimentally more difficult but the observed electronic structure is perfectly one-dimensional and shows non-Fermi-liquid behaviour. We will contrast the physics of these two samples to each other and draw conclusions on the stability of the charge density wave ground state and the low-dimensional electron gas.



Th-D11

Surface States Dimensionality Transition of Bi(111) on a curved crystal

Jorge Lobo-Checa¹, Federico Mazzola², Lucas Barreto³, Frederik Schiller¹, Justin W. Wells², Martina Corso¹, Luis Alejandro Miccio¹, Ignacio Piquero-Zulaica¹, Nickolas C. Plumb⁴, Philip Hofmann⁵, J. Enrique Ortega^{1,5,6}

¹Centro de Física de Materiales (CSIC-UPV/EHU), San Sebastián, Spain, ²Dep. of Physics, Norwegian Univ. of Science and Technology, Trondheim, Norway, ³Dep. of Physics and Astronomy, Interdisciplinary Nanoscience Center, Aarhus University, Aarhus, Denmark, ⁴Swiss Light Source, Paul-Scherrer-Institut, Villigen, Switzerland, ⁵Dep. Física Aplicada I, Universidad del País Vasco, San Sebastián, Spain, ⁶Donostia international Physics Center, San Sebastián, Spain

Bismuth is a semimetal whose surface shows better metal behaviour than its bulk counterpart due to the presence of metallic-like surface states. These are spin-split given its large atomic weight and spin orbit interaction [1]. Depending on the crystal termination these states behave as two dimensional (2D), delocalized states, or one dimensional (1D), localized states [2]. Such modification of the electron wavefunction is induced by the presence of step arrays, by repulsive scattering at steps and confinement within terraces [3] and has been widely explored for Shockley states in noble metals [3-5]. Semimetals have not received such a widespread attention but the investigating of this 2D to 1D transition is particularly interesting since Bi is very close to being a topological insulator and great interest has emerged in topologically guaranteed 1D surface states. We present a study that finely explores the 1D-2D transition in Bismuth surface states using a curved crystal (see FSM images). Such special samples allows for a smooth variation of the surface orientation, which translates into a smooth variation of the step separation, i.e. the step potential barriers. The evolution of the electronic structure is investigated by state-of-the-art ARPES and correlated to the local structure obtained from STM and LEED. We find that this transition is unexpectedly different from the noble metal curved surfaces because we do not observe umklapps and the surface states are referred to the rhombic (111) direction of the crystal instead of the projection of the L point on the surface.

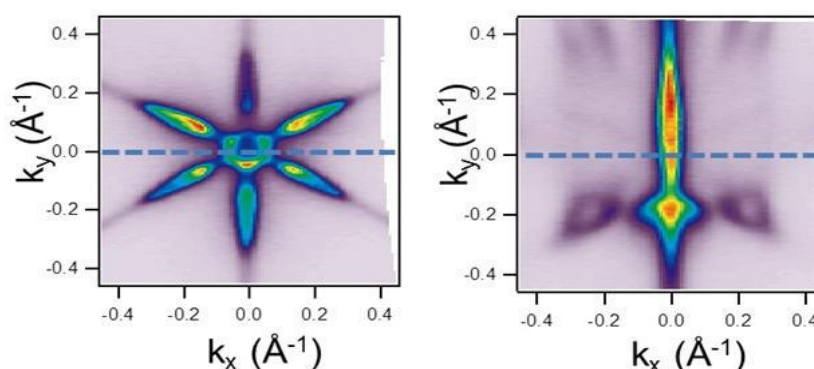
1 Ph. Hofmann, Prog. In Surf. Sci. 81,191 (2006).

2 J. W. Wells et al., PRL, 102, 096802 (2009).

3 L. Bürgi et al., PRL 81, 5370 (1998).

4 J. E. Ortega et al., PRB 87, 115425 (2013).

5 J. Lobo-Checa et al., PRB, 84, 245419 (2011).



Th-D12

Electronic structure of TlBi alloy formed on Si(111)

Kazuyuki Sakamoto¹, Hirotaka Ishikawa¹, Toru Hazama¹, Takashi Hayashida¹,
Yuichi Oda¹, Yuchi Yaoita¹

¹Chiba University, Chiba, Japan

In this paper, we present the electronic structure of a heavy element alloy created on a semiconductor substrate. Heavy element films are known to show various interesting spin-orbit coupling related physical properties. For example, peculiar Rashba-Bychkov (RB) effects that result from the symmetry of the surface are reported in case of heavy element monolayer films adsorbed on solid surfaces [1], and the creation of two-dimensional topological insulators is expected in case of heavy element alloys forming a honeycomb structure [2]. By using angle-resolved photoelectron spectroscopy, we have measured the electronic structure of a heavy element alloy TlBi film formed by the adsorption of 1 ML of Tl and 1 ML of Bi on a Si(111) substrate. The creation of TlBi alloy was confirmed by the binding energies of the core-levels of both elements and the valence-band electronic structure. Although the LEED pattern of the TlBi alloy suggests its atomic structure to be incommensurate, the electronic structure follows the (1x1) periodicity of Si(111). This indicates that the created alloy strongly interacts with the substrate, and thus does not behave like an isolated honeycomb structure film. In the band structure, a huge valley with a rather linear dispersion is observed at the K point of the Si(111)-(1x1) surface Brillouin zone, and a giant RB splitting is observed at the M point. By analyzing the valley structure, we found that the Fermi velocity of this system is comparable to that of graphene. We will also discuss the origins of both the valley structure and the giant RB effect based on the symmetry of the surface.

[1] K. Sakamoto et al., Nat. Commun. 4, 2073 (2013).

[2] F.-C. Chuang et al., Nano Lett. 14, 2505 (2014).

Th-D13

Surface states on vicinal Beryllium surfaces: two-dimensional quantum well states

Lukasz Walczak¹, Victor Joco², Miguel Angel Valbuena³, Balasubramanian Thiagarajan⁴, Pilar Segovia^{1,5}, Enrique Garcia Michel^{1,5}

¹Departamento de Física de la Materia Condensada, Universidad Autónoma de Madrid, Madrid, Spain, ²Centro de Microanálisis de Materiales, Universidad Autónoma de Madrid, Madrid, Spain, ³Instituto Catalan de Nanotecnologia, Bellaterra, Barcelona, Spain, ⁴MAX-Lab, Lund University, Lund, Sweden, ⁵Departamento de Física, Condensed Matter Physics Center (IFIMAC), Universidad Autónoma de Madrid, Madrid, Spain

Vicinal metal surfaces are an important example of a nanostructured system with long-range order. The case of noble metal surfaces vicinal to the (111) or (100) directions has been studied in detail. Group II metals (like Be and Mg) present many specific properties of interest. These metals exhibit large surface band gaps, which hold several prominent surface states with a high density of states. In the case of the flat (10-10) surface of both metals, different surface states are seen both for normal and off-normal emission (surface A point).

We report in this work an investigation on the electronic properties of Be surfaces vicinal to the (10-10) direction using LEED, Angle Resolved Photoemission Spectroscopy (ARPES) and synchrotron radiation. The sample long-range order was characterized by LEED, which showed superstructure spot splitting. We have characterized the electronic structure along steps (Gamma M surface direction) and perpendicular to steps (Gamma A surface direction) for several photon energies and for a range of different miscut angles. We identify several surface state bands, for both normal and off-normal emission (surface A point). The binding energy of the surface state near the surface A point depends on the crystal miscut angle, so that the surface state becomes slightly shallower than for a flat surface, as expected assuming a partial lateral confinement by the step superlattice. Concerning the surface state observed at normal emission, we observe the appearance of additional subbands, whose dispersion is compatible with lateral confinement induced by the step superlattice (delocalization parallel to steps and confinement along the direction normal to steps). The results for different miscut angles are discussed and interpreted within standard models for vicinal metal surfaces.

Th-D14

Anomalous d-like Surface Resonance on Mo(110) Analyzed by Time-of-Flight Momentum Microscopy

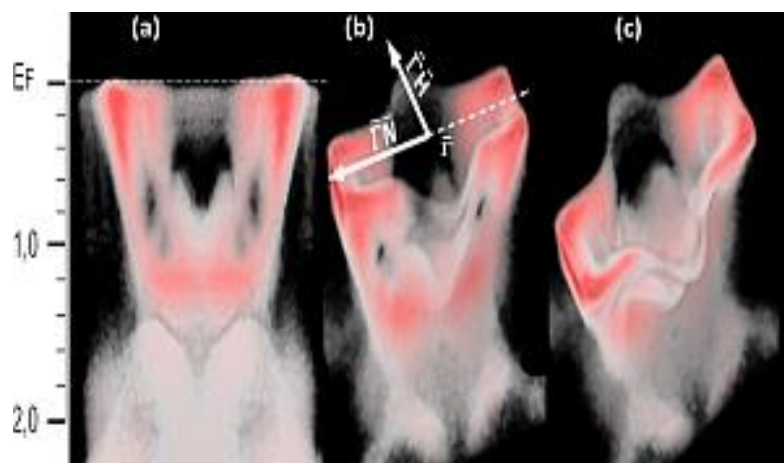
D. Kutnyakhov¹, S. Chernov¹, K. Medjanik¹, C. Tusche², S. A. Nepijko¹, A. Oelsner³, J. Braun⁴, J. Minár^{4,5}, S. Borek⁴, H. Ebert⁴, H. J. Elmers¹, J. Kirschner², G. Schönhense¹

¹Institut für Physik, Johannes Gutenberg-Universität Mainz, Mainz, Germany, ²Max Planck Institut für Mikrostrukturphysik, Halle, Germany, ³Surface Concept GmbH, Mainz, Germany, ⁴Department Chemie, Ludwig-Maximilians-Universität München, München, Germany, ⁵New Technologies-Research Center, University of West Bohemia, Pilsen, Czech Republic

The electronic surface states on Mo(110) have been investigated using time-of-flight momentum microscopy with synchrotron radiation in single-bunch mode at BESSY ($h\nu=35$ eV). This novel angle-resolved photoemission approach yields a simultaneous acquisition of the E-vs-k spectral function in the full surface Brillouin zone and several eV energy interval. (k_x, k_y, E_B) 3D-maps with 3.4 \AA^{-1} dia. And 2 eV width reveal a rich structure of d-like surface resonances in the spin-orbit induced partial band gap (see figure [1]). Calculations using the one-step model in its density matrix formulation predict an anomalous state with Dirac-like signature and Rashba spin texture crossing the bandgap at the Γ -point and $E_B = 1.2$ eV. Experiment shows that the linear dispersion persists away from the Γ -point in an extended energy- and k_{\parallel} -range. Analogously to a similar state previously found on W(110) [2] the dispersion is linear along H- Γ -H and almost zero along N- Γ -N. The similarity is surprising since spin-orbit interaction is 5 times smaller in Mo. A second point with unusual topology was found midway between Γ and N. Band symmetries are probed by linear dichroism [1]. Funded by BMBF (05K13UM1, 05K13WMA).

Figure caption: 3D data matrix of the E-vs-k spectral function showing the topology of the surface resonances on Mo(110); raw data as observed by the ToF k-microscope. The perspective views (a-c) uncover many subtle details of the k-space object. Binding-energy scale and k_{\parallel} -directions are denoted in (a,b), red color marks enhanced intensity.

[1] Chernov et al., Ultramicroscopy, in print; [2] Miyamoto et al., PRL 108 (2012) 066808



Th-E09

Model catalysts of nitrogen-doped graphitic carbons for oxygen reduction reaction

Donghui Guo¹, Takahiro Kondo¹, Riku Shibuya¹, Chisato Akiba¹, Shunsuke Saji¹, Junji Nakamura¹

¹Department of Materials Science, University of Tsukuba, Tsukuba, Japan

Nitrogen-doped graphitic carbons are expected as non-Pt fuel cell catalysts for oxygen reduction reaction (ORR). However, the active sites are still under debate, which is due to the complexity of carbon catalysts, such as co-existence of different types of nitrogen species and the degree of conjugative system. Here we designed nitrogen doped graphite (HOPG) model catalysts with different type of nitrogen species and their concentration to clarify the ORR active site. The ORR measurements of the HOPG model catalysts indicated that the active site was created by pyridinic nitrogen (N bonded to two carbon atoms). It was also found that carbon dioxide adsorbs on the HOPG model catalysts with pyridinic-N. The ORR active site was thus ascribed to carbon atoms with Lewis base properties created by pyridinic-N. The local electronic structure of carbons near pyridinic nitrogen were discussed based on the results of scanning tunneling spectroscopy (STS) measurements.

Th-E10

Electrochemical switchable device based in ferrocene-SAMs for memory devices

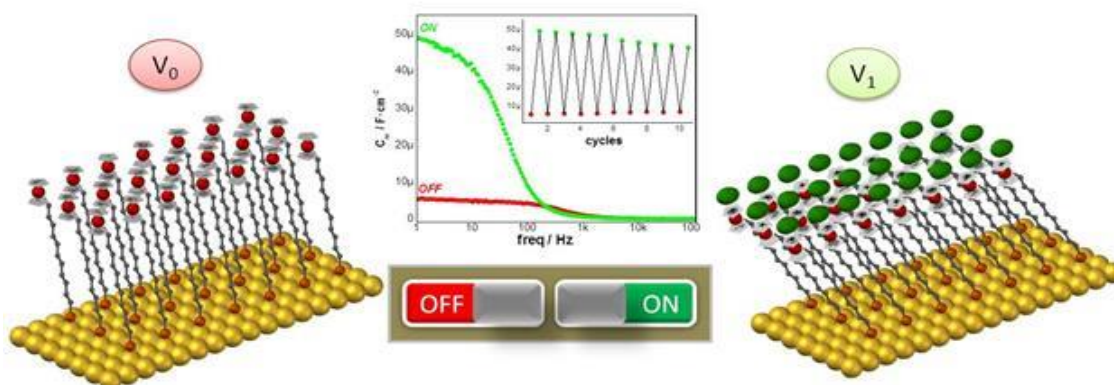
Elena Marchante¹, Núria Crivillers¹, Marta Mas-Torrent¹, Concepció Rovira¹,
Jaume Veciana¹

¹ICMAB-CSIC, Bellaterra, Barcelona, Spain

Inside the field of Molecular Electronics, the use of molecular switches has emerged as a simple device for the development of logic devices based on them. For this purpose, the molecules should present reversible properties that can be interconverted in response to an external stimulus. One of the mainly used methodologies for the study of these molecules consists on the self-assembly formation of monolayers (SAM) at metal substrates.

SAMs of electroactive molecules behaving as electrochemical switches with optical and magnetic response have been previously described. In our case, gold substrates are modified with an electro-active self-assembled monolayer. We have chosen ferrocenyl-alkanethiols compounds due to their optimal electrochemical properties. Furthermore, different ionic liquids are used as electrolytes for the high conductivity, nonvolatility and high thermal stability. Nevertheless, the most attractiveness of the ionic liquids relies in their capability to be immobilized in a polymeric matrix forming ion-gels, and their application as solid electrolytes.

In this work, by means of ionic liquids and ion-gels as electrolytes, and through the application of a DC bias, the redox state of the SAM is changed. In this way, the interfacial capacitance is measured by electrochemical impedance spectroscopy (EIS) and used as the output of the system. The results obtained represent a feasible methodology for the future integration of molecular electrochemical switches in real electronic devices.



Th-E11

Self-assembled monolayers on oxidized platinum as platforms for biosensors

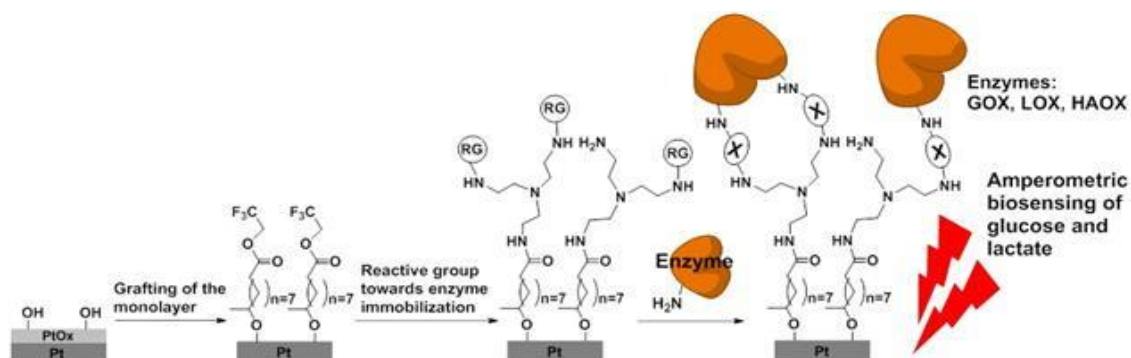
Jose Maria Alonso Carnicero¹, Abraham A. M. Bielen¹, Maurice C. R. Franssen¹, Han Zuilhof^{1,2}

¹Wageningen University, Laboratory of Organic Chemistry, Wageningen, Netherlands, ²Department of Chemical and Materials Engineering, King Abdulaziz University, Jeddah, Saudi Arabia

Self-assembled monolayers (SAMs) provide an excellent platform for the fabrication of biosensors as they offer a good control over the accessibility and orientation of the immobilized sensing element (usually a biomolecule). SAMs can be formed on many inorganic materials but the examples on truly conductive substrates are restricted to thiols on noble metals (Au, Ag, Pt or Pd). Moreover the thermal and hydrolytic stability of those SAMs are limited. Therefore, alternatives that rely on different surface chemistries should be investigated. Pt and Pt oxide seem appropriate materials to explore since they have a wide range of applications including catalysis, electrochemistry and biosensing. Besides they are compatible with silicon processing in micro and nanofabrication techniques, which does not occur for Au.

Herein we describe the fabrication of glucose and lactate amperometric biosensors through the engineering of oxidized Pt electrodes with ester terminated 1-alkenes followed by the covalent attachment of oxidase enzymes: glucose oxidase (GOX), lactate oxidase (LOX) and human hydroxyacid oxidase (HAOX). Different coupling protocols are tested in order to tune the amount of immobilized enzyme. Drop-casting of enzyme solution on N-hydroxysuccinimide (–NHS) or aldehyde (–CHO) functionalized surfaces produces electrodes with a (sub)-monolayer coverage of enzyme while higher coverages are obtained by cross-linking the enzymes in the presence of glutaraldehyde or bis-NHS derivatives. Electrode surfaces are characterized by static contact angle (CA), infrared reflection absorption spectroscopy (IRRAS), X-ray photoelectron spectroscopy (XPS) and atomic force microscopy (AFM).

J. M. Alonso, B. Fabre, A. K. Trilling, L. Scheres, M. C. R. Franssen, H. Zuilhof. Covalent Attachment of 1-Alkenes to Oxidized Platinum Surfaces. *Langmuir* 2015, 31, 2714–2721



Th-E12

Thin films of water-based biopolymers for protection of reactive surfaces

Christian Fernández-Solis¹, Michael Rohwerder¹, Andreas Erbe¹

¹Max-Planck-Institut für Eisenforschung GmbH, Düsseldorf, Germany

Corrosion of metals is a natural occurring electrochemical phenomenon that constitutes a ubiquitous problem in modern society, especially for infrastructure and industry. Polysaccharides and polypeptides represent two of the most abundant polymer groups in nature, with interesting properties. Both classes of polymers can take up water. We explore using such water-soluble biomacromolecules to create thin films on metals as an alternative to advance towards greener functional materials for protection of reactive surfaces.

Thin films were deposited on zinc substrate, utilising solutions of alginate, chitosan and gelatine. The coatings were characterised using infrared spectroscopy (IR), scanning electron microscopy (SEM) and atomic force microscopy (AFM). Scanning Kelvin probe (SKP) measurements were performed to study the delamination kinetics of the system after creation of an artificial defect. Additionally, water uptake and ion permeability of the layer were analysed using electrochemical impedance spectroscopy (EIS).

AFM and SEM of coated substrate showed a complete, homogeneous coverage of the surface. SKP measurements recorded an apparent delamination front. The variation of potentials can be attributed to effects of Donnan potential in the coating. Potentials constantly remain above the corrosion potential expected for freely corroding zinc. EIS data recorded over 400 min showed water uptake, where alginate-based coating incorporates a significantly higher amount of water compared to chitosan and gelatine. The final capacitances of all coatings are very similar. However, no secondary processes were observed for any of these films, but water diffusion into the protective layer. Complementary linear polarisation resistance measurements showed a decrease of corrosion current about 1/50 compared to bare substrate. The water-based biopolymers coatings studied in this work exhibited charge transfer resistance values comparable to that of hydrophobic coatings. However, corrosion is delayed by retention of corrosive ions within the coating layer.

Th-E13

Fundamental Investigations of Sweet Oilfield Corrosion

Hadeel Hussain¹, Matthew Acres¹, Chris Muryn^{1,2}, Rob Lindsay³

¹Photon Science Institute, University of Manchester, Manchester, United Kingdom, ²School of Chemistry, University of Manchester, Manchester, United Kingdom, ³Corrosion and Protection Centre, University of Manchester, Manchester, United Kingdom

Dissolved CO₂ is a primary reagent for internal (sweet) corrosion of oilfield equipment fabricated from carbon steel. The resulting aqueous phase species (carbonic acid) stimulates corrosion primarily through supplying reactant for the cathodic process (H₂(g) evolution); iron dissolution (Fe(s) → Fe²⁺(aq)) occurs at anodic sites. Solid corrosion products may also appear as a consequence of CO₂ induced corrosion, with their formation dependent upon a range of parameters, e.g. pH and temperature. If adherent to the carbon steel substrate, such solids can significantly reduce the rate of corrosion, and so are integral to material sustainability.

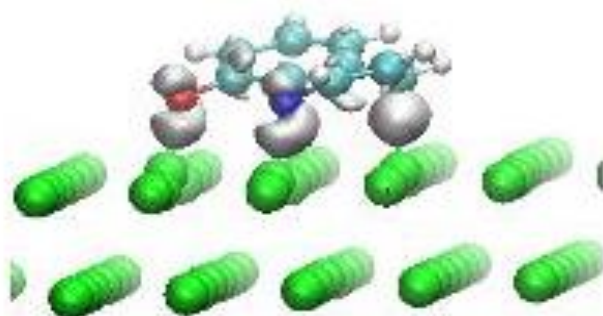
Given the potential importance of sweet corrosion scales, there is significant on-going effort to understand them. Substantial progress has been made, in particular as regards the composition and morphology of established scales. Lacking, however, are nanoscale details about the nucleation and growth of these scales, including the surface structure/chemistry prior to scale initiation. On this basis, we have adopted a surface science type approach in attempt to address these topics. Using UHV-STM, we have examined the adsorption of H₂O/CO₂ onto Fe(110), finding significant variation as a function of both exposure and substrate temperature. Long range ordered phases are observed, as well as more local features (e.g. islands), apparently arising from mass transport of substrate material. Such results demonstrate the dynamic nature of the iron substrate, even when exposed to technologically insignificant quantities of pertinent species, suggesting that our nanoscale mechanistic understanding of sweet oilfield corrosion is at best currently highly limited.

Th-E14

Corrosion Inhibition Studies at the Atomic Scale:
8-Hydroxyquinoline on pure Aluminum and OxideFatah Chiter^{1,2}, Corinne Lacaze-Dufaure¹, Hao Tang², Nadine Pébère¹¹CIRIMAT, Toulouse, France, ²CEMES, Toulouse, France

Since the beginning of the 1990s, intense research efforts are being undertaken to find new environmentally friendly compounds as corrosion inhibitors of aluminum and aluminum alloys. Experimentally, it was shown that 8-hydroxyquinoline (8-HQ) acts as an effective corrosion inhibitor for different metals and alloys, such as magnesium [1], copper [2] and aluminum [3-5]. The aim of the present work is to correlate theoretical approaches at atomic scale to experimental ones in order to extract the factors which are favorable to the inhibition processes. A better understanding of the corrosion inhibition mechanisms will help to rationalize the search of new species that could provide corrosion protection close to that afforded by non organic inhibitors. We present here density functional studies of the adsorption and bonding of 8-HQ molecule and its derivatives that could be present in acidic, alkaline and neutral media, on clean aluminum surface and on the aluminum oxide surface at different coverages. The molecule/substrate system was modeled by a periodic supercell and dispersed corrected computations were performed. The interactions between the surface and the molecules are discussed in term of adsorption sites and topology. Moreover, a detailed analysis of the energies and of the electronic structure of the organic-metal interface leads to the determination of the nature of the bonding (physisorption or chemisorption modes). It is really meaningful because it governs the surface properties of the system. The reduction of oxygen was also investigated with and without the presence of the organic inhibitors on the aluminum and aluminum oxide surfaces. It is connected to the corrosion inhibition mechanism.

- [1] H. Gao, et al. Corrosion Science 52 (2010) 603-1609.
- [2] G.P. Cicileo, et al. Corrosion Science 40 (1998) 1915-1926.
- [3] C. Casenave, et al. Materials Science Forum 192-194 (1995).
- [4] L. Garrigues, et al. Electrochimica Acta 41 (1996) 1209-1215.
- [5] S.V. Lamaka, et al, Electrochimica Acta 52 (2007) 7231-7247.



Th-A15

Substrate-induced structural effects in graphene nanoislands on Ni(111)

Aran Garcia-Lekue^{1,2}, Marc Olle³, Gustavo Ceballos³, Juan José Palacios⁴, Aitor Mugarza³, Pietro Gambardella⁵, Daniel Sánchez-Portal^{1,6}

¹Donostia International Physics Center (DIPC), Donostia, Spain,

²IKERBASQUE, Basque Foundation for Science, Bilbao, Spain, ³Catalan Institute of Nanotechnology (ICN2), Barcelona, Spain, ⁴IFIMAC, Universidad Autónoma de Madrid, Madrid, Spain, ⁵Department of Materials, ETH Zurich, Zurich, Switzerland, ⁶Centro de Física de Materiales (CFM), CSIC-UPV/EHU, Donostia, Spain

Edges play a fundamental role in shaping the morphology and electronic properties of graphene nanostructures.[1,2] Understanding and defining the edge morphology is therefore important to tune the growth of graphene nanostructures as well as to modulate the electronic properties of graphene in confined geometries. In free-standing graphene, crystallographically oriented edges are of either zigzag (zz) or armchair (ac) type. A very different scenario arises in epitaxially grown graphene, where the interaction with the substrate can stabilize armchair, zigzag and reconstructed edges and induce complex graphene-metal boundaries. In this work, we combine density functional theory (DFT) calculations and experiments by scanning tunneling microscopy (STM) to reveal the most stable edge structures of graphene on Ni(111) as well as the role of stacking-driven activation and suppression of edge reconstruction.[3] DFT calculations show that depending on the position of the outermost carbon atoms relative to hollow and on-top Ni sites, zigzag edges have very different energies. Triangular graphene islands (TGIs) are exclusively bound by zigzag hollow edges. In hexagonal islands (HGIs), which are constrained by geometry to alternate zigzag hollow and zigzag top edges along their perimeter, only the hollow edge is stable, whereas the top edges spontaneously reconstruct into the (57) pentagon-heptagon structure. Moreover, the edge energetics fully accounts for the shape of the HGIs observed experimentally and suggests that the temperature driven transition from TGIs to HGIs is an activated process related to the existence of an energy barrier for the 57 pentagon-heptagon reconstruction.

[1] E. Loginova et al., New J. Phys. 11, 063046 (2009)

[2] A. Garcia-Lekue et al., Phys. Rev. Lett. 112, 066802 (2014)

[3] A. Garcia-Lekue et al., J. Phys. Chem. C 119, 4072 (2015)

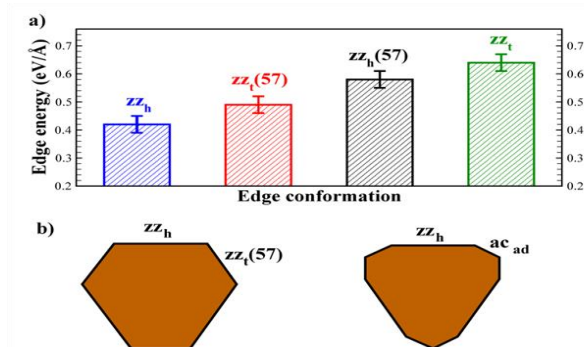


Figure (a) Formation energies of graphene zz edges on Ni(111). (b) Equilibrium shape of graphene nanoislands on Ni(111) obtained by minimizing the edge energy.

Th-A16

Enhanced chemical reactivity of pristine graphene strongly interacting with a substrate: chemisorbed CO on graphene/Ni(111).

Mario Agostino Rocca^{1,2}, Marco Smerieri², Edvige Celasco^{1,2}, Giovanni Carraro^{1,2}, Angelique Lusuan^{1,2}, Jagriti Pal^{1,2}, Gianangelo Bracco^{1,2}, Letizia Savio², Luca Vattuone^{1,2}

¹Università di Genova, Genova, Italy, ²IMEM CNR, Genova, Italy

Graphene is usually considered a chemically inert material. Theoretical studies of CO adsorption on free standing graphene predict indeed adsorption energies < 0.1 eV. In spite of this it has been recently demonstrated that it can be used effectively in gas sensing applications [1,2]. Applications in chemistry have been envisaged, too [3,4], but much larger adsorption energies are then needed. Chemisorption can take place at defects, which however lower the graphene quality [5]. For catalytic applications chemisorption at pristine graphene films would thus be highly desirable. We show by High Resolution Electron Energy Loss Spectroscopy and Scanning Tunnelling Microscopy that non-dissociative chemisorption of CO does indeed occur at cold, pristine graphene grown on Ni(111) [6]. The adlayer remains stable when heating the sample up to 125 K and CO desorbs eventually when heating further. Some CO coverage survives to flashes up to 225 K. This unexpected result is qualitatively explained by the modification of the density of states close to the Fermi energy induced by the relatively strong graphene-substrate interaction. The value of the adsorption energy allows to estimate an equilibrium coverage of the order of 0.1 ML at 10 mbar pressure, thus paving the way to the use of graphene as a catalytically active support under realistic conditions.

- [1] F. Schedin et al. Nature Materials 2007, 6, 652-655
- [2] T. O. Wehling, et al. Nano Letters 2008, 8, 173-177
- [3] L. Liao, H. Peng, Z. Liu, JACS 2014, 136, 12194.
- [4] L. Ferrighi, M. Datteo, C. Di Valentin, JPCC 2014, 118, 223.
- [5] B. Huang, et al. J. Phys. Chem. C 2008, 112, 13442-1446
- [6] M. Smerieri et al. ChemCatChem XX, XXX (2015)

Th-A17

Engineering edge structure and electronic properties of graphene nanoislands by Au intercalation

Michele Gastaldo¹, Gustavo Ceballos¹, Aitor Mugarza¹¹Catalan Institute of Nanoscience and Nanotechnology (ICN2), Bellaterra (Barcelona), Spain

Exciting electronic and magnetic phenomena have been predicted for graphene nanostructures with atomically precise edges, such as the induction of band-gaps [1], spin-polarized edge states [2] and finite magnetization [3]. The supporting substrate has a crucial role both in tuning and modifying the electronic and magnetic properties of graphene, and also in determining the atomic structure, when bottom-up growth methods are applied. We have previously shown that on a Ni(111) surface, the interaction with the substrate determines the edge termination and shape of graphene nanoislands: by selecting post-annealing temperature, triangular islands with zig-zag edges or hexagonal islands with alternated zig-zag and reconstructed pentagon-heptagon (zz(57)) edges are obtained [4]. The strong interaction with the Ni substrate induces gapped spin polarized bands in graphene, and leads to spin and edge-dependent electron scattering [5]. In this work, we use scanning tunneling microscopy to study the effect of Au intercalation on such islands. Following graphene growth, Au is deposited and the sample annealed to 400-500°C. Graphene nanoislands are found floating on or embedded in the Au overlayer, with some islands laying on different Au atomic layers. Hexagonal islands now present only zig-zag edges, implying that the interaction with Au is not strong enough to induce the zz(57) reconstruction. The capability of laterally displacing graphene nanoislands by using the STM tip [Fig.1a] evidences chemical decoupling from the substrate, while electronic decoupling is evidenced by the characteristic intervalley scattering patterns observed inside the islands [Fig.1b].

- [1] J. Cai et al., Nature, 466 470 (2010)
- [2] Y. Li et al., Phys. Rev. Lett., 110 216804 (2013)
- [3] J. Fernández-Rossier et al., Phys. Rev. Lett., 99 177204 (2007)
- [4] M. Olle et al., Nano Lett., 12 4431 (2012); A. Garcia-Lekue, J. Phys. Chem. C, 119 4072 (2015)
- [5] A. Garcia-Lekue et al., Phys. Rev. Lett., 112 66802 (2014)

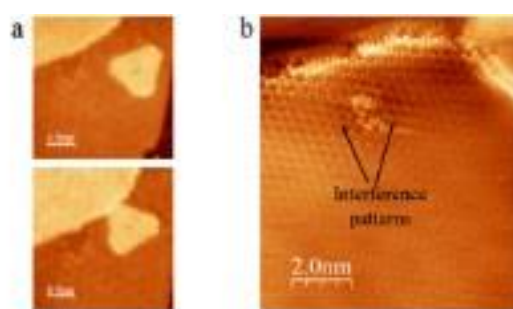


Figure 1: a) consecutive STM scans showing the displacement of a graphene island over the surface of Au due to interaction with the tip. $V_b=120$ mV, $I_t=0.3$ and 0.2 nA for upper and lower image, respectively. b) Intervalley scattering at the edge and around an impurity of a graphene flake leads to interference patterns superimposed on the atomically resolved lattice. $V_b=25$ mV, $I_t=0.58$ nA.

Th-A18

Characterization of the interface between graphene on SiC(0001) and adsorbed or intercalated cobalt islands by STM field emission resonance spectroscopy

Anastasia Sokolova¹, Alexander Schneider¹

¹FAU Erlangen-Nuremberg, Erlangen, Germany

The understanding of the interaction between metal and graphene is fundamental for graphene based devices. Here we use scanning tunneling spectroscopy (STS) of field emission resonances (FERs) to investigate the electrostatic properties and the chemical interaction between metal islands and graphene.

For cobalt ad-islands we see the expected shift of the FER states to higher energies due to the increased work function with respect to graphene/SiC(0001). However, a detailed analysis of the resonance energies with respect to the distance from the metal island reveals that states with lower quantum number n ($n = 1, 2$) reflect abruptly the change in chemical properties at the lateral metal-graphene interface. On the other hand, states with higher n show the influence of a positive space-charge region in the graphene that has a width of approximately 2 nm.

The work function of a single graphene layer on cobalt is lower than that of graphene on SiC(0001) [1]. Consequently one would expect down shift of the resonance energies, when going from pure graphene to cobalt covered by graphene. However, our data clearly shows a shift of the resonances to higher energies, which indicates bilayer graphene on top of the island. Additionally, the lateral dependence of FER energies shows a distinct feature for $n = 1, 2$, which we assign to different substrate coupling of the graphene layer when going from monolayer graphene on SiC(0001) to bilayer on Co.

[1] G. Giovannetti et al., PRL 101, 026803 (2008)

Th-A19

Switchable graphene-substrate coupling through formation/dissolution of an intercalated Ni-carbide layer

Laerte Patera^{1,2}, Cristina Africh¹, Cinzia Cepek¹, Giovanni Zamborlini^{2,3},
Alessandro Sala⁴, Tevfik O. Montes⁴, Andrea Locatelli⁴, Giovanni Comelli^{1,2,4}

¹IOM-CNR Laboratorio TASC, Trieste, Italy, ²Department of Physics, University of Trieste, Trieste, Italy, ³Peter Grünberg Institute (PGI-6) and JARA-FIT, Research Center Jülich, Jülich, Germany, ⁴Elettra-Sincrotrone Trieste S.C.p.A., Trieste, Italy

Chemical vapor deposition (CVD) on metal surfaces is widely recognized as the most versatile and promising technique for large scale production of high-quality graphene films [1]. Among possible substrates, Ni plays a major role, also because of the small metal-graphene lattice mismatch, which allows for epitaxial growth. Nevertheless, we have recently demonstrated that not only the epitaxial phase, but also rotated graphene flakes can be produced [2]. By varying the temperature, it is possible to control the solubility of carbon into Ni bulk, resulting in the reversible formation or dissolution of a nickel-carbide layer between the metal and the rotated graphene domains. This approach allows obtaining a switchable graphene-substrate coupling.

Here, we give a complete characterization of the different graphene structures on Ni(111). By Scanning Tunneling Microscopy (STM) and Low Energy Electron Microscopy (LEEM), we were able to characterize the morphology of graphene phases at the nano- and meso-scales. Photo Emission Electron Microscopy (PEEM) and spatially resolved Angle Resolved Photo Electron Spectroscopy (μ -ARPES) were used to probe the electronic structure of all phases, directly elucidating the changes in graphene's electronic structure.

Based on these results and on our previous investigations of the influence of growth parameters on the final morphology of the graphene layer, the tailored synthesis of graphene with controlled interaction with the Ni substrate is demonstrated.

1. Novoselov, K. S. et al. A roadmap for graphene. *Nature* 490, 192–200 (2012).
2. Patera, L. L. et al. In Situ Observations of the Atomistic Mechanisms of Ni Catalyzed Low Temperature Graphene Growth. *ACS Nano* 7, 7901–7912 (2013).

Th-A20

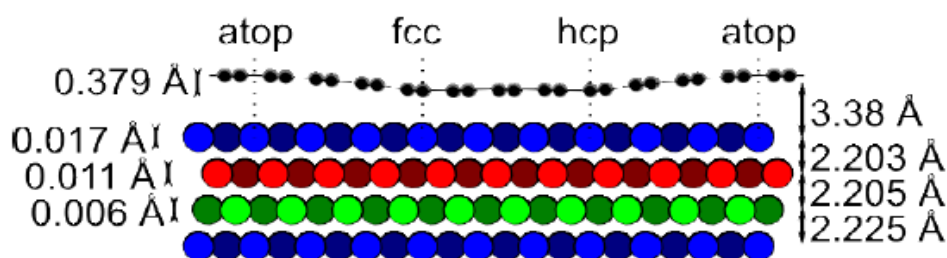
Graphene on Ir structure by synchrotron X-rays

Gilles Renaud¹, Fabien Jean², Nils Blanc², Johann Coraux²¹Univ. Grenoble Alpes / CEA-Grenoble, Grenoble, France, ²Univ. Grenoble Alpes / Institut Néel CNRS, Grenoble, France

The exceptional properties of graphene can be tailored by small structural modification, such as those induced by the epitaxy on a substrate or by defects. A combined CVD/TPG growth of graphene on Ir(111) was claimed to yield graphene of the highest quality. We have demonstrated that the resulting graphene has tiny imperfections such as small biaxial strain, rotations, shears, and the coexistence of commensurate and incommensurate domains. These deviations from perfection could only be detected by X-ray diffraction. These structural variations are mostly induced by the increase of the lattice parameter mismatch when cooling down the sample from the graphene preparation temperature. Although graphene only weakly interacts with Ir, its thermal expansion was found positive, contrary to free-standing graphene, and was found to follow that of Ir over large temperature ranges. The detailed atomic structure of graphene was quantitatively determined by Surface X-Ray Diffraction. The graphene undulation is found to be of small amplitude (0.38 Å), and to be in phase with the Ir (0.017 Å) one. The structure agrees well with recent ab initio calculations. The average graphene-iridium distance is 1.5 times the distance between two Ir(111) planes. The structure was also studied during growth and during the creation of defects. Large strains, above 2%, are present in graphene during its growth on Ir(111) and when it is subjected to oxygen etching and ion bombardment. Our results unravel the microscopic relationship between point defects and strain in epitaxial graphene and suggest new avenues for graphene nanostructuring and engineering its properties through introduction of defects and intercalation of atoms and molecules between graphene and its substrate. The organized growth of metallic nanoparticle on the graphene's moiré has also been investigated by GISAXS and X-ray diffraction.

Phys. Rev. B 86 (2012) 235439

Phys. Rev. Lett. 111 (2013) 085501

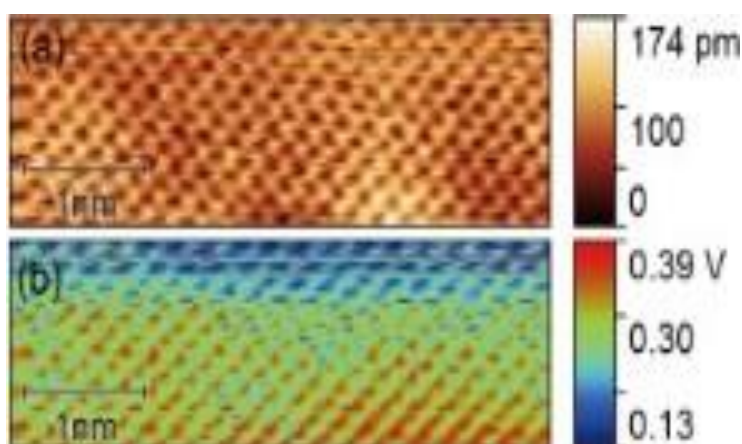


Th-A21

Graphene on C-terminated face of 4H-SiC studied by noncontact scanning nonlinear dielectric potentiometry

Kohei Yamasue¹, Hirokazu Fukidome¹, Kazutoshi Funakubo¹, Maki Suemitsu¹, Yasuo Cho¹¹Tohoku University, Sendai, Japan

Graphene synthesis by the thermal decomposition of hexagonal SiC substrates has been studied towards the future mass-production of graphene-based electronic devices. Graphene sheets are grown on both Si-face and C-face. On Si-face, large-scale and uniform monolayer graphene sheets are obtained. However, the carrier mobility of graphene on Si-face has remained much smaller than an expected value. In contrast, on C-face, much higher mobility has been measured than on Si-face, while graphene sheets are disordered and multi-layer. Here, we investigate graphene on C-face of 4H-SiC by using noncontact scanning nonlinear dielectric potentiometry (NC-SNDP) by simultaneously imaging topography and potentials in an atomic-scale. The sample was prepared by annealing an n-type 4H-SiC substrate in Ar atmosphere. Figure 1 shows simultaneous NC-SNDP images of (a) topography and (b) potential. In contrast to Si-face, we could not see any super-periodicity on C-face. We find that the height of top-layer graphene was spatially fluctuated. This implies that the structures below the top-layer are spatially inhomogeneous. However, this cannot be attributed to different number of graphene layers underlying the top-layer, because the height variation is about 20 pm, which is much smaller than the interlayer distance of graphene. The measured potential also spatially varied, ranging from +0.1 V to +0.4 V, and the spatial average was +0.27 V. NC-SNDP is sensitive to potentials induced by electric dipole moments. The sp^2 configuration of the C atoms in graphene layers has no dipole moment. Thus, our results suggest that the dipole moments exist on the interface. The detected dipoles were oriented from surface to bulk. The existence of these positive dipoles is consistent with workfunction reduction by graphene formation on C-face, which has been shown in a previous first-principles study. Thus, our results suggest that interfacial electronic structures are spatially inhomogeneous in graphene on C-face.



Th-A22

Atomic and electronic structure of epitaxial graphene on SiC: from the flat surface to sidewall nanoribbons

Antonio Tejeda^{1,2}, Amina Taleb-Ibrahimi², Walt de Heer³, Claire Berger³,
Edward Conrad³

¹Laboratoire de Physique des Solides, CNRS, Univ. Paris Sud, Univ. Paris-Saclay, Orsay, France, ²Synchrotron SOLEIL, Gif sur Yvette, France, ³GeorgiaTech, Atlanta, United States

On a first step, we demonstrate that graphene grown on the (000-1) (C-face) of SiC exhibits the presence of the ideal linear dispersion characteristic of graphene [1]. This system presents several graphene sheets rotated by different angles, giving rise to a non Bernal stacking. Such rotations break the stacking symmetry of graphite and lead to each single sheet behaving like an isolated graphene plane.

On a second step, we have focused on the electronic properties of ribbons of graphene grown on facets of the SiC(0001) surface. It is possible to take advantage of graphene grown on patterned SiC steps [2], where the edge is settled by growth instead by cutting an already existing graphene sheet. We have observed by photoemission a region with a gap opening greater than 0.5 eV in an otherwise continuous metallic graphene sheet [3]. Our morphological characterization by STM and cross sectional TEM allows to understand the origin of the band gap in mini-ribbons bordering a central extended ribbon [4]. On the nanoribbon, where our STM measurements show a well-defined edge [5], transport measurements have also shown that charge carriers travel at room temperature on a length scale greater than ten micrometers [5], which is similar to the performance of metallic carbon nanotubes, and opens a promising future for graphene electronics.

[1] M. Sprinkle et al., Phys. Rev. Lett. 103, 226803 (2009).

[2] M. Sprinkle et al., Nature Nanotechnology 5, 727 (2010).

[3] J. Hicks et al., Nature Physics 9, 49 (2012).

[4] I. Palacio et al., NanoLett. 15, 182 (2015).

[5] J. Baringhaus et al., Nature 506, 349 (2014).

Th-A23+24

CVD graphene growth and characterisation by in-situ and in-operando STM studies

Cristina Africh¹

¹CNR-IOM, Trieste, Italy

Most of the unique properties exhibited by graphene when deposited on a metal surface are strongly influenced by the morphology of the layer and its interaction with the substrate. For this reason, a detailed understanding of growth mechanisms at the atomic level is a key step towards reliable control of such properties. In the literature, this issue is mainly addressed by post-growth experiments, which rarely yield undisputable answers. We investigated graphene growth by Chemical Vapor Deposition on nickel under in-operando conditions by acquiring scanning tunneling microscopy movies at rates up to video-frequency. Combining STM results with X-ray photoelectron spectroscopy and density functional theory calculations, we identified the underlying atomic scale mechanisms and the relevant growth parameters that drive the process towards the synthesis of graphene layers of well-defined morphology [1]. Graphene structure was thoroughly characterized both during and after growth [2,3]. The role of defects, vacancies and heteroatoms, in determining the graphene properties, including chemical activity, is elucidated.

[1] L.L. Patera et al, ACS Nano 9 (2013) 7901-7912

[2] F. Bianchini et al, J. Phys. Chem. Lett. 5 (2014) 467-473

[3] L.L. Patera et al, Nano Letters 15 (2015) 56-62

Th-B15

Ultra-thin film x-ray diffraction using high energy photons

Florian Bertram¹, Olof Gutowski¹, Uta Ruett¹¹DESY, Hamburg, Germany

With recent developments on modern synchrotron radiation sources and new 2D detectors high energy x-rays (> 60 keV) become more and more interesting for studying the structure of surfaces, interfaces and ultra-thin films.

Using high energy photons the Bragg angles become smaller and therefore a larger part of the q-space can be covered by a single detector image. Using a grazing incident geometry its is possible to obtain reciprocal space maps containing several crystal truncation rods with a simple azimuthal scan at a fixed detector position within very short time scales[1]. This fact makes it an ideal method to study processes in-situ.

Here we demonstrate how this method can be applied to diffraction measurements on epitaxial ultra-thin films. As a model case we use epitaxial iron oxide thin films on a MgO(001) substrate with thicknesses ranging from 5 up to 30 nm.

We will compare the data obtained using high photon energies to the energies conventionally used for surface and thin film diffraction experiments (10 - 20 keV). In addition to that we will show how this method can be used to study the structure of thin films in-situ during the growth process.

[1] Gustafson et al., Science 343 (6172): 758-761

Th-B16

Plasticity induced wear mechanisms in fretting wear of Ti-6Al-4V

Abdul Latif Mohd Tobi¹, Wei Sun¹, Philip Shipway¹

¹University of Nottingham, Nottingham, United Kingdom

In seeking to develop frameworks within which behaviour in fretting wear can be categorised, there is a need to understand plasticity driven wear mechanisms. The effect of changes in the contact surface geometry due to the wear process will change the stress distribution across the contact surface. Fretting wear damage is strongly dependent upon the elastic-plastic shakedown response of materials on the surfaces; specifically, the high wear rate regime in fretting is due to the occurrence of global surface shear plasticity, whilst the low wear regime is governed by local asperity plasticity. This paper presents a finite element based wear modelling methodology, along with computational device which facilitates the capture of plasticity accumulation on a particular profile of wear scar at a specific number of cycles. As part of this method, the effect of wear itself is suppressed once a given number of wearing cycles have been achieved. Alongside this, the accumulated plastic hardening from the wear model is preserved, and between these two modelling devices, the prediction of plasticity accumulation at various stages of the wear process can be made. This method highlights the pressure-geometric profile based induced plastic deformation without the effect of active surface modification from the wear model. The predicted plastic accumulation from the analysis is quantified and compared with the surface morphology, micrograph, and nano-indentation analyses from the experimental results. It is found that the combination of surface geometrical modification along with the contact pressure redistribution contributes to different mechanisms of wear on the same fretting surface. The observed changes in fretting wear behaviour is a result of a combined effect of plasticity accumulation and subsequently the formation of compacted oxide debris on the surface in the early stage of fretting wear, whilst the asperity Archard's based wear, dominates the later stages of fretting wear.

Th-B17

Magnetic resonance force microscopy designed for application at low and ultra-low temperature

Soonho Won¹, Jinhee Heo¹, Youngmok Rhyim¹

¹Korea Institute of Materials Science, Changwondaero, Seongsangu, Changwon, Gyeongnam, South Korea

Mechanically detected NMR as an imaging technique was firstly suggested in 1991 in a theoretical approach by Sidles. Since then, several groups have successfully setup experiments in mechanically detected magnetic resonance and the technique was referred to “magnetic resonance force microscopy” (MRFM). Until now, substantial progress in MRFM has been achieved a 100 million-fold improvement in volume resolution over conventional MRI. But, there are no commercially available MRFM systems and up to date few groups have reported details of the MRFM system’s design.

We report a compact MRFM insert designed particularly for application at low and ultra-low temperatures. Overall features are ultra-compact, highly rigid body and sensitive interferometric deflection detection. Also, the insert is compatible with any commercially available cryostat. Except for commercial cryostat, all parts were developed by us. To verify the performance of the insert, we have obtained MRFM spectra in a diphenyl-picryl-hydrazyl sample at T=4.2K and in vacuum.

Th-B18

Atomic Force Microscopy tip monitoring methods based on higher harmonic vibrations of the cantilever

Enrique Rull Trinidad¹, Urs Staufer¹, Francesc Perez-Murano², Jordi Fraxedas³

¹Technical University of Delft (TUD), Delft, Netherlands, ²Instituto de Microelectrónica de Barcelona (IMB-CNM, CSIC), Bellaterra, Spain, ³Institut Catala de Nanociència i Nanotecnologia (ICN2) and Consejo Superior de Investigaciones Científicas (CSIC), Bellaterra, Spain

The measurement of surface texture by Atomic Force Microscopy (AFM) is influenced by the tip shape with the tip radius being the most important parameter. Hence, it is important to know the tip radius for a correct interpretation of experimental results versus tip wear. Even more important is to know the changes of the tip radius “in operando” during imaging. We present a study that investigates continuous monitoring methods that can be implemented in automated amplitude modulation (AM)-AFM operation modes and which allow tracking the evolution of the tip. It is well known that the dynamics of tip-surface interaction depends on contact stiffness and this interaction depends on the tip radius. Hence, monitoring the dynamics of the cantilever should allow extracting tip radius information as can be observed from numerical models.

Here, we use a multi-frequency analysis to present a method based on the use of higher harmonics, which are generated in the repulsive regime as a result of the nonlinear interactions between the tip and the studied surface. An advanced Lock-in technique allows obtaining very small signals above the first flexural eigenmode of the cantilever and to simultaneously measure several harmonics (8-10 first harmonic frequencies). We observe that the amplitudes of the higher harmonics increase for increasing values of the tip radius. We have applied this method to commercial rectangular microfabricated silicon cantilevers in the 3-50 N/m range (50-400 kHz) with sharp tips (tip radius below 20 nm). This method is based on computational analysis and includes real-time data processing to perform an average of higher frequencies amplitudes. It detects when the harmonic spectra has changed and finds the relationship between changes in the non-linear tip sample interaction and changes in the tip radius.

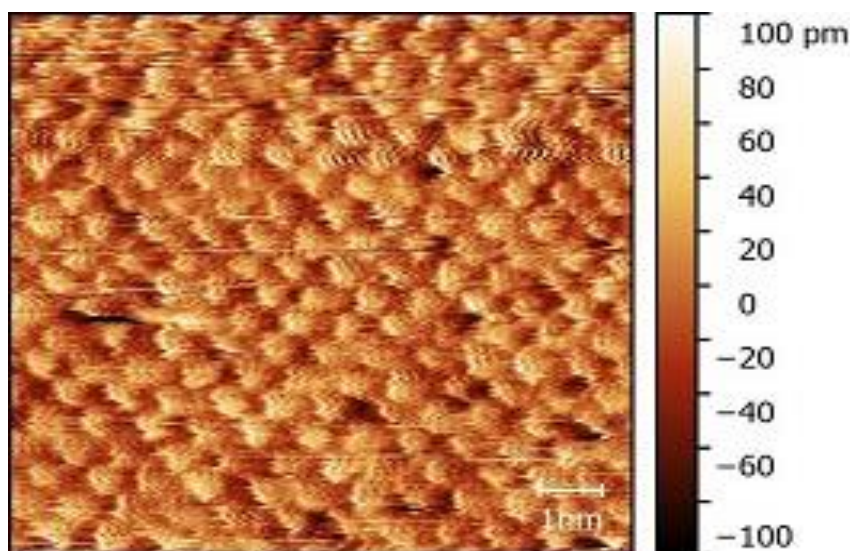
We acknowledge funding from the EU commission through the aim4np project (FP7 NMP Programme).

Th-B19

Autopilot for FM-AFM

Kfir Kuchuk¹, Itai Schlesinger¹, Uri Sivan¹¹Department of Physics and The Russell Berrie Nanotechnology Institute, Technion, Israel Institute of Technology, Haifa, Israel

One of the most challenging aspects of operating an atomic force microscope (AFM) is finding good feedback parameters. This statement applies particularly to frequency-modulation AFM (FM-AFM), which utilizes three feedback loops to control the cantilever excitation amplitude, cantilever excitation frequency, and piezo extension. These loops are regulated by a set of feedback parameters that the user must tune to optimize stability, sensitivity, and noise in the imaging process. Optimization of these parameters is difficult, primarily due to non-linear coupling between the frequency and piezo feedback loops, which requires simultaneous optimization of the four PI parameters regulating these loops. Moreover, the PI parameters must generally be optimized without knowing the tip-sample interaction. Users presently optimize these parameters by a tedious manual process of trial and error. Here, we report on the development and implementation of an algorithm that computes these parameters automatically. We analyze a linear model of the FM-AFM feedback system and derive the total feedback loop transfer function. The algorithm reads experiment-specific parameters, analyzes the poles and zeros of the transfer function, and finds four PI parameters for the frequency and piezo control loops that optimize the bandwidth and step response of the total feedback loop. The calculated parameters are consistently excellent and rarely require further tweaking by the user. The quality of these parameters is demonstrated by figure 1, which shows the raw data image of mica in aqueous NaCl solution imaged by FM-AFM using the unmodified feedback parameters calculated by the presented algorithm. The new algorithm saves the precious time of experienced users, facilitates utilization of FM-AFM by casual users, and removes the main hurdle on the way to a fully automatic FM-AFM microscope.



Th-B20

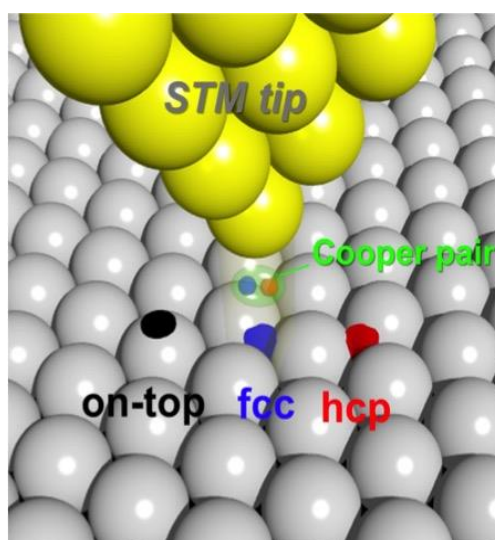
Site-dependent Josephson current from tunneling to atomic contact: Scanning tunneling microscopy and spectroscopy study

Howon Kim¹, Yukio Hasegawa¹¹University of Tokyo, Kashiwa, Japan

Electron transport in a quantum coherent conductor can be characterized by the set of transmission probability, $\{\tau_i\}$, which is relevant to conductance channels through the junctions. The accurate determination of the $\{\tau_i\}$ for the junctions is crucial to understand the conduction mechanism of electron in both normal-state and superconducting state. Although there has been many efforts with various methods to unveil the relation between channel distributions and their contributions to the electron transport through the superconductor-superconductor (S-S) junction at atomic-size junctions, direct observation of that relation is still challenge because of the lack of the geometric information at the atomically-formed junctions. Here, we investigated atomic-scale S-S junctions by using scanning tunneling microscopy and spectroscopy with highly stable and precise control of a tip. In our local conductance measurements between superconducting Pb islands on Ge(111) and Pb layers on the end of PtIr tip apex, we observed evolution of not only the normal-state conductance [1] but also a zero-bias peak from tunnel to atomic contact, which corresponds to the Josephson current, with a decrease in the tip-substrate distance. Additionally, we found that the amounts of Josephson supercurrent and their evolutions from tunneling to contact were strongly depending on the contact between tip-apex atom and atomic sites on the surface crystalline lattice of the substrate. With a help of multiple Andreev reflection analysis through the S-S junctions, the observed spatial variation of Josephson current can be explained in terms of atomic-sites dependent distributions of conductance channels. Our new observations based on the precisely-controlled STM measurements together with theoretical supports at the S-S junctions can be expected to shed a new light to understand conduction mechanism in the small superconducting device and their applications.[2]

[1] H. Kim and Y. Hasegawa, Phys Rev Lett, accepted (2015)

[2] H. Kim and Y. Hasegawa, submitted (2015)



Th-B21

Developments of a total-reflection high-energy positron diffraction station at the KEK Slow Positron Facility

Ken Wada¹, Masaki Maekawa², Yuki Fukaya³, Atsuo Kawasuso², Izumi Mochizuki¹, Tetsuo Shidara⁴, Toshio Hyodo¹

¹Institute of Materials Structure Science, High Energy Accelerator Research Organization (KEK), Tsukuba, Japan, ²Quantum Beam Science Center, Japan Atomic Energy Agency, Takasaki, Japan, ³Advanced Science Research Center, Japan Atomic Energy Agency, Tokai, Japan, ⁴Accelerator Laboratory, High Energy Accelerator Research Organization (KEK), Tsukuba, Japan

The positron is the antiparticle of the electron. It has the same mass and spin as an electron, but has a positive charge equal in magnitude to that of the electron's negative charge. An experiment station for total-reflection high-energy positron diffraction (TRHEPD), which is the positron counterpart of reflection high-energy electron diffraction (RHEED), was installed in 2010 [1,2] at the Slow Positron Facility, High Energy Accelerator Research Organization (KEK). Taking advantage of the positron total-reflection from the surface with the Bragg's condition, the TRHEPD experiments are delivering new information on the topmost and immediate sub-surface atomic configurations [3].

A pulsed 50-Hz electron beam (55 MeV, 0.6 kW) from a dedicated linear accelerator (linac) is impinged on a Ta converter and causes fast positron-electron pair creation through bremsstrahlung. The fast positrons are thermalized in W foils and then emitted spontaneously from the foils with an energy of 3 eV determined by the negative work function for the positron. The moderated positrons are accelerated by an electric field to an energy of 15 keV along the grounded beam line. The positrons are guided magnetically to the TRHEPD experiment station, and released into a nonmagnetic region. Then a brightness-enhancement unit with a second moderator is effectively used to achieve a small-diameter and highly-parallel 10-keV beam with a sufficient flux. Several results [3-5] have been obtained efficiently by users of this facility.

(Everybody is invited to use KEK Slow Positron Facility through approval of his/her research proposal.)

- [1] K. Wada et al., Eur. Phys. J. D 66, (2012) 37.
- [2] M. Maekawa et al., Eur. Phys. J. D, 68 (2014) 165.
- [3] Y. Fukaya et al., App. Phys. Express 7. (2014) 056601.
- [4] I. Mochizuki et al., Phys. Rev. B 85 (2012) 245438.
- [5] Y. Fukaya et al., Phys Rev. B 88 (2013) 205413.

Th-B22

Total Reflection High-Energy Positron Diffraction (TRHEPD): A Powerful Tool for Surface Studies

Ayahiko Ichimiya¹, Yuki Fukaya², Izumi Mochizuki¹, Ken Wada¹, Masaki Maekawa³, Atsuo Kawasuso³, Tetsuo Shidara⁴, Hiroko Ariga⁵, Kiyotaka Asakura⁵, Toshio Hyodo¹

¹ Institute of Materials Structure Science, High Energy Accelerator Research Organization (KEK), Tsukuba, Japan, ²Advanced Science Research Center, Japan Atomic Energy Agency, Tokai, Japan, ³Quantum Beam Science Center, Japan Atomic Energy Agency, Takasaki, Japan, ⁴Accelerator Laboratory, High Energy Accelerator Research Organization (KEK), Tsukuba, Japan, ⁵Catalysis Research Center, Hokkaido University, Sapporo, Japan

The total reflection high-energy positron diffraction (TRHEPD) is an extremely powerful tool for crystal surface studies. Using the TRHEPD, we have determined several crystal surface structures and surface properties such as surface phase transitions and surface Debye temperatures. Since a positron is a positive charged particle, crystal potential is repulsive for fast positrons. This means that total reflection takes place for positron beams at a certain incident angle for a crystal surface [1-3]. At the total reflection condition, penetration depth of positron beams is less than 0.1 nm. Therefore we are able to detect only the topmost surface structures and properties without disturbance from the bulk by this method. Recently evidence that only the topmost layer structure is selectively detected by the TRHEPD is reported for the Si(111)(7×7)(the dimer-adatom-stacking-fault: DAS) surface by Fukaya et al. [4] using a brightness-enhanced intense positron beam constructed at the Slow Positron Facility, KEK [5]. Moreover, recent works on the Ge(001)(4×2)-Pt surface [6] and the silicene on the Ag(111) surface [7] have demonstrated that the method is also sensitive to the immediate subsurface structures. We present summary of the TRHEPD results including coming ones on a TiO₂ surface, graphene, and Ge/Au nanowire. We also discuss potential of TRHEPD for crystal surface studies in comparison with the conventional diffraction methods.

- [1] A. Ichimiya, Solid State Phenom. 28/29, 143 (1992).
- [2] A. Kawasuso and S. Okada, Phys. Lett. 81, 2695 (1998).
- [3] A. Kawasuso et al. e-J. Surf. Sci. Nanotechnol. 1, 152 (2003).
- [4] Y. Fukaya et al., Appl. Phys. Express 7, 056601 (2014).
- [5] K. Wada et al., J. Phys. Conf. Series 443, 012082 (2013).
- [6] I. Mochizuki et al., Phys. Rev. B85, 245438 (2012).
- [7] Y. Fukaya et al., Phys. Rev. B88, 205413 (2013).

Th-B23

An improved positron diffraction: total-reflection high-energy positron diffraction (TRHEPD) and its applications

Toshio Hyodo¹, Yuki Fukaya², Izumi Mochizuki¹, Ken Wada¹, Masaki Maekawa³, Atsuo Kawasuso³, Tetsuo Shidara¹, Hiroko Ariga⁴, Kiyotaka Asakura⁴, Ayahiko Ichimiya¹

¹High Energy Accelerator Research Organization (KEK), Tsukuba, Japan,

²Japan Atomic Energy Agency / Tokai, Tokai, Japan, ³Japan Atomic Energy Agency / Takasaki, Takasaki, Japan, ⁴Hokkaido University, Sapporo, Japan

Total-reflection high-energy positron diffraction (TRHEPD) is the positron counterpart of reflection high-energy electron diffraction (RHEED). This method, formerly called as reflection high-energy positron diffraction (RHEPD), was proposed by Ichimiya in 1992, and first demonstrated by Kawasuso and Okada in 1998. A TRHEPD station with a brightness-enhanced intense positron beam is now in operation at the Slow Positron Facility, KEK [1].

The unique features of TRHEPD are:

- (1) Since electrostatic potential inside every solid is positive, a positron beam tends to be pushed out of a solid in contrast to an electron beam which tends to be pulled in.
- (2) When the incidence glancing angle is smaller than a critical angle, the positron is totally reflected.
- (3) The range of the glancing angle for the total reflection overlaps well with that for the diffraction.
- (4) By increasing the glancing angle across the critical angle, information on the immediate subsurface is also available and the depth of interest is adjustable.
- (5) The diffraction patterns are free from the background from the deeper layers because the inelastic scatterings prevent a positron from contributing to the diffraction pattern.

The extremely high sensitivity of TRHEPD to the topmost- and immediate subsurface of solids is demonstrated by using measurements and calculations for the reconstructed Si(111)-(7×7) surface [2]. Also presented are the structure analyses of the Ge(001)-(4×2)-Pt [3] and of silicene on the Ag(111) surface [4], as well as on-going researches on rutile-TiO₂(110)-(1×2) surface, nanowire structure of Ge(001)-(8×2)-Au, and grapheme on metals.

[1] M. Maekawa, K. Wada, et al., Eur. Phys. J. D 68, 165 (2014).

[2] Y. Fukaya, M. Maekawa, et al., Appl. Phys. Express 7, 056601 (2014).

[3] I. Mochizuki, Y. Fukaya, et al., Phys. Rev. B 85, 245438 (2012).

[4] Y. Fukaya, I. Mochizuki, et al., Phys. Rev. B 88, 205413 (2013).

Th-B24

Combined molecular beam and matrix isolation methodology for the separation, trapping and storage of nuclear spin isomers of water

Jonathan Vermette¹, Pierre-Alexandre Turgeon¹, Patrick Ayotte¹, Gil Alexandrowicz²

¹Chimie, Université De Sherbrooke, Sherbrooke, Canada, ²Schulich Faculty of Chemistry, Technion-Israel Institute of Technology, Haifa, Israel

Efficient separation methodologies, yielding water samples strongly enriched in the ortho-H₂O nuclear spin isomers (NSI), could find applications ranging from laboratory astrophysics to nuclear magnetic spectroscopy/imaging. However, they must circumvent the interconversion between the ortho and para NSI (which is forbidden in the isolated H₂O molecule) in order to maintain highly enriched out-of-equilibrium NSI populations. Using molecular beam techniques, water vapor was strongly enriched in ortho-H₂O by focusing in a hexapolar magnetic lens. The NSI populations were probed directly in the supersonic jet using REMPI-TOF allowing the enrichment efficiency as well as the occurrence of NSI conversion in the supersonic expansion to be quantified. The trapping and storage of these water samples strongly enriched in ortho-H₂O by magnetic focussing was achieved and characterized using matrix isolation spectroscopy. We will demonstrate that ortho:para ratio as high as 15:1 can be achieved using magnetic focusing and that significant enrichments can be maintained for several hours in Ar and Kr matrices at cryogenic temperatures. This methodology should allow controlled laboratory investigations of NSI conversion mechanism and rates in/on amorphous ice films providing invaluable molecular-level insight into the spin isomer interconversion in astrophysical ices.

Th-C15

Epitaxy and self-assembly of perylene on Ag(110) surface

Kirill Bobrov¹, Natalya Kalashnyk¹, Laurent Guillemot¹¹CNRS, Orsay, France

We present a STM study of perylene adsorption on the Ag(110) surface at monolayer coverage regime as a function of molecule density. We found that the monolayer structure is determined by a specific balance between the intermolecular attraction within the monolayer and the intrinsic ability of individual perylene molecules to recognize favourable adsorption sites on metal substrates. The recognition effect was found to be strong enough to provide a surface registry for the monolayer by anchoring some of the perylene molecules to specific adsorption sites of the (110) lattice. Still, the local intermolecular interaction was strong enough to accommodate the anchoring phenomenon and to arrange all the molecules into the ordered 2D network.

We have found that the site recognition effect was always counterbalanced by the intermolecular interaction. The monolayer structure and symmetry varied as a function of perylene coverage accounting the specific balance. On the other hand, the specific balance preserved the epitaxial character of the self-assembled monolayer throughout the whole coverage range (0.10-0.12 ML).

We have found that the interplay of the molecule-molecule and molecule-substrate interactions of moderate strength bestows great flexibility to the monolayer and plays a key role in formation of the well-tailored interface. We anticipate that the ability of perylene to form epitaxial self-assembled structures can be very useful in engineering well-tailored organic interfaces.

Th-C16

Self-Assembly of Aromatic Carboxylic Acids on Ag and Cu at the Liquid-Solid Interface

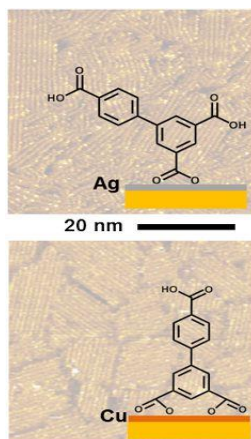
Manfred Buck¹, Hannah Aitchison¹, Hao Lu^{2,3}, Michael Zharnikov², Thomas Potter¹, Herbert Früchtl¹

¹University of St Andrews, St Andrews, United Kingdom, ²University of Heidelberg, Heidelberg, Germany, ³Max Planck Institute for Polymer Research, Mainz, Germany

On weakly interacting surfaces such as Au or HOPG aromatic carboxylic acids adsorb in a flat lying geometry which enables the formation of two-dimensional hydrogen bonded networks. In contrast, an upright orientation can be obtained on more strongly interacting surfaces such as Ag and Cu, thus resulting in monolayers of densely packed molecules. The driving force for the formation of these self-assembled monolayers (SAMs) is the maximisation of coverage arising from the strength of the metal-organic coordination bond between the carboxylic acid moiety and the substrate.

While networks have been extensively studied both in ultrahigh vacuum and at the solid/liquid interface, studies of SAMs based on aromatic carboxylic acids are very scarce. However, since this class of molecules also represent key constituents of surface based metal-organic frameworks (SURMOFs) understanding their assembly behaviour at the solid/liquid interface is of interest. Our studies focus on carboxylic acid based SAMs on Au(111)/mica surfaces modified by a Cu monolayer or a Ag bilayer formed electrochemically by underpotential deposition. The SAMs prepared from solution are characterised ex situ by scanning tunneling microscopy, X-ray photoelectron spectroscopy and near-edge X-ray absorption fine structure spectroscopy.

The difference in the strength of the carboxylate-substrate bond between Cu and Ag affects the balance between molecule-substrate and intermolecular interactions and as a consequence yields very different SAM structures for both surfaces. One example discussed is biphenyl-3,4',5-tricarboxylic acid which, on Cu, adsorbs in a bipodal bidentate geometry whereas a monopodal bidentate geometry is found on Ag as illustrated in the Figure. Compared to its smaller homologue benzene-1,3,5-tricarboxylic acid unexpectedly pronounced differences in both the preparation conditions on Cu and the film structure on Ag are observed.



Th-C17

Novel push-pull thiophene-based chromophores: synthesis, self-assembled monolayers and characterization

Lionel Patrone¹, Volodymyr Malytskyi^{1,3}, Jean-Manuel Raimundo³, Jean-Jacques Simon²

¹IM2NP, CNRS UMR 7334 Aix-Marseille Université, ISEN-Toulon, Maison des Technologies, Toulon, France, ²IM2NP UMR CNRS 7334 Aix-Marseille Université, Campus de St Jérôme, Marseille, France, ³CINaM UMR CNRS 7325, Aix-Marseille Université, Marseille, France

Organic donor-acceptor (D/A) “push-pull” chromophores are of considerable interest because of their potential use in nonlinear optics, LEDs, field-effect transistors with impressive dielectric performances as self-assembled nanodielectrics [1], and photovoltaics (PV) [2]. Most often, the 1-dimension D/A pair is connected via a π -conjugated spacer like thiophene that has led to a wide range of applications in materials science [3]. Meanwhile, self-assembling properties of push-pull onto surface for such applications are not well studied. Correct arrangement of these molecular structures on a surface should improve their properties for electro-optical devices. In this context we have developed a multi-step synthesis of new push-pull molecules bearing a thiol reactive group enabling to form self-assembled monolayers (SAMs) on gold or ITO surfaces. Combining various donor, acceptor, and spacer moieties we could tune the push-pull optical and electronic properties, e.g. the LUMO position by the choice of the acceptor, as shown by cyclic voltammetry and UV-visible absorption spectroscopy. Push-pull products exhibit high light absorption (λ_{max} ~550nm & ~610nm) interesting for PV applications. SAMs with gold nanoparticles are prepared on gold and ITO surfaces and growth kinetics of successive layers is followed using cyclic voltammetry and UV-visible absorption. Dense SAM formation of such non-charged chromophores is for the first time clearly demonstrated by spectroscopy (XPS, UV-vis.), ellipsometry, scanning probe microscopy (STM, AFM), and electrochemical measurements. Besides, good film quality is highlighted, and local I-V characteristics measured by STM are consistent with the structure of the SAM-organized push-pull molecules standing upright at the surface [4]. This unique combination of properties makes this SAM a system of choice for the foreseen applications such as in the field of PV energy conversion.

[1].L.Wang et al., Nat.Mater. 5(2006)893

[2].V.Malytskyi et al., RSCAdv. 5(2015)354

[3].I.F.Perepichka, D.F.Perepichka, Handbook of Thiophene-Based Materials: Applications in Organic Electronics and Photonics 2009 ©J.Wiley&Sons, Ltd.

[4].V.Malytskyi et al., RSCAdv. 5(2015)26308.

Th-C18

Probing Photostationary States of Photochromic SAMs by Two-Photon Photoemission Spectroscopy

Cornelius Gahl¹, Wibke Bronsch¹, Daniel Przyrembel¹, Martin Weinelt¹¹Freie Universität Berlin, Berlin, Germany

Self-assembled monolayers (SAMs) of azobenzene-decorated alkanethiols represent a versatile class of systems for the functionalization of a metal surface with molecular switches. Varying the length of the alkyl linker allows to control the coupling strength of the azobenzene moiety to the metal substrate. In addition, the interaction between the azobenzene chromophores can be controlled via dilution, e.g. by intermixing bare alkanethiols without a chromophore. Thereby the optical properties as well as the efficiency of the trans-cis photoisomerization become tunable.[1]

In this contribution we investigate optical switching in SAMs of azobenzene-decorated undecane thiol diluted with dodecanethiol on Au(111) by means of two-photon photoemission (2PPE) spectroscopy. Along with changes in the electronic structure, we observe a pronounced isomerization-induced shift of the work function of up to 250 meV.

In order to reversibly tune the photostationary state between predominantly trans and predominantly cis we vary the intensity ratio of femtosecond UV pulses and a 450 nm continuous-wave laser which does not contribute to the 2PPE signal.

[1] T. Moldt, D. Brete, D. Przyrembel, S. Das, J. R. Goldman, P. K. Kundu, C. Gahl, R. Klajn, and M. Weinelt, Tailoring the Properties of Surface-Immobilized Azobenzenes by Monolayer Dilution and Surface Curvature, *Langmuir* 31 (2015), 1048-1057

Th-C19

2D Solution processed host-guest arrays for the elaboration of donor-acceptor systems

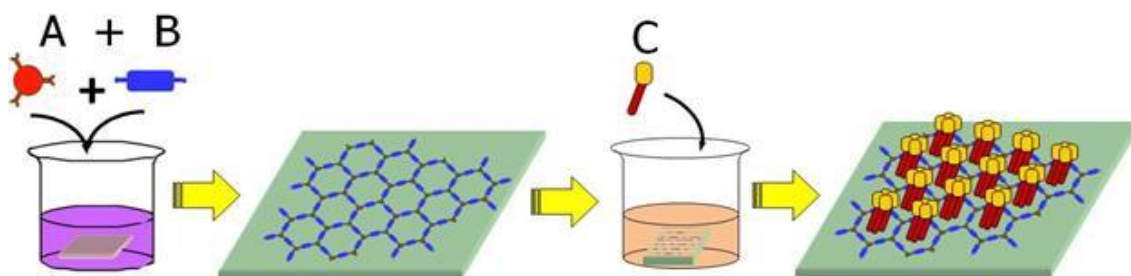
Andrés Lombana¹, Philippe Lang¹, Nicolas Battaglini¹, Samia Zrig¹

¹Université Paris Diderot, ITODYS, UMR 7086 CNRS, Paris, France

Self-assembly of organic molecules is a promising way to the elaboration of electronics and optoelectronic devices at the nanometer scale. In this regard, surface supramolecular chemistry provides a versatile approach to build systems at a molecular level by using the reversibility and relative strength of multiple non-covalent interactions. Particularly, we aim to build host-guest networks with electron donor and acceptor molecules located very close to each other and thus able to form and dissociate photo-excitons.

Molecular arrangements can be formed by molecules able to bind each other by complementary triple H-bonds as it is the case of the porous two-dimensional network formed by the self-assembly of PTCDI and Melamine molecules upon a Au(111) surface. Here we demonstrate the formation of such network by ambient Scanning Tunneling Microscopy (STM) following an original, non-vacuum solution based protocol that yields room temperature and room pressure stable samples. Furthermore, we show the functionalization of the pores of the network by a porphyrin molecule synthesized with a thioester moiety strongly binding to the Au(111) surface and a butyl spacer between the anchor group and the porphyrin core. Polarisation-Modulation Reflection and Absorption InfraRed Spectroscopy (PM-RAIRS) studies performed in this system show that the relative orientation of the porphyrin core is different from that of an intrinsic porphyrin monolayer without an organic template below. This hints to some kind of interactions between the porphyrin and the PTCDI molecules in this Host-Guest system.

In summary, we elaborated a promising host-guest donor-acceptor suited for further studies of optoelectronic properties such as exciton generation and charge separation.



Th-C20

2D folding and self-assembly of peptides on surfaces

Sabine Abb¹, Gordon Rinke¹, Ludger Harnau¹, Rico Gutzler¹, Duy Le², Talat Rahman², Stephan Rauschenbach¹, Klaus Kern^{1,3}

¹Max Planck Institute for Solid State Research, Stuttgart, Germany, ²University of Central Florida, Dept. Physics, Orlando, USA, ³Ecole Polytechnique Fédérale de Lausanne, Lausanne, Switzerland

In the past decade, the self-assembly of molecules on surfaces via hydrogen bonding and metal coordination has been studied extensively with small, specifically designed organic molecules, yielding a huge variety of self-assembled nanostructures. Peptides and proteins are the building blocks for functional structures in biological systems. Their specific assembly and folding behavior is programmed by the amino acid sequence and guided by the same non-covalent interactions such as hydrogen bonding, van-der-Waals interaction and ionic interaction. Electrospray ion beam deposition (ES-IBD) enables us to deposit these non-volatile molecules intact in ultra-high vacuum (UHV) where they can be investigated with high precision by STM.

Here, we report on the investigation of peptide self-assembly on metal surfaces and demonstrate 2D folding and sequence controlled self-assembly. In the gas phase, bradykinin, a nine amino acid peptide, has a variety of different conformations. Deposition on the surface, changing from Cu(111) to Cu(100) and Cu(110), induces 2D folding of bradykinin. This refines the different conformations to one surface-specific conformation, while it also enables the self-assembly into compact, self-passivated dimers. Peptides with sterically demanding residues cannot fold and self-passivate on the surface, as shown for angiotensins (At). Therefore, these peptides can be used as bio-organic building block self-assembly. While At-I does not assemble into long range ordered structures, it contains a promising binding motif that can be activated by removing two amino-acids, yielding At-II. Upon deposition of a submonolayer coverage of At-II we observe self-assembly into a long-range ordered chiral honeycomb network on Au(111) at 40K.

By a combination of high resolution STM and atomistic MD simulation, we are able to provide atomistic models and propose design rules for peptide nanostructures on surfaces. Our approach of ES-IBD and high resolution STM investigation combined with MD and DFT modelling opens the door for rationally designed peptide nanostructures at surfaces.

Th-C21

1,4-Phenylene Diisocyanide Adsorption on Metals Investigated by Broad Band Sum frequency Generation Spectroscopy and Scanning Tunneling Microscopy: From Single Crystals to Supported Nanoparticles

Ahmed Ghalgaoui¹, Martin Sterrer¹

¹Institute of Physics, University of Graz, Graz, Austria

We have investigated the adsorption of 1,4-Phenylene Diisocyanide ((PDI), NC-C₆H₄-NC) on single crystal metal surfaces (Au(111) and Pt(111)) and metal nanoparticles supported by an insulating layer (Au/FeO/Pt(111)). Both, gas-phase and liquid-phase deposition methods were applied. The role of PDI concentration and Au nanoparticle size on the surface structure/adsorption mode of PDI has been investigated by Scanning Tunneling Microscopy (STM) and Broad Band Sum Frequency Generation (BBSFG) Spectroscopy. The PDI molecule adsorbs either with both isocyanide groups interacting with the surface, leading to a flat adsorption geometry, or by only one isocyanide group, assuming a vertical adsorption structure. The frequency domain SFG measurements in the –NC stretching region show that PDI deposited from the gas-phase always binds with both –NC groups to Au(111), independent of surface coverage. In the case of liquid-phase deposition, PDI molecules adsorb in the flat adsorption geometry at low concentration, but change to the vertical geometry upon increasing the concentration. This concentration dependence is absent on Pt(111), where PDI exclusively adsorbs in the vertical geometry. Finally, the influence of Au particle size on the adsorption structure of PDI will be discussed.

Th-C22

The study of self-assembling of polar C₆₀F₁₈ molecules on Au(111)

Vladimir Stankevich¹, Kaushik Bairagi², Amandine Bellec², Ratibor Chumakov¹,
Konstantin Menshikov¹, Jerome Lagoute², Cyril Chacon², Yann Girard², Sylvie
Rousset², Vincent Repain², Alexey Lebedev¹, Leonid Sukhanov¹, Nikolai
Svechnikov¹

¹NRC "Kurchatov Institute", Moscow, Russian Federation, ²Paris Diderot
University, Paris, France

It was established experimentally using scanning tunneling microscopy (STM) that at room temperature C₆₀F₁₈ molecules with electric dipole moment (EDM) of ~ 10 D form on the steps of Au(111) a film structure with ordered islands having a lateral size of 10-100 nm. Namely, there were found the following features of a self-assembling process of polar C₆₀F₁₈ molecules on a metal surface:

- molecular orientation - EDMs are perpendicular to the surface and the fluorine atoms are pointed towards the surface,
- islands grow in both directions from the gold step edges,
- molecular surface structure is a close-packed hexagonal lattice with an intermolecular distance of 1.0 ± 0.1 nm (C₆₀F₁₈ molecular size = 1 nm),
- formation of island-type structures with amorphous island boundaries,
- non-linear dependence of molecular apparent height versus bias voltage,
- the apparent height of a separate molecule is lower than that of a molecule in the self-assembled system,
- transition from a two-dimensional film structure to a three-dimensional one with film growth.

Also, we compare our experimental data with theoretical models describing polarized point dipoles adsorption on a metal surface [1, 2]. The influence of molecular dipole-dipole, dipole-surface, dispersion interactions and polarization effects on self-assembly process is discussed. The fulfilled investigations help to advance our understanding of surface properties of high EDM molecules on metal surfaces, like C₆₀F₁₈ ones on Au(111) as an example, and to further make use of this class of materials in nanoelectronics, non-linear optics, etc.

[1] A. Kokalj, Phys. Rev. B 84 (2011) 045418.

[2] A. Natan, L. Kronik, H. Haick, R. T. Tung, Adv. Mater. 19 (2007) 4103.

Th-D15+16

Spin-orbit-induced spin textures of unoccupied states

Markus Donath¹¹Muenster University, Muenster, Germany

The term „spintronics“ is used in information technology, where the electron spin plays a functional role in electronic devices. Lifting the spin degeneracy of electronic states can be achieved by spin-orbit interaction. For this purpose, a broken inversion symmetry is needed, which appears, in particular, at the surface. Therefore, the current scientific interest is strongly focused on surface systems comprising heavy elements with strong spin-orbit interaction. In view of applications in electronic devices, making use of, e.g., spin-dependent transport or optical properties, the electronic states and their spin texture below and above the Fermi level are of interest.

In this contribution, I will present studies of the spin-dependent unoccupied electronic structure of spin-orbit-influenced systems, obtained by spin- and angle-resolved inverse photoemission [1]. For $\text{Ti/Si}(111)$, a number of surface states had been predicted, which, for some k values, come close to the Fermi level and, therefore, are interesting for transport properties. Fascinating k -dependent spin textures have been observed: Giant spin splittings, spin-polarized valleys, rotating spin textures, and a spin structure with a peculiar twist [2]. However, puzzling spin results for the surface alloy $\text{Bi/Ag}(111)$ [3] and even a tunable spin polarization from a highly symmetric, unpolarized state on $\text{W}(110)$ [4] put the experimentally derived spin information to the test. Spin results from states with mixed orbital symmetries have to be taken with a pinch of salt. Vice versa, these at first puzzling data reveal details about the orbital character of the involved states. The interpretation of these demanding experimental results was made possible by excellent theoretical support.

[1] Stolwijk et al., RSI 85, 013306 (2014)

[2] Stolwijk et al., PRL 111, 176402 (2013); PRB 90, 161109(R) (2014)

[3] Wissing et al., PRL 113, 116402 (2014)

[4] Wortelen et al., PRB 91, 115420 (2015)

Th-D17

Rashba splitting in image potential state of Au(001) investigated by high energy-resolution circular dichroism two-photon photoemission spectroscopy

Takeo Nakazawa^{1,2}, Ryuichi Arafune², Maki Kawai¹, Noriaki Takagi¹

¹The University of Tokyo, Kashiwa-Ho-Ha, Kashiwa-Shi, Chiba, Japan,

²National Institute for Materials Science, Namiki, Tsukuba, Ibaraki, Japan

Rashba spin-orbit interaction (SOI) is one of the hottest topics in surface science. Experimentally, Rashba SOI has been investigated using angle resolved photoemission spectroscopy, and thus the information on the electronic states are limited to the occupied states. In order to utilize the information for the realization of spintronics, the SOI in the unoccupied states and its dynamics must be measured in equivalent quality as for the occupied states. The image potential state (IPS) is a typical unoccupied surface state and a model system for understanding the hot-electron dynamics. Although Rashba splitting in the IPS has not been observed, theoretical calculations predicted that a measurable splitting should appear in the IPS of Au(001) [1].

We present here the first experimental evidence, by using two-photon photoemission spectroscopy (2PPES), that the Rashba effect certainly occurs in the $n = 1$ IPS on Au(001). Owing to the small splitting and the broad intrinsic linewidth of the state, the high energy-resolution (better than 10 meV) alone is not sufficient to measure the Rashba splitting, unfortunately. To measure the Rashba splitting in the IPS, we have introduced the circular dichroism (CD) technique into 2PPES for distinguishing the spin texture. The 2PPE intensity shows the momentum dependent CD; the strong CD appears at the large electron momentum. The spin direction orients perpendicular to both the surface normal and the momentum of the electron. These experimental results clearly show the characteristic feature of the Rashba SOI.

[1] J. R. McLaughlan et al., J. Phys.: Condens. Matter 16, 6841 (2004).

Th-D18+19

Interfacing 3D topological insulators with surface perturbations: from single adatoms to self-assembled molecular overlayers

Paolo Sessi¹

¹Universität Würzburg, Würzburg, Germany

Topological insulators are a new class of materials insulating in the bulk, but which host on their surface linearly dispersing Dirac states. Contrary to the trivial surface states usually found at surfaces in metals and semiconductors, topological states cannot be destroyed by the presence of defects and adsorbates as long as time-reversal symmetry is preserved. Furthermore, the strong spin-orbit coupling inherent to these systems perpendicularly locks the spin to the momentum, resulting in a chiral spin texture which give them unconventional properties such as forbidden backscattering and results in spin currents intrinsically tied to charge currents. This makes topological insulators attractive materials for spintronics and magneto-electric applications as well as a promising platform to explore unconventional states of matter.

Since these properties manifest at boundaries, scanning probe techniques are ideal tools to visualize them with both high spatial and energy resolution.

In my talk, I will first describe experiments that, through quantum interference, allow not only to visualize the presence of these unconventional boundary states, but also to demonstrate some of their unusual properties [1].

I will then discuss more recent efforts focused on their controlled manipulation, which is required to make them useful for new technologies and can be achieved by direct coupling to well defined external perturbations. In particular, I will show how local magnetic order can be established at very dilute concentrations using 3d adatoms [2] and how the creation of charge puddles associated with their random distribution can be avoided by embedding the magnetic moments into molecules to create self-assembled networks of different symmetries [3,4].

[1] P. Sessi et al. Phys. Rev. B 88,161407(R) (2013);

[2] P. Sessi et al. Nature Communications 5,5349 (2014);

[3] P. Sessi et al. Nano Letters 14, 5092 (2014);

[4] T. Bathon et al. Nano Letters 15,2442 (2015)

Th-D20

Adsorption of organic and metallorganic molecules on Bismuth Selenide: investigating the robustness of surface states

Marco Caputo¹, Simone Lisi², Mirco Panighel³, Lama Khalil¹, Giovanni Di Santo⁴, Evangelos Papalazarou¹, Andrzej Hruban⁵, Marcin Konczykowski⁶, Ivana Vobornik⁷, Jun Fuji⁷, Andrea Goldoni⁴, Marino Marsi¹

¹Laboratoire de Physique des Solides, Université Paris-Sud, Orsay, France,

²Dipartimento di Fisica, Università di Roma La Sapienza, Roma, Italy, ³ICN2-Institut Catala de Nanociencia i Nanotecnologia, Barcelona, Spain, ⁴Laboratory Micro & Nano Carbon Consorzio INSTM UTrieste-ST c/o ELETTRA -

Sincrotrone Trieste S.C.p.A., Trieste, Italy, ⁵Institute of Electronic Materials Technology, Warsaw, Poland, ⁶Laboratoire des Solides Irradiés, CNRS-UMR 7642 & CEA-DSM-IRAMIS, Ecole Polytechnique, Palaiseau, France, ⁷Istituto Officina dei Materiali (IOM)-CNR, Laboratorio TASC, Trieste, Italy

Topological insulators constitute a new class of materials that is attracting the attention of scientific community in the latest years. While semiconductor in the bulk, 3D topological insulators (Bi_2Se_3 and Bi_2Te_3 among the others) possess surface states crossing the Fermi level protected by time-reversal symmetry. Strong spin-orbit coupling characteristic of such heavy elements locks the spin to the momentum, forbidding backscattering for electrons occupying their surface states. All these features make Topological insulators an ideal candidate in the field of spintronics.

Organic molecules have demonstrated their potential in the same field. Molecular-based spin valves have already been realized, while metallophthalocyanines (MPc) paved the way for the so-called molecular magnetism. New physics can arise by the interaction of metalorganic molecules and topological insulators, with completely new perspectives in the field of spintronics.

Here we show results from an Angle Resolved Photoemission Spectroscopy (ARPES) study of the prototypical Cobalt Phthalocyanine (CoPc)/ Bi_2Se_3 and Metal-free Phthalocyanine (2HPc)/ Bi_2Se_3 interfaces. Special care will be devoted to the different modification of the surface states induced by the adsorption of the metalorganic and the metal-free molecules.

Th-D21

Surface atomic structure and reactivity of prototypical topological insulators and topological crystalline insulators

Lada Yashina¹, Mikhail Kuznetsov², Andrei Volykhov¹, Jaime Sanchez-Barriga³,
Oliver Rader³

¹Lomonosov Moscow State University, Moscow, Russian Federation, ²Institute of Solid State Chemistry of the Ural Branch of the Russian Academy of Sciences, Russia, Ekaterinburg, Russian Federation, ³Helmholtz-Zentrum Berlin für Materialien und Energie, Berlin, Germany

Understanding how topologically protected surface states behave at surfaces and interfaces requires knowledge of the atomic structure. The long-term stability of functional properties of topological insulator materials is crucial for the operation of future topological insulator based devices. These two issues are considered for second generation of topological insulators and topological crystal insulators.

Bi₂Se₃, Bi₂Te₃ and Sb₂Te₃ present an iconic example of topological insulators with layered structure of tetradimite. Employing photoelectron diffraction and holography, we find bulklike chalcogen termination with a very small surface relaxation (<1%) in agreement with density functional theory simulations.

Water and oxygen are to be the main sources of surface deterioration by chemical reactions. In the present work, we investigate the behavior of the topological surface states on Bi₂X₃ (X = Se, Te), Sb₂Te₃ and mixed crystals by valence-band and core level photoemission in a wide range of water and oxygen pressures. We find that no chemical reactions occur in pure oxygen and in pure water for Bi₂X₃. The presence of water, however, promotes the oxidation in air, and we suggest the underlying reactions supported by density functional calculations. The surface reactivity is found to be negligible, which allows expanding the acceptable ranges of conditions for preparation, handling and operation of future Bi₂X₃-based devices. Sb₂Te₃ and mixed crystals containing Sb react with water and show much higher reactivity towards oxygen and water. The underlying mechanisms are discussed.

SnTe, (Pb,Sn)Se and (Pb,Sn)Te are topological crystalline insulator with rocksalt structure. Two surface orientations are typically can be obtained for such materials as (001) and (111). In contrast to (111) for (001) surfaces no surface reconstruction, no trivial surface states and small SCLS of -0.3 eV were found. This class of materials is much more unstable chemically toward oxidation by atmospheric or residual oxygen, that may restrict essentially their applications. The comparative reactivity is discussed.

Th-D22

BiAg₂ Rashba surface alloy: Spin-flip electron scattering

S. Schirone¹, E.E. Krasovskii^{2,3,4}, G. Bihlmayer⁵, R. Piquerel¹, P. Gambardella^{1,6,7}, A. Mugarza¹

¹ICN2-Catalan Institute of Nanoscience and Nanotechnology, Bellaterra, Spain, ²Dpto. de Física de Materiales, Facultad de Ciencias Químicas, UPV/EHU, San Sebastián-Donostia, Spain, ³Donostia International Physics Center (DIPC), San Sebastián-Donostia, Spain, ⁴IKERBASQUE, Basque Foundation for Science, Bilbao, Spain, ⁵Peter Grünberg Institut and Institute for Advanced Simulation, Forschungszentrum Jülich and JARA, Jülich, Germany, ⁶ICREA-Institució Catalana de Recerca i Estudis Avançats, Barcelona, Spain, ⁷Department of Materials, ETH Zurich, Zurich, Switzerland

Spin-orbit interaction (SOI) in metallic surfaces can break the spin degeneracy and lead to the emergence of particular spin textures that are related to the entanglement between spin and orbital momentum. This can give rise to interesting electron scattering phenomena where backscattering is forbidden by time reversal symmetry, as observed for topological surface states [1].

Here we study effect of the spin texture on electron scattering at surfaces characterised by a strong Rashba interaction. In the BiAg₂ surface alloy, which is characterised by the strongest to date Rashba effect [2,3], we find that an SOI-driven spin-flip mechanism opens new backscattering channels, allowing the scattering to states of opposite spin.

The alloy is formed on the Ag(111) surface after the deposition of 1/3 monolayer of Bismuth, which induces a ($\sqrt{3}\times\sqrt{3}$)R30° reconstruction. The scattering has been studied using Scanning Tunnelling Microscopy and Spectroscopy (STM/STS). In this way we have studied electron confinement by measuring the interference patterns formed by surface electrons scattered from monoatomic steps [fig. 1].

We find that scattering is determined by i) an unconventional orbital/spin texture of the surface bands, which gives rise to transitions with combined orbital and spin flips, and ii) by its chemical composition, which defines a heterogeneous electron localization and potential landscape. The negligible leakage we observe across some step structures indicate a strong confinement effect, comparable to that observed in metals with marginal SOI such as Ag(111) [4].

The results describe a scenario that is far more complex than the conventional Rashba-type two dimensional free-electron gas.

[1] J. Seo, et al., Nature 466, 343 (2010).

[2] C. Ast, et al., Phys. Rev. Lett. 98, 186807 (2007).

[3] G. Bihlmayer, et al., Phys. Rev. B 75, 195414 (2007).

[4] J. E. Ortega, et al., Phys. Rev. B 87, 115425 (2013).

[5] S. Schirone, et al., Phys. Rev. Lett. 166801, 1 (2015).

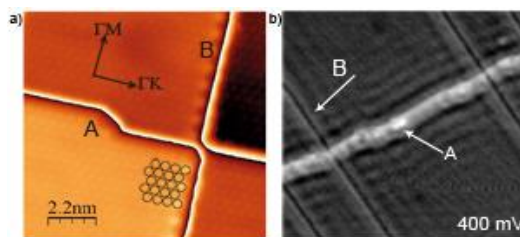


Figure 1: (a) Monoatomic steps perpendicular to the ΓM (A) and ΓK (B) directions. The atomically resolved image (bottom) shows the Bi sites as protrusions. Set point: $I = 0.59$ nA, $V_b = 1000$ mV (top) and 28 mV (bottom). (b) dI/dV map acquired at 0.2V, showing interference patterns formed by A and B steps. Image size: 40.6×40.6 nm². Setpoint: $I = 0.59$ nA, $V_b = 0.2$ V.

Th-D23

Spin Dynamics of Hot Carrier in the Topological Insulator
 Bi_2Se_3

C. Cacho¹, A. Crepaldi², M. Battiato³, J. Braun⁴, F. Cilento², M. Zacchigna⁵, C. Richter⁶, O. Heckmann⁶, E. Springate¹, Y. Liu⁷, S. Dhesi⁷, H. Berger⁸, P. Bugnon⁸, K. Held³, M. Grioni⁸, H. Ebert⁴, K. Hricovini⁶, J. Minar⁴, F. Parmigiani²

¹Central Laser Facility, Didcot, United Kingdom, ²Elettra - Sincrotrone, Trieste, Italy, ³Institute of Solid State Physics, Vienna University, Vienna, Austria, ⁴Department Chemie, Munchen University, Munchen, Germany, ⁵CNR-IOM, Trieste, Italy, ⁶Laboratoire de Physique des Matériaux, Cergy-Pontoise University, Cergy-Pontoise, France, ⁷Diamond Light Source, Didcot, United Kingdom, ⁸Institute of Condensed Matter Physics, EPFL, Lausanne, Switzerland

Topological Insulators (TIs) are attracting widespread scientific interest particularly for their surface electronic spin structure [1]. The prospect of photoinduced spin polarized current for spintronic device requires an in depth understanding of the out-of-equilibrium electronic dynamics [2-3]. What are the empty states available above Fermi and how do the hot carriers relax between bulk and surface? Here we report a time- spin- resolved ARPES study [4] on n-doped Bi_2Se_3 in order to explore the electronic relaxation above the Fermi level in both spin channels. The ARPES measurement is performed with a spin-resolved electron Time-of-Flight analyzer which allows us to resolve the spin of the photoelectron over several orders of magnitude on the photoemission signal.

Our experiment reveals for the first time the existence of a spin polarized surface resonance state (SRS) in Bi_2Se_3 with a topologically trivial character. This out-of-equilibrium measurements are very well reproduced by fully relativistic ab-initio spin resolved photoemission calculations [5] populated by a hot Fermi-Dirac distribution ($T_e = 850$ K). Furthermore the study of the energy and spin dependent relaxation of the hot carriers allows us to disentangle the bulk and surface electron thermalization. The difference in cooling rates of both systems is attributed to the presence of the SRS acting as a bottleneck in the relaxation process which also results in a weak coupling between the topologically protected surface state and the bulk conduction bands. Our findings may have important implications for the optical control of spin currents in TIs and points towards the possibility of independently manipulating the surface and bulk spin states.

1. Xu et al., Science 332, 560 (2011)
2. Sobota et al., PRL 108, 117403 (2012)
3. Wang et al., Science 342, 453 (2013)
4. Cacho et al., PRL (2015) accepted
5. Sánchez-Barriga et al., PRX 4, 011046 (2014)

Th-E15

Functional Group Adsorption on Calcite {10.4}: A combined DFT and XPS Study

Evren Ataman¹, Martin Andersson¹, Marcel Ceccato¹, Nicolas Bovet¹, Susan Stipp¹

¹Nano-Science Center, Dept. of Chemistry, Univ. of Copenhagen, Denmark

Calcium carbonate is a very common mineral in nature. It is a main constituent of geological formations, such as limestone and chalk; it plays an essential role for marine organisms; it is widely used in industrial products and encountered in everyday life, for example as scale in pipes and tea kettles. As a result, there is a vast literature concerning the interactions of various organic molecules with surfaces of calcite - the most stable polymorph of calcium carbonate. However each study focuses on adsorption of only a few molecules and therefore reaches conclusions of limited general applicability. Our aim was to present the big picture, with a comprehensive study of adsorption of a range of organic molecules, to answer two fundamental questions: How do the common functional groups of organic molecules interact with calcite? And what is the effect of side groups on adsorption?

For this purpose, we derived adsorption energies and geometries for 38 oxygen, nitrogen and sulfur containing molecules on calcite {10.4}, using density functional theory with semiempirical dispersion corrections (DFT-D2). Our results show that carboxylic acids (R-COOH) have the strongest interactions, followed by primary amines (R-NH₂) and alcohols (R-OH). Thiols (R-SH), nitriles (R-CN) and aldehydes (R-CHO) have the weakest interactions. We also investigated the effects of replacing the H atom with methyl (-CH₃), ethyl (-C₂H₅) and phenyl (-C₆H₅) side groups. From the adsorption energies, within the transition state theory approximation, we derived desorption temperatures for all molecules and results agree well with 8 measurements from temperature programmed X-ray photoelectron spectroscopy (XPS). We believe that the results of this work can be used by both experimentalists, as a guide for strength of interaction for various organic molecules, and by theoreticians, as a benchmark for adsorption of organic molecules, especially on ionic surfaces.

Th-E16

Ab initio study of gas and hydrocarbon adsorption on Fe₃C surfacesDavid Muñoz Ramo¹, Stephen J. Jenkins¹¹Department of Chemistry, University of Cambridge, Cambridge, United Kingdom

The study of iron carbide surfaces is interesting from both a fundamental and technological point of view. For example, carbide formation on top of iron is a key ingredient in the Fischer-Tropsch reaction for the conversion of synthesis gas into liquid hydrocarbons. Also, carbonaceous deposit growth on iron surfaces is involved in clogging of pipes or engine fouling and failure; understanding of the reactions occurring at the carbide surface may shed light on ways to control these processes, either to favour them or to prevent them from happening.

In this work, we characterize the adsorption of different gases and hydrocarbon species on a typical iron carbide, Fe₃C, using computational methods. We model the surfaces of Fe₃C at the atomistic level, with periodic slabs of about 15 Å thickness and different areas. We use Density Functional Theory and the PBE functional, including a semiempirical van der Waals correction to improve accuracy.

Through this modelling approach we obtain the different relative surface energies of different Fe₃C symmetries. In the case of stoichiometric surfaces, the 001 surface is the most stable one. However, when nonstoichiometric surfaces are considered, an iron-depleted 010 surface is stabilized over the 001 surface due to the additional relaxation gained from exposed carbon atoms. Regarding gas interaction with the surface, carbon reduces the activity of the surface in comparison with pure iron surfaces, as we observe lower adsorption energies and higher dissociation barriers for simple atmospheric and combustion gases like CO, N₂, O₂ or H₂. Small organic molecules like ethanol or toluene adsorb exothermically in a canted configuration due to van der Waals interactions with the surface. Adsorption of these hydrocarbons may provide a starting point for carbonaceous deposition.

Th-E17

Adsorption of H₂O at Cleaved Sr_{n+1}Ru_nO_{3n+1} and Ca₃Ru₂O₇ (001) Surfaces

Daniel Halwidl¹, Bernhard Stöger¹, Jiri Pavelec¹, Florian Mittendorfer^{1,2},
Wernfried Mayr-Schmölzer^{1,2}, Zhiming Wang¹, David Fobes³, Jin Peng³,
Zhiqiang Mao³, Michael Schmid¹, Josef Redinger^{1,2}, Ulrike Diebold¹

¹TU Wien, Institute for Applied Physics, Wien, Austria, ²TU Wien, Center for Computational Materials Science, Wien, Austria, ³Tulane University, New Orleans, USA

Complex ternary perovskite oxides are increasingly used in solid oxide fuel cells and catalysis. Therefore it is highly desirable to obtain a better understanding of their surface chemical properties. We use low-temperature STM, XPS and DFT to investigate the adsorption of H₂O on Sr_{n+1}Ru_nO_{3n+1} (n=1,2) and Ca₃Ru₂O₇. On Sr_{n+1}Ru_nO_{3n+1} dosing 0.05 L of water at 105 K leads to dissociation of the molecule forming an (OH)_{ads} group and an O_{surf}H group. While no long-range diffusion was observed at 78 K, we observe a locally restricted movement of the (OH)_{ads} around the O_{surf}H, as predicted in earlier work [1]. The activation energy for this movement was measured by STM to be E_{act}=175.2 ± 9.1 meV, in excellent agreement with our DFT calculation (180 meV). Increasing the water dose to 0.2 L leads to the onset of molecular adsorption. On Ca₃Ru₂O₇ dosing water at 105 K also leads to dissociation, but no such movement as on Sr_{n+1}Ru_nO_{3n+1} is observed.

Annealing to room temperature leads to diffusion, enabling interactions and the formation of 1D chains on both materials. At higher doses water forms various superstructures that depend on the coverage, temperature and annealing time. This work was supported by the Austrian Science Fund (FWF project F45) and the ERC Advanced Grant "OxideSurfaces".

[1]J. Carrasco et al., Phys. Rev. Lett. 100, 016101 (2008)

Th-E18

Surface chemistry of water on magnetite thin films

Petr Dementyev¹, Jan Seifert¹, Francisco Ivars¹, Francesca Mirabella¹,
Swetlana Schauermann¹, Hans-Joachim Freund¹

¹Fritz-Haber-Institut der Max-Planck-Gesellschaft, Berlin, Germany

Solid metal oxides ubiquitously interact with liquid and gaseous water. In order to get an insight on fundamental processes underlying the oxide-water interface, we study surface chemistry of magnetite, which is a naturally abundant and widely employed material. Single-crystal adsorption calorimetry (SCAC) and infrared reflection-absorption spectroscopy (IRAS) are our molecular beam techniques, which in combination provide an opportunity to investigate both thermodynamics and kinetics of elementary chemical reactions at surfaces.

Two well-defined Fe₃O₄ (111) and (100) films grown on Pt crystals are examined towards adsorption of water under UHV conditions. As revealed by SCAC, water is chemisorbed on the iron oxide while only weak interaction is seen on bare platinum. IRAS experiments confirm formation of surface hydroxyls on magnetite. However, adsorption energy of water on (111) surface differs from that on (100) film. Dissociation of water is found to be fully reversible whereas saturation surface coverage changes much with the temperature.

Thus, we directly measured the energetics of water adsorption on the metal oxide surfaces and assigned it to the certain chemical transformations. The SCAC data revise those derived in previous adsorption-desorption studies and exhibit sharp coverage dependence. We also show quantitatively that the one oxide surface termination is more reactive than the other one.

Th-E19

Adsorption and Reactivity of Single Metal Adatoms at the Fe₃O₄(001) Surface

Roland Bliem¹, Adam Zavodny¹, Jessica van der Hoeven², Eamon McDermott¹, Michael Schmid¹, Peter Blaha¹, Ulrike Diebold¹, Gareth Parkinson¹

¹Vienna University of Technology, Vienna, Austria, ²Utrecht University, Utrecht, Netherlands

The Fe₃O₄(001) surface is an ideal system to study single metal adatoms and their interaction with gases. This surface exhibits a ($\sqrt{2}\times\sqrt{2}$)R45° reconstruction based on subsurface Fe vacancies [1], which provides strong adsorption sites stabilizing single metal adatoms up to temperatures of 700K [2,3]. The stability of the adatoms in ultra-high vacuum allows to study the interaction of various metals with gases. This can provide valuable insights for heterogeneous catalysis, such as information about adsorption strengths or the nature of deactivation processes.

We present a room temperature scanning tunneling microscopy (STM) study of various metal adatoms (Co, Rh, Ir, Ni, Pd, Pt, Ag, Au) at the Fe₃O₄(001) surface and their interaction with low pressures of CO, NO, and O₂. CO adsorbs strongly on Pd [4] and Pt, causing adatom mobility and sintering, whereas this is not the case for Co, Rh, Ir, Ni, Ag, and Au. With O₂, only Rh adatoms show a comparably strong adsorption and sintering. In contrast, NO adsorbs on all metals that were exposed to it (Rh, Ir, Pt, Ni), inducing mobility but hardly any sintering. These results allow determining trends in the interaction between metal adatoms and gases, which are interpreted with support of density functional theory calculations. We propose that elements within one subgroup of the periodic table behave similarly. While Au and Ag seem inert to CO and O₂ exposure, Pt and Pd adatoms adsorb CO strongly. Adatoms in the Co subgroup interact more strongly with O₂.

[1] R. Bliem et al. Science 346, 1215-1218 (2014).

[2] Z. Novotny et al. Phys. Rev. Lett. 108, 216103 (2012).

[3] R. Bliem et al. ACS Nano 8, 7531-7537 (2014).

[4] G.S. Parkinson et al. Nature Mater. 12, 724–728 (2013).

Th-E20

Density Functional Theory study of adatom adsorption on metal supported thin Zirconia films

Wernfried Mayr-Schmölzer¹, Florian Mittendorfer¹, Josef Redinger¹¹Center for Computational Materials Science, TU Vienna, Vienna, Austria

Zirconium dioxide is a material with many interesting properties, which make it useful for various technological applications, for example as a solid electrolyte in solid-oxide fuel-cells or as an oxygen gas sensor. Therefore a detailed understanding of adsorption on the Zirconia film is crucial for these applications. We present results of DFT calculations of the adsorption of metal adatoms on a thin zirconium oxide film supported by a Pt₃Zr substrate. This alloy is very stable and can be used to experimentally grow thin ZrO₂ films by oxidation [1]. We employ differently sized model cells, a small $\sqrt{3}$ and a much larger $\sqrt{19}$ cell. All calculations were performed using the Vienna Ab-Initio Simulation Package (VASP) employing standard PBE and van-der-Waals density functionals [2]. We study the binding mechanism and interaction of various metal atom adsorbates including noble metals such as Au, Ag, and the transition metals Ni and Pd with the oxide surface. Using the small model cell we find the weakest adsorption energy for Au (1.4eV) while the other metals show significantly higher values. With the exception of Ag the calculated trends correspond well with our results on bulk ZrO₂ surfaces. To assess the unexpected results for Ag we furthermore investigate the influence of film thickness and the oxide/metal interface on the adsorption properties such as charge state of the adatom. This work has been supported by the Austrian Science Fund under the project number F4511-N16.

[1] Antlanger, M. et al, Phys Rev B 86, 035451 (2012)

[2] Klimes, J. et al, J. Phys.: Cond Matt. 22 022201 (2010)

Th-E21

Sub-surface incorporation of 3d metal atoms into Bi(111) films studied by density-functional theory

N.J. Vollmers¹, U. Gerstmann¹, C. Klein², P. Zahl³, D. Lükermann⁴, G. Jnawali², H. Pfnür⁴, C. Tegenkamp⁴, P. Sutter³, M. Horn-von Hoegen², W.G. Schmidt¹

¹Lehrstuhl für theoretische Physik, Universität Paderborn, Paderborn, Germany,

²Fakultät für Physik und Center for Nanointegration (CENIDE), Universität Duisburg-Essen, Duisburg, Germany, ³Center for Functional Nanomaterials, Brookhaven National Laboratory, New York, USA, ⁴Institut für Festkörperphysik, Leibniz Universität Hannover, Hannover, Germany

Substrate-stabilized Bi(111) bilayers and Bi(111) surfaces have been studied intensively for some time due to the occurrence of strong spin-orbit split surface states. Recently it has been shown that the Bi(111) surface provides a well-defined incorporation site in the first bilayer that traps highly coordinating atoms like transition metals (TMs) or noble metals [1]. All deposited atoms assume sub-surface interstitial sites.

Here we use density-functional theory to gain a microscopic understanding of the sub-surface incorporation and its implication for the Bi surface electronic properties. The Quantum-ESPRESSO package [2] is used for the calculations, employing the PBE functional for the description of the electron exchange and correlation. Relativistic effects are taken into account on different levels of theory: While for structure relaxation a scalar-relativistic description is found to be sufficient, spin-orbit coupling affects the details of the electronic structure and is dealt with here using a numerically highly efficient PAW-based implementation [3]. It is found that 3d TMs penetrate the surface barrier-free, thereby causing no morphological changes at the surface. All isolated atoms assume exactly the same seven-fold coordinated interstitial position, and provide metallic near-surface state, by only weakly perturbing the surface band structure.

[1] C. Klein et al., Phys. Rev. B (in press).

[2] P. Giannozzi et. al., of Phys.: Condens. Matter 21, 395502 (2009)

[3] U. Gerstmann et al., Phys. Rev. B 89, 165431 (2014).

Th-E22

Diindenoperylene adsorption on Cu(111) studied with density-functional theory

Hazem Aldahhak¹, Eva Rauls¹, Wolf Schmidt¹¹Lehrstuhl für Theoretische Physik, Universität Paderborn, Paderborn, Germany

The formation of diindenoperylene (DIP) thin films on metal substrates has intensively been investigated in the context of the miniaturization of organic optoelectronic devices, due to the high charge carrier mobility, good film forming properties and thermal stability of the molecules [1, 2]. Thereby, interesting terrace-width dependent adsorption characteristics have been observed on Cu(111): On narrow terraces (<15nm), the DIP molecules assemble in a co-directionally oriented adsorption pattern, the symmetry of which is not dictated by the hexagonal substrate symmetry [3]. On wider terraces, in contrast, completely different adsorption patterns with a short-range order determined by the underlying substrate are observed. We performed first principles calculations and investigated the balance between intermolecular and molecule-substrate interactions of DIP molecules on planar surfaces and near step-edges. A detailed analysis of the potential energy surface is presented. Our calculations show a strong influence of the substrate on the geometric and the electronic properties of single molecules and indicate an important role of the step-edges for molecular self-assembly and film growth. In combination with the scanning tunneling microscopy (STM) measurements, long-range ordered arrangements of DIP molecules are found to be most favorable irrespective of the terrace width. The role of the configurational entropy in stabilizing the energetically less favored short-range order structures has been presented as well [4,5].

[1] Zhang et al., Surface Science, 603(2009) 3179.

[2] De Oteyza et al., Journal of Physical Chemistry C 112, 18 (2008) 7168.

[3] De Oteyza et al., Phys. Chem. Chem. Phys. 11, 8741 (2009).

[4] H. Aldahhak, et al., Phys. Chem. Chem. Phys. DOI: 10.1039/C4CP05271D (2015).

[5] H. Aldahhak et al., Surf. Sci., in press, (2015).

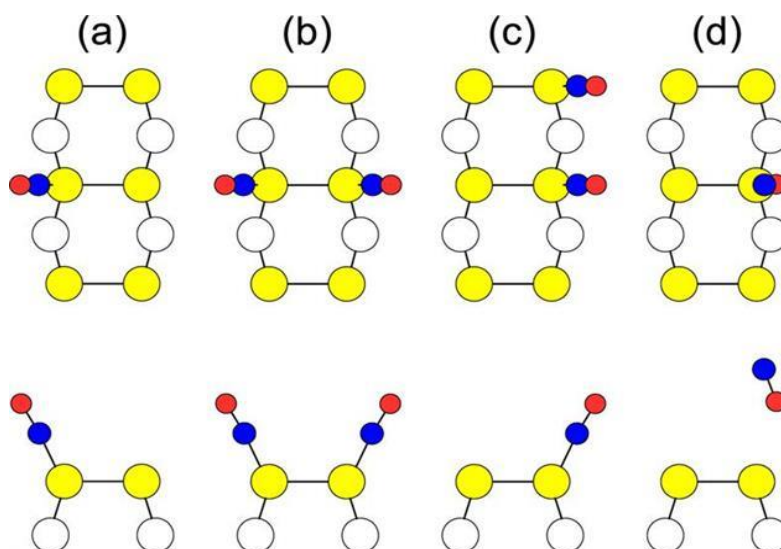
Th-E23

Adsorption and thermal dissociation of CO Molecules on Si(001)-2x1 and Si(111)-7x7

Ja-Yong Koo^{1,3}, Ms. Eonmi Seo^{1,3}, Daejin Eom¹, Hanchul Kim²¹Korea Research Institute of Standards and Science, Daejeon, South Korea,²Department of Physics, Sookmyung Women's University, Seoul, South Korea,³Korea University of Science and Technology, Daejeon, South Korea

It has been well known that CO molecules do not adsorb on Si(001) and Si(111) at temperatures higher than room temperature (RT). We investigated initial adsorption of CO molecules on Si(001) by scanning tunneling microscopy (STM) and density functional theory calculations. All the observed STM features due to CO adsorption are identified as terminal-bound CO configurations. The initial sticking probability of CO molecules on Si(001)-2x1 at RT is $\sim 1 \times 10^{-4}$ monolayer/Langmuir. Thermal annealing at 900 K for 5 min results in the dissociation of the adsorbed CO molecules with the probability of 60-70% instead of dissociation, indicating a strong chemisorption state. The unique adsorption state with a large binding energy, a tiny sticking probability, and a finite adsorption barrier is in stark contrast with the previous low-temperature (below 100 K) observations of a weak binding, a high sticking probability, and a barrierless adsorption.

Adsorption of CO molecules on Si(111)-7x7 by STM shows both bright and dark features on the adatom sites. Though with very small sticking probabilities, every dangling bond on the Si(111) surface can bind with the C atom of a CO molecule at RT. The most two reactive sites are corner and center adatoms in the faulted triangle of Si(111)-7x7. The initial sticking probability of CO molecules on Si(111)-7x7 at RT is estimated to be $\sim 1 \times 10^{-4}$ monolayer/Langmuir, which is similar to that on Si(001)-2x1. We expect that the adsorbed CO molecule on the adatom stands upright, while the O atom of a CO molecule on the restatom rebonds weakly with the dangling bond of a nearby Si adatom. From the sticking probability, the average reactivities of Si dangling bonds on Si(111)-7x7 are expected to be similar to those on Si(001)-2x1. Thermal annealing of the CO/Si(111)-7x7 results in the C incorporation on this surface.



Th-E24

Reactivity mechanism of exchange-split infinite graphene
from first-principles methodMary Clare Sison Escano¹¹University of Fukui, Fukui, Japan

Graphene, being inert to many kinds of molecules, has been doped and/or cut (producing semi-infinite nanoribbons) to improve its reactivity. In this research, an unconventionally reactive exchange-split infinite graphene (or ESIG) and its reactivity mechanism are studied using density functional theory calculations with van der Waals interaction. Using oxygen as a probing molecule, the adsorption energy is compared among free-standing graphene, nitrogen-doped graphene and ESIG (all in 2x2 unit cell). It is found that ESIG binds oxygen ~0.20eV more than that of free-standing graphene and ~0.05eV more than that of nitrogen-doped. Analysis of the density of states (DOS) reveals that the exchange-splitting caused by magnetic substrate (Ni), shifted the minority electrons to higher energies creating DOS at the Fermi level (EF). The DOS at EF is localized or delocalized depending on the position of the graphene on Ni. Such dispersion explains the observed different adsorption energies for different ESIG configurations. Finally, the energy required for transition from exchange-split graphene to non-spin-polarized graphene is higher than the oxygen binding energies. Ways to control the reactivity via the exchange-splitting are proposed. It is seen that this study can provide basis of the use of surface magnetism in 2D non-precious catalysts based on carbon.

Posters

Theme	From	To
Poster session, Monday 31 August		Pg. 344
· Graphene and carbon-based nanomaterials	P-Mo-001	P-Mo-032
· Superconductivity in 2D materials	P-Mo-033	
· Surface magnetism	P-Mo-034	P-Mo-036
· Materials for energy: photovoltaics, solar and fuel cells, etc.	P-Mo-037	P-Mo-053
· Metal, alloy and quasicrystal surfaces	P-Mo-054	P-Mo-060
· Novel and advancement of experimental and computational methods	P-Mo-061	P-Mo-068
· Oxide surfaces and thin/ultra-thin oxide films	P-Mo-069	P-Mo-094
Poster session, Tuesday 1 September		Pg. 430
· Molecules at surfaces	P-Tu-001	P-Tu-047
· Polymer surfaces and interfaces	P-Tu-048	P-Tu-059
· Self-assembly at surfaces	P-Tu-060	P-Tu-074
· Surface dynamics	P-Tu-076	P-Tu-081
· Adsorption and desorption	P-Tu-082	P-Tu-098
· Surface diffusion and growth	P-Tu-099	P-Tu-107
Poster session, Thursday 3 September		Pg. 522
· Band structure of surfaces	P-Th-001	P-Th-003
· Colloids and interfaces	P-Th-004	P-Th-007
· Electronic properties of surfaces	P-Th-009	P-Th-027
· Liquid/solid and liquid/liquid interfaces	P-Th-028	P-Th-031
· Optoelectronic excitations at surfaces	P-Th-032	
· Semiconductor surfaces	P-Th-034	P-Th-041
· Surface phases and phase transitions	P-Th-042	P-Th-045
· Surface structure	P-Th-046	P-Th-054
· Strong correlations at surfaces	P-Th-055	
· Topological insulators	P-Th-056	P-Th-057
· Tribology and mechanical properties at the atomic scale	P-Th-058	
· Catalysis under ideal and real conditions	P-Th-059	P-Th-073
· Corrosion at the atomic scale	P-Th-075	
· Electrochemistry at surfaces	P-Th-076	P-Th-082
· Real-time processes at surfaces	P-Th-083	
· Surface chemical reactions, kinetics and heterogeneous catalysis	P-Th-084	P-Th-099
· Surface structure (II)	P-Th-100	

P-Mo-001

Study of bromine molecules in intercalated compounds of fluorinated graphite

Igor Asanov¹, Tatiana Asanova¹, Dmitry Pinakov¹

¹Nikolaev Institute of Inorganic Chemistry, Novosibirsk, Russian Federation

The state of bromine atoms intercalated into fluorinated graphite was investigated by XPS, EXAFS and Raman techniques. Intercalated compounds of fluorinated graphite (ICFG) offer promise for application in optoelectronics, sensors, supercapacitors and as nanocontainers of volatile compounds. Besides, graphite fluorination is a perspective route for synthesis of graphene compounds. Study of intercalation compounds is of scientific interest in search of ways of modification of electronic properties of the matrix. Investigations of intercalated compounds of graphite with Br₂ have shown remarkable properties related to formation of ordered bromine structure, phase transitions and hole doping of matrix. Likewise, ICFG shows the presence of several types of molecule ordering between layers and the possibility of mutual transformations. We performed the study of bromine atoms in ICFG of composition C₂F_x*yBr₂ with 1>x>0.08 and y<0.13 from room to liquid nitrogen temperature range. Based on XPS and XANES of C K- and F K-edges data, the structural model of fluorinated graphene layer (FGL) has suggested that consists of shorts C-F chains separated by conjugated C-C chains. XPS points to the presence of several bromine states, related to intercalated Br₂ as well as Br atoms forming covalent bond with carbon of the graphene and different structural defects in FGL. The angular dependence of XANES and EXAFS of Br K edge was applied to study an orientation of intercalated Br₂ molecules relative to FGL. Results showed that Br₂ axis is tilted at an angle 57° relative to surface normal of FGL that considerably different from intercalated graphite. Based on EXAFS data the presence of polymeric Br chains between FGL is suggested. The temperature dependence of Raman spectra gives an indication of phase transformation of Br₂ molecules between FGL.

P-Mo-002

Graphene and Other Overlayers Forming Interference Lattices: a Unified Theoretical Treatment

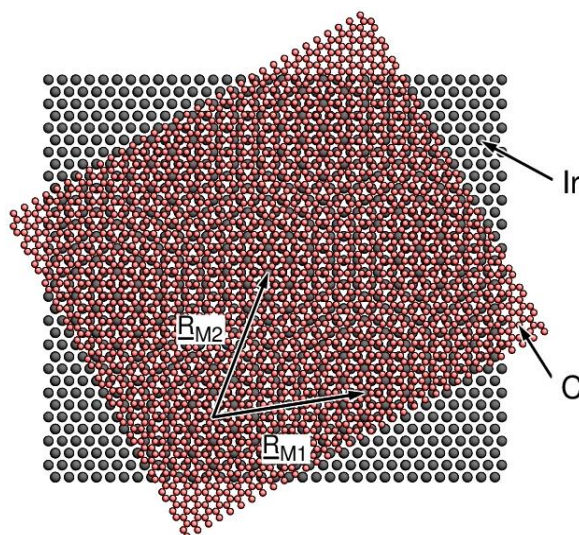
Klaus Hermann¹

¹Fritz-Haber-Institut der MPG, Berlin, Germany

Complex overlayer structures at single crystal surfaces have been observed where long-range order, expressed by additional approximate surface periodicity with very large unit cells, was found. Examples are Pb(111)-C60 near $(\sqrt{(403/7)} \times \sqrt{(403/7)})R22.8^\circ$ [1], Ag(111)-3S near $(\sqrt{7} \times \sqrt{7})R19.1^\circ$ [2], or graphene at different hexagonal metal surfaces, such as Ir(111) [3]. This phenomenon can be characterized by spatial interference resulting in 2-dimensionally periodic Moiré patterns which consist of similar local surface regions (moirons). We have generalized a previously proposed formalism [4] of determining such Moiré patterns based on concepts of higher-order coincidence (HOC) lattices together with 2-dimensional Fourier theory. The extended formalism provides simple mathematical relations allowing to compute 2-dimensional Moiré lattices of any order in their dependence on layer rotation and scaling with respect to a given HOC lattice structure.

For isotropically scaled ($p \times p$) overlayers the general formalism confirms a singularity near $p = 1$ resulting in very large moiré lattices observed for graphene on hexagonal metal substrate where the measured moiré lattice constants [3] agree quantitatively with theory. For rotated (1×1) $R\alpha$ overlayers the formalism yields a singularity for $\alpha = 0^\circ$ which confirms the large moiré lattices found for superimposed graphene layers with the measured moiré lattice constants being reproduced by the present theory. Moiré lattices resulting from combined isotropical scaling and rotation, observed for C60 at Pb(111) [1], can also be quantitatively accounted for by the present formalism. Further, the formalism can explain giant moiré lattice shifts due to overlayer shifting which occur for graphene at stepped metal surfaces [3].

- [1] H.L. Li, et al., Phys. Rev. B 80 (2009) 085415.
- [2] M. Yu, et al., J. Phys. Chem. 111 (2007) 3152.
- [3] E. Loginova, et al., Phys. Rev. B 80 (2009) 085430.
- [4] K. Hermann, J. Phys.: Condensed Matter 24 (2012) 314210.



P-Mo-003

Research of sensor activity of the nitro group modified carbon nanotube to some metal atoms

Natalia Polikarpova¹, Irina Zaporotskova¹, Sergei Boroznin¹, Pavel Zaporotskov¹

¹Volgograd State University, Volgograd, Russian Federation

To date, nanometer scale objects are being widely applied in various fields of science and technology. The discovery of carbon nanotubes (CNTs) is among the most significant achievements of modern science. CNTs possess unique electronic properties, high sorption activity and are effective adsorbents of different particles. There exist a great number of studies on the wide range of gas sensors, the basic principle of which is the adsorption of gas molecules in which the molecule gives or takes away an electron in a nanotube, which leads to changes in the electrical properties of CNTs that can be detected and registered. Devices with boundary-modified carbon nanotubes can perform as sensors.

In previous research we studied interaction between carbon nanotube modified with a carboxyl group and alkali metal atoms [1]. In this study we investigated the mechanism of boundary modification in single-walled carbon nanotube with a nitro functional NO₂ and calculated the interaction of this boundary-modified system with atoms and ions of alkali metals: lithium, sodium and potassium. The calculations were performed using the MNDO method and DFT. The process was simulated as incremental movement of the selected atoms or metal ions to the atom O of the functional group. The energy curves of the nanosystems with selected atoms or ions enabled to determine the basic characteristics of the interaction (the distance and energy). Analysis of the results allowed to conclude the following: since the interaction distance corresponding to the minimum on the energy curves is rather large, it can be assumed that interaction between the boundary-modified nanotubes and selected metals is characterized as a weak van der Waals interaction. This fact shows that the sensor probe could be used repeatedly and would not be subject to destruction, which would have happened in case a chemical reaction in the system had occurred.

P-Mo-004

Investigation of carbon nanotubes modified by amino group

Irina Zaporotskova¹, Natalia Poikarpova¹, Pavel Zaporotskov¹, Sergei Boroznin¹, Dinara Vilkeeva¹

¹Volgograd State University, Volgograd, Russian Federation

The ability of carbon nanotubes to adsorb particles of various origin and conductivity enables them to be used as chemical and biological sensors. Sensors can be designed on the base of devices modified by carbon nanotubes. The atomic force microscope with the tip of the cantilever modified by carbon nanotube with a specific boundary functional group can serve as a sample of this device.

To investigate the possibility of the probe formation the binding process of amino group $-NH_2$ to an open boundary of semi-infinite carbon nanotubes (6, 0) and (6, 6) was studied.

Calculations showed that the amino group binds to the nanotube (6,6) at an angle of 114° . The length of the C-N was equal to 1,35 Å, N-H -1 Å. For the binding process of nanotube (6,0) the following parameters were revealed: angle = 122° ; bond lengths: C-N = 1,33 Å; N-H = 1 Å.

The binding process between the amino group $-NH_2$ and the selected carbon atom at the open boundary of nanotubes (6,6) and (6,0) was simulated in increments of 0,1 Å perpendicularly to the edge of the tube and with orientation to the C atom. As a result, the energy curves were constructed for the systems "nanotube - $-NH_2$." The energy minimum on the curves indicates chemical bond formation between the tube and the functional group. It is found that the moment - NH_2 binds to the tubulene electron density is transferred from the C-atom to the nitrogen atom of the amino group. As a result, change in the number of carriers enables conductivity in the system and the nanotubular system acts as the probe sensor.

The investigation proved the possibility to modify carbon nanotubes by amino groups to design sensors based on them.

P-Mo-005

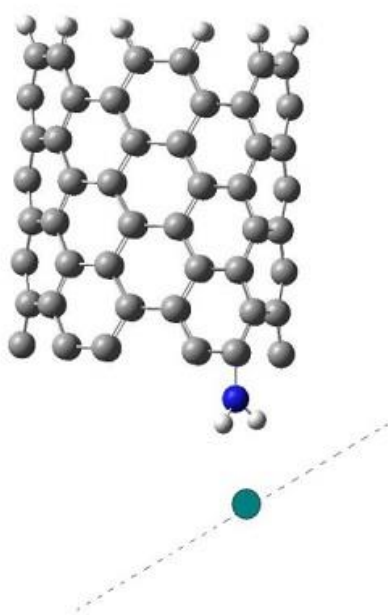
Investigation of sensor activity of the amino group boundary-modified CNT to some metal atoms

Pavel Zaporotskov¹, Irina Zaporotskova¹, Sergei Boroznin¹, Natalia Polikarpova¹

¹Volgograd State University, Volgograd, Russian Federation

It is known that gas sensors can be based on pure single and multi-walled carbon nanotubes and nanotubes modified with functional groups. We assume that modified carbon nanotubes that are applied as elements in sensor devices (probes) are not limited to the detection of gases. Boundary-modified nanotubes can be used to identify other chemical elements, for example metals and ions that make up salts and alkalis.

We investigated sensory properties of the probe based on the amino group modified CNT with respect to atoms and ions of sodium, potassium, lithium, magnesium. We studied the process of random surface scanning to detect an atom (or ion) under investigation and calculated the activity of the selected nanotubes modified with the boundary functional group in relation to the selected element. The process of a metal atom (ion) approach to the functional group was modeled in increments parallel to the border of the modified nanotubes at a distance of 2,0 Å (Fig. 1). Analysis of the interaction energy curves found that tubules with the selected functional group become sensitive to the selected metal atoms (ions). The curves show characteristic minimum indicating the interaction between a metal atom and the modified system "CNT - amino group." The results indicate the possibility of using modified carbon nanotubes as sensors for certain elements and radicals whose presence can be experimentally detected by change in the potential of the probe system based on nanotubes modified with the functional group.



P-Mo-006

Structural Characterization of sidewall graphene nanoribbons by Scanning Tunneling Microscope and Scanning Transmission Electron Microscope

Maya Narayanan Nair¹, Irene Palacio¹, Arlensiu Celis^{1,2}, Alexandre Gloter², Alberto Zobelli², Muriel Sicot³, Daniel Malterre³, Meredith Nevius⁴, Walt A. de Heer⁴, Claire Berger⁴, Edward H Conrad⁴, Amina Taleb-Ibrahimi¹, Antonio Tejeda^{1,2}

¹UR1 CNRS/Synchrotron Soleil, Gif-Sur-Yvette, France, ²Laboratoire de Physique des Solides, Université Paris-Sud, Orsay Cedex, France, ³Institut Jean Lamour, Université de Lorraine, Vandoeuvre-lès-Nancy, France, ⁴School of Physics, The Georgia Institute of Technology, Atlanta, USA

The new templated growth technique of graphene nanoribbons grown on silicon carbide facets has attracted much attention as it allows growing narrow nanoribbons with smooth edges as required for graphene based nanoelectronics [1]. Recently, 40nm wide graphene nanoribbons grown in this way on 4H-SiC facets have exhibited an exceptional ballistic transport at room temperature [2]. Our photoemission experiments have also demonstrated a band gap opening in these ribbons [3]. In order to understand both the observed ballistic transport and the band gap opening, we have performed a detailed morphological characterization using Scanning Tunneling Microscopy (STM) and High Resolution Scanning Transmission Electron Microscopy (HR-STEM). By combining these two techniques, we can access the last-layer topography and cross sectional view, the nature of the edges, their orientation and their termination into the buffer layer or into the SiC substrate. Here we show that the ribbons grown on the facet are decoupled from the substrate and bordered by 1-2nm miniribbons on top and bottom edges. STEM-EELS measurements with spatial resolution allow to localize the band gap opening in the miniribbons, in agreement with photoemission experiments. The observed bandgap is opened by quantum confinement in agreement with our DFT calculations [4].

- [1]. M. Sprinkle et al, Nat. Nanotech, 5, (2010) 727
- [2]. J. Baringhaus et al, Nature, 506 (2014) pp. 349-354.
- [3]. J. Hicks et al, Nat. Phys, 9 (2013) pp. 49-54.
- [4]. I. Palacio et al, Nano Lett, 15 (2015) pp. 182 –189

P-Mo-007

Carbon nanotubes for improving the properties of lubricating oils

Irina Arkharova¹, Irina Zaporotskova¹

¹Volgograd State University, Volgograd, Russian Federation

We assumed that doping of oil with carbon nanotubes will be change some of oil's properties such as an indicator of viscosity, improvement of chemical stability. For this reason the study of some properties of the received composite mixes is important.

The doping of lubricating oils – semi-synthetic engine oil – with the carbon nanotubes, taken in various mas. % of additives, was carried out: 0,01; 0,1; 0,5 mas. %.

The physical and chemical characteristics were investigated:

- 1) Viscosity of composite mix at the temperature $T=25\text{ }^{\circ}\text{C}$ (an initial state);
- 2) Viscosity of composite mix after its aging at $T=160\text{ }^{\circ}\text{C}$ on the mode of oxidation of the investigated samples of composite mix during 24 hours;
- 3) The oxidation stability has been determined by the parameters "acidity" and "acid number", these parameters have been carried out for the investigated samples of composite mix in an initial state and after aging.

The way of development functional and operational characteristics of lubricants by doping with carbon nanotubes was suggested. Results of researches showed that doping of carbon nanotubes causes change of such physical and chemical characteristics of lubricant as viscosity, acidity and acid number, alkaline parameter. Doping of lubricant with carbon nanotubes stops oxidation process and leads to decrease of acidity and acid number in an initial state and for a state after aging. Besides, the carbon nanotube's presence has increased alkaline parameter after aging of composite mix that provides ability of oil to neutralize collateral sulphurous products and after aging during its exploitation. Thus, the researches proved positive influence of carbon nanotubes on the main functional characteristics of lubricants that allow us to recommend CNTs as new additives of liquid lubricant composite mixes.

P-Mo-008

Electron dynamics in graphene by ultrafast Tr-ARPES

Cephise Cacho¹, R. T. Chapman¹, I. Gierz², A. Cavalleri², J.C. Johannsen³, S. Ulstrup⁴, P. Hofmann⁴, E. Springate¹

¹Central Laser Facility, Didcot, United Kingdom, ²MPI for the Structure and Dynamics of Matter, Hamburg, Germany, ³Institute of Condensed Matter Physics (EPFL), Lausanne, Switzerland, ⁴Department of Physics and Astronomy, Aarhus University, Aarhus, Denmark

Graphene's electronic and optical properties are intrinsically governed by the conical dispersion of the π -bands localized at the K-point. Ultrashort pulses of high energy photons are required to explore the electronic dynamics in the Dirac cone. Artemis is a user facility offering an ultrafast XUV beamline and a photoemission end-station for Time- and Angle- Resolved PhotoEmission Spectroscopy (tr-ARPES) with mid-IR pumping [1].

A quasi-free-standing monolayer of graphene (MLG) is optically pumped with a ~ 30 fs pulse. Within the excitation pulse duration, electron-electron interactions lead to the formation of a thermalized distribution of hot carriers [2]. Subsequently the electronic temperature cools down via optical phonon and supercollisions interaction [3]. A large carrier multiplication factor is observed for n-doped graphene [4], showing that the Dirac carrier dynamics can be controlled by tuning the doping level. With sufficient pumping fluence we observe a population inversion across the Dirac point [5-6] supporting the potential of graphene for applications in THz amplification.

AB-stacked bilayer graphene (BLG) is predicted to open a small band gap with great importance for electronic device applications. Such a gap gives rise to a bottleneck in the decay of hot carriers that is confirmed by comparing the relaxation times in BLG and MLG [7]. Furthermore, the BLG band structure can be controlled by exciting the BLG E_{1u} lattice vibration. At resonance excitation the peak electronic temperature and cooling time are significantly reduced [8]. Based on DFT frozen phonon calculations it is confirmed that this anomalous dynamics corresponds to the modification of a gap structure at the Dirac point.

1. Frassetto, Op.Exp. 19, 19169 (2011)
2. Ulstrup, J.Phys.:Condens.Matter (2015)
3. Johannsen, PRL 111, 027403 (2013)
4. Johannsen, NanoLett. 15, 326 (2015)
5. Gierz, NatureMaterials 12, 1119 (2013)
6. Gierz, J.Phys.:Condens.Matter (2015)
7. Ulstrup, PRL 112, 257401, (2014)
8. Gierz, PRL, (2015)

P-Mo-009

High-quality graphene on sapphire grown in UHV

Gloria Anemone¹, Esteban Climent-Pascual², Hak Ki Yu^{3,4}, Amjad Al Taleb¹,
Félix Jiménez-Villacorta², Carlos Prieto², Alec M. Wodtke^{3,4}, Alicia de
Andrés², Daniel Farías^{1,5,6}

¹Departamento de Física de la Materia Condensada, Universidad Autónoma de Madrid, Spain, ²Instituto de Ciencia de Materiales de Madrid. Consejo Superior de Investigaciones Científicas, Madrid, Spain, ³Institute for Physical Chemistry, University of Göttingen, Göttingen, Germany, ⁴Max Planck Institute for Biophysical Chemistry, Göttingen, Germany, ⁵Instituto de Ciencia de Materiales “Nicolás Cabrera”, Universidad Autónoma de Madrid, Spain, ⁶Condensed Matter Physics Center (IFIMAC), Universidad Autónoma de Madrid, Spain

We report a new method to produce in UHV high-quality, transparent graphene/sapphire samples, using Cu as a catalyst. The starting point is a high-quality graphene layer prepared by CVD on Cu(111)/Al₂O₃. Graphene on sapphire is obtained in-situ by dewetting and evaporation of the Cu film in UHV. He-diffraction, atomic force microscopy, Raman spectroscopy and optical transmission have been used to assess the quality of graphene in metal free area. We used helium atom scattering as sensitive probe of the crystallinity of graphene on sapphire. The observation of high reflectivity and clear diffraction peaks demonstrates the presence of flat and homogeneous graphene domains over lateral scales of microns, consistent with scanning force microscopy results. The uniformity of the graphene has been also investigated by Raman mapping. The G to 2D peak ratio presents the same value for graphene/Cu/sapphire and for graphene/sapphire after Cu elimination. This indicates a similar quality of the graphene layer in both cases, independently of the presence of Cu. The high transparency measured (80%) in the visible range makes this system suitable for many applications. Our method also allows preparation of graphene/sapphire samples with Cu nanoparticles wrapped under graphene, making them potentially useful for catalysis studies.

P-Mo-010

Atomic and electronic structure of SWCNT encapsulated by TbBr₃

Alexander Rashkovskiy¹, Anatoly Kovalev¹, Dmitry Wainstein¹, Andrey Kumskov³, Nikolay Kiselev³, Ivan Verbitsky², Andrey Eliseev²

¹I.P. Bardin Central Research Institute for Ferrous Metallurgy "CNIICHERMET", Moscow, Russian Federation, ²Moscow State University, Moscow, Russian Federation, ³Shubnikov Institute of Crystallography RAS, Moscow, Russian Federation

Single wall carbon nanotubes (SWCNT) encapsulated by TbBr₃ one-dimensional nanocrystals were fabricated by capillary filling from anhydrous salt melt, followed by slow crystallization. Comparative study of both pristine and infilled SWCNTs is presented. HRTEM analysis has shown, that synthesized composites have a perfect structure with well-defined atomic arrangement of encapsulated compound within the nanotube channel. A thermally activated slow-motion diffusion process of the TbBr₃ molecules occurs along the interstitial channels during TEM investigation. The filling ratio of the carbon nanotubes exceeded 70% according to both TEM and XPS experiments. The influence of the intercalated material on the electronic structure of the nanotubes was investigated by HREELS, REELS, EELFS and XPS techniques. Analysis of photoelectron spectra reveals that the binding energy of C1s and Tb3d are shifted, suggesting an electronic interaction between Tb and neighboring C atoms of the CNTs. The investigation of nearest atomic surrounding by EELFS at the Tb M edge (922.5 eV) also confirmed that Tb is inserted into CNTs during synthesis and interacts with carbon atoms. Moreover, we show that there are two types of Tb anions and Br cations bonded to sp²-hybridized carbon. Intensity of plasmon peaks on REELS spectra measured for TbBr₃@SWCNT was lower and shifted towards higher energy losses than for pristine ones. This phenomenon originates from decreasing the DOS of conduction electrons in the carbon nanotubes and a partial charge transfer, which suggest a plausible Tb(3d)–C(1s) hybridization.

P-Mo-011

Carbon-Based Materials as Foundation to Realize Designer Materials

Wilson Agerico Diño^{1,2}, Hiroshi Nakanishi¹, Hideaki Kasai^{3,4}, Yousuke Kawahito⁵

¹Department of Applied Physics, Osaka University, Suita, Japan, ²Center for Atomic and Molecular Technologies, Osaka University, Suita, Japan, ³National Institute of Technology, Akashi, Japan, ⁴Institute of Industrial Science, The University of Tokyo, Meguro-ku, Japan, ⁵Joining and Welding Research Institute, Osaka University, Ibaraki, Japan

Carbon comprises a vast number of compounds and assumes a variety of forms when two or more atoms are brought together. As such, carbon is a good strategic element of choice as a building block, offering a rich playground for realizing designer materials [1], with applications as varied as catalysis, (spin)electronics, fuel storage and transport, joining and welding, to name a few. For example, by inducing spin polarization [2,3] of a strip of carbon material, we could subsequently use it to detect the presence or absence of particulates, e.g., hydrogen [2], amino acids [4,5], in the environment. By inducing structural changes of a strip of carbon material, and subsequently use it to store particulates, e.g., hydrogen [6], or facilitate the joining and welding of dissimilar materials, e.g., thermoplastics and metals, without the use of adhesives [7,8]. At the meeting, we will present a more detailed discussion, emphasizing the unique role played by the Surface/Interface for providing a special environment (foundation) for realizing Designer Materials [1,9], that are not realizable in the bulk, and the strategic choice of particular elements as building blocks, viz., carbon.

- [1] H. Kasai et al., e-J. Surf. Sci. Nanotech. 12 (2014) 203.
- [2] cf., e.g., W.A. Diño et al., J. Phys. Soc. Jpn. 72 (2003) 2413.
- [3] cf., e.g., W.A. Diño et al., J. Magn. Magn. Mater. 272-276 (2004) 1602.
- [4] cf., e.g., T. Roman et al., Eur. Phys. J. D 38 (2006) 117.
- [5] cf., e.g., T. Roman et al., Thin Solid Films 509 (2006) 218.
- [6] cf., e.g., T. Roman et al., Jpn. J. Appl. Phys. 45 (2006) 1765.
- [7] cf., e.g., T. Roman et al., Solid State Commun. 132 (2004) 405.
- [8] cf., e.g., M. David et al., J. Phys.:Condens. Matter 18 (2006) 1137.
- [9] cf., e.g., www.dyn.ap.eng.osaka-u.ac.jp/web/publications.html.

P-Mo-012

High quality of graphene grown on oxidized copper foils by chemical vapour deposition

Van Lam Do¹, Regis Y. N. Gengler¹, Petra Rudolf¹¹Zernike Institute for Advanced Materials, Groningen, Netherlands

Graphene grown on copper foils by chemical vapour deposition (CVD) has seen a lot of improvement recently and several reports point to a crucial role of oxygen in realizing graphene with fewer defects. Here we report that the oxidation of copper foils before growth is a key factor to produce high quality of graphene. Copper foils were oxidized either in air at room temperature or by annealing in oxygen. Graphene was then grown by CVD using methane as a carbon precursor. AFM images confirm the presence of graphene and also showed more uniform and aligned of graphene domains as compared to the one grown on clean copper foils. Raman spectra of graphene grown on both clean copper foil and oxidized copper foil clearly indicate the improvement in quality of graphene in the latter case.

P-Mo-013

Wettability of graphene surface

Akira Akaishi^{1,2}, Jun Nakamura^{1,2}

¹The University of Electro-Communications (UEC-Tokyo), Chofu, Tokyo, Japan,

²CREST, Japan Science and Technology Agency, Kawaguchi, Saitama, Japan

Understanding of the wettability of graphitic surfaces is of great importance for the practical applications of graphene-based materials since the water wettability is closely related to whether the surface is hydrophobic or hydrophilic. One of the characteristic measures of wettability is a contact angle that is the angle of the edges of a water droplet placed on target surfaces. In recent studies, it is reported that the water contact angle of the graphene surfaces becomes relatively small by removing surface contamination. This observation is also confirmed by estimating the water contact angle with molecular dynamics (MD) simulations. The wettability of pristine graphene surfaces remains unsettled.

We have examined the structure of water molecules on graphene surfaces with MD simulations. The simulations are prepared with a graphene sheet and a water droplet, which are dropped initially on the graphene surface. With increasing the number of water molecules, the droplet covers the surface and the layered-structure of molecules on the surface is formed. This indicates that, at a level of empirical model, a graphene surface is capable of wetting.

The formation of water layers on the surface can be seen by the density profile of water molecules. The density distribution of oxygen and hydrogen atoms of water along the axis perpendicular to the graphene surface indicates the existence of the layers. Moreover, the distinct peaks of the hydrogen atom distributions indicate that the oxygen-hydrogen (O-H) bonds are not randomly formed but are certainly oriented. The angle distribution of O-H bonds shows that hydrogen bonds are formed between the water layers on the graphene surface. In other words, the water molecules in the layers tend to form the hydrogen bonding only within the layers. Above the second layer, there are no unpaired hydrogen bonds that are pointing perpendicular to the layer plane.

P-Mo-014

Elastic modulus of Extreme Ultraviolet exposed single-layer graphene

Baibhav Mund¹, An Gao¹, Jacobus Sturm¹, Chris Lee¹, Fred Bijkerk¹

¹XUV Optics Group, MESA+ Institute for Nanotechnology, University of Twente, Enschede, The Netherlands

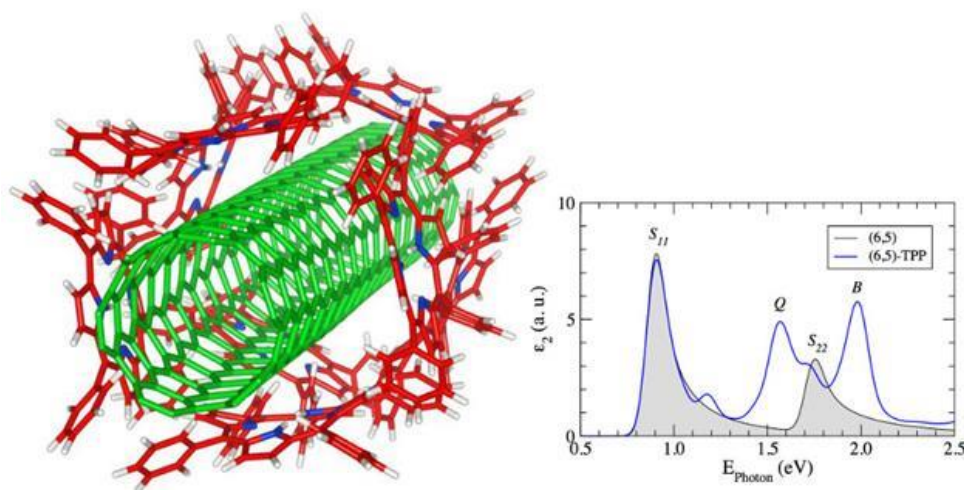
In the Extreme Ultraviolet (EUV) range, transmission optics must be supported by ultra-thin membranes to limit absorption losses. Graphene has remarkable physical strength, and very high EUV transmission, making it a good candidate to support transmission optics. However, its longevity under EUV radiation is unknown. To test how the mechanical strength of graphene is modified by EUV exposure, we measured and compared the elastic modulus of free-standing single-layer CVD grown graphene membranes before and after EUV exposure. The elastic modulus of graphene was obtained via nano-indentation in an atomic force microscope. The results show that the 2D effective elastic modulus of a pristine graphene membrane is approximately 83 ± 11 N/m which is about four times lower than the intrinsic elastic modulus of supported graphene (340 ± 5 N/m). This can be attributed to the fact that CVD graphene results in grain boundaries lined with defects and poor adhesion of graphene to the substrate, reducing the mechanical strength of single-layer graphene. Surprisingly, after EUV exposure, the elastic modulus of the graphene membrane rises to about 212 ± 18 N/m, despite an increase in defect density, as indicated by Raman spectroscopy. The apparent increase in the elastic modulus is attributed to two factors: an additional hydrocarbon layer is deposited on the graphene during EUV exposure, effectively increasing the thickness of the membrane, and the graphene is more effectively bound to the substrate. Using an effective medium model, the elastic modulus of the exposed graphene was calculated to be 309 ± 56 N/m close to the literature value.

P-Mo-015

Single- and double-wall carbon nanotubes fully covered with tetraphenylporphyrins: Stability and optoelectronic properties from ab-initio calculations

Walter Orellana¹¹Universidad Andres Bello, Santiago, Chile

The noncovalent functionalization of carbon nanotubes (CNTs) with porphyrin chromophores has proven to be an efficient method to combine the strong photoabsorption of porphyrin with the CNT electron transport and charge separation properties. This supramolecular assembly has been explored recently as light-harvesting donor/acceptor complexes. Some schemes proposed for such a functionalization include the CNT encapsulation in micelles of surfactant or in polymers. Indeed, CNT-porphyrin complexes obtained from a micelle-swelling technique have shown an extremely efficient energy transfer from the photosensitized porphyrin to the nanotubes. However, some key parameters like the TPP concentration on the CNT surface and the stability of the compounds are not yet clarify. In the present work we investigate single- and double-wall CNTs noncovalently functionalized with free-base tetraphenylporphyrin (TPP) molecules using dispersion-corrected density functional theory calculations and linear optical response. Our goal is to give insight in the stability of such complexes with temperature and also determine its electronic properties and optical response. We consider both metallic and semiconducting CNTs in order to identify possible chirality dependence in the TPP adsorption strength, particularly those with chiral indexes (10,10), (16,0), and (6,5). Our results show that the TPP molecules tend to cover the whole CNT surface, exhibiting quite large binding energy of about 2 eV/TPP. The TPP binding strength would depend on the CNT diameters instead of chirality. The semiconducting CNT-TPP compounds show optical response characterized by a strong absorption associated to the TPP bands, where band intensities are related with the number of TPP molecules adsorbed on the CNT surface. In addition, molecular dynamic simulations show that all compounds under study are stable at 100°C, preserving this stability at temperature as high as 500°C. This work was supported by the funding agency CONICYT-PIA under the Grant Anillo ACT-1107.



P-Mo-016

Carbon Nanotube Network Film as a Compliant and Transparent Electrode

Seung-Youl Kang¹, Jaehyun Moon, Seong Deok Ahn

¹Electronics and Telecommunications Research Institute, Daejeon, South Korea

We investigated the compliant characteristics of carbon nanotube network films on dielectric elastomers. Compared with other stretchable or compliant electrodes such as corrugated metal electrodes, conducting polymers, metal nanowires and so on, carbon nanotube electrodes have a very high strain value as well as a good transparency. We fabricated carbon nanotube electrodes onto dielectric elastomers by a filtration-transfer process. The obtained electrodes showed a large strain more than 150 % at a high transparency of 85 %. This high strain value is competitive with carbon grease which is a typical compliant electrode. And we investigated the compliant characteristics of carbon nanotube network films with various areal densities of carbon nanotubes. Through SEM measurements and microscopic investigation of the actuation of carbon nanotube electrodes, it could be found out that if the density of carbon nanotubes on the electrodes increased, the interaction between carbon nanotubes also did and the expansion of carbon nanotube mats during the actuation of elastomers was reduced. On the other hand, if the density decreased too much, the connection between the network of carbon nanotubes was broken during the actuation, the compliant characteristics was deteriorated. Therefore, carbon nanotube films had a good enough performance at a relatively lower density and so showed a higher transparency.



P-Mo-017

Theoretical study on quantum capacitance of charged bilayer graphene with applied electric field

Yutaro Mori¹, Emi Minamitani¹, Yasunobu Ando¹, Kasamatsu Shusuke², Kaoru Kanayama¹, Kosuke Nagashio¹, Satoshi Watanabe¹

¹Department of Materials Engineering, The University of Tokyo, Tokyo, Japan,

²The Institute for Solid State Physics, The University of Tokyo, Kashiwa, Japan

Bilayer graphene (BLG) is one of the promising materials for the channel in the field effect transistor (FET) owing to the controllability of band gap by electric field. In the FET structure, the electronic states of the BLG are determined by the doping from the source electrode, and the modification of the band structure and the electronic polarization by the gate voltage. Some of us measured the quantum capacitance, the Fermi level shift to store the doped charge in the finite DOS, to estimate the DOS around the Fermi level. However, it is experimentally impossible to distinguish the quantum capacitance from other capacitive properties. Thus, we examine the dielectric properties of BLG using the density functional theory (DFT). First, the electronic structures of BLG under applied electric field but without doped charge were calculated within the DFT. Next, the electronic structures of BLG with doped charge under applied electric field were calculated by the effective screening medium method within the DFT. The value of local relative permittivity of BLG is larger than two even in the middle of the two graphene layers. So we conclude that the BLG can be regarded as a single dielectric material. Figure1 shows the energy required to modify the band structure of BLG. Since this energy is in the order of 10 meV, we can say that the effect of the band structure change in the quantum capacitance measurement of BLG is negligible. In addition, we find that the band gap under the electric field slightly changes by the carrier doping: The band gap first increases with the doping, then decreases as the doping further increases.

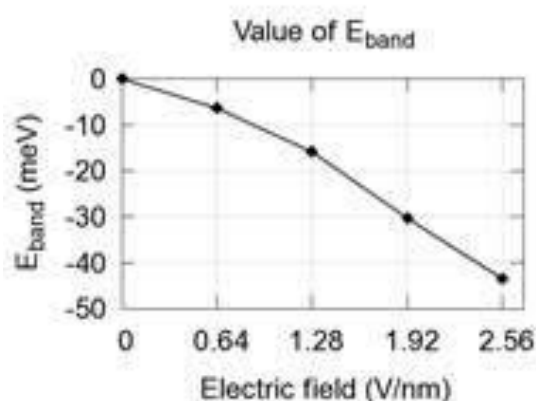


Figure1 Relationship between electric field and energy for the band structure modulation

P-Mo-018

Morphology of Transferred Graphene Affected by Surface Steps in Copper Substrate

Masamichi Yoshimura¹, Takashi Nagamori¹, Seiya Suzuki¹

¹Toyota Technological Institute, Nagoya, Japan

Graphene, a two-dimensional honeycomb lattice of carbon, has excellent electronic properties and is desirable for the electrical device applications. Recently, the growth of graphene on Cu by chemical vapor deposition (CVD) has attracted attentions for mass production. However, the graphene grown by CVD needs to be transferred from Cu substrates to device-compatible substrates for fabricating electrical devices. In the present study the graphene structure before and after the transfer process is in detail investigated by atomic force microscopy (AFM), and the effect of steps in Cu substrate is investigated.

Prior to growth, Cu foils were pre-annealed at a high pressure (~0.4 MPa) at 1050 °C under the flows of Ar and H₂. Then single-crystal graphenes were synthesized by introduction of CH₄ at atmospheric pressure. The graphene on Cu was first spin-coated with PMMA (~50 nm thick) and was irradiated by UV light. After the irradiation, the second PMMA layer (~300 nm thick) was spin-coated over the first PMMA layer. The Cu substrate under the graphene was etched by floating in 0.2 M (NH₄)₂S₂O₈ solution and was rinsed with deionized water a few times. The resulting PMMA/Graphene film was transferred on SiO₂ (300 nm)/Si substrate and dried. The PMMA layer was dissolved in mixed solution of acetone, isopropyl alcohol and methyl isobutyl ketone. AFM observation of the identical hexagonal graphene before and after the transfer process was conducted. The surface before transfer shows rough step-terrace structures formed by high pressure pre-annealing, while that after transfer shows wrinkles of the graphene. Although their periods are somewhat different from each other, their orientations coincide well with each other. Thus we conclude that the transferred graphene structure is strongly affected by the step-terrace structure of the substrate Cu.

P-Mo-019

Covalent modification of carbon-based surfaces with electroactive organic radicals

Gonca Seber¹, Alexander Rudnev², Marta Mas-Torrent¹, Jaume Veciana¹, Núria Crivillers¹, Concepció Rovira¹

¹Institut de Ciència de Materials de Barcelona, Bellaterra, Spain, ²Department of Chemistry and Biochemistry, University of Bern, Bern, Switzerland

The isolation of the graphene monolayer sheets in 2004 lead to the realization of its attracting properties, like high electrical and thermal conductivity, optical transparency and mechanical strength [1]. Since then there has been an increased interest in trying to utilize graphene for electronic device applications such as transistors, memory devices, biosensors, solar cells, batteries etc., as well as in the field of spintronics [2]. Several synthetic strategies have been established to functionalize graphene with organic molecules in order to tune its electronic properties [3]. In this work, a novel polychlorinated triphenylmethyl (PTM) radical has been synthesized and used for the functionalization of carbon substrates. Electrografting was employed for covalently attaching this novel PTM radical derivative to glassy carbon and HOPG substrates. The modified substrates have been characterized by cyclic voltammetry, Raman spectroscopy, AFM and STM.

[1] Novoselov, K.S.; Geim, A.K.; Morozov, S.V.; Jiang, D.; Zhang, Y.; Dubonos, S.V.; Grigorieva, I.V.; Firsov, A.A. *Science* 2004, 306, 666.

[2] Georgakilas, V.; Otyepka, M.; Bourlinos, A.B.; Chandra, V.; Kim, N.; Kemp, K.C.; Hobza, P.; Zboril, R.; Kim, K.S. *Chem. Rev.* 2012, 112, 6156-6214.

[3] Chua, C.K.; Pumera, M. *Chem. Soc. Rev.* 2013, 42, 3222-3233.

P-Mo-020

Ballistic transport in self-assembled graphene nanoribbons

Frederik Edler¹, Jens Baringhaus¹, Johannes Aprojanz¹, Walt A. de Heer²,
Claire Berger², Christoph Tegenkamp¹

¹Institut für Festkörperphysik, Leibniz Universität Hannover, Hannover, Germany, ²Georgia Institute of Technology, Atlanta, USA

The patterning of graphene into nanoribbons is essential for the development of future graphene based electronic devices. For such ribbons with a well-ordered edge geometry the presence of one-dimensional edge states has been predicted. We use a selective graphitization process on SiC-mesa structures to produce graphene nanoribbons with a width of 40 nm. The local electronic properties of the ribbons are investigated by means of a 4-tip STM/SEM system, allowing the precise positioning of all tips on the nanometer range to perform local transport measurements. Additionally, the STM tips can be used for STS measurements to gain an insight into the local density of states. This reveals two peaks in the local density of states at the edges of the ribbons which can be attributed to the zeroth subbands in the band structure of a ferromagnetic zig-zag graphene nanoribbon. Transport experiments on the very same ribbon show a conductance close to e^2/h for a wide temperature range from 30 K up to room temperature and probe spacings between 1 - 10 μm . Description within the Landauer formalism is possible assuming ballistic transport dominated by a single channel. Transport in the second zeroth subband is only detectable for probe spacings smaller than 1 μm due to the short localization length of carriers in this subband. This manifests in the increase of the conductance to $2 e^2/h$ at probe spacings below 200 nm.

Remarkably, 4- and 2-point probe configurations result in almost identical conductance values as expected for a ballistic conductor measured with fully invasive probes. This invasiveness can be used to give further evidence for the ballistic nature of transport by introducing additional passive probes in a 2-point probe configuration. Every additional passive probe doubles or triples the observed resistance, strongly indicating single-channel ballistic transport.

P-Mo-021

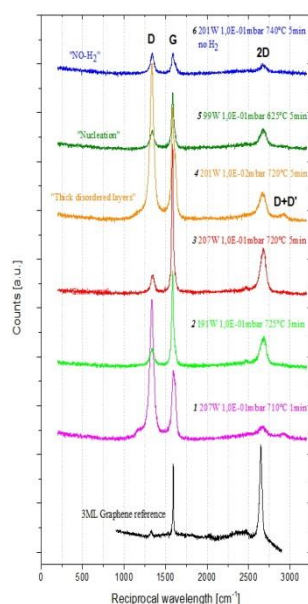
Remote Plasma Enhanced - Chemical Vapor Deposition (rPE-CVD) of Graphene on Various Substrates

Marc González Cuxart¹, Eric Pellegrin¹¹Institut Català de Nanociència i Nanotecnologia, Barcelona, Spain

Mechanical exfoliation of highly oriented pyrolytic graphite (HOPG) has been the most common method of producing single layers of graphene. However, the lateral dimensions of monolayer samples are typically limited to the micro-scale. Since large area graphene films on insulating substrates are required for practical applications, several techniques have been explored such as chemical vapor deposition (CVD) on transition metals, graphitization of SiC wafers under high vacuum, and reduction of oxidized graphite films.

Plasma Enhanced Chemical Vapor Deposition (PE-CVD) [1-3] makes the deposition method more tunable as it allows for an independent control of the reaction parameters and the growth parameters, which should lead to a better control of the size and shape of the nanostructures. Moreover, converting the precursor gas into a plasma state involves, by definition, a higher amount of active carbon radicals in the reaction process and thus enhances the deposition rate. By means of using a highly reactive deposition technique such as a hydrocarbon plasma, one can decrease the exposure time and/or decrease the substrate temperature. This latter feature opens the deposition process towards a wider variety of substrates with lower melting points. Last but not least, a remote plasma is – by definition - generated at a distance from the substrate, thus minimizing preferential perpendicular growth directions that the electrical fields may induce in a traditional plasma setup.

CELLS-ALBA together with ibss Group, Inc. has adapted the GV10x downstream inductively coupled RF plasma source typically used for cleaning hydrocarbon contaminated from SEM chambers to also remove carbon deposits on optical precision surfaces [4]. For these applications the feedstock gas of the plasma consists of a chemically active agent such as oxygen or hydrogen converting carbon into CO₂, CO, or hydrocarbons gas via a corresponding oxidation or reduction process, respectively.



P-Mo-022

Domain boundaries in merged graphene nanoislands
on Ni(111)

Sofia Parreiras^{1,2}, Cesar Moreno², Maximiliano Martins³, Roberto Paniago¹,
Gustavo Ceballos², Aitor Mugarza²

¹Universidade Federal De Minas Gerais - UFMG, Belo Horizonte, Brazil,

²Institut Català de Nanociència i Nanotecnologia - ICN2, Barcelona, Spain,

³Centro de Desenvolvimento da Tecnologia Nuclear - CDTN, Belo Horizonte, Brazil

The edge structure and stacking of graphene with respect to the substrate determine the properties of the graphene-metal interface as the equilibrium shape and growth kinetics and the interfacial electronic structure. Depending on the atomic structure, edges can induce band gaps by quantum confinement [1], or 1D spin-polarized states [2]. The Ni(111) substrate is particularly interesting due to the small mismatch between the two lattices and the strong interaction which can lead to the growth of isolated nanoislands with atomic-scale control on the morphology and edge structure [3]. The strong interaction stabilizes different type of edges depending on their stacking, and the capability of controlling it leads to a shape selection.

In this work we study how the bulk and edge structure of isolated graphene nanoislands grown on Ni(111) are affected by the coalescence at higher coverage. Graphene islands were prepared by CVD, exposing 10^{-8} mbar of propene to a surface at RT. After that the surface was post-annealed at 500°C for 5 min. At low coverage we observe isolated, slightly truncated triangular islands with the same orientation [3]. Atomically resolved STM images reveal that the long edges are zig-zag and the short ones are reconstructed pentagon-heptagon. The two C sublattices of the bulk are in the minimum energy top-hcp stacking and the nearly isoenergetic top-fcc stacking only appears for small enough size. For higher coverage, the islands' merging stabilizes top-fcc domains. The domain boundaries can be continuous with a smooth transition, or a well-defined periodic defect structure, as found for monolayers [4]. The edge structure of the merged islands will depend on the orientation and the bulk stacking of the local domain.

1.Y.W. Son et al., PRL 2006, 97, 216803

2.J. Fernández-Rossier et al., PRL 2007, 99, 177204

3.A. Garcia-Lekue et al., JPCC 2015, 119, 4072-4078

4.J. Lahiri et al., Nature Nanotech. 2010, 5, 326-329

P-Mo-023

On-surface assembly of graphene nanoribbons

Eduard Carbonell¹, Richard Balog^{1,2}, Maciej Topyla¹, Manuel Vilas⁴, Martina Corso^{1,2,3}, Jingcheng Li¹, Diego Peña⁴, Nacho Pascual^{1,2}

¹CIC Nanogune, Donostia-San Sebastian, Spain, ²IKERBASQUE, Bilbao, Spain,

³Centro de Física de Materiales, Donostia-San Sebastian, Spain, ⁴Universidad Santiago de Compostela, Santiago de Compostela, Spain

Graphene Nanoribbons (GNRs) are one dimensional graphene structures that have emerged as an approach to open a bandgap in graphene. Among the different families of GNRs, armchair GNRs (AGNRs) are a promising candidate for semiconducting applications as they possess a width dependent gap.

Bottom-up fabrication of GNRs has shown encouraging results as a controllable process to tailor the dimensions and the edge structure of nanoribbons with atomic precision. One of the most successful methods has been the on-surface reaction of brominated bianthracene monomers to form 7-AGNRs. Upon adsorption on a gold substrate, these monomers undergo a substrate mediated Ullmann coupling and a cyclodehydrogenation step that yields the resulting 7-AGNRs.

In this work we expand the possibilities of this reaction in order to produce different widths of AGNRs from the same molecular precursor. Owing to a cascade intermolecular dehydrogenation between 7-AGNR, we are able to produce high quality 14-, 21- and 28-AGNRs. By means of Low Temperature Scanning Tunneling Microscope, we identify the reaction pathway and study the electronic properties of all the different resulting species of AGNRs.

Moreover, thanks to a custom-built precursor and the aforementioned on-surface reaction, we are able to synthesize semiconducting nanoribbons with attached periodically confined structures. This coupled nanoribbon-quantum dot system is a very interesting platform for potential optoelectronic applications.

P-Mo-024

Sorption properties of carbon nanotubes with different concentration of boron impurities

Sergei Boroznin¹, Irina Zaporotskova¹, Natalia Polikarpova¹

¹Volgograd State University, Volgograd, Russian Federation

The discovery of carbon NTs in the early nineties was followed by intensive investigation into their electronic structure and energy spectrum parameters as well as physical and chemical properties. Due to high surface activity nanotubes can be used as basis for fabricating various types of composites. However, apart from carbon nanotubes, current research focuses on theoretical and experimental investigation of non-carbon nanotubes, namely recently discovered boron-carbon nanotubes with different concentration of boron in it (25% or 50%). In this paper we present the results of theoretical research into the properties of two types of boron-carbon nanotubes (BCNTs) within the framework of an ionic-built covalent-cyclic cluster model and an appropriately modified MNDO quantum chemical scheme as well as DFT method. We studied the mechanism of Cl, O and F atoms sorption on the external surface of single-walled arm-chair nanotubes. We defined the optimal geometry of the sorption complexes and obtained the sorption energy values. Further, we considered the possibility of multiple regular adsorption of these atoms on the BCNT surface. We modeled the process of superlattice formation by gas atoms above the nanotube surface. The electron density is located near the surface atoms of the tube.

P-Mo-028

Improvement of strength properties of dental materials by using carbon nanotubes

Lusine Elbakyan¹, Irina Zaporotskova¹¹Vjlgograd State University, Volgograd, Russia

Nowadays polymeric materials have found wide application in medicine. It is suggested the technology of creating new polymeric dental composite materials on the basis of fast-curing dental plastics "Carbodont" by reinforcing it with carbon nanotubes. The use of carbon nanotubes as reinforcing element allows you to create a new composite material with unique properties and characteristics that will ensure its use in the production of high-quality and reliable materials. Carbon nanotubes, which has unprecedented mechanical properties are considered as effective means of improving the strength properties of composite polymer materials. Were the calculations and experiments to determine the optimal concentration of carbon nanotubes to create a composite polymeric material having improved operational characteristics.

DFT-calculations had been done with to determine the feasibility of adsorption mechanism of interaction of components of Carbodont with the surface of carbon nanotubes was performed [1] of the process of interaction of the basic polymer components of Carbodont (methyl methacrylate, butyl methacrylate, methacrylic acid) and single-layer carbon nanotube.

The results of measuring the hardness of a polymeric composite material based on dental plastic "Carbodont" reinforced carbon nanotubes, led to the conclusion that with the introduction of carbon nanotubes in a total volume of the polymer matrix of Carbodont in the amount of 0.05 % provides a significant improvement in the operational characteristics of dental plastics without critical deterioration of its color characteristics. Theoretical calculations based on DFT method proved that the mechanism providing a good pairing polymer base matrix with reinforcing carbon nanotubes, is adsorption interaction of the main components of Carbodont with the surface of carbon nanotubes. Such polymer systems are useful for creating dentures, fabricating orthodontic appliances, temporary dentures, individual impression trays.

[1] Zaporotskova I.V., Carbon and non-carbon nanomaterials and composite structures on their basis: structure and electronic properties. – Volgograd. Of VolSU, 2009, 490 p.

P-Mo-029

Transport properties of polycrystalline CVD graphene during Gallium deposition

Pavel Procházka^{1,2}, Jindřich Mach^{1,2}, Jakub Piastek¹, Miroslav Bartošík^{1,2},
Zuzana Lišková^{1,2}, Tomáš Šikola^{1,2}

¹Institute of Physical Engineering, Brno University of Technology, Faculty of Mechanical Engineering, Brno, Czech Republic, ²CEITEC BUT, Brno University of Technology, Brno, Czech Republic

Graphene-metal nanoparticle composites form a novel class of materials suitable for an enhancement of the device performance in numerous applications such as plasmon-based photonics [1], plasmon enhanced graphene-based photodetectors [2], plasmon assisted photocatalysis [3], sensors [4] and solar cells [5].

Gallium is one of the possible candidates for future graphene-metal devices. It is a sp metal that predominantly forms ionic bonds with graphene. Hence, there is not a strong hybridization between the pz orbitals of graphene and valence electrons of Ga. Also, a weak bonding charge yields a minimal distortion of the graphene lattice. Furthermore, Ga and carbon atoms are also insoluble, a characteristic that preserves the graphene structure. Additionally, Ga may even produce a "catalytic" effect in preserving and reconstructing the sp² structure of graphene. Finally, Ga is one of the relatively few metals that are themselves Raman active. The interface Ga-graphene electrons transfer from Ga to graphene which may enter the π^* state, giving a " π -doping" effect.

In this presentation we show how the transport properties of polycrystalline graphene produced by Chemical Vapor Deposition (CVD) were changing during deposition of Ga atoms by an e-beam effusion cell under UHV conditions. It has been found that the Dirac point of nanostructures determined in situ from I-Vg curves moves significantly with the Ga coverage towards lower voltage values (at maximum from +70 to -70 V). Influence of specific gases as oxygen and nitrogen, and water vapour on such behaviour will be reported as well.

[1] R. Zan, et al, Small, 7, 2868-2872, (2011).

[2] T. Echtermeyer, et al., Nat. Commun., 2, 458-464, (2011).

[3] Y. Wen, et al, Nanoscale, 3, 4411-4417, (2011).

[4] H. Jiang, Small, 7, 2413-2427, (2011).

[5] V. D. Dao, et al., Nanoscale, 10.1039/C3NR03219A (2013).

P-Mo-030

Charge transfer between separated graphene sheets studied by Kelvin probe force microscopy in ambient conditions

Martin Konečný^{1,2}, Miroslav Bartošík^{1,2}, Pavel Procházka^{1,2}, Jindřich Mach^{1,2},
Peter Varga^{1,2}, Tomáš Šikola^{1,2}

¹Institute of Physical Engineering, Brno University of Technology, Brno, Czech Republic, ²CEITEC BUT, Brno University of Technology, Brno, Czech Republic

The electrical communication in terms of charge transfer between separated graphene sheets on insulating substrates may have a great impact on the functionality of future graphene nanoelectronic devices. Therefore, the understanding of these phenomena will play a crucial role in design of such devices. Here, we report on the possible utilization of scanning probe force microscopy for injection of electrical charge into an isolated graphene sheets transferred on SiO₂/Si wafers, and on characterization of charge transfer enhanced under controlled ambient conditions. The charge transfer itself is monitored by surface potential measurements using Kelvin probe force microscopy (KPFM). It is shown that the discharging and transport of charges increase as a function of relative humidity, and consequently, we propose that the charge-transport is mainly realized through water adsorbed on the SiO₂ surface. The experimental work will be supported by relevant charge transfer simulations.

P-Mo-032

Adsorption behaviors of nano-porous activated carbon produced from agricultural residues

Kamal Khalil¹, Omar Allam¹¹Chemistry Department, Faculty of Science, Sohag University, Sohag, Egypt

Activated carbon (AC) as carbon-based nano-porous material is very effective adsorbent for many organic compounds, as well as large number of inorganic metal ions including toxic or hazardous. AC is generally termed as "The Universal Adsorbent" because it is useful for treating municipal drinking water, as well as, a variety of waste streams including pesticide wastes, hazardous industrial wastes, municipal waste-waters, petroleum refinery and textile waste-waters [1]. There are a vast number of investigations reported in literature for conversion of agricultural biomass to ACs [1, 2]. This work aims to get rid, usefully utilize the available residues in production of efficient adsorbents and to explore their surface reactivity. In addition, this will help climate change mitigation.

In the work dried agriculture residue obtained from crop grown in Upper Egypt were crushed, then impregnated with ZnCl₂ solution of different concentrations. After aging and drying the materials were thermally treated at 400, 500 and 500°C for 1h in flow of N₂ gas. The obtained materials were characterized by FTIR, XRD and combined TGA-DTA analysis, and N₂ adsorption/desorption measurement and its related analyses. High BET surface area values in the range of (1470-1830 m²/g) with very high mesoporous contents were obtained. Parameters that control the formation of micro/meso pore structure were correlated to the activation temperature and ZnCl₂ solution concentration. The adsorption behavior and kinetics of the obtained materials towards methylene blue and phenol were examined. High adsorption capacity amounts to 383 mg/g for methylene blue; and 106 mg/g for phenol where obtained, respectively.

This approach facilitates production of different activated carbons to face different pollutants and help environmental removal of the agriculture residues.

1.O. Ioannidou, A. Zabaniotou, Renewable and Sustainable Energy Reviews 11 (2007) 1966–2005.

2.D. Mohan, A. Sarswat, Y.S. Ok, C.U. Pittman, Bioresource Technology 160 (2014) 191–202.

P-Mo-033

Control of microstructure of clad wire with multifilament attacked inside

Haguk Jeong¹, Jong-beom Lee¹¹Korea Institute of Industrial Technology, Incheon, South Korea

Superconducting wire is made of superconducting materials which, when cooled below its transition temperature, has zero electrical resistance. In recent, most of superconductors are formed in filament or tape shape. The superconducting wire in the filament form, many number of monofilament wires are packed inside a second tube which is then subjected to several plastic deformations like extrusion, swaging, rolling, drawing to obtain the desired cross-section and longitudinal-shape. In order to obtain desired cross-section and longitudinal-shape in long wire with multifilament structure, manufacturing process parameters must be precisely controlled during the creation of the wire. In the deformation process, the most important factor is to keep the interface states in harmony with material having different mechanical properties. Hydrostatic extrusion technique is very useful process for fabrication of hybrid or clad structured wire with multifilament stacked inside, because uniform metal flow, between materials having different properties each other, can be easily obtained during the deformation. In the present study, a warm hydrostatic extrusion process, prior to fabricate wire, was applied to fabricate some kind of clad composites (Cu, Al, Ti, CNT) with multifilament structure. In order to investigate the effect of the interface states depending on several process conditions, extrusion schedule prior to work, likes heat-treatment condition, surface condition, schedule of working passes were accurately controlled. As control the process conditions, electrical and thermal properties, interface structure and microstructure in cross-section were varied as expected.

P-Mo-034

XMCD-PEEM and ARPES study of the twinned Ni_{49.7}Mn_{29.1}Ga_{21.2}(100) martensite crystal

Yaroslav Polyak¹, Vladimír Cháb¹, Oleg Heczko¹, Jaromír Kopeček¹, Jan Honolka¹, Ján Lančok¹, Josef Kudrnovský¹, Václav Drchal¹, Ladislav Fekete¹, Vitaliy Feyer²

¹Institute of Physics CAS, Prague, Czech Republic, ²Sincrotrone Trieste, Basovizza, Italy

We have studied the magnetic domain microstructure at the surface of a weakly off-stoichiometric Ni_{49.7}Mn_{29.1}Ga_{21.2}(100) martensite monocrystal by means of X-Ray Magnetic Circular Dichroism (XMCD) in conjunction with the photoemission electron microscopy (PEEM). The measurements were performed at NanoESCA beamline of the synchrotron radiation (SR) facility Elettra in Trieste. The in-plane and out-of-plane magnetic domains were clearly resolved in the recorded XMCD-PEEM images. The element selective magnetic microstructure was observed only at the Mn L_{2,3} X-ray absorption edge. The magnetic moment in Ni_{49.7}Mn_{29.1}Ga_{21.2}(100) single martensite crystal is mainly localized on Mn sites while Ni atoms carry only a small magnetic moment. The magnetic domain contrast in the twinned martensitic phase was also observed with the help of the magnetic force microscopy (MFM) which is in very good agreement with the results of the XMCD-PEEM measurements. The dramatic change of the magnetic domain pattern was obtained after annealing of the sample at 820 K. Low-energy electron diffraction (LEED) measurements were performed to check the surface structure of Ni_{49.7}Mn_{29.1}Ga_{21.2}(100) single crystal. LEED imaging of the twinned martensite exhibits the characteristic superlattice diffraction pattern indicating a periodic modulation of 5M pseudotetragonal structure. We have calculated the electronic structure and angular-resolved photoemission spectra (ARPES) of a weakly off-stoichiometric Ni_{49.7}Mn_{29.1}Ga_{21.2}(100) Heusler alloy from the first principle applying the tight-binding linear muffin-tin orbital (TB-LMTO) method. The disorder, caused either by non-stoichiometry, or by swapping of atoms between sublattices is considered within the framework of the coherent potential approximation (CPA). Matrix elements are included in the electric dipole approximation. Theoretical results are compared with the k-space measurements provided with the linear horizontal and vertical as well as circular left and right polarized SR in order to clarify the distinct features of the Fermi surface map in the martensitic phase.

P-Mo-035

Enhanced magnetic anisotropy in self-organized (Fe,Co) nanodots

Cyril Chacon¹, Jean.Baptiste Marie¹, Yann Girard¹, Pr Vincent Repain¹, Jérôme Lagoute¹, Sylvie Rousset¹, Emiliano Fonda², Philippe Ohresser², Hélène Magnan³

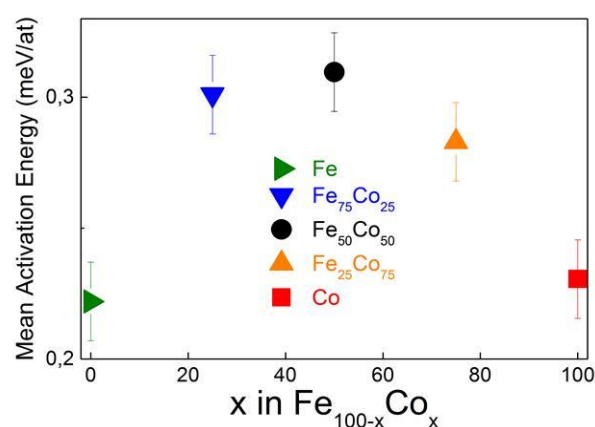
¹Laboratoire MPQ / Université Paris Diderot et CNRS, Paris, France,

²Synchrotron Soleil, Gif-sur-Yvette, France, ³SPCSI / IRAMIS / CEA, Gif-sur-Yvette, France

The design of self-organized nanodots with superior magnetic properties up to room temperature remains a major challenge. These nanostructures are forecast as models candidates for the next generation of hard-disks. In particular, nanodots made of cobalt and iron are expected to have unrivaled magnetic properties such as high anisotropy and ordering temperature or strong magnetization. However, it is rather challenging to know the exact structure and chemical composition of these clusters and only few experimental techniques are able to give valuable information down to the nanometer scale.

In this study, we have investigated the growth and the magnetic properties of nano-clusters obtained by co-deposition on a Au(111) substrate. The herringbone reconstruction acts as a guide for nucleation and self-organization of the bi-metallic clusters. The evolution of the cluster's morphologies in function of the Co concentration has been revealed by STM, XMCD, and AC-magnetic susceptibility measurements were performed thanks to a in-situ MOKE set up in order to get the average magnetic anisotropy energy per atom for each (Co,Fe) co-deposition.

The growth of (Co,Fe) clusters on the Au(111) surface observed by STM revealed a morphological transition from single layer to bilayer islands with the Co concentration as well as a structural change. The magnetic measurements show a clear dependence of the blocking temperature of these superparamagnetic nanodots on the sample composition. As a consequence, the energy of activation is enhanced up to a factor of three and the highest value is reach for a composition with the same amount of each element (see figure). A complete study of the Fe₅₀Co₅₀ composition using XMCD at low temperature and with high magnetic field will be given. Finally, a comparison with (Co,Pt) nanodots or similar core-shell or systems obtained by subsequent deposition will be given.



P-Mo-036

Ballistic electron emission microscopy: a tool for ultrathin films magnetic imaging with a nanometer resolution

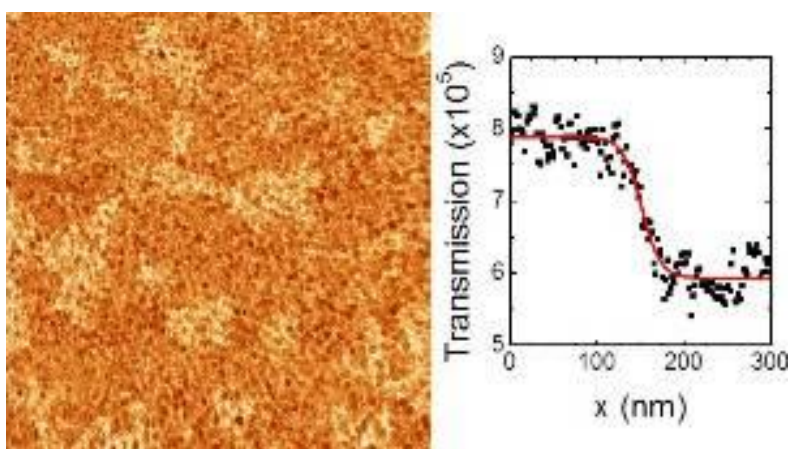
Stanislas Rohart¹, Ian Aupiais¹, André Thiaville¹¹Université Paris-Sud, Orsay, France, Orsay, France

Magnetic imaging in perpendicular magnetization layers is a real challenge as the typical length scale, the so-called Bloch domain wall parameter can be as small as few nanometers. Beyond domain walls, research perspectives on skyrmions create a real need for versatile tools for imaging. Here we demonstrate the ability of ballistic electron emission microscopy based on a scanning tunneling microscope to image domain walls and nanodomains (100-200 nm diameter) with a resolution of a few nanometers, in buried ultrathin magnetic layers.

We study domains and domain walls in a Au/Co(1.2 nm)/Pt sandwich, which presents a perpendicular magnetization easy axis. The asymmetric stacking, with large spin-orbital layers should promote Dzyaloshinskii-Moriya interaction, consequently lower domain wall energy and thus stabilize ultra small domains. The sandwich is deposited on a Si(111)/Au Schottky diode needed to filter the ballistic electrons in the BEEM and a Au/Co(1.2 nm)/Au sandwich, always magnetized in a uniform state, which acts as a spin analyzer and allows imaging the out-of-plane magnetization component of the magnetic layer under study. The magnetic domains have been created by sweeping a perpendicular magnetic field under the control of a magneto-optical microscope.

We have observed a high density (several on any of the $2 \times 2 \mu\text{m}^2$ images) of small domains which indicates that domain wall energy should be small in this sample. Profiles made on domain walls show the high quality of the images and give a domain wall width of 21 nm in good agreement with expectations. These images augur well for future studies, particularly on skyrmions.

Image: $2 \times 2 \mu\text{m}^2$ BEEM image showing magnetic domains. The profile taken on a domain wall shows a 21 ± 2 nm domain wall width.



P-Mo-037

This paper has been withdrawn by the author.

P-Mo-039

In-situ electrochemical atomic force microscopy study of the evolution of Pt-Co thin film catalyst during electrochemical aging test

Ivan Khalakhan¹, Mykhailo Vorokhta¹, Michal Václavů¹, Roman Fiala¹, Iva Matolínová¹, Vladimír Matolín¹

¹Charles University in Prague, Prague, Czech Republic

A Pt-Co thin film catalyst was prepared by using simultaneous magnetron sputtering of Pt and Co and showed high activity on a cathode side of a proton exchange membrane fuel cell (PEMFC). By combining for the first time in situ electrochemical atomic force microscopy (EC-AFM) technique with ex-situ energy dispersive X-ray spectroscopy (EDX) and photoelectron spectroscopies (XPS and SRPES) we accelerate electrochemical aging test and have shown that the Pt-Co thin film catalyst transforms under electrochemical aging test, forming Pt skin layer due to Co leaching. The similar transformation process was proved to occur in real membrane electrode assembly of the fuel cell.

P-Mo-040

Elaboration and characterisation of ZnO-Cu thin films
by thermal evaporationDergham Driss¹, Salim Hassani¹, Ouchaabane Mohamed¹, Lakoui Fouaz¹¹Advanced Technology Development Center (CDTA), Algiers, Algeria

ZnO, and ZnO-Cu thin films were synthesis by thermal evaporation technique, the samples were annealed at 300°C, 500°C, for one hour, the as deposited samples were characterized by X-ray diffraction (XRD), scanning electron microscopy (SEM), UV-VIS Spectroscopy and nanoindentation were used to study the optical and Nano hardness properties, of the films, respectively. The transmittance of ZnO-Cu thin films in the visible region was $\geq 90\%$, the grain size of the thin films was estimated from the Scherer's formula [1] by measuring the Full Width at Half Maximum peak Intensity (FWHM). Annealing at 300°C has no effect on the optical properties as annealing at 500°C improves the transparency of the films, on the other hand, the resistivity of the films increases for 300°C then decreases

P-Mo-041

Influence of the electrosynthesis method on the supercapacitive properties of polypyrrole

Ms Franciele Wolfart², Deepak P. Dubal¹, Marcio Vidotti², Pedro Gómez-Romero¹

¹Institut Català de Nanociència i Nanotecnologia - ICN2, Bellaterra, Barcelona, Spain, ²Universidade Federal do Paraná - UFPR, Curitiba, Brazil

Polypyrrole (PPy) is indeed one of the most investigated conducting polymers due to great specific advantages such as relatively easy polymerization, low cost, environmental and thermal stability, high conductivity and charge storage capability. Among the many applications for the use of PPy we can mention sensors and biosensors, anti-corrosion coatings, energy storage and drug delivery [1,2]. It is well known that the properties of PPy such as morphology, size and shape of nanostructures, conductivity etc. can be tuned by the synthetic methods used. Various approaches regarding the synthesis of polypyrrole have been reported before [2,3]. Among them, electropolymerization is a widespread method for the synthesis of PPy with the special advantage of variable modes of polymerization/deposition, namely, cyclic voltammetry (CV), galvanostatic (GS) and potentiostatic (PS) deposition [2]. With this investigation, we have probed the influence of different modes of electropolymerization on the supercapacitive properties of PPy films. To begin with, the electropolymerization of PPy on carbon cloth has been carried out using different electrochemical technique: CV, PS and GS modes. Later, these PPy films were studied by different physico-chemical techniques, such as XPS spectroscopy, SEM and TEM in order to study the surface morphology and structure and consequent effect on capacitive behaviour. The electrochemical properties of PPy films were investigated by cyclic voltammetry and galvanostatic charge/discharge techniques. Interestingly, different modes of electropolymerization significantly affect the supercapacitive properties of PPy thin films. Amongst the different electrodeposition modes presented here, PPy synthesized by potentiostatic mode exhibits maximum specific capacitance of 166 F/g with specific energy of 13 Wh/kg that was attributed to the presence of different oxidized states of PPy detected in the XPS analysis. Thus, the present investigation provides evidence on the suitability of electrodeposition methods for PPy films which can be used as promising materials for supercapacitors.

[1] *Reac.Funct.Polym.*,2001,47,125-139.

[2] *Chem.Soc.Rev.*,2000,29,(5),283-293.

[3] *Electrochim.Acta.*,2014,122,93-107.

P-Mo-042

Effects of Nb-doped MgH_2 in H desorption energy: A DFT approachEstefania German¹, Alfredo Juan¹¹IFISUR-CONICET, Bahia Blanca, Argentina

Magnesium hydride is one of the most promising candidates as hydrogen storage media in the automotive industry due to its very high capacity (7.6 wt%) and low cost. Nevertheless, a slow hydriding and dehydrogenating kinetics and a high dissociation temperature limit its practical application. The mechanical alloy of MgH_2 with transition metal elements has been experimentally proved to be an efficient method. We have studied the preferential site for Nb dopants on MgH_2 bulk, MgH_2 (001) and (110) surfaces to improve H desorption energy. Calculations have been carried out within the frame of DFT as implemented in the VASP code.

The studied bulk structure was simulated using a supercell containing 96 atoms and MgH_2 surfaces using a (2 x 2) slab with a 20 Å vacuum in the vertical direction. In order to avoid edge effects, the dopant was located at the center of the supercell, considering substitutional and interstitial configurations. Occupation energy is calculated to recognize the preference site of dopants in the structures and the relative stability of the systems. Positive values were obtained for all systems, this implies that the overall stability of doped bulk and surfaces is reduced comparing to pure systems. The dopant prefers to occupy interstitial sites, in these cases the energy cost to remove one H atom at 0 K is about 36% minor than in pure MgH_2 bulk and (001) surface, and 96% minor for (110) surface.

The more appropriate system for H desorption is MgH_2 (110) surface containing one interstitial Nb atom. The Mg-H bonds decrease their strength about 27% because of the dopant presence makes easier the dehydrogenation process. Dehydrogenation is improved due to the Nb occupation energy is low as well as the H desorption energy. Nb-H bonds are formed and Mg-H bonds are weakens allowing the process.

Table. Occupation energy (E_{occ}), dehydrogenation energy (E_{de}), overlap population (OP) and Metal-H distance (d) for MgH_2 bulk, surface (001) and (110) pure and doped systems.

System	E_{occ}	E_{de}	Mg-H OP-d (Å)	Nb-H OP-d (Å)
<i>bulk</i>				
MgH_2	-	1.634	0.272/1.86	-
$\text{MgH}_2\text{+Nb (S)}$	3.478	1.217	0.146/2.01	0.515/1.86-1.97
$\text{MgH}_2\text{+Nb (I)}$	2.514	1.046	0.109/2.07-2.09	0.428/1.90-1.99
<i>Surface (001)</i>				
MgH_2	-	1.376	0.427/1.80	-
$\text{MgH}_2\text{+Nb(S)}$	2.170	0.725	0.249/1.88	0.382/1.89-2.00
$\text{MgH}_2\text{+Nb(I)}$	1.950	0.888	0.170/2.06	0.438/1.90-2.00
<i>Surface (110)</i>				
MgH_2	-	1.590	0.240/1.90	-
$\text{MgH}_2\text{+Nb(S)}$	3.023	-0.610	0.127/2.04	0.453/1.95-2.00
$\text{MgH}_2\text{Nb(I)}$	1.643	0.070	0.176/ 2.05	0.429/ 1.83-1.90

P-Mo-043

Analysis of thin films Pd-catalysts prepared for DFAFC

Igor Bieloshapka¹, Petr Jiricek², Andrii Rednyk³, Mykhailo Vorokhta⁴

¹Institute of Physics, Academy of Sciences; MFF, Charles University, Prague, Czech Republic, ²Institute of Physics, Academy of Sciences, Prague, Czech Republic, ³MFF, Charles University, Prague, Czech Republic, ⁴MFF, Charles University, Prague, Czech Republic

Direct formic acid fuel cell (DFAFC) operating at low temperature (below 70°C) are promising source of electric power for the range of applications [1]. DFAFC has the advantages of high electromotive force (theoretical open circuit potential 1.48V), limited fuel crossover, and reasonable power densities at low temperatures [2].

A critical problem of Pd based catalysts is too high cost of this precious metal. Recently it was shown that Pd catalysts are better to work with DFAFC [3]. The non-reactive magnetron sputtering was used to prepare Pd thin films on anode. The sputtering was carried out in Ar atmosphere with total pressure of 4×10^{-1} Pa. Before starting the deposition the sputtering chamber was always evacuated up to 5×10^{-4} Pa. The described sputtering conditions gave a growth rate of the Pd films of 1 nm/min. Surface properties of these samples were characterized by X-ray photoelectron spectroscopy (XPS). XPS was performed in an ultrahigh vacuum experimental chamber operating at base pressures $< 8 \times 10^{-10}$ mbar. The XPS is applied for determination of surface composition and a content of Pd bonding. The Fuel Cell (FC) tests were performed by using a home-made device with pneumatically compressed graphite cell using 1000 kPa piston pressure. Membrane electrode assembly has active area of 1.5 cm² formed from the 0.05 mm thick Nafion membranes (DuPontInc., Nafion NR-212, perfluorosulfonic acid-PTFE copolymer), which was sandwiched by the catalyzed anode and cathode without hot pressing. The commercial carbon graphite gas diffusion layer with different coating of Pd layers was used as anode in a FC.

Obtained experimental data show chemical bondings of anode system elements after forming of the Pd layer during magnetron sputtering. Results help to understand preparation procedures of DFAFC catalytic system by magnetron sputtering.

P-Mo-044

Structural studies of hydrogenated silicon films prepared by RF magnetron sputtering

Fouzia Zeudmi Sahraoui¹, Aissa Kebab¹, Jamal Dine Sib¹, Yahia Bouizem¹,
Djamal Benlekhal¹, Iarbi chahed¹

¹University of Oran, Oran, Algeria

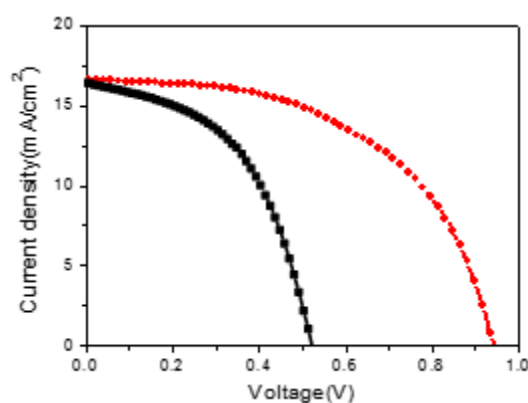
Hydrogenated nanocrystalline silicon films have become the subject of great attention due to their remarkable properties for microelectronics and solar cells technology. The structural changes in intrinsic silicon thin films deposited by radiofrequency (rf) magnetron sputtering at room temperature ($T_s = 35^\circ\text{C}$) are investigated as a function of the rf-power. The aim of this work is to get more insight into the effect of the rf-power. By varying the rf-power from 200 W to 500 W, and keeping all other parameters of the plasma constant (the total pressure is fixed at 4 Pa, the plasma gas mixture of 30% Argon and 70% H₂ and the target-sample holder distance of 50 mm). The composition and the microstructure of the films were analysed by X-ray diffractometry (XRD), atomic force microscopy (AFM), optical transmission measurements (OT) and spectroscopic ellipsometry. The results indicate that the films have nanocrystalline structures and the grain size decreases (5 to 2 nm) with increasing rf-power (200 to 500 W). The crystals are oriented generally towards the (111) plane, parallel to the sample surface. Analysis of the surface layers reveal that the Root Mean Square (RMS) surface roughness for the samples increases (11 to 43 nm) with increasing rf-power and the film thickness grows (1.4 to 3.7 μm).

P-Mo-045

Significant efficiency improvement of the ZnO nanorod arrays based perovskite solar cell through acid treatment

Bingjie Feng¹, Yang Xu¹¹Hubei University, Wuhan, China

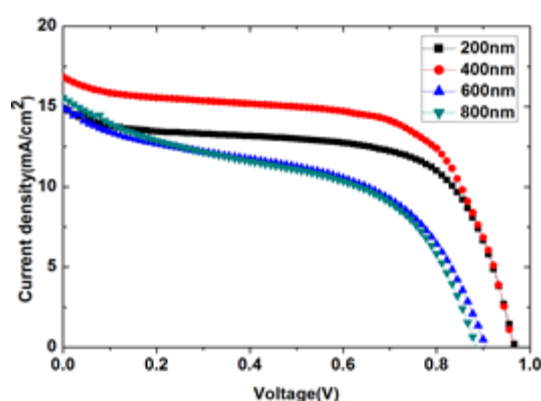
A research on the acid processed ZnO nanorod arrays based perovskite solar cell shows an impressive increase on the open-circuit voltage while the short-circuit current remains to be at the same level. The support structure for the light absorbing layer was constructed with a spin-coated ZnO seed layer and ZnO nanorod array using hydrothermal method. The enhancement of the V_{oc} can be related to the surface etching of the ZnO nanorod arrays. For further improvement of the cell performance, a series of different kinds of acid and process cycle time is conducted for an optimal treat time and the thickness of the ZnO nanorod arrays was also studied as well. As a result, samples without acid treatment acquired $V_{oc} \sim 0.53$ V, $J_{sc} \sim 16.45$ mA/cm² and FF $\sim 50\%$ which form an efficiency of about 4.38%, while a significant performance improvement of about 8.36% was achieved together with $V_{oc} \sim 0.94$ V, $J_{sc} \sim 16.6$ mA/cm² and FF $\sim 53\%$ for the sample with a nanorod thickness of ~ 800 nm under 1 time HCl treatment.



P-Mo-046

Effect of TiO₂ scaffold thickness on the photovoltaic performance of perovskite solar cellsHao Wang¹, Bingjie Feng¹¹Hubei University, Wuhan, china

Hybrid trihalide perovskite solar cells, which directly convert solar energy to electrical energy, exhibit the high power conversion efficiency (PCE), low cost, possibility of delivering all-solid-state photovoltaic devices, and represent promising renewable alternative to fossil fuels and traditional silicon-based solar cells. In typical mesoporous structural perovskite solar cells, the TiO₂ mesoporous layer provides a scaffold for the organolead halide and also transport the photogenerated electrons from the perovskite to conductive substrate and then to the external circuit. The thickness of the scaffold TiO₂ layer is an important factor for the photovoltaic performance of the perovskite solar cells. Here, the influence of TiO₂ scaffold thickness on the photovoltaic performance of perovskite solar cells were investigated. The thickness of the mesoporous TiO₂ scaffold was adjusted by varying the concentration of TiO₂ paste during spin coating. It was found that the PCE of perovskite solar cells increases from 8.89% to 10.03% when the thickness of scaffold layer rises from 200 nm to 400 nm, and then it drops gradually from 10.03% to 6.58% and further to 6.38% when the scaffold thickness increases from 400 nm to 600 nm and finally to 800 nm. The optimum PCE of 10.03%, short-circuit current density (J_{sc}) of 16.97 mA/cm², open-circuit voltage (V_{oc}) of 0.96 V and fill factor of 0.61 were achieved in cell with scaffold thickness of 400 nm. It should be contributed to the proper thickness of TiO₂ scaffold to absorb enough light from the organolead halide perovskite that covered onto the TiO₂ scaffold, exhibit fast transportation of electrons as well as the minimized recombination between the electrons and the holes.



P-Mo-049

Oxygen adsorption on the C60 cage of PC60BM and its influence on the O 1s XPS and NEXAFS spectra

Barbara Brena¹, Iulia Emilia Brumboiu¹, Leif Ericsson², Rickard Hansson², Ellen Moons², Olle Eriksson¹

¹Department of Physics and Astronomy, Uppsala University, Uppsala, Sweden,

²Department of Engineering and Physics, Karlstad University, Karlstad, Sweden

Organic photovoltaics (OPVs) have been steadily developing in recent years as a viable alternative to existing technologies [1,2,3]. The low production cost, short energy payback time and high energy return factors, alongside the possibility of large scale production of flexible devices all give OPVs very interesting prospects for the energy market [1,2,3]. Before this type of technology can actually become competitive, the stability issues of both the electron donor and the electron acceptor [3] must be addressed.

As a continuation to a C1s near edge x-ray absorption fine structure (NEXAFS) study of the electron acceptor PC₆₀BM (a fullerene derivative) [4], the current work addresses the oxidation of its C₆₀ molecular moiety. Oxidation has been proposed as a possible degradation mechanisms in the case of PC₆₀BM [5, 6]. Specifically, we have analysed in detail several final products of oxygen adsorption by means of density functional theory. For each relaxed molecular structure the O 1s NEXAFS and O 1s x-ray photoelectron (XPS) spectra have been calculated in the same theoretical framework. Our study shows that when the exclusive presence of oxygen is known, a combined O1s XPS and NEXAFS experiment can provide information on both the nature of the adsorbate (molecular or atomic oxygen) as well as of the bonding configuration at the adsorption site [7].

[1] N. Espinosa et al., Energy Environ. Sci., 5 (2012), 5117-5132

[1] N. Espinosa et al., Sol. Energy Mater. Sol. Cells, 95 (2011), 1293-1302

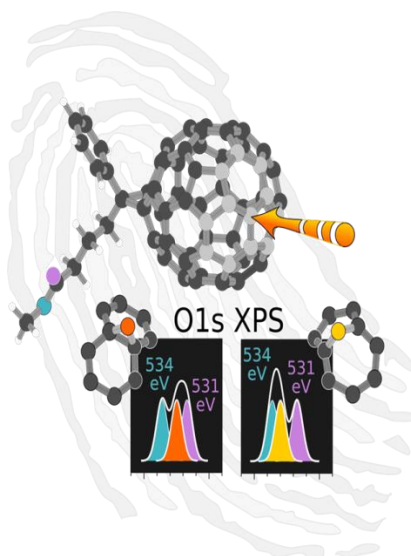
[2] M. Jørgensen et al., Adv. Mat., 24 (2012), 580-612

[4] I. E. Brumboiu et al., Chem. Phys. Lett, 568-569 (2013), 130-134

[5] M. O. Reese et al., Adv. Funct. Mater., 20 (2010), 3476-3483

[6] G. Volonakis et al., Org. Electron., 14 (2013), page 1242-1248

[7] I. E. Brumboiu et al., J. Chem. Phys., 142 (2015), 054306



P-Mo-050

Spectroscopic impedance analysis of Metal-Insulator-semiconductor based on Al₂O₃ dielectric thin films on silicon for solar cells applications

Lyes Zougar¹, Samira SALI¹, Salim Kermadi¹, Khadidja Mahdid¹, Messaoud Boumaour¹, Mohamed Kechouane²

¹Research Center in Semiconductors Technology for Energy, Algiers, Algeria,

²Houari Boumediene University, Faculty of Physics, Algiers, Algeria

Aluminum oxide thin films have received an increasing amount of interest because of their application for the surface passivation of crystalline solar cell. Surface passivation of c-Si solar cell with aluminum oxide is a good candidate for both p-and n type silicon due to its very high negative fixed charge density in combination with a low level of interface state density. The thin films Aluminum oxide were deposited on n-type silicon substrates by the spray ultrasonic technique at temperatures ranging from 300 to 420°C. After deposition and after anneal at 400°C in N₂ atmosphere for 30 mn, we analyzed the electrical properties of Al/Al₂O₃/n-Si (MOS) capacitor by impedance spectroscopy in wide frequency range. Effect of the deposition temperature on interface state density D_{it} and fixed charge density Q_f is investigated. The equivalent circuit model consisting of a parallel resistor (R_p) and capacitor (C_p) in series was found to give a well fit to the measured data of MOS capacitor. The values of resistors and capacitor were obtained from the Cole-Cole plots indicating a single semicircle. Keywords: Spectroscopic impedance; surface passivation; solar cells; Al₂O₃ dielectric thin films; spray ultrasonic

P-Mo-051

Solar cell metallization: from the electroless Ni nucleation to the NiSi setting up

Elise Delbos^{1,2}, Hanane El Belghiti^{1,2}, Damien Aureau², Muriel Bouttemy²,
Arnaud Etcheberry²

¹KMG Ultra Pure Chemicals, Saint-Fromond, France, ²Institut Lavoisier de
Versailles, Versailles, France

The increase of solar cells efficiency is of great interest for the scientific and industrial communities. Several researches are managed these years to elaborate new absorbers or optimize existing configurations (multi-layers, surface roughening...). Another challenging field concerns the replacement of silver contact lines, currently made by serigraphy, by cheaper materials and processes without damaging the cells efficiency. Our objective is to develop a nickel/copper lines elaboration method for Silicon cells technology, based on electroless and electrolytic deposition processes. First, an electroless nickel-phosphorus layer is deposited to ensure a barrier role against detrimental copper diffusion throughout the silicon substrate. Then, this nickel-phosphorus layer is annealed to obtain specifically NiSi composite, necessary to guarantee the desired contact adherence and the low contact resistance (14 $\mu\Omega\text{cm}$).

Initially, to optimize the process, an accurate understanding of the nickel-phosphorus electroless mechanism is necessary. The main step consists in controlling the nickel nucleation on silicon at very short times. Therefore, we propose a specific study dedicated to these preliminary steps, carried-out on textured PV silicon, with a multiple approach. The surface evolution is characterized combining complementary methods: imaging by SEM, surface chemistry by XPS and nano-Auger. In addition, the evolution of the silicon open circuit potential versus time, in electroless nickel solution, is studied in-situ. The correlation between the OPC value and the progressive nickel coverage of the silicon surface will be presented. A second critical point is the determination of the optimal nickel-phosphorus layer thickness and annealing conditions to form a high efficiency nickel silicide. Thus, SEM, EDS and XPS profiling are employed to determine the influence of both nickel-phosphorus coverage ratio with plating time and initial nickel-phosphorus thickness on the Ni diffusion depth throughout the silicon during annealing under Ar/5% H₂ atmosphere.

Acknowledgements: The authors thank the ANR (ANR-11-PRGE-004) for funding and INES for providing silicon substrates.

P-Mo-052

Structural Study of radiation induced Ni-Mg nanoparticles in Ni/MgO catalysts

Nassira Keghouche¹, Nora Ouafek¹, Emérite Jaqueline Belloni²

¹Laboratoire Microstructures et Défauts dans les Matériaux. Université Frères Mentouri - Constantine, Constantine, Algeria, ²Laboratoire de Chimie Physique, UMR CNRS/UPS 8000, ELYSE, Université Paris-Sud université Paris 11, CNRS, Orsay, France

Intermetallic compounds have received attention because of their potential applications in the energy field. Several new and good hydrogen storage alloys were studied. Among them, the most promising candidates are Mg-based metallic hydrides in view of their major advantages such as low specific weight, low cost and high hydrogen storage ability. In the nanometric scale, these materials exhibit size dependant properties. Particularly, their absorption/desorption capacity is enhanced. When these phases are present in catalysts, their activity in hydrogenation reactions can be improved.

In the present study, Ni/MgO catalysts are prepared by ionic exchange of Ni²⁺ ions with magnesium oxide followed by calcination (T=100-600°C) and H₂ reduction or by gamma irradiation. The structural and surface properties of samples are studied by XRD, TEM, HRTEM, SAED, FTIR and XPS techniques, at several stages of their preparation.

The XRD patterns reveal the presence of MgO, Ni₂Mg, MgNi₂ and Mg(OH)₂. The later phase disappears progressively after calcination. The HRTEM correlated to SAED study demonstrates that Ni-Mg intermetallic phases are untimely alloyed in the nanometric scale (2-4 nm). In addition NiO is detected by TEM, which indicates the presence also of highly dispersed nickel.

Key words: Intermetallic phases ; Ni-Mg ; nanoparticles ; XRD ; TEM

P-Mo-053

Conductive and transparent ZnO-based multilayer thin film electrodes for solar cell applications

Salim Hassani¹, Racha Hadj Ali², Ibtissem Djemai², Fouaz Lekoui¹, Mohamed Kechouane², Ahmed Taleb²

¹Centre de Développement des Technologies Avancées (CDTA), Baba Hassen Algiers, Algeria, ²Université des Sciences et Technologies Houari Boumediene (USTHB), Bab Ezzouar, Algiers, Algeria

Conductive and transparent multilayer thin films consisting of three alternating layers of Metal oxide/Metal/Metal oxide were prepared for applications as transparent conductive oxide (TCO) in Dye Sensitized Solar Cells (DSSC). Specifically in this work, two types of multilayer systems were investigated: ZnO/Cu/ZnO and ZnO/Au-Pd/ZnO. The films were prepared by successive deposition steps consisting of vacuum thermal evaporation followed by heat treatment at 450 °C. The thickness of the metallic interlayer (Cu or Au-Pd) was varied in order to optimize the optical and electrical properties of the stack. Morphology and microstructure of the films were investigated by SEM and XRD. Electrical properties were investigated by four point probe and the transmittance values were measured using a spectrophotometer. The best conductivity was found when Cu films were used as interlayer while a better transmittance is measured for multilayer stacks containing Au-Pd interlayer. An optimized configuration of the ZnO/Me/ZnO multilayer film system is discussed as a good candidate for application as electrode in solar cells.

P-Mo-054

Experimental study on the heat transfer performance of titanium fiber porous materials

Liu Shifeng¹

¹Xian University of Architecture and Technology, Xi'An, China

The titanium fiber porous materials of different parameters were prepared by sintering process. The key point of this project is researching the influence of materials structure parameters of thickness, porosity, wire diameter and sintering time to its pool boiling heat transfer performance. The result show that: the heat transfer effect reached to the best when the sintering time was 2h; the heat transfer performance of titanium fiber porous materials didn't show the trend of increasing or decreasing with the change of its wire diameter and thickness; the heat transfer effect reached to the best when the porosity was 50%.

P-Mo-055

Stainless steel surfaces studied by XPEEM

Lisa Rullik¹, Yuran Niu², Eleonora Bettini³, Alexei A. Zakharov², Jinshan Pan⁴,
Edvin Lundgren¹

¹Lund University, Lund, Sweden, ²MAX IV Laboratory, Lund, Sweden, ³AB Sandvik Materials Technology, Sandviken, Sweden, ⁴KTH Royal Institute of Technology, Stockholm, Sweden

Steels have been subject to major research efforts because of their industrial importance. Even though new steels have been developed continuously there is a significant demand for more advanced steels with improved corrosion resistance. To improve the corrosion resistance it is crucial to understand the composition, thickness and stability of their passive films. Especially duplex stainless steels are a challenge regarding their passive films because of their two-phase microstructure, usually consisting of an equal amount of ferrite and austenite. Thermal or mechanical treatment can lead to a deviation from this ratio and the formation of new phases.

Numerous spectroscopy and microscopy techniques, have been used to study the passive layer. However, questions about the chemical composition and the relation to the underlying microstructure remain. By approaching this issue with XPEEM (X-ray Photoemission Electron Microscopy) it allows to map the lateral variations of the different alloying elements and their chemical states, which are present at the surface region. Further, XPEEM can be used in combination with MEM (Mirror Electron Microscopy), which provides information about the sample's topography and work function differences. By relating the information of these techniques austenitic and ferritic phases as well as inhomogeneities within the surface layer can be identified.

In this contribution, we will present recent result from an XPEEM study on super duplex stainless steels that were studied after polishing, polished and immersed in 1-M NaCl solution for 2h, and polished and electrochemical polarized at 0.9V against Ag/AgCl in 1-M NaCl solution for 30min. Partitioning of the different alloying elements and differences in the oxide layer thickness depending on the phase were observed. Furthermore, the chemical states of the different elements were studied by μ -XPS (micro-X-ray Photoelectron Spectroscopy) and μ -XAS (micro- X-ray absorption spectroscopy) to support the XPEEM results.

P-Mo-056

Effect of B content on the amorphization process of the mechanically alloyed Fe-Nb-B powders

Nadia Bensebaa¹, Thaouanza Chabi¹, Safia Alleg¹, Sonia Azzaza¹, Joan Josep Sunol², Jean Marc Grenèche³

¹Laboratoire de Magnétisme et de Spectroscopie des solides Département de Physique, Faculté des Sciences, Université Badji Mokhtar, Annaba, Algeria,

²Dep. de Física, Universitat de Girona, Campus Montilivi, Girona, Spain,

³Laboratoire de Physique de l'Etat Condensé, CNRS UMR 6087, Université du Maine, Le Mans Cedex 9, France

Nanocrystalline Fe₈₇Nb₈B₅ and Fe₈₂Nb₈B₁₀ powder mixtures were prepared by mechanical alloying from elemental Fe, Nb and B powders in a planetary ball mill Retsch PM400 [1-4]. Scanning electron microscopy, X-ray powder diffractometry, transmission mössbauer spectroscopy and differential scanning calorimetry were carried out to investigate morphological, structural, magnetic properties changes and thermal stability during the milling process. After 50 h of milling, the end product is an amorphous matrix with a proportion of 53% and 67% for Fe₈₇Nb₈B₅ and Fe₈₂Nb₈B₁₀ alloys, respectively, where nanocrystalline bcc Fe (Nb, B), Nb (B) and bcc Fe₂B phases are embedded. The DSC scan reveals the existence of several exothermic and endothermic peaks related to the structural relaxation, recovery and grain growth. The endothermic peaks at about 609°C can be attributed to the magnetic transition of Fe₂B phase.

[1] Suryanarayana C Mechanical alloying and milling. Marcel Dekker. 457, 2004.

[2] Bensebaa N, Alleg S, Bentayeb FZ, Bessais L, Greneche JM Microstructural characterization of Fe-Cr-P-C powder mixture prepared by ball milling. J. Alloys Compd. 388:41-48, 2005.

[3] Alleg S, Azzaza S, Bensalem R, Suñol JJ, Khene S, Fillion G Magnetic and structural studies of mechanically alloyed (Fe50Co50)62Nb8B30 powder mixtures. J. Alloys Compd. 482: 86-89, 2009.

[4] Souilah S, Alleg S, Djebbari C, Suñol JJ Magnetic and microstructural properties of the mechanically alloyed Fe57Co21Nb7B15 powder mixture. Mat. Chem. Phys. 132: 766-772, 2012.

P-Mo-057

Fabrication and Shape Control of a Single Ag Nanoparticle Using Scanning Tunneling Microscopy

Satoshi Katano¹, Masaki Hotsuki¹, Yoichi Uehara¹¹Tohoku University, Sendai, Japan

Metal nanoparticles (NP) have received much attention because of their unique electronic and optical properties. In particular, the strong enhancement of the electric field associated with localized surface plasmon (LSP) excitations on noble metal NPs plays a key role in various applications such as biosensing devices. The enhancement of the electric field is known to be sensitive to the size, shape and separation distance of the metal NPs. Thus, it is necessary to control these geometric parameters precisely in order to utilize metal NPs as a nano-scale optoelectronic device. In this paper we report the creation and shape control of a single silver NP (AgNP) on Si(111) by scanning tunneling microscope (STM).

All experiments were performed in the ultrahigh vacuum (UHV) chamber. The based pressure was 10^{-10} Torr. The Si(111) sample was cut from n-type wafers and was cleaned by the flash heating in UHV. The STM tip was an Ag wire which was sharpened by the electrochemical etching in solution of $\text{HClO}_4/\text{CH}_3\text{OH}$.

A single AgNP was created reproducibly beneath the STM tip by the application of the voltage pulse (-6 V). The large size of AgNP is formed preferentially when the lower voltage was used. Furthermore, we found that AgNP was stretched in a direction toward the STM tip by applying the positive voltage pulse. Note that this kind of structural change occurs when the voltage exceed 4 V. Regarding the bias dependence, we assume that the STM tip-induced AgNP modification is associated with the field evaporation. In the presentation, we also report the result of the STM light emission spectroscopy applied to the AgNP/Si(111) system.

P-Mo-058

Stress Control Factor of Tungsten Thin Film by Chemical Vapor Deposition

Dong-Hoon Han¹, Kyunghwan Lee¹, Seon-Woo Kim¹, Sunsoo Lee¹, Yoonbon Koo¹, Kyengmo Koo¹, Youngchae Seo¹, Jeonghoon Nam¹, Kangsoo Kim¹

¹Samsung Electronics Co. LTD, Hwasung, South Korea

As a feature size of memory devices decreased, demands of a stress control of the films has grown. W film has high tensile stress (~2GPa) with usual procedure of CVD in the memory fabrication. So, finding the control factor of the W film stress is important without loss of pattern fill capability and electrical resistivity. In this paper, the effects of nucleation layer and underlying film on the W film properties, e.g. stress and resistivity were presented. W nucleation layers were deposited by using two different reaction schemes, one is with dibolane reducing agent and the other is with silane. And titanium nitride and tungsten nitride were prepared as underlying film. It was found that electrical resistivity and stress has a correlation and stress is managed by controlling concentration of reducing agent in the specific deposition sequence. From these results W film stress which has thickness ~1500Å was reduced to 1.5GPa with keeping fill capability. By using X-ray diffraction (XRD) and X-ray reflectivity (XRR), effect of tungsten phase and density were analyzed.

P-Mo-059

Structural and EPR studies of Cr doped ZnO thin films

Osman Gürbüz¹, Sadık Güner²¹Yıldız Technical University, Istanbul, Turkey, ²Fatih University, Istanbul, Turkey

Wide band gap II–VI semiconductors have been the focus of interest of many research groups during the past few years due to the possibility of their applications in light-emitting diodes (LEDs), sensors and laser diodes. Among the II–VI functional semiconductor materials, zinc oxide (ZnO) has attracted significant interest because of its wide band gap, large exciton binding energy, high chemical stability, and environment friendly applications [1]. Due to their catalytic, optical, electrical, optoelectronic, gas sensing, Piezoelectric, and photo-electrochemical properties, ZnO is not only attractive for fundamental research but also for practical applications [2]. The effect of Cr doping on the structural and optoelectronic properties of Cr: ZnO thin films were investigated. The elemental composition of virgin and doped films was determined by Energy Dispersive X-ray Spectroscopy (EDS) system. The crystal structure analyses were carried out by Rigaku SmartLab diffractometer. All measurements were performed by using the same input parameters, such as 2 θ range of 20–60°. We using the Debye-Scherrer method to obtain crystallite size of our samples. The surface morphology of the films was observed by scanning electron microscope (SEM). Optical properties of the films were studied by transmittance measurements using a UV–Vis spectrophotometer. The optical transmittance edge presents a blueshift to the region of higher photon energy, when Cr doping concentrations increases. In I–V studies, we conducted in-plane bulk resistivity measurements by applying the FPP method. Four probe measurements of as deposited films showed high resistance values for the Cr: ZnO thin films in absence of increasing concentration depicted in Table II. It was observed that the electrical resistivity of the films decreased first as the concentrations increased and reached a minimum value, $3.22 \times 10^{-4} \Omega \text{ cm}$ from Cr:ZnO-5 film, which is due to not only increase in the carrier concentration and Hall mobility, but it has bad crystallite structure.

P-Mo-060

Thermal processes on Surface and in Bulk: $[\text{Pt}(\text{NH}_3)_4][\text{MCl}_6]$
(M is Re or Os)Tatyana Asanova¹, Igor Asanov¹¹Institute of Inorganic Chemistry SB RAS, Novosibirsk, Russian Federation

Investigation of thermal processes on surface and in bulk of complex compounds is of important task, solution of which widens an understanding solid state chemistry, thermal reduction of metal/s and formation of nanoparticles. A family of compounds with general formula $[\text{M1}(\text{NH}_3)_4][\text{M2Cl}_6]$ (where M1 is Pd or Pt and M2 is Ir, Pt, Re or Os) attracts interest as precursor for preparing alloy nanoparticles and as complexes for studying solid state chemistry under high temperature. The complex salts have been studied by XPS, HAXPES and XAFS in temperature range of 25-500°C.

In the paper we present results of investigation for $[\text{Pt}(\text{NH}_3)_4][\text{M2Cl}_6]$ (M2 is Re or Os) in compared to early studied $[\text{Pd}(\text{NH}_3)_4][\text{M2Cl}_6]$ (M2 is Pt, Os, Ir). It was found that the complex salts under heating behave differently. Thermal decomposition of $[\text{Pt}(\text{NH}_3)_4][\text{M2Cl}_6]$ is similar for both M2 (Re and Os) and differs from these of $[\text{Pd}(\text{NH}_3)_4][\text{M2Cl}_6]$ (M2 is Pt, Ir) by absent of ligand exchange between cation and anion of the complex salts. At the time for all the salts on the surface cation and anion metals (M1 and M2) are reduced at the same temperature while in the bulk the M1 is reduced first. Alloy nanoparticles were shown to be formed only from $[\text{Pd}(\text{NH}_3)_4][\text{PtCl}_6]$. The other complex salts under heating produce inhomogeneous products consisting of monometallic, bimetallic nanoparticles with different chemical ordering. The latter was additionally studied by HAXPES from analysis of element depth profile vs temperature.

P-Mo-061

Bias Dependent Potential of High-k thin films obtained from Operando Photoelectron Spectroscopy

Yoshiyuki Yamashita¹, Hideki Yoshikawa¹, Toyohiro Chikyow¹

¹National Institute for Materials Science, Tsukuba, Japan

Although gate stack structures with high-k materials have been extensively investigated, there are some issues to be solved for the formation of high quality gate stack structures. Here, we employ operando photoelectron spectroscopy (OP-PES). This method allows us to investigate the bias voltage dependent electronic states while keeping device structures intact [1,2]. In the present study, we employed OP-PES and have investigated electronic states and potential distribution in metal/high-k gate stack structures under device operation [3]. When metal gate layer is Ru, most of applied voltage was applied to Si substrate, which was ideal for a metal/high-k gate stack structure. In the case of gate metal layer of Pt, the HfO₂ peak in Hf 3d and the substrate Si 1s peak were shifted by almost the same amount. Analysis of the observed shifts indicated that most of the potential drop at the Pt/HfO₂ interface. In order to clarify the origin of the potential drop at the Pt/HfO₂ interface, O1s spectra were measured. Angle resolved photoelectron spectroscopy in O1s revealed that the SiO₂ and/or PtO layer was formed at the Pt/HfO₂ interface. Thus, the formation of the oxide layer at the interface is the origin the potential drop observed at the Pt/HfO₂ interface.

[1] Y. Yamashita, K. Ohmori, S. Ueda, H. Yoshikawa, T. Chikyow, and K. Kobayashi, e-J. Surf. Sci. Nanotech. 8, 81 (2010)

[2] Y. Yamashita, H. Yoshikawa, T. Chikyow, and K. Kobayashi, J. Appl. Phys. 113, 16370 (2013).

[3] Y. Yamashita, H. Yoshikawa, T. Chikyow, and K. Kobayashi, J. Appl. Phys. 115, 043721 (2014).

P-Mo-062

Dependence of fogging electron current at a specimen surface on the bias-voltage

Taku Noda^{1,2}, Yoshifumi Hagiwara¹, Masatoshi Kotera¹, Raynald Gauvin²¹Osaka Institute of Technology, Osaka, Japan, ²McGill University, Montreal, Canada

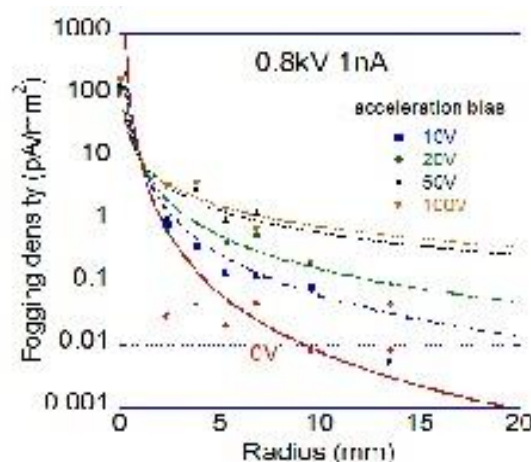
Although electron beam (EB) is used in various surface analyses, if a specimen is an insulator, electrons may be accumulated in the specimen and it is charged negatively. This charging gives bad influences on the performance of specific applications. It has been understood that this charging mainly occurred locally in the specimen around the EB incident point. However, backscattered electrons from the specimen hit various optical components in the specimen chamber, especially pole piece of the objective lens, and the re-backscattered electrons expose the specimen surface in a large area as a global charging phenomenon. We call them fogging electrons (FGEs).

To understand the influence of the FGEs, in the present study we measured radial distribution of FGE current at the specimen surface in an ordinary scanning electron microscope.[1] The FGE current is measured by concentric annular electrodes, centered at the EB irradiation point, and it is made on a commercially available printed circuit board. The current at every electrode is measured by an electrometer (R8252), and with dividing it by the area of each electrode, current density is obtained.

Figure shown as "0V" is the density distribution when all electrodes are grounded. In order to analyze the energy distribution of FGEs, positive potential (acceleration bias) is applied to the electrodes. FGEs were attracted toward electrodes by the acceleration bias. The current density increases with the increase of the acceleration bias, as shown in the figure. It is expected that by subtracting one distribution from another distribution, radial distribution of band-pass filtered FGEs can be obtained.

[1] Y. Ohara et al., Abstracts of EIPBN2012 (2012).

This work was supported by KAKENHI (A) 25249052.



P-Mo-063

Dependence of charging of insulator film by electron beam irradiation on the bias-voltage

Masashi Tokai¹, Yuki Handa¹, Masatoshi Kotera¹¹Osaka Institute of Technology, Osaka, Japan

In the present study surface potential distribution is measured for 300 nm-thick FEP resist film on 70 nm-thick Cr layer on a bulk glass substrate. As shown in the figure, if the EB accelerating voltage is 30kV and the current is 30nA, the potential distribution obtained by fogging electrons distribute in a large lateral distance. In this experiment the Cr layer is biased from -100 to +200V. In a simple discussion, at the bias of -100V, electrons with less than 100eV are repelled by the surface, and a positive potential is obtained. On the contrary, at the bias is positive, as it is 200V, fogging electrons existing over the specimen surface are attracted and injected into the specimen surface. In this situation the surface charges negatively, and the distribution reaches a very wide range of around 4mm in the present study.

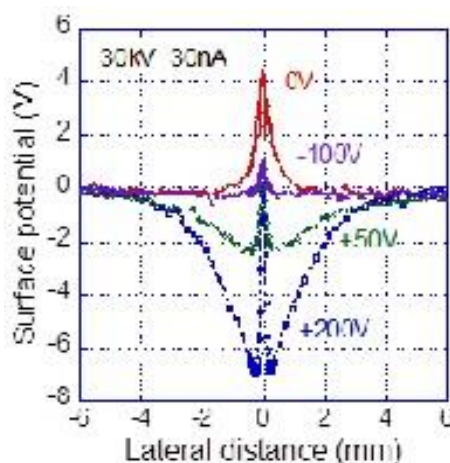
Since the potential is made by charges at the surface, assuming that the capacitance is the same, these potential distributions can be subtracted each other. By comparing measured potential distributions, it is found that fogging electrons with higher energy has narrower spatial distribution.

[1] M. Kotera et al., J.V.S.T. B29, 06F316 (2011).

This work was supported by KAKENHI (A) 25249052.

It is known that insulator charges up during electron beam (EB) exposure. However, the quantitative mechanism and the value of charging potential are not well known. We have been constructing an electrostatic force microscope (EFM) system to clarify them in our scanning electron microscope specimen chamber.[1]

We have pointed out that not only the direct electron accumulation at the point of EB irradiation, but also there is a large contribution of fogging electrons on the charging. Fogging electrons are produced by multiple backscattered electrons between specimen surface and optical components of the SEM, mainly the objective lens plate.



P-Mo-064

Simulation of charging process of PMMA film on Si substrate under electron beam irradiation

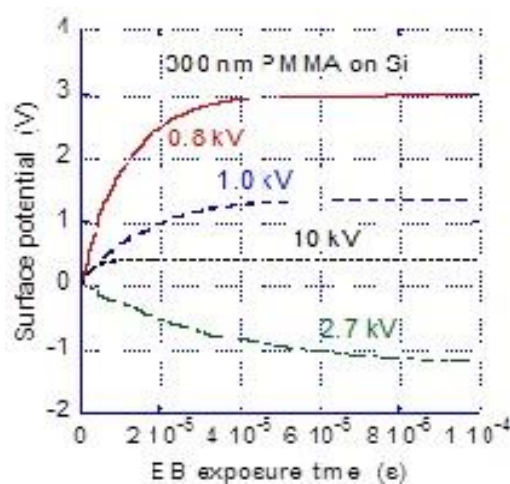
Akihiro Fukuzawa¹, Masatoshi Kotera¹

¹Osaka Institute of Technology, Osaka, Japan

Electron beam (EB) has been widely used for characterization of specimen surface. However, if the electric conductivity of the materials to be measured is low, they charge-up during the EB irradiation. In order not only to avoid the charging, but also to make use of the characteristics in the application, quantitative knowledge of the charging process is important. In the present study, a simulation model is introduced to express a time-dependent charging process of PMMA film on Si substrate under EB irradiation.

Spatial distributions of the electron deposition and the energy deposition in PMMA are obtained by a Monte Carlo simulation of electron trajectories. The potential distribution in and above the PMMA layer is obtained by solving the Poisson equation. The electron beam induced conduction is calculated based on the energy deposited. The thickness of PMMA is 300 nm, and the acceleration voltage of EB varies from 0.8 to 20 kV and the beam current is 50 pA. The electron density distribution of EB is assumed to be a Gaussian, where the radius at 1/e of its maximum is 100 nm. Since the trajectories of electrons less than several eV cannot be treated by the Monte Carlo simulation, electron diffusion by drift is considered by the transport equation. The local electric conductivity is given by the energy deposited by the beam, and the charge drift is calculated by the equation of continuity, and the final charge distribution is obtained in a time step. A typical time step is 1 ns, and after numerous loops of the calculation, the time dependent surface potential is obtained. Surface potential averaged within the radius of irradiated EB is obtained, and the potential variation as a function of EB exposure time is plotted in the figure.

This work was supported by KAKENHI (A) 25249052.



P-Mo-065

X-ray tubes for investigations of macro and micro properties of surface

Andrey Trubitsyn¹, Evgeniy Grachev¹, Vladimir Ivanov¹, Boris Polonskiy¹, Victor Bochkov²

¹Ryazan State Radio Engineering University, Ryazan, Russian Federation,

²Pulsed Technologies Ltd., Ryazan, Russian Federation

A range of X-ray tubes is developed for the purpose of providing the surface and protective coating researches at the macro and micro-level.

In the late 90-s a group of the authors developed a compact device for the X-ray photoelectron spectroscopy (XPS) on the basis of the original conic energy analyzer with a coaxially built-in powerful (1 kW) X-ray tube. The XPS module was attached to a gate oxide cluster tool for the process of optimization in the cleaning/oxidation sequence. At the present time, an improved design of the energy analyzer with higher energy resolution is suggested [1].

Fine-focused reflection X-ray tubes produced according to the original technologies with operating voltage up to 500 kV (Fig. 1) are used for the shadow fluoroscopy and the X-ray tomography of objects with different nature including defects in multilayer protective coatings.

Developed transmission-type microfocus X-ray tubes with original design and power up to 100 W are used for study of surface and near-surface layers by the methods of shadow fluoroscopy, X-ray tomography and diffraction analysis. Advanced experimental data can be achieved by using the copyrighted software with a wide range of the smoothing and background subtraction techniques for the X-ray image and diffraction pattern processing.

The copyrighted application software "FOCUS" [2] is used for the computer simulation of electron-optical schemes of X-ray tubes.

The research was performed by the grant of Russian Science Foundation (the project number 15-19-00132).

[1] Kasko I, Oechsner R., Schneider C., Pfitzner L., Ryssel H., Trubitsyn A., Kratenko V. Abstracts of ECASIA'97 7-th European Conference on Application of Surface and Interface Analysis.- Goteborg, Sweden, 1997.- P.158.

[2] Trubitsyn A. The software "FOCUS" to simulate axi-symmetrical and planar electron (ion) optical systems // Abstracts of the Eighth International Conference on Charged Particle Optics (CPO-8). Software Demo Session.-Singapore, 2010 .- P.208-209.



P-Mo-066

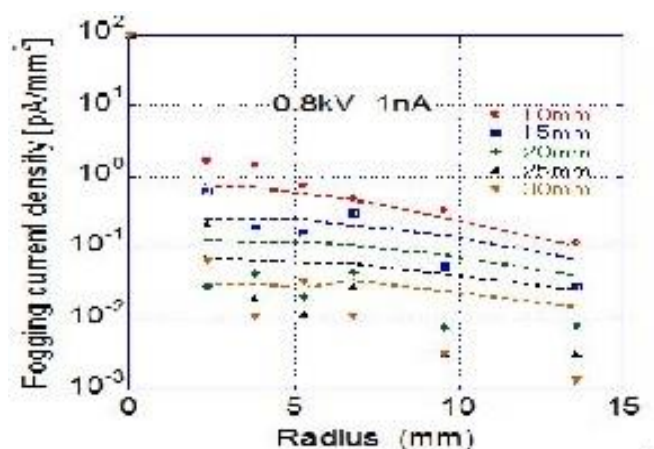
Simulation of fogging electron trajectories in Scanning Electron Microscope

Taiki Nishino¹, Masatoshi Kotera¹

¹Osaka institute of Technology, Osaka-City, Japan

Scanning electron microscope (SEM) has been used in various fields, and it is one of indispensable instruments in surface science. For a discussion of the spatial resolution, electron spreading in the specimen has been evaluated precisely in more than 10 years. However, recently it is known that fogging electrons (FGEs) made by multiple re-backscattering events between specimen surface and optical components of SEM, especially the objective lens plate, in the vacuum can be a cause of degradation of the spatial resolution. The fogging electrons spread so much, as several 10 mm, and they may be a cause of an unexpected global charging in the optical system.

The spatial distribution of fogging electron current can be measured by using a specimen with many concentric annular electrodes, and the results are plotted in the figure. For a quantitative understanding the phenomena occurring for FGEs, we made a simulation. The simulation takes account not only backscattered electrons, but also secondary electrons in vacuum. It is confirmed that the simulation gives appropriate values on their yields for materials at all energy range from 4eV to 30keV. By tracing not only in the specimen and in the objective lens plate, but also in vacuum electron trajectories are calculated by the Monte Carlo simulation. If electrons stop in the specimen, they flow as the current, and the current density is compared with the results. In the figure the FGE current density is shown as a function of radius for various working distances, which is a distance between the specimen surface and the objective lens plate. The acceleration voltage of electron beam is 0.8kV and the current is 1nA. The agreement is fair, but if the radius is large, the difference is large, especially at larger working distances. This work was supported by KAKENHI (A) 25249052.



P-Mo-067

Accurate explicit formulae for higher harmonic force spectroscopy by FM-AFM

Kfir Kuchuk¹, Uri Sivan¹

¹Department of Physics and The Russell Berrie Nanotechnology Institute,
Technion - Israel Institute of Technology, Haifa, Israel

AFM measurements are presently utilized to generate atomic resolution 3D force maps that carry unprecedented information on the interfacial properties of soft matter, water structure and ion ordering. In FM-AFM the force is usually reconstructed from the resonance frequency shift, which in the small amplitude regime is proportional to the derivative of the force with respect to tip-surface distance. Nonlinear interaction between an AFM tip and a sample gives rise to oscillations of the cantilever at integral multiples (harmonics) of the fundamental resonance frequency. These harmonics have been shown to be related to higher derivatives of the force, and thus carry valuable information on the interaction and particularly on short range forces in addition to the information detectable by fundamental harmonic FM-AFM. Utilization of higher harmonics for force spectroscopy has thus far been relatively limited due to theoretical and experimental complexities. In particular, existing approximations of the interaction force in terms of higher harmonic amplitudes required up till now simultaneous measurements of many harmonics to achieve satisfactory accuracy, which is usually difficult. We address this challenge mathematically and derive accurate, explicit formulae for both conservative and dissipative forces in terms of an arbitrary single harmonic. The equations relate measured higher harmonic amplitudes to conservative and dissipative force as a function of tip-sample separation, generalizing the widely applied Sader-Jarvis force reconstruction formula for the fundamental harmonic. Additionally, we prove that each harmonic in FM-AFM carries complete information on the force, obviating the need for multi-harmonic analysis. Finally, we show that higher harmonics may be used to reconstruct short range forces more accurately than the fundamental harmonic when the oscillation amplitude is small compared with the interaction range.

P-Mo-068

Energy distributions of the secondary and backscattered electrons from polymethylmethacrylate irradiated by an electron beam. A Monte Carlo simulation

Maurizio Dapor^{1,2}

¹European Centre for Theoretical Studies in Nuclear Physics and Related Areas (ECT*-FBK), Trento, Italy, ²Trento Institute for Fundamental Physics and Applications (TIFPA-INFN), Trento, Italy

The study of the electronic and optical properties of the matter is paramount for our comprehension of physical and chemical processes which occur in solids. Radiation damage, investigation of chemical composition, and electronic structure study, represent a few examples of the role played by the electron-matter interaction mechanisms. The electron spectroscopies include a wide range of techniques. They are based on scattering processes in which the initial state consists of electrons impinging upon solid-state targets, and final states are characterized by non-interacting particles. This work describes a Monte Carlo code which appropriately takes into account the stochastic behavior of electron transport in solids and treats event-by-event all the elastic and inelastic interactions between the incident electrons and the particles of the solid target. The code is used to simulate the energy distributions of the secondary and backscattered electrons from polymethylmethacrylate (PMMA) irradiated by an electron beam. Several values of the initial kinetic energy of the incident electrons, in the range from 100 to 1000 eV, are considered, and the evolution of the shape of the spectra investigated. The simulation of the backscattered and secondary electron spectra also allows calculating the backscattering coefficient and the secondary electron yield of PMMA as a function of the initial energy of the incident electrons. Results of the simulation are compared with the available experimental data.

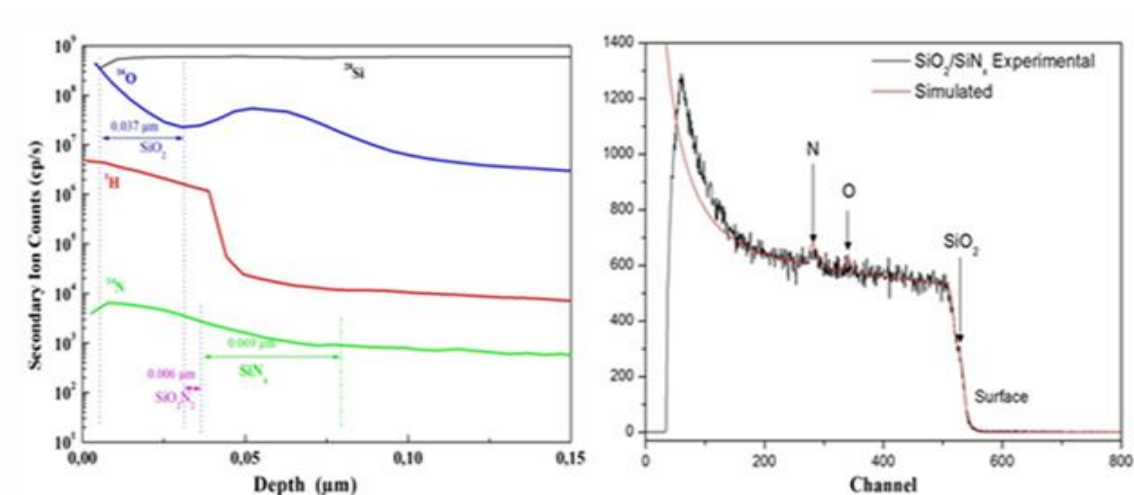
P-Mo-069

Compositional study by SIMS and RBS of oxidized silicon nitride prepared by PECVD

Samir Meziani¹, Abderrahmane Moussi¹, Linda Mahiou¹, Ratiba Outemzabet²

¹Centre de Recherche en Technologie des Semi-conducteurs pour l'Energétique, Algiers, Algeria, ²Université des Sciences et Technologies Houari Boumedienne, Algiers, Algeria

Stoichiometric silicon nitride (SiN) layers were grown on multicrystalline silicon (mc-Si) by Plasma Enhanced Chemical Vapour Deposition (PECVD) at temperature 380°C and flow gas ratio $R = 6$ for ammoniac (NH₃) and silane (SiH₄) gas mixture. After a deposition process, these layers were oxidized in dry oxygen ambient at 950°C. Then thermal annealing at different annealing temperature was made. Secondary ion Mass Spectroscopy (SIMS) and Rutherford Backscattering Spectroscopy (RBS) were employed for analyzing quantitatively chemical composition and stoichiometry in oxide/nitride (ON) stacked films. The effect of annealing temperature on the chemical composition of ON structure is investigated. It is shown that high-oxygen contents exist on the surface. Indeed, this is due to the oxidation growth effect on nitride. It was observed that after oxidation and annealing SiN, we have found thickness of 0.037 μm , 0.069 μm for SiO₂ and SiN, respectively, with the presence Si₂O₂N thin film with thickness of 0.006 μm .



P-Mo-070

Desorption of D₂O and D₂ molecules in hydrogen removal of surface oxide layers on Ru(001)

T. Goto¹, G. Yasutomi¹, T. Yamauchi¹, Akira Izumi¹, A. Namiki¹, H. Oizumi², T. Anazawa², O. Suga², I. Nishiyama²

¹Kyushu Institute of Technology, Fukuoka, Japan, ²Association of Super-Advanced Electronics Technologies (ASET), Kanagawa, Japan

We have studied removal of oxides by D(g) atoms from Ru(001) surface for a temperature range $200 \leq T \leq 600$ K. When the O-saturated Ru(001) surface is exposed to D(g) atoms, both D₂O and D₂ molecules are found to desorb from the surface. The desorption rates become increased with T, indicating the hydrogenation of adsorbed O atoms is activated by T. The D₂O desorption rate curves exhibit a delayed peaking, suggesting two consecutive hydrogenation reactions via formation of intermediate OD(ad) species. On the other hand, the desorbed D₂ molecules exhibit gradual increase in their rates until the rate of the D₂O desorption become zero, after which the D₂ desorption levels off. Possible pathways for the D₂ desorption are discussed.

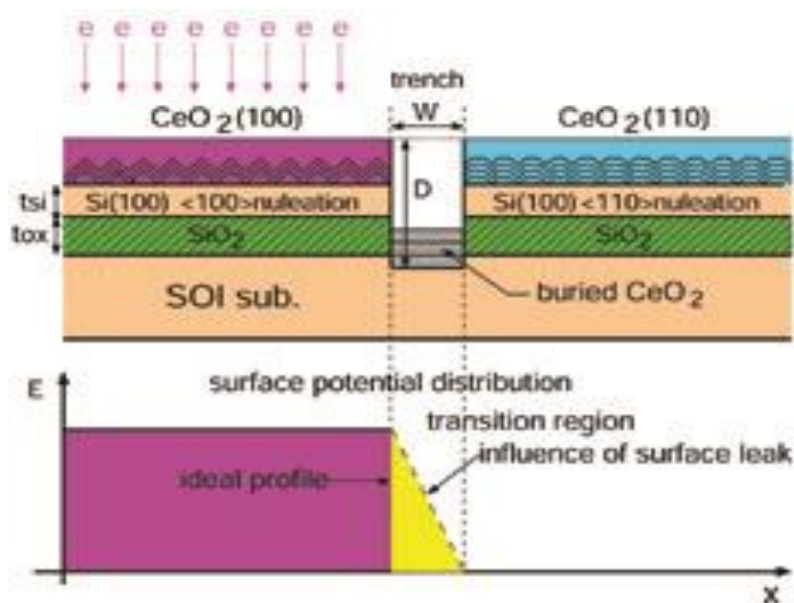
P-Mo-071

Hybrid orientation structure of CeO₂(100) and (110) regions grown on SOI substrates with lithographically formed trenches

Tomoyasu Inoue¹, Shigenari Shida¹

¹Iwaki Meisei University, Iwaki, Japan

Epitaxial growth of CeO₂ layers on Si substrates has been studied for the application to microelectronics. We have found that orientation selective epitaxial (OSE) growth of CeO₂(100) and (110) layers on Si(100) is capable by controlling surface potential distribution. With the aim of application to hybrid orientation technology for higher speed CMOS devices, we are studying the hybrid orientation structure of the CeO₂(100) and (110) regions on Si(100) substrates using electron beam-induced OSE growth by reactive magnetron sputtering. Two separate areas of growth are seen, with CeO₂(100) layers found to grow in areas irradiated by electrons during the growth process, and the CeO₂(110) layers growing in the areas without irradiation. The lateral orientation mapping by X-ray diffraction measurements reveals the existence of transition regions between these two orientation areas. The width of the transition region is found to decrease proportionally as the logarithm of the underlying Si substrate resistivity. To make a breakthrough in the limitation in reduction of the transition region width, we propose a new method of OSE growth on silicon on insulator (SOI) substrates with lithographically formed trenches. The trenches prevent spread of the potential distribution to the neighboring Si islands. We report the experimental results showing perfect isolation between OSE grown regions having different crystallographic orientations, optimizing the Si layer thickness of SOI and the cross-sectional geometry of the trenches.



P-Mo-072

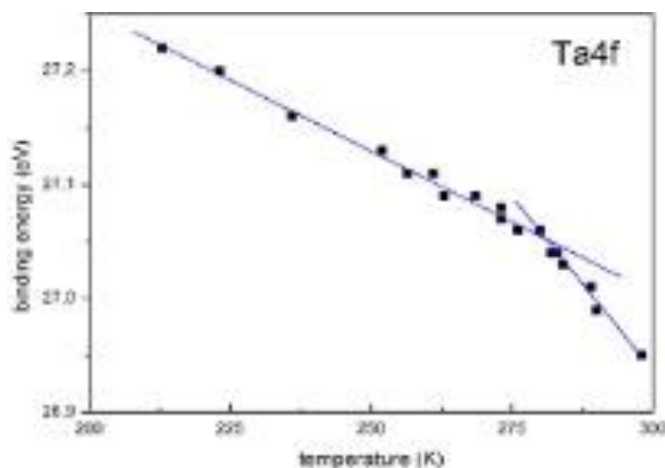
Temperature-dependent surface charging of epitaxial lithium tantalate films

Federico Gramazio¹, Jaume Roqueta¹, Guillome Sauthier¹, Nuria Bagues¹, José Santiso¹, Jordi Fraxedas^{1,2}

¹Catalan Institute of Nanotechnology and Nanoscience (ICN2), Barcelona/Bellaterra, Spain, ²Consejo Superior de Investigaciones Científicas (CSIC), Barcelona/Bellaterra, Spain

We have grown epitaxial lithium tantalate films on SrTiO₃ substrates by pulsed laser ablation of stoichiometric LiTaO₃ ceramic targets. The films, with thickness within the 15 to 45 nm range, crystallize in a highly oriented single phase, as depicted from X-ray diffraction (XRD) measurements, with well-resolved thickness fringes. High-resolution transmission electron microscopy (TEM) measurements evidence a layered structure with long c-axis parameter $c = 1.764$ nm fully coherent with the substrate in-plane structure. Although the crystal structure has not been yet completely elucidated, we can conclude that it differs from the known rhombohedral perovskite structure of LiTaO₃ (with pseudocubic cell parameter $a=0.375$ nm). Ex situ XPS measurements, performed with a PHOIBOS150 hemispherical analyzer using 400 W monochromatic AlK α radiation show that the core level lines exhibit a rigid shift towards higher binding energies, characteristic of surface charging, when the sample temperature is decreased below room temperature (RT). The overall observed shift between RT and a given temperature vary as a function of the film thickness. Figure 1 shows the dependence of the binding energy of the Ta4f_{7/2} line (referred to the system Fermi level) as a function of temperature. Two clearly differentiated regimes can be observed, with a crossover at about 280K. These preliminary results are in line with early investigations from Ehre and co-workers [1], who have experimentally shown that the sign of the surface charge of Z-cut wafers of LiTaO₃ changes at 265 K, by tracking water freezing by optical microscopy, in spite of the different crystal structure.

[1] Ehre, D., Lavert, E., Lahav, M. and Lubomirsky, I., Science 327 (2010) 672.



P-Mo-073

Defects in sol-gel derived tin dioxide thin films - a way to control the oxide's electronic and chemical properties

Maciej Krzywiecki^{1,2}, Lucyna Grządziel², Adnan Sarfraz¹, Georgi Genchev¹,
Andreas Erbe¹

¹Max-Planck-Institut für Eisenforschung GmbH, Düsseldorf, Germany, ²Silesian University of Technology, Institute of Physics, Gliwice, Poland

Nowadays, tin dioxide (SnO₂) thin layers are well known candidates as a basis for photovoltaic, sensor, and electronic applications. In the form of tin (IV) oxide the layers are basically wide-band gap semiconductors with high transparency in the visible range.

The applications mentioned above depend on the electronic properties of SnO₂ as well as on their chemical composition and surface morphology. In order to be able to consciously use the oxides' potential there is a need for thorough characterization with complementary methods.

Due to the vast range of applications, numerous SnO₂ film preparation techniques have been employed, such as chemical vapour deposition, rheotaxial growth, and vacuum oxidation or atomic layer deposition. However these techniques are expensive and technologically complicated. Therefore there is a need for search of relatively cost effective alternatives.

In presented work SnO₂ films were prepared by sol-gel process following a spin-coating step on silicon substrates. The surface chemical composition and basic electronic properties were studied by X-ray photoelectron spectroscopy combined with ion depth etching. X-ray diffraction and scanning microscopy techniques (atomic force microscopy and scanning electron microscopy) were used to yield information on the surface topography and internal structure of the films respectively. The optical properties and auxiliary electronic properties were determined by means of spectroscopic ellipsometry.

Obtained results indicate that the defect sites recognized by photoemission experiments strongly affect not only the composition of the oxide but also its electronic structure. Moreover, presented deposition technology allows controlling the degree of stoichiometry and composition depth profile. This in turn, enables the ability for easy and cost-effective manipulation of oxide's properties tuned for particular application.

P-Mo-074

Interaction of CO₂ with well-ordered CaO(001) thin films

Ms. Xuefei Weng¹, Yi Cui¹, Brian Solis², Joachim Sauer², Shamil Shaikhutdinov¹, Hans-Joachim Freund¹

¹Fritz-Haber-Institut der Max-Planck-Gesellschaft, Berlin, Germany, ²Institut für Chemie, Humboldt Universität zu Berlin, Berlin, Germany

Interaction of CO₂ with CaO has been a subject of interest in chemistry for many years as CaO plays an important role in CO₂ absorption for many technological applications.¹ However, fundamental understanding of CO₂ adsorption on CaO surfaces is still missing, and has only recently received attention in surface science. Very recently, preparation of well-ordered thin CaO(001) films on Mo(001) was reported.² The STM and XPS results indicated that film ordering at elevated temperatures is accompanied by Mo diffusion to the sub-surface region which in turn affects CaO interaction with O₂.³ As such, this system provides additional opportunity to study effect of metal dopants on chemical reactions at oxide surfaces. Here, we studied CO₂ adsorption on CaO(001) films by IRAS and TPD as a function of annealing and exposure conditions, and the film thickness as well. The experimental data were corroborated by DFT calculations. The results show the formation of strongly bonded surface species which are identified as carbonates. It appears that the CO₂ adsorption on CaO is not much affected by sub-surface Mo, and CO₂ readily adsorbs on regular surface. To prove this, CaO films were grown on Pt(100) which showed similar results.

[1] R. Besson, M. R. Vargas and L. Favregeon, CO₂ adsorption on calcium oxide: An atomic-scale simulation study, *Surf. Sci.*, 2012, 606, 490–495

[2] Y. Cui, X. Shao, M. Baldofski, J. Sauer, N. Nilius and H-J Freund, Adsorption, activation, and dissociation of oxygen on doped oxides, *Angew. Chem. Int. Ed.*, 2013, 52, 11385-11387

[3] Y. Cui, Y. Pan, L. Pascua, H. Qiu, C. Stiehler, H. Kühlenbeck, N. Nilius and H-J Freund, Evolution of the electronic structure of CaO thin films following Mo interdiffusion at high temperature, *Phys. Rev. B*, 2015, 91, 035418

P-Mo-075

Structural and electrical characterization of titanium oxynitride deposited by reactive magnetron sputtering

Rodrigo César¹, Angélica Barros¹, Ioshiaki Doi¹, Andressa Rosa¹, José Diniz¹,
Jacobus Swart¹

¹University of Campinas - UNICAMP, Campinas, Brazil

Titanium dioxide (TiO₂) thin film has been studied due to its qualities, adequate for wide range of applications as biosensor, especially as Field Effect Devices due to its chemical stability, bio-compatibility, high dielectric constant (high k) along with the ability to form hydrogen bonds (which provides a high sensitivity). Some works report that with the introduction of nitrogen in TiO₂ it is possible to obtain titanium oxynitride (TiO_xN_y) films with better mechanical, optical and electrical properties if compared with the conventional TiO₂, which could be attributed to the variation in the N/O ratio. Other applications of the titanium oxynitride are: solar selective absorbers, barrier diffusion, MEMS, cutting tools and wear resistant coatings. There are several ways of obtaining TiO_xN_y such as sol-gel, e-beam, PECVD and sputtering, but the major advantage of sputtering is that the flow of reactive gases can be controlled precisely and the deposition is in room temperature.

In this work the titanium oxynitride films were deposited by reactive magnetron sputtering of various N/O flow ratio. The samples were manufactured on p-type (100) Si wafers as substrates. For structural characterization was used Raman spectroscopy and was possible to note the rutile and anatase crystal structure for all samples. The atomic force microscopy (AFM) shows roughness below 1 nm, the ellipsometry technique determined the thickness of the 91 nm and refractive index of 2.4 for all samples. For electrical characterization MOS capacitors were fabricated and capacitances versus voltage (CxV curve) were carried out in order to determine which N/O flow rate exhibited the best dielectric film. The films show high dielectric constant around 70, charge density (Q₀/q) of the 10⁺¹² cm⁻² and flat-band voltage (V_{FB}) of -0.8V. These values are interesting for field effect devices application.

P-Mo-076

Growth and thermal effects of Co on CeO₂(111)

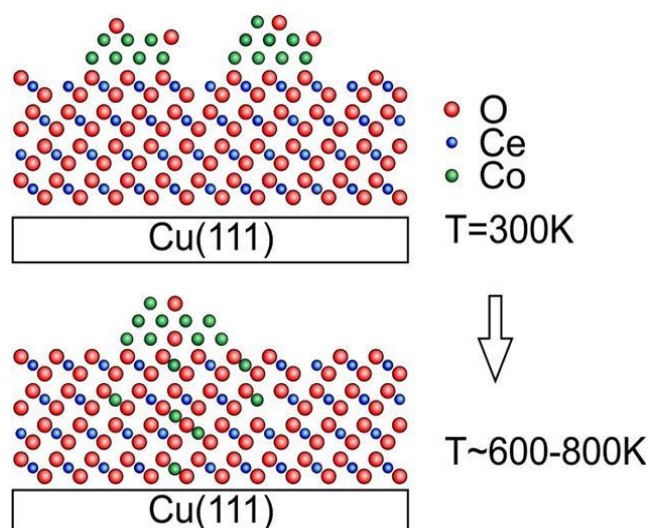
Gábor Vári¹, László Óvári², Christian Papp³, Hans-Peter Steinrück³, János Kiss², Zoltán Kónya^{1,2}

¹Department of Applied and Environmental Chemistry, University of Szeged, Szeged, Hungary, ²MTA-SZTE Reaction Kinetics and Surface Chemistry Research Group, Szeged, Hungary, ³Chair of Physical Chemistry II, University of Erlangen-Nürnberg, Erlangen, Germany

Nowadays, ceria is an essential material in catalysis as a support, promoter or catalyst. Ceria-supported cobalt is an efficient noble metal-free catalyst for CO oxidation or the steam reforming of ethanol (SRE). The interaction of cobalt with an ultrathin CeO₂(111) film prepared on Cu(111) was investigated by X-ray photoelectron spectroscopy (XPS) and low energy ion scattering spectroscopy (LEIS). Previous LEIS studies on (oxidized) cerium deposits using other metallic substrates reported serious difficulties related to the neutralization of noble gas ions. For this reason, special attention was paid here to reveal possible matrix effects for the neutralization (“neutralization effects”) [1]. Co grows three-dimensionally on the ceria film at room temperature. Cobalt is oxidized to Co(II), together with the formation of Ce(III) in the ceria for small Co coverages (0.2 ML). An increasing fraction of cobalt remained metallic after deposition of larger amounts of cobalt. Annealing to higher temperatures induced the diffusion of Co(II) ions into the ceria film, and for metallic cobalt, presumably agglomeration occurs. Above 750 K, oxidation of significant amounts of Co⁰ to Co(II) is found, which is diffusing into the ceria film, and partly also in the copper crystal underneath. The interaction of cobalt with a reduced CeO_x (1.5 < x < 2) film on Cu(111) was also studied by XPS and LEIS. The oxidation of cobalt proceeded to a lesser extent on the reduced surface. Furthermore, the thermal induced migration of Co into the ceria film was slowed down by the hindered redox reaction between cobalt and cerium [2].

[1] G. Vári, L. Óvári, J. Kiss, Z. Kónya, Phys. Chem. Chem. Phys. 17 (2015) 5124.

[2] G. Vári, L. Óvári, C. Papp, H.-P. Steinrück, J. Kiss, Z. Kónya, J. Phys. Chem. C 119 (2015) 9324.



P-Mo-077

Initial surface oxidation of Zr: XPS, PEEM, FIM, FEM and DFT studies

Ivan Beshpalov¹, Martin Datler¹, Sebastian Buhr¹, Johannes Zeininger¹, Peter Blaha¹, Günther Rupprechter¹, Yuri Suchorski¹

¹Vienna University of Technology, Vienna, Austria

Zr and Zr-alloys are widely used in nuclear technology, as e.g. cladding of fuel rods in nuclear reactors [1, 2]. The properties of the thin oxide films usually formed on the Zr surface under operating conditions are thus important for the technological applications. Therefore, the initial stage of zirconium oxidation is extensively studied over decades using various surface analysis techniques. Mostly the composition, the structure and the oxidation state are studied and much less the kinetics and the mechanism of the oxide formation [2, 3]. However, the Zr hcp-to-bcc phase transformation occurring at temperatures usual in nuclear reactors remains mainly disregarded in the Zr oxidation studies. In addition, the knowledge about the role of Zr-suboxides remains still scarce and controversial.

In the present contribution we present μm - to nm-scale studies of initial stages of the zirconium oxide formation using XPS, PEEM, FIM, and FEM. Corresponding DFT calculations are in accord with the experimental findings which include the formation of Zr-suboxides.

The hcp-to-bcc" phase transformation in Zr is visualized by PEEM for the first time and the role of the resulting structure and surface morphology changes in the ZrO_x formation as well as the role of Zr suboxides in the Zr-based oxidic supports of catalytically active noble metals are discussed.

[1] Corrosion of Zirconium Alloys in Nuclear Power Plants, International Atomic Energy Agency, TECDOC-684, 1993

[2] N. Stojilovic, E.T. Bender, R.D. Ramsier, Prog. Surf. Sci. 78 (2005) 101, and references therein.

[3] G. Bakradze, L.P.H. Jeurgens, E.J. Mittemeijer, J. Appl. Phys. 110 (2011) 24904

P-Mo-078

Formation of NiO Nanoclusters on MgO Monolayers induced by Segregation of Interfacial Oxygen.

Mario Agostino Rocca^{1,2}, Marco Smerieri², Letizia Savio², Jagriti Pal^{1,2}, Riccardo Ferrando^{1,2}, Luca Vattuone^{1,2}, Sergio Tosoni³, Livia Giordano³, Gianfranco Pacchioni³

¹Università di Genova, Genova, Italy, ²IMEM CNR, Genova, Italy, ³Università di Milano Bicocca, Milano, Italy

Nanoparticles deposited at oxide surfaces are important for their applications in several fields of technology and life science. It is therefore mandatory to achieve a complete characterization of their structural, electronic and chemical properties, which are well known to depend on particle size and production conditions [1,2].

Here we report a combined low temperature STM and DFT investigation of the aggregation of Ni clusters on MgO /Ag(100). We recently demonstrated how to grow nearly perfect, extended, monolayer MgO films [3,4], which are an ideal substrate for the deposition of nanoparticles. Upon Ni deposition at 300 K we find 3D growth on the clusters, as expected. At 200 K, however, a bimodal distribution of the cluster size is detected and also small, 2D objects (from 2 to 6 Ni atoms in size) are imaged. The latter ones cannot be identified with metallic Ni nanoparticles since they are not 3-dimensional (contrary to expectation already for Ni₄) and since the Ni-Ni distance is too large. DFT indicates that they consist of Ni_xO_y particles with different stoichiometries, which can form thanks to the availability of atomic oxygen accumulated at the MgO/Ag interface [4]. Besides being of relevance in view of the large use of Ni nanoclusters in catalysis, this finding gives a further proof of the peculiar behavior of oxide films grown at metal surfaces in the ultrathin limit.

[1] Schauermann, S.; Nilius, N.; Shaikhutdinov, S.; Freund, H.-J., *Accounts of Chemical Research* 2013, 46, 1673-1681.

[2] Henry, C. R., *Progress in Surface Science* 2005, 80, 92-116.

[3] Jagriti Pal, Marco Smerieri, Edvige Celasco, Letizia Savio, Luca Vattuone, Mario Rocca, *Phys. Rev. Lett.* 2014, 112, 126102.

[4] Pal, J.; Smerieri, M.; Celasco, E.; Savio, L.; Vattuone, L.; Ferrando, R.; Tosoni, S.; Giordano, L.; Pacchioni, G.; Rocca, M., *Journal of Physical Chemistry C* 2014, 118, 26091-26102.

P-Mo-079

Cleaning and Profiling of STO oxide with new ion source

Damien Aureau¹, Karl Ridier², Arnaud Fouchet², Arnaud Etcheberry¹

¹Institut Lavoisier, Versailles, France, ²Gemac, Versailles, France

XPS spectroscopy gives information about the chemical composition and the chemical environment of the atoms situated at surfaces and is a direct measurement of band offsets. Nevertheless, surface contaminants (water, adsorbed molecules) at the surface could provide a non-negligible contribution which modifies the analysis, especially for organics or oxides. In order to obtain clean surface, ion bombardment is used to clean and profile the surfaces. Nevertheless, the traditional ion etching with mono-atomic argon ions tends to modify the materials, challenging the analysis. We will present a new method for surface cleaning and profiling with cluster ion gun where the energy per atom is much less important. Consequently, this last etching appears to be much more gentle for any surfaces and doesn't seem to change binding energies of the elements. The capacity to remove only the carbon contamination and then to control a progressive etching atoms by atoms is really promising to investigate various ultrathin films. First results based on model system based on SrTiO₃ will be presented

P-Mo-080

Upconversion luminescence of Er^{3+} sensitized by Yb^{3+} ions in Zn_2TiO_4 crystals

Toshihiro Nonaka¹, Shin-Ichi Yamamoto¹

¹Ryukoku University, Otsu, Japan

Various light-emitting devices have been developed in recent years, and it is known that their emission generally occurs in accordance with the principles of down-conversion. However, the excitation energy required to obtain luminescence is usually higher than the energy released at the time of light irradiation. This study focuses on up-conversion (UC) technology as an alternative approach that avoids this problem. Oxides can be formed from many materials by air sintering after coating a substrate with a metal–organic decomposition (MOD) solution. This enables the preparation of thin films by simple processes such as spin coating. The up-conversion (UC) phosphor produced by the MOD method has a multifunctional potential for use in applications such as displays and solid-state lighting. In this study, a simple TiO_2 – ZnO mixed oxide system was examined for use as the base material and host crystal of rare-earth (RE) elements for UC phosphor. The maximum emission luminescence of the UC phosphor was obtained when the mixing ratios of the base materials TiO_2 : ZnO and additive materials Yb_2O_3 : Er_2O_3 were 1 : 1 and 0:06 : 0:06, respectively. When the mixing ratio of the phosphor, Ti : Zn : Yb : Er, was 1 : 1 : 0:06 : 0:06, 550 nm green and 650 nm red emissions were produced. The UC emission intensity could be controlled by varying the mixing ratio of the rare-earth materials.

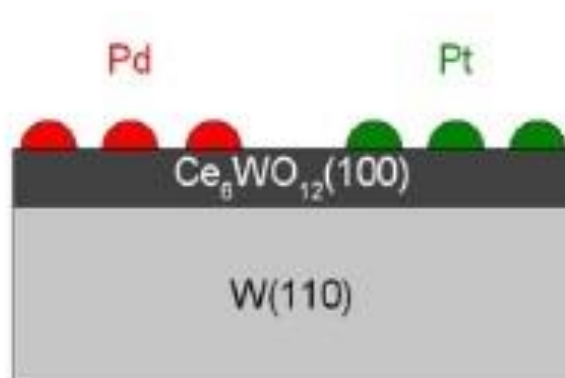
P-Mo-081

Growth of transition metals on cerium tungstate model catalyst layers

Tomas Skala¹, Vladimir Matolin¹

¹Charles University in Prague, Faculty of Mathematics and Physics, Prague 8, Czech Republic

Growth and thermal stability of two model catalytic metal/oxide systems were investigated by photoelectron spectroscopy with conventional X-ray lamp and synchrotron radiation as excitation sources. The mixed-oxide support was a cerium(III) tungstate epitaxial thin layer grown in situ on the W(110) single crystal. Active particles consisted of palladium and platinum 3D islands deposited on the tungstate surface at 300 K. Both metals were found to interact weakly with the mixed oxide support and the original chemical state of both support and metals was mostly preserved. Electronic and morphological changes of the model layers are discussed during the metal growth (Pd or Pt) and after post-annealing at temperatures up to 700 K. Partial transition-metal coalescence and self-cleaning from the CO and carbon impurities were observed.



P-Mo-082

Atomically flat Fe-doped cobalt ferrite single crystal islands with μm -sized magnetic domains

L. Martín-García¹, A. Quesada², C. Munuera³, M. Foerster⁴, L. Aballe⁴, J. de la Figuera¹

¹Instituto de Química Física Rocasolano, CSIC, Madrid, Spain, ²Instituto de Cerámica y Vidrio, CSIC, Madrid, Spain, ³Instituto de Ciencia de Materiales de Madrid, CSIC, Madrid, Spain, ⁴Alba Synchrotron Light Facility, CELLS, Barcelona, Spain

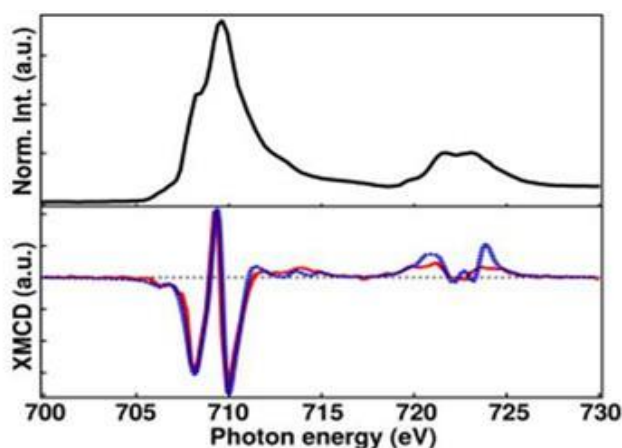
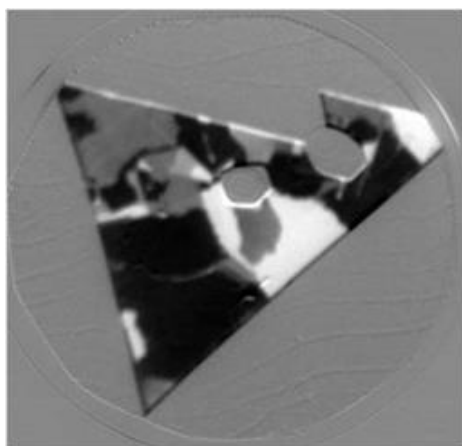
CoFe_2O_4 (CFO) is an oxide of the spinel family. Stoichiometric CFO is electrically insulating and ferrimagnetic, with a high anisotropy and a large magnetostriction [1]. Changing its structure, for example by substitution of the different cation sites, offers the possibility of manipulating its physical properties. In particular, upon Fe doping, its electrical resistivity decreases linearly while its magnetic moment increases in a non-linear fashion [2,3]. The capacity of tuning the physical properties of CFO by doping makes it a promising material for spintronic devices.

We here present Fe-doped CFO single crystal islands grown on Ru(0001) by reactive molecular beam epitaxy (MBE). In situ low-energy electron microscopy (LEEM) permits tailoring the epitaxial growth in order to obtain micron-sized defect-free crystals of nm thickness. The magnetic domains distribution and the magnetic moments were studied by X-ray absorption (XAS) and X-ray Magnetic Circular Dichroism (XMCD) at the CIRCE beamline at the ALBA Synchrotron. Contributions to the XMCD spectra of the different cationic species were determined by simulations using the CTM4XAS 5.5 program. The stability of the films in air permits ex situ studies such as AFM and MFM in order to obtain valuable complementary information.

[1] V. A.M. Brabers, Ferrimagnetic insulators, in Handbook of Magnetism, Ed. Kronmüller and S. S. Parkin.

[2] Junichi Takaobushi et al., Phys. Rev. B 76, 205108 (2007).

[3] J. A. Moyer et al., Phys. Rev. B 84, 054447 (2011).



P-Mo-083

A photoemission study of adsorbates on TiO₂

Daniel Payne^{1,2}, Yu Zhang^{1,2}, Chi Lun Pang^{1,2}, Helen Fielding¹, Geoff Thornton^{1,2}

¹UCL, London, United Kingdom, ²London Centre for Nanotechnology, London, United Kingdom

Photoexcitation of electron-hole pairs across the ~3 eV band gap of TiO₂ is thought to initiate redox reactions which underlie many of the applications of this material [1]. Subsequently, it is necessary to understand the properties of both the ground and excited states of TiO₂. Excited electrons are typically difficult to study [2], however, one technique capable of doing so is two-photon photoemission (2PPE). Using ultra-fast lasers, both the energy and dynamics of excited states may be interrogated by this pump-probe technique. In this study, 2PPE is combined with ultraviolet and x-ray photoemission spectroscopy to characterise the electronic structure of the rutile TiO₂(110) surface.

Typical ultra-high vacuum preparation techniques, such as argon sputtering and high temperature annealing, lead to the reduction of TiO₂. As a result of this sub-stoichiometry, bridging oxygen vacancies are formed. These are active sites for chemical reactions on the surface, and are associated with the appearance of Ti 3d band gap states ~1 eV below the Fermi level [3]. This reduced surface is easily hydroxylated via the dissociation of water at oxygen vacancies, healing the surface structure without influencing the band gap states [4].

We report a photoemission study on the effect of small inorganic molecules on the TiO₂(110) surface. The core levels, valence band and defect states are characterised using ultraviolet and x-ray photoemission spectroscopy. Hence, changes in the 2PPE spectra are attributed unambiguously to the unoccupied density of states.

[1] K. Onda et al., Science 308, 1154 (2005).

[2] M. Henderson, Surf. Sci. Rep. 66, 185 (2011).

[3] C. L. Pang, R. Lindsay, G. Thornton, Chem. Revs. 113, 6 3887 (2013).

[4] C. Di Valentin, G. Pacchioni, A. Selloni, Phys. Rev. Lett. 97,16 (2006).

P-Mo-084

Engineering the Oxide/Metal interface through the insertion of a buffer layer: CoO growth onto metastable Co/Fe(001) bilayers

Andrea Picone¹, Michele Riva¹, Dario Giannotti¹, Alberto Brambilla¹, Lamberto Duò¹, Franco Ciccacci, Marco Finazzi¹

¹Dipartimento di Fisica, Politecnico di Milano, Milano, Italy

Ultrathin oxide films deposited on metallic substrates have attracted great interest in recent years, mainly because they provide high quality templates for advanced studies in the field of heterogeneous catalysis and magnetism [1,2]. The oxide/metal interface plays a fundamental role on the structural, chemical, and physical properties of the resulting heterostructures. Deposition of oxide layers on Fe leads to a particularly complex interface chemistry, because the highly reactive substrate undergoes to a substantial oxidation upon reactive deposition (i.e. metal deposition in an oxidizing atmosphere). A suitable strategy to control the interface composition is the use of a metallic buffer layer in between the substrate and the oxide adlayer. The buffer layer should possess specific characteristics, such as a good epitaxial relation with both the metallic substrate and the oxide adlayer, as well as good passivating properties in order to prevent an extensive substrate oxidation. Here it is demonstrated that a buffer layer of metastable body centered cubic Co [3] deposited on the Fe(001) surface provides a good template for the growth of high quality CoO films, protecting at the same time the Fe substrate from uncontrolled oxidation. Atomically flat Co oxide films are obtained and investigated at atomic scale level by Scanning Tunneling Microscopy.

[1] S.Valeri and G. Pacchioni, eds., Oxide Ultrathin Films (Wiley-VCH Verlag, Weinheim, 2011).

[2] M. Finazzi, L. Duò, and F. Ciccacci, eds., Magnetic Properties of Antiferromagnetic Oxide Materials: Surfaces, Interfaces and Thin Films (Wiley-VCH Verlag, Weinheim, 2010).

[3] A. Picone et. al., Phys. Rev. Lett. 113, 046102 (2014).

P-Mo-085

Structural study of several conducting SrTiO₃ crystal surfaces

Xavier Torrelles¹, M. Salluzzo², Z. Ristic³, J. Drnec⁴, R. Felici⁴, R. Di Capua⁵, N. Plumb⁶, M. Radovic⁶

¹ Institut de Ciència de Materials de Barcelona, ICMAB (CSIC), Cerdanyola del Vallès, Spain, ²CNR-SPIN, Complesso Universitario di Monte Sant Angelo, Napoli, Italy, ³Ecole Polytechnique Fédérale de Lausanne, Lausanne, Switzerland, ⁴ESRF, Grenoble, France, ⁵CNR-SPIN, Unità di Napoli, Napoli, Italy, ⁶Paul Scherrer Institut, Swiss Light Source, Villigen, Switzerland

The two-dimensional electron gases (2DEGs) that can be induced at interfaces between the widegap band-insulator SrTiO₃ (STO) and other bulk insulators, like LaAlO₃, have renewed a widespread interest in the physical properties of STO surfaces.

SrTiO₃ is one of the most widely studied perovskite oxides and is characterized by a number of interesting electronic properties, including superconductivity, ferroelectricity under strain, or even exotic magnetism when combined with LaAlO₃ layers. Apart of that, recent, ARPES studies showed that the (001) SrTiO₃ surface shows a 2DEG [1] with properties similar to the one observed in the case of interfaces obtained by depositing a (001) LAO film on a (001) STO substrate [2]. One of the specific feature of the electronic properties of the STO surface hosting a 2DEG is a splitting of the 3d_{xy} and 3d_{xz,yz} bands [1,3], having respectively 2D and a 3D characters, and a rumpling of the TiO₂ and SrO planes which is linked to the electronic reconstruction [4]. Remarkably, 2DEGs were recently observed also at the interfaces between (110) or (111) STO single crystals and LAO thin films [4].

These results are very interesting, suggesting that these 2D-surface states can be manipulated by changing the crystallographic orientation of the STO surface. For example, the ideal (111) plane has a 2D-trigonal symmetry, consequently it forms a 2D-honeycomb lattice similar to graphene and some topological insulators.

Here we will show some GIXRD preliminary results on metallic STO(111), STO(110) and ST(001) surfaces to try to unravel some of the structural pieces that could explain this electrical behavior.

[1] F. Santander-Syro, et al. , Nature 469 (2011) 189.

[2] M. Salluzzo et al., Adv. Mater., 25 (2013) 2333

[3] N. C. Plumb et al., arXiv. 1302.0708, (2013).

[4] G. Herranz et al., Nature Communications 2 7(2012) 758.

P-Mo-086

Stabilization of the $\langle 1-10 \rangle$ step structure on vicinal $\text{TiO}_2(110)$

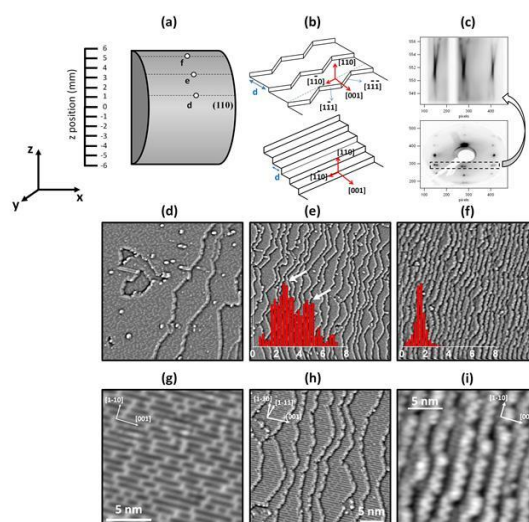
Alejandro Miccio¹, Martin Setvin², Ignacio Piquero³, Mikel Abadía³, Celia Rogero³, Frederik Schiller³, Jorge Lobo-Checa³, Michael Schmid², Ulrike Diebold², Enrique Ortega^{1,3}

¹Donostia International Physics Center, DIPC, San Sebastian, Spain, ²TU Wien, Vienna, Austria ³Centro de Física de Materiales, Centro Mixto CSIC-UPV/EHU

Vicinal surfaces have frequently demonstrated their enormous potential from both the scientific and the technological point of view. They exhibit distinct chemical and physical properties due to their high density of atomic steps, being also useful as nanoscale templates to control the growth of low dimensional structures, such as nanodots or nanostripes. In this context, a vast majority of studies on the chemistry and electronic properties of $\text{r-TiO}_2(110)$ have been carried out on the flat surface, whereas much less effort has been focused on stepped planes. Moreover, as low atomic coordination sites, the step edges are chemically and electronically very active, and hence stepped surfaces may become technologically relevant, e.g., as a way of tailoring new chemical properties of r-TiO_2 .

Recent studies on stepped $\text{r-TiO}_2(110)$ pointed out the existence of characteristic vacancies (Oedge) at the $\langle 1-11 \rangle$ -like step edge [1], different from the bridging vacancies that show up on (110) planes (Obr). Using a r-TiO_2 crystal with a shallow curvature around the (110) symmetry, we have investigated stepped $\text{r-TiO}_2(110)$ vicinal planes with a smoothly varying miscut angle. Our Scanning Tunneling Microscopy (STM) and Low Energy Electron Diffraction (LEED) analysis have shown zig-zagged step arrays exhibiting energetically stable $\langle 1-11 \rangle$ mini-facets, which evolve into straight, monatomic $\langle 1-10 \rangle$ steps at higher step densities. The latter appear saturated with bright features that remain after water adsorption, suggesting the presence of Oedge vacancies. Such assignment also agrees with the analysis of the $\text{Ti}3d+$ photoemission peak across the curved surface.

[1] U. Martinez, et al., Phys. Rev. Lett. 109, 155501 (2012)



P-Mo-087

Optical and gas sensing properties of nanostructure SnO₂ synthesized by microwave plasma

Somchai Thongtem¹, Arrak Klinbumrung², Titipun Thongtem¹

¹Chiang Mai University, Chiang Mai, Thailand, ²University of Phayao, Phayao, Thailand

SnO₂ nanoparticles were successfully synthesized by a 900 W microwave plasma method. X-ray diffraction (XRD) was used to specify the tetragonal cassiterite SnO₂ crystal structure with the lattice constant of $a = 0.4735$ nm and $c = 0.3207$ nm. The morphology of 30 min processed SnO₂ was investigated by scanning electron microscopy (SEM) and transmission electron microscopy (TEM), and founded nanoparticles with diameter around 12 nm. Selected area electron diffraction (SEAD) result was in accordance with that of the XRD. Ultraviolet-visible (UV-vis) absorption spectroscopy and photoluminescence (PL) were employed to examine the optical properties of the as-synthesized product of 3.50 eV energy gap and 395 nm emitting wavelength. Gas sensing performance exposing to NH₃ was tested at different working temperatures and gas mixture concentrations. For the gas concentration of 1,055 ppm and the working temperature of 350 °C, the nanoparticles has the highest sensitivity of 10.7. In this research, respond-recovery reversibility performance was also determined and discussed. Keywords: SnO₂; X-ray diffraction; Spectroscopy; Gas sensor.

P-Mo-088

Local Restriction of Co Diffusion through Ultrathin SiO₂ Layer by Substrate Modification by Focussed Ion Beam

Jan Cechal^{1,2}, Josef Polcak^{1,2}, Adam Závodný², Tomas Sikola^{1,2}

¹CEITEC, Brno University of Technology, Brno, Czech Republic, ²Institute of Physical Engineering, Brno University of Technology, Brno, Czech Republic

Cobalt deposited on a thin oxide layer on a Si substrate forms a smooth continuous layer if the deposition is carried out at room temperature. At elevated temperatures the Co atoms penetrate the oxide layer and form a thin CoSi₂ layer underneath the oxide. In the contribution we show that the diffusion can be controlled by local modification of the substrate by focussed ion beam. Counterintuitively, the surface-to-bulk diffusion is restricted at the modified areas and, hence, Co stays at the surface there. We discuss the physical origin of this phenomenon in terms of either ion beam induced amorphization of the bulk silicon or presence of implanted Ga atoms both leading to an increase of activation energy for formation of CoSi₂ nuclei.

P-Mo-090

Dissociation of formic acid on metal oxide surfaces probed by UHV-IRRAS and complimentary techniques

Heshmat Noei¹, Oscar Gamba², Maria Buchholz³, Yuemin Wang⁴, Gareth Parkinson², Martin Muhler⁴, Ulrike Diebold², Christof Wöll³, Andreas Stierle¹

¹DESY Nanolab, Hamburg, Germany, ²TU Vienna, Vienna, Austria, ³Karlsruhe Institute of Technology, Karlsruhe, Germany, ⁴Ruhr-University Bochum, Bochum, Germany

Carboxylate groups are frequently used to anchor photosensitizers and other functional molecules to oxide substrates. As a result the binding of HCOOH, the simplest carboxylic acid, to oxides substrates is an important model system with regard to understanding the grafting of more complex molecules via carboxylate groups with this important oxidic substrate. Here, the interaction of formic acid with different oxide single crystal surfaces (TiO₂(101), ZnO(10-10), Fe₃O₄(001)) has been monitored by infrared reflection absorption spectroscopy (IRRAS). The high-quality IR data are further combined with other complimentary techniques, such as X-ray photoelectron spectroscopy (XPS), low energy electron diffraction (LEED) and scanning tunneling microscopy (STM). We found that the interaction of HCOOH with TiO₂(101), ZnO(10-10) and Fe₃O₄(001) leads to dissociative adsorption yielding different formate species via an acid-base reaction on oxide surfaces. The adsorption geometry of reacted formate species will be discussed in detail.

P-Mo-091

Sandwich heterostructures of antimony trioxide and bismuth trioxide films: structural, morphological and optical analysis

Simona Condurache-Bota¹, Mirela Praisler¹, Raluca Gavrilă²

¹Dunarea de Jos University of Galati, GALATI, Romania, ²National Institute for R&D in Microtechnologies (IMT Bucharest), Bucharest, Romania

Thin film heterostructures can be advantageous since they either exhibit novel or a combination of the properties of their components. Here we propose sandwich-type of heterostructures made of antimony trioxide and bismuth trioxide thin films, which were deposited on glass substrates by thermal vacuum deposition at three substrate temperatures, 50 degrees apart. Their morphology and optical properties are studied as compared to the corresponding monolayers. It was found that even small substrate temperature changes strongly influence their morphology, increasing their roughness, while the optical transmittance shows a slight decrease as compared with the individual layers. The corresponding absorption coefficient exhibits intermediate values as compared to the component oxides, while the energy bandgaps for the indirect allowed transitions move towards the Infrared when overlapping the antimony and bismuth trioxides.

P-Mo-092

Near-infrared energy bandgap bismuth oxide thin films and their in-depth morpho-structural and optical analysis

Simona Condurache-Bota¹, Nicolae Tigau¹, Mirela Praisler¹, Gabriel Corneliu Prodan², Raluca Gavrilă³

¹Dunarea de Jos University of Galati, GALATI, Romania, ²Ovidius University of Constanta/Institute for Nanotechnologies and Alternative Energy Sources, Constanta, Romania, ³National Institute for R&D in Microtechnologies (IMT Bucharest), Bucharest, Romania

Bismuth oxide thin films generally exhibit high energy bandgap and high refractive indexes, depending on the deposition method and the corresponding deposition parameters. Such a material has already found some uses in Optoelectronics. Here we present the analysis of bismuth oxide thin films prepared by thermal evaporation of pure bismuth onto glass substrates in vacuum, followed by thermal oxidation in air. The substrate temperature during the initial bismuth deposition was varied from room temperature up till 200 deg. Celsius. In-depth transmission electron microscopy analysis was performed for the films, since bismuth exhibits a complex behavior upon oxidation, by giving several non-stoichiometric oxides along with different polymorphs of its stoichiometric bismuth trioxide. Not only the identification of the crystalline structure was done, but also the grain size and distribution was analyzed, such that the optical properties of the films could be explained and exploited for various applications. The refractive index of the films vary around 2.0 and the energy bandgap, as resulted from the Wemple-Didomenico model varies around 1.5 eV, corresponding to the near-infrared, making such films useful for thermal energy capture.

P-Mo-093

Water adsorption and freezing on ferroelectric oxide thin films

Laura Rodríguez^{1,2}, Kumara Cordero¹, María José Esplandiu^{1,2}, Carlos Escudero³, Victoria Pérez³, Annalisa Calò^{1,4}, Neus Domingo¹, Albert Verdaguer^{1,2}

¹ICN2- Institut Català de Nanociència i Nanotecnologia, Campus UAB, Bellaterra, Spain, ²CSIC-Consejo Superior de Investigaciones Científicas, ICN2 Building, Campus UAB, Bellaterra, Spain, ³ALBA Synchrotron Light Source, Barcelona, Spain, ⁴CIC nanoGUNE, Donostia-San Sebastian, Spain

Freezing of liquid water begins with an embryo ice formation. Although there are different nucleation mechanisms which induce that, the process also depends on temperature. In pure water, spontaneous icing can happen below -35°C by a mechanism called Homogeneous Nucleation. At higher temperatures, icing starts by activation due to the presence of any catalytic particle or surface. This mechanism known as Heterogeneous Nucleation, mostly leads the troposphere freezing processes.

But not all surfaces facilitate nucleation with the same efficiency because nucleation is also influenced by the surface-water interfacial energy. Moreover, the presence of electric fields or surface dipoles has been considered important for ice nucleation. For example, the water freezing temperature varies widely depending on whether it is onto polar or non-polar amino acid crystals: the former is far more efficient at inducing water freezing.

Recent experiments on pyroelectric materials have shown that water freezes differently on positively and negatively charged surfaces. However, this phenomenon has yet to be explained and yet to be explored at the molecular level. Ferroelectric oxides thin films can be used as model surfaces to study water adsorption and freezing dependence on surface polarization. In this contribution, we show a combination of Near-ambient X-ray photoelectron spectroscopy (XPS), Atomic Force Microscopy (AFM), Environmental Scanning Electron Microscopy (ESEM) and optical microscopy measurements. We compare water adsorption and ice nucleation on ferroelectric oxides thin films with the same composition but different surface polarization.

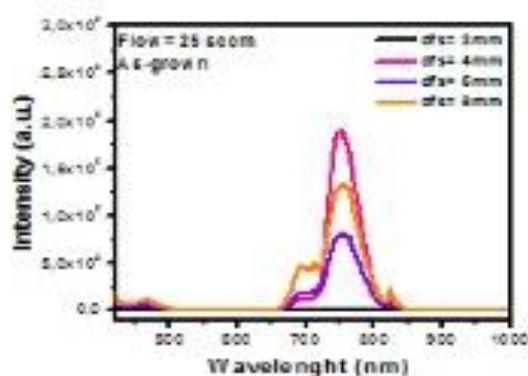
P-Mo-094

SiO_x films deposited by HFCVD: Annealing effect on the compositional and optical properties

Jose Alberto Luna Lopez¹, Diana Elizabeth Vazquez Valerdi¹, Alfredo Benitez Lara¹, Godofredo Garcia Salgado¹, Jesus Carrillo López¹, Alvaro David Hernandez de la Luz¹, Miguel Angel Dominguez Jimenez¹

¹BUAP, Puebla, Mexico

In this work, non-stoichiometric silicon oxide (SiO_x) films as-grown and after further annealing are characterized by different techniques. The SiO_x films are obtained by hot filament chemical vapor deposition technique at different hydrogen flow (25, 50, 75 and 100 sccm). Transmittance spectra of the SiO_x films showed a wavelength-shift of the absorption edge, thus indicating an increase in the optical energy band gap, when the hydrogen flow decreases. After thermal annealing this shifted is to high energies. Fourier transform infrared spectroscopy reveals, so that, the film composition changes with the hydrogen flow, also the vibrational band stretching have a behavior in agreement with the thickness obtained with profilometry. On the other hand FTIR spectra show vibrational bands related to the presence of hydrogen in as grown SiO_x films where this band is more intense as the hydrogen flow is increased, but disappears after thermal annealing. SiO_x films as-grown exhibit broad photoluminescence (PL) spectra with main peaks at 650 and 850 nm with high intensity and this is enhanced when the hydrogen flow decreases, with annealing the PL intensity quenches, at the same time that the presence of hydrogen disappears. These results lead to good possibilities for proposed novel applications in optoelectronics devices.



P-Tu-001

Heat-induced formation of molecular coordination networks of porphyrin derivatives on Au(111): Towards tuning the dimensionality

Tuan Anh Pham¹, Fei Song¹, Mariza N Alberti², Carlo Thilgen², Francois Diederich², Meike Stöhr¹

¹Zernike Institute for Advanced Materials, University of Groningen, Groningen, Netherlands, ²Laboratorium für Organische Chemie, ETH Zürich, Zürich, Switzerland

In the fast growing research field of on-surface molecular self-assembly, coordination bonding is currently considered as an important tool for the construction and design of low-dimensional molecular networks on metal surfaces, also in view of their prospective usage in future electronic devices.[1] To date, most of the reported metal-ligand coordination units stabilizing surface-supported metal organic frameworks (MOFs) are based on the combination of organic ligands bearing pyridyl, cyano, hydroxyl or carboxyl endgroups and transition-metal atoms such as Cu, Fe, Co or Ni.[2] However, the construction of such MOFs on Au surfaces with native Au atoms (without adding transition metal atoms) is hardly reported and thus, not well-understood. Here, we show that MOFs comprising porphyrin derivatives can be formed on Au(111) upon annealing. Both a threefold and a fourfold coordination motif stabilizing the MOFs were found. These findings were compared to MOFs made from the same cyano-functionalized porphyrin derivatives and Co atoms. For this, Co atoms and porphyrin derivatives were deposited on Au(111).[3] In both cases (native Au atoms and additional Co atoms), the same structures were observed what evidences that indeed a coordination bonding is formed between the cyano groups and gold atoms. Moreover, we also investigated the influence of the position of the substituents (cis- vs. trans-isomers) on the MOF formation on Au(111). We could successfully demonstrate that the dimensionality of the MOF can be tuned from 1D to 2D depending on the chosen isomer.

[1] H. Spillmann, A. Dmitriev, N. Lin, P. Messina, J.V. Barth, K. Kern, J. Am. Chem. Soc., 125, 10725 (2003).

[2] N. Lin, S. Stepanow, M. Ruben, J.V. Barth, Top. Curr. Chem., 287, 1 (2009).

[3] T.A. Pham, F. Song, M.N. Alberti, N. Trapp, C. Thilgen, F. Diederich, M. Stöhr, submitted (2015).

P-Tu-003

Post-deposition Hydrogen treatment effect on surface roughness and hydrophobicity of amorphous silicon films

Yamina Brahmi¹, Larbi Filali¹, Jamal Dine Sib¹, Yahia Bouizem¹, Djamal Benlekhal¹, Aissa Kebab¹, Larbi Chahed¹

¹University of Oran, Oran, Algeria

Amorphous silicon films were deposited by radiofrequency (rf) magnetron sputtering. Then, the films were treated by pure hydrogen gas at different pressures (1, 2 and 3 Pa) for 20 min, to investigate its effect on surface hydrophobicity (or un-wettability) and roughness. Fourier transform infrared-attenuated total reflection (FTIR-ATR) spectroscopy was used to evaluate presence of Si-H bonds at the surface. Results obtained by the atomic force microscopy (AFM) showed a sharp decrease (the non-treated film had a root mean square value of 81.74 nm, which then dropped significantly to 13.02 nm for the 1 Pa hydrogenated film) in surface roughness as a result of hydrogenation. Optical transmission results revealed that optical properties were not affected. Contact angle measurements showed an enhanced hydrophobicity by 15 degrees for the 1 Pa hydrogenated film, and then it decreased for the 2 Pa and 3 Pa hydrogenated films. This result indicates that the decrease in roughness compromised the hydrophobization process.

P-Tu-004

Analysis of the intra-molecular components of the inelastic electron tunneling signal by means of first-principles calculations

Giuseppe Foti¹, Héctor Vazquez¹

¹Institute of Physics, Academy of Sciences of the Czech Republic, Prague, Czech Republic

Inelastic electron tunneling spectroscopy (IETS) reveals the effect of the interactions between tunneling electrons and vibrations on the conductance of molecular junctions. Previous works addressing the origin of the inelastic signal have identified propensity rules describing the probability of having such processes [1, 2]. A local analysis of the propensity rules allows a deeper understanding of the sub-molecular mechanisms governing the relation between molecular vibrations and conductance. Here we determine by means of first-principles calculations [3] the intra-molecular contributions [4] at the origin of the inelastic signals in a benzene-based molecular junction. This detailed analysis reveals how the partial contributions of each atom and bond in the molecule add up or cancel each other providing a unique insight into the sub-molecular origin of the intensity of IETS peaks.

[1] A. Troisi et al., J. Chem. Phys. 125 (2006) 214709

[2] M. Paulsson et al. Phys. Rev. Lett. 100 (2008) 226604

[3] T. Frederiksen et al. Phys. Rev. B 75 (2007) 205413

[4] A. Gagliardi et al. Phys. Rev. B 75 (2007) 174306

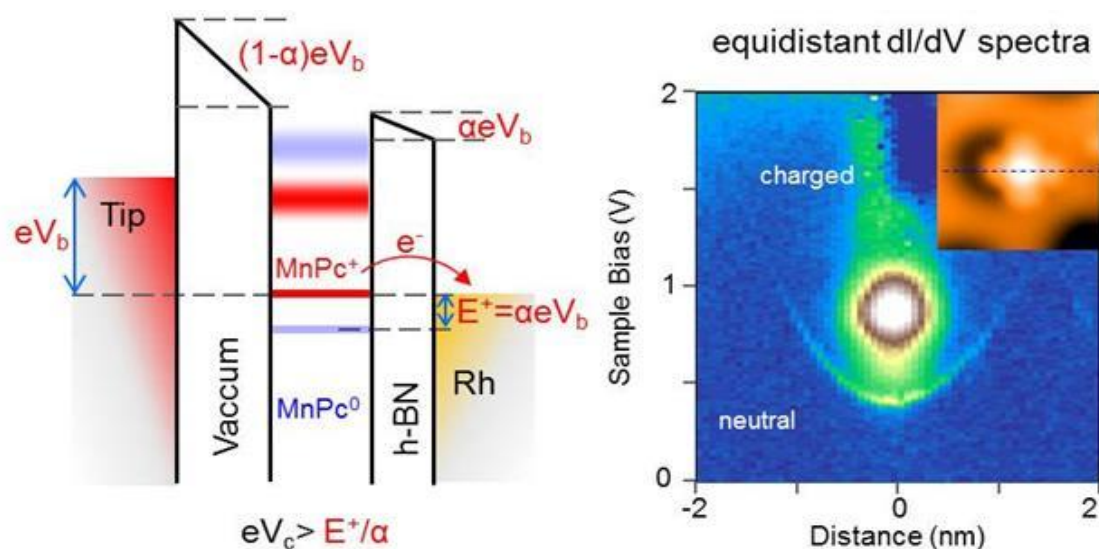
P-Tu-005

Interplay between Molecular Orbitals and Charging Effect of Manganese Phthalocyanine on Atomic Thin Insulator

Liwei Liu¹, Thomas Dienel¹, Roland Widmer¹, Oliver Groening¹

¹Empa, Swiss Federal Laboratories for Materials Science and Technology, Duebendorf, Switzerland

Sub-monolayer coverage of manganese phthalocyanine (MnPc) on hexagonal boron nitride (h-BN) on Rh(111) is studied by low-temperature scanning tunneling microscopy (STM) and spectroscopy (STS). The adsorbed molecules are categorized into three distinct types with very different bias-dependent-topographic signatures. Among the three kinds of MnPc, one shows pronounced charging behavior because of the low lying of highest-occupied molecular orbital (HOMO) level to the Fermi level on the decoupling h-BN substrate. The charging has dramatic different influence on the d orbital depending on whether it starts at low or high bias. Moreover, two adsorption orientations with small difference of the HOMO energies have their respective preferential charging behavior. Our results show how molecular adsorption and orbitals influence the charge states and subsequently, how charging effect affects orbital state on the seemingly inert h-BN ultrathin insulating substrate.



P-Tu-006

Bending of pentacene on Fibonacci modulated Cu film

M. Lahti¹, K. Pussi¹¹Lappeenranta University of Technology, Lappeenranta, Finland

Pentacene ($C_{22}H_{14}$, Pn) is a p-type organic semiconductor consisting of five linearly bonded benzene rings. It is an archetypal p-type molecule for organic field effect transistors and it has received much attention because of its unusually high intrinsic charge carrier mobility without doping. Significant deviation from a conventional planar adsorption configuration was only reported for Au(110) [1] and Al(001) [2] surface. Otherwise, only minor bending of the molecule, with the central ring closer to the surface have been reported.

A thin film of copper on the fivefold surface of Al–Pd–Mn forms a structure that is uniaxially commensurate with the aperiodic structure of the substrate. This structure has been analyzed using low-energy electron diffraction and is found to consist of a vicinal surface of a body-centered tetragonal (bct) (100) structure.[3]

We have studied the bending of a pentacene molecule adsorbed on this aperiodic copper surface with DFT and also how the distance between the nearest neighboring molecule affects the bending.

The magnitude of bending varies with coverage, and values between 0.47–0.78 Å has been calculated for an average bending measured between the the center of the molecule and a plane bisecting the H atoms at either ends. The adsorption energy also varied with the coverage. Lowest values were calculated for low coverage.

[1] Bavdek, G.; Cossaro, A.; Cvetko, D.; Africh, C.; Blasetti, C.; Esch, F.; Morgante, A.; Floreano, L. Pentacene Nanorails on Au (110). *Langmuir* 2008, 24, 767–772.

[2] Anu Baby, Guido Fratesi, Shital R. Vaidya, Laerte L. Patera, Cristina Africh, Luca Floreano, and Gian Paolo Brivio, *J. Phys. Chem. C* 2015, 119, 3624–3633

[3] K Pussi, M Gierer and R D Diehl, *J. Phys.: Condens. Matter* 21 (2009) 474213; K. M. Young, J. A. Smerdon, H. R. Sharma, M. Lahti, K. Pussi, and R. McGrath, *Phys. Rev. B* 87, 085407 (2013).

P-Tu-008

Reactivity of Metal-Organic Coordination Networks for CO₂ activation

Daniel Hurtado^{1,2}, Ane Sarasola^{3,4}, Gustavo Ruano^{1,2}, Klaus Kern^{2,6}, Andrés Arnau^{3,5}, Magalí Lingenfelder^{1,2}

¹Max Planck-EPFL Laboratory for Molecular Nanoscience, EPFL, Lausanne, Switzerland, ²Institut de Physique de la Matière Condensée, EPFL, Lausanne, Switzerland, ³Donostia International Physics Center(DIPC), Donostia, Spain, ⁴Departamento de Física Aplicada I, UPV/EHU, Bilbao, Spain, ⁵Departamento de Física de Materiales UPV/EHU y Centro de Física de Materiales CFM, Donostia, Spain, ⁶Max Planck Institut für Festkörperforschung, Stuttgart, Germany

Photosynthesis, the model system for energy conversion, uses CO₂ as its starting reactant to convert solar energy into chemical energy, i.e. organic molecules or biomass. The first and rate-determining step of this process is the immobilization and activation of CO₂, a carboxylation reaction catalyzed by the enzyme RuBisCO. The active center of the RuBisCO is Mg²⁺ ion surrounded by amino acids that anchor the ribulose and provide the CO₂ as a cofactor. In this way, inorganic carbon is transformed into organic carbon-based molecules. Metal-organic structures observed in nature, can be replicated in the laboratory by self-assembly. Inspired by the active site of the enzyme RuBisCO, we designed the first network using an alkaline earth metal (Group 2): magnesium (Mg). Here we present a method for producing stable networks of Mg and organic molecules by direct deposition onto a clean metal substrate. We track their reactivity and dynamic response to CO₂, O₂ and H₂ by Scanning tunneling microscopy (STM) under Ultra High Vacuum (UHV) conditions. Specific phase transformations are identified upon gas exposure at room temperature. Additionally, we have performed Density Functional Theory calculations aimed at understanding the reactivity of Mg atoms against CO and CO₂ adsorption when they are coordinated to three or four terephthalic acid (TPA) organic ligands forming a Mg-TPA ionic network. In particular, we have studied the preferential adsorption sites based on the analysis of the energetics of adsorption, as well as the changes induced in the Mg-TPA network upon adsorption.

P-Tu-009

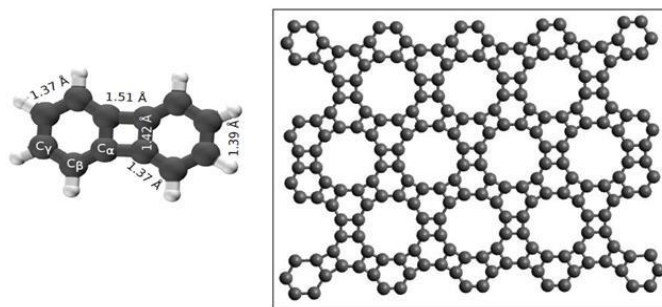
Biphenylene: a building block for 2D graphene-like gap-provided molecular network

Roberta Totani¹, Johann Lüder², Monica de Simone³, Ieva Bidermane², Cesare Grazioli^{3,4}, Teng Zhang², Marcello Coreno⁵, Henrik Ottosson⁶, Barbara Brena², Luca Lozzi¹, Carla Puglia²

¹Department of Physical and Chemical Sciences, University of L'Aquila, L'Aquila, Italy,

²Department of Physics and Astronomy, Uppsala University, Uppsala, Sweden, ³CNR-IOM, Laboratorio TASC, Sincrotrone Trieste, Trieste, Italy, ⁴Department of Chemical and Pharmaceutical Sciences, University of Trieste, Trieste, Italy, ⁵CNR-ISM, Trieste, Italy, ⁶Department of Chemistry, Uppsala University, Uppsala, Sweden

Covalently-bonded 2D carbon networks are graphene-inspired materials, which can combine the outstanding properties of graphene with other important characteristics like, for example, an intrinsic band gap, whose lack in graphene puts severe limits on its applications. The most reliable technique to grow this kind of materials is a bottom-up procedure, exploiting the surface-confined self-assembly of functional molecular building blocks, used as precursors. Their interaction with appropriate surfaces (generally coinage metals) induces an ordering of the precursors in molecular networks of specific design. Biphenylene is cyclic hydrocarbon that can be regarded as the very initial precursor of a 2D porous graphene-like molecular network, called biphenylene carbon (BPC, Figure 1). Density Functional Theory (DFT) calculations demonstrated that BPC is characterized by nonzero band gap and by bands with good dispersion and delocalized frontier orbitals, so it could be an ideal structure for many electronic applications. In order to study the behavior of biphenylene as precursor directly on a surface, in this work we show an x-ray photoemission and absorption (XPS and XAS) investigation on biphenylene films, deposited on a Cu(111) crystal. The occupied core and valence levels and the non-occupied states of the film are examined, to study the electronic properties of biphenylene in solid phase. Considering the importance of the biphenylene-substrate interaction in 2D molecular network formation, the film has been investigated in the multilayer and monolayer coverages to clarify the intermolecular (multilayer) and molecule – substrate (monolayer) dynamics. The obtained results have been compared with spectra of the single biphenylene molecule, provided by gas phase measurements and DFT calculations. This allowed to show the modifications induced in the film molecular electronic structure due the molecule–molecule and the molecule–substrate interactions. Furthermore, we have performed a XAS characterization of the overlayer orientation, whose knowledge is crucial for implementing thin film molecular electronics.



Left: Biphenylene molecule with theoretical bond lengths between C atom.
Right: BPC

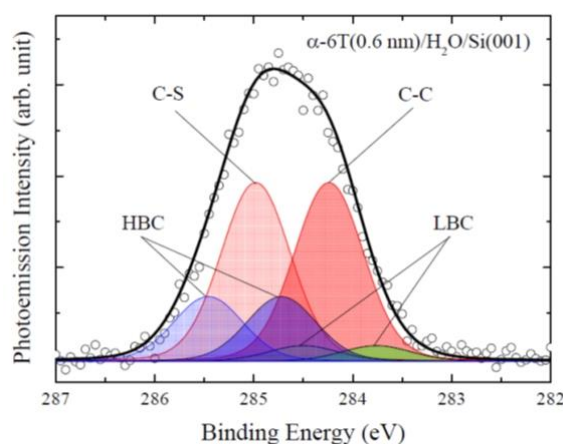
P-Tu-010

Electronic structure of sexithiophene ultrathin films grown on passivated Si(001) surfaces

Shinya Ohno¹, Hiroya Tanaka¹, Kazuma Tanaka¹, Kazutoshi Takahashi², Masatoshi Tanaka¹¹Yokohama National University, Yokohama, Japan, ²Synchrotron Light Application Center, Saga University, Honjo, Japan

Molecular organic semiconductor materials such as conjugated oligothiophenes have been extensively studied due to their potential application in electronic and optoelectronic devices [1]. Here, we focused on α -sexithiophene (α -6T), which contains six thiophene rings linked together in para positions. It has been reported that α -6T molecules dissociate on a clean Si(001) surface [2]. Therefore, we here used passivated Si(001) surfaces. In our previous study, we first determined the molecular orientation of α -6T on three passivated Si(001) surfaces: oxidized Si(001), water-adsorbed Si(001) and ethylene-adsorbed Si(001) by means of optical measurements [3]. Our ultraviolet photoelectron spectroscopy (UPS) study showed that the work function decreases upon the deposition of α -6T in the case of oxidized Si(001), while it is almost unchanged for ethylene-adsorbed Si(001) at the thickness lower than 0.5 nm [4]. The amount of the change in the work function is intermediate for water-adsorbed Si(001). It is likely that the molecular orientation is directly associated with the work function change. In the present study, we investigated the core levels (Si 2p, O 1s, C 1s, S 2p) using high-resolution photoelectron spectroscopy with synchrotron radiation. Figure 1 shows the C 1s state for the water-adsorbed Si(001). We identified two components other than the bulk component: one is the high binding energy component (HBC) shifted toward higher binding energy, and the other is the low binding energy component (LBC) shifted toward lower binding energy. Our results indicate that the HBC and LBC is associated with the orientation parallel to the surface and that perpendicular to the surface, respectively.

- [1] D. Fichou, J. Mater. Chem. 10 (2000) 571.
 [2] R. Lin et al., J. Chem. Phys. 117 (2002) 321.
 [3] H. Toyoshima et al., Surf. Sci. 616 (2013) 36.
 [4] K. Hiraga et al., Appl. Surf. Sci. 307 (2014) 520.



P-Tu-011

Soft bombardment with argon cluster on crystalline Si-H: Model system to study molecules at surfaces

Damien Aureau¹, Muriel Bouttemy¹, M. Jackie Vigneron¹, Arnaud Etcheberry¹

¹Institut Lavoisier, Versailles, France

All the studies performed on chemically modified surfaces must deal with the presence of organic contaminants that modify, alter and change the conclusions made. This paper proposes to study in details the contaminants thanks to the use of a perfectly controlled platform, H-Si(111), with an adapted tool, XPS spectroscopy with a new MAGCIS gun allowing depth profile with monoatomic and polyatomic argon ions. The possibility to change energy by atoms from some eV to thousands of eV allows to study in details cleaning, modification or real etching of the surface. Such approach helps to discriminate the nature of the elements detected and to see the impact of any bombardment on the Silicon signals. XPS experiments were performed on a Thermo-VG Escalab 250iXL spectrometer at the "CEFS2 center". A mono-chromatized Al K α X-ray line was used. We will show that cluster ion etching allows a really progressive etching with separate regimes from cleaning to etching while traditional monoatomic bombardment modifies the surface during cleaning steps. The fact the Carbon peaks continuously decrease while the oxygen peak remains important clearly shows that the etching remove only carbon contamination. Such behavior also reveals that the main part of the oxygen peak is related to traces of silicon oxide (Si-Ox formation at the interface) and not to adsorbed oxygenated molecules. The results presented here can directly impact the work of many groups who have been limited by contaminants in their analyses. Such approach is a also a new exciting and promising tool to study in details monolayers on surface by its capacity to remove successively the elements at different z-position.

P-Tu-012

Induced infrared absorption due to H₂, D₂, O₂, and CO₂ adsorbed on porous NaCl films

Koichiro Yamakawa¹, Katsuyuki Fukutani²

¹Department of Physics, Gakushuin University, 1-5-1 Mejiro, Toshima-ku, Tokyo, Japan, ²Institute of Industrial Science, The University of Tokyo, 4-6-1 Komaba, Meguro-ku, Tokyo, Japan

The adsorption states of molecules on alkali halide surfaces have been extensively studied for decades. Dai and Ewing used deposited NaCl films as substrates in order to investigate adsorption isotherms of homonuclear diatomic molecules by detecting induced infrared absorption [1-3]. In the present study, we observed induced infrared absorption due to H₂, D₂, O₂, and CO₂ adsorbed on porous NaCl films and discuss frequency shifts of their infrared inactive modes from the gas phase values.

The experimental apparatus consists of a UHV chamber with a liquid helium cryostat, a Fourier transform infrared spectrometer, and a compartment of a HgCdTe detector. NaCl porous films were deposited on a CaF₂(111) surface at 16 K. Subsequently, each gas of H₂, D₂, O₂, and CO₂ was dosed on the films, and infrared spectra were measured in the transmission configuration at 13 K. A strong absorption band due to the antisymmetric stretch of CO₂ was observed at 2343 cm⁻¹, and was attributed to CO₂ directly adsorbed on a NaCl film. In addition, we observed absorption bands at 1278 and 1384 cm⁻¹, which are attributed to induced infrared absorption of CO₂. When NaCl films were exposed to H₂, D₂, and O₂, absorption bands due to the symmetric stretch modes of the molecules were observed at ~4110, ~2960, and 1549 cm⁻¹, respectively. Whereas the band frequencies of H₂ and D₂ showed large red-shifts of ~50 and ~30 cm⁻¹, respectively, from the gas phase values, those of CO₂ and O₂ were red-shifted only slightly. We evaluate the frequency shifts of these bands and discuss the physisorption states of the molecules.

[1] D. J. Dai and G. E. Ewing, J. Chem. Phys. 98, 5050 (1993).

[2] D. J. Dai, J. Chem. Phys. 104, 2461 (1996).

[3] D. J. Dai, J. Chem. Phys. 104, 6338 (1996).

P-Tu-013

Quasi-one dimensional pentacene structures on
prepatterned vicinal silicon surface

Paweł Nita¹, Paweł Dyniec¹, Roberto Otero², hab. Mieczysław Jałochowski¹

¹Maria Curie-Skłodowska University, Lublin, Poland, ²IMDEA Nanociencia,
Madrid, Spain

Engineering of molecular nanostructures, especially one-dimensional (1D) molecular chains on silicon surfaces is of great importance, since it may integrate functionalities of organic species with the main-stream semiconductor electronics. However, on bare silicon, self-assembly of molecules into ordered structures is inhibited by the dangling bonds projecting out of the surface [1]. From the other hand, it was shown that 1D nanostructures on metal surfaces can be used as templates to direct molecular chain growth [2]. The same approach might also work on vicinal silicon surfaces, since 1D, metal-induced chain structures have been successfully realized on them [3].

Here, we report first, experimental results showing self-assembly of pentacene (Pn) molecules into regular, quasi-1D, chain-like structure on Si(553) surface prepatterned with lead atoms [4]. As deduced from STM images, at 1 ML coverage, pentacene molecules create two equivalent, most densely packed phases, which differ in orientation with respect to [11-2] direction. Both phases consist of array of three Pn rows within single (111) terraces. Along each row, the molecules adopt head to head orientation with the long axis parallel to step edges [5]. This work was supported by Polish Science Foundation Grant No. HOMING PLUS/2013-8/10.

[1] M. Kasaya et al., Surf. Sci. 400 (1998) 367.

[2] P. W. Murray et al., Phys. Rev. Lett 80 (1998) 988.

[3] F. J. Himpsel, et al., J. Phys.: Condens. Matter 13 (2001) 11097.

[4] M. Kopciuszynski et al., Phys Rev B 88 (2013) 155431.

[5] P. Nita et al., to be submitted.

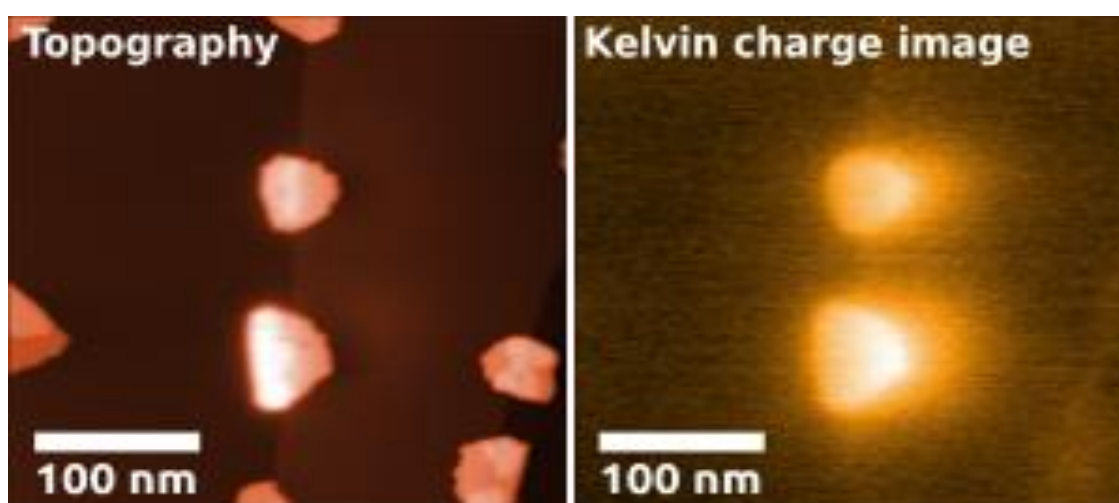
P-Tu-014

Charging C₆₀ islands on NaCl(001) by the AFM tipBrice Hoff¹, Claude R. Henry¹, Clemens Barth¹¹Centre national de la recherche scientifique (CNRS) / Aix-Marseille Université, Marseille Cedex 09, France

Since their experimental discovery in 1985, buckminsterfullerenes have been subject for many investigations in superconductivity, biochemistry and in photovoltaic. Based on weak van der Waals forces C₆₀ can self-assemble into a solid with a fcc lattice at room temperature, which has fascinated research ever since as exemplified by the large amount of scanning tunneling microscopy (STM) and noncontact atomic force microscopy (nc-AFM) work on supported C₆₀ films. A fascinating property of the single C₆₀ molecule is that due to its large electron affinity and low activation energy for electron attachment the molecule is a good electron acceptor. With respect to bulk C₆₀, calculations exhibit a semi-conducting character of the solid, with the electron affinity being even higher. The direct capture of electrons by single molecules can be realized in principle by crossing an electron beam with a molecular beam of C₆₀, which yields important information of about, e.g., the lifetime of C₆₀ anions. Charging bulk C₆₀ has been indirectly realized by intercalating potassium atoms into C₆₀ islands. The question is if charges can be directly transferred into bulk C₆₀.

In this contribution it is shown that by a combination of nc-AFM, electrostatic force microscopy (EFM) and frequency modulated Kelvin probe force microscopy (FM-KPFM) individual C₆₀ islands can be explicitly charged on demand with electrons (see two charged C₆₀ islands in the right 'Kelvin charge image' of the figure). We exemplify this by controlled charge manipulation experiments conducted at room temperature and in ultrahigh vacuum (UHV) on C₆₀ islands, which were grown on insulating bulk NaCl(001) [1]. We document the charging of single C₆₀ islands and discuss time dependent discharge processes at charged C₆₀ islands, which appear within hours of observation.

[1] B. Hoff, C. R. Henry, C. Barth, submitted (2015)



P-Tu-015

Interplay between molecule-molecule and molecule-substrate interaction: Pentacene on Pb/Si(553) surface

Mariusz Krawiec¹, Paweł Nita¹, Roberto Otero², Mieczysław Jałochowski¹¹Institute of Physics, Maria Curie-Skłodowska University, Lublin, Poland,²Instituto Madrilenio de Estudios Avanzados en Nanociencia (IMDEA Nanociencia), Ciudad Universitaria de Cantoblanco, Madrid, Spain

Molecular nanostructures play an important role in the field of nanoelectronics. One of the examples is pentacene ($C_{22}H_{14}$), a p-type π -conjugated chain molecule, featuring good carrier mobility. The properties of pentacene on various metal and semiconductor surfaces have been studied in recent years. On metals pentacene usually forms regular structures and interacts rather weakly. On semiconductor surfaces, due to chemical activity of the surfaces, the adsorption of pentacene results in strong bonding, and leads to disordered structures. Recently, we have discovered that pentacene self-assembles into arrays of one-dimensional chains on Pb decorated vicinal Si(553) surface. The ordering is very regular over macroscopic area of the sample. In the present work, using first-principles density functional theory, we study geometry and stability of pentacene molecules on Pb passivated Si(553) surface. We pay attention to the molecule-molecule and molecule-substrate interaction, and discuss their interplay at various surface coverage of pentacene. The DFT calculations suggest that this interplay is responsible for different orientations of pentacene with respect to the surface, i.e. horizontal vs. vertical.

This work was supported by Polish Science Foundation Grant No. HOMING PLUS/2013-8/10.

P-Tu-016

The work function changes of Ag(100) surface induced by cobalt phthalocyanine

Agata Sabik¹, Franciszek Golek¹, Grażyna Antczak¹¹Institute of Experimental Physics, University of Wrocław, Wrocław, Poland

The adsorption phenomena of organic π – conjugated molecules on metal surfaces attracts huge interest due to their possible application in electronic devices. The metal – phthalocyanines (MPcs) are widely studied as they exhibit promising electronic, optical and magnetic properties [1]. The study of work function changes ($\Delta\phi$), in particular, provides information about formation of interface dipoles and allow to probe various surface processes. Usually in metal – MPc interfaces the charge transfer occurs, which induces extra changes in $\Delta\phi$ [2]. We characterize the electronic, adsorption and desorption properties of CoPc on Ag(100) by means of the work function changes using diode (Anderson) method. The structural properties are probed by low energy electron diffraction (LEED). We explore how the CoPc adsorption influences the shape of $I - V$ characteristic and probe the $\Delta\phi$ as a function of coverage. The $\Delta\phi$ measurements reveal the minimum which is associated with coverage of 1 ML. The depth of the minimum varies with substrate temperature and is connected with charge donation from substrate to the molecule. Subsequent layers partly reduce the decrease in the work function caused by the first layer formation. The $\Delta\phi$ behavior depends on the sample temperatures during deposition. Probing the $\Delta\phi$ as function of annealing temperature allows determining the desorption parameters of CoPc from Ag(100).

[1] G. de La Torre, C. G. Claessens, T. Torres, Chem. Commun. 20, 2007, 2000

[2] E. Salomon, P. Amsalem, N. Marom, M. Vondracek, L. Kronik, N. Koch, T. Angot, Phys. Rev. B 87, 2013, 075407

P-Tu-017

Large X ray circular dichroism in adsorbed films of homochiral organic molecules

Juan José de Miguel¹, Francisco Jesus Luque¹, Iwona Agnieszka Kowalik², Miguel Angel Niño³, Dimitri Arvanitis⁴, Rodolfo Miranda¹

¹Department of Condensed Matter Physics, University Autonoma Madrid, Madrid, Spain, ²Institute of Physics, Polish Academy of Sciences, Warsaw, Poland, ³IMDEA-Nanoscience Madrid, Madrid, Spain, ⁴Department of Physics and Astronomy, Uppsala University, Uppsala, Sweden

Chiral molecules are fascinating objects lying behind some deep, still unexplained puzzles of Nature such as the fundamental asymmetry found in living beings, which only utilize molecules with a specific helicity, called enantiomers. One of the main characteristics of these molecules is their optical activity, that has long been known and studied for the visible and UV wavelengths but not so much in the X ray range.

Enantio-pure ultrathin films of chiral 1,2-diphenyl-1,2-ethanediol deposited on Cu(100) at 100 K have been studied using circularly polarized x rays absorption (XAS) at the carbon K edge. XAS excites element-specific core electrons to empty levels in the ground state thus probing the molecule's electronic configuration. The different features present in the absorption spectra have been identified and assigned to specific electronic transitions. The LUMO corresponds to the well-known π^* resonance of the C unsaturated bonds. Several other components also with π character follow in energy, which are assigned to the C–H bonds in the molecules, whereas broader features at higher energies correspond to σ -type C–C bonds.

Pairs of spectra with circularly polarized X-rays of opposite helicity were acquired and compared. Several clearly dichroic features have been observed and assigned to C–C and C–H π orbitals; the dichroic asymmetry shows opposite sign for the two enantiomers studied. Cross-check measurements using the non-chiral meso-DPED enantiomer confirm the direct relationship between the circular dichroism and the molecular handedness. Further photoemission microscopy (PEEM) experiments making use of the magnetic circular dichroism effect have also allowed us to image the magnetic state of the sample substrate –an epitaxial Fe film deposited on W(110)– and detect the enantiosensitive modifications induced by the adsorption of the chiral molecules. These findings lend additional support to the existence of some link between the molecular chirality and the electronic spin.

P-Tu-018

Coverage-dependent molecular packing and electronic structure of DNTT and Picene monolayer on Au(111)

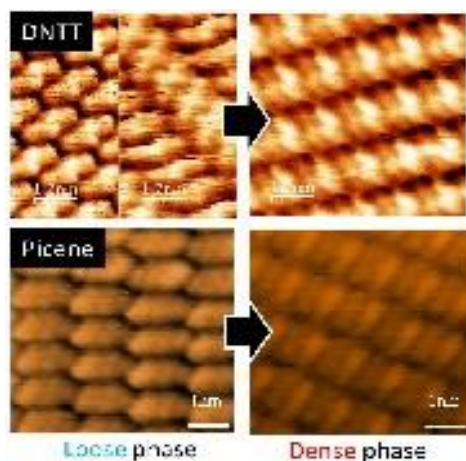
Yuri Hasegawa¹, Takuya Hosokai², Yutaka Wakayama³, Yoichi Yamada¹, Masahiro Sasaki¹

¹Institute of Applied Physics, University of Tsukuba, Tsukuba, Japan, ²National Institute of Advanced Industrial Science and Technology (AIST), Tsukuba, Japan, ³International Center for Materials Nanoarchitectonics National Institute for Materials Science (NIMS WPI-MANA), Tsukuba, Japan

Small organic compounds with strong intermolecular interaction, such as rubrene, picene, and DNTT, are promising materials for the organic thin film transistors. Single-crystalline films of these materials are also available and their carrier transport properties have become comparable to those of an amorphous Si. However, molecular-scale understanding of the film structure of these materials has not been well clarified. In this paper, we investigated the molecular-scale structure of the well-defined monolayers of DNTT and picene on Au(111) surface, at room temperature.

It is found with increasing amount of molecule that both molecular monolayers undergo a structural phase transition from a loosely packed phase consisting of face-on molecules to a densely packed phase with slightly tilted and dimerized molecules. All the monolayer phases does not seem to strongly interact with the substrate, since the herringbone reconstruction of Au(111) surface underneath the monolayer is always visible in the STM image of the monolayers.

Upon this reconstruction of the monolayer, electronic structure of both molecules also changes as suggested by means of UPS measurements. The rising edge of HOMO peak of the dense phase is found to shift to 0.3 eV and 0.5 eV toward lower binding energy compared to the loose phase, for picene and DNTT, respectively. This is possibly due to a splitting of HOMO level in the dense phase. We also calculated the HOMO level for the loose and dense phases and indeed found the splitting of HOMO in the dense phase. In addition, ARUPS measurement of the dense phase revealed the possible band dispersion of HOMO orbital, of about several tens meV. These observations demonstrate the control of the electronic properties of the organic monolayer by tailoring the molecular packing, i.e., the overlapping of the molecular orbitals.



P-Tu-019

Change in molecular orientation of metal phthalocyanines on heteroepitaxial growth using templating layer

Heeseon Lim^{1,2}, Sehun Kim¹, Jeong Won Kim²

¹Korea Advanced Institute of Science and Technology, Daejeon, Rep. of Korea,

²Korea Research Institute of Standards and Science, Daejeon, Rep. of Korea

Organic materials features low-cost, flexibility and large-scale fabrication, and their interfaces give essential information on device performance such as charge transport and mobility in OLED and OPVs. Especially, the molecular orientation can affect the electronic structure at interface and ultimately the device performance in OPVs. Thus, through the control of molecular orientation at interface, it is anticipated how the material characteristics such as light absorption, charge transport and energy level alignment in a device can be changed as we wish. One of the methods to control the molecular orientation is to use a templating layer such as PTCDA, pentacene, and CuX. Especially, CuI shows the best performance as templating layer and it can also modify the anodes in organic solar cells. To reveal the templating effect of CuI on heteroepitaxial growth, we investigate the change in the molecular orientation of metal phthalocyanine (MPc; M=Cu, Zn) on ITO with and without CuI templating layer using ultraviolet photoelectron spectroscopy (UPS), near edge X-ray absorption fine structure (NEXAFS), X-ray diffraction (XRD), and atomic force microscopy (AFM). It turns out that on CuI template layer, the orientation of CuPc molecules is changed and it represents relatively “lying-down” orientation with intermolecular π - π overlap being aligned in vertical direction, while the orientation of ZnPc molecules hardly changes (“standing-up”). This is because the CuPc and CuI layers have stronger interaction than ZnPc and CuI layers. Consequently, in bilayer OPVs consisting of CuPc as donor and C₆₀ as acceptor, the carrier transport across the donor-acceptor interface is enhanced by the insertion of CuI templating layer. In addition, the optical absorption in CuPc molecules is increased due to aligned transition matrix elements along the surface. Overall the lying down orientation of CuPc on CuI will improve photovoltaic efficiency.

P-Tu-020

Changing the Quantum Well Structure of Oxide-Supported Au Nanoislands by Molecular Adsorption: Chemisorption versus Physisorption

Christian Stiehler¹, Wolf-Dieter Schneider¹, Niklas Nilius², Hans-Joachim Freund

¹Fritz-Haber-Institute of the Max-Planck-Society, Berlin, Germany, ²Carl von Ossietzky Universität Oldenburg, Oldenburg, Germany

Electron quantization is a fundamental phenomenon that accompanies the transition from bulk metals to nanoclusters. The associated opening of an energy gap at the Fermi level crucially affects various properties of the nanostructures, e.g. its electrical and optical behavior and its performance in catalytic reactions [1]. Scanning tunneling microscopy and spectroscopy have been employed to analyze the impact of molecular adsorption on the quantized electronic structure of individual metal nanoparticles, containing between 50-200 atoms [2,3]. For this purpose, isophorone and CO₂, as prototype molecules for physisorptive and chemisorptive binding, were dosed onto monolayer Au islands grown on MgO ultrathin films [4]. An attachment of molecules was exclusively observed to the metal-oxide boundary. The Au quantum well states experience distinct energy shifts upon molecular adsorption, whereby adjacent states move apart in the CO₂ case but decrease their mutual spacing in isophorone-covered islands. Additional infrared reflection absorption spectroscopy measurements clearly reveal a fully reversible activation process of gas-phase CO₂ to oxalate species at the rim of the clusters, induced by electron-transfer processes between the Au islands and molecules [5].

[1] M. Valden et al., Science 281, 1647 (1998)

[2] X. Lin et al., Phys. Rev. Lett. 102, 2068011 (2009)

[3] C. Stiehler et al., Phys. Rev. B 88, 115415 (2013)

[4] C. Stiehler et al., submitted (2015)

[5] F. Calaza, C. Stiehler et al., Angew. Chem., in press (2015)

P-Tu-021

Effect of the Type of Fluorofunctional Organosilicon Compounds onto the Surfaces on its Hydrophobic Properties

Joanna Karasiewicz¹, Hieronim Maciejewski^{1,2}

¹Adam Mickiewicz University, Faculty of Chemistry, Poznań, Poland, ²Adam Mickiewicz University Foundation, Poznań Science and Technology Park, Poznań, Poland

Non-wettable surfaces with high water contact angles (WCAs) have received tremendous attention in recent years both in the context of protective coatings, antifoam agents and polymeric materials for special applications. It is possible to modify a surface of different materials to obtain strong hydrophobicity by combining specific features of chemical compound, especially low surface energy and particular topographic characteristics. Here we present the methods of glass surface modification using different organosilicon compounds from the group of fluorinated silanes, polysiloxanes and silsesquioxanes. In addition to octafluoropentyloxypropyltrimethoxysilane, we have used in our study also two siloxane copolymers of the same length of siloxane chain and the same number of octafluoropentyloxypropyl groups, however differing in the type of reactive groups (trimethoxysilylethyl or glycidoxypropyl ones), as well as two silsesquioxanes (POSS) with the analogous type of groups. The choice of such derivatives was based on results of our earlier studies. The hydrophobisation method involves the condensation reaction of the hydroxyl groups on the modified surface with reactive groups in the organofunctional compounds. Moreover, the present study was aimed at determining the effect of the modification way on the developed hydrophobic properties of the substrate. To meet this aim, modifications were performed by using solutions of organosilicon derivatives only and by adding nanosilicas. The measure of hydrophobicity is contact angle determined by drop profile tensiometry. The examined fluorocarbofunctional organosilicon derivatives are good precursors for the synthesis of highly hydrophobic materials and coatings. In some cases, obtained values of contact angles exceeded 150°, which are typical values for superhydrophobic surfaces.

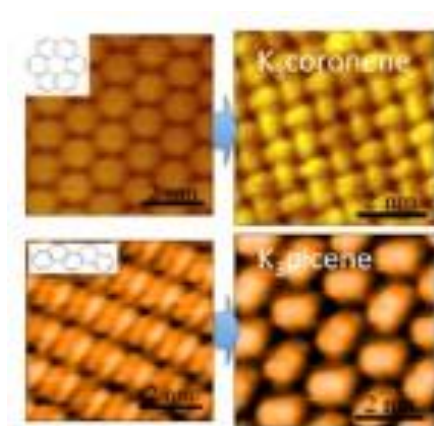
P-Tu-022

STM studies on Alkali Doping of Organic Monolayers

Yoichi Yamada¹, Masahiro Yano¹, Yuri Hasegawa¹, Masahiro Sasaki¹¹University of Tsukuba, Tsukuba, Japan

Electronic modifications of the organic materials by doping of foreign metals have been one of the key technologies in the current organic electronics. While many of researches in this line have been concentrating on the electronic points of view, structural aspects with respect to the doping have not been well explored. However, structural viewpoints are of crucial importance in the weakly bound organic systems. In this work, we studied two doping systems, K-doping of aromatic molecules (coronene, picene) and K-doping of phthalocyanines (Pcs). Exotic phase transitions, such as a superconducting (SC) transition and the insulator-metal-insulator transition, have been reported for these systems, respectively. We modeled these systems by a well-defined monolayer with metal dopants, on the inert substrates. STM investigations on the model systems have revealed a significant structural modification of the molecular layer upon the metal doping.

In the case of K-doping of coronene and picene, noticeable reconstruction of the monolayer takes place at the doping level of the "optimum" doping for the SC transition, i.e. 3 atoms/molecule. The reconstructed phase appears to be consisting of the standing-up molecules, suggesting that the K atoms are intercalating in between the molecular plane. The reconstruction also gives rise to a new density of states just below the Fermi level, possibly reflecting the onset of the metallization of the system. In the case of K-doping of Pcs, subtle reordering of the monolayer was found at the doping level of 1 and 2 atoms/molecule followed by disordering of the whole layer above 3 atoms/molecule. On the other hand, no metallicity was found in the photoemission spectrum at any doping level. The observation of the reordering and disordering of the Pc layer seems to be corresponding to the reported increase and decrease in the conductivity of the Pc films.



P-Tu-023

Thermal evolution of hydrogenated phthalocyanine molecules on copper

Ane Sarasola^{2,3}, Mikel Abadia¹, Ruben González-Moreno^{1,2}, Giacomo Lovat⁴, Luca Floreano⁴, Celia Rogero^{1,2}, Aran García-Lekue^{2,5}

¹Centro De Física De Materiales (CSIC-UPV/EHU), San Sebastian, Spain,

²Donostia International Physics Center (DIPC), San Sebastian, Spain, ³1Dpto. Física Aplicada, Universidad del País Vasco UPV/EHU, San Sebastian, Spain,

⁴CNR-IOM, Laboratorio Nazionale TASC, Trieste, Italy, ⁵IKERBASQUE, Basque Foundation for Science, Bilbao, Spain

Using a combination of X-ray photoelectron spectroscopy (XPS) and density-functional theory (DFT) calculations, we determine the hydrogenation and subsequent dehydrogenation of phthalocyanine molecules on a copper surface. Several XPS measurements of different metalated phthalocyanine molecules grown on Cu(110) have put in evidence the unexpected presence of a pyrrolic nitrogen component in the submonolayer regime. Our calculations demonstrate that the double peak observed in the XPS experiments is not a final-state effect, i.e. is not due to the splitting of the LUMO level [1]. Rather, the reaction of the ZnPc molecules with the extra H atoms in the chamber [2] gives rise to H₃ZnPc molecules, which having two inequivalent N atoms produce a double peak in the XPS spectra. This additional XPS peak in the N1s core level region is often observed when evaporating phthalocyanine or porphyrin molecules on many other surfaces [3]. Subsequently, we investigate the thermal evolution of the system. By comparing the evolution of the experimental XPS peaks as a function of the temperature with the DFT-based core level shift calculations, we conclude that the evolution of the system upon annealing is related to the dehydrogenation of the H₃ZnPc molecules following a two-step process.

[1] P. Borghetti et al. ACS Nano 12, 12786 (2014)

[2] F.D. Natterer et al., Surf. Sci. 615, 80 (2013)

[3] S. Yu. Et al. J. Chem Phys 136, 154703 (2012); A. Garcia-Lekue et al., J. Phys. Chem C 116, 15378 (2012)

P-Tu-025

An in situ XPS study of biomolecules co-adsorbed with water on gold

Astrid Jürgensen¹, Hannes Raschke¹, Norbert Esser², Roland Hergenröder¹

¹Leibniz-Institut für Analytische Wissenschaften - ISAS e.V., Dortmund, Germany, ²Leibniz-Institut für Analytische Wissenschaften - ISAS e.V., Berlin, Germany

The interaction of proteins and peptides with solid surfaces is important in a wide range of natural and technological processes. An adsorbed layer of such biological molecules introduces complex reactive functionality to the substrate which has a wide variety of applications, including catalysis, sensors, and bio-compatible materials. Amino acids, the basic building blocks in the formation of peptides and proteins, are of interest in surface science and nanotechnology, since their structure is simple enough to serve as a model for the chemisorption of biomolecules. In particular, L-cysteine interacts strongly with noble metals, and the model system of L-cysteine on gold has been studied extensively. It offers a good starting point to investigate the more complex interaction of small peptides such as glutathione (GSH) with different metal surfaces. A challenge in studying model bio-surface systems is that the relevant applications take place in aqueous solution near room temperature. Of particular interest is the structure of the first few monolayers on the surface, as these layers determine most interfacial properties, including the adsorption and reaction of biomolecules at surfaces. However, despite this importance, the actual processes involved are still not well understood.

Here we present the first results of an in situ study on the interaction of water and small biomolecules using near-ambient pressure x-ray photoelectron spectroscopy (NAP-XPS) with a conventional Al K α x-ray source. Thin films of L-cysteine and glutathione were grown on polycrystalline gold from aqueous solution or via vapour deposition. They were characterized in UHV and in a water vapour atmosphere up to a pressure of 1 mbar. The effect of a water vapour atmosphere on the composition and structure of the films was investigated.

P-Tu-026

Control parameters in a local epoxidation reaction using scanning probe lithography

Vincent Mesquita¹, Julien Botton², Lionel Patrone¹, Mathieu Abel¹, Silviu Balaban², Olivier Chuzel², Jean-Luc Parrain², Sylvain Clair¹

¹Aix-Marseille Université, CNRS, IM2NP UMR 7334, Marseille, France, ²Aix-Marseille Université, CNRS, ISM2 UMR 7313, Marseille, France

The main objective of this study is to show how the probe of an atomic force microscopy (AFM) can locally and selectively initiate a chemical reaction on a surface. Scanning probe lithography (SPL) is a highly promising tool for the creation of specific nanosized patterns on a surface with high spatial resolution.[1] We have recently reported a novel approach to chemically selective lithography using an AFM probe with immobilized manganese complex homogeneous catalyst, potentially opening access to a diversity of nanoscale transformations of the surface-bound functional groups [2]. This new concept was proven for local epoxidation of alkene-terminated self-assembled monolayer (SAM) on silicon using H₂O₂ as an oxidant and a catalytic silicon AFM tip charged with manganese complexes with 1,3,7-triaza-cyclononane type ligand in double heterogeneous conditions. The reaction was revealed by selective grafting of N-octylpiperazine molecules or other compounds like ferrocene, fullerene or porphyrin derivatives onto the modified areas of the surface.

We have further studied the influence of the physicochemical parameters on the reaction yield of this chemical model reaction, like the applied force, the reaction time or the catalyst configuration. We could achieve a resolution limit of ~30nm. We found that the catalytic system is very robust and could successfully be used for grafting laterally an equivalent surface of at least 450µm², but also vertically for sequential grafting of a 3D pyramidal edifice of up to three molecular layers high.

P-Tu-027

Computational modelling of Lindqvist polyoxomolybdate on Au (111)

Zhongling Lang¹, Anna Clotet¹, Josep M. Poblet¹

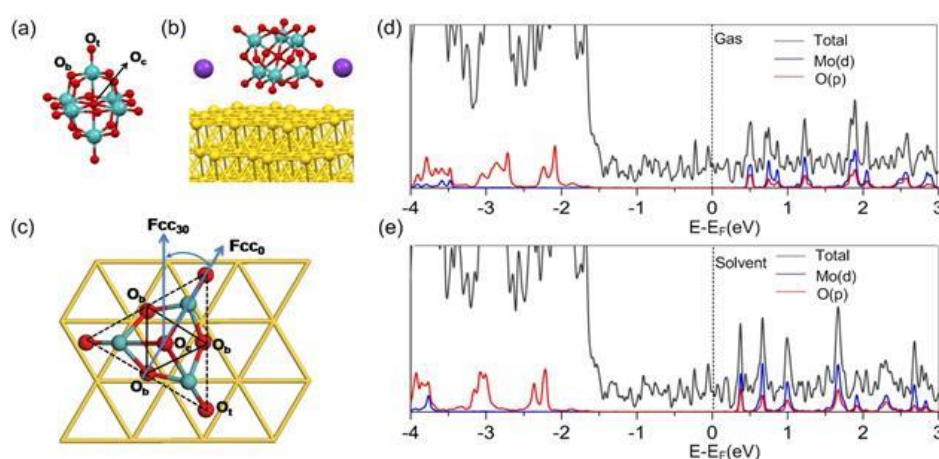
¹Departament de Química Física i Inorgànica, Universitat Rovira i Virgili, Tarragona, Spain

Adsorption of polyoxometalates (POM) on surfaces provides a new platform for their application in catalysis. It is necessary to know first the behaviour of POMs on the surface. After our previous studies of α -Keggin ($[\text{SiW}_{12}\text{O}_{40}]^{4-}$) on Ag surfaces [1,2], we investigate the Lindqvist adsorption ($[\text{Mo}_6\text{O}_{19}]^{2-}$) on Au(111). Thus, different active sites were explored using a periodic plane wave DFT based method. The most favorable adsorption sites (Fcc30 and Hcp30) for the anion $[\text{Mo}_6\text{O}_{19}]^{2-}$ on the Au(111) surface was determined with six O atoms (3Ot and 3Ob) directly linking with Au. The computed surface-POM (Au–Ox) distances are in the range 2.32–2.46 Å, which overestimate the interaction between the POM and the surface. The solvent model (using VASP) and the counteranions (2K^+) were introduced to correct the effect of the environment, which is crucial for ionic species. The Au–O distances increase to 2.71–2.87 Å, which is in agreement with those found in $[\text{AlW}_{11}\text{O}_{39}]^{9-}$ on gold nanoparticles. The electronic structures and Bader charges show that this POM on Au(111) is stable enough and it is difficult to be spontaneously reduced both in gas and solvent phases. The introduction of the solvent and the counteranions can correctly describe the geometry and electronic properties of this system. This strategy could be applied to other POMs in order to unravel the catalytic mechanism mediated by the adsorption of POMs.

Figure 1: (a) Oxygen labels of $[\text{Mo}_6\text{O}_{19}]^{2-}$; (b) Representation of $[\text{K}_2\text{Mo}_6\text{O}_{19}]$ on Au(111); (c) Representation of Fcc0 site and the rotation motion to Fcc30 site; (d) and (e) Density of States and Projected Density of States for $\text{K}_2\text{Mo}_6\text{O}_{19}$ on Au(111) in gas and solvation phase, respectively.

[1] X.Aparicio-Angles, P.Miro, A.Clotet, C.Bo, J.M.Poblet, Chem.Sci., 2012, 3, 2020–2027.

[2] X.Aparicio-Angles, A.Clotet, C.Bo, J.M.Poblet, Phys.Chem.Chem.Phys., 2011, 13, 15143–15147.



P-Tu-028

Interaction of copper phthalocyanine with Sn and In reconstructed Si(111) surfaces - STM study

Petr Zimmermann¹, Pavel Sobotik¹, Karel Majer¹, Pavel Kocan, Ivan Ostadal¹

¹Charles University in Prague, Prague, Czech Republic

Metalophthalocyanines (MPc) are small conjugated organic molecules with a broad range of applications in printing and dyeing, solar cells or organic semiconductors. Their strong photoabsorption and charge transfer abilities make them interesting for applications in silicon microtechnology. Moreover, they are currently being investigated for use in novel areas such as cancer treatment or quantum computing. In our contribution we present the results of our STM investigations of CuPc interaction with In and Sn reconstructed Si(111) surfaces. Both metals can produce structurally and electronically diverse reconstructions of the Si(111) surface. We report on the nature of CuPc interaction with the Sn- $\sqrt{3}\times\sqrt{3}$, Sn- $2\sqrt{3}\times2\sqrt{3}$, In- 4×1 , In- $\sqrt{3}\times\sqrt{3}$ and In- $\sqrt{31}\times\sqrt{31}$ reconstructions: the In $\sqrt{3}\times\sqrt{3}$ surface is simple and semiconducting while the Sn- $\sqrt{3}\times\sqrt{3}$ is conducting, the Sn- $2\sqrt{3}\times2\sqrt{3}$ and In- $\sqrt{31}\times\sqrt{31}$ surface have a complex unit cell, the In- 4×1 surface contains 1D conducting wires. A common trait in the interaction of CuPc with these surfaces is the key role of surface defects and structural dislocations in anchoring of the molecules. Si substitutional defects and dislocations play a special role in producing interesting bi-stable configurations and ordered arrays. Behaviour of CuPc molecules on these different reconstructions will be compared and discussed.

P-Tu-029

On-surface reactions of porphyrin molecules on Au(111)

Nino Hatter¹, Laëtitia Farinacci¹, Sonja Schubert¹, Benjamin W. Heinrich¹,
Katharina J. Franke¹

¹Institut für Experimentalphysik, Freie Universität Berlin, Berlin, Germany

Chemical reactions on surfaces are strongly influenced by the nature and properties of the substrate. Its catalytic activity may reduce the reaction barrier, increase the reaction yield, but also lead to a different product. Porphyrin is the parent compound of the class of porphyrines, consisting of a conjugated tetrapyrrole macrocycle. The central H-atoms can be easily substituted by a transition metal atom, which endows the molecule with paramagnetic properties. Here, we present a low-temperature scanning tunneling microscopy/spectroscopy (STM/STS) study of free-base porphyrin adsorbed on Au(111). The molecules tend to stay isolated on the surface, suggesting an electrostatic repulsion between each other. All molecules exhibit the same electronic structure around the Fermi energy. Annealing to 630 K leads to a modification of monomers as well as to the formation of covalently linked dimers and oligomers. In agreement with previous experiments on Ag(111) [1], we identify different types of porphyrin dimers, which can be distinguished by their shape and electronic structure. Subsequent deposition of Fe onto the surface at room temperature leads to a self-metalation [2,3] of the monomers and dimers. In their metallic center, we detect inelastic excitations in the differential conductance spectra, which are fingerprints of magnetic excitations. The differential conductance steps are broadened in the metalized dimers. This points to a stronger interaction with the substrate as a consequence of the larger π -electron system, which enhances the hybridization of molecular states with the electronic bands of the substrate.

[1] A. Wiengarten et al., J. Am. Chem. Soc. 2014, 136 (26), 9346-9354

[2] J.M. Gottfried et al. J. Am. Chem. Soc. 2006, 128, 5644

[3] W. Auwärter et al. ChemPhysChem 2007, 8, 250

P-Tu-031

Para-hexaphenyl-dicarbonitrile on Au(111) and graphene: A STM and nc-AFM study

Juan Carlos Moreno Lopez¹, Stefano Gottardi¹, Leticia Monjas², Leonid Solianyik¹, Jun Li¹, Kathrin Müller¹, Fei Song¹, Tuan A. Pham¹, Anna K. H. Hirsch², Meike Stöhr¹

¹Zernike Institute for Advanced Materials, University of Groningen, Groningen, Netherlands, ²Stratingh Institute for Chemistry, University of Groningen, Groningen, Netherlands

Nowadays, organic thin films are used in several commercial applications, among others, in photovoltaic cells, light-emitting devices and field-effect transistors. To improve the performance of these commercial devices, a clear understanding of the mechanisms that govern molecular adsorption on inorganic surfaces is needed. A promising strategy for building functional molecular 2D architectures is based on the autonomous organization of molecules without human intervention, called molecular self-assembly. This approach opens up the possibility to meet the demands of cheaper, lighter, and sustainable materials. Real-space observation with sub-molecular resolution of the molecular arrangement on surfaces is a very helpful prerequisite to obtain insight into the forces that govern 2D molecular self-assembly.

In this work, by means of low-temperature Scanning Tunneling Microscopy (LT-STM) and non-contact Atomic Force Microscopy (nc-AFM), we studied the formation of porous molecular networks from para-hexaphenyl-dicarbonitrile (P6) on both Au(111) and graphene surfaces. For deposition of P6 on Au(111) held at room temperature, the molecules arrange in a rhombohedral nanoporous network stabilized by a combination of dipolar coupling and hydrogen bonding interactions. By either thermal annealing or deposition of metal atoms, the formation of a metal-coordinated honeycomb network is induced on Au(111). In contrast, when the molecules are deposited on graphene no porous network forms. Instead, a densely-packed phase held together by dipolar coupling and hydrogen bonding is observed which is similar to the one found for bulk P6. While thermal annealing does not modify the arrangement, the deposition of metal atoms can induce changes of the molecular arrangement in dependence of the sort of metal atoms deposited. These results are compared with the ones obtained on Au(111) and the reported in literature.

P-Tu-033

Effects of an oxygen adlayer on the on-surface Ullmann polymerization of halobenzenes on Cu(110)

Gianluca Galeotti¹, Marco Di Giovannantonio², Nicola Angelo Rana³, Maryam Ebrahimi¹, Josh Lipton-Duffin^{1,4}, Dmitrii F. Perepichka⁵, Giorgio Contini², Federico Rosei^{1,5}

¹Centre Énergie, Matériaux et Télécommunications, INRS, Varennes, Canada,

²Istituto di Struttura della Materia, CNR, Rome, Italy, ³Physics department, University of Roma Tor Vergata, Rome, Italy, ⁴CARF, Institute for Future Environments, Queensland University of Technology, Brisbane, Australia,

⁵Department of Chemistry and Center for Self-Assembled Chemical Structures, McGill University, Montreal, Canada

Extended on-surface networks of π -conjugated organic polymers have been intensely studied in recent years. The combination of monolayer thickness and tunable band-gaps make them perfect candidates for low-cost flexible organic electronic devices. Until recently most on-surface polymerization reactions have exploited the catalytic properties of transition metal surfaces, using well known reactions such as Ullmann coupling to produce polymers on conducting substrates [1]. Of particular interest in on-surface Ullmann coupling is the role of the halogen; its electronegativity and mobility on the surface plays a non-negligible role in the reaction kinetics and in the structure of the products.

To study this effect we have investigated the effect of switching the halogen in the same reaction, and have explored its role in Ullmann coupling on bare and oxidized Cu(110). Both the choice of halogen and the oxygen passivation allow direct control over the reactants' mobility and activation barriers, and provide a means of tuning the speed and temperature of the coupling reaction. We report on a particularly interesting behaviour when using iodated precursors: subsequent to carbon-iodine cleaving, selective replacement of the oxygen in the substrate oxide takes place with gentle annealing, whereas the same effect is not observed with brominated precursors. Higher temperature annealing destroys the organic network, by oxidation and desorption of CO_x species.

[1] M. Bieri et al., JACS 2010, 132; J. Bjork et al., JACS 2013, 135; R. Gutzler et al. Nanoscale, 2014, 6

P-Tu-034

Unstable configuration of CuPc molecules on the Sn/Si(111)-($\sqrt{3}\times\sqrt{3}$) surface studied by scanning tunneling microscopy

Karel Majer¹, Petr Zimmermann¹, Pavel Sobotík¹, Pavel Kocán¹, Ivan Ošřádal¹

¹Charles University in Prague, Prague, Czech Republic

Phthalocyanines are conjugated organic molecules with strong photoabsorption and charge transfer properties which make them a promising material for a wide range of applications – e.g. organic transistors, organic solar cells or novel methods of cancer treatment. Our STM investigations of CuPc adsorbed on the Sn/Si(111)-($\sqrt{3}\times\sqrt{3}$) surface have shown that some molecules are adsorbed in unstable „fuzzy“ configurations. The „fuzzy“ appearance in STM is indicative of tip-induced molecular fluctuations during scanning. Moreover, „fuzzy“ molecules can switch into two non-fluctuating configurations. Molecules with multistable adsorption configurations could be used as molecular switches in nanoelectronic circuits. We discuss the role of adsorption site on adsorption configuration and present our results of current-fluctuation measurements employed to study the fluctuations of „fuzzy“ CuPc molecules. We observed multistable behavior of CuPc molecules and studied the effect of the electric field and tunneling current on molecular fluctuations.

P-Tu-036

Molecular electronics functional units on Si(100)

Wojciech Koczorowski², Maciej Bazarnik^{1,2}, Agnieszka Racis³, Leszek Jurczyszyn³, Marian W. Radny^{2,4}, Karina Morgenstern⁵, Ryszard Czajka²

¹Department of Physics, University of Hamburg, Hamburg, Germany, ²Institute of Physics, Poznan University of Technology, Poznan, Poland, ³Institute of Experimental Physics, University of Wroclaw, Wroclaw, Poland, ⁴School of Math. and Phys. Sciences, The University of Newcastle, Callaghan, Australia, ⁵Chair of Physical Chemistry I, Ruhr-University Bochum, Bochum, Germany

Molecular electronics proposes to use single molecules as functional units within larger circuits. Electronic industry is based on Si(100), therefore finding molecules, which can act as a switch on silicon is essential. Furthermore a development of contacts by nanowires at desired positions on the surface is necessary. A weak interaction between the functional unit of the adsorbed molecules and the surface is crucial for the molecules' isomerisation capabilities. The platform approach seems to be the most promising in achieving this. Diffusion of metallic adsorbates on Si(100) is causing an instability of nanowires grown at sub 0.1 monolayer coverage. Activation of certain sites on silicon surface is possible due to preabsorption of small molecules. In this contribution we show by a combination of scanning tunneling microscopy and density functional theory that: realizing a photo-switch is possible for anilino-nitroazobenzene molecule that adsorbs as in the platform approach, also Pb and Al nanowires growth may be induced by preadsorption of benzonitrile molecules. Our study demonstrates a very compact photo-switch on a Si(100) surface, and molecules induced nanowire growth as prototypes of a molecular functional units for further incorporation into devices.

We gratefully acknowledge financial support from the Polish Ministry of Science and Higher Educations under project nr IP2012 031772.

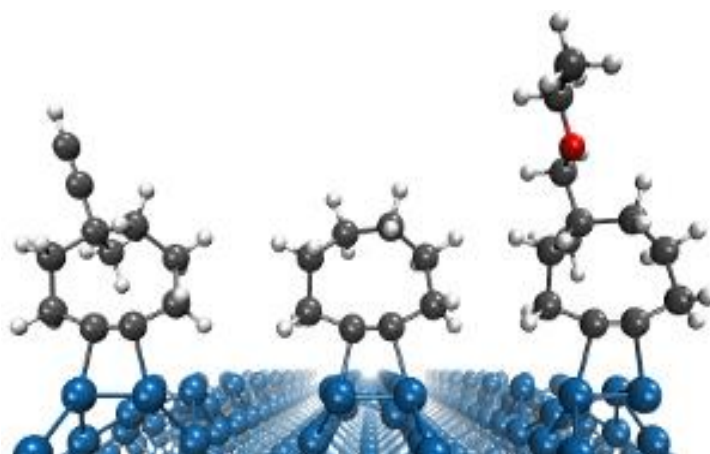
P-Tu-037

Computational investigation of adsorption and dynamics of molecules for organic-semiconductor interfaces on Si(001)

Josua Pecher¹, Ralf Tonner¹¹Fb. Chemie, Philipps-Universität Marburg, Marburg, Germany

Organic/semiconductor interfaces play an important role in the development of new materials and devices. In particular, the use of cyclooctyne (Fig. 1, center) derivatives on the silicon(001) surface promises to be an ideal starting point for the construction of such interfaces. Adsorption structures and their thermodynamical aspects have been determined experimentally[1] for cyclooctyne on Si(001), while an analysis of the kinetic processes and the general behaviour of the derivatives remains to be done. We compare the adsorption dynamics of two selected cyclooctyne derivatives (Fig. 1, left and right) to the unsubstituted molecule with density functional theory methods and analyze their bonding and reactivity on the surface in order to predict the suitability as building blocks for internal interfaces.

[1] G. Mette, M. Dürr, R. Bartholomäus, U. Koert, U. Höfer, Chem. Phys. Lett. 2013, 556, 70.



P-Tu-039

Hydrogenation of polycyclic aromatic hydrocarbons studied with scanning tunneling microscopy

Anders Lind Skov¹, Jakob Jørgensen¹, Liv Hornekær¹

¹Aarhus University, Aarhus C, Denmark

Scanning tunneling microscopy (STM) has been used to study the hydrogenation of the polycyclic aromatic hydrocarbon (PAH) coronene (C₂₄H₁₂). PAHs are thought to exist in significant quantities throughout the interstellar medium (ISM) and have been suggested to account for up to 20% of the carbon in the ISM [1]. PAHs therefore play an important part in the chemical environment of the ISM and observations have suggested that they can act as a catalyst for the formation of H₂, since a correlation between PAH emission and H₂ formation rates has been observed in certain parts of the ISM [2]. Density functional theory (DFT) calculations have suggested that neutral PAHs can act as a catalyst for H₂ formation through superhydrogenation of the molecules [3]. This has previously been confirmed experimentally using temperature programmed desorption measurements of deuterated coronene on graphite [4]. Here we attempt to use STM to follow the hydrogenation of coronene with the aim to investigate the catalytically active sites of the coronene molecule. Coronene films were deposited on graphite under UHV conditions and subsequently characterized with cryo-STM, at 6 K. The films were subsequently exposed to 2300 K atomic hydrogen and then characterized with STM at 6 K. STM images of the coronene films showed clear submolecular resolution of the coronene molecules both before and after exposure to hydrogen. Changes to the electronic structure were mainly observed at edges of the coronene molecules suggesting that these sites are the most active. The experimental results are compared with DFT calculations.

[1] G. C. Clayton et al., *Astrophys J*, 2003, 592, 947-952.

[2] E. Habart et al., *Astron Astrophys*, 2003, 397, 623-634.

[3] E. Rauls and L. Hornekær, *Astrophys J*, 2008, 679, 531-536.

[4] J. D. Thrower et al., *Astrophys J*, 2012, 752.

P-Tu-040

Electronic characterization of the gas phase iron phthalocyanine by means of soft x-ray spectroscopy and multiplet calculations

Johann Lüder¹, Ieva Bidermane^{1,2}, Roberta Totani³, Cesare Grazioli^{4,5}, Monica de Simone⁴, Marcello Coreno⁶, Antti Kivimäki⁴, John Åhlund¹, Luca Lozzi³, Barbara Brena¹, Carla Puglia¹

¹Department of Physics and Astronomy, Uppsala University, Uppsala, Sweden,

²Institut des Nanosciences de Paris, UPMC Univ. Paris, Paris, France,

³Department of Physical and Chemical Sciences, University of L'Aquila, L'Aquila, Italy, ⁴CNR-IOM, Laboratorio TASC, Trieste, Italy, ⁵Department of Chemical and Pharmaceutical Sciences, University of Trieste, Trieste, Italy,

⁶CNR-ISM, Basovizza Area Science Park, Trieste, Italy

Understanding the building blocks of functional materials is essential to achieve profound tailored functionality. Metal-organic macro-cycles like metal-porphyrins and -phthalocyanines can be such building blocks. Regarding magnetic properties, the iron phthalocyanine is of particular interest for applications in molecular spintronic and as single molecular magnet.

We present a characterization of the gas phase Fe 2p x-ray adsorption spectroscopy measurements (XAS) in conjunction with those of the N and of the C 1s x-ray photoelectron spectroscopy (XPS). The results can be considered as a fingerprint of the unperturbed molecule. The comparison of the gas phase measurements with those conducted on the molecular film revealed great similarities. Multiplet calculations yielded additional insights into the electronic features of the molecules in the gas phase and in the molecular film.

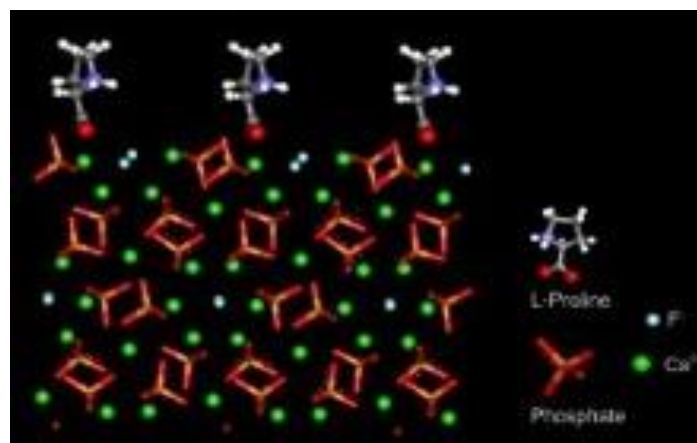
P-Tu-042

GIXRD study about adsorption behavior of aqueous proline solution on fluorapatite (100) surface

Anna Kupka¹, Xavier Torrelles², Hermann Gies¹, Klaus Merz¹

¹Ruhr-University Bochum, Bochum, Germany, ²Institute of Material Science of Barcelona, UAB, Bellaterra, Spain

The famous Miller experiment to model the primordial soup demonstrated that amino acids can form spontaneously as the essential building blocks of life in solutions. It is, however, still an open question how self-recognition processes influence the transformation of these amino acids. It has been proposed that inorganic materials play a key role in this process. Our work has been motivated by the relevance to know the interaction processes between essential organic molecules with inorganic materials to form new essential building blocks of life. Former GIXRD studies analyzing rocking curves of the crystal truncation rods (CTR's) of the fluorapatite (100) – aqueous glycine interface proved the geometric structural arrangement and the crystalline order of adsorbed water and glycine molecules. The adsorption process on the mineral surface is site competitive as both the glycine and water molecules show equal affinity toward surface Calcium cations. The glycine molecules interact directly with the fluorapatite (100) surface, where one of their carboxylate groups coordinates with the surface Calcium cations. On this basis, we investigated the aggregation process of proline in solution on the (100) surface of fluorapatite. At the synchrotron radiation facilities ESRF (BM25, SpLine) and SOLEIL (SIXS) we measured CTRs of the clean surface as well as concentrated aqueous solution sets of D- and L-proline diluted in H₂O and D₂O. These GIXRD-experiments present the possibility to determine the structure of the fluorapatite (100) surface in presence of proline in aqueous and deuterated aqueous solutions and compare them with the respective interface structure of glycine in aqueous solution. This permits to determine the active sites of adsorption of the organic molecules on the fluorapatite surface and yield detailed information about the 3-dimensional structure of the interface between the mineral and a sorbate layer of proline molecules which act as nucleation seed for crystallization.



P-Tu-043

Comparative study of carbon monoxide oxidation on model titania and lithium fluoride supported gold nanoparticles

Soslan Khubezhov¹, Inga Tvauri¹, Ivan Silaev¹, Bela Gergieva¹, Galina Grigorkina¹, Viktoria Magkoeva¹, Aleksan Bliev¹, Tamerlan Magkoev¹

¹North-Ossetian State University, Vladikavkaz, Russian Federation

To further understand the extent to which the effect of titania support is important in catalytic performance of Au/TiO₂ catalyst, comparative study of carbon monoxide oxidation over Au/TiO₂ and Au/LiF model catalysts in the same experimental ultra-high vacuum condition has been done. Titania and lithium fluoride films have been grown on the Mo(110) surface, former – by well-known procedure of reactive evaporation of Ti in an oxygen ambient, whereas the latter – by thermal evaporation of bulk LiF crystal. Subsequently, gold has been deposited onto the formed films. Size and morphology of the particles have been controlled by combination of evaporation flux, substrate temperature and post-deposition treatment. Techniques used include RAIRS, TPD, XPS, AFM and AES. It was found that Au particles of 2 to 5 nm mean size on as-deposited LiF film exhibit much lower catalytic (CO+O₂) efficiency compared to Au particles of about the same size and morphology on TiO₂ film. However, when the LiF film, before Au deposition, has been pretreated by 100 eV electron flux, CO oxidation on Au/LiF proceeded more efficiently than on Au/TiO₂. In this case it is necessary, however, that the amount of metallic Li, released by electron bombardment, does not exceed concentration corresponding to about 0.15 monolayers. At higher Li content catalytic activity is dramatically quenched. For larger Au particles exceeding 10-15 nm, regardless whether or not they are on the as-deposited or pretreated LiF film, carbon monoxide oxidation efficiency is considerably lower than on Au/TiO₂ model catalyst. The higher catalytic activity for small Au particles on pretreated LiF film can be reconciled in terms of charge transfer effect within the (Au+CO+O₂) complex enhanced by the F-center, presumably being, among the other defect sites, the preferred Au particle nucleation center at low coverage.

The work was supported by The Russian Ministry of Education and Science (Goszadanie) and Government of RSO-Alania-2015.

P-Tu-044

Steering the Conformation of Polypeptides by Adsorption on Cu₂N

Daniel P. Rosenblatt¹, Sebastian Koslowski¹, Sabine Abb¹, Markus Etzkorn¹,
Stephan Rauschenbach¹, Klaus Kern^{1,2}, Uta Schlickum¹

¹Max-Planck-Institut für Festkörperforschung, Stuttgart, Germany, ²Institut de Physique de la Matière Condensée, Ecole Polytechnique Fédérale de Lausanne (EPFL), Lausanne, Switzerland

Surface chemistry and geometry provide powerful tools to immobilize small molecules at specific locations on a surface and bestow functionality upon them. Large molecules such as proteins require a higher degree of control due to the enormous conformational freedom that is a result of their flexibility. In recent investigations of the protein cytochrome-C (CytC) deposited on metallic substrates by electrospray ion beam deposition (ES-IBD) it has been shown that the adsorption conformation of the unfolded protein is strongly influenced by surface mobility and the charge state of the gas phase protein ion.[1,2] However, this approach still leaves the proteins free to adopt random conformations sampled from a large, continuous conformation space.

Here we present scanning tunneling microscopy (STM) investigations of the conformations of individual CytC molecules deposited by ES-IBD on a Cu₂N template monolayer on Cu(100). At close to monolayer coverage, Cu₂N forms a dense array of approximately square 5x5 nm islands, separated by a grid of narrow bare Cu strips.[3] We demonstrate that this substrate can be used as a template that favors unfolded protein conformations along the exposed Cu strips. This significantly reduces their conformational freedom, leading to a discrete distribution of stretched out, straight conformations following the Cu grid. We used a simple model with limited molecule on-surface mobility and generated the corresponding distribution of surface conformations. In spite of the model's simplicity, the results are in good agreement with the observed distribution of conformations.

[1] Z. Deng et al., Nano Lett. 12 (2012) 2452-2458

[2] G. Rinke et al., Nano Lett. 14 (2014) 5609-5615

[3] F. M. Leibsle et al., Surf. Sci. 317, 309 (1994)

P-Tu-045

Controlling Protein Conformation on Surfaces by Soft-Landing Electrospray Ion Beam Deposition

Stephan Rauschenbach¹, Gordon Rinke¹, Ludger Harnau¹, Klaus Kern^{1,2}

¹Max-Planck-Institute for Solid State Research, Stuttgart, Germany, ²EPFL, Institut de Physique de la Matière Condensée, Lausanne, Switzerland

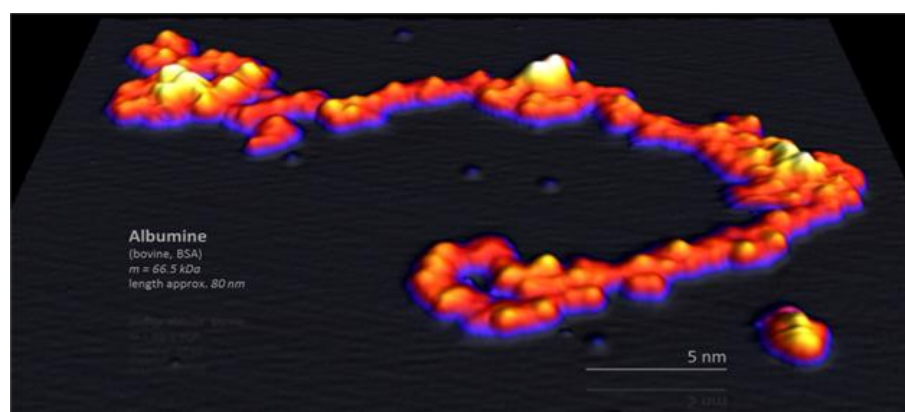
The physical, chemical, and biological properties of macromolecules like proteins are strongly dependent on their conformation. The degrees of freedom of the flexible scaffold generate a huge conformational space. We use soft-landing electrospray ion beam deposition (ES-IBD) to transfer proteins to a surface,[1] which allows us to choose their conformation from folded or unfolded species present in solution. The protein is imaged at the single molecule level by scanning tunneling microscopy (STM) with sub-nanometer resolution. The interpretation of the results is supported by molecular dynamics simulations of the landing process. Folded proteins appear as globular structures in STM. Unfolded proteins at the surface reveal submolecular details at the single amino acid level.[2] We steer the conformation of unfolded proteins on the surface by selecting the solution conformation, charge state, deposition energy, template surfaces, or surface diffusion.[3] In the absence of diffusion, the final conformation is reached through a mechanical deformation of the gas phase conformation during the ion-surface-collision. By actively selecting a charge state the mechanical stiffness and gas phase conformation is chosen. The hyperthermal deposition energy is a measure for how much the polymer is altered upon collision. We achieve conformations spanning a wide range from fully extended unfolded to completely compact in two dimensions.

This work adds a new dimension of control to the processing of macromolecular materials in vacuum, with the potential to reach otherwise inaccessible conformational states in a highly pure, well controlled environment.

[1] S. Rauschenbach, et al.: Electrospray Ion Beam Deposition of Clusters and Biomolecules. *Small* 2, 540-547 (2006)

[2] Z. Deng, S. Rauschenbach: A Close Look at Proteins: Submolecular Resolution of Two- and Three-Dimensionally Folded Cytochrome c at Surfaces. *Nano Lett.* 12, 2452-2458 (2012)

[3] G. Rinke, S. Rauschenbach, et al.: Active Control of Protein Conformation on Metals by Hyperthermal Surface Interaction. *Nanoletters* 14, 5609-5615 (2014)



P-Tu-046

Theoretical investigation of carboranethiols on gold (111) surface

Ersen Mete¹, Gül den Güney¹, Ayş en Yılmaz², Fatih Danış man²

¹Department of Physics, Balı kesir University, 10145 Balı kesir, Turkey,

²Department of Chemistry, Middle East Technical University, Ankara, Turkey

The isolated and full monolayer adsorption of various carboranethiol compounds on gold (111) surface has been investigated using the density functional theoretical calculations. The effect of differing molecular dipole moment orientations on the self-assembly property of carboranethiols was examined and interpreted for the formation of film structures. We have studied relative stabilities, the binding characteristics and the electronic properties of the low energy adlayer geometries of carboranethiol isomers on gold (111) surface.

This work has been financially supported by TUBITAK under Grant No. 213M182.

P-Tu-047

Self-assembly and on-surface coupling of carbonyl-bridged triphenylamines

Maximilian Ammon¹, Zechao Yang¹, Tim Sander¹, Patrick Seitz¹, Milan Kivala², Sabine Maier¹

¹Department of Physics, University of Erlangen-Nürnberg, Erlangen, Germany,

²Department of Chemistry and Pharmacy, University of Erlangen-Nürnberg, Erlangen, Germany

Carbonyl-bridged triphenylamines are ideal precursors for the on-surface synthesis of planar nitrogen-doped π -systems on metal surfaces. In addition, the bridging carbonyl groups are suitable for Schiff-base type coupling reactions, which proceed, compared to the Ullman coupling, at lower temperatures and leave no reaction side products on the surface. [1]

Here we present a low-temperature scanning tunnelling microscopy study on the self-assembly and covalent coupling of amino-functionalized carbonyl-bridged triphenylamin derivatives. On Au(111), we find hydrogen-bonded porous networks of triphenylamines after evaporation at room temperature. The observed hydrogen-bonding motif indicates a weak molecule-surface interaction. In contrast on Ag(111) and Cu(111), the strong interaction between the carbonyl group and the metal promotes metal-ligand bonded networks at room temperature. Independent of the molecular interaction in the self-assembly, similar covalently-linked structures were observed after post annealing on both the Ag(111) and Au(111) sample. After an intermediate dimer phase, wire-like covalent structures with a length of several nanometres are obtained.

[1] Weigelt, S. et al., *Angewandte Chemie* 119, 9387–9390 (2007).

P-Tu-048

Preparation of Highly Porous Spherical Nanocomposite of Poly(methyl methacrylate) and TiO₂ by Electro spraying Approach

Hyunsuk Lee¹, Donghyun Paik², Yongjin Kim¹, Johnhwan Lee¹, Sejun Park¹,
Kyungho Choi¹, Youngjin Choi¹, Sung-Wook Choi²

¹Amorepacific R&D Center, Yongin, South Korea, ²The Catholic University of Korea, Bucheon, South Korea

Highly porous PMMA microspheres impregnated by TiO₂ nanoparticles were fabricated by electro-spraying process. The size and the morphology of the micro-structure was well-controlled by varying the PMMA concentration, co-solvent ratio, PMMA/TiO₂ ratio and the relative humidity. SEM images showed that the resulting microspheres exhibited highly-porous structure and spherical morphology with an average size of $3.03 \pm 0.94 \mu\text{m}$. Energy dispersive X-ray mapping confirmed that the TiO₂ nanopowders were homogeneously distributed throughout the composited microspheres. The water repellency of the porous particles was determined by measuring the contact angle and the oil absorption with respect to the porosity was also tested using triglyceride oil. This study clearly indicates that the well-defined architecture and the controllable porosity of the PMMA/TiO₂ microspheres could be potentially advantageous in the applications to catalyst, sensor and cosmetics.

P-Tu-049

Hydrophobic recovery in plasma-polymerized polymers vs conventional polymers after plasma treatment in different gases

Jerson Peralta¹, Francesc Benitez¹, Arturo Lousa¹, Joan Esteve¹

¹Universitat de Barcelona - Departament Física Aplicada i Òptica, Barcelona, Spain

It is well-known that the surface properties of polymers can be modified by bombardment of energetic species (photons, electrons, ions). Usually this modification is effected by a plasma treatment in reactive or non-reactive gases such as oxygen, nitrogen, argon, helium or air, and it leads to an increase in the surface energy of the polymers by creating polar groups on its surface. These results in a hydrophilic behaviour which is beneficial in order to increase the adhesion of any coating deposited on top of the polymer. However, the effect of this modification is limited in time, with a progressive recovery of the original low surface energy of the polymer, an effect known as 'hydrophobic recovery'. We have demonstrated that hydrophobic recovery is much lower in plasma polymerized polymers (PP-polymers) as compared to conventional polymers. A comparison is established between the properties obtained by plasma modification of equivalent organosilicon polymers: plasma polymerized hexamethyldisiloxane (PP-HMDSO) and its conventional analogue, chemically polymerized polydimethylsiloxane (PDMS). We have found that the ageing of plasma treated PP-HMDSO is extremely low, thus resulting in no significant hydrophobic recovery within several years, whereas the ageing of plasma treated PDMS is several orders of magnitude faster, thus producing regeneration of the original hydrophobicity in a few hours. The relation of the density and cross-linking degree of the polymer with the different recovery rates measured is discussed and related to the mechanisms of hydrophobic recovery.

P-Tu-050

Surface modification of electrospun nanofiber by laser treatment

Masume Ayazi¹, Nadreh Golshan Ebrahimi, Saiede Khalaji, Emad Jafari

¹Tarbiat Modares University, Tehran, Iran

Porous polymeric electrospun nanofibrous have some advantages in bioapplications. In this research electrospun of poly(vinyl alcohol) (PVA) and chitosan fibers structure with nanoscale diameters were prepared. Nanoroughness structures were fabricated under various condition of electrospinning. To fix nanofiber structure were crosslinked by glutaraldehyde. Although electrospun beaded nano/micro fibers has nanoroughness structure, laser micromachining is possible to control fabrication of hole with hexagonal array on the mat. Laser treatment of electrospun fibers induces higher roughness and more porosity of surface. Surface roughness of different electrospun fibers and structure of the laser irradiated holes were be quantified by SEM and AFM images. It was found that laser parameters have influenced on the size of porosity. Moreover, The effect of roughness and pore structure on wettability of crosslinked samples were shown in this study.

P-Tu-052

Interaction between dimethyl methylphosphonate (DMMP) and polydimethylsiloxane (PDMS)-coated TiO₂: towards development of effective MALDI matrix

Eun Ji Park¹, Sang Wook Han¹, Myung-Geun Jeong¹, Dae Han Kim¹, Ju Ha Lee¹, Bo Ra Kim¹, Soong Yeon Kim¹, Ki Jung Park¹, Il Hee Kim¹, Young Dok Kim¹

¹Department of Chemistry, Sungkyunkwan University, Suwon, South Korea

In this work, TiO₂ nanoparticle was used as matrix for dimethyl methylphosphonate (DMMP) detection in matrix assisted laser desorption ionization mass spectroscopy (MALDI-MS) and its efficiency was compared with that of polydimethylsiloxane (PDMS)-coated TiO₂ nanoparticle. Two different sampling methods, dried droplet and thin-layer method, were used for each matrix and the efficiency of the matrices was determined in terms of DMMP signal intensity in MALDI-MS. In both sampling methods, DMMP signal significantly increased by using PDMS-coated TiO₂ instead of bare TiO₂. FT-IR result verified that the enhancement of DMMP signal upon PDMS coating is the result of weaker interaction between DMMP molecule and the PDMS-covered surface than that with bare TiO₂. A weaker interaction between DMMP and matrix can facilitate desorption of DMMP from the matrix surface in the MALDI process, yielding a higher sensitivity to DMMP in the MALDI-MS

P-Tu-053

Hydrophilic Treatment for Intraocular Lens Injectors By Graft Copolymerization

William Lee^{1,2}, Pei-Lin Lu², Ih-Houng Loh²

¹AST Products, Inc., BILLERICA, United States, ²ICARES Medicus, Inc., Hsinchu, Taiwan, R.O.C.

For nearly six decades, surgeons have used intraocular lenses (IOLs) to replace the existing crystalline lens because it has been clouded over by a cataract, or as a form of refractive surgery to change the eye's optical power. The very first IOL for cataract surgery was implanted by Sir Harold Ridley on November 29, 1949. As most of the early cataract surgery cases had a disastrous outcome, IOL implantation fell into disrepute and it was not until some 30 years later that advances in IOL design, surgical technique, viscoelastics and surgical instrumentation began to make IOL implantation a safer procedure. At present, IOL implantation is the accepted routine for cataract surgery and there have been major advances in IOL technology in recent years. The goal of cataract surgery in the 21st century has moved from restoring sight to correcting refractive error and improving the quality of the patient's vision postoperatively. Beside the IOL itself, the invention and evolution of one of the key technology components, the IOL injector as a disposable medical device, has enabled the delivery of IOLs into the eyes via smaller incisions. This presentation will highlight the development of a novel hydrophilic treatment by graft copolymerization that is essential to enable a safer, simpler and effective IOL implantation into the patient's eye. The technique has enabled the preparation of a hydrophilic and lubricious surface that is thin, biocompatible, autoclavable and durable in wet storage. Moreover, this treatment can be easily applied onto arbitrary shapes of IOL injectors.

P-Tu-054

Characterization of amorphous hydrogenated carbon (a-C:H) layers industrially deposited on common high-density polyethylene (HDPE)

Alberto Catena¹, Simonpietro Agnello², Franco Mario Gelardi², Stefan Wehner¹,
J Christian Berthold Fischer¹

¹University of Koblenz-Landau, Koblenz, Germany, ²University of Palermo, Palermo, Italy

Common high density polyethylene (HDPE), previously cleaned with oxygen plasma, has been gradually deposited from 5 nm up to 1000 nm with amorphous hydrogenated carbon (a-C:H) layers. This series has been performed in a direct deposition method by radio frequency plasma enhanced chemical vapor deposition (RF-PECVD) with acetylene plasma as carbon source resulting in a robust layer type (r-DLC). Surface morphologies have been studied in detail by atomic force microscopy (AFM), chemical composition by Raman spectroscopy and wettability by contact angle measurements. On top of the surfaces individual grains are detected which evolve in dimension with increasing layer thickness. A characteristic bottom texture is additionally found on each surface, which is the same for every deposition. These observations suggest that the grains and the characteristic bottom texture belong to two different features: the evolution of the grains is indicative of the layers growth, whereas the bottom textured protrusions are conserved from the oxygen plasma cleaned HDPE material features. Raman analysis revealed a rearrangement of the carbon entities in the layers for high carbon depositions, related to a growth of the sp² hybridized carbon structures despite the sp³ ones, with a parallel dehydrogenation of the samples. Contact angle measurements suggest that at the first steps of the deposition process reorganization of the layer structure takes place, due to the intermixing of soft plastic material and hard carbon deposition. These findings provide a better understanding of robust a-C:H depositions as a protection of soft polymer materials.

P-Tu-056

Characterization of degradation of PMMA by SEM and FTIR analyzes

El Hadi Belhiteche¹, Mohand Amokrane Handala¹, Nora Kireche³

¹Université Mouloud Mammeri, Tizi-Ouzou, Algeria, ²Université Mohamed Boudiaf, M'sila, Algeria, ³Université de Bouira, Bouira, Algeria

Insulating solids are the basic elements for electrical equipments. It is of high importance to increase the knowledge of dielectric materials characteristics on which depend the reliability of high voltage electrical systems. The trend today is to obtain cheap, clean and more efficient materials. This experimental study is conducted on characterization by scanning electron microscopy (SEM) and FTIR (Fourier Transform Infrared) of polymethyl methacrylate (PMMA) subjected to dielectric barrier discharges (DBD). Under this electrical stress, PMMA degrades, hydroxyl groups are then formed. Micrographs obtained by SEM showed the development of tree shaped forms on the surface of the dielectric material, an unusual phenomenon in the case of DBD. Index Terms - Degradation, dielectric barrier discharge, FTIR analysis, PMMA, SEM, trees.

P-Tu-057

Improved adhesion of sputtered coatings on PC by RF oxygen plasma pretreatments

Joan Esteve¹, Jerson Peralta¹, Francesc Benitez¹, Arturo Lousa¹

¹Universitat de Barcelona, Barcelona, Spain

In the present work RF oxygen plasmas were used to modify polycarbonate (PC) surface chemistry, in order to improve adhesion of later sputtered coatings. We have studied the influence of the polymer RF self-bias voltage on the evolution of static contact angle measurements and the subsequent adhesion of the coatings. The chemical modifications of the polymer induced by the plasma treatment, were evaluated by Fourier transform infrared spectroscopy with an attenuated total reflectance configuration and by X-ray photoelectron spectroscopy analysis. The correlation between the surface activation achieved with the previous treatments and the adhesion of subsequent sputtered coatings were evaluated by means of the pull-off test applied to the coatings. The plasma treatments produced an increase in the polymer surface wettability due to formation of oxygen containing groups in the near-surface layer of the PC. The contact angle and pull-off test measurements suggested that surface activation of PC effectiveness, tends to increase when self-bias voltage was increased up to values of 350 V for short activation treatment processes.

P-Tu-058

Refining biodegradable polyhydroxybutyrate (PHB) with amorphous hydrogenated carbon (a-C:H)

J. Christian Fischer¹, Stefan Wehner¹

¹University Koblenz-Landau, Koblenz, Germany

Bioplastic materials, especially when they are bio generated and biodegradable represent a promising alternative for common petroleum-based plastics. These bioplastics are ideal materials for packaging in food industry, agricultural usage or in the medical field. In many cases the parent plastic material suits mechanical requirements but exhibits poor surface features leading for instance to bacterial adhesion. Furthermore unfavorable barrier properties and enhanced degradation in contact with water can limit the use of these bioplastic materials. These disadvantages can be avoided by appropriate surface modifications. The coating of parent material with thin films of amorphous hydrogenated carbon (a-C:H) via plasma-enhanced chemical vapor deposition (PECVD) is a frequently used technique. The surface morphologies of a 50 µm thick foil of the bioplastic polyhydroxybutyrate (PHB) coated with two different carbon-types of various thicknesses are examined by SEM and AFM. The sp³-enriched r-type results in a more robust layer, while the sp²-enriched f-type is more flexible. Carbon layers of r-type up to around 450 nm are intact, further deposition results in cracking and exfoliation of the DLC film due to increasing internal stress. Furthermore the effect of various alcohols on bioplastic samples coated with a 100 nm DLC-film is performed. The surface structures of uncovered materials and isolated thin films have been analyzed. Significant differences of the contact side depending on the used solvent are found. This provides further insights into the interaction of hard carbon coatings and soft plastic materials.

P-Tu-059

Antimicrobial biopolymeric composites containing flavonoids and silver nanoparticles

Rodica Cristescu¹, Anita Visan¹, Gabriel Socol¹, Alexandru Mihai Grumezescu², Mariana Carmen Chifiriuc³, Dan Mihaiescu⁴, Ryan D. Boehm⁵, Dina Yamaleyeva⁵, Michael Taylor⁵, Roger J. Narayan⁵, Douglas B. Chrisey⁶

¹National Institute for Lasers, Plasma & Radiation Physics, Lasers Department, Bucharest-Magurele, Romania, ²Faculty of Applied Chemistry and Materials Science, Department of Science and Engineering of Oxide Materials and Nanomaterials, Politehnica University of Bucharest, Bucharest, Romania, ³Faculty of Biology, Microbiology Immunology Department, University of Bucharest, Bucharest, Romania, ⁴Faculty of Applied Chemistry and Materials Science, Organic Chemistry Department, Politehnica University of Bucharest, Bucharest, Romania, ⁵Department of Biomedical Engineering, University of North Carolina, Chapel Hill, United States, ⁶Department of Physics and Engineering Physics, Tulane University, New Orleans, United States

Antimicrobial resistance has become a global public health issue due to the spread of resistance genes and the ability of microbial strains to grow in biofilms, which are highly tolerant to limiting conditions such as antibiotics. Eradication of biofilm-associated infections requires either high concentrations of antimicrobial agents, which are commonly associated with an increased incidence of undesired side effects (e.g., local or systemic allergies, dysbiosis, and diarrhea), or combinations of various therapeutic agents. In order to circumvent the emergence of resistant bacteria, other classes of compounds are investigated as a potential alternative to conventional antibiotics. The purpose of this study was to investigate the efficiency of various bioactive polymeric composites against planktonic and adherent microorganisms. The following combinations were tested: biopolymer (polyvinylpyrrolidone), flavonoid (quercetin dehydrate/resveratrol)-biopolymer, silver nanoparticle-biopolymer, and flavonoid-silver nanoparticle-biopolymer composite thin films; the films were deposited using matrix assisted pulsed laser evaporation (MAPLE). A pulsed KrF* excimer laser source ($\lambda = 248$ nm, $\tau = 25$ ns, $\nu = 10$ Hz) was used to deposit the aforementioned composite thin films, which were further characterized using Fourier transform infrared spectroscopy, atomic force microscopy (AFM) and scanning electron microscopy (SEM). The antimicrobial activity of the obtained bioactive thin films was quantified using two assays to quantify the microbial culture mass (e.g., spectrophotometric measurements to determine the density of microbial cell cultures) and cell number (e.g., viable cell count assays). Both AFM and SEM confirmed that MAPLE may be used to create thin films with chemical properties corresponding to the input materials as well as surface properties that are appropriate for medical use. The large-spectrum antimicrobial activity of the obtained flavonoid-containing films demonstrated the potential use of these hybrid systems for the development of novel antimicrobial agents, biomaterials, or other medically-relevant surfaces.

P-Tu-060

Electronic effects in Gd thin films on W(110) at sub-monolayer coverage studied by STM

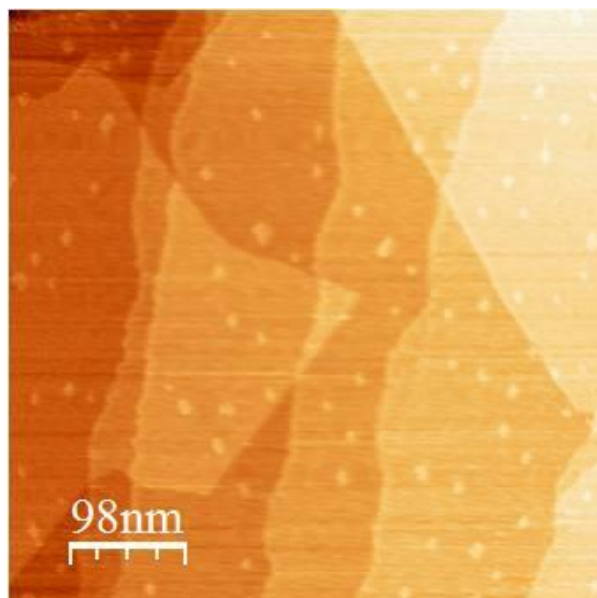
Danielle Schweke¹, Henry Realpe², Yishai Manassen²

¹Nuclear Research Center Negev, Beer Sheva, Israel, ²Ben-Gurion University, Beer Sheva, Israel

Formation of Gd thin film upon W(110) substrate has been studied by scanning tunneling microscopy (STM). A small amount of Gd (about 0.3ML) was deposited by e-beam evaporation at a high deposition rate, at room temperature, and the sample was subsequently annealed at 650 °C for about 15 min. STM images recorded after cooling indicate the formation of a Gd epitaxial layer, partially covering the W(110) surface, and the nucleation of small Gd clusters homogeneously scattered upon the sample surface, as seen in figure 1. The clusters are mostly rectangular in shape and of a few nanometers size.

The boundaries of the Gd film observed are straight lines, lying along specific directions and crossing the W(110) terraces. We show that the apparent film is indeed composed of self-organized chains of Gd atoms, oriented along the [1-10] direction of the W(110) substrate, whose formation is governed by electronic interactions. The chains extend to several hundreds of nanometers.

The Gd film thus formed appears as "transparent", due to electronic effects, and the topography of the W(110) surface underneath is clearly discerned. In extended areas, a superposition of at least two Gd thin films is observed, although the overall coverage thus formed is less than a full mono-layer. This noticeable feature is discussed, as well as additional features, such as the unusual shape of the Gd islands observed.



P-Tu-061

Microscopic and spectroscopic studies for the self-assembled 2D chiral honeycomb structures of unnatural amino acids on Au(111)

Graduate Student Sena Yang¹, Hangil Lee²

¹KAIST, Daejeon, South Korea, ²Sookmyung Women's University, Seoul, South Korea

Here, we have studied two-dimensional self-assembled structures of an unnatural amino acid, (S)- β -methyl naphthalen-1- γ -aminobutyric acid (γ^2 -1-naphthylalanine) on Au(111) surface at 150 K using scanning tunneling microscopy (STM) and high resolution photoemission spectroscopy (HRPES). Interestingly, according to our STM images, at initial stage, we found interlocking chiral honeycomb structures which are counter-clockwise and clockwise configurations in single domain. On the other hand, naphthalene forms chiral domains separated by a step at low coverage. By further increasing the amounts of adsorbed γ^2 -1-naphthylalanine, a well-ordered square closed packing structure was observed. In addition, we found the other structure that molecules were trapped in the pore of the hexagonal molecular assembly. At high coverages, naphthalene can form a well-ordered hexagonal closed packing structure. In addition, the HRPES analysis results indicates that there are no bonding between γ^2 -1-naphthylalanine and Au (111) and γ^2 -1-naphthylalanine can form self-assembled structures by intermolecular interactions. Therefore, we suggest that modifying molecule can potentiate to build well-ordered self-assembly structures.

P-Tu-062

Surface Functionalization of Oxide- covered Zinc and Iron with Phosphonated Phenylethynyl Phenothiazine

Julian Rechmann¹, Adnan Sarfraz¹, Alissa C. Götzinger², Elena Dirksen², Thomas J. J. Müller², Andreas Erbe¹

¹Max-Planck-Institut für Eisenforschung GmbH, Department of Interface Chemistry and Surface Engineering, Düsseldorf, Germany, ²Heinrich-Heine-Universität Düsseldorf, Chair of Organic Chemistry, Düsseldorf, Germany

Phenothiazines are redox-active, fluorescent molecules with potential applications in molecular electronics. Phosphonated phenylethynyl phenothiazine can be easily obtained in a four-step synthesis, yielding a molecule with a head group permitting surface linkage. Upon modifying hydroxylated zinc and iron both covered with their native oxide, ultrathin organic layers were formed and investigated by using infrared (IR) reflection spectroscopy, X-ray photoelectron spectroscopy (XPS), time-of-flight secondary ion mass spectrometry (ToF-SIMS), contact angle measurement and ellipsometry. While stable and densely packed monolayers with upright oriented organic molecules were formed on oxide- covered iron, multilayer formation is observed on oxide- covered zinc. ToF-SIMS measurements reveal a bridging bidentate bonding state of the organic compound on oxide- covered iron, whereas monodentate complexes were observed on oxide- covered zinc. Cyclic voltammetry (CV) indicates redox-activity of the multilayers, whereas the monolayers show sufficient stability towards corrosive aqueous environment at open circuit potential (OCP). The protected phosphonic acids are suitable head groups to link phenothiazine by covalent bonds to oxide- covered transition metals. By π - π -interactions, phenothiazines form dense and close packed monolayers on oxide- covered iron, which may assist in corrosion protection, which is of big interest in steel related industries. On the other hand, the indicated redox-activity of multilayers on oxide- covered zinc and the possible tunability of the HOMO-LUMO levels in combination with its low electron affinity make phenothiazines promising candidates for organic semiconductors.

P-Tu-064

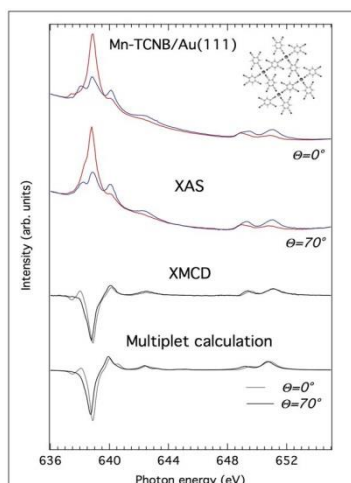
Magnetic Coupling and Single-Ion Anisotropy in Surface-Supported Mn-based Metal-Organic Networks

Luca Giovanelli¹, Adrien Savoyant¹, Mathieu Abel¹, Francesco Maccherozzi², Ksari Younal¹, Mathieu Koudia¹, Roland Hayn¹, Fadi Choueikani³, Edwige Otero³, Philippe Ohresser³, Jean-Marc Themlin¹, Sarnjeet Dhesi², Sylvain Clair¹

¹IM2NP-CNRS-University of Aix-Marseille, Marseille, France, ²Diamond Light Source, Didcot, United Kingdom, ³Synchrotron SOLEIL, Saint-Aubin, France

π -conjugated macrocycles such as phthalocyanines hosting a single transition metal atom have shown great versatility in producing 2D magnetic arrays. This includes the possibility to modify the magnetic state of the central metal atom through ferromagnetic (FM) coupling to the substrate and by adsorption of smaller molecules [1]. An alternative approach for the synthesis of magneto-organic nanostructures consists in manipulating the magnetic properties of transition metal atoms through selective bonding to functional ligands in surface-supported, self-assembled metal organic networks [2]. In the present study the electronic and magnetic properties of Mn coordinated to 1,2,4,5-tetracyanobenzene (TCNB) have been investigated by combining STM and XMCD performed at low temperature (3 K). When formed on Au(111) and Ag(111) substrates the Mn-TCNB networks display similar geometric structures. Magnetization curves reveal FM coupling of the Mn sites with similar single-ion anisotropy energies, but different coupling constants. Low-temperature XMCD spectra show that the local environment of the Mn centers differs appreciably for the two substrates. Multiplet structure calculations were used to derive the corresponding ligand field parameters confirming an in-plane uniaxial anisotropy. The observed inter atomic coupling is discussed in terms of super-exchange as well as substrate-mediated magnetic interactions [3]. In the figure are displayed the angular dependence of the XAS and resulting XMCD over the Mn L_{2,3} edge for Mn-TCNB/Au(111). T=3 K. B=6 T. $\Theta = 0^\circ$ correspond to normal incidence and $\Theta = 70^\circ$ to grazing incidence. The bottom curves are obtained by ligand field multiplet calculations.

- [1] C. Wackerlin et al., Angew. Chem. Int. Ed. 2013, 52, 1
 [2] T. R. Umbach et al., Phys. Rev. Lett. 109, 267207 (2013), N. Abdurakhmanova et al., Phys. Rev. Lett. 110, 027202 (2013)
 [3] L. Giovanelli et al. J. Phys. Chem. C 118 (2014) 11738



P-Tu-065

Photo-switchable conductivity of spiropyran SAMs on Au surface

Sumit Kumar¹, R.Y.N. Gengler¹, Jochem Van Herpt², Ben L. Feringa², Petra Rudolf¹, R.C. Chiechi²

¹Zenikhe institute for Advanced Materials, University of Groningen, Groningen, Netherlands, ²Stratingh Institute for Chemistry, University of Groningen, Groningen, Netherlands

Spiropyrans are photochromic molecules that show a large change in dipole moment upon photo-switching. Photo-switchable molecules have found numerous applications in a wide range of novel smart materials, optical memories, photonic devices and logic units. The relatively nonpolar spiropyran (SP) can be reversibly switched with UV light to a polar, zwitterionic merocyanine (MC) isomer that has a much larger dipole moment. The reverse reaction is induced by visible light. Here we report photo-switchable conductivity of a spiropyran-functionalized gold surface. We developed ordered spiropyran self-assembled monolayer (SAMs) on template striped Au surface. The SAMs were characterized by contact angle measurements and X-ray photoelectron spectroscopy (XPS). The conductivity of SAMs were studied by using liquid Eutectic Ga–In (EGaIn) as a non-damaging, top-contact electrode. The XPS analysis of the film revealed the presence of bound thiolate, which confirms the chemisorptions of the SAM on Au. The current density changes in the order of magnitude as the surface undergoes SP to MC form transformation under UV-visible radiation.

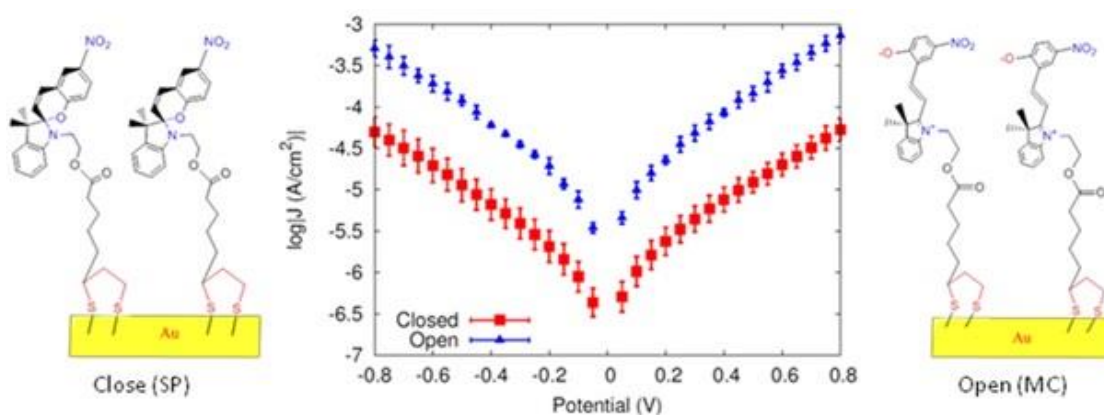


Fig. 1. Current-density versus voltage plots of EGaIn/Ga₂O₃//SAM/Au junctions SAMs of spiropyran in the open (blue) and closed (red) forms.

P-Tu-067

Kinetic effects and packing densification in a supramolecular self-assembly: a Kinetic Monte Carlo approach

Sylvain Clair¹, Laurent Nony¹, Franck Bocquet¹, Mathieu Abel¹, Manuel Cobian², Christian Loppacher¹

¹Aix-Marseille Université, CNRS, IM2NP UMR 7334, Marseille, France, ²Ecole Centrale de Lyon ECL, CNRS, LTDS UMR 5513, Lyon, France

Investigations on the self-assembly of nitro-benzenediboronic acid molecules on NaCl(001), KCl(001) and RbCl(001) at room temperature by means of nc-AFM experiments have revealed well-ordered extended networks with equivalent superstructures and equivalent substrate sites, and molecular lattice constants of 11.9 Å, 13.5 Å and 13.9 Å on NaCl, KCl, and RbCl, respectively. These dimensions are too large compared to the size of individual molecules (~7.4 Å) to account for relevant lateral intermolecular interactions. Based on these intriguing observations, we proposed a simplified supramolecular model where each individual molecule was free to diffuse and rotate up to a certain intermolecular distance corresponding to the experimental observation. Shorter intermolecular distances were allowed only for well-aligned molecules (with hindered rotation), a condition imposed by otherwise steric repulsion. Higher bonding energy was assigned to the dense phase as compared to the large superstructure. Kinetic Monte Carlo simulations with CARLOS program [1] were performed to test the possibility of maintaining a large size supramolecular unit cell despite lower bonding energy. By varying the rotation to diffusion ratio we observed that the large superstructure can be indeed kinetically favored for slow rotating molecules only. Longer time-scale simulations, however, reproduced in all cases the dense, energetically favored phase.

[1] CARLOS is a general-purpose program for Kinetic Monte Carlo simulations, written in C by J. J. Lukkien, <http://carlos.win.tue.nl/>

P-Tu-068

STM study of the Si(111)/I-(1x1) surface as a metal-like passivated Si substrate for growth of nanostructures

Peter Matvija¹, Pavel Kocán¹, Ivan Ošťádal¹, Pavel Sobotík¹

¹Faculty of Mathematics and Physics of Charles University in Prague, Praha, Czech Republic

Controlled growth of thin films on highly reactive silicon surfaces has been a challenge for decades. High density of surface dangling bonds, however, hinders the adsorbate diffusion and its self-organization. In our work, we use the I-(1x1) layer as a passivating agent, which saturates all dangling bonds of the Si substrate [1]. We use room-temperature scanning tunneling microscopy to study structures formed on the Si(111)/I-(1x1) surface after deposition of submonolayer amounts of three elemental adsorbates: Mn, In and Sn. Behavior of the adsorbates – however diverse – in all cases resembles interaction with metal substrates. Importantly, massive enhancement of adatom diffusivity is observed in all studied cases.

[1] P. Matvija, P. Sobotík, I. Ošťádal, P. Kocán, Appl. Surf. Sci., 331 (2014) 339-345

P-Tu-069

Formation of metal-organic frameworks by subtle interplay between molecular epitaxy, H-bonding and thermal treatment

Nataliya Kalashnyk¹, Yangchun Xie¹, Kawtar Mouhat², Frédéric Dumur², Didier Gigmes², Sylvain Clair¹

¹Aix-Marseille University, CNRS, IM2NP UMR 7334, Marseille, France, ²Aix-Marseille University, CNRS, ICR UMR 7273, Marseille, France

Self-assembly based on the paradigm that atoms and molecules can self-organize spontaneously via intermolecular and adsorbate-substrate interactions, is of utmost interest in many technological areas. Generally, the inner forces driving molecular self-assembly at surfaces are non-covalent in nature but it is desirable to form stronger bonds such as metal-ligand. We report on the self-assembly of an indacene-tetrone derivative on the Cu(111) surface studied with UHV-STM at room temperature. The molecule contains four peripheral oxygens, and is adsorbed with the diagonal oxygen atoms along close-packed rows of Cu(111) surface. This molecular growth is epitaxial since this oxygen-oxygen distance corresponds to three interatomic distances between bulk copper atoms. Furthermore, due to the C₃ symmetry of the substrate the molecules can adsorb with three different orientations at surface. The presence of two equivalent diagonal pairs of oxygens but with distinct adsorption configuration leads to additional three molecular orientations which are chiral with respect to the previous ones. Consequently, they form chiral clockwise or anticlockwise windmill patterns by maximizing intermolecular H-bonding. After subsequent annealing a new windmill structure is formed. Two neighboring windmill units of the annealed structure are interconnected by a pair of copper adatoms while in the initial structure they are linked by one shared molecule. Further annealings lead to more complex structures based on similar intermolecular bonding schemes but with increasing adatom to molecule ratio. This study demonstrates the possibility to tune self-assemblies based on H-bonding towards more complex structures with stronger metal-ligand interactions controlled by molecular epitaxy, substrate nature and thermal treatment.

P-Tu-071

Self-assembly of low-symmetry aromatic molecules in 2D

Fabrizio De Marchi¹, Maryam Ebrahimi¹, Josh Lipton-Duffin^{1,2}, Jennifer MacLeod^{1,3}, Federico Rosei^{1,4}

¹Centre Énergie, Matériaux et Télécommunications, Institut National de la Recherche Scientifique, Varennes, Canada, ²Central Analytical Research Facility (CARF), Institute for Future Environments, Queensland University of Technology, Brisbane, Australia, ³School of Chemistry, Physics, and Mechanical Engineering, Queensland University of Technology, Brisbane, Australia, ⁴Center for Self-Assembled Chemical Structures, McGill University, Montréal, Canada

The self-assembly of molecular networks on surfaces could represent a future route for the production-scale manufacture of nano-sized structures. However, before this process could be widely adopted, an increased effort is required to improve our capacity to predict the final structure of the self-assembled film. To this end, density functional theory (DFT) simulations are an important tool for both predicting the interactions between molecules, and in unraveling the details of assemblies when the relevant experimental techniques, such as scanning probe microscopy, fail to unambiguously identify them. We report herein our investigation of indole 2-carboxylic acid (I2CA) and 5,6-dihydroxy indole 2-carboxylic acid (DHICA). Both molecules, once deposited on the surface, form large structures stabilized by non-covalent interactions. Due to the presence of the low-symmetry pyrrole ring, indoles are asymmetric molecules, and for each intermolecular bond geometry, a number of molecular configurations can be possible. I2CA assembles in dimer pairs, relatively independent from preparation condition, arranged in long lamellar structures across the surface. We have applied periodic boundary condition DFT to elucidate this structure, and find that the position of the nitrogen atoms in the pyrrole ring of the indoles have a non-negligible effect on the energetics of the system, despite the fact that the intermolecular geometry is stabilized primarily through the –COOH groups. A similar approach is used for DHICA, where the increased functionalization increase both the number of possible bonding motifs and the number of phases obtained. In particular, on Ag(111) DHICA forms long linear structures, whose growth is limited in width due to the low symmetry of the molecule. This work demonstrates the power of symmetry reduction in the monomer for creating spatially confined assemblies, as well as illustrating the increased possibilities for molecular conformations in continuous films when such a symmetry reduction is applied.

P-Tu-072

Dynamics of dimethyl-disulfide on Au(111)

Scott Holmes¹, Richard Palmer¹, Quanmin Guo¹¹University of Birmingham, Birmingham, United Kingdom

The dynamics of dimethyl-disulfide (DMDS) adsorbed on the Au(111) surface has been investigated at a variety of temperatures using a low temperature scanning tunnelling microscope (LT-STM). On adsorption, the breaking of the sulfur-sulfur bond allows the incorporation of a gold atom to form a $(\text{CH})_3\text{S-Au-S}(\text{CH})_3$ moiety [1], which forms the building block of a wide variety of self-assembled surface structures. At low coverage, the dominant phase is formed of chains of these $(\text{CH})_3\text{S-Au-S}(\text{CH})_3$ units in the trans conformation. As the temperature is varied between 77K and 230K, diffusion of these molecular units becomes possible. At the lowest temperatures (below 130K) only single units undergo diffusion, with diffusion of longer chains becoming common only at higher temperatures (frequent short chain diffusion events at 170K). This leads to interesting diffusive dynamics, where the motion of small chains is constrained by larger, more stable chains. In addition to diffusion of the molecular units, conformational changes are found to be induced both thermally and by the STM tip. When triggered by the STM tip this 'switching' occurs collectively, and only on one side of the chain structures; this is not expected given the symmetry of the $(\text{CH})_3\text{S-Au-S}(\text{CH})_3$ units. A possible explanation lies in the positioning of the molecular unit with respect to the underlying substrate.

[1] Peter Maksymovych, D C Sorescu, and J T Yates, Jr. Phys. Rev. Lett. 97 146103 (2006)

P-Tu-073

Thermal stability of surface-confined assemblies comprising functional cross-shaped molecules – insights from Monte Carlo modeling

Adam Kasperski¹, Paweł Szabelski¹¹Maria Curie-Skłodowska University, Department of Theoretical Chemistry, Lublin, Poland

The self-assembly of star-shaped organic molecules on solid surfaces provides an effective approach to construct 2D functional nanostructures such as supramolecular networks with programmable architecture and functions. As it has been often observed experimentally, small changes in geometry and functionality of a building-block can directly influence the morphology and stability of the resulting two-dimensional molecular assemblies. In this contribution, we used the Monte Carlo simulation method in the Canonical Ensemble to explore the effect of shape and intramolecular distribution of interaction centers within a model cross-shaped building-block on the thermal stability of the resulting low-dimensional structures [1]. Specifically, for the cruciform molecular units [2] we calculated heat capacities as a function of temperature and linked the position of the corresponding peak maxima with the structural parameters of the molecules. Additionally, for the selected tectons we performed the simulations in the Grand Canonical ensemble and estimated the associated phase diagrams. The obtained results indicate, that the heat capacities and the phase behaviour of the studied systems strongly depend on the properties of the building molecule, such as the number and position of interaction centers and molecular symmetry. The insights from this study can be helpful in designing molecular architectonics on solid surfaces, especially when building blocks such as porphyrins and phthalocyanines are at play.

This research was supported by the Polish Ministry of Science and Higher Education (Diamond Grant, No. DI2011 011941).

[1] A. Kasperski, D. Nieckarz, P. Szabelski, *Surface Science* (2015), DOI: 10.1016/j.susc.2015.02.005.

[2] A. Kasperski, P. Szabelski, *Copernican Letters* 4 (2013) 67-73.

P-Tu-074

Disaccharide self-assembly on metal surfaces

Sabine Abb¹, Ludger Harnau¹, Christian Schön¹, Juan Cortés², Stephan Rauschenbach¹, Klaus Kern^{1,3}

¹Max Planck Institute for solid state research, Stuttgart, Germany, ²Laboratory for Analysis and Architecture of Systems, Toulouse, France, ³Ecole Polytechnique Fédérale de Lausanne, Lausanne, Switzerland

Saccharides are involved in almost every biological process, including signal transducing, cell-adhesion, cell localization and differentiation, and play a role in nearly every human disease. However, the interactions of saccharides adsorbed on a surface are not well understood on a molecular level. Intriguingly, the chemical structure among the monosaccharide building blocks appears very similar - they all are structural and stereo isomers of the chemical sum formula $C_6H_{12}O_6$. Their vastly different behavior follows from rather subtle differences in the placement of OH-groups in the molecules. In this study we investigated the self-assembly of disaccharides, namely sucrose (α -D-glucopyranosyl-(1 \rightarrow 2)- β -D-fructofuranoside) and trehalose (α -D-glucopyranosyl-(1 \rightarrow 1)- α -D-glucopyranoside), on Cu(111) and Cu(100) by STM. Electrospray ion beam deposition (ES-IBD) enables us to deposit these non-volatile molecules intact on the surface in ultra-high vacuum as negatively charged molecular ions. After deposition of a submonolayer coverage, we observe self-assembly of ordered 1D and 2D nanostructures. For sucrose, the molecule is imaged as two protrusions with different contrast corresponding to the two monosaccharide-rings, while trehalose molecules are imaged as single droplike feature. The disaccharide assembly is driven by hydrogen bonding of the many hydroxyl groups of the molecule. While both disaccharides show similar behavior on the specific surfaces, trehalose interacts more strongly with the surface and does not readily form large assemblies. Based on our observations combined with molecular dynamics and energy landscape calculations, we can propose a model for the different disaccharide assemblies elucidating the influence of the isomers on the assembly behavior.

P-Tu-076

Molecular dynamics simulations of the high-speed copper nanoparticles interaction with the aluminum surface

Viktor Pogorelko¹, Dmitry Tikhonov², Alexander Mayer³

¹Chelyabinsk State University, Chelyabinsk, Russian Federation, ²Chelyabinsk State University, Chelyabinsk, Russian Federation, ³Chelyabinsk State University, Chelyabinsk, Russian Federation

Interaction of high-speed atomic clusters, nano- and micro-particles with a solid surface is actively investigated recently. Interest in these studies is due to the possibility of using such particles flow for surface modification (change of the surface relief, functional coating, etc.). As an example, a copper coating of the aluminum surface is widely used in order to increase the conductivity of the surface layer. On the other hand, action of high-speed nanoparticles can lead to a substantial plastic deformation and deformation hardening in a surface layer of substrate. In the present work, a molecular dynamics study of a high-speed impact of nanoparticles with aluminum surface is carried out. Main attention is given to the nanoparticles impacts leading to either modification (deformation hardening) of the aluminum surface layer or implantation of the nanoparticles material. At nanoparticles velocities of about 1000 m/s, there are severe plastic deformation and melting of material of the bombarding nanoparticles and the target parts that are adjacent to the site of the collision; which results in an efficient adhesion of the nanoparticles material. The effects of the size, shape, material and kinetic energy of the nanoparticles on the mechanical properties of the aluminum surface are investigated. Also, the optimal parameters of collision that provide the material adhesion of the nanoparticles material to the aluminum surface are determined.

This work is supported by the Ministry of Education and Science of the Russian Federation (competitive part of State Task of NIR CSU No. 3.1334.2014/K).

P-Tu-077

New Insights into the O₂/Al(111) Dissociative Adsorption and Abstraction Dynamics

Koji Shimizu¹, Hiroshi Nakanishi¹, Wilson Agerico Diño^{1,2}

¹Department of Applied Physics, Osaka University, 2-1 Yamadaoka/Suita/Osaka, Japan, ²Center for Atomic and Molecular Technologies, Osaka University, 2-1 Yamadaoka/Suita/Osaka, Japan

Oxygen molecule is common for chemical reactions and aluminum is widely used material for various applications, and it is believed that their physical properties are well understood, yet the reaction of O₂/Al(111) seems to be still under debate. Experiments [1-3] report low initial sticking of O₂/Al(111) and widely separated O adsorbates (ca. 80 Å) at low coverages. On the other hand, theoretical studies employing density functional theory (DFT) [4] found an absence of absolute energy barriers for adsorption in almost all of the configurations considered. Subsequently, various studies have been done to explain the experimental findings, taking into account spin constraints [5] and different exchange-correlation functional [6,7]. We, however, ascribe the problems to dynamical aspects. In this study, we perform quantum dynamical calculations on top of the corresponding spin-polarized potential energy surface (PES) obtained by DFT calculations for the relevant system. Our calculation results show that the rotational motion of the scattered molecule is greatly affected by the strong orientational anisotropy of the PES. This contributes to the low initial sticking [8]. We also found strong corrugation/surface site dependence for the adsorption. In addition to these potential energy anisotropies, the dynamical calculations on top of the substantial interplay between molecular motions and surface vibration would provide new insights into the reaction of O₂/Al(111). At the conference, we will present a more detailed discussion.

- [1] H. Brune, et al., PRL 68 (1992) 624.
- [2] L. Österlund, et al, PRB 55 (1997) 15452.
- [3] M. Kurahashi, et al., PRL 110 (2013) 246102.
- [4] Y. Yourdshahyan, et al., PRB 65 (2002) 075416.
- [5] J. Behler, et al., PRB 77 (2008) 115421.
- [6] F. Libisch, et al., PRL 109 (2012) 198303.
- [7] H-R. Liu, et al., J. Chem. Phys. 135 (2011) 214702.
- [8] K. Shimizu, et al., J. Phys. Soc. Jpn. 82 (2013) 113602.

P-Tu-078

Dispersion of surface phonons in a xenon monolayer physisorbed on the graphite basal plane and its probing by scattering of helium atoms

Azamat Khokonov¹, postgraduate Zeitun Akhmatov¹

¹Kabardino-Balkarian State University, Nalchik, Russian Federation, ²Institute for Nuclear Research of the Russian Academy of Sciences, Troitsk, Moscow, Russian Federation

Atomic beam diffraction experiments are used to study the incommensurate-commensurate transition of Xe atoms adsorbed on a graphite surface [1]. In [2] proposed a simple model for the transverse vibrations of the monolayer and calculated diffraction inelastic scattering in single-phonon approximation.

On the necessity to take into account of multiple helium atoms scattering due to high corrugation surface profile and multiphonon processes in this problem was justified by Siber and Gumhalter [3]. Both the lattice dynamical calculations and the molecular dynamics simulations have been done for nonstatic graphite (0001) surface. For oscillations graphite substrate used an analytical model proposed in [4]. Obtained dispersion curves were used for calculation of helium atoms inelastic diffraction in frame of multiple scattering generalization of eikonal-like quasiclassical approach [5].

This work was supported in part by State Scientific Program № 2262 of Russian Federation.

[1] G. Bracco, P. Cantini, A. Glachant and R. Tatarek. Surf. Sci. 125 (1983) L81.

[2] Khokonov A.Kh., Kokov Z.A., Karamurzov B.S. Surf. Sci. 496 (2002) L13.

[3] Siber A., Gumhalter B. Surf. Sci. 529 (2003) L269.

[4] Khokonov A. Kh. Bulletin of the Russ. Acad. of Sci. Physics. 78 (2014) 762.

[5] Bogdanov A.V., Dubrovskiy G.V., Krutikov M.P., Kulginov D.V., Strelchenya V.M. Interaction of Gases with Surfaces. Detailed Description of Elementary Processes and Kinetics. Springer-Verlag (1995).

P-Tu-079

Ultrafast Exciton Dynamics in Thin Sexithiophene Films

Wibke Bronsch¹, Malte Wansleben¹, Kristof Zielke¹, Sebastian Baum¹,
Cornelius Gahl¹, Martin Weinelt¹

¹Freie Universität Berlin, Berlin, Germany

Sexithiophene/Gold is a model system for an organic semiconductor/metal interface [1]. Exciton formation and relaxation as well as charge transfer processes across those interfaces are of high relevance in molecular electronics. Therefore we studied the optical properties and the electron and exciton dynamics in thin sexithiophene (6T) films on a Au(111) surface by differential reflectance spectroscopy (DRS) and time-resolved two-photon photoelectron spectroscopy (2PPE). Our DRS studies show that the S1 absorption band of a 1ML 6T film on Au(111) is significantly red-shifted with respect to 6T in solution. Whereas this shift stays the same for increasing coverage, the spectral shape of the S1 band changes. Already for a 10ML thick film a clear vibrational substructure of the S1 band is observable. Following up these results we performed coverage-dependent 2PPE measurements with different excitation energies to investigate the influence of the vibrational degree of freedom on the exciton energetics and dynamics.

[1] Varene et al., Phys. Rev. Lett. 109 (2012), 207106

P-Tu-080

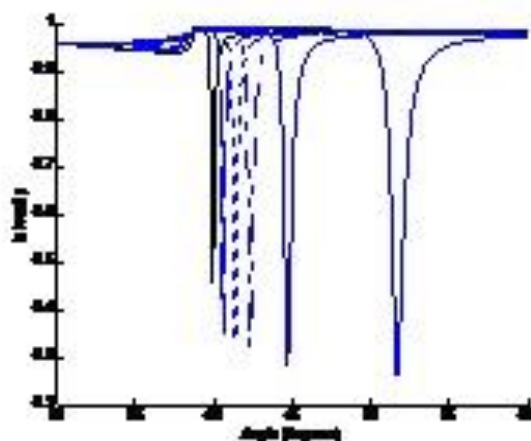
Hemoglobin dielectric parameters studied by SPR technique

Khaled Ayadi¹

¹Université de SETIF, SETIF, Algeria

The advances of method for optical blood analysis need to know the properties of dispersion and absorption of human blood. It is also important for the diagnosis and prognosis of human therapeutic and applications in the field of medical studies, hematology, and the current medical diagnostic. The information on optical properties of human blood is fundamental for many medical applications. In particular, the hemoglobin in red blood cells plays an important role by transporting oxygen throughout the human body. The optical properties of the blood may be described by the intrinsic optical parameters: absorption coefficient, scattering coefficient, which they depends on the complex refractive index (\tilde{n}). Because in the visible range is sensitive to the hemoglobin concentration, optical investigations of hemoglobin are important for medical diagnostics and treatment. A simple method for determining the optical properties of oxyhemoglobin in human blood is proposed. The method is based on a variation of the complex propagation constant of guided wave in a thin-film optical waveguide. We present an optical sensor based on Surface Plasmon Resonance and study the variation of reflectivity of hemoglobin with deference concentration and in various wavelengths. The relation between the light and the thin film is given by

Fig: Reflectivity of the system Prism/Ag/Blood (With different concentrations of Hb)10 g/dl (Concentration of Hémoglobine)



P-Tu-081

Effect of Vibrational Excitation on Chemical Reaction Dynamics of Water and Silicon Surface by First-Principles Molecular Dynamics Simulation

Naoki Yokoyama¹, Takeshi Nishimatsu¹, Yuji Higuchi¹, Nobuki Ozawa², Hiroo Yugami², Momoji Kubo¹

¹Institute for Materials Research, Tohoku University, Sendai, Japan, ²Graduate School of Engineering, Tohoku University, Sendai, Japan

Hydrogen is highly efficient and environmentally-friendly fuel, which is expected as resource to replace fossil fuels. However, manufacturing process of hydrogen requires a large amount of heat supply and produces carbon dioxide as a by-product. A new hydrogen production method is essential for creating more environmentally-friendly energy system. Chemical reaction of water and silicon surface has been proposed as the new hydrogen production method. This reaction can produce hydrogen at relatively low temperature without harmful by-products. However, higher reaction efficiency is still required for practical realization. For promoting chemical reaction, we focused on molecular vibrational excitation by IR laser [1]. To verify the usefulness of the vibrational excitation, we investigated the effect of vibrational excitation of water molecule on the chemical reaction of water and silicon surface by first-principles molecular dynamics (FPMD) simulation. We used our developed FPMD code "Violet" [2]. This program is effective to simulate chemical reaction dynamics. The previous research showed hydronium ion and hydroxide ion were produced by vibrational excitation of water molecules [3]. Then, we performed simulation of attack process of water molecule, hydronium ion, and hydroxide ion to SiH cluster. In attacking process of water molecule and hydroxyl ion, hydrogen production reaction was not observed. Attacking process of hydronium ion is shown in Fig. 1. First, hydronium ion approached to SiH cluster (Fig. 1(a),(b)), and O-H bond was dissociated (Fig. 1(c)). Then, hydrogen and water molecule were produced (Fig. 1(d)). We proposed that hydronium ion generated from vibrational excitation of water molecule by IR laser is possible to promote the hydrogen production reaction of water and silicon surface.

[1] M. Kitada, Japan Patent Kokai 2007-314384.

[2] T. Shimazaki and M. Kubo, Chem. Phys. Lett., 503, 316 (2011).

[3] N. Toyama et al, Chem. Phys. Lett., 420, 77 (2006).

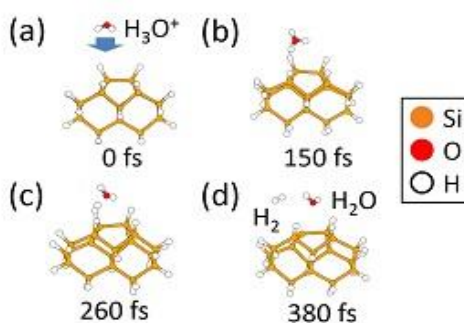


Fig. 1. H₂ production process from H₃O⁺ and Si surface

P-Tu-082

PTCDA molecules on Terraces and at Steps Sites of the KCl and NaCl Surfaces

Hazem Aldahhak¹, Eva Rauls¹, Wolf Gero Schmidt¹

¹Lehrstuhl für Theoretische Physik, Universität Paderborn, Paderborn, Germany

The adsorption of PTCDA ($C_{24}H_8O_6$) on metal substrates has for a long time been used as model system for understanding molecular self-assembly. Ionic crystals as substrate provide the additional possibility to study the molecular properties with little perturbation by substrate screening or strong substrate-adsorbate bonds [1]. Here, we present density-functional theory calculations on the adsorption and the adsorbate-substrate interactions between PTCDA and planar as well as stepped NaCl or KCl surfaces. The adsorption is dominated by van-der-Waals and electrostatic forces. This leads to a site-specific adsorption of the molecule on the surface, resulting in commensurate long-range ordered structures [2]. The influence of the substrate and bonding mechanism on the molecular electronic structure is investigated in detail and compared with the experimental data available [3-5]. Our calculations for different kinds of step-edge defects show the importance of these surface defects for initiating the adsorption of organic molecules on ionic surfaces.

- [1] V. W. Henrich, P.A Cox, The surface of metal Oxides, vol.1, Cambridge University Press, 1996.
- [2] H. Aldahhak et al, Surf. Sci. 617, 242, 2013.
- [3] Q. Que et al., J. Phys. Chem. C 118, 29911, 2014.
- [4] H. Karacuban et al. Nanotechnology, 22, 295305, 2011.
- [5] A. Paulheim et al., Phys. Chem. Chem. Phys.15, 4906, 2013.

P-Tu-083

Temperature-induced processes for size-selected metallic nanoparticles on surfaces

Mathias Getzlaff¹, Hendrik Bettermann¹, Torsten Veltum¹, Matthias Werner¹,
Wolfgang Rosellen¹

¹University of Düsseldorf, Düsseldorf, Germany

Most of the properties of nanoparticles significantly depend on their size. For alloy systems the stoichiometry also plays an important role. In this contribution we report on the temperature dependent processes and shape of size-selected deposited metallic nanoparticles. This investigation is carried out by STM. The nanoparticles consist of ferromagnetic materials (Fe, Co, Ni) and binary alloys of them with different stoichiometry. They are produced by an arc cluster ion source (ACIS). Due to a high degree of charged particles using this technique, it is possible to realize a mass-filtering by a subsequent electrostatic quadrupole. The particles with diameters between 5 and 15 nm are deposited under UHV and softlanding conditions on a W(110) surface. They are heated in situ by a resistive heater integrated in the manipulator. The heating process itself is carried out up to different temperatures and for different duration. Desorption as well as melting occurs. The resulting behavior significantly depends on the size, the material and the stoichiometry. The influence of the anisotropy of the W(110) surface additionally plays an important role which can be proven by a non-isotropic melting of the nanoparticles.

P-Tu-084

Study on Effect of Corrosion on Outgassing of ITER Vacuum Vessel In-Wall Shielding Materials

Abha Maheshwari¹, Haresh Pathak¹, Bhoomi Mehta¹, Rahul Laad¹, Gurlovleen Phull¹, Moin Shaikh¹, Ulhas Dethe¹, Sunil Dani¹

¹ITER-India, Gandhinagar, India

In-Wall Shield Blocks (IWS) will be inserted between inner and outer wall of the ITER Vacuum Vessel (VV) and comprise of number of plates stacked together with fasteners. Although these blocks will be submerged in water passing through the double wall of VV, Outgassing Rate (OGR) of IWS materials plays a significant role in leak detection. On a leak detector there will be a spillover of mass 3 and mass 2 to mass 4 which creates a background reading. Helium background will have contribution of Hydrogen too. So it is necessary to ensure the low OGR of Hydrogen. To achieve an effective leak test it is required to obtain a background below $1 \times 10^{-9} \text{ Pam}^3\text{s}^{-1}$. Hence giving a maximum hydrogen Outgassing Rate $1 \times 10^{-7} \text{ Pam}^3\text{s}^{-1}\text{m}^{-2}$ for IWS at Room Temperature is the requirement for IWS materials. 3 coupons of each IWS material have been manufactured with the same technique which is being used in manufacturing of IWS blocks. OGR depends on absorption and adsorption of gases which is related to Surface Roughness. Surface Roughness of sample may get changed after corrosion and subsequently OGR will also get affected. Water flowing between the walls of VV will promote the corrosion of IWS. IWS is not accessible until life of the machine after closing of VV so it is necessary to examine the effect of this corrosion on OGR. IWS coupons with known OGR have been immersed in water applying the same conditions which will be followed in ITER. Following a sequence of different operating conditions, OGR of these coupons has been measured again and studied the effect of corrosion. This paper will describe OGR Measurement, Surface Roughness Requirement of these coupons, Corrosion under ITER operating conditions and again the measurement of OGR to study the effect of corrosion on OGR of IWS materials.

P-Tu-085

Effect of hydrogenation of amorphous silicon surfaces on protein adsorption

Larbi Filali¹, Yamina Brahmi¹, Jamal Dine Sib¹, Yahia Bouizem¹, Djamal Benlekhal¹, Aissa Kebab¹, Larbi chahed¹

¹University of Oran, Oran, Algeria

We studied in this work, the adsorption of proteins on thin layers of amorphous silicon, depending on the surface conditions. We have a set of samples of sputtered silicon thin films, with different hydrogen concentration at the surface. Infrared spectroscopic analysis with the ATR method, ellipsometry and scanning electron microscopy revealed that the adsorption on the surfaces is enhanced on samples with highest hydrogen surface concentration. This result leads to the conclusion that the adsorption is caused by hydrogen bonds at the film / protein interface, which seems to be the dominant effect compared to surface roughness and wettability, which were found to decrease as hydrogen surface concentration increases.

P-Tu-086

Vacuum ultraviolet photon-stimulated desorption surface spectroscopy of polymers using a laser-produced plasma emission

Masanori Kaku¹, Masahito Katto¹, Atushi Yokotani¹, Wataru Sasaki², Shoichi Kubodera¹

¹University of Miyazaki, Miyazaki, Japan, ²NTP, Inc., Miyazaki, Japan

Photo-dissociation processes of solid materials such as polymers have not well been understood. In contrast, simple molecules such as H₂, O₂, N₂ and CO have been investigated by using synchrotron radiation. The facility is, however, usually large and in limited use. We have demonstrated a spectrally continuous vacuum ultraviolet (VUV) emission source in the wavelength between 115 and 200 nm using a laser-produced plasma (LPP) as a spectroscopic emission source. Despite lower brightness and coherence compared with those of synchrotron radiation, the LPP emission source can be easily operated in a compact size in a small-scale laboratory. We, therefore, have proposed new photon-stimulated desorption surface spectroscopy using such broadband VUV emissions using the LPP. Adsorbed atoms or molecules on material surfaces should be desorbed and dissociated as a result of absorption of the wavelength-selected high-energy VUV photons. Material surfaces would be analyzed by detecting desorbed and dissociated atoms or molecules. This photon-stimulated desorption surface spectroscopy should have superior characteristics over conventional thermal desorption spectroscopy in terms of energy and spatial resolutions with minimum heat effect. In this paper, we report new photon-stimulated surface spectroscopy using the LPP. The irradiation wavelength dependence of mass spectra of polyethylene and polyvinyl chloride samples were demonstrated. We have found that the characteristic differences of the mass spectra were obtained in the wavelength shorter than 200 nm in each sample. Dissociation of atoms or molecules from material surfaces depended on bond energy or molecular structure.

P-Tu-088

DFT study of the Si/Al ratio in the adsorption of O₂, N₂ and CO₂ on faujasite

Gerard Alonso¹, Ramón Sayós¹, Xavier Giménez¹, Pablo Gamallo¹

¹University of Barcelona, Barcelona, Spain

Zeolites are adsorbent materials commonly used as gas separators. The main factor that controls the activity of the zeolite is the so-called Si/Al ratio that represents the quantity of AlO₂⁻ units per cell. A totally silicated zeolite has no total net charge but the presence of aluminum atoms originates negative charges that need alkali or alkali earth cations to get balanced. Faujasite is a zeolite that belongs to the FAU framework with a Si/Al ratio of 2.4 and widely used in processes that involve capture of CO₂. In this study we report the main density functional theory (DFT) results about the interaction of N₂, O₂ and CO₂ molecules with Faujasite at different Si/Al ratios (i.e., from fully silicated faujasite to Si/Al ratio of 3.36). Periodic DFT calculations have been performed by means of Vienna ab-initio Simulation Package (VASP) using the Perdew, Burke and Ernzerhof (PBE) functional. Van der Waals interactions have been accounted using the DFT-D2 dispersion correction formulated by Grimme. This study details how the presence of Al/Na⁺ pairs affect the diffusion barriers of adsorbents found in the porous material as well as their binding energies. The values obtained here are important in order to get some light about the mechanism that describes correctly the CO₂ capture in flue gas mixtures, the common outgoing gases in many industries. More specific details on the results obtained will be given in the meeting.

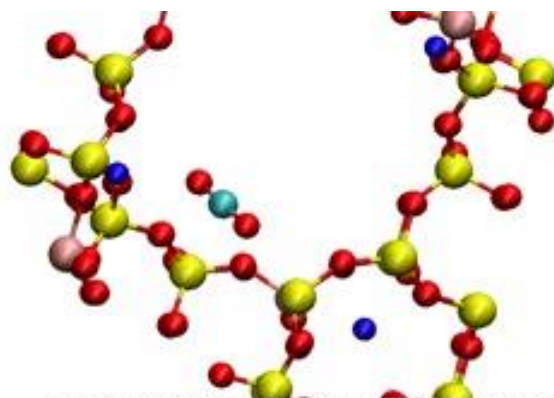


Figure 1. Faujasite Detail with CO₂ molecule adsorbed into a Site II Na⁺

P-Tu-089

Adsorption of silicon on Ag(111) studied with XPS and LEED

Dah-An Luh^{1,2}, Chiao-Yin Yeh¹, Tsai-Feng Yu¹, Chia-Hsin Wang², Yaw-Wen Yang²

¹Department of Physics, National Central University, Jhongli, Taiwan, ²National Synchrotron Radiation Research Center, Hsinchu, Taiwan

Silicene, the silicon version of graphene, has become a subject of great interest since graphene was discovered. Free-standing silicene is not stable in nature and not realized so far. Several studies have reported the growth of silicene on Ag(111). However, in addition to silicene, those studies, mostly with STM and LEED, revealed the various phases of Si/Ag(111), of which the structural models are not available or under intense debates. In this work, we have investigated the growth of Si on Ag(111) with varied Si coverage and growth conditions. Several surface reconstructions were obtained and characterized with LEED and XPS. Based on the evolutions of the LEED images and the XPS spectra, the origins of the various components of Si 2p were assigned. The assignments agree with a growth model in which the Ag atoms migrate to the surface of the Si layer on Ag(111) at an elevated temperature.

P-Tu-090

Investigation of local electronic structures of Cesium ion in clay minerals using Fluorescence XAFS measurements

Mitsunori Honda¹, Iwao Shimoyama¹, Shinishi Suzuki¹, Tsuyoshi Yaita¹

¹Japan Atomic Energy Agency, Ibaraki, Japan

Influence of local electronic structures of cesium in two kinds of clay minerals (vermiculite and kaolinite) in which the different ability to fix cesium is investigated by near edge x-ray absorption fine structure (NEXAFS) at the Cs L₃ adsorption edge. The NEXAFS measurement is known to have element selectivity due to inner shell excitation, but the L₃ edge of cesium NEXAFS measurement was difficult by a very small amount of Titanium which is existed in clay minerals because Cs L₃ edge (5.01 keV) and Ti K edge (4.96 keV) are extremely close. In this study, we succeed in getting Cs L₃ edge NEXAFS spectra which completely distinguished Ti which was minor component in clay minerals and Cs using fluorescence NEXAFS measurements which we have recently developed in KEK-PF BL27A. Herewith, we clarified that difference in interaction in clay minerals was reflected in electronic structure of the Cs. In addition, we performed the comparison with the standard material of Cs compounds which were an ionic solids. As the result of NEXAFS spectra, we found that a difference appeared in the spectrum of the standard materials. This indicates different orbital hybridization of Cs between the clay minerals and standard ionic solids because electronic structures in the Cs NEXAFS reflect orbital hybridization around Cs sites and suggests some contribution of covalent character for strong fixation of Cs in clay minerals. From the result, the electronic structure of Cs in clay minerals reflected that orbital hybridization was different from the ionic solid which was a Cs standard material and we have achieved that the contribution of covalent attachment occurred.

P-Tu-091

Characterization of green fluorescent protein monolayers utilizing controllable self-assembled monolayers

Shin-ichi Wada^{1,2}, Jumpei Kajikawa¹, Hironori Hayashita¹, Ryosuke Koga¹, Atsunari Hiraya^{1,2}

¹Department of Physical Science, Hiroshima University, Higashi-Hiroshima, Japan, ²Hiroshima Synchrotron Radiation Center, Hiroshima University, Higashi-Hiroshima, Japan

It is important to understand the function and interaction of proteins immobilized onto surfaces in order to not only investigate characteristics of proteins conveniently but also realize ideal protein monolayers for applications like biosensors, immunosensors, molecular electronic devices and microarrays. Self-assembled monolayers (SAMs) have attractive potential as one of promising candidate surface on which proteins can be introduced as they are. Because it is expected that one can introduce proteins onto surfaces nondestructively by inserting the soft organic monolayers between hard metal substrates and soft proteins. In this study, protein layers formed on SAMs were evaluated using green fluorescent protein (GFP) by means of optical emission, XPS and NEXAFS measurements. From the results of the emission measurements obtained from GFP layers on SAMs with different terminal functional groups, we can easily check the function of GFP (that is, confirm fluorescence spectra characteristic to GFP). It was quantitatively analyzed that the amount of GFP adsorption onto the SAM surfaces can be remarkably controlled by using SAMs in which oligo ethylene glycol is inserted. The orientation of GFP on SAMs was also examined by NEXAFS spectroscopy at SR facility at Hiroshima University, HiSOR. Sharp peaks which correspond to the N/O(peptide) 1s to the π^* transitions only show clear incident angle dependence in both N and O K-edges. It is quite important that incident angle dependence appears and the orientation was evaluated even for huge molecular system like GFP. This incident angle dependence describes that GFP forms an oriented monolayer on the SAM. Although a GFP molecule has 237 peptide bonds around it, by the analysis of polarization dependence using the natural symmetric structure of GFP, it was found that GFP molecules are immobilized on the SAM surface with the averaged tilting angle of 65 degrees from the surface normal.

P-Tu-092

Theoretical study of NO adsorption on Cu(110) and O(2x1)/Cu(110) surfaces

Antón X. Brión-Ríos^{1,2}, Daniel Sánchez-Portal^{1,3}, Pepa Cabrera-Sanfelix^{1,4}

¹DIPC (Donostia International Physics Center), Donostia-San Sebastián, Spain,

²Departamento de Física de Materiales, UPV/EHU, Facultad de Química, Donostia-San Sebastián, Spain, ³Centro de Física de Materiales (CFM-MPC), Centro Mixto CSIC-UPV/EHU, Donostia-San Sebastián, Spain, ⁴IKERBASQUE, Basque Foundation for Science, Donostia-San Sebastián, Spain

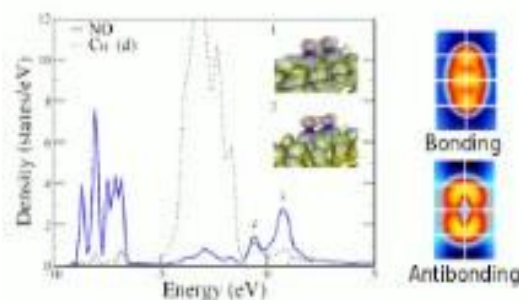
Previous work showed the preferred tilted adsorption of Carbon monoxide (CO) on O(2x1)/Cu(110) surface [1]. As a consequence of the tilting, the dipole attraction between CO molecules resulted in the formation of one-dimensional molecular rows along the [1-10] direction. Recent scanning tunneling microscope (STM) experiments on nitric oxide (NO) adsorption on Cu(110) reveal also two possible orientations, vertical or tilted, depending on temperature [2]. In this work we studied the interaction between NO molecules on Cu(110) and O(2x1)/Cu(110) using Density Functional Theory (DFT). Our results shows that NO interacts strongly with the Cu(110) surface, losing its spin polarization at all coverages. The dimer configuration is favored on a confronted tilted geometry (figure 1) along the [1-10]. On O(2x1)/Cu(110) surface NO adsorbs between CuO rows, in a way that N atoms produce a spontaneous pulling of the row Cu atoms. In this case, vertical and tilted adsorption along the [001] direction are energetically degenerate and the NO molecule show a spin polarization of $\frac{1}{2} \mu_B$. In spite of the low energetic cost to tilt the molecule, we do not find any evidence that the formation of dimers or molecular rows are favored on the O(2x1)/Cu(110) surface [3].

[1] M. Feng, P. Cabrera-Sanfelix, C. Lin, A. Arnau, D. Sánchez-Portal, J. Zhao, P. M. Echenique and H. Petek, ACSnano. 5, 8877-8883 (2011)

[2] A. Shiotari, Y. Kitaguchi, H. Okuyama, S. Hatta and T. Aruga, Phys. Rev. Lett. 106, 156104 (2011)

[3] Antón X. Brión-Ríos, Daniel Sánchez-Portal, Pepa Cabrera-Sanfelix, Phys. Chem. Chem. Phys. submitted.

Figure 1: PDOS representation. NO dimer on Cu(110) along the [1-10] direction. Interaction between $2\pi^*$ molecular orbitals around the Fermi level.



P-Tu-093

The formation and thermal stability of adsorbed HCOO groups on O/Pd(100) surfaces

Imre Kovács¹, János Kiss², Frigyes Solymosi²

¹College of Dunaújváros, Dunaújváros, Hungary, ²MTA-SZTE Reaction Kinetics and Surface Chemistry Res. Group, University of Szeged, Szeged, Hungary

The formation of adsorbed HCOO was confirmed during several catalytic reaction conditions. Surface HCOO species were easily formed by the decomposition of formic acid so its chemical and physical properties has been widely studied on transition metal surfaces. While on the group VIII and Ib metals HCOO was produced by this way, the lack of HCOO formation on clean Pd(100) was the only exception [1]. The HCOOH/Pd(100) adsorbed layer readily decomposed to CO and H₂ but no HCOO was found by UPS. However, preadsorbed K induces its formation and it is stable up to 480 K. According to our results: on precovered O(a) the HCOOH adsorption produces bands at 4.2, 7.9-8.7, 10.9, 13.4 eV in UPS due to formate. In presence of O(a) the formate species is stable up to 300 K. The product distribution changed; i.) The main products were CO₂ and H₂O which desorbed with a coincidence peak temperature at 310K. ii.) An additional new HCOOH peak appeared at 320 K due to recombination. HCOO(a) can be produced by the surface reaction between O(a) + H₂CO, too. The stability of HCOO in such a surface layer was far below than in the previous way, 230-240 K. Based on our TDS and AES results, we estimated the surface concentrations of adsorbed species and we can conclude that more adsorbed oxygen is necessary for the formation HCOO from H₂CO which is reflected in the lower stability.

[1] F. Solymosi, I. Kovács; Surface Science 296 (1993) 171

P-Tu-094

Atomistic thermodynamics study of SHCH₃ molecule adsorption and dissociation on the Fe(100) surface; GGA-PW91 and van der Waals corrections method comparison.

Sherin Saraireh¹

¹Al-Hussain bin Talal University, Ma'an, Jordan

This study represents a detailed Density Functional Theory (DFT) periodic-slab study on the adsorption and stability of SHCH₃ molecule on the Fe(100) surface. Model structures with the SHCH₃ adsorption via the Sulfur, Hydrogen and carbon atoms corresponding to top, bridge and hollow pure on-surface adsorptions were examined and the favorable structures have been found. Dissociation of the molecule into SH-CH₃ and H-SCH₃ species into different sites on the Fe(100) surface have been determined also. All the calculations of these structures were carried out using Vienna ab initio simulation package (VASP). The initial DFT calculations (without van der Waals corrections) were performed using the generalized gradient approximation (GGA) which was parameterized with the Perdew–Wang 91 (PW91) functional. Then the structures were examined using the optB88-vdW exchange-correlation functional to account for van der Waals corrections which has shown to strongly affect the adsorption energies of both physisorbed and chemisorbed species. The surfaces were modeled using p(4 × 4) supercells in order to minimize the lateral interactions between the repeating supercells due to VASP's implementation of periodic boundary conditions. The near surface structure was modeled using five metal layers, the bottom two of which were kept fixed during the optimization. The differential charge density distribution and the partial density of state were also examined. Comparing the differential charge density distribution for molecule adsorption on the Fe(100) surface to show the electronic exchange that will occur between the atoms of the SHCH₃ and the surface. A stability temperature-pressure diagram is constructed for a wide range of chlorine chemical potentials to mimic real operational conditions.

P-Tu-095

Study of surface screening by adsorbates on LiNbO₃ single crystals in different environments by Near Ambient Pressure XPS.

Rohini Kumara Cordero Edwards¹, Laura Rodríguez¹, Carlos Escudero²,
Virginia Pérez², Gustau Catalán¹, Neus Domingo¹, Albert Verdager¹

¹Institut Català De Nanociència I Nanotecnologia (ICN2), Bellaterra, Spain,

²ALBA Synchrotron Light Source, Barcelona, Spain

Ferroelectrics are characterized by having a permanent dipolar moment (polarization) that can be reversed by an external electric field. Though it can, in principle, be used to make ferroelectric memories. Understanding interplay between ferroelectric phase stability, screening and atomistic processes at the surface is a key to control low-dimensional ferroelectricity. A crucial insight is that the interplay between polarization and surface adsorbates works in both directions: adsorbates influence polarization, but the orientation of the polarization also determines the type of adsorbates that bond to the surface. Experiments show that ferroelectric surfaces with opposite polarity have different properties for adsorbing molecules. Lithium Niobate (LiNbO₃) is a uniaxial ferroelectric material, often periodically poled (PPLN) – with P+ and P- domains with a period of about 5 to 35µm – for nonlinear optics applications. In this work we are showing Near Ambient Pressure X-ray Photoelectron Spectroscopy (XPS) measurements performed at the line CIRCE in ALBA. We studied water absorption on LiNbO₃ and PPLN single crystal as a function of the polarization and temperature of the sample and water vapor pressure in the chamber. We observed that water deposition rates, and the discharge effects due to water is strong dependence on the sign of the polarization of the crystals.

P-Tu-096

Preparation and structure of Ni/mixed oxides nanoparticles

Malika Doghmane¹, Fatiha Seridi¹, Sabah Chettibi¹, Nassira Keggouch²

¹Laboratory of Material, Physics University 8, Guelma, Algeria, ²Laboratory Microstructure and defects in materials, University Constantine 1, Algeria,

The objective of this study is the optimization of experimental conditions for the preparation of monometallic nanoparticles deposited on mixed oxide and study of physicochemical properties of these ultra divided materials. These are then tested in industrial interest catalytic reactions. In this work, we have optimized the preparation of nanoparticles of nickel deposited on mixed oxide by ion exchange. The kinetic of impregnation is followed by UV visible and pH metric. They are characterized by XRD and SEM as well as TPR at different stages of elaboration. The study of the effect of the support ($\text{Al}_2\text{O}_3\text{-CeO}_2$, $\text{TiO}_2\text{-CeO}_2$...) is interesting and remarkable

P-Tu-097

Effect of oxygen adsorption on the electron emission probability from Cs/GaAs (001) in vacuum

Andrey Zhuravlev^{1,2}, Vitaly Alperovich^{1,2}

¹Novosibirsk State University, Novosibirsk, Russia, Novosibirsk, Russia,

²Rzhanov Institute of Semiconductor Physics, Novosibirsk, Russia, Novosibirsk, Russia

The GaAs surface with adsorbed cesium is a model system for studying the mechanisms of metal-semiconductor interface formation and a basis for preparing p-GaAs(Cs,O) photocathodes with the state of negative effective electron affinity. Cesium adsorption on the surface of GaAs (001), when the effective affinity remains positive ≥ 0.05 eV, causes nonmonotonic dependence of the electron escape probability P [1]. However, P remains small $\leq 10\%$ even at the maximum. Causes maximum depending $P(\theta)$ and low probability values output are not understood. It can be assumed that the escape probability at Cs coverage > 0.5 ML decreases due to the scattering of momentum and energy of emitted electrons in the single-particle and collective excitations in metallic cesium clusters, which are formed at high coverages. The goal of this work is to verify this hypothesis in an experiment with the adsorption of oxygen on the Cs/GaAs(001) surface, which destroys of the metal cesium bonds in clusters. Experiments were carried out in ultra-high vacuum setup on highly doped epitaxial layers of p-GaAs. Clean the GaAs (001) surfaces were prepared by chemical removal of oxides and subsequent annealing in vacuum. The escape probability and the electron affinity under adsorption of cesium and oxygen on the GaAs (001) surface were determined by the photoemission quantum yield spectroscopy adapted for systems with parameters varying over time [1]. For Cs/GaAs and GaAs (Cs,O) surfaces the escape probability versus the electron affinity are compared. These dependencies have the hysteresis form. It is found that when Cs coverages > 0.5 ML oxygen adsorption causes an increase of the probability of electron emission into the vacuum. Subsequent adsorption of cesium on the surface of GaAs/(Cs,O), leading to the re-formation of the electron gas in cesium clusters again causes a decrease of the electrons escape probability in the vacuum.

[1] A.G. Zhuravlev et al., Appl. Phys. Lett. 105, 251602 (2014).

P-Tu-098

Evaluation of activated carbon prepared by pyrolysis of sawdust of wood on the adsorption of acetaminophen

Naima Gherbi¹, Amel Dib¹, Rania Marouani¹, Angel Berenguer Murcia², Jaime Garcia², A. Hassein Meniai¹, Diego Cazorla-Amoro²

¹Laboratoire de l'Ingénierie des Procédés d'Environnement, University de Constantine 3, Algeria, Constantine, Algeria, ²Departamento de Química Inorgánica, Universidad de Alicante, Alicante, Spain

Activated carbons were prepared by the pyrolysis of sawdust of wood impregnated by phosphoric acid at 450 °C. Materials were characterized for their surface chemistry by elemental analysis, "Boehm titrations", point of zero charge measurements, Infrared spectroscopy, XPS; as well as for their porous and morphological structure by nitrogen and CO₂ adsorption. The physical properties of adsorption capacity for acetaminophen (AA) were examined at 37 °C in vitro, the results show that the retention process is rapid (after 20min), the optimal pH is 4; and the maximum adsorption capacity is 0.386 g AA per g of activated carbon, for an solid-liquid ratio equal to 5g/l the efficiency of retention is 99.39%.

P-Tu-099

Nucleation and initial film growth of pentacene on amorphous mica

Adolf Winkler¹, Levent Tumbek¹, Alberto Pimpinelli²

¹Graz University of Technology, Graz, Austria, ²Rice University, Houston, USA

In this contribution, we discuss several features observed in adsorption, diffusion, nucleation and initial film growth of pentacene molecules on amorphous mica, which might be exemplary for the interaction of large organic molecules with solid substrates. A thorough understanding of these processes is of utmost importance for tailoring organic thin films for application in organic electronics. Pentacene was deposited on sputter amorphized mica (001) via physical vapor deposition under ultrahigh vacuum conditions. Thermal desorption spectroscopy was applied to determine the adsorption and desorption kinetics. With ex-situ atomic force microscopy the morphology of the ultrathin films was measured, allowing to determine the number of islands and the island size distribution. The island density was measured as a function of deposition temperature and deposition rate. From these measurements, the following results could be obtained: (a) Nucleation cannot be described by the classical diffusion limited aggregation (DLA) model; we propose an attachment limited aggregation model (ALA). (b) The molecules do not directly adsorb on the surface but rather via a hot precursor. (c) A new universal correlation between the rate dependence of the island density and the island size distribution was worked out, which will have great impact on the general understanding and description of organic film growth.



P-Tu-100

Diffusion on one-dimensional lattice with NN and NNN lateral interactions between the adsorbed particles

Alexander Tarasenko¹, Lubomir Jastrabik¹

¹Institute of Physics, v.v.i., Prague, Czech Republic

Diffusion of particles adsorbed on the one dimensional sawtooth lattice is investigated using theoretical approach and kinetic Monte Carlo simulations. The concentration dependencies of the center-of-mass and Fickian diffusion coefficients are calculated for some representative values of the lateral interactions between the adsorbed particles. We thoroughly compared the analytical dependencies with the KMC numerical data. The perfect coincidence of the data obtained by the two quite different methods clearly demonstrates that the analytical expressions for the diffusion coefficients derived in the framework of the approach based on the non-equilibrium statistical operator exactly describe the particle migration in the lattice gas systems.

P-Tu-101

Ultraviolet photoelectron spectroscopy study of Cu(200 nm)/Si substrates treated by Ar ion sputtering and vacuum annealing

Xxx Ajjasaijian¹, Yuki Kotanigawa¹, Yudai Ohtomo¹, Shuichi Ogawa¹, Yuji Takakuwa¹

¹Tohoku University, Sendai, Japan

A photoemission-assisted Ar plasma (PAP) ion source, in which DC discharge plasma is triggered by photoelectrons emitting from the UV-irradiated surface, has been developed for improving surface roughness down to nanometers scale. Therefore, the PAP discharge current (I_{PAP}) is very sensitive to the work function (ϕ) of the substrate, which governs the photoelectron yield, making it possible to monitor in situ the surface chemical states of the substrate during the PAP treatment. In this study, ultraviolet photoelectron spectroscopy (UPS) with 21.22 eV was employed to measure the changes of ϕ , amount of adsorbed oxygen, and density of states near the Fermi level for the polycrystalline Cu(200 nm)/Si treated by PAP Ar ion sputtering and vacuum annealing to consider the surface flattening mechanism with a reaction model of the Cu substrate with PAP Ar ion. With increasing temperature during annealing under $\sim 10^{-7}$ Pa, ϕ remained almost unchanged at 4.9 eV up to 250°C and then showed a considerable increase followed by a very gradual saturation at 5.2 eV above 300°C, indicating the thermal reduction of Cu oxide. However, the O 2p intensity demonstrated that oxide still remained at 400°C. On the other hand, when irradiating the Cu surface with 600-eV Ar ion at RT, ϕ decreased gradually after an initial quick increase and then saturated at ca. 4.7 eV, which was ascribed to the clean Cu surface. Such a behavior of ϕ interprets well the time evolution of I_{PAP} that showed a recovery after the initial rapid decrease and then almost saturated. A significant flattening effect of Cu surface was achieved after the saturation of I_{PAP} . Based on this agreement, we proposed a reaction model that flattening of Cu surface is accomplished due to the enhancement of surface migration of Cu atoms after the Cu oxide removal.

P-Tu-102

Electronegativity-dependent removal of tin from different surface materials

Malgorzata Pachecka¹, Chris Lee¹, Marko Sturm¹, Fred Bijkerk¹

¹University of Twente, Industrial Focus Group XUV Optics, MESA+ Institute for Nanotechnology, Enschede, Netherlands

In Extreme ultraviolet lithography (EUVL), a tin plasma is used to generate light. The plasma creates a rather hostile environment, with plasma-facing surfaces subjected to an amount of background gas species, and tin. In particular, it is important that tin can be removed from the mirror surface to prevent reflectivity loss. Achieving this relies on understanding how the environment interacts with the mirror surface. We assumed that successful etching with atomic radicals could be predicted from electronegativity considerations. Given a surface material, M, and a contaminant, N, then etching with radical species would be successful if $\chi_N - \chi_M \geq 0$. To test this hypothesis, different materials (Sc, Ti, Al, Cr, Nb, V, W, Si, Mo, Ag, B, Ru, Au, C), that cover a range of electronegativities, were deposited onto a silicon wafer. Tin was then evaporated onto the surfaces, followed by etching with hydrogen reactive species. The deposition and removal of tin was studied using in situ ellipsometry. The surface roughness of the original surface, the tin-covered surface and the cleaned surface was analyzed using atomic force microscopy (AFM). Finally, the amount of tin remaining after etching was quantified using X-ray fluorescence spectroscopy (XRF). We show that for metals, our hypothesis appears to be supported. Clean-ability depends on the relative electronegativities of the cap material and tin. Tin can be fully chemically etched from surfaces with the electronegativity lower than tin, while incomplete tin etching is observed for materials with electronegativity higher than tin.

P-Tu-103

Step dynamics on sidewalls of nanowires: step curvature and Ehrlich-Schwoebel effects

Yuri Hervieu¹, Sergey Filimonov¹¹Tomsk State University, Tomsk, Russian Federation

We consider lateral growth of nanowires (NWs) as a sequential formation of monoatomic steps at the NW base and their propagation along the nanowire sidewall upwards to the NW top. The elongation rate of a NW and step velocities are determined from the solution of the surface diffusion equation subject to the relevant boundary conditions at the steps, at the NW base, at the NW top, and on the substrate surface [1]. The step curvature and Ehrlich-Schwoebel (ES) effects as well as elastic step-step repulsion are taken into account. We show that due to the step curvature there might exist the supersaturation at the step relatively to the nanowire top. In this case the step propagation is suppressed when the step is approaching the top. Therefore, the sidewall becomes unstable against step bunching that might trigger the transition from cylindrical to pencil-like NWs observed during the Au-assisted MBE growth of GaAs and InAs [2]. The existence of the ES barrier leads to the increased adatom concentration behind the step, which gives rise to the accelerated formation of new steps. On the other hand the ES barrier promotes “detachment” of the leading step from the bunch and prevents bunching of the “detached” steps. At a sufficiently high ES barrier this leads to the formation of a tapered nanowire with a non-tapered section at the top as observed, e.g., in the InP NWs growth by the Au-assisted selective area MOMB [3].

This work was supported by the Russian Foundation for Basic Research (grant 13-02-12160).

[1] V.G. Dubrovskii, Yu.Yu. Hervieu, J. Cryst. Growth 401 (2014) 431.

[2] M.C. Plante, R.R. LaPierre, J. Appl. Phys. 105 (2009) 114304.

[3] Y. Greenberg et al, J. Cryst. Growth 389 (2014) 103.

P-Tu-104

Interaction of Au(200 nm)/Si surface with photoemission-assisted plasma ion source: the surface flattening effect of He⁺, Ar⁺, Kr⁺, and Xe⁺ ions

Kotanigawa Yuki¹, AJIASAIJIAN¹, Ogawa Shuichi¹, Takakuwa Yuji¹

¹Tohoku University, Sendai, Japan

Flattening Au surfaces within a few nanometers is of practical importance for many applications such as optical device and MEMS assembly and DNA tip. For this sake, we have developed a photoemission-assisted plasma (PAP) ion source, in which DC discharge plasma was triggered by photoelectrons emitting from UV-irradiated substrates with a Xe excimer lamp. In the PAP ion source, the kinetic energy of ion impinging on the substrate can be lowered below a few tens eV for PAP glow discharge and furthermore reduce as low as a few tenth eV for PAP Townsend discharge. In this study, we investigated the interaction between the Au(200 nm)/Si substrate and PAP He⁺, Ar⁺, Kr⁺, and Xe⁺ ions with low energies to clarify the Au surface flattening mechanism of PAP ion. The initial surface roughness of Au(200 nm) films deposited on the front mirror-polished and rear roughened Si substrate was measured by AFM as 7 nm (A surface) and 240 nm (B surface), respectively. The ion irradiation treatment of the Au surface was performed under PAP glow discharge. At a total ion charge of 0.8 C for B surface, He⁺, Kr⁺, and Xe⁺ ions showed a flattening effect of -15.3%, -10.8%, and -6.4%, respectively, whereas roughening of +1.7% was observed for Ar⁺ ion. For the case of A surface, He⁺, Kr⁺, and Xe⁺ ions still improved the surface roughness by -18.3%, -3.5%, and -9.2%, respectively, although Ar⁺ ion was not available for flattening. The observed dependence of the Au surface flattening effect on the ion species is not interpreted in terms of a simple energy transfer model, in which He⁺ ion is expected to be less effective for Au. To clarify the flattening mechanism of PAP ion, we consider separately the sputtering effect and the enhancement effect of surface migration during PAP treatment.

P-Tu-105

Microstructural, Mechanical and Tribological Investigations of Nb-C-N and Nb-Al-C-N Coatings Obtained by Thermo-Reactive Deposition Technique

Eray Abakay¹, Şaduman Şen¹, Uğur Şen¹

¹Sakarya University, Sakarya, Turkey

In this study the microstructural, mechanical and tribological properties of Nb-C-N and Nb-Al-C-N coatings with different Al contents were investigated. The coatings were deposited on AISI 4140 steel substrates by a duplex surface treatment involving nitriding and thermo-reactive deposition and diffusion (TRD) technique. The TRD process was performed by pack method at the temperature of 1000 °C for 2 h. The thickness of the coating layers formed on the substrates approximately 6.68 µm for all compositions. The depth of the coated layer Microstructural properties of these coatings investigated by X-ray diffraction analysis (XRD), Raman spectroscopy, scanning electron microscopy (SEM) and energy dispersive x-ray spectroscopy (EDS). The results showed that the coating exhibited a dense and smooth microstructure with NbCN, NbN and AlN phases. Mechanical properties were investigated by micro hardness and Rockwell C adhesion tests. Addition of aluminum to the coating bath was resulted to increasing of hardness but decreasing of adhesion strength quality. Unlubricated sliding wear tests of coatings were realized by ball-on-disc method against alumina ball under 2.5, 5 and 10 N loads at 0.1 m/s sliding speed. The wear debris and the wear tracks were analyzed by SEM and 3D-stylus profilometry. According to the results, wear rate of the coatings decreased with increasing of aluminum ratio.

P-Tu-106

Scanning electron microscopy study of ice nucleation and growth on mineral and metal surfaces

Sarah Delage¹, Patrick Ayotte¹

¹Université de Sherbrooke, Sherbrooke, Canada

Interest into the role of mineral dust particles as ice nuclei (IN) soared recently due to our increasing awareness of the impact of ice clouds in the global radiation budget which remains a major source of uncertainty in climate forcing [IPCC 2014]. Our poor understanding of the ice formation mechanisms and rates in the atmosphere hampers mitigation efforts and the elaboration of regulatory guidelines for the emission of particulate matter. Previous laboratory investigations, using microscopic and spectroscopic methods, pointed out numerous physico-chemical properties (composition, size, hydrophobicity) influencing the nucleation rates of ice by mineral aerosols under various environmental conditions (water vapor super-saturation ratio, temperature). Despite continuing efforts [1], our understanding of the impact of structural, chemical and morphological properties of dust particles on ice nucleation remains incomplete. Cryogenic environmental scanning electron microscopy (Cryo-eSEM) offers the opportunity to explore the dependence of ice nucleation and growth kinetics on the structure and morphology of particulate matter, as well as the surface chemistry of single crystal surface with emphasis on the role of defects, under controlled conditions. Furthermore, this approach allows us to investigate the impact of morphological characteristics of individual IN with their propensity for heterogeneous ice nucleation and growth, and to correlate these attributes with the morphological properties of ice crystallites, under conditions relevant to the atmosphere. In this context, we use Cryo-eSEM to study ice nucleation by two types of aerosols using water vapor deposition under condition relevant to the upper troposphere/lower stratosphere. Recent results of our ongoing study of ice nucleation and growth at the surface of hydrophilic mineral single-crystals and dust particles (in particular muscovite, as its potency at inducing ice nucleation is well established [2]) will be compared and contrasted with that occurring at hydrophobic metallic surfaces.

[1] Zepeda, Yeh & Orme. Rev. Sci. Instrum., 72, 4159-63 (2001)

[2] Eastwood et al. J. Geophys. Res., 113, D22203 (2008)

P-Tu-107

Low temperature selective growth of GaN single crystals on pristine and graphene modified SiO₂ substrates

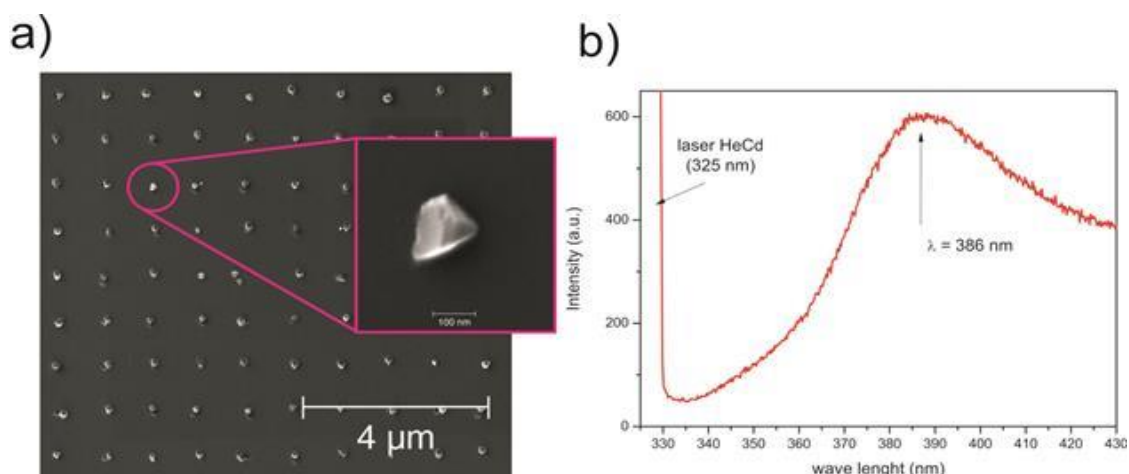
Jindřich Mach^{1,3}, Tomáš Šamořil^{1,2}, Pavel Procházka¹, Miroslav Bartošík^{1,3},
Stanislav Voborný^{1,3}, Kirill Andrejevič Ermakov³, Tomáš Šíkola^{1,3}

¹BUT Brno, Brno, Czech Republic, ²Tescan a.s., Brno, Czech Republic,
³CEITEC, Brno, Czech Republic

We will report on a simple hybrid method for the selective growth of GaN nanostructures on pre-patterned silicon substrates covered with native oxide. The patterning was performed by a Ga focused ion beam (FIB) to create nucleation centers in form of an array of pits and grooves. Using ultra-low energy (50 eV) ion-beam assisted physical vapour deposition [1, 2] a self-organized growth of GaN single crystals at these nucleation sites was achieved at 300°C. The size control of GaN single crystals was provided by a sequential deposition of Ga atoms and low energy nitrogen ions. Compared to our previous experiments we have significantly improved spatial selectivity of the growth (no small crystallites on a substrate between the ordered nanocrystals). The characterization of these crystals was performed using SEM and AFM (morphology) and by electron backscatter diffraction – EBSD (crystallographic structure). A good quality of the nanocrystals was also confirmed by a photoluminescence signal possessing a peak at the expected wavelength (390 nm) and measured by scanning confocal μ Raman spectroscopy. In addition, an influence of a graphene layer laid upon silicon substrates on the selective growth will be discussed as well.

[1] MACH, J.; ŠAMOŘIL, T.; VOBORNÝ, S.; KOLÍBAL, M.; ZLÁMAL, J.; SPOUSTA, J.; DITTRICHOVÁ, L.; ŠÍKOLA, T.. Review of Scientific Instruments, (82), Vol. 8, p.p. 083302, (2011).

[2] MACH, J.; ŠAMOŘIL, T.; KOLÍBAL, M.; ZLÁMAL, J.; VOBORNÝ, S.; BARTOŠÍK, M.; ŠÍKOLA, T., Review of Scientific Instruments, (85), Vol. 8, p.p. 083302-1, (2014).



P-Th-001

Charge-Density-Wave Orderings in LaAgSb₂ - A Photoemission Study

Maya Narayanan Nair¹, Irene Palacio¹, R.F Luccas², P. C Canfield³, E.G Michel², A. Taleb-Ibrahimi¹, A Tejada^{1,4}

¹UR1 CNRS/Synchrotron Soleil, Gif-Sur-Yvette, France, ²Dept.Fisica de la Materia Condensada, Universidad Autonoma de Madrid, Madrid, Spain, ³Ames Laboratory-US, DOE and Dept. of Physics and Astronomy, Iowa State University, USA, ⁴Laboratoire de Physique des Solides, Université Paris-Sud, France

The growing interest of RAgSb₂ family (R=rare earth) is due to the observed highly anisotropic electronic and magnetic properties and the low temperature physical properties. These properties are correlated to their anisotropic atomic structure. In LaAgSb₂, anomalies in the resistivity and magnetic susceptibility have been observed [1]. An evidence of a Peierls transition that accounts for these anomalies has been observed by X-ray diffraction experiments [2]. X-ray scattering measurements have shown a periodic charge and lattice modulation below 207K along the a direction of tetragonal structure. Further lowering in temperature, an additional CDW ordering was observed along the c direction. Here we report the modifications of the Fermi surface as a function of the temperature using high resolution angle-resolved photoemission spectroscopy (ARPES).

[1] K. Myers, S. Bud'ko, I. Fisher, Z. Islam, H. Kleinke, A. Lacerda, and P. Canfield, Journal of Magnetism and Magnetic Materials 205, 27 (1999).

[2] C. Song, J. Park, J. Koo, K. -B. Lee, J. Y. Rhee, S. L. Bud'ko, P. C. Canfield, B. N. Harmon and A. I. Goldman, Phys. Rev. B 68, 035113 (2003)

P-Th-002

Electronic structure of Au/Pt(001): observation of 1D surface states

Silvina Bengió¹, Lukasz Walczak², Ivana Vobornik³, Pilar Segovia², Enrique García Michel²

¹Conicet and Centro Atómico Bariloche, Bariloche, Argentina, ²Departamento de Física de la Materia Condensada, Universidad Autónoma de Madrid, Madrid, Spain, ³Istituto Officina dei Materiali (IOM)-CNR, Laboratorio TASC, Area Science Park, Trieste, Italy

The electronic and structural properties of Au, Pt and their alloys in the nm size range have been a subject of continuous interest over many years, due to their many interesting properties, including an specific electronic behavior, complex reconstructions and catalytic activity [1,2]. We report an ARPES study of the electronic structure of Au deposited on reconstructed Pt(001) in the range of 1-7 ML, including an analysis of the Fermi surface and combined with structural information from LEED. Au grows epitaxially on Pt(100) following a quasi layer-by-layer growth mode. We monitor the electronic band structure near the surface X point vs. Au coverage. For 1 ML Au coverage we identify the formation of a hybridized electronic state related to the Pt sp band and the incipient Au sp band. Starting at 2-3 ML coverage, we identify contributions from the Au sp band, from the surface of Au, and from the underlying substrate (Pt sp and d bands). The Au surface states exhibit a quasi one dimensional character with a (1x7) LEED reconstruction. On the basis of STM and LEED data, we traced it back to the surface reconstruction of the Au layer, which adopts a similar termination as in bulk Au(100), namely a rotated hexagonal topmost atomic layer, corrugated to accommodate to the (100) Au layers underneath. Our results provide us with a complete picture and understanding of the electronic structure of Au/Pt(100), including sp Au band formation, hybridization, electronic confinement, surface charging and the mode of surface growth, and with implications in the understanding of the distinct electronic behavior of Au layers and particles in the nm size range.

[1] M. Chen, Y. Cai, Z. Yan, and D.W. Goodman, J. Am. Chem. Soc. 128, 6341 (2006).

[2] S. Bengió et al. Phys. Rev. B 86: 045426 (2012).

P-Th-003

Study of Half-Metallic Ferromagnetism of MgSe Doped with Zr in Zinc Blende Phase Using First Principles

Muhammad Rashid¹, Altaf Karim¹

¹Department of Physics, CIIT, Islamabad, Islamabad, Pakistan

First-principles full-potential linearized augmented plane wave (FLAPW) method is used to study the electronic structure and magnetic properties of zinc blende (ZB) $\text{Mg}_{0.75}\text{Zr}_{0.25}\text{Se}$. Wu–Cohen generalized gradient approximation (WC-GGA) and the modified Becke-Johnson local density approximation (mBJLDA) were employed within the framework of spin-polarized density functional theory (DFT). We investigated the ferromagnetic (FM) and antiferromagnetic (AFM) phases and found that $\text{Mg}_{0.75}\text{Zr}_{0.25}\text{Se}$ is stable in the ferromagnetic structure. Structural properties are computed by total energy minimization. Our results show that the cohesive energy of ZB $\text{Mg}_{0.75}\text{Zr}_{0.25}\text{Se}$ is greater than that of ZB MgSe. The electronic and magnetic properties calculated for ferromagnetic phase exhibit half-metallic ferromagnetism. The calculated total magnetic moments are $2.0 \mu_B$ and, which agree with the Slater–Pauling rule quite well. It is observed that the p–d hybridization reduces the local magnetic moment of Zr from its free space charge value and produces smaller local magnetic moments on the non-magnetic Mg and Se sites. The values of the $N0\alpha$ and $N0\beta$ exchange constants confirm the magnetic nature of these compounds.

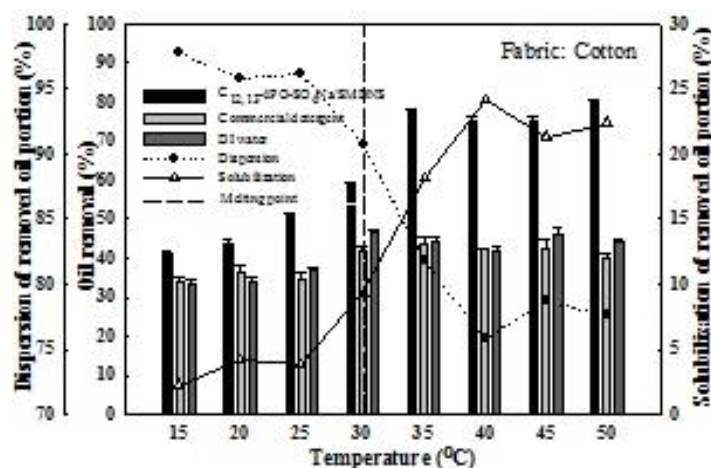
P-Th-004

Mechanisms and Performance of Methyl Palmitate (Solid Fat Soil) Detergency under Microemulsion-Based Formulation

Jarussri Chanwattanakit¹, John F. Scamehorn², David A. Sabatini², Sumaeth Chavadej^{1,3}

¹The Petroleum and Petrochemical College, Chulalongkorn University, Bangkok, Thailand, ²Institute for Applied Surfactant Research, University of Oklahoma, Norman, USA, ³Center of Excellence on Petrochemical and Materials Technology, Chulalongkorn University, Bangkok, Thailand

In this work, the correlation of oily soil detergency performance with oil/water interfacial tension (IFT), oil dispersion and oil solubilization at different temperatures above and below the melting point of methyl palmitate was investigated using two fabrics of cotton and polyester as compared with a commercial detergent product and de-ionized water. A selected formulation of an anionic extended surfactant (a branched alkyl polypropoxylated sulfate, C_{12,13}-4PO-SO₄Na) and sodium mono- and dimethyl naphthalene sulfonate (SMDNS) as a hydrophilic linker was able to form a middle phase microemulsion at a minimum of total surfactant concentration of 0.015 wt% with a weight ratio of C_{12,13}-4PO-SO₄Na:SMDNS = 1:0.1625. At a temperature higher than the melting point of methyl palmitate (30°C) and under the Winsor Type III microemulsion condition, the maximum oil removal was found to correspond to the minimum system IFT. Above the melting point, the oil removal (about 80%) almost remained unchanged with increasing temperature from 30 to 50 °C whereas it increased significantly from 58% to 80% with increasing temperature. The studied formulation provided a much higher oily soil detergency as compared to both commercial and de-ionized water systems. For any temperature below the melting point, on any studied fabrics, the oil removal was significantly lower than that of any system at a temperature higher than the melting point and it decreased with decreasing washing temperature. Under the studied formulation, the solubilization capacity increased with increasing temperature especially at high temperatures whereas the dispersion of detached oil was extremely high and decreased greatly with increasing temperature. The results suggest that the removal of methyl palmitate under liquidified oil results from the mechanisms of both roll up and solubilization while the oil removal mechanism of solidified oils is governed the detachment and dispersion stability of solid particles.



P-Th-007

Different surface interactions in new self-assembled structures of gold nanorods and polysaccharides

Heloise Ribeiro de Barros¹, Izabel Riegel-Vidotti¹, Leandro Piovan¹, Mário Meneghetti², Ábner Nunes², Guilherme Lanzi Sassaki³, Diego Araujo Sabry³

¹Paraná Federal University/ Chemistry Department, Curitiba, Brazil, ²Alagoas Federal University/ Biotechnology and Chemistry Department, Maceió, Brazil,

³Paraná Federal University/ Biochemistry Department, Curitiba, Brazil

The advances in nanoscience and nanotechnology brought attention to the development of nanomaterials for biological applications. Gold nanorods (AuNRs) are of great interest due their surface plasmon (SPR) and geometrical characteristics. Besides, AuNRs are very suitable for exploring self-assembled structures in constructing nanodevices for biosensing, especially in the biomedical field. Cetyltrimethylammonium bromide (CTAB) is the most commonly employed surfactant for obtaining AuNRs. However, CTAB is cytotoxic and is responsible for AuNRs instability in buffer solutions which restrict its use for biological applications. Therefore, it is fundamental the development of surface modification methodologies for the removal or encapsulation of CTAB in order to obtain AuNRs with reduced cytotoxicity and high stability in different physiological media. Biopolymers are very promising interacting materials for AuNRs since they are biodegradable, biocompatible, have low toxicity and present a variety of functional groups that are distributed in a complex molecular microstructure. In our work, gum arabic (GA) and a sulfated chitosan (ChiS) exhibited remarkable features in encapsulating CTAB/AuNR producing novel self-assembled structures. Their inherent microstructure properties, the variety of functional groups in both polysaccharides, in particular the sulfate groups in ChiS and the carboxylic groups in GA, as well as the highly branched structure of GA are responsible for the efficient interactions of these polysaccharides and the CTAB/AuNRs. Combining the results obtained by UV-Vis spectroscopy, FTIR, zeta potential and transmission and scanning electron microscopies we were able to discuss in details the possible surface interactions between GA or ChiS with CTAB/AuNR. Therefore, our work contributes to the understanding of the driving forces that are prone to control the self-assembling of the studied materials providing useful considerations in the development of new gold building blocks.

P-Th-009

Influence of electronic and plasmonic structure of planar TiAlN/Ag metamaterials on its heat conductivity

Anatoly Kovalev¹, Dmitry Wainstein¹, Alexan Rashkovskiy¹, Raul Gago², Jose Endrino³

¹I.P. Bardin Central Research Institute for Ferrous Metallurgy, Moscow, Russian Federation, ²Instituto de Ciencia de Materiales de Madrid, Madrid, Spain, ³School of Aerospace, Transport and Manufacturing (SATM), Cranfield University, Cranfield, UK

The planar metamaterials based on interleaved TiAlN/Ag bilayers with thicknesses of individual layers varying from 100 to several nm were obtained by magnetron sputtering. Degradation of Ag-Ag bonds metallicity with metal layers thickness decreasing was measured by XPS of inner and outer electrons levels. The features of plasmons and phonons oscillations propagation were studied by EELS with excitation by 1.5 keV electron beam. Degradation of volume resonant plasmons and their localization near interfaces are observed at Ag layer thickness decreasing. There is shown also that the energy of acoustic phonons decreases with decreasing of Ag layers thickness within nanoscale region. In contrast, the energy of optical phonons increases with nanostructuring of Ag layers. We suppose that longitudinal plasmons (LP) couple only to transverse optical (TO) phonons, while transverse plasmons (TPs) couple only to longitudinal optical (LO) phonons. Lowering of free electrons density in thinner Ag layers together with plasmon-phonon energy exchange on interfaces are explaining thermal barrier properties of nanolaminate metal-dielectric metamaterial.

The research was partially supported by RSF research project No. 14-12-00170

P-Th-010

Investigation of behaviour of copper during transition passive state to transpassive state by in situ spectroscopic techniques

Cigdem Toparli¹, Adnan Sarfraz¹, Andreas Erbe¹

¹Max-Planck-Institut für Eisenforschung GmbH, Düsseldorf, Germany

Copper is one of the most widely used metals in the industry, because of its availability and corrosion stability. The stability is caused by spontaneous formation of an ultrathin film as a corrosion product, e.g. as passive film on the metal surface, which prevents oxidation [1]. Therefore, understanding the mechanism of corrosion processes on copper surface is vital. The electrochemically passive state can break down by applying higher potential – the material then enters the transpassive regime. During this transition, electrochemical splitting of water occurs, which also includes oxygen evolution on the surface. This study focuses to understand this transition from passive to transpassive state. The transition was investigated by electrochemistry coupled spectroscopic ellipsometry and Raman spectroscopy. From the analysis of ellipsometric data we are able to investigate the thickness changes and electronic structure changes during the passive-transpassive transition, while Raman spectroscopy gives also information about the layer itself. For the analysis of ellipsometric data, a similar approach was used as described previously [2]. Based on literature data for the dielectric function of Cu [2], Cu₂O, CuO [2] and water [2], ellipsometric spectra for Cu covered with different oxide layers of different thicknesses were simulated. This analysis is applied under potentiodynamic polarization and for potentiostatic steps. As a result, the change in oxide thickness is determined, which changes with the electrode potential. Further, dielectric function of the oxide films is deduced from a subsequent full fit of the ellipsometric spectra. Ellipsometric results are complemented by Raman spectroscopic data and ex situ surface analysis.

[1] J. Kunze, V. Maurice, L. H. Klein, H.-H. Strehblow, P. Marcus, Corrosion Science 46 (2004) 245-264.

[2] M. Hans, A. Erbe, S. Mathews, Y. Chen, M. Solioz, F. Mücklich, Langmuir 29 (2013) 16160-16166.

P-Th-011

Influence of plasmon structure of multilayer metal-insulator-metal coatings on light reflection

Dmitry Wainstein¹, Anatoly Kovalev¹, Alexandr Rashkovskiy¹, Raul Gago², Jose Endrino³

¹I.P. Bradin Central Research Institute for Ferrous Metallurgy, Moscow, Russian Federation, ²Instituto de Ciencia de Materiales de Madrid, Madrid, Spain, ³School of Aerospace, Transport and Manufacturing (SATM), Cranfield University, Cranfield, UK

The multilayer (Ti₃₄Al₆₆)N/Ag metal-insulator-metal (MIM) heterostructures with different thicknesses of individual layers varied from several to several hundred nanometers were fabricated by DC-magnetron sputtering. The microstructure investigations were performed by HRTEM. The phase composition and crystallography of individual layers were studied by X-ray diffraction. The reflection indexes were measured from infrared to ultraviolet radiation in the photons energies range from 1 to 5 eV, or from 1240 to 248 nm. The spectroscopy of plasmon losses and plasmon microscopy allowed us to measure the plasmons losses characteristic energies and their surface distribution. The energies of plasmons peaks and their locations are strongly depending on Ag layers thickness in the MIM nanocomposite. The surface plasmon with energy about 4 eV was observed in the centre of Ag layer while thickness was 20 nm. The plasmons were localized at the metal/dielectric interface for Ag layers 5 nm and less. The reflectance spectral profiles edges positions at long and short waves are correlated with plasmons energies and features of their spatial distribution. The MIM based on the (Ti₃₄Al₆₆)N/Ag light absorber can find applications in design optical filter and photovoltaic energy conversion devices, etc.

The research was partially supported by RSF research project No. 14-12-00170

P-Th-012

An MIES study of variation in the local electronic structure during alkali-promoted oxygenation of GaAs(001) surfaces

Kenji Yamada¹, Hirofumi Takikawa²¹Ishikawa National College of Technology, tsubata, Japan, ²Toyohashi University of Technology, Tempaku-cho, Japan

Negative electron affinity (NEA) surfaces of O/Cs/GaAs(0 0 1) have found applications as efficient photocathodes. Metastable-induced electron spectroscopy (MIES) and Ultraviolet Photoelectron Spectroscopy (UPS) have been employed to extract top-layer electronic density of states of the Ga-rich GaAs(001)(4x2) surfaces co-adsorbed with Cs and oxygen. The quality of the GaAs surface was evaluated ex situ by X-ray photoelectron spectroscopy (XPS) and Auger electron spectroscopy (AES). The p-type GaAs(001) specimen were cleaned by repeated Ar⁺ ion sputtering followed by annealing. This surface is known to have a Ga top-layer with the (4x2) arrangement of double Ga dimers. At the saturation coverage of Cs, an MIES spectrum showed well-developed Cs 6s-induced states just below EF. Upon admission of oxygen at exposures less than 1L onto the surface, the Cs 6s intensity abruptly decreased and O 2p-induced states appeared with multiple peak structures, implying direct bonding of oxygen with substrate atoms even at an early oxygenation stage. The variation of the Cs 6s intensity as a function of oxygen exposure reflects the extent of charge outflow from these states to promote oxygen dissociation. Annealing effects on the oxygen bonding have also been measured by MIES. We found that direct charge transfer from alkali-induced states to oxygen promoting the initial oxygen uptake process depends much upon the substrate. At the Cs/GaAs(001) surface, the charge transfer occurs slowly, and oxygen atoms are incorporated into the bonding with substrate atoms.

P-Th-013

Work function studies of gold surfaces for the KATRIN experiment using a custom high vacuum Kelvin Probe

Martin Babutzka¹, Kerstin Schöning¹¹Karlsruhe Institute of Technology (KIT), Eggenstein-Leopoldshafen, Germany

The Karlsruhe Tritium Neutrino Experiment KATRIN will perform a model-independent measurement of the electron antineutrino mass. Therefore the energy spectrum of the beta electrons of a gaseous molecular tritium source will be examined. To achieve the sensitivity goal of 0.2 eV/c² (90 % CL) the potential of the tritium source plasma must be temporally and spatially stable within $\sigma < 20$ mV. This requirement applies, in particular, for the work function of the so called “Rear Wall” in the source section, because the potential of its gold-coated surface dominantly determines the plasma potential. A system based on the Kelvin Probe principle will be used to measure the spatial distribution and the temporal behavior of the Rear Wall surface. This Kelvin Probe needs a high precision to detect work function variations on the millivolt scale. In order to scan the whole surface, the samples are placed on a 2-D motorized stage and within a high vacuum system to reproduce the environmental conditions for the Rear Wall at KATRIN. Such a custom system has been designed and built up at the Tritium Laboratory Karlsruhe. In this work the requirements on and the realization of the Kelvin Probe setup are presented. Additionally the results of its commissioning as well as the results of the work function measurements of final Rear Wall candidates will be discussed.

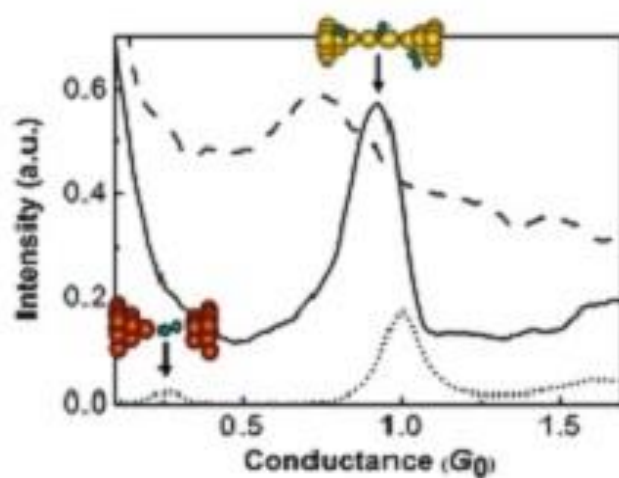
P-Th-014

Electron transport of single hydrogen molecule bridging between Au, Ag and Cu electrodes

Yu Li¹, Satoshi Kaneko¹, Manabu Kiguchi¹

¹Department of Chemistry, Tokyo Institute of Technology, Tokyo, Japan

Single molecular junctions (SMJs) have attracted wide attention as novel properties can appear due to their peculiar geometrical and electronic characters. Hydrogen SMJs have been studied as model systems of SMJs using transition metals. Although coinage metals should be used as electrodes for application, there are little studies using coinage metals due to their low reactivity toward molecules. In present study, we have studied the electron transport properties and the atomic structures of hydrogen SMJs utilizing Au, Ag, Cu. We fabricated SMJs with mechanically controllable break junction (MCBJ) technique in an ultrahigh vacuum (UHV) at 10 K. The typical conductance histograms of Au, Ag and Cu atomic contacts are shown in Fig. 1, which constructed from conductance traces during the breaking process in the presence of H₂ molecule. The prominent peaks appeared around 1 G₀ (=2e²/h), which corresponds to each metal atomic contact. While the feature was observed below 1 G₀ for Au and Ag electrodes, a prominent peak was observed around 0.3 G₀ for Cu electrodes. By measuring the dI/dV curves, we detected the vibration mode between metal and hydrogen for Au, Ag, Cu contacts, which suggested the bridging of H₂ molecule between metal electrodes. The conductance histograms and dI/dV curves indicated that hydrogen SMJs with a certain atomic configuration were preferentially formed only for Cu contacts. To study configuration of hydrogen SMJs, we investigated the length of the SMJs by plateau length. The plateau length analysis revealed that the Au and Ag form single atomic chain (SAC) but Cu does not. Since SAC has more adsorption sites than atomic contacts, the adsorption and incorporation of the H₂ molecule to SAC leads to a variety of conductance states for Au and Ag contacts.

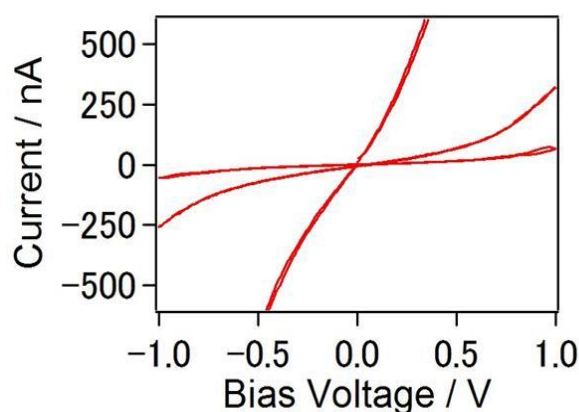


P-Th-015

Metal-Molecule Interface of the Single Molecular Junction studied with Current-Voltage Characteristics

Yuki Komoto¹, Shintaro Fujii¹, Tomofumi Tada², Manabu Kiguchi¹¹Department of Chemistry, Tokyo Institute of Technology, Tokyo, Japan,²Chemical Resources Laboratory, Tokyo Institute of Technology, Yokohama, Japan

Recently, electronic properties of single molecular junctions have been extensively investigated in the fields of the molecular electronics. However, many studies focused on conductance of the junctions at a certain bias voltage. It is necessary to measure current-voltage (I-V) characteristics toward practical application for molecular devices. The purpose of this research is to measure I-V characteristics of single molecular junctions. We characterized molecular junctions of p-benzenediamine, 1,4-butanediamine, p-benzenedithiol (BDT), and 4-aminobenzenethiol (ABT) to examine the effect of molecular backbones, anchoring groups, and molecular asymmetry on the I-V characteristics. We used scanning tunneling microscope-based break junction technique to prepare single molecular junctions. While the molecular junction was prepared, bias voltage was swept. We repeated this process and obtained over 1000 I-V curves for the single molecular junctions. We described the charge transport properties based on a single level resonant tunneling model (the Breit-Wigner model) and found good fits for statically averaged I-V characteristics to get molecular dependent energy level-alignment and electronic coupling. We observed molecular dependent I-V characteristics caused by differences of molecular backbones and anchoring groups. Figure 1 represents typical I-V curves of the BDT junctions, we found three conductance states whose zero bias conductance are 0.4, 2.4 and 30mG₀. The difference in conductance states is ascribed to preferential binding geometries of the metal-S contacts. Electronic coupling of high conductance state is 10 times larger than that of low conductance state. The difference in the conductance states is due to electronic coupling at the metal-molecule interface rather than variations in the energy level alignment within the Breit-Wigner model. For asymmetric ABT junctions, we obtained almost symmetric I-V curves against our expectation. In conclusion, we measured I-V curves of the molecular junctions. Statistical analysis of the I-V curves revealed that the difference in the conductance states is caused by binding geometries.



P-Th-016

Scattering-Energy and -Angle Landscape of the Spin-Filter Efficiency of W(001)

Dmytro Kutnyakhov¹, S Borek², J Braun², J Minàr², H Ebert², Hans-Joachim Elmers¹, G Schönhense¹

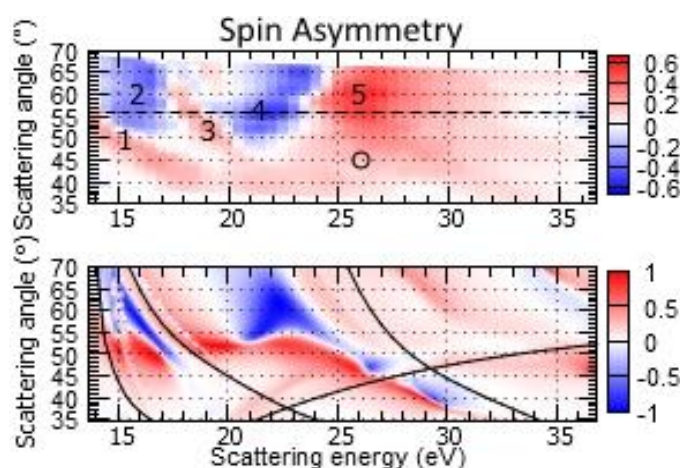
¹Institut für Physik, Johannes Gutenberg-Universität Mainz, Mainz, Germany,

²Department Chemie, Ludwig-Maximilians-Universität München, München, Germany

Extending previous work on the novel imaging spin-filter technique based on electron diffraction from W(001) in the specular (00) LEED spot [1,2] we studied the scattering energy (E) and angle of incidence (θ)-landscape of the spin sensitivity S, and reflectivity I/I_0 . The setup includes a spin-polarized GaAs electron source and a delay-line detector for spatially resolving detection. The resulting energy-angular landscapes show rather good agreement with theory (relativistic layer KKR SPLEED code [3,4]). We identify several regions of high asymmetry and figure of merit, opening a path to development of new modification of the multichannel spin-filter for electron spectroscopy and momentum microscopy with higher performance. The E- θ -landscape of the spin asymmetry for W(001) (see figure) agrees rather well with the data calculated by the relativistic layer-KKR SPLEED code. Concerning the figure of merit the W(001) results [5] are comparable with the landscapes for Ir(001) [6] and a pseudomorphic monolayer of Au on Ir(001) [7].

[1] Tusche et al., APL 99 (2011) 032505 ; [2] M. Kolbe et al., PRL 107 (2011) 207601; [3] Feder in Polarized Electrons in Surface Physics (World Scientific, 1985); [4] Ebert et al., Rep. Prog. Phys. 74 (2011) 096501 ; [5] Kutnyakhov et al., PRB 91 (2015) 014416 ; [6] Kutnyakhov et al., Ultramicroscopy 130 (2013) 63 ; [7] Kirschner et al., PRB 88 (2013) 125419.

Figure caption: E- θ -landscape of the measured (top) and calculated (bottom) spin-orbit asymmetry. Numbers 1–5 denote pronounced structures that can be identified in experiment and theory and black lines denote sharp characteristic intensity maxima in the calculation that originate from surface resonances. The circle corresponds to the working point used in [1] and [2]. Dashed line at 56 degree reveals a favorable +/- feature for switching the asymmetry by a slight variation of the scattering energy.



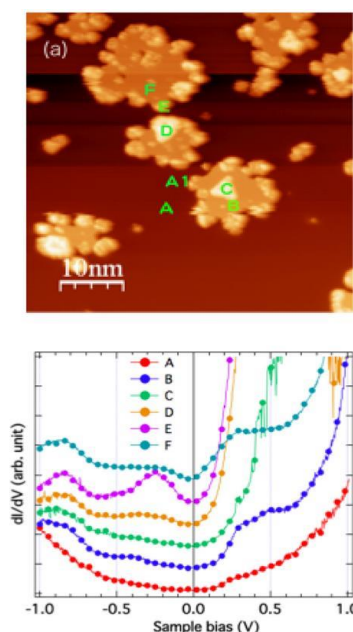
P-Th-017

Electronic and magnetic properties of Sm nanostructure

Galif Kutluk¹, M Nakatake¹, M Arita¹, M Sawada¹, H Sumida², Y Kooda², H. Namatame¹

¹Hiroshima University, Higashi-Hiroshima, Japan, ² Mazda Motor Corporation, Aki-gun, Japan

The lanthanide metal and their compounds have been a challenge to solid-state physicists for many years because of their unusual electronic, magnetic, and structural properties. Relatively small changes in a chemical environment may induce a change in the valence states of the lanthanide metal. Due to a lack of experimental data, a means of preventing the valence fluctuation of Sm by isolation from the substrate has been not fully developed. Thus, the nature of the valence transition has not been fully understood. Graphite is selected as the substrate here, since the inertness of the graphite surface may offset the sensitivity of the valence states of Sm to relatively small changes in the chemical environment, and the metallic properties of the graphite enable electron spectroscopy and microscopy experiments without the problem of surface charging. We report the structural (geometrical) and temperature dependence of valence state of Sm in the coverage range of 0.1~20Å by utilizing the PES, XMCD, STM and STS. The STM/STS would be an effective tool to minutely investigating the structural dependence of electronic structure of such sample of Sm. Since the STS is able to reveals the electronic structure in spatial resolution of a nanometer size, furthermore the STS is also able to provides an information about the empty state in the vicinity of Fermi level. Figure 1 shows STM and STS spectra recorded for the Sm coverage of 0.8Å at a temperature of 77K, The unoccupied feature is observed around 0.4eV, which seems to consist of two components of the magnetic exchange splitting, although these two components are not fully resolvable here, it is obviously not a single peak structure. Whereas, such a structure of unoccupied state has not been observable for the Sm coverage less than 0.3Å. This feature coincides with the DFT prediction of P. Strange.



P-Th-019

Electrical characteristics according to the tensile strain of stretchable substrates for soft electronics

Bock Soon Na¹, Chan Woo Park¹, Soon-Won Jung¹, Ji-Young Oh¹, Sang Seok Lee¹, Jae Bon Koo¹

¹Electronics and Telecommunications Research Institute, Daejeon, South Korea

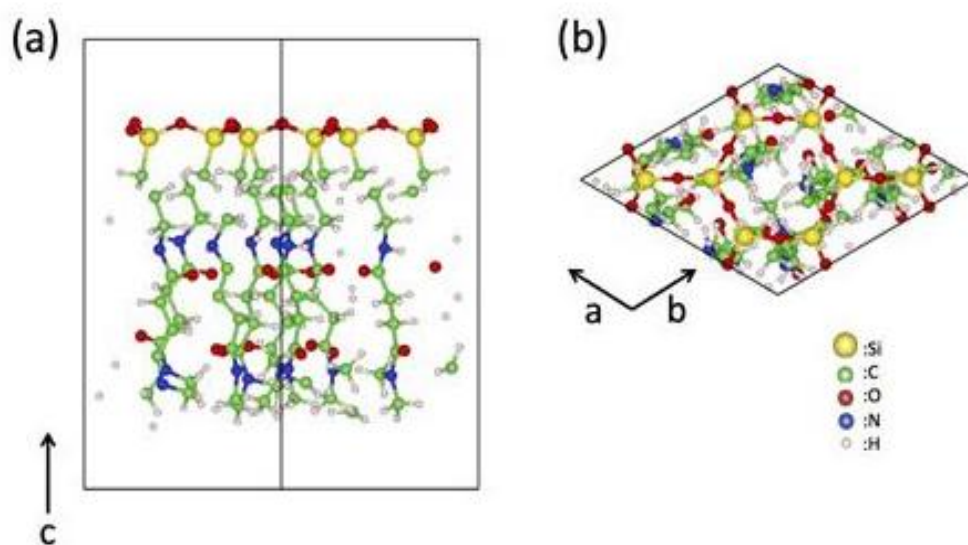
Stretchability will significantly expand the application scope of electronics, particularly display, sensors, soft and human friendly devices, and so on. The realization of stretchability in electronics is one of the most interesting challenges. As a strategy for this promising electronics that maintain proper functions under a large amount tensile strain. Here, we report a new method to fabricate stretchable substrates using a thick rigid island and thin wavy membrane of parylene, wavy interconnects which configured into a wavy silicon mold. In this process a thick rigid island of polyimide is produced by conventional photolithography on the wavy parylene and then metal was evaporated for interconnects. Within the thick rigid islands, we can locate electronic devices so that the influence of an external stress can be minimized, while most stress is absorbed by the thin wavy membrane and interconnects regions. Lastly, transferred on to a stress-free elastomeric polydimethylsiloxane (PDMS). In previous methods for stretchable substrates, a supporting elastomeric substrates is first stretched, then metal interconnects are deposited or transferred onto the pre-strained substrates. But this method is less practical because it is precisely control the structure of wavy profiles over a very large substrates area. The non-uniform distribution of pre-strain also makes it difficult to obtain high reliability. Here this stress-free wavy substrates demonstrate achievement in high reliability, good stretchability. For monitoring the variation of resistance with tensile strain, substrates were stretched on a house-made stretching stage. These were strained up to 40% their original length without compromising their functionality.

P-Th-020

Electronic Structures of a Cerasome Model

Masato Oda¹¹Wakayama University, Wakayama, Japan

Recently, drug delivery systems (DDSs) have attracted much attention. The aim of DDS is to reduce undesirable side effects of drug therapy. The construction of the DDS requires materials to capsule a drug and to release it around the diseased area. Lipid bilayer vesicles, so-called liposomes, are typical DDS materials. However, liposomes do not have enough stability because all the lipids are connected via van der Waals interactions. As a result of this low stability, liposomes cannot reach the diseased part intact. To overcome this problem cerasomes, i.e., liposomes featuring surfaces reinforced with a siloxane bond network, have been developed. It has been shown that a cerasome can capsule a drug and is much more stable than a liposome. Thus, cerasomes are promising materials for DDS. Although there are lots of research for application, basic properties of the cerasome such as microscopic structures and electronic states at its surface have not been cleared yet. The purpose of this study is to investigate the basic surface properties of a simple model of the cerasome. To model the cerasome, we approximate a spherical vesicle to a plane membrane and assume closed packing configuration. We calculate the electronic structures of the model using the first principles method based on the density functional theory. Comparing the electronic DOS of the membrane model with that of the lipid molecule, we reveal that there are mid-gap states in the membrane model that are not in the molecule. These mid-gap states are caused by antibonding states of Si-C bonds that connect the siloxane network and the organic parts of the lipid.



P-Th-021

Conductance in self-assembled terbium-silicide nanowires probed by multi-tip STM

Frederik Edler¹, Ilio Miccoli¹, Herbert Pfnür¹, Stephan Appelfeller², Mario Dähne², Christoph Tegenkamp¹

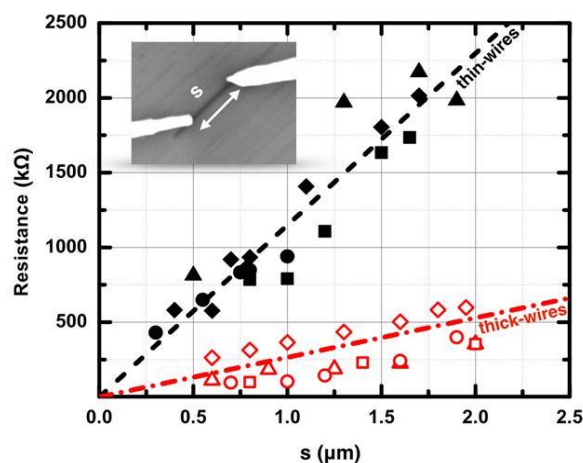
¹Institut für Festkörperphysik, Leibniz Universität Hannover, Hannover, Germany, ²Institut für Festkörperphysik, Technische Universität Berlin, Berlin, Germany

In the last three decades, metal silicide wires have played a dominant role in electronics as ohmic contacts and gate electrodes because of their extremely low-resistivity, contact-resistance and good-adhesion on Silicon (Si). However, the “ultimate” scaling of Si technology towards the sub-10nm regime makes pivotal the investigation of silicide properties down to the atomic scale, where exotic phenomena (e.g. Luttinger liquid behaviour or Peierls transitions) are often observed, while apart from that the interaction with the substrate is known to influence their conductance nature [1]. In parallel, it has become promising to look for new bottom-up approaches, such as strain-mediated self-assembly, to circumvent the current limits of lithographic techniques in producing ultra-small defect-free nanostructures. Rare-earth (RE) metal silicides are of special interest, because they can be grown in form of long (up to several microns) but extremely thin nanowires (NWs) on Si(001) substrates. The 1D growth mechanism relies on the peculiar uniaxial lattice matching of nearly all RE metals with Silicon. Structural and electronic properties for dense arrays of RE₂Si₃ NWs were reported for several materials (eg. Tb, Dy, Ho, Er, Gd, Sm and Y), however, their transport properties are seldom studied and hardly correlated with details of their atomic structure [2,3]. In this work, we have grown single and equally spaced bundles of TbSi₂ NWs on vicinal Si(001) substrates and comprehensively characterized by means of a multi-probe scanning tunnelling microscope (STM). STM and STS revealed the growth of metallic wires. Thereby, two characteristic classes of wires are formed. The analysis of their resistances as a function of probe distances at room temperature support the growth of two classes and reveal resistivities of around 500 μΩcm.

[1] Zeng et al. Nat.Mater.7 (2008) 539

[2] Qin et al. NanoLett.12 (2012) 938

[3] Inacu et.al NanoLett.13 (2013) 3684



P-Th-022

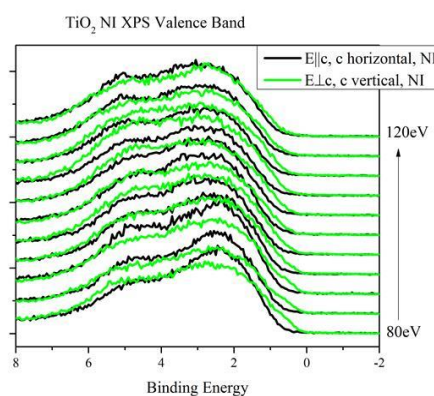
Electronic structure of rutile TiO_2 - a polarisation dependent investigation of orbital character of the bulk valence band structure

Stephen Callaghan¹, Patrick Casey¹, Alexander Generalov², Alexei Preobrajenski², Cormac McGuinness¹

¹School of Physics, Trinity College Dublin, College Green, Dublin 2, Ireland, Dublin, Ireland, ²MAX IV, Lund University, Lund, Sweden

Synchrotron-radiation based photoelectron spectroscopy investigations of the bulk valence band structure of rutile $\text{TiO}_2(100)$ single crystals are presented. In the rutile tetragonal unit cell the metal cation is coordinated octahedrally (MA_6) (with a tetragonal distortion), while the oxygen anion has planar trigonal coordination (M_3A). All M_3A planes share the c-axis but successive M_3A planes are rotated by 90° about the c-axis, giving a net four-fold symmetry about $[001]$. Due to M_3A coordination, sp^2 hybridization of the central anion gives rise to three σ -like M-A bonds derived from anion p_x and p_z atomic orbital projections and one π -like M-A bond from p_y perpendicular to the M_3A plane. The anisotropic spatial orientation of these bonds and their differing orbital character gives an anisotropic charge density with a uniaxial symmetry along the c-axis. Polarization-dependent electronic and optical responses measurable via optical spectroscopy and x-ray absorption spectroscopy measure a resulting natural linear dichroism which also manifests in photoemission. Synchrotron-radiation based photoemission spectroscopies were performed on single crystals of $\text{TiO}_2(100)$ at beamline D1011 at MAXlab. Photon energy dependent soft x-ray valence band photoemission spectroscopy is used in various angle-resolved photoemission geometries to probe the detailed specific orbital character of the rutile TiO_2 occupied electronic bulk bandstructure, where for the first time in rutile [1] the anisotropic bonding and consequent linear dichroism in photon based spectroscopies that result is exploited in order to elicit the orbital character of valence band states through polarization-dependent photoemission with respect to the rutile c-axis (fig1). Polarization dependent normal emission and normal incident geometries, the latter to maximise the contrast in the photoemission matrix elements, were measured and all exhibiting substantial linear dichroism throughout the valence band at differing photon energies as the bulk electronic structure is probed. These measurements are compared with theoretical electronic band structure calculated via density functional theory.

[1] For anatase see Emori et al, Phys.Rev.B 85, 035129 (2012)



P-Th-023

Unexpected spectral properties in the band structure of a two dimensional layered dichalcogenide: 1T-TiS₂

Miguel Angel Valbuena¹, Stephane Pons¹, S. Conejeros², P. Alemany², Enric Canadell³, E. Frantzeskakis⁴, J. Avila⁴, Maria Carmen Asensio⁴, H. Berger¹, Marco Grioni¹

¹Institute of Condensed Matter Physics (ICMP), Ecole Polytechnique Fédérale de Lausanne (EPFL), Lausanne, Switzerland, ²Departament de Química Física and Institut de Química Teòrica i Computacional (IQTCUB), Universitat de Barcelona, Barcelona, Spain, ³Institut de Ciència de Materials de Barcelona (ICMAB-CSIC), Bellaterra (Barcelona), Spain, ⁴Synchrotron SOLEIL, L'Orme des Merisiers, Gif sur Yvette, France

Two dimensional transition metal layered dichalcogenides (TMDC) have been subject of study over decades because of their low dimensional character and the electronic instabilities and phase transitions they exhibit at low temperatures. They continue to be still a focus of interest because of their exceptional variety of ground states and competing phases. 1T-TiS₂ is a two dimensional bad metal, or semiconducting system with an indirect band gap, whose transport properties are derived from carriers coming from a very few populated Ti 3d band located at M points. In contrast with the widely studied isostructural 1T-TiSe₂ compound which develops a 2x2 Charge Density Wave (CDW) transition related to the formation of an exciton condensate phase, there is a lack of recent studies on 1T-TiS₂ system, where a priori not electronic instabilities and phases transitions were predicted and reported. In this contribution we present a comprehensive study of the electronic structure of 1T-TiS₂ system by Angle Resolved Photoemission Spectroscopy (ARPES) and Density Functional Theory (DFT) calculations. Our experimental results reveal a series of new and unique unexpected spectral features that opens a new scenario of different competing phases in this material: Low energy electronic correlations, CDW fluctuations or even the formation of a two dimensional high mobility electron gas are invoked to take into account the exceptional electronic band structure of this material.

P-Th-024

Electronic properties of interfacial region in Polyethylene-MgO nanocomposite

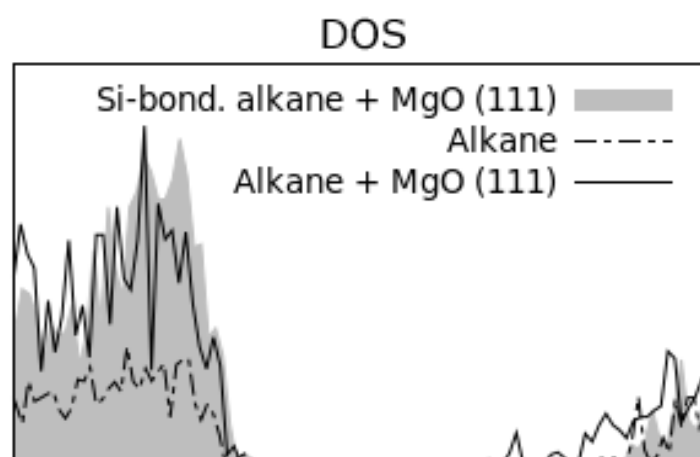
Elena Kubyshkina¹, Lars Jonsson¹

¹KTH Royal Institute of Technology, Stockholm, Sweden

Nanocomposite materials are expected to become a new generation of materials in a variety of applications. We focus here on polyethylene-MgO nanocomposite. The polyethylene-MgO nanocomposite is a promising material for high voltage electrical insulation. It has been reported to have superior to the pure polyethylene properties such as reduced space charge formation, higher partial discharge resistance and decreased conductivity. [1] As a step towards understanding the influence of nano-sized particles on the electrical properties of nanocomposites, we model an interfacial region in MgO-polyethylene nanocomposite. We exploit density functional theory to calculate densities of states of several possible interface configurations: MgO (100) and hydroxylated MgO (111) surfaces in the presence of alkane chains $C_{12}H_{26}$ representing polyethylene, and MgO (111) surface chemically bonded to an alkane chain with a silicon atom. The considered systems are modeled as double-layered two-dimensional periodic structures. The hybrid functional HSE06 [2] is used for the study. We report here a high impact of silicon coverage of MgO (111) surface on the electronic structure of the interface. Pure hydroxylated MgO (111) surface exhibits a big amount of trap states in the band gap region. The study shows that these states are completely removed in the case when $C_{12}H_{26}$ is bonded to the surface through a silicon atom. When there is no chemical bond between the alkane and hydroxylated MgO (111) the trap states are not changed. In case of MgO (100)- $C_{12}H_{26}$ interface the trap states are reduced, but still present.

[1] "Nanodielectrics: A panacea for solving all electrical insulation problems?", Solid Dielectrics (ICSD), 2010 10th IEEE Int. Conf. on, (2010).

[2] Krukau, Aliaksandr V. et al., "Influence of the exchange screening parameter on the performance of screened hybrid functionals", J. Chem. Phys. 125, 224106 (2006).



P-Th-026

Structural and electronic properties of GdAg₂ and GdAu₂ surface alloys

Alexander Correa Aristizabal^{1,2}, Bin Xu^{3,4,5}, Matthieu Verstraete^{3,4}, Lucia Vitali^{2,6}

¹Donostia International Physics Center (DIPC), Donostia, Spain, ²Departamento de física de materiales, Universidad del País Vasco EHU/UPV, San Sebastian, Spain, ³Département de Physique, Université de Liège, Sart Tilman, Belgium,

⁴European Theoretical Spectroscopy Facility (<http://www.etsf.eu>), San Sebastian, Spain, ⁵Department of Physics and Institute for Nanoscience and Engineering, University of Arkansas, Fayetteville, Arkansas, ⁶Ikerbasque Foundation for Science, Bilbao, Spain

We report here on the synthesis and electronic characterization of two ferromagnetic alloy layers, namely GdAg₂ and GdAu₂. These form on the surface of Ag(111) and Au(111) exposed at high temperature to the physical vapor of gadolinium atoms. Due to lattice incommensurability with the supporting substrates their growth leads to the formation of Moiré patterns [1, 2]. By means of a scanning tunneling microscope we have locally investigated the structural and electronic properties of these two alloy layers. In particular, we have measured the density of states close to the Fermi level at two different temperatures, 4K and 77K i.e. well below and above the ferromagnetic transition temperature of these layers [1]. Density functional theory calculations have been performed to predict the electronic properties of these alloys as their band structure, work functions and spin-orbit coupling strengths. We will explain the difference in the electronic properties between the two alloys and the observed temperature effects in terms of in-layer coupling strength in the alloys and their hybridization with the underlying Ag and Au substrates.

[1] L.Fernandez, M.Blanco Rey, M.Llyn, L.Vitali, A.Magaña, A.Correa, P.Ohresser, J.E.Ortega, A.Ayuela, F.Schiller, Nano Letters, 14, 2977 (2014)

[2] A.Correa, PhD thesis, San Sebastian 2015

P-Th-027

Ultrafast Electron Spin Dynamics at the Fermi Level in Fe_3O_4 Thin films

Cephise Cacho¹, Christine Richter², Marco Battiato³, Jean-Michel Mariot⁴,
Olivier Heckmann², Hubert Ebert⁶, Jan Minar⁶, Fulvio Parmigiani⁵, Karol
Hricovini²

¹Central Laser Facility, STFC, Rutherford Appleton Laboratory, Harwell, Oxford, United Kingdom, ²Univeristé de Cerg-Pontoise, Cergy-Pontoise, France,

³Institute of Solid State Physics, Vienna University of Technology, Vienna, Austria, ⁴Laboratoire de Chimie Physique–Matière et Rayonnement, Univ. Paris 6/CNRS, Paris, France, ⁵CNR, Laboratorio TASC INFM, Trieste, Italy, ⁶Ludwig Maximilians Universität, Germany

Magnetite, Fe_3O_4 (FO), belongs to the family of half-metals characterized by an insulating gap for one spin state resulting in a fully spin-polarised transport at the Fermi level, which attracts a high interest for spintronic devices. In spite of intensive theoretical and experimental studies, the magnetic and electronic properties of FO remain controversial. We studied the demagnetisation process in FO by spin- and time-resolved pump-probe photoemission experiments using the third harmonic (4.65 eV) of Ti-Sapphire laser with a repetition rate of 250 kHz. For the maximum of the photoexcitation we observe a clear reduction of the spin polarisation in a region of ~ 200 meV around the Fermi level. At higher binding energy no variation is observed up to a 1000 fs delay indicating that the spin polarisation reduction observed comes from the electron dynamics and not from the demagnetization. The Boltzmann equation for out-of-equilibrium dynamics combined with the calculated spin-resolved electronic density-of-states fully describes the decay of the excited electrons as well as the variation of the spin polarisation.

P-Th-028

Potential-dependent adsorption states of aromatic thiol molecules at liquid-Au interface studied by surface reflectance spectroscopy

Ippei Sakurada¹, Masatoshi Tanaka¹, Shinya Ohno¹

¹Yokohama Nat'l Univ., Yokohama, Japan

Function of biomolecules on solid surface in electrolyte solutions should be investigated in terms of electronic states for the development of biosensors, bioelectronics devices and so on. The molecules immobilized by such as Au-S bonding on an electrode are subject to high electric field in an electric double layer. Therefore, how the molecules are affected by an applied potential is an important problem. To elucidate the effect on functional groups of biomolecules, it is a good way to examine the behavior of aromatic thiol molecules immobilized on the electrode by optical methods. In this study, potential-dependent adsorption states of thiophenol, 4-mercaptobenzoic acid (4-MBA), and 4-aminothiophenol (4-ATP) molecules on Au-films in electrolyte solution have been investigated mainly by means of surface differential reflectance spectroscopy (SDRS) and cyclic voltammetry (CV). SDRS is defined as $\Delta R/R(V) = (R(V) - R(0))/R(0)$, where $R(V)$ is the reflectance at applied potential V . SDRS is sensitive to the optical transitions with transition moments perpendicular to the surface. Neither oxidation nor reduction was found in the range of the applied potential in CV measurements. In SDR spectra of thiophenol/Au-film, a negative peak around 4.1 eV is observed at negative potential. This peak is caused by the reductive desorption of thiophenol molecules from Au-film. In SDR spectra of 4-MBA/Au-film, the potential-dependent structures are observed around 3.5, 4.25, 4.7 eV. The sign of the peak is positive at positive potential, and vice versa. This feature is interpreted to reflect the potential-dependent inclination of the molecule, probably caused by the interaction between carboxylate ion of the molecule and the Au surface. Similar effect is expected for 4-ATP/Au-film, however, potential dependence of SDR spectra is less prominent.

This work has been supported by JSPS Grant-in-Aid for Scientific Research (B) Number 25286016.

P-Th-029

Structural Dynamics Study of Hydration Shells in Aqueous Solution with Electrochemical Control

Fang Niu¹, Andreas Erbe¹

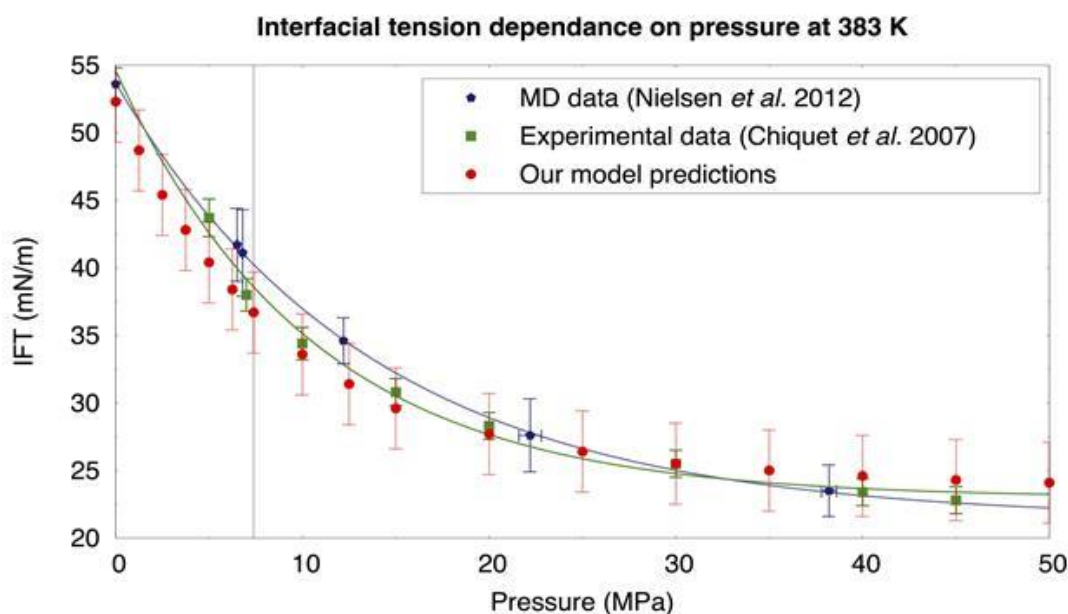
¹Max-Planck-Institut für Eisenforschung GmbH, Düsseldorf, Germany

Structural changes of the hydration shell of surfaces formed in aqueous solutions are essential to many chemical and biological phenomena. Infrared spectroscopy is a powerful tool to investigate the hydration shells, via their vibrational modes, and to further analyze water dynamics at an interface. Here, we present a study using electrochemical attenuated total reflection spectroscopy, of the vibrational spectra of water under different electrode potentials and consequently different states of the solid/liquid interface. In acidic solution, germanium undergoes a transition from a hydrophilic to a hydrophobic, H-terminated surface when polarized at sufficiently negative potentials. Appearance and growth of OH stretching modes with electrode potential are observed for Ge(100) surfaces, which can be interpreted as related to changes in the hydrogen-bonding pattern at the interface. Further results are presented for saline electrolyte with different hydrogen ion concentration, which show clearly a pH-dependent transition of the crucial surface termination change.

P-Th-030

Predicting CO₂-H₂O interfacial tension using COSMO-RSAlessandro Silvestri¹, Martin P Andersson¹, Susan L S Stipp¹¹Nano-Science Center, Department of Chemistry, University of Copenhagen, Copenhagen, Denmark

Knowledge of the interaction between pore fluids and mineral surfaces, and the interfacial tension (IFT) that results, is of importance for predicting the behaviour of rock formations during and after CO₂ geological storage. The interfacial tension controls the capillary forces that hold either the supercritical CO₂ or the water with dissolved CO₂ in the pores and that move them through the pore throats. Molecular modelling is a valuable tool to complement experimental IFT determination and it can help us interpret results and gain insight under conditions where experiments are difficult to perform. Here, we report predictions for CO₂-water interfacial tension performed using density functional theory (DFT) calculations combined with the COSMO-RS implicit solvent model. We predicted the IFT dependence as a function of pressure (0-50 MPa) and temperature (273-383 K). The CO₂-water IFT values determined by the model agree well with experimental and molecular dynamics (MD) results (see the attached figure). The results of this study suggest that our model can be used as a fast alternative to time consuming computational approaches in the prediction of the CO₂-water IFT over a range of temperatures and pressures relevant for CO₂ geological storage.



P-Th-031

Structure of a Core-Shell Type Colloid Nanoparticle in Aqueous Solution Studied by XPS from a Liquid Microjet

Giorgia Olivieri¹, Alok Goel¹, Matthew Brown¹

¹Laboratory for Surface Science and Technology, Department of Materials, ETH Zürich, Zurich, Switzerland

With the developments of near ambient pressure photoemission (NAPP) and the liquid microjet, X-ray photoelectron spectroscopy (XPS) measurements at the liquid-nanoparticle interface are now possible. This significant advance allows soft matter physicists working in the field of colloid nanoscience the opportunity to perform surface science experiments long deemed impossible. Recently, we have used XPS in conjunction with a liquid microjet to study the electronic and geometric structures of a 12 nm core-shell type nanoparticle (NP), $\text{Al}_x\text{O}_y@\text{SiO}_2$, suspended in aqueous solution. At pH lower than ~ 4 , electrophoretic mobility measurements (zeta potential) suggest that the NPs are positively charged. The Al 2p spectrum is consistent with two unique electronic structures that we assign to neutral sites $>\text{Al}-\text{OH}$ at higher kinetic energy (KE) and to protonated species $>\text{Al}-\text{OH}_2^+$ at lower KE. We discuss the origin of this shift in terms of electrostatic effects. As we move towards the ability to follow a chemical reaction at the liquid-NP interface with XPS the natural next step, after having characterized the NP in aqueous solution, is to follow the adsorption of a simple molecule on the NPs surface. This has been achieved by adding varying concentrations of formic acid (HCOOH) into the solution. The C 1s spectrum shows the presence of two components, formic acid and formate (HCOO^-), the latter of which is adsorbed to the NPs surface. A corresponding change in the Al 2p region occurs with adsorption: there is a significant increase in the low KE species that we assign to $>\text{Al}-\text{OOCH}$. We discuss the limitations of this new technique to follow chemical reactions and postulate potential new directions for the field.

P-Th-032

The antibacterial effect of TiO₂ coatings deposited by open air atmospheric pressure plasma jet with a TTIB sol precursor on surgical stainless steel.

Christin Rapp¹, Alexander Knospe², Christian Buske², Erich Wintermantel¹

¹Technische Universität München, Garching, Germany, ²Plasmatreat GmbH, Steinhagen, Germany

Microorganisms in hospitals are becoming an increasing problem and especially surfaces are a breeding ground for them. Due to the photocatalytic effect of titanium dioxide (TiO₂) it is an often suggested material for antibacterial surface coatings. The use of an open air atmospheric pressure plasma jet (APPJ) offers a simple and variable method to deposit TiO₂ coatings. The coatings were deposited in three different ways: (i) by spraying the liquid precursor into the plasma flame, (ii) by applying the precursor on the surface and (iii) treating it subsequently with plasma and by evaporating and discharging the precursor directly into the plasma flame. Efficiency of all coatings was tested by the degradation of Rhodamine B and by bacterial tests with *Escherichia coli*. To evaluate the structure and the chemical properties X-ray Diffraction (XRD), X-ray Photoelectron Spectroscopy (XPS), Fourier Transform Infrared Spectroscopy (FT-IR), Scanning Electron Microscopy (SEM), and Contact Angle Measurements were performed. The layers are in an excited state immediately after the coating, indicated by very low water contact angles (CA) and almost constant angles with diiodmethane resulting in high surface energy, with a large polar fraction. Over time the water CA increases, when the layer is stored in the dark, suggesting that the excitation of the surface fades with time. The antibacterial effect here is present with visible light. It was determined, that the antibacterial effect of the sprayed and applied coatings is more pronounced than the one with the evaporated coating. However, the evaporated coatings showed a very thin and excited titanium dioxide layer compared to the applied one where the surface is much rougher. According to the results the sprayed and the evaporated coatings are very promising for use as medical surfaces.



P-Th-034

Band energy alignment studies at heterojunction by X-ray photoelectron spectroscopy (XPS)

Jisheng Pan¹

¹Institute of Materials Research and Engineering, Singapore, Singapore

The performance of any type of hetero-junction device is determined by two kinds of interface parameters: the band discontinuities and the built-in potential. Therefore, determining heterojunction band offsets and tuning them to a desired application would have an obvious impact on the optimization of the devices. Many techniques such as electrical and optical techniques as well as photoemission spectroscopy (PES) have been developed to determine the interfaces and to understand the microscopic origin of the interface properties. PES is more widely used technique to study band alignment of heterojunction, probably due to its capability to simultaneously detect interface chemical and electronic properties which can be exploited for fully understanding of distinct correlations between the thin film material characteristics and device performance. In one of PES methods, the valence band offset (VBO) of interface is determined by combination of core level and valence band spectra. The conduction-band offset (CBO) is then deduced from VBO and suitable reference gap values of two materials at interface. However, the determination of band alignment in this way requires careful consideration of many possible effects. In this paper, we have studied the effects of chemical shift, differential charging, band bending and photoemission final state on the determination of heterojunction band offsets using this method. The method has been applied to determinate energy-band alignments of molybdenum disulphide (MoS_2) monolayer on high-k dielectric oxides. The VBO at monolayer $\text{MoS}_2/\text{Al}_2\text{O}_3$ (ZrO_2) interface was measured to be 3.31 eV (2.76 eV), while the CBO was 3.56 eV (1.22 eV). For bulk $\text{MoS}_2/\text{Al}_2\text{O}_3$ interface, both VBO and CBO increase by 0.3 eV, due to the upwards shift of Mo 4d_{z²} band. The symmetric change of VBO and CBO implies Fermi level pinning by interfacial states. Our finding ensures the practical application of both p-type and n-type MoS_2 based complementary metal-oxide semiconductor.

P-Th-035

Polarity of polar and semipolar GaN by X-ray photoelectron diffraction

O. Romanyuk¹, S. Fernández-Garrido², P. Jiricek¹, I. Bartos¹, L. Geelhaar², O. Brandt², T. Paskova³

¹Institute of Physics, Academy of Sciences of the Czech Republic, Prague, Czech Republic, ²Paul-Drude-Institut für Festkörperelektronik, Berlin, Germany,

³Department of Electrical and Computer Engineering, North Carolina State University, Raleigh, USA

The polarity is an inherent property of wurtzite nitrides and is well known to have a detrimental effect on optoelectronic devices due to associated piezoelectric and spontaneous polarization fields. As the conventional X-ray diffraction (XRD) does not provide the information about polarity, different alternative methods have been developed for assessment of the polarity of the grown structures. For polar GaN, several destructive methods have been established. For the semipolar GaN, however, polarity determination methods have not well established yet. A fast and non-destructive method based on X-ray photoelectron diffraction (XPD), providing a local crystallography, has recently been developed and tested on free-standing GaN crystals [1] and GaN nanowires [2]. Method, based on simple geometrical considerations, utilizes a polar angle dependence of emitted photoelectrons excited by MgK α radiation from the anions' core-levels. Intensity distribution from the selected azimuths of GaN lattice allows polarity determination for polar GaN{0001} as well as for semipolar {10-11}, {20-21}, and {11-22} crystals [3]. By employing comparative analysis of the measured polar angle dependences of N 1s intensities with that of free-standing GaN epilayers the polarity of polar and semipolar GaN epitaxial films and nanostructures grown on foreign substrates can be accurately determined.

Support by the Academy of Sciences of the Czech Republic (project no. M100101201) is highly appreciated. T. Paskova acknowledges the support by NSF (No. DMR-1207075).

[1] O. Romanyuk, P. Jiříček, T. Paskova, I. Bieloshapka, and I. Bartoš, Appl. Phys. Letts. 103, 091601 (2013).

[2] O. Romanyuk, S. Fernández-Garrido, P. Jiříček, I. Bartoš, L. Geelhaar, O. Brandt, and T. Paskova, Appl. Phys. Lett. 106, 021602 (2015)

[3] O. Romanyuk, P. Jiříček, T. Paskova, and I. Bartoš, J. Appl. Phys. 116, 104909 (2014).

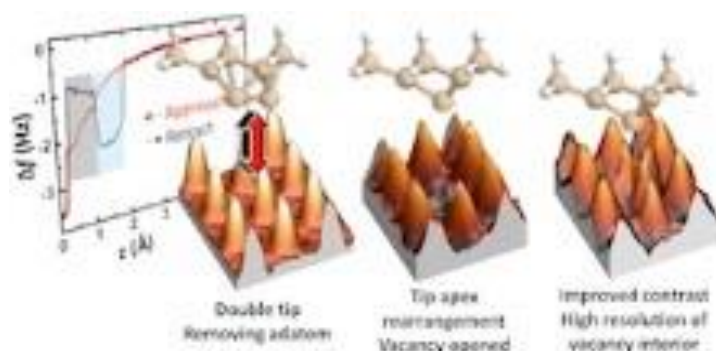
P-Th-036

Force-driven single-atom manipulation on a low-reactive Si surface for tip sharpening and resolving of subsurface dangling bonds

Jan Berger^{1,2}, Evan Spadafora¹, Pingo Mutombo¹, Pavel Jelínek^{1,3}, Martin Švec¹

¹Academy of Sciences of Czech republic, Prague, Czech Republic, ²Czech Technical University in Prague, Prague, Czech Republic, ³Graduate School of Engineering, Osaka University, Osaka, Japan

Atomic manipulation of the delta-doped B:Si(111)-($\sqrt{3}\times\sqrt{3}$)R30° surface was carried out using the Kolibri sensor based low temperature nc-AFM. To create a vacancy, a Si adatom was removed via a controlled vertical displacement of the probe. We succeeded to close the vacancy site by precisely placing a Si atom back, thus demonstrating that this process is completely reversible. During the manipulations, the rearrangement of atoms at the tip apex occurs, leading to a sharpening of the tip. This enables us to look deeper inside the vacancy. It appeared that the removal of a Si adatom exposes subsurface Si dangling bond (DB) triplets, surrounding the B dopant in the first bilayer. DFT calculations reproduced nicely the experimental results and suggest that the tip is likely terminated by two Si atoms at the apex. Moreover, it is shown that the closing of the vacancy was possible only when atomic manipulation was performed with the tip placed off-center the vacancy site.



P-Th-037

Initial growth of Ba on Ge(001) - a DFT study

Agnieszka Puchalska¹, Wojciech Koczorowski², Marian Wojciech Radny^{2,3},
Leszek Jurczyszyn¹

¹Institute of Experimental Physics, University of Wrocław, Wrocław, Poland, Wrocław, Poland, ²Institute of Physics, Poznań University of Technology, Poznań, Poland, Poznań, Poland, ³School of Mathematical and Physical Sciences, University of Newcastle, Australia, Newcastle, Australia

An ordered alkaline earth submonolayer on a clean Si(001) surface provides a template for growth of the atomically sharp, crystalline Si-oxide interface that is ubiquitous in the semiconductor-based electronic industry. It has been suggested that submonolayers of Sr or Ba on Ge(001) could play a similar role as on structurally identical Si(001), overcoming known limitations of the Ge(001) substrate such as amorphization of its oxidation layers. We have performed ab-initio DFT, plane-waves, pseudopotential computational studies on the low coverage adsorption and aggregation of Ba on the Ge(001) substrate. Several important conclusions have emerged from these calculations. For small concentrations [below 1 mono-layer (ML)] of Ba adatoms on Ge(001) the formation of a pair Ba adatoms (dimer) at a bridge site between two adjacent germanium dimer rows is clearly preferred. These pairs form a chain-like structure on the surface that run across the Ge dimer rows and is also thermodynamically the most stable Ba adatom configuration. The obtained results are compared with newly collected the experimental (atomic resolution scanning tunneling microscopy) data. Our results are crucial for understanding the on-top Ba adsorption on clean Ge(001) which is believed to be an initial step in the formation of the Ba based passivation layer on the Ge(001) substrate.

LJ, MWR and WK acknowledge NCN for support (Project N-N202-195840).

P-Th-038

Stability and Electronic band structure of SnSi Nanocrystals in a Si Matrix

Andrey Klavsyuk¹, Denis Nagayuk¹, Alexander Saletsky¹, Alexander Tonkikh², Nikolai Zakharov², Peter Werner²

¹Faculty of Physics, Moscow State University, Moscow, Russian Federation,

²Max Planck Institute of Microstructure Physics, Halle(Saale), Germany

Semiconductor alloys have been extensively used for engineering material properties through tuning the alloy composition. The SnSi and SnGe systems are characterized by the existence of cubic and tetragonal phases of Si and Sn, respectively; and a low mutual solubility in the solid phase. For example, SnGe has attracted considerable attention owing to the indirect-direct band gap crossover in the Ge-rich GeSn alloys [1, 2], which has recently resulted in demonstration of lasing from GeSn alloys metamorphically grown on Si [3]. A zinc blende crystallographic structure of SnSi nanocrystals generated by molecular beam epitaxy is observed by electron microscopy techniques in a Si matrix. Our ab initio modeling demonstrates that the strain in precipitates caused by a matrix is an important criterion for the arrangement of Si and Sn atoms in the zinc blende phase in the nanocrystals. The compressive strain in these nanocrystals makes it energetically preferable for Sn atoms to have Si atoms as first neighbors in the cubic lattice. Consequently, the zinc blende lattice possesses the lowest formation enthalpy among all other compositions of disordered $\text{Sn}_x\text{Si}_{1-x}$ alloys. Our first-principles calculations have shown strong dependence of electronic band structure of $\text{Sn}_{0.5}\text{Si}_{0.5}$ nanocrystals of the lattice parameter.

This work was supported by the Russian Foundation of Basic Researches (grant RFBR 15-32-20560).

- [1] J. D. Gallagher, C. Xu, L. Jiang, J. Kouvetakis, J. Menendez, Appl. Phys. Lett. 103, 202104 (2013).
- [2] A.A. Tonkikh, C. Eisenschmidt, V.G. Talalaev, N.D. Zakharov, J. Schilling, G. Schmidt, P. Werner, Appl. Phys. Lett. 103, 032106 (2013).
- [3] Wirths, S.; Geiger, R.; von den Driesch, N.; Mussler, G.; Stoica, T.; Mantl, S.; Ikonik, Z.; Luysberg, M.; Chiussi, S.; Hartmann, J. M.; Sigg, H.; Faist, J.; Buca, D.; Grützmacher, D. Nat. Photonics 9, 88–92 (2015).

P-Th-039

Atomic structure of Ir nanowires on Ge(001)

Nikolay Kabanov¹, Alexander Saletsky¹, Andrey Klavsyuk¹¹Faculty of Physics, Moscow State University, Moscow, Russian Federation

A new approach to the creation of integrated circuit, combining metal nanowires and structures on the silicon surface shows opportunity for a new generation of fast and reliable electronic and photonic devices [1]. Since the conventional lithographic techniques have reached their limits, the most promising is the creation of such structures as a result of self-organization. Recent works [2-5] have shown that deposition of 4d, 5d-transition metals on Ge(001) leads to formation of atomic wires up to a few micrometers. Atomic structure of the nanowires on the surface of Ir/Ge(001) formed as a result of self-organization, has been studied using a scanning tunneling microscope (STM) and ab initio calculations. It was found that the nanowires consist of Ir dimers, which are oriented perpendicular to surface. Based on the STM images several models of the Ir nanowires on the surface of the Ge (001) have been proposed and then by performing ab initio calculations we have determined wire and surface structure.

This work was supported by the Russian Foundation of Basic Researches (grant RFBR 15-32-20560)

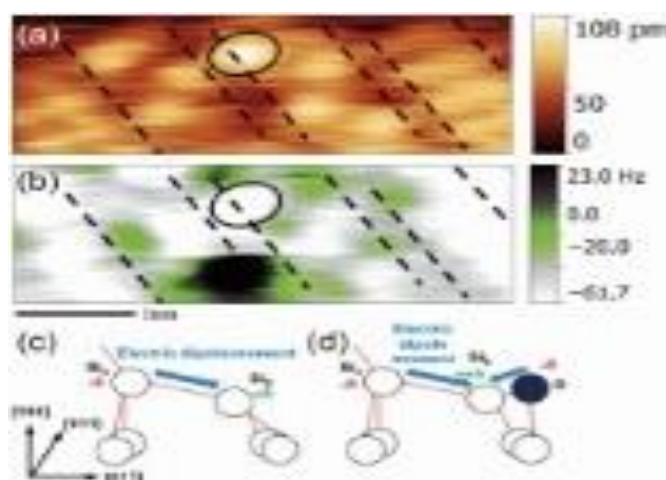
- [1] Tijs F. Mocking, Pantelis Bampoulis, Nuri Oncel, Bene Poelsema & Harold J.W. Zandvliet, Nature Communications 4, 2387 (2013).
- [2] D. E. P. Vanpoucke and G. Brocks, Phys. Rev. B 81, 085410 (2010).
- [3] A. van Houselt, T. Gnielka, J. M. A. de Brugh, N. Oncel, D. Kockmann, R. Heid, K.-P. Bohnen, B. Poelsema, and H. J. Zandvliet, Surface Science 602, 1731 (2008).
- [4] D. E. P. Vanpoucke and G. Brocks, Phys. Rev. B 77, 241308 (2008).
- [5] A. A. Stekolnikov, F. Bechstedt, M. Wisniewski, J. Schafer, and R. Claessen, Phys. Rev. Lett. 100, 196101 (2008).

P-Th-040

Non-contact scanning nonlinear dielectric microscopy study of oxygen-adsorption on a Si(100)-(2x1) surface

Kohei Yamasue¹, Masataka Suzuki¹, Yasuo Cho¹¹Tohoku University, Sendai, Japan

The oxidation of a Si(100) surface is important, because modern electronic devices are typically fabricated on the Si(100) surface. In this study, noncontact scanning nonlinear dielectric microscopy (NC-SNDM) is used to investigate an initial oxidation of a Si(100)-(2x1) surface. We simultaneously imaged topography and electric dipole moment distribution of the surface in an atomic-scale. In our experiment, we partially oxidized a clean Si(100)-(2x1) surface by exposing it to oxygen gas at room temperature in ultrahigh vacuum. Figure 1 [Suzuki et al. (submitted)] shows (a) topography and (b) dipole moment distribution of the surface after oxygen-exposure. In the topography, zig-zag patterns are observed along the dimer rows, in which the dimers were alternately buckled probably due to a non-local action of oxygen-adsorption. The dimers had negative dipole moments oriented from surface to bulk. These negative moments are explained by charge transfer between the dimer atoms. As illustrated in Fig. 1(c), a dipole moment exists in a dimer and the moment is oriented from negatively charged upper atom (Si α) to positively charged lower atom (Si β). The normal component of the moment is detectable by NC-SNDM. Among the buckled dimers, we found that the upper dimer atom circled in Figs. 1(a) and 1(b) protruded about 0.2 Å from the other upper atoms. According to the previous study by Uchiyama and Tsukada, as illustrated in Fig. 1(d), the protrusion of Si α results from the insertion of an oxygen atom into a back-bond of Si β and the inserted oxygen atom also protrudes relative to Si β . The observed negative dipole on the circled atom is explained by the difference in electronegativity of silicon and oxygen atoms. Since an oxygen atom has higher electronegativity, the oxygen atom deprives electrons from Si β . Thus, the normal component of the dipole moment remains totally negative, which explains our experimental result.



P-Th-041

Investigation of MOVPE-prepared GaP(111)B by surface analytics and ab initio DFT calculations

Peter Kleinschmidt¹, Pingo Mutombo², Oleksandr Romanyuk², Marcel Himmerlich³, Theresa Berthold³, Weihong Zhao¹, Andreas Nägelein¹, Matthias Steidl¹, Agnieszka Paszuk¹, Sebastian Brückner¹, Oliver Supplie¹, Stefan Krischok³, Thomas Hannappel¹

¹Photovoltaics Group, Institute of Physics, TU Ilmenau, Ilmenau, Germany,

²Institute of Physics, Academy of Sciences of the Czech Republic, Prague, Czech Republic, ³Technical Physics I, Institute of Physics and Institute of Micro- and Nanotechnologies, TU Ilmenau, Ilmenau, Germany

Aiming at nanowire-based optoelectronic devices we have investigated suitable semiconductor growth substrates. Typically, for subsequent III-V nanowire growth using the vapor-liquid-solid approach, III-V crystals, or (to reduce cost) III-V-on-Si substrates are employed. However, due to surface energetics, B-type polarity III-V substrate material (i.e. the (-1-1-1) face) is required. Our approach is to prepare GaP(111)B crystals or GaP/Si(111) heterofilms [1] for subsequent nanowire growth. It is well-known that the surfaces resulting from MOVPE processing can exhibit entirely different surface reconstructions compared to ones prepared in UHV [2]. For this purpose, we have studied the MOVPE-prepared GaP(111)B surface by STM, XPS, UPS and LEED, accessible via a dedicated, contamination-free MOVPE-to-UHV transfer. Experimental studies were supported by ab initio calculations based on density functional theory (DFT). While our measured LEED patterns exhibited only integer order diffraction spots (in contrast to the complex LEED patterns reported for GaP(111)B crystals annealed in UHV [3]), our STM measurements of MOVPE-prepared GaP(111)B revealed an atomically flat surface with locally ordered domains of ($\sqrt{3} \times \sqrt{3}$) and c(4x2) reconstructions, and bright protrusions which were identified as trimers with specific orientation. With higher annealing temperature at the end of the MOVPE process, the number of trimers in the STM images is reduced, while XPS shows an increasing Ga content at the surface. Ab initio DFT predicts stable (2x2) or c(4x2) structures. Under extremely Ga-rich conditions, a Ga-terminated ($\sqrt{3} \times \sqrt{3}$) surface is found to be stable. Valence band structures of P-rich and Ga-rich surfaces were measured by UPS and correlated with the total density of states resulting from the stable structure models.

[1] A. Paszuk et al., Appl. Phys. Lett. (2015), accepted.

[2] P. Kleinschmidt et al., Physical Review B 83 (2011), 155316.

[3] K. Hattori et al., Surface Science 525 (2003), 57.

P-Th-042

Superhard nanocomposite AlO_x / TiAlSiCN coatings with high thermal stability and oxidation resistance

Konstantin Kuptsov¹, Alexander Sheveyko¹, Philipp Kiryukhantsev-Korneev¹, Dmitry Shtansky¹

¹National University of Science and Technology «MISIS», Moscow, Russia

Multicomponent nanostructured coatings remain material of choice for a wide variety of high-temperature applications. High thermal stability and oxidation resistance are important characteristics for such applications. Superhard TiAlSiCN coatings with “comb”-like nanocomposite structure, in which fine $(\text{Ti,Al})(\text{C,N})$ columnar grains were separated by well-developed amorphous SiCN interlayers, recently developed in our group exhibited the highest thermal stability reported to date for nanocomposite coatings. In the first part we discuss the reasons for the exceptionally high thermal stability of the TiAlSiCN coatings. Their main drawback is a relatively large temperature gap between thermal stability (1300°C) and oxidation resistance (1000°C), which limits their use at high temperatures. In the second part we compare three different approaches to increase the oxidation resistance of TiAlSiCN coatings: deposition of a thin Al top-layer, Al ion implantation into the surface of TiAlSiCN coatings, and deposition of a thin AlO_x top-layer. To evaluate thermal stability, the coatings were vacuum annealed at different temperatures up to 1600°C . The structure and phase composition of as-deposited and annealed coatings were studied by XRD, TEM, SEM, GDOES, XPS and Raman spectroscopy. The coatings were characterized in terms of their hardness, Young's modulus and elastic recovery. The coatings were also annealed in air at 1000 , 1100 , and 1200°C for 1 h and their oxidation behavior was studied using SEM and GDOES. Obtained results show that the TiAlSiCN coatings retained their “comb”-like nanocomposite morphology and hardness (above 37 GPa) up to 1300°C . Deposition of a thin top amorphous AlO_x layer was shown to increase the oxidation resistance of the TiAlSiCN coatings from 1000 to 1100°C . In contrast, the deposition of a thin Al top-layer and Al ion implantation resulted in a negative effect. The phase transformations in the range of 900 - 1600°C and factors affecting coating oxidation are discussed.

P-Th-043

Theoretical analyses of 4x1-8x2 phase transition on In-adsorbed Si(111) surface with continuous displacement model

S.T.A. Abdulmawla¹, H. Kaji¹, K. Kakitani¹

¹Okayama University of Science, Ridai-cho, Japan

The 4x1-8x2 phase transition on the In-adsorbed Si(111) surface has been discussed in the light of the Peierls transition or the Charge Density Wave transition. These suggest that this transition is the second order phase transition. On the other hand, the recent experimental results revealing coexistence of the two phases or hysteresis of diffraction intensities suggest that this transition is the first order.[1,2] We analysed this system with the continuous displacement model that is extended from the Ising model proposed by Yagi et al.[3] and succeeded to reproduce the metal-insulator transition accompanying with this structural phase transition.[4] The calculation results showed the properties on our model at equilibrium states were similar to the properties of the original Ising model, however, the details of the phase transition including in our continuous displacement model were not clarified necessarily. In this work, we perform the computer simulation with the Monte Carlo method and the molecular dynamic method to reveal the details of the phase transition including in the continuous displacement model. This model has similar behaviour to the Ising model, however, it includes the huge anisotropy and the frustrated many-body interaction. We calculate the distribution for the properties as functions of the local and global order parameters and discuss the nature in the continuous displacement model.

- [1] F. Klasing, T. Frigge, B. Hafke, B. Krenzer, S. Wall, A. Hanisch-Blicharski, and M. Horn-von Hoegen, *Physical Review B* 89 (2014) 121107.
- [2] H. Zhang, F. Ming, H.-J. Kim, H. Zhu, Q. Zhang, H. H. Weitering, X. Xiao, Ch. Zeng, Jun-H. Cho, and Zh. Zhang, *Physical Review Letters* 113 (2014) 196802.
- [3] Y. Yagi, and A. Yoshimori, *Journal of Physical Society of Japan*, 74 (2005) 831.
- [4] Y. Yagi, H. Kaji, K. Kakitani, and S. Osanaga, *Journal of Physics: Conference Series* 100 (2008) 072039.

P-Th-044

The equation of state of monolayer of inert gases and their mixtures on the basal plane of graphite

Zeitun Akhmatov¹, Azamat Khokonov¹, Murat Khokonov¹, Vitali Tarala²¹Kabardino-Balkarian State University, Nalchik, Russian Federation, ²North-Caucasus Federal University, Stavropol, Russian Federation

Monolayer of inert gases and their mixtures on graphite (0001) surface are of interest as two-dimensional system with great diversity of surface structures and phase transitions between them [1]. The $\sqrt{3} \times \sqrt{3}$ R 30° structures of krypton and xenon commensurate with the graphite substrate has been studied experimentally and theoretically [1, 2]. Using molecular dynamic method we have obtained equations of state for monolayers of krypton and xenon on the basal graphite plane which connects two-dimensional pressure with specific ad-atom volume. Our approach is based on the calculation of time averaging the force virial [3]. In the case of binary central potential the method reduces to the convolution of radial distribution function with binary radial force as it was used in [4]. We have taken into consideration three-particle potential for nearest neighbours which is expressed by two algebraically independent polynomials invariant under transformations of the group $O(3) \times S_3$ composed of the radius vectors of particles [5]. Thermodynamic parameters calculations with three – particle forces gives the difference from binary approximation about 10% for xenon (e.g. critical temperature) and practically do not change binary results for krypton.

This work was supported in part by State Scientific Program № 2262 of Russian Federation.

[1] Unertl W.N. Physical Structure. Handbook of Surface Science V1 (1996).

[2] Toennies J. P., Vollmer R. Phys. Rev. B40 (1989) 3495.

[3] Khokonov A. Kh., Khokonov M. Kh., M. V. Dottueva. Bulletin of the Russ. Acad. of Sci. Physics. 78 (2014) 777.

[4] Khokonov A.Kh., Dolov M.Kh., Kochesokov G.N., Khamukova L.A. High Temperature. 47 (2009) 763.

[5] Osipenko I. A., Kukin O. V., Gufan A. Yu., Gufan Yu. M. Physics of the Solid State. 55 (2013) 2405.

P-Th-045

Interaction between impurities and charge density wave in the phase transition of atomic wires

Hyungjoon Shim¹, Geunseop Lee¹, Jung-Min Hyun², Hanchul Kim²

¹Inha University, Incheon, South Korea, ²Sookmyung Women's University, Seoul, South Korea

A Si(111)-In surface, an array of indium atom wires, is an extensively studied quasi-one-dimensional (quasi-1D) system undergoing a charge density wave (CDW) transition accompanied by a structural transition. Oxygen impurities were known to raise the transition temperature (T_c), but its mechanism remained veiled. We have investigated the interaction between the oxygen impurities and the CDW to reveal how the oxygen impurities assist the condensation of the CDW and how the CDW condensation affect reciprocally the impurities near the phase transition. Scanning tunneling microscopy images showed that the oxygen adsorbates were immobile but could be displaced from their symmetric sites at low temperatures near T_c . This displacement, driven by the CDW, renders the oxygen defects capable of pinning the 1D CDWs between their pairs in each wire and triggering the nucleation of the 2D CDW domains. The asymmetry directions of the O defects were adjusted in concert with the phase of the condensed CDW. This flexibility is responsible for the enhanced condensation of the CDW and the increase of the T_c by the oxygen adsorption. First-principles calculations showed that the asymmetric interstitially-incorporated O defects can assist the formation of hexagon structure of the CDW phase. The underlying mechanisms will be discussed.

P-Th-046

Bound State Resonances at high velocities, a coherent skipping motion above the surface

Philippe Roncin¹, Asier Zugarramurdi¹, Maxime Debiossac¹, Anouchah Momeni¹, Petru Lunca-Popa¹, Hocine Khemliche¹, Andrei Guenadievitch Borisov¹

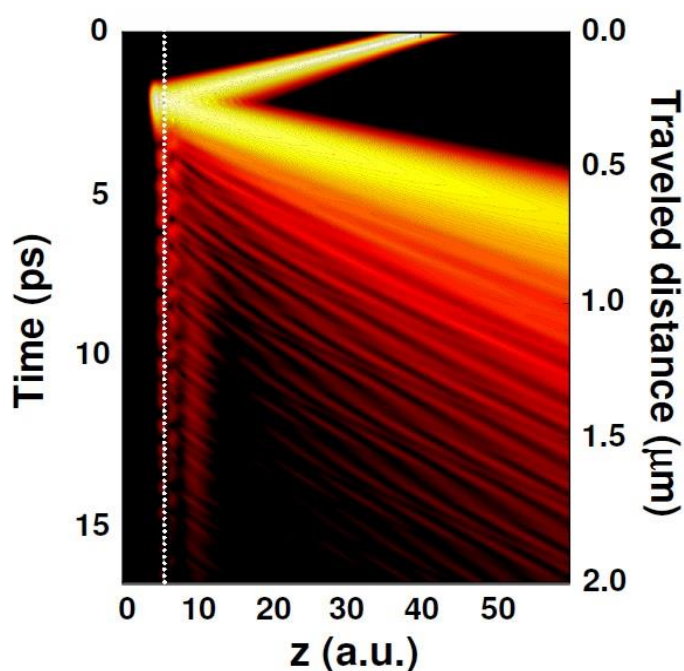
¹CNRS, Orsay, France

Grazing incidence fast atom diffraction (GIFAD) is similar to RHEED in terms of geometry and detection efficiency while it is similar to helium atom scattering (HAS) in terms of exclusive interaction with the topmost surface layer. One of the great success of HAS was the discovery, in the 1930's, of sharp resonances in the smooth variations of the diffracted intensities. These were rapidly interpreted as bound states resonance occurring when the exchange of a reciprocal lattice vector brings the atom into the bound states of the helium-surface potential well deriving from the Van der Waals attraction forces. These have been measured with high accuracy with spin echo technique. We have investigated [1] these states bound by few meV at the comparatively large velocities $v \sim 0.1$ a.u. associated with 300 eV helium atoms. One interesting aspect is that the diffracted intensity is associated with the interference between the beams that are directly scattered with those which are temporarily trapped into the bound state. The situation looks similar to the well-known skipping motion[2] at the surface but here, the trajectories cannot be described by classical physics as only few bound state exist. The distances spanned during a vibration period τ ($\tau \sim 1$ ps for He-LiF) given by $L \sim v\tau$. The observed resonance width is ~ 0.5 meV suggesting coherence length larger than $0.2 \mu\text{m}$. The results are compared with a wave packet calculations developed for GIFAD[3].

[1] M.Debiossac, et al. Phys. Rev. Lett. 112, 023203 (2014)

[2] J.Villette et al. Phys. Rev. Lett. 85, 3137 (2000)

[3] Zugarramurdi and. Borisov Phys. Rev. A 86, 062903 (2012)



P-Th-047

Periodic quantum chemical calculations for the structure and stability of divalent metal fluoride surfaces

Zeinab Kaawar¹, Beate Paulus¹¹Freie Universität Berlin, Berlin, Germany

Divalent metal fluorides have attracted continuous attention due to interesting electronic, catalytic and optical properties. For example, ZnF_2 is one of the important optical materials that have been investigated mainly looking at the effects on optical properties induced by doping [1]. The alkaline-earth fluorides CaF_2 , SrF_2 and BaF_2 constitute an important class of relatively simple ionic crystals whose optical and lattice-dynamical properties are of much theoretical and experimental interest [2,3]. In the first part of our work, we use CO as probe molecule to characterize ZnF_2 surfaces. We calculate adsorption properties for CO on different ZnF_2 low index surfaces using periodic DFT calculations with the B3LYP functional as implemented in the programme package Crystal09 [4], and subsequent dispersion correction [5, 6]. Additionally a wave function-based correlation treatment at the MP2 level was performed with the Cryscor programme [7]. In the second part, we investigate the bulk and surface structure of group II metal fluorides CaF_2 , SrF_2 and BaF_2 and characterize the surface cations by adsorbing HF molecules on top of the surfaces.

[1] Wu, X., and Wu, Z., Eur. Phys. J. B, 2006, 50, 521-526.

[2] G.A. Samara, Phys. Rev. B 13 (1976) 4529.

[3] R.M. Hazen, L.W. Finger, J. Appl. Cryst. 14 (1981) 234.

[4] R. Dovesi, V. R. Saunders, C. Roetti, R. Orlando, C. M. Zicovich-Wilson, F. Pascale, B. Civalleri, K. Doll, N. M. Harrison, I. J. Bush, P. D'Arco, and M. Llunell. CRYSTAL09 User's Manual. University of Torino, Torino, 2010.

[5] S. Grimme, J. Comput. Chem. 27 (2006) 1787.

[6] S. Grimme, J. Antony, S. Ehrlich, H. Krieg, J. Chem. Phys. 132 (2010) 154104.

[7] C. Pisani, M. Schütz, S. Cassassa, D. Usvyat, L. Maschio, M. Lorenz, A. Erba, Phys. Chem. Chem. Phys. 14 (2012) 7615.

P-Th-048

Theoretical and experimental study of molecular Deuterium diffractive scattering from Methyl-Si(111)

Cristina Díaz¹, Alberto S. Muzas¹, Marcos del Cueto¹, Terry J. Frankcombe², Fernando Martín^{1,3}, Zack M. Hund⁴, Kevin J. Nihill⁴, Steven J. Sibener⁴

¹Universidad Autónoma de Madrid, Madrid, Spain, ²Australian National University, Canberra, Australia, ³Instituto Madrileño de Estudios Avanzados en Nanociencia (IMDEA-Nanoscience), Madrid, Spain, ⁴University of Chicago, Chicago, USA

During the last decade, organic-terminated Si surfaces have attracted a great deal of attention in surface science. These kind of surfaces exhibit improved oxidative and electrochemical stability, relative to hydrogen-terminated silicon, for applications such as photoelectrodes in electrochemical cells [1] or biosensing electronics [2]. Thus, methyl terminated functionalized silicon surfaces have emerged as the best alternative to hydrogen termination ones [3]. Very recent diffraction experimental results on CH₃-Si(111) have shown [4] a remarkable rotational excitation for D₂, which is not observed in the diffraction spectra measured for H₂. Aiming to understand the mechanism behind of this behaviour, we have simulated these experimental spectra. In a first step we have constructed a suitable potential energy surface (PES), using a Modified Shepard interpolation method [5]. Subsequently, we have performed classical (scattering) and quantum (diffraction) dynamics. First dynamics results already show that our six-dimensional PES reproduces accurately the anisotropy of the system. Classical scattering results show rotational excitation probabilities (from J=0 to J=2) of the order of 30% for D₂, and less than 10% for H₂, within the incidence experimental energy range. Quantum rotational inelastic diffraction peaks (RIDs) probabilities show the same trend as that observed experimentally.

[1] X. Shen et al. ACS Nano 4, 5869 (2010).

[2] T. L. Lasseter et al. J. Am. Chem. Soc. 126, 10220 (2004).

[3] R. D. Brown et al. Phys. Rev. Lett. 110, 156102 (2013).

[4] Z. M. Hund et al. to be published

[5] T. J. Frankcome et al. J. Chem. Phys. 137, 144701 (2012).

P-Th-049

Laser Irradiated ZnO for biosensor applications

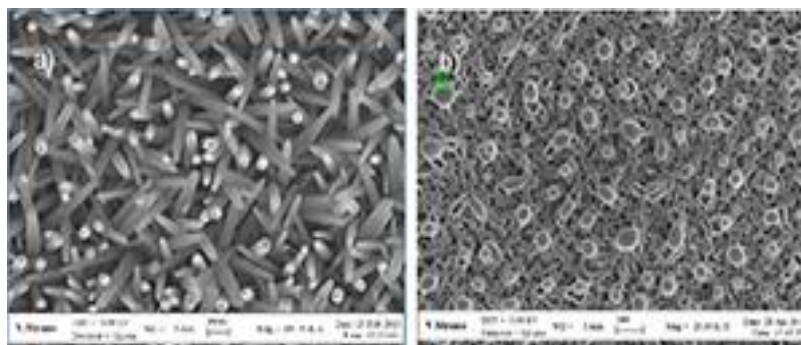
Giorgia Fiaschi¹, Salvo Mirabella², Vicky Strano², Giorgia Franzó², Adrian Chitu³, Luca Maiolo⁴, Yigal Komem^{3,5}, Yosi Shacham-Diamand¹

¹Dept. of Phys. Elect., Engineering Faculty, Tel Aviv University, Tel Aviv, Israel,

²MATIS IMM-CNR and Dipartimento di Fisica e Astronomia, Università di Catania, Italy, ³Applied Physics and Applied Mathematics Department, Columbia University, New York, USA, ⁴Istituto per la Microelettronica e i Microsistemi, Consiglio Nazionale delle Ricerche, Rome, Italy, ⁵Faculty of Materials Engineering, Technion - Israel Institute of Technology, Haifa, Israel

Among semiconductors and metal oxides, ZnO attracts interest due to its unique properties [1] and the possibility of synthesizing ZnO nanostructures via low-cost methods, such as chemical bath deposition (CBD). Here we present a study on the effect of laser irradiation of ZnO nanorods grown by CBD, in an aqueous solution of Zn nitrate and hexamethylenetetramine (HMTA) [2]. After deposition, the ZnO samples were irradiated by excimer laser ($\lambda = 308$ nm) with energy density at the sample level in the range of 130-1018 mJ/cm². The effects of the irradiation on the properties of ZnO are investigated by field emission scanning electron microscope (SEM) and photoluminescence (PL). The SEM analysis reveals a remarkable change in the morphology of the surface with respect to the increasing of the laser energy density. After the irradiation, formation of uniform microstructures is observed, in particular the formation of melt induced balls-like shape at the tips of the ZnO nanorods. This unique morphology is prospective for chemical and biological sensors. The PL analysis shows a UV excitonic emission, attributed to free excitons recombination [3], with a variable PL intensity. As-grown ZnO nanorods show a peak in the visible region, attributed to defects with levels in the energy gap [4]. This peak decreases with the increasing of the laser energy density, suggesting that after the annealing the intrinsic defects, such as O vacancies, are removed or filled. The laser processed ZnO nanorods properties can potentially provide special conditions for immobilization of enzymes, paving the way for the construction of electrochemical biosensors with enhanced analytical performance.

- [1] A. Janotti et al., Rep. Prog. Phys. 72 (2009)
- [2] V. Strano et al., J. Phys. Chem. C, 118 (2014)
- [3] V.A. Fonoberov et al., Phys. Rev. B 73 (2006)
- [4] E. Barbagiovanni et al., Appl. Phys. Lett. 106 (2015)



P-Th-050

Synthesis and structural characterization of ultrathin heavy fermion compounds Ce-Pt on Pt(111)

Koichiro Ienaga¹, Sunghun Kim¹, Yukio Takahashi¹, Toshio Miyamachi¹, Fumio Komori¹

¹The University of Tokyo, Chiba, Japan

Studies of f-electron compounds have revealed many intriguing phenomena concerning strongly-correlated electrons, including Fermi liquid, magnetic order and heavy Fermion superconductivity. These electronic states are mainly determined by the hybridization between localized f-electron states and itinerant s/p electrons. For modifying the electronic state in bulk materials, the hybridization has been tuned so far by external pressure and element substitution. Recently, unusual phenomena due to strong electron interaction have been reported in epitaxial alternate layers and surface compounds formed on metal substrates [1,2]. These studies suggest that nano-scale structural control is a new way to change the electron correlation and thus to discover novel electronic states. One of the interesting candidates for the thinnest strongly-correlated system is CePt₅ grown on a Pt(111) substrate[2,3,4]. However, the growth of the films thinner than two unit layers has been controversial. To synthesize well-ordered CePt₅ films of a few unit layers, we have studied their growth process on Pt(111) by using scanning tunneling microscopy and low-energy electron diffraction. The films were prepared by depositing Ce atoms on the substrate at 300 K followed by annealing up to 800 K. We find that the deposited Ce atoms start mixing with the substrate by annealing around 600 K, and the CePt₅ film is gradually ordered during the annealing process. A film of one unit layer is successfully realized.

[1] H. Shishido et al., Science 327, 980 (2010).

[2] M. Klein et al., Phys. Rev. Lett. 106, 186407 (2011).

[3] C. J. Baddeley et al., Phys. Rev. B 56, 12589 (1997).

[4] J. Kemmer et al., Phys. Rev. B 90, 195401 (2014).

P-Th-051

Blister mechanism in extreme ultraviolet multilayer mirrors

R.A.J.M. van den Bos¹, C.J. Lee¹, F. Bijkerk¹¹Industrial Focus Group XUV Optics, MESA+ Institute for Nanotechnology,
University of Twente, Enschede, Netherlands

Multilayer mirrors form an important optical component in soft X-Ray or XUV optical systems, which, for example, can be found in lithography, synchrotrons, and telescopes. Hydrogen ions or radicals can be useful to remove contaminants from the mirror surfaces. However under certain exposure conditions, hydrogen interaction can cause delamination, leading to the formation of blisters on the mirror surface. To prevent this, a complete understanding of the blister formation process is needed. Currently, there are two competing hypotheses for blister formation: hydrogen-induced swelling, and hydrogen-induced stress relaxation. To determine which process is more likely, multilayer structures were exposed to controlled fluences of low energy ionic (50-200 eV) and atomic hydrogen. By analysing the size distribution of the blisters, we calculate that the induced strain in the blister layer typically reaches values of several percent, far beyond the elastic limit. The pressure required to create such a blister is rather large, indicating that hydrogen-induced swelling is unlikely to be the only cause of blistering. On the other hand, analysis of the changes in substrate curvature shows that hydrogen exposure is associated with stress relaxation, supporting the hydrogen-induced stress relaxation model.

P-Th-052

Toward 3D holographic imaging of surface atoms by CTR scatterings at SPring-8, BL13XU

Hiroo Tajiri¹

¹Japan Synchrotron Radiation Research Institute, Kouto, Sayo, Japan

The SPring-8 standard undulator beamline BL13XU for surface and interface structures offers high-flux optics suitable for surface X-ray diffraction, e.g. X-ray beam over 10^{13} photons/s in 0.1 mm size is available, and ultra-high vacuum MBE systems for sample preparations and in-situ observations. On the other hand, it is needless to say that the establishment of both experimental environments and analytical methods is important. Therefore, we are preparing a program package supporting a model-free analytical method, c.f. 3D atomic imaging of surfaces and interfaces by crystal truncation rod (CTR) scatterings, which is based on CTR scattering holography proposed by Toshio Takahashi [1]. An ordinary structure analysis program based on least squares fit for structure refinement is supported too and opened for users.

[1] Toshio Takahashi et al., Surf. Sci. 493 (2001) 36.

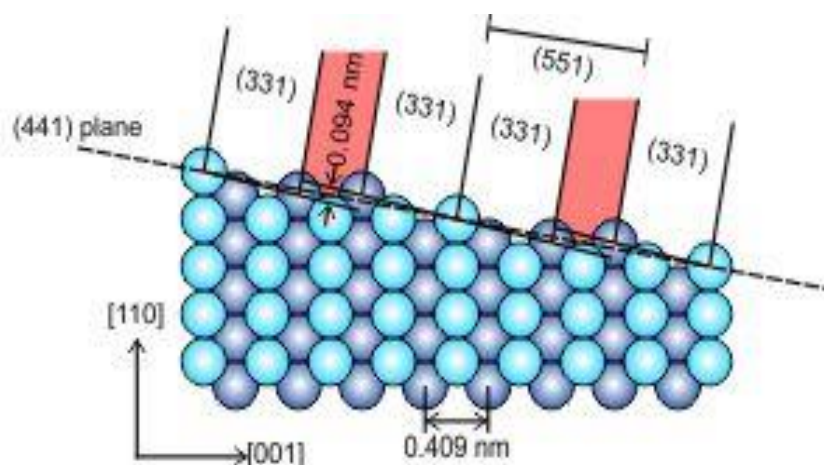
P-Th-053

On the microscopic structure of the Ag(441) surface

Thorsten Wagner¹, Daniel Roman Fritz¹, Robert Zimmerleiter¹, Peter Zeppenfeld¹

¹Johannes Kepler University Linz, Linz, Austria

Regularly stepped (vicinal) surfaces provide a convenient path to control the number of defects of a surface. They can be easily prepared by a slight miscut of a low index surface. In the case of an fcc($nn1$) surface with small integer n it is even expected that the large number of steps will dominate the surface properties. Here we report on a study of the Ag(441) surface with a combination of scanning tunneling microscopy (STM) and high resolution electron diffraction (SPA-LEED). The STM data suggest a statistical distribution of the step width which can be described in general by a Γ -probability distribution. In fact, the steps are not randomly distributed but are interacting. The detailed statistical analysis of the images also reveals that the terraces are formed by an integer number of (331) building blocks whereas the actual steps are given by (551) microfacets. Complementary to the STM data, reciprocal space maps (RSMs) were recorded using SPA-LEED. In order to compare the electron diffraction data to the real space information from the STM experiment, we carried out simulations of the reciprocal space maps in the framework of the simple kinematic approximation. In this particular case of narrow, interacting steps one has to be cautious to carry out a correct interpretation of the experimental RSM based on the simple analysis of the splitting of the rods and their tilt angle. Especially the latter is strongly influenced by the correct alignment of the SPA-LEED.



P-Th-055

Fermi surface analysis of the low temperature phases of
 α -Sn/Ge(111)

Antonio Tejeda^{1,2}, Irene Palacio², Yoshi Otshubo², Amina Taleb-Ibrahimi²,
Enrique Garcia Michel³, Arantzazu Mascaraque⁴

¹Laboratoire de Physique des Solides, CNRS, Univ. Paris Sud, Univ. Paris-Saclay, Orsay, France, ²Synchrotron SOLEIL, Gif sur Yvette, France,

³Universidad Autonoma de Madrid, Cantoblanco, Spain, ⁴Universidad Complutense de Madrid, Madrid, Spain

Since the discovery of a Mott transition associated to a $(\sqrt{3}\times\sqrt{3})R30^\circ$ symmetry below 30 K on Sn/Ge(111) [1], interest on the electronic correlation at surfaces has been renewed. In this work we report a detailed analysis of the valence band electronic structure of Sn/Ge[111] as a function of temperature by angle resolved photoemission spectroscopy [2]. The pseudo Fermi surface and the $E(k)$ relations as a function of the temperature demonstrate the existence of three different phases below room temperature: a Mott insulator state at 5 K with $(\sqrt{3}\times\sqrt{3})R30^\circ$ symmetry, a Charge Ordered Insulator (COI) phase at 40 K with (3×3) symmetry and a metallic state at 200 K with (3×3) symmetry. These results confirm our previous STM measurements [3] and corroborate the coexistence of the COI phase with the metallic and Mott phases.

[1] R. Cortés et al., Phys. Rev. Lett. 96, 126103 (2006).

[2] I. Palacio et al., To be published.

[3] R. Cortés et al., Phys. Rev. B 88, 125113 (2013).

P-Th-056

Theoretical calculation of electronic structures of SnTe and PbTe monolayers with supports

Katsuyoshi Kobayashi¹

¹Ochanomizu University, Tokyo, Japan

Recently, topological crystalline insulators (TCIs) have much attention. TCI is a concept introduced by Fu. Electronic states of insulators are classified according to topological numbers defined by point group symmetries of crystals such as mirror symmetry. The first realistic materials of TCI are SnTe and its alloy with Pb. They were theoretically proposed and have been experimentally verified. They are three-dimensional materials. Recently two-dimensional (2D) materials of TCI are theoretically predicted, and their new applications were proposed [1]. However, they have not been materialized experimentally. We theoretically calculated electronic states of 2D TCI thin films with supports and show their results in this presentation. The proposal of 2D TCI is based on electronic-state calculations for free-standing thin films [1]. When we make some experiments or devices using 2D TCI, it would be necessary to place them on substrates or embed in materials. In contrast to the topological insulators whose topological character is protected by the time-reversal symmetry, the topological character of TCI is guaranteed by crystal symmetries of systems which are easily broken by the interaction with substrates and environments. Therefore, it is important to study the effect of substrates and environments on electronic structures of 2D TCI. In this presentation we show our theoretical calculations of SnTe and PbTe monolayers with supports. First we calculate free-standing SnTe and PbTe monolayers by a density-functional method. We find that the planar structure is unstable and the mirror symmetry is lost. Therefore, we need supports for stabilizing the planar structure. We choose alkali-halide surfaces as supports. Our theoretical calculations show that when a SnTe monolayer is sandwiched between two NaBr surfaces, the system is a 2D TCI.

[1] J. Liu, et al., Nature Mat. 13 (2014) 178.

P-Th-057

Surface Superconductivity in Metastable Phase of Topological Insulator Bi_2Se_3 Quenched after High-Pressure-High-Temperature Treatment

Sergei Buga^{1,2}, Vladimir Kulbachinskii^{2,3,4}, Vladimir Kytin³, Nadezhda Serebryanaya^{1,2}, Sergei Tarelkin¹, Vladimir Blank^{1,2}

¹Technological Institute for Superhard and Novel Carbon Materials, Moscow/Troitsk, Russian Federation, ²Moscow Institute of Physics and Technology, Moscow/Dolgoprudny, Russian Federation, ³M.V. Lomonosov Moscow State University, Moscow, Russian Federation, ⁴Moscow Engineering Physics Institute, Moscow, Russian Federation

High-pressure studies of topological insulators like tellurides and selenides of V group elements (Bi, Sb) attract much attention due to transformation into superconducting phases enabling Majorana fermions to emerge. We obtained for the first time bulk polycrystalline samples of metastable phase of Sb_2Se_3 topological insulator by a rapid quenching after a high-pressure-high-temperature treatment at a pressure of 7.7 GPa in the temperature range of 1373 - 1573 K and investigated their electrical and magnetic properties in the temperature range of 0.5-300 K. Unlike pristine material, the quenched metastable phase of Sb_2Se_3 possesses superconductivity transition with $T_{c_onset} = 2.5$ K at normal pressure. In the temperature range of 50 - 3 K the electrical conductivity decreases as a square root function of temperature that is typical feature of degenerate semiconductors due to quantum corrections to electron-electron interaction and proper to 2D superconductors. The low critical current value of about 2 mA in the metastable Sb_2Se_3 phase and an absence of the detectable heat capacity effect at the superconducting transition also indicate a low-dimensional character of superconductivity which may refer to the surface of the crystal grains. We observed a zero-field magnetic susceptibility cusp at temperatures in the range of 77-300 K and a linear positive magnetoresistance at $T < 100$ K. It was most pronounced at $T < 10$ K. These effects indicate the topological insulator state. Thus the metastable phase of Sb_2Se_3 topological insulator obtained by high-pressure-high-temperature treatment possesses surface superconductivity and may be interesting for Majorana fermions search.

P-Th-058

Influence of Si addition on the properties and wear behavior of nc-AlCrN/a-Si_xN_y hard coatings deposited onto WC-Co turning inserts by LARC

Marián Haršáni¹, Tomáš Vopát², Martin Sahul¹, Ľubomír Čaplovič¹, Miroslav Béger³

¹Slovak University of Technology, Faculty of Materials Science and Technology in Trnava, Institute of Materials Science, Trnava, Slovakia, ²Slovak University of Technology, Faculty of Materials Science and Technology in Trnava, Institute of Production Technologies, Trnava, Slovakia, ³LISS, a.s., Rožnov pod Radhoštěm, Czech Republic

The aim of this paper was to study structure, properties and wear behavior of nc-AlCrN/a-Si_xN_y with 1.0, 3.6 and 5.0 at. % of Si deposited onto WC-Co turning inserts. The nanocomposite coatings were prepared by the Lateral rotating cathodes arc (LARC®) technology. The increase of the Si in the coatings leads to a lower tool wear during turning. The tool wear of coated turning carbide inserts was determined in long-term tool life test on the DMG CTX alpha 500 CNC turning center. In the experiment, the same cutting conditions were set. At the earliest, the optimum cutting speed for turning inserts was studied by experiments. The tool wear was measured on Zoller Genius 3s universal measuring machine. The results show a different tool life of coated turning inserts, structure and properties such as nanohardness, adhesion and thermal stability of the nc-coatings depending on the Si content.

P-Th-059

Temperature induced structural changes of Co-Rh/ceria catalysts

Erika Varga¹, Péter Pusztai², Albert Oszkó¹, János Kiss^{1,3}, András Erdőhelyi¹, Zoltán Kónya^{2,3}

¹Department of Physical Chemistry and Materials Science, University of Szeged, Szeged, Hungary, ²Department of Applied and Environmental Chemistry, University of Szeged, Szeged, Hungary, ³MTA-SZTE Reaction Kinetics and Surface Chemistry Research Group, Szeged, Hungary

Temperature dependent structural properties as well as metal-metal and metal-support interactions were studied in connection with Co-Rh/ceria powder catalysts. X-ray photoelectron spectroscopy (XPS), low energy ion scattering (LEIS), high-resolution transmission electron microscopy (HRTEM) and X-ray diffraction (XRD) were applied to study the catalysts in simple temperature controlled experiments. It was revealed that high temperature reduction (773 K) induces the intensity decrease of Co 2p and Rh 3d signals in XPS, and Co decreases the ceria average particle size from 27.6 nm to 10.7 nm at 10% Co content. However, when the reduced samples were heated under N₂ flow, an intensity increase for Co and its entire reoxidation were presented by XPS, and the emergence of a new Rh 3d_{3/2} component at 308.8 eV was also observed. Our conclusions are that the mobile oxide ions of ceria have significant effect on the supported metals: at elevated temperature they segregate to the surface and oxidize the partially reduced Co particles, and a novel O-spill over from ceria to Rh also takes place. Intensity changes detected by XPS after reduction are caused by the diffusion of Co into the ceria and agglomeration of Rh under heating. Rh enhances the reduction of Co and hinders its tendency to disrupt ceria particles. Co on the other hand inhibits Rh agglomeration.

P-Th-060

Surface Hydrogen Induced CO₂ Conversion Mechanism at Cu(775) Step Surface

Yeonwoo Kim¹, Hangil Lee²

¹KAIST, Daejeon, South Korea, ²Sookmyung Women's University, Seoul, South Korea

Heterogeneous catalytic system for methanol synthesis using the Cu/ZnO/Al₂O₃ is industrially important CO₂ conversion catalyst in order to satisfy the world-wide demands of methanol as well as to untangle the activation of CO₂. From the recent studies, there have been numerous improvements in terms of the active sites which described as 'active copper with step sites' decorated by ZnOx. In spite of these improvements, circumstantial mechanistic routes are still unknown and debated even its initial stage. In this study, we simplified the system to the only bare Cu(111) and Cu(775) surfaces to systematically describe the mechanistic effects of step sites. The reaction was conducted using CO₂/H₂ gas mixture at 1 torr with varying temperature by infrared reflection absorption spectroscopy (IRRAS).

P-Th-061

Preparation, characterization and catalytic behavior of cobalt spinel ferrite obtained by hydrothermal treatment

Laaldja Meddour-Boukhobza¹, Yasmina Hammiche-Bella², Amar Djadoun³, Amel Benada⁴, Aline Auroux⁵¹LMCCCO, Faculté de Chimie, USTHB, Alger, Algeria, ²LMCCCO, Faculté de Chimie, USTHB, Alger, Algérie, ³Laboratoire de Géophysique, FSTGAT, USTHB, Alger, Algérie, ⁴LMCCCO, Faculté de Chimie, USTHB, Alger, Algérie, ⁵CNRS, IRCELYON, Lyon, France

Ferrite materials are a large family of mixed oxides which have the potential applications in catalysis. Several routes are used for the preparation of spinel ferrites. In this study, a series of cobalt spinel ferrite compounds were prepared using coprecipitation method at room temperature followed by a hydrothermal treatment at 150°C for different times varied between 2 and 22 hours. The powders were characterized by Thermogravimetric and Differential Thermal Analysis (TGA/DTA), X-Ray Diffraction (XRD) and Temperature Programmed Reduction (TPR). The TGA/DTA (fig.1) results showed a thermal instability of the precursor and two selected samples, counting a weight loss attributed to a decomposition of hydroxide species, which involves the formation of impure spinel phase during the hydrothermal treatment. XRD study of products (fig.2) obtained at different times revealed the presence of mixture single oxides in addition to the spinel phase. The relative proportion of CoFe_2O_4 increases from 68,2% after a hydrothermal treatment of 2 hours to a maximum of 93% at a residence time of 16 hours in autoclave as reported in Table 1. The crystallite size and lattice parameters (Tab.1) were found to exhibit an irregular variation with increasing the synthesis time which may indicate a complex progress in the growth of the crystals. This behavior is also observed on the catalytic proprieties of the solids in the total oxidation of ethanol (fig.3). The comparison of the isoconversion temperatures leads to the conclusion that the most active sample is obtained at a hydrothermal treatment time of 5h, it is characterized by the lower crystallite size value and contains 76.1% of CoFe_2O_4 phase. A correlation between the catalytic activity and the TPR results (fig.4) is attempted, concluding that the lower the reduction temperature is, the lower are the isoconversion temperatures.

Sample	HT-2h	HT-5h	HT-8h	HT-12h	HT-16h	HT-19h	HT-22h
% CoFe_2O_4	68.2	76.1	86.3	82.1	93.0	71.9	83.2
Crystallite size (nm)	18.95	14.23	20.53	19.87	19.31	22.49	54.86
L. Parameter (Å)	8.3850	8.3853	8.3490	8.3711	8.3686	8.3903	8.3405
T10 (°C)	177.5	177.5	199.6	224.8	211.7	210	211.7
T50 (°C)	235	209.5	235	271.8	262.8	262.8	308.5
T90 (°C)	249.7	223	247.7	295.7	273.4	305.5	323.3

Table 1. Quantitative analysis and XRD data and temperatures of 90% isoconversion levels of the samples prepared by hydrothermal treatment at different times.

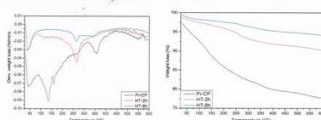


Figure 1. TGA-DTA curves of the solids: precursor (P-CP); after 2 hours hydrothermal treatment (HT-2h); after 8 hours hydrothermal treatment (HT-8h).

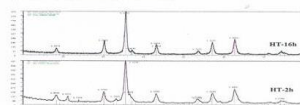


Figure 2. XRD diffractograms of the hydrothermal prepared solids at 150°C for 2 hours (HT-2h) and 16 hours (HT-16h).

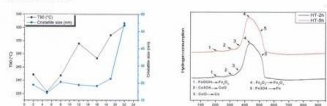


Figure 3. Crystallite size and isoconversion temperatures versus hydrothermal treatment time.

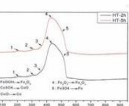


Figure 4. TPR profiles of two selected temperatures versus hydrothermal treatment time.

P-Th-062

Annealing effects on reactivity of oxide supported Rh nanoclusters in the decomposition of methanol

Meng-Fan Luo¹, Ting-Chieh Hung¹, Ting-Wei Liao¹, Zhenhe Liao¹, Po-Wei Hsu¹, Pei-Yang Cai¹

¹National Central University, Taoyuan, Taiwan

Decomposition of methanol on Rh nanoclusters grown from vapor deposition at 300 K on a thin film of Al₂O₃/NiAl(100) was studied with various surface probe techniques including STM, RHEED, TPD and IRAS. The as-prepared Rh clusters had mean diameter 1.0 - 3.5 nm and mean height 0.4 - 0.8 nm; they were structurally ordered, had a fcc phase and grew with their facets (001) parallel to the θ -Al₂O₃ surface. On annealing the clusters to 450 and 700 K, the clusters remained in the same orientation but large clusters (diameter ≥ 2 nm) varied in diameter. The decomposition of methanol on the Rh clusters proceeded through only dehydrogenation. The production of CO and hydrogen per surface Rh site was significantly enhanced on the clusters annealed to 450 and 700 K. The enhancement can be as great as two times the production on the as-prepared Rh clusters. The origin of the intriguing annealing effect is discussed with annealing-induced alternation in the clusters' structures, the reaction processes and the oxide-clusters interaction.

P-Th-063

Photocatalytic activity of gold nanoparticles on titanium oxide prepared by solution plasma method

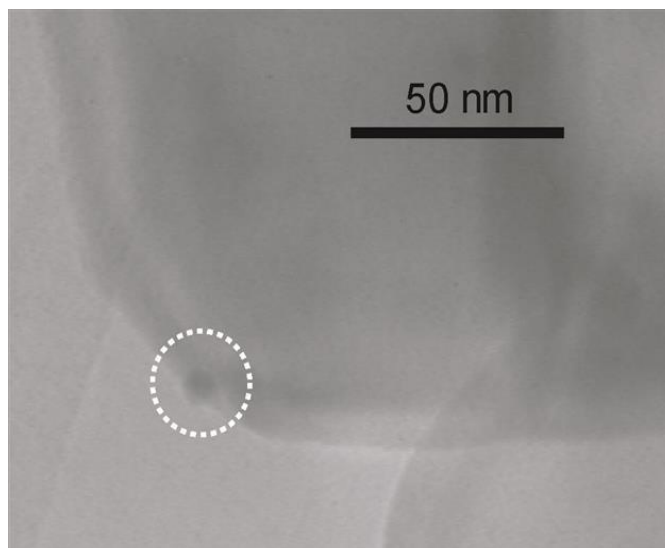
Tsuyoshi Mizutani¹, Satoshi Ogawa¹, Muneaki Yamamoto¹, Hirofumi Nameki²,
Tomoko Yoshida³, Shinya Yagi¹

¹Nagoya University, Nagoya, Japan, ²Aichi Center for Industry and Science Technology, Gamagori, Japan, ³Osaka City University, Osaka, Japan

Gold nanoparticles on titanium oxide have been paid attention as a plasmonic photocatalyst [1]. This composite material is generally prepared by impregnation or photoreduction methods. Both of these methods have to use chlorauric acid as starting material for gold nanoparticles and therefore it is difficult to remove chlorine atoms completely. It is said that these residual chlorine atoms may reduce the catalytic activity. We try to prepare the gold nanoparticles on titanium oxide by solution plasma method which is new preparation method for nanoparticles in solution [2]. The solution plasma method can prepare the gold nanoparticles completely without chlorine because in this method a gold wire is used as a raw material for gold nanoparticles. We apply the solution plasma method to ammonium solution in which titanium oxide powder is dispersing. The ammonium solution is used to enhance the deposition of gold nanoparticles on the titanium oxide surface by decrease of electric double layers on there particles. The ammonium molecules on the sample can be easily removed by calcination after the preparation. We measure morphologies of the prepared sample by transmission electron microscope (TEM) observation. TEM result shows the almost spherical gold nanoparticles are deposited on the titanium oxide surface and the particle diameter is about 5 nm. Typical TEM image is shown in Figure 1. The photocatalytic activity of hydrogen production from aqueous ethanol is measured by gas chromatography under visible light irradiation. We will prepare a reference sample, which has same diameter and deposition amount of gold nanoparticles, by photoreduction method to discuss about the effect of residual chlorine on photocatalytic activity.

[1] H. Yuzawa et al. Appl. Catal. B Environ. 115-116 (2012) 294-302.

[2] X. Hu et al. Cryst. Growth Des. 12 (2012) 119-123.



P-Th-064

Spatially- and component-resolved reaction kinetics on a μm -scale: CO oxidation on Pd model catalysts

Martin Datler, Ivan Beshpalov, Günther Rupprechter, Yuri Suchorski¹

¹Vienna University of Technology, Vienna, Austria

Most of the practically useful catalysts are complicated heterogeneous systems exhibiting strong local variations of catalytic activity. Since theoretical calculations cannot yet provide reliable predictions for the local reaction kinetics even on the mesoscopic (mkm) scale, the problem of laterally-resolved studies of reaction kinetics is still up-to-date. Recently, it was demonstrated that information about local reaction kinetics for individual mkm-sized grains of a polycrystalline Pt foil can be obtained “just by imaging” using PEEM [1, 2]. We extend herewith this approach to model catalysts consisting of Pd powder supported by metal and oxidic supports. The kinetic data for the individual μm -sized Pd powder agglomerates were obtained by digital analysis of PEEM video-sequences recorded in situ during the ongoing CO oxidation reaction. From the same video-sequences, the data for the individual (100) and (110) domains of the supporting Pt foil were obtained. The Pd powder agglomerates and the supporting Pt domains behave in the combined Pdpowder/Ptfoil sample independently from each other with respect to the CO oxidation, at least in the 10-5 mbar pressure range. The propagating reaction fronts move within grain boundaries for Pt domains and also remain confined to the Pd agglomerates. Substituting the supporting Pt foil by oxidic support allows to elucidate the effect of the support via comparison of the catalytic behaviour of individual metal- and oxide-supported Pd powder agglomerates.

[1] Y. Suchorski, C. Spiel, D. Vogel, W. Drachsel, R. Schlögl, G. Rupprechter, Chem.Phys.Chem. 11 (2010) 3231.

[2] D. Vogel, Ch. Spiel, A. Suchorski, A. Trinchero, R. Schlögl, H. Grönbeck and G. Rupprechter Angew. Chem. Int. Ed. 51 (2012) 10041.

P-Th-067

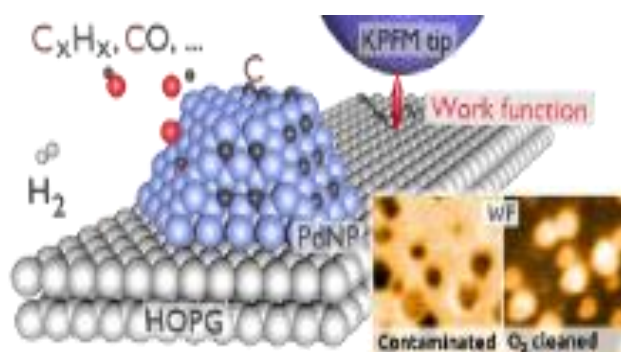
Carbon contamination of metal nanoparticles detected by Kelvin probe force microscopy

Fayçal Mechehoud¹, Henrik Grönbeck², Clemens Barth¹

¹Centre national de la recherche scientifique (CNRS) / Aix-Marseille Université, Marseille, France, ²Chalmers University of Technology, Göteborg, Sweden

In many catalytic reactions, carbon can be split from carbon containing gas like CO at metal nanoparticles (NPs), which may lead to a contamination and poisoning of the NPs. However, in many cases, dissolved carbon inside NPs is needed, like in the Fischer-Tropsch process at FeNPs or the hydrogenation of hydrocarbons at PdNPs (PdNPs). Although carbon contamination and dissolution are a 'known phenomena', experimental studies accomplished by, e.g., Auger electron spectroscopy, core electron energy loss spectroscopy, and static secondary ion mass spectroscopy always left behind some ambiguity in the interpretation of the results. An important but almost undiscovered aspect is how the carbon contamination scales with the NPs size, shape and composition. Recently, we have shown that Kelvin probe force microscopy (KPFM) can detect carbon at PdNPs grown on HOPG via measuring the WF of the NPs [1]: when PdNPs are left in the ultrahigh vacuum (UHV), they get contaminated over a time of a week by splitting carbon from carbon containing gas of the UHV at low-coordinated sites of the NPs (left graphics). The carbon gets dissolved inside the NPs, which reduces their high WF by more than 500 meV (left WF image). High temperature annealing in molecular oxygen cleans the NPs such that the initial WF is recovered (right WF image). In this contribution, we extend our research on the carbon contamination at PdNPs but also AuNPs. We discuss the contamination when leaving the NPs in UHV and upon explicit contaminating NPs by cracking ethylene. By a comparison between experiment and DFT calculations the basic mechanisms involved in the WF reduction of the NPs by carbon will be explained. In general, the role of KPFM in heterogeneous model catalysis will be discussed.

[1] E. Palacios-Lidon, C. R. Henry and C. Barth - ACS Catal. 4, 1838-1844 (2014)



P-Th-068

Step edges on ceria stabilize Pt²⁺ ions

Andrii Tovt¹, Filip Dvořák¹, Mikhaylo Vorokhta¹, Tomáš Skála¹, Iva Matolínová¹,
Josef Mysliveček¹, Vladimír Matolín¹, Fabio Ribeiro², Matteo Farnesi
Camellone², Tran Nguyen Dung², Stefano Fabris²

¹Charles University in Prague, Faculty of Mathematics and Physics, Prague,
Czech Republic, ²CNR-IOM DEMOCRITOS, Istituto Officina dei Materiali,
Consiglio Nazionale delle Ricerche and SISSA Trieste, Trieste, Italy

Ceria activated with Pt²⁺ ions provides exceptional reactivity in advanced catalytic applications including catalysis by single atoms. Controlling the morphology of thin-film ceria substrates, and employing scanning tunneling microscopy and photoelectron spectroscopy we observe that Pt²⁺ ions are stabilized at monolayer-high step edges on CeO₂(111) surface. Pt²⁺ ions are thermally stable and do not sinter upon exposition to CO. Density functional theory calculations demonstrate the driving force for Pt segregation at step edges and the stabilization of Pt²⁺ in PtO₄ moieties decorating the steps. On the other hand, both the experimental and the theoretical results confirm that oxygen vacancies on ceria do not stabilize Pt²⁺. Our study demonstrates the importance of step edges for obtaining up to 5% coverage of monodispersed and fully ionized platinum on the ceria surfaces. We propose step engineering as a general approach towards stabilizing single metal atoms or ions on oxide surfaces.

P-Th-069

Photocatalytic reduction of NO with ethanol on Au/TiO₂Gyula Halasi¹, Tamás Bánsági¹, Frigyes Solymosi¹¹MTA-SZTE Reaction Kinetics and Surface Chemistry Research Group,
Szeged, Hungary

The primary subject of the present work is to examine the effect of illumination on the NO+C₂H₅OH reaction over Au nanoparticles deposited on TiO₂, which was found to be active for the generation of hydrogen in the photocatalytic processes. Attention is paid to the detection of surface intermediate formed in the photoreaction. An attempt will be also made to perform experiments in visible light. While the thermal reaction between NO and C₂H₅OH on Au/ TiO₂ catalyst occurred with measurable rate only at and above 473-523 K, illumination of the system induced the reaction even at room temperature. By means of IR spectroscopy the formation of absorption bands at ~2180 and ~2210 cm⁻¹ were observed. The first is attributed to the NCO species locating on Au particles, the second one to NCO residing on the TiO₂ support. A fraction of NO was converted into N₂O, another one to N₂. At the same time the photo-induced decomposition of C₂H₅OH also occurred yielding CH₃CHO, H₂, CO and CH₄. Separate studies revealed that all these products react with NO as a result of illumination. However, the photoreduction of NO with all substances is slower than that measured with C₂H₅OH. Taking into account the changes in the products of photoinduced decomposition of C₂H₅OH in the presence of NO, it appears that the amount of H₂ underwent a most significant decrease. It is assumed that adsorbed H atoms formed in the photoinduced dissociation of C₂H₅OH is responsible for the reduction of NO. As the work function of TiO₂ (~4.6 eV) is less than that of Au (5.31 eV), the occurrence of an electron transfer from TiO₂ to the Au particles is assumed, which is enhanced by illumination. Lowering the bandgap of TiO₂ by N incorporation made possible the reaction to occur in visible light.

P-Th-070

Catalytic properties of Fe-HMS materials in the phenol oxidation

Khalida Chellal¹, Khaldoun Bachari², Frida Sadi¹

¹Laboratoire d'Etude Physico-chimiques des Matériaux et Application à l'Environnement. Faculté de Chimie. U.S.T.H.B. Algérie, Alger, Algeria, ²Centre de Recherche Scientifique et Technique en Analyses Physico-Chimiques (C.R.A.P.C.), Alger, Algeria

Iron-incorporated mesoporous silica material Fe-HMS (Si/Fe = 50) was synthesized at ambient temperature by using hexadecylamine as templating agent. The characterization by several spectroscopic techniques has shown that iron is present mainly as nanometric clusters. The catalytic performance of Fe-HMS was studied for phenol hydroxylation and wet phenol oxidation with H₂O₂ at 313K. The effect of pH, H₂O₂: PhOH molar ratio and stability of the catalyst on the oxidation process was investigated. In the phenol oxidation, the activity of the catalyst increase with increasing acidity of the reaction mixture to pH 3.4 and the amount of leached iron species was only 1.95 ppm. A reusing test indicates that the recovered catalyst by drying in air at 423 K preserved its activity. Fe-HMS has high catalytic activity and very high selectivity to dihydroxybenzene for the hydroxylation of phenol. We have found that hydroquinone is the predominant product under these experimental conditions. As the reaction went on, hydroquinone is consumed and small amounts of benzoquinone appeared at the end of reaction.

P-Th-071

High UV-light photocatalytic activity of Ag₃PO₄ synthesized by simple precipitation and hydrothermal methods

Titipun Thongtem¹, Nuengruethai Ekthammathat², Miss Saowalak Krungchanuchat¹, Assistant Anukorn Phuruangrat³, Somchai Thongtem¹

¹Chiang Mai University, Chiang Mai, Thailand, ²Bansomdejchaopraya Rajabhat University, Bangkok, Thailand, ³Prince of Songkla University, Songkhla, Thailand

Silver orthophosphate (Ag₃PO₄) was successfully synthesized by a hydrothermal method at 100-150 °C and a precipitation method at room temperature without adding a surfactant. Phase, morphology, vibration modes and optical property of the products were characterized by X-ray diffraction (XRD), Fourier transform infrared (FTIR) spectroscopy, Field emission scanning electron microscopy (FE-SEM) and photoluminescence (PL). Upon synthesizing at the pH of precursor solution of 8, pure cubic Ag₃PO₄ phase was detected. Size and morphology of the products were controlled by the synthetic method and temperature. In this study, Ag₃PO₄ was used to study photocatalytic degradation of rhodamine B (RhB) organic dye molecules. The photocatalytic activity of Ag₃PO₄ synthesized by the hydrothermal method has higher efficiency than Ag₃PO₄ synthesized by the room-temperature reaction. The product synthesized in the precursor solution with the pH 8 at 150 °C for 24 h has the highest photocatalytic activity of 99.55 % decolorization of RhB within 2h.

P-Th-072

Synthesis and characterization of Co, Ce and Co+Ce incorporated mesoporous SBA-15 and KIT-6 catalysts

Plamen Stefanov¹, Tanya Tsoncheva², Genoveva Atanasova¹, Anton Naydenov¹

¹Institute of General and Inorganic Chemistry, Bulgarian Academy of Sciences, Sofia, Bulgaria, ²Institute of Organic Chemistry with Centre of Phytochemistry, Bulgarian Academy of Sciences, Sofia, Bulgaria

Microporous zeolites are most widely applied catalyst supports due to the uniform pore sizes, good stability, high surface area and large pore volume. The possibility of incorporating heteroatoms into the structure and their ion exchange capacities make zeolites unique materials in catalytic processes. SBA-15 is a highly ordered, two-dimensional hexagonal mesoporous silica. KIT-6 is a new type of mesoporous material with 3-D cubic structure. The present work focuses on the synthesis, incorporation and characterization of Co, Ce and Co+Ce - SBA-15 and Co, Ce and Co+Ce -KIT-6 mesoporous materials. The synthesized materials were characterized by nitrogen physisorption, XRD, TEM, UV-Vis and temperature programmed reduction. The concentration and chemical state of the incorporated Co and Ce were determined by XPS.

P-Th-073

HRTEM study of NiCe/Al₂O₃ nanoparticles

Sabah Chettibi¹, Fatiha Seridi¹, Nassira Keghouche²

¹Lab. of Materials Physics, Univ. 8 Mai 45, Guelma, Algeria, ²Lab. Microstructure and Defects in Materials, Univ. Constantine 1, Algeria

The preparation and characterization of ultra divided materials is a field in full expansion. The great proportion of the surface metal atoms in contact with the environment and the redox potential lower than that of the bulk state, make these materials of first importance in catalysis. In this work, we studied oxide supported Ni-Ce nanoparticles, prepared under γ radiation. The radiolytic process has been proven to be a powerful tool to generate nanoparticles of controlled size and monodispersed. The HRTEM images of Ni-0.5% Ce/ Al₂O₃ nanoparticles present two forms of nickel on oxide support, a veil of elongated particles and dispersed spherical particles with a size about 3-5 nm. When tested in the benzene hydrogenation, they exhibit catalytic properties with higher efficiency.

P-Th-075

Initial surface transformations on hydrated bioactive glasses: insight from MD simulations

Antonio Tilocca¹

¹University College London, London, United Kingdom

The interaction between a bioactive glass and a biological aqueous host plays a key role in steering in the dissolution of key soluble species that trigger the tissue regeneration and interfacial bonding ability of these materials. The glass-water interaction initially results in rapid exchange between alkali ions and protons and formation of a silica-rich layer. Whereas the formation of this layer on highly bioactive glasses such as 45S5 is established, its structural properties and mechanism of formation are less clear. A fundamental understanding of these issues can be gained through atomistic simulations. Building up from our previous work in using simulations to rationalise the behaviour of bioactive glasses at a fundamental level, including atomic-scale models of the 45S5/water interface, here we present simulations focused on an ion-exchanged bioactive glass, revealing the effect of Na/H exchange on the structural features of the alkali-depleted glass. The present simulations provide a high-resolution picture of the structural evolution of the glass during this stage and help unveiling the mechanism of the corresponding surface processes that occur following implant of the glass in an aqueous biological environment.

P-Th-076

Some features on the electrosynthesis of nanostructured Nb₂O₅ anodic films

Leonid Skatkov¹, Larisa Liashok², Valeriy Gomozyov², student Irina Tokareva², Boris Bayrachniy²

¹PCB "Argo", Beer Sheva, Israel, ²NTU "KhPI", Kharkov, Ukraine

Niobium oxide (V) with nanostructured surface is considered to be a prospective material for serving of the basis for creation of a range of nano-, microsystems and touch technology products. However, however procedure of pore formation and self-organization within niobium anodic oxidation have not yet been precisely determined. The present paper is aimed at investigation of specific features of electrosynthesis of Nb₂O₅ nano-structured anodic films and development of theoretical approaches to description of the processes occurred herewith. Within the survey it has been defined that niobium anodic oxidation is limited to solid-phase diffusion of reaction agents in oxidic layer. It has been taken an effort to develop a universal model of formation of barrier- and porous-type niobium anodic oxide. This model helps to evaluate a nature of pores germination, initial stage of their growth as well as temporal progress of the pores geometric shape. Within the survey it has been defined, that morphology of synthesized films substantially depends on the electrolyte contents, voltage and anodic oxidation duration. Thus, at niobium anodic oxidation in a solution of 1 M H₂SO₄ + 0,5 M HF at 60 V within 2 hours it is generated porous anodic film of Nb₂O₅, while at extension of electrosynthesis duration up to 5 hours or HF concentration up to 1 M it is generated secondary structures, which completely cover surface of Nb₂O₅ porous anodic films.

P-Th-077

FeNi electrodeposited on meso and macroporous silicon

Souad Ouir^{1,2}, Ghania Fortas², Sabrina Sam², Noureddine Gabouze²

¹USDB1, Route De Soumaa, Blida, Algeria, ²CRTSE, Algiers, Algeria

In this work, we report on electrodeposition of FeNi into porous silicon (PS) formed on n-type Si with different resistivity. mesopore and macropores silicon layers were formed at constant current density. FeNi films were electrodeposited by applying a constant bias potentiel. The electrodeposited thin films were characterized by scanning electron microscopy (SEM) and Energy Dispersive Spectroscopy (EDS). SEM images of the FeNi deposits show that cylindrical or tubular forms are obtained depending on the morphology of PS. Moreover, it has been shown that the distribution of the FeNi nanosized depends strongly on the potentiel deposition. According to the results a grow mechanism is discuted.

P-Th-078

Electrochemical co-reduction of tellurium (IV) with copper (I), copper (II) or zinc (II) ions from Ethaline ionic liquid

Adriana-Simona Catrangiu¹¹University Politehnica , Bucharest, Romania

The electrochemical deposition of CuTe and ZnTe compounds was studied in an eutectic consisted in choline chloride - ethylene glycol mixture (Ethaline) at 60°C. The working electrodes were Pt, Cu or glassy carbon. CuCl, CuCl₂·2H₂O and TeO₂ precursors were dissolved in ionic liquid in the 5-30 millimolar concentration range. Cyclic voltammetry studies for Zn²⁺ containing electrolytes displayed three cathodic processes as limiting currents or peaks: Te⁴⁺ reduction, codeposition of ZnTe, and deposition of a Zn-rich binary telluride. A disproportionation reaction leading to an equilibrium between Cu⁺ and Cu²⁺ occurs whether CuCl or CuCl₂ is introduced, so a supplementary cathodic peak assigned to Cu²⁺/Cu⁺ couple is recorded at very positive potentials. The corresponding anodic waves or peaks were also identified. Voltammograms had shapes which depend on the electrodeposition conditions (nature of electrode, electrolyte composition, scan rate). The shape of impedance spectra depended also on applied potential. Nyquist curves showed that the support first covers with a Te film, and then the more cathodic polarization produces a co-reduction of Te⁴⁺ with Cu⁺, Cu²⁺ or Zn²⁺ as binary compound. The formation of metal-rich compound at excessive negative polarization is indicated by lowest value of maximum phase angle in Bode curves. The Cu/Te and Zn/Te ratios in the deposited films were successfully controlled by carrying out electrolyses with corresponding ionic ratios in Ethaline bath using Cu or carbon steel electrodes. Film morphology and crystalline structure were evidenced by atomic force microscopy and X-ray diffraction, respectively.

P-Th-080

Treatment of effluent of water paints industry by electrocoagulation

K. Zoulikha¹, D. Zerrouki¹, Nassila Sabba¹, M. Taleb Ahmed¹

¹Laboratoire Génie de la Réaction, GE-FGMGP-USTHB, Alger, Algeria

This work has concerned the study of the effectiveness of electrocoagulation applied in batch using electrodes of aluminum, for the treatment of five synthetic solution of pure hues of different colors and for real discharge painting water from (ENAP / Algeria). Its efficiency is evaluated by measurement of indicators of pollution namely turbidity, concentration and COD (for the actual discharge). The electrocoagulation process was developed to overcome the disadvantages of industrial water treatment technologies. This process is very efficient in the removal of heavy metals, suspended particles, and organic matter. Parametric study was followed including: pH of the medium concentration of the pollutant load processing time, current density on the electrochemical treatment process.

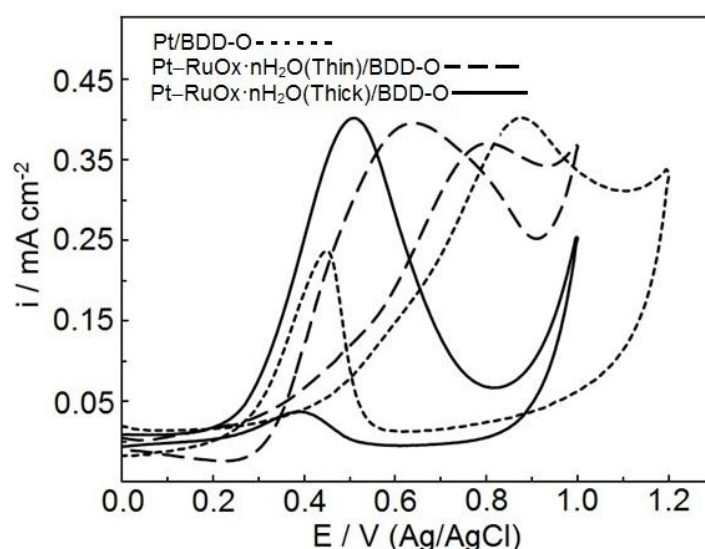
P-Th-081

Effect of hydrous ruthenium oxide modification of conductive diamond substrate on the electrocatalytic performances of supported Pt particles

Tanta Spataru¹, Loredana Preda¹, Cecilia Lete¹, Petre Osiceanu¹, Alexandru Ioan Caciuleanu¹, Nicolae Spataru¹

¹Institute of Physical Chemistry of the Romanian Academy, Bucharest, Romania

The present work was aimed at studying the possibility of using direct electrochemical deposition for obtaining boron-doped diamond (BDD)-supported Pt–RuOx · nH₂O electrocatalysts with high activity for methanol oxidation. Highly boron-doped (ca. 10²¹ atoms/cm³) polycrystalline diamond films grown on Si wafers by microwave plasma-assisted chemical vapor deposition were used as supports for the deposition of Pt–RuOx · nH₂O composites by a two-step electrochemical procedure. First, hydrous ruthenium oxide was deposited by cyclic voltammetry from an aqueous solution containing RuCl₃ and in the second step, platinum deposition was achieved from a H₂PtCl₆ solution, by applying consecutive potentiostatic pulses. Prior to hydrous ruthenium oxide deposition, BDD electrodes were subjected either to a cathodic hydrogenation treatment or to an anodic oxidation one, in order to achieve hydrogen-terminated or oxygen-terminated surfaces. The effect of the chemical termination of the conductive diamond surface on the overall hydrous ruthenium oxide deposition process was investigated, as well as that of the RuOx · nH₂O loading on the electrocatalytic performances of deposited platinum. XPS measurements were employed in order to check the influence of the oxide substrate on the nature of deposited platinum species, both for thin and thick intermediary oxide layers. In order to appraise the effect of the hydrous ruthenium oxide substrate on the electrocatalytic performances of deposited platinum, the activity for methanol oxidation of the Pt–RuOx · nH₂O/BDD-O electrodes was checked by cyclic voltammetry and by long-term polarization measurements. Compared to the case of platinum electrodeposited on bare BDD, it was found that the presence of the oxide results in a co-catalytic effect. With an eye to fuel cell applications, the influence of the oxide coating on the resistance to fouling during methanol oxidation of the supported Pt particles was also scrutinized and preliminary results were reported.



P-Th-082

Heavy metals extraction and separation by electrodeposition on a steel substrate from wastewater

Addi Yassine¹

¹ENPEI-USTHB, Algiers, Algeria

Heavy metals contaminated waste water sludge is classified as hazardous solid waste [1]. For this reason it needs to be properly treated to prevent releasing heavy metals to the environment. The sludge was treated in a batch reactor [2] by sulfuric acid to extract the contained heavy metals (Cu; Cd; Ni and Zn). The effects of sulfuric acid concentration and solid to liquid ratio on the heavy metal removal efficiencies were investigated. The experimental results showed that the total and individual heavy metal removal efficiencies increased with increasing sulfuric acid concentration, but decreased with increasing solid to liquid ratio. For 5g/L solid to liquid ratio, more than 99,9% of heavy metals can be removed from the sludge by treating with 0,5 M sulfuric acid in 2h. The separation, of metals extracted by sulfuric acid from the sludge, is carried out by plating on steel substrate [3]. The electrode position is performed in two different media: acid and basic media. A comparative study of the two plating media was studied.

[1] B.Johnke, B.Wiebusch, Fuel Energy Abstract.1997. 38. 350

[2] M.A.Styllanou; D.Kollia,K.J.Haralambous. V.J.Inglezaki. ,K.G.Moustakas. M.D.Loizidou, Desalination 2007. 215. 73-81

[3] Mortaga M.Abou-Krishna, Applied surface science 2005. 252. 1035-1048

P-Th-083

High temperature real time observation of AuNPs by SEM on silicon oxide

Petr Bábor^{1,2}, Radek Duda^{1,2}, Jan Čechal¹, Stanislav Průša^{1,2}, Jan Polčák^{1,2},
Peter Varga^{1,2}, Tomáš Šíkola^{1,2}

¹Institute of Physical Engineering, Brno University of Technology, Brno, Czech Republic, ²CEITEC BUT - Brno University of Technology, Brno,

Gold nanoparticles (AuNPs) play a key role during the vapor-liquid-solid (VLS) growth of Si nanowires. At the beginning of the VLS growth, AuNPs have to be melted to form an alloy with Si. Therefore, it is essential to know the behavior of AuNPs on substrates at the enhanced temperatures. As the growth direction of the Si nanowires can be guided by the silicon oxide at elevated temperatures, the knowledge on limits of the oxide stability are needed [1]. We have studied the silicidation of AuNPs deposited from a colloidal solution on thermal silicon oxide at temperatures up to 1100 K by real time observation using Scanning Electron Microscopy. In addition, X-ray Photoelectron Spectroscopy and Time of Flight Low Energy Ion Scattering were employed as well to find chemical and morphological changes of AuNPs during annealing. In the contribution the mechanisms of AuNPs interaction with the silicon oxide at specific temperatures will be discussed in detail.

[1] Quitoriano, N.J. & Kamins, T.I., 2008. Integratable nanowire transistors. Nano letters, 8(12), p.4410-4414.

P-Th-084

Bond length effects during the dissociation of O₂ on Ni(111)Ian Shuttleworth¹¹Nottingham Trent University, Nottingham, United Kingdom

The interaction between O₂ and Ni(111) has been investigated using spin-polarised density functional theory. A series of low activation energy (103 to 315 meV) reaction pathways corresponding to precursor and non-precursor mediated adsorption have been identified. It has been seen that a predominantly pathway-independent correlation exists between O-Ni bond order and the O₂ bond length. This correlation demonstrates that the O-O interaction predominantly determines the bonding of this system.

P-Th-085

The role of dual perimeter catalytic sites of metal on metal oxide support

Pussana Hirunsit¹, Masahiro Ehara^{2,3}, Kajornsak Faungnawakij¹

¹National Nanotechnology Center (NANOTEC), Patumthani, Thailand, ²Institute for Molecular Science (IMS), Okazaki, Japan, ³Kyoto University, Kyoto, Japan

The catalytic activity of supported metal nanoparticles depends on the metal-support interaction and the metal particle size. This work theoretically elucidates the role of the interface perimeter site between metal cluster and the metal oxide support using density functional theory (DFT) calculations. We particularly focus on the Ag cluster and alumina support, Ag/ θ -Al₂O₃(110), for H₂ activation[1] and Cu cluster on Cr₂O₃(001), MnO(200) and Fe₃O₄(311) for methoxy dehydrogenation[2] which is the key rate-limiting step of methanol steam reforming (MSR). The heterolytic cleavage of both reactions is thermodynamically and kinetically preferred compared with that on pure metal catalyst. For the H₂ activation on Ag/ θ -Al₂O₃(110), the examined factors which potentially influence H₂ activation at the dual perimeter site including the low coordination and the intrinsic reactivity of Ag atoms, the role of the alumina support, and the hydroxylation of the alumina support are discussed. The calculation results also clearly demonstrate the significance of the dual catalytic sites of Cu and metal oxides for methoxy dehydrogenation and how metal oxide species has an impact on MSR catalytic activity.

[1] Hirunsit, P., et al., Cooperative H₂ Activation at Ag Cluster/ θ -Al₂O₃(110) Dual Perimeter Sites: A Density Functional Theory Study. The Journal of Physical Chemistry C, 2014. 118(15): p. 7996-8006.

[2] Hirunsit, P. and K. Faungnawakij, Cu-Cr, Cu-Mn, and Cu-Fe Spinel-Oxide-Type Catalysts for Reforming of Oxygenated Hydrocarbons. The Journal of Physical Chemistry C, 2013. 117(45): p. 23757-23765.

P-Th-087

CO Desorption of MgO/Mo(001) Revisited – a TPD Study Combined with STM

Stefanie Stuckenholtz¹, Christin Büchner¹, Markus Heyde¹, Hans-Joachim Freund¹

¹Fritz-Haber-Institut der Max-Planck-Gesellschaft, Berlin, Germany

The desorption of CO from MgO(001) has been studied in the past decades in great detail, still there is an ongoing debate about the exact desorption energies between theory and experiment.[1] The CO desorption of MgO(001) serves as a model for the interaction of CO with an ionic surface.[1] To study this reaction, a model catalysis system of thin MgO films on Mo(001) was used. Magnesium oxide (MgO) is a widely studied model catalyst due to its AB composition and the simple rock salt crystal structure. Our ultra-high vacuum (UHV) setup contains a combined scanning tunneling microscope (STM) and noncontact atomic force microscope (nc-AFM) operated at 5 K. Additionally, the setup includes a new temperature programmed desorption (TPD) setup working at low temperatures ($T(\text{min}) < 20 \text{ K}$), specially constructed for a portable sample design. With this setup we are able to image the same sample before and after TPD experiments. Here, the desorption of CO from MgO/Mo(001) films of different thickness has been studied. Additionally, the morphology of the samples was studied with STM. The desorption peak positions of earlier studies could be confirmed and we could show with our setup that the surface structure is stable during experiments.[2, 3] The presented results combine the available TPD data on the CO desorption from the MgO(001) surface with STM data and augment the findings from literature.

[1] A. D. Boese, J. Sauer, Phys. Chem. Chem. Phys. 15, 16481 (2013).

[2] R. Wichtendahl, M. Rodriguez-Rodrigo, U. Härtel, H. Kuhlenbeck, H.-J. Freund, Phys. Status Solidi A 173, 93 (1999).

[3] Z. Dohnálek, G. A. Kimmel, S. A. Joyce, P. Ayotte, R. S. Smith, B. D. Kay, J. Phys. Chem. B 105, 3747 (2001).

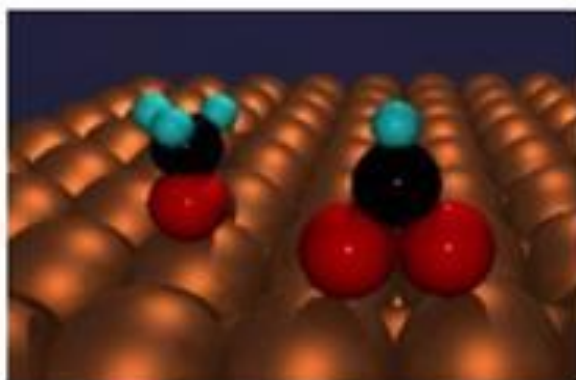
P-Th-088

Ligands vs Ensembles in Catalysis and Surface Reactivity – the d-band theory challenged

Michael Bowker¹, Neil Perkins¹

¹Cardiff Catalysis Institute, Cardiff University, Cardiff, United Kingdom

Orthodoxies abound in science and this includes catalysis and surface science. One of the latest is the d-band theory of surface reactivity and catalysis. The theory basically states that reactivity scales with the energetic position and the width of the d-band. I will give an example which shows that a delocalised d-band theory does not properly describe the reactivity pattern for alloys. I will show that for the Cu-Pd alloy system, the reactivity is mainly dictated by ensemble effects and that the local chemical identity of the two alloy components DOMINATES the reactive behaviour. The examples chosen to illustrate this proposal are the reactivity of ethanol and formic acid with single crystal Cu-Pd alloy surfaces. These form ethoxy and formate surface intermediates of very different stability from each other, and each with different stability and decomposition mechanisms on the two individual metals.



P-Th-089

H-Abstraction from Methane in H-ZSM5 Zeolite

Maria Rutigliano¹, Nico Sanna³, Amedeo Palma²¹CNR-Nanotec, Bari, Italy, ²CNR-ISMN, Roma Monterotondo, Italy, ³CINECA, Roma, Italy

The interaction of methane with an extra-framework oxygen atom in acidic Zeolite (H-ZSM5) porous substrate has been investigated by means of Density Functional Theory plus Dispersion energy calculations and reaction path has been obtained exploiting Climbing Image Nudged Elastic Band method (c-NEB). Zeolite was modelled by its crystallographic structure subject to periodic boundary condition. Relaxation of the zeolite cage is fundamental for a correct energetics. The reaction path for the H - abstraction reaction of methane, in presence of an open shell oxygen atom within the zeolite along (010) straight channel leads to the formation of a slightly distorted H₂O water molecule and CH₃ radical. These in bulk calculations support the interesting idea that open shell systems, involving an extra cage Oxygen atom, favour the H-abstraction from small hydrocarbons.

P-Th-090

Influence of step sites in the water-gas shift reaction on copper surfaces

Hector Prats Garcia¹, Leny Álvarez¹, Pablo Gamallo¹, Francesc Illas¹, Ramón Sayós¹

¹Universitat De Barcelona, Barcelona, Spain

The water-gas shift reaction (WGSR: $\text{CO} + \text{H}_2\text{O} \rightarrow \text{CO}_2 + \text{H}_2$, $\Delta_r H^0 = -41.2$ kJ/mol, 298.15 K) is an industrial important reaction for H_2 production, where iron oxide-based and copper-based catalysts are used at high- and low-temperature stages, respectively. Metallic copper is a typical benchmark catalyst for this reaction; however, a more detailed exploration of the molecular mechanism of the WGSR catalysed by Cu including the effect of step sites on the calculated energy profiles seems necessary. To this end, Density Functional Theory calculations have been carried out using a Cu(321)-stepped surface, which has different low-coordinated atoms and includes a rather high heterogeneity of adsorption sites (such as terraces, nearby kinks and steps), being obviously less stable than the Cu(111) low Miller index surface studied previously by Mavrikakis et. al and in a recent work by our research group, but provides a more realistic model of the real catalysts. With this surface model, we consider the same reaction scheme of Fajin et al., using a 2x2 supercell to study the adsorption energies at low-coverage limit with the PBE functional, including also the effect of van der Waals (vdW) interactions, and adding new processes like the diffusion of the main adsorbates or adsorption of the reactants on other sites, which are necessary to understand the kinetics of the WGSR reaction over Cu(321) via new kMC simulations. Finally, we compare the energetics of the WGSR and the results of these kMC simulations for both the plane Cu(111) and the stepped Cu(321) surfaces. Conclusions and comparison with the available experimental data will be presented at the meeting.

P-Th-091

Atomic and electronic structure of guanine on Ge(100)

Do Hwan Kim¹, Young-Sang Youn², Hye Jin Lee³

¹Daegu University, Gyeongsan, South Korea, ²Korea Atomic Energy Research Institute, Daejeon, South Korea, ³Kyungpook National University, Daegu, South Korea

We investigated the chemical reaction of guanine molecule with Ge(100) surface using density functional theory (DFT) calculations and scanning tunneling microscopy (STM) observation. Focusing on the multifunctionality of guanine molecule, possible reaction pathways through each functional group were compared. Competitive reaction among the different reaction sites in guanine may lead to either mono- or multi- dentate product. The calculations reveal that the C=O dative bonded structure following N-H dissociation is the most stable among the possible adsorption configurations. The N-H bonding at N1 position is the most favorable N-H dissociative reaction site. The experimentally observed STM features were explained on the basis of the electron charge density around the adsorbed guanine molecules and the reacting Ge atoms.

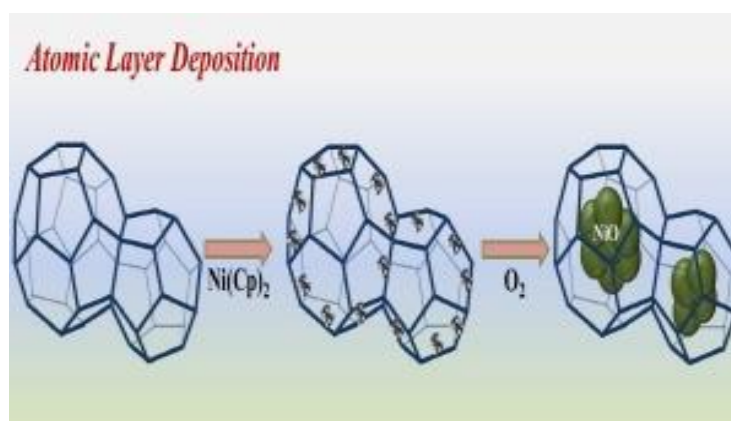
P-Th-092

Surface modification of mesoporous chromium terephthalate MIL-101 with NiO nanoparticles via atomic layer deposition

Myung-Geun Jeong¹, Dae Han Kim¹, Ju Ha Lee¹, Sang Wook Han¹, Eun Ji Park¹, Bo Ra Kim¹, Soong Yeon Kim¹, Il Hee Kim¹, Ki Jung Park¹, Young Dok Kim¹

¹Department of Chemistry, Sungkyunkwan University, Suwon-si, South Korea

The porous chromium terephthalate MIL-101 was modified with NiO nanoparticles via atomic layer deposition (ALD) using bis-(cyclopentadienyl)nickel ($\text{Ni}(\text{Cp})_2$) as a metal precursor and oxygen as an oxidizing agent, respectively. NiO-modified MIL-101(Cr) with various ALD cycles were characterized by transmission electron microscopy (TEM), N_2 and Ar isotherm, X-ray photoelectron spectroscopy (XPS), inductively coupled plasma-atomic emission spectroscopy (ICP-AES) and thermal gravimetric analysis (TGA). We provide compelling evidence that the deposited NiO nanoparticles were distributed inside internal mesoporous cages as well as on the external surface of MIL-101(Cr). From insight into surface chemistry, NiO ALD did not affect the chemical state of coordinatively unsaturated metal sites in the MIL-101(Cr) and accompanied the slight accumulation of residual carbon by a ligand of $\text{Ni}(\text{Cp})_2$ precursor. The deposited NiO nanoparticles enhanced the thermal stability of MIL-101 and provided catalytic activity for CO oxidation. In conclusion, we suggest that ALD can be an effective and versatile strategy for enhancing chemical competency of metal-organic-framework (MOF) and providing new functionality to them.



P-Th-093

Encapsulation on Pd- and Pd-Au on TiO₂(110)Michael Bowker¹, Ryan Sharpe¹¹Cardiff Catalysis Institute, Cardiff University, Cardiff, United Kingdom

The effect of sputtering, annealing and oxidation on the surface properties of TiO₂(110), and on the same surfaces with nanoparticles present, has been investigated. The clean crystal sputters to leave a very reduced surface with Ti²⁺ as the dominant species, but when annealed in vacuum, the surface is mainly Ti^{3+,4+}. Oxidation reduces the surface Ti³⁺ considerably. When Pd nanoparticles are present on all the titania surfaces, then the particles become encapsulated by a film of titanium oxide, and this is particularly noticeable in ISS where the Pd:Ti ratio drops by a factor of 300 after annealing to 750 K, indicating complete coverage of the Pd nanoparticles by the oxide film. This happens most easily for the nanoparticles deposited on the reduced surfaces (beginning at ~673K), but even occurs for the very oxidized surface, but at 100K higher in temperature. Thus reduced Ti from the subsurface region can migrate onto the Pd surface to form the sub-oxide, the sub-oxide being a thin TiO-like layer. When we form Au/Pd layers on the surface then the effects of thermal treatment depend strongly on the preparation method. The surfaces prepared tend to be dominated by Au after annealing, and for these encapsulation is suppressed.

P-Th-094

Effect of SrWO₄ Micro/Nanostructures morphology on the Photodegradation of Rh B

Nadine Dirany¹, Sylvie Villain¹, Jean Raymond Gavarri¹, Madjid Arab¹

¹Université De Toulon- IM2NP UMR CNRS, La Garde, France

During recent years, tungstate Strontium scheelite structure have been extensively studied because of their properties and potential applications in various field, particularly the catalysis and the photocatalysis. These properties and associated applications depend on the size and morphology of the individual particles. The aim of this work is to see the influence of the micro - nanocrystals morphologies on photocatalytic transformation/ decomposition of Rhodamine B (and blue mythelene) in aqueous medium. For that, we synthesized strontium tungstate SrWO₄ (SWO) micro-nanostructures with two morphologies including spindles and spheres. The SWO powders have been synthesized at room temperature with aqueous mineralization processes. All obtained samples were characterized by X-ray diffraction XRD, Scanning electron microscopy SEM to identify the structure and the morphology. XRD and SEM results demonstrate that the as obtained SrWO₄ particles are high purity, well crystallized and exhibit a relatively uniform morphology. The photocatalytic activities were conducted for the two morphologies under UV excitation and reported as a function of time and concentration. The photodegradation reactivity was discussed as a function of the morphology and the crystallization degrees. The influence of calcination temperature on photocatalytic activities of the tetragonal SrWO₄ for two morphologies was investigated within the limits of the stability of the morphology.

P-Th-095

In situ study of oxide supported gold nanoparticles by surface X-ray scattering techniques

Venkatesan Dhanasekaran¹, Andrea Resta¹, Beri Mbenkum³, Yves Garreau^{1,2},
Alessandro Coati¹, Alina Vlad¹

¹Synchrotron SOLEIL, L'Orme des Merisiers, Saint Aubin, France, ²Université Paris Diderot, Sorbonne-Paris-Cité, MPQ, UMR 7162 CNRS, France,
³NANOARC Ltd., NanoArchitecture & Consulting, New Zealand

Gold nanoparticles have been extensively studied for their high catalytic activity in CO oxidation reaction. The preparation technique of the nanoparticles and the type of support has great impact on the catalytic behavior of the system. To effectively monitor the effect of size on CO oxidation, we study gold nanoparticles synthesized by micelle nanolithography, a technique well adapted to yield minimal size distribution of nanoparticles. Here, we synthesized 3nm and 15nm gold nanoparticles using the micelle nanolithography technique. To achieve monodisperse metal-loaded micelles on MgO (001) substrates we employ spin-coating and observe quasi-hexagonal ordered micelles in the SEM. Atomic oxygen and hydrogen were used to remove the polymer and reduce the gold ions and enable, nanoparticle formation. We made a systematic approach to study the effect of atomic hydrogen and oxygen during the formation of the nanoparticles by means of surface X-ray scattering techniques at SixS Beamline, Synchrotron SOLEIL, France. Grazing incidence X-ray diffraction (GIXRD) was used to determine the crystalline nature of the nanoparticles and their lattice constants. 3nm gold particles formed using atomic hydrogen, annealed at 700°C showed (111) epitaxy on MgO (001) substrate, which was not observed for the nanoparticles formed using atomic oxygen. In addition, x-ray reflectivity (XRR) and grazing incidence small angle x-ray scattering (GISAXS) techniques were used to complement the diffraction data. The activity of these nanoparticles towards the CO oxidation is under investigation using a flow reactor at SixS Beamline, Synchrotron SOLEIL.

P-Th-096

This paper has been withdrawn by the author.

P-Th-097

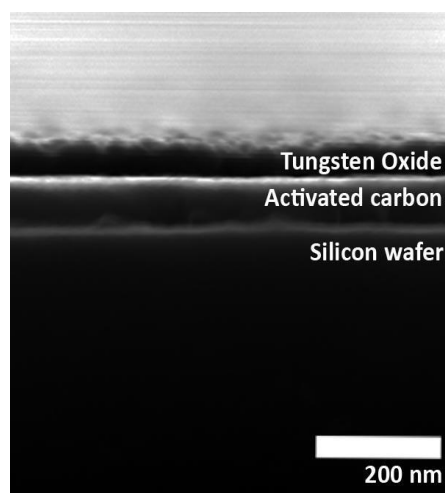
Methanol oxidation over pure and pt-doped tungsten oxide supported on activated carbon

Jan Polášek¹, Karel Mašek¹, Viktor Johánek¹, Anna Ostroverkh¹, Vladimír Matolín¹

¹Charles University in Prague, Prague, Czech Republic

Hydrogen production via methanol decomposition to H₂, CO and CO₂ is studied not only as model reaction but also for its practical uses, for example in direct methanol fuel cells. In this work, we examine both pure and Pt-doped tungsten oxide as a catalyst for hydrogen production by partial methanol oxidation.

Tungsten oxide, both pure and doped with platinum was prepared by reactive magnetron sputtering on silicon and activated carbon substrates. Activated carbon substrate was prepared by magnetron sputtering and subsequent etching in the oxygen plasma. Temperature programmed reaction (TPR) of MeOH and O₂ in microreactor system was used to measure catalytic activity and selectivity to the production of hydrogen and carbon monoxide/dioxide. Samples surface and porosity were characterised by nitrogen adsorption. Their composition, chemical state and morphology were investigated before and after reaction with x-ray photoelectron spectroscopy (XPS) and scanning electron microscopy. TPR on pure tungsten oxide showed that presence of activated carbon as a substrate led not only to increased activity towards hydrogen production, but also to lower ratios of unwanted carbon monoxide and dioxide to the hydrogen production. We found that while using carbon as a support, lower amount of deposited tungsten oxide led to higher overall catalytic activity. XPS showed no significant changes in the chemical state of the sample before and after the TPR. Presence of small amount of platinum in the tungsten oxide led to the increased production rate of hydrogen, but also higher fraction of carbon monoxide/dioxide in the products. This reaction needed some time to stabilize as the sample undergoes chemical changes during this stabilisation phase. Platinum present as PtO and PtO₂ after preparation is reduced to its metallic state and strong interaction between platinum and tungsten oxide can be seen by XPS after this reduction.



P-Th-098

STM Study of Chirality Transfer Complexes on Pt(111)

Yi Dong¹, Jean-Christian Lemay¹, Peter McBreen¹¹Laval University, Québec, Canada

Adsorbed chiral molecules (chiral modifiers) can interact stereoselectively with prochiral co-adsorbates on reactive metal surfaces (1). This is used in one of the most common methods to perform asymmetric heterogeneous catalysis. The chiral modifier provides stereoselection through non-covalent assembly with a substrate, forming isolated complexes with well-defined geometries. We will present a variable temperature STM study of individual bimolecular complexes formed by enantiopure adsorbates and three representative prochiral substrates on Pt(111). The results reveal sub-molecularly resolved and time-resolved stereospecific data for competing complexation geometries. Time-lapsed STM measurements of individual substrate molecules sampling a set of interaction geometries provide new insight on the dynamics of stereocontrol. The results reveal that a single prochiral substrate can probe various sites on the surface due to diffusion and prochiral switching. This shows the importance of considering interconversion between complexation geometries to fully understand the stereocontrol operated by the chiral modifier.

P-Th-099

Initial oxidation behavior of Ni₃Al (210) surface induced by supersonic oxygen molecular beam at room temperature

Ya Xu¹, Junya Sakurai¹, Yuden Teraoka², Akitaka Yoshigoe², Masahiko Demura¹, Toshiyuki Hirano¹

¹National Institute for Materials Science, Tsukuba, Japan, ²Japan Atomic Energy Agency, Sayo-cho, Japan

The initial oxidation behavior of a clean Ni₃Al (210) surface was studied at 300 K using a supersonic O₂ molecular beam (O₂ SSMB) having an O₂ translational energy of 2.3 eV, and real-time photoemission spectroscopy performed with high-brilliance synchrotron radiation. The evolution behaviors of the O 1s, Ni 2p, Al 2p, and Ni 3p spectra were examined over time during irradiation with the O₂ SSMB. The spectral analysis revealed that both the Al atoms and the Ni atoms on the surface were oxidized; however, the oxidation of Al progressed much faster than that of Ni. The oxidation of Al began to occur at an oxygen coverage of 0.26 monolayer (ML) (1 ML was defined as the atomic density of the Ni₃Al (210) surface) and saturated at an oxygen coverage of 2.5 ML. In contrast, the oxidation of Ni commenced at an oxygen coverage of 1.6 ML and slowly progressed to saturation, which occurred at an oxygen coverage of 4.9 ML. Further, the thickness of the Al oxide layer was estimated to be 3.9 Å, while that of the Ni oxide layer was 1.6 Å at the final saturated oxygen coverage.

P-Th-100

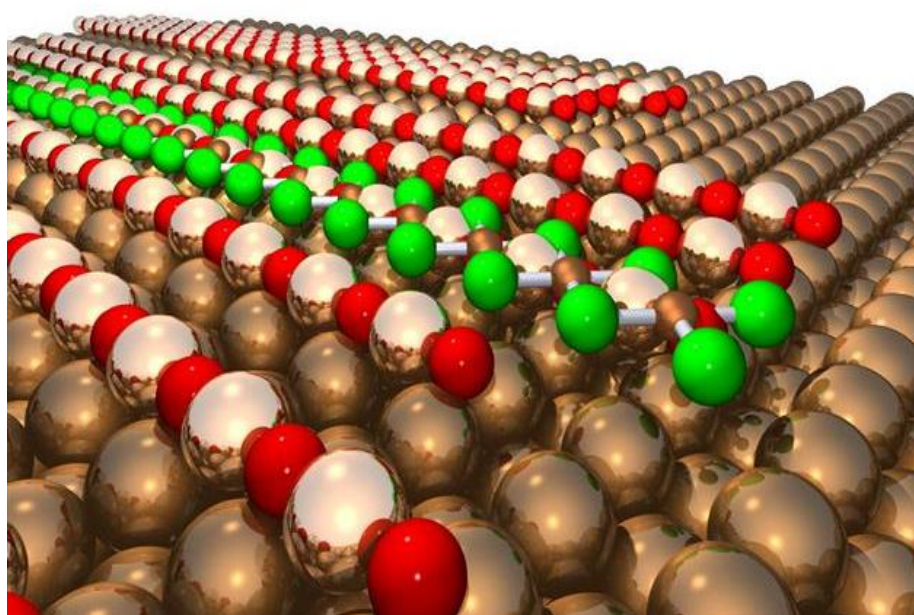
An STM/XPS study of the oxychlorination of Cu(111) and Cu(110) surfaces

Hatem Altass¹, Philip Davies³, Albert Carley²

¹ Umm Aquraa University, Makkah, Saudi Arabia, ²Cardiff University, Cardiff, UK, ³Cardiff University, Cardiff, UK

The reaction of chlorine containing molecules with copper is relevant to a number of industrially important reactions including the Deacon process, an important route by which HCl from waste streams can be converted into chlorine gas. The Deacon process is catalysed by a copper chloride/copper oxide catalyst but the mechanism remains controversial at least partly because of our incomplete understanding of the behaviour of copper chloride surface phases. Similarly, polychlorinated dibenzo-p-dioxins (PCDD), and polychlorinated dibenzo-furans (PCDF) (referred to collectively as PCDD/F's) are known to be generated during combustion processes and over copper surfaces on carbon fly ash particles. PCDD/F's are environmentally harmful compounds and there is considerable debate on the mechanism and the nature of the copper phases involved

We are investigating the role of surface oxygen in determining the chloride phases formed at copper single crystals. On Cu(110) a new short lived Cu(II) surface phase was identified (Fig 1.) which may account for some aspects of the unusual catalytic behaviour of the copper chlorides. The present work discusses the chloride phases formed on Cu(111) surfaces and compares reactivity and stability to those observed on Cu(110).



Index of authors

Plenary speakers

Flores, Fernando	Pg. 13
Friend, Cynthia	Pg. 11
Salmerón, Miquel	Pg. 09
Wodtke, Alec M.	Pg. 10
Xue, Qi-Kun Xue	Pg. 12

Oral presentations and posters

A

Abadía, Mikel	P-Mo-086, P-Tu-023, We-C08	Alonso Carnicero, José M.	Th-E11
Abakay, Eray	P-Tu-105	Alonso, Gerard	P-Tu-088
Aballe, Lucía	Mo-E05, Mo-A03, Th-B12, P-Mo-082	Alperovich, Vitaly	P-Tu-097
Abb, Sabine	P-Tu-044, P-Tu-074, Th-A05, Th-C20	Al-Salik, Yahya	Mo-E01+02
Abdollahi, Amir	Th-B04	Altass, Hatem	P-Th-100
Abdulmawla, S.T.A.	P-Th-043	Altshuler, B. L.	Mo-A14
Abel, Mathieu	P-Tu-026, P-Tu-064, P-Tu-067	Álvarez, Leny	P-Th-090
Abufager, Paula	Tu-C06	Amati, Matteo	Mo-E07
Acres, Matthew	Th-E13	Ammon, Maximilian	Mo-C08, P-Tu-047, Th-C09
Acres, Robert G.	Tu-E15	Anazawa, T.	P-Mo-070
Adachi, Koshi	We-E07, We-E08, We-E09	Anders, Frithjof	Tu-C02
Adler, Florian	Mo-D16	Andersen, Jesper N	Mo-B06, Mo-B10
Aebi, Philipp	Tu-C15	Andersson, Martin P.	Mo-C11, Tu-D19, Tu-D20, Th-E15, P-Th-030
Affronte, Marco	Tu-A06	Ando, Yasunobu	P-Mo-017, Tu-B19
Africh, Cristina	Th-A19, Th-A23+24	Anemone, Gloria	P-Mo-009
Aghamohammadi, Mahdieh	We-B01+02	Angurell, Inma	Mo-E05
Agnello, Simonpietro	P-Tu-054	Antczak, Grażyna	Tu-D05, P-Tu-016
Agnoli, Stefano	Th-A11	Aochi, Joji	Th-C01
Åhlund, John	Tu-D09, P-Tu-040	Apolloner, Florian	We-E03
Ahmadi, Sareh	Mo-B02	Appelfeller, Stephan	P-Th-021
Ahmed, Mahmoud	Tu-B04	Aprojanz, Johannes	P-Mo-020
Ahn, Seong Deok	P-Mo-016	Arab, Madjid	Th-A06, P-Th-094
Aiglinger, Markus	Tu-C18	Arafune, Ryuichi	Mo-D12, Th-D17
Aitchison, Hannah	Th-C16	Ardini, Jacopo	Mo-E14
Ajiasaijian, Xxx	P-Tu-101, P-Tu-104	Argent, Stephen	Th-C12
Akaishi, Akira	P-Mo-013, Th-A02	Ariga, Hiroko	Th-B22, Th-B23
Akhmatov, Zeitun	P-Tu-078, P-Th-044	Arita, M	P-Th-017
Akhtar, Mohammad Waseem	We-B04	Arkharova, Irina	P-Mo-007
Akiba, Chisato	Th-E09	Arman, Mohammad A.	Mo-B10, Tu-B01
Al Ghamdi, Hamdan	Mo-E01+02	Arnarson, Logi	Mo-E12
Al Taleb, Amjad	P-Mo-009	Arnau, Andrés	Tu-C01, Tu-A03, P-Tu-008
Albani, Marco	Tu-D07	Arrigo, Rosa	Tu-D10
Alberti, Mariza N.	P-Tu-001	Aruga, Tetsuya	Mo-D04
Alcami, Manuel	Mo-A07, Tu-C01, We-C07	Aruta, Carmela	Tu-B09+10
Aldahhak, Hazem	P-Tu-082, Th-E22	Arvanitis, Dimitri	Tu-C03, P-Tu-017
Aleman, P.	P-Th-023	Asakawa, Kanta	Tu-B06, Tu-B20
Alexandrowicz, Gil	Tu-D02, We-D11, Th-B24	Asakura, Kiyotaka	Th-B22, Th-B23
Alfè, Dario	Tu-A20	Asano, Masato	Th-E08
Allam, Omar	P-Mo-032	Asanov, Igor	P-Mo-001, P-Mo-060
Alleg, Safia	P-Mo-056	Asanova, Tatiana	P-Mo-001
Allegretti, Francesco	Tu-E15	Asanova, Tatyana	P-Mo-060
Allison, William	Tu-D02, We-E04	Asaoka, Hidehito	We-E02
		Asensio, Maria Carmen	P-Th-023
		Ataman, Evren	Th-E15
		Atanasova, Genoveva	P-Th-072
		Ataran, Sara	Mo-B11
		Atkinson, Paola	Tu-D01
		Aufray, Maëlen	Th-C05
		Aulbach, Julian	Mo-D16

Aulická, Marie
Aupiais, Ian
Aureau, Damien

Aureau, Damien
Auroux, Aline
Auwärter, Wilhelm
Auwärter, Willy
Avila, J.
Ayadi, Khaled
Ayazi, Masume
Ayotte, Patrick

Azzaza, Sonia

B

Bábor, Petr
Babutzka, Martin
Bachari, Khaldoun
Bachelier, Nicolas
Backofen, Rainer
Bagués, Núria
Bagus, Paul
Bahr, Stephan
Bai, Shandan

Bairagi, Kaushik
Balaban, Silviu
Baldanza, Silvia
Baldelli, Steve
Balestrino, Giuseppe
Baletto, Francesca
Baljović, Miloš
Ballav, Nirmalya
Balmes, Olivier
Balog, Richard
Bamroongwongdee, Chanut
Bánsági, Tamás
Baraldi, A.
Baraldi, Alessandro
Barcaro, Giovanni
Baringhaus, Jens
Barja, Sara

Barrena, Esther

Barreto, Lucas
Barrett, Nick
Barros, Angélica
Barros, Heloise Ribeiro de
Barth, Clemens
Barth, Johannes

Barthélémy, Agnès
Bartos, I.
Bartošík, Miroslav

Basagni, Andrea
Battaglini, Nicolas
Battiato, M.
Battiato, Marco
Baum, Sebastian
Bayrachniy, Boris
Bazarnik, Maciej
Béger, Miroslav
Belhaj, Mohamed
Belhiteche, El Hadi
Belianinov, Alex
Bellec, Amandine

Tu-B15
P-Mo-036
P-Mo-079, P-Tu-011,
Th-E07
P-Mo-051
P-Th-061
Tu-E15
Tu-A18, We-C07
P-Th-023
P-Tu-080
P-Tu-050
Tu-E05, Th-B24,
P-Tu-106
P-Mo-056

P-Th-083
P-Th-013
P-Th-070
Tu-C06
Tu-D07
Th-B03, P-Mo-072
Th-B14
Th-B11
We-E07, We-E08,
We-E09
Th-C22
P-Tu-026
Mo-E14
Tu-B04
Tu-B09+10
Tu-E03+04
We-A04
Tu-C16, We-A04
We-D03
P-Mo-023, Tu-A24
Mo-E11
P-Th-069
We-C11
Tu-A20
Tu-B17
P-Mo-020
Mo-A07, Tu-C01,
Tu-A03
Tu-C03, We-B01+02,
Th-C11
Th-D11
Th-B05
P-Mo-075
P-Th-007
P-Tu-014, P-Th-067
Tu-E15, Tu-A18,
We-C07
Mo-B05
P-Th-035
P-Mo-029, P-Mo-030,
P-Tu-107
Th-A09, Th-A11
Th-C19
Th-D23
P-Th-027
P-Tu-079
P-Th-076
Mo-C09, P-Tu-036
P-Th-058
Tu-B23
P-Tu-056
Tu-B09+10
Th-C22

Belloni, Jaqueline
Benada, Amel
Benedek, Giorgio
Bengiό, Silvina
Benitez Lara, Alfredo
Benitez, Francesc
Benlekhal, Djamel

Bensebaa, Nadia
Berenguer Murcia, Ángel
Bergamaschini, Roberto
Berger, Claire

Berger, H.
Berger, Jan
Bergvall, Anders
Berkó, András
Bermúdez, María Dolores
Berthold, Theresa
Berti, Giulia
Bertoglio, Maxime
Bertram, Cord
Bertram, Florian

Bertrand, Francois
Bespalov, Ivan

Bettermann, Hendrik
Bettini, Eleonora
Biagi, Roberto
Biberian, Jean-Paul
Bibes, Manuel
Bidermane, Ieva
Bielen, Abraham A. M.
Bieloshapka, Igor
Bihlmayer, G.
Bijkerk, F.
Bijkerk, Fred
Binks, David
Bischoff, Felix
Björk, Jonas
Black, Andrés
Blaha, Peter
Blanc, Nils
Blanco, Cristina
Blank, Vladimir
Bliem, Roland
Bliev, Aleksandr
Blomberg, Sara
Blumenschein, Felix
Blunt, Matthew
Bobrov, Kirill
Bochkov, Victor
Bocquet, Franck
Bocquet, Francois
Bocquet, Marie-Laure
Boeckmann, Hannes
Boeglin, Alex
Boehm, Ryan D.
Bohr, Jakob
Bolou, Hervé
Bondino, Federica
Bongiorno, Angelo
Borek, S.
Borek, Stephan
Borg, Anne
Borghetti, Patrizia
Borisov, Andrei

Boroznin, Sergei

P-Mo-052
P-Th-061
We-E03
P-Th-002
P-Mo-094
P-Tu-049, P-Tu-057
P-Mo-044, P-Tu-003,
P-Tu-085
P-Mo-056
P-Tu-098
Tu-D07
Th-A22, P-Mo-020,
P-Mo-006
Th-D23, P-Th-023
P-Th-036
Tu-A25
Tu-E23
We-E11
P-Th-041
We-A09
Mo-B07
Tu-D02
Mo-B02, Tu-E16,
Th-06, Th-B15
Tu-C14
Mo-E10, P-Mo-077,
P-Th-064
P-Tu-083
P-Mo-055
Tu-A06, Tu-A07
Mo-B07
Mo-B05
P-Tu-009, P-Tu-040
Th-E11
P-Mo-043
Th-D22
P-Th-051
P-Mo-014, P-Tu-102
We-B09
Tu-E15, Tu-A18
Tu-C16, Th-C10
Tu-A03
P-Mo-077, Th-E19
Th-A20
Tu-A09
P-Th-057
Th-E19
P-Tu-043
Mo-B11, Tu-E07
Tu-A25
Th-A12, Th-C12
Th-C15
P-Mo-065
P-Tu-067
Tu-A12
Tu-C06
Tu-C10
Mo-D14
P-Tu-059
Tu-D16
Mo-D14
We-B08, Th-A11
Tu-B09+10
Th-D14, P-Th-016
Mo-A04
Tu-E17
Mo-C03+04
Tu-A17, Tu-D01,
P-Th-046
P-Mo-003, P-Mo-004,
P-Mo-005, P-Mo-024

Botton, Julien	P-A09-026	Caputo, Marco	Mo-A09, Th-D20
Bouizem, Yahia	P-Mo-044, P-Tu-003, P-Tu-085	Carbonell, Eduard	P-Mo-023
Boumaour, Messaoud	P-Mo-050	Cardenas, Luis	Tu-C14
Bourgeois, Sylvie	We-D09	Carla, Francesco	Th-E06
Bouttemy, Muriel	P-Mo-051, P-Tu-011	Carley, Albert	P-Th-100
Bovet, Nicolas	P-Tu-D16, Tu-D20	Carlomagno, Ilaria	We-D04
	Th-E15	Carlsson, Per-Anders	We-D03
Bowker, Michael	Mo-E11, P-Th-088, P-Th-093	Carraro, Giovanni	Th-A16
Bozhko, S.	Mo-A14	Carrétéro, Cécile	Mo-B05
Bracco, Gianangelo	Th-A16	Carrillo López, Jesus	P-Mo-094
Brackmann, Christian	Tu-E07	Casanovas, Albert	Mo-E06
Brahmi, Yamina	P-Tu-003, P-Tu-085	Casarin, Maurizio	Th-A09
Brambilla, Alberto	Mo-B01, P-Mo-084, Tu-D03, We-A09	Casey, Patrick	P-Th-022
Brandbyge, Mads	Tu-A18	Cassidy, Andrew	Tu-A26
Brandt, O.	P-Th-035	Castellanos-Gómez, Andrés	Mo-A15
Braun, J.	Th-D14, Th-D23, P-Th-016	Catalan, Gustau	Th-B03, P-Tu-095, Th-B04
Braun, Jürgen	Mo-A04	Catena, Alberto	P-Tu-054
Braun, Lukas	Mo-A10	Catrangiu, Adriana-Simona	P-Th-078
Brena, Barbara	Mo-A08, P-Mo-049, P-Tu-009, P-Tu-040	Cattelan, Mattia	Th-A09, Th-A11
Brion, Antón	Tu-E16, P-Tu-092	Cavalleri, A.	P-Mo-008
Bronsch, Wibke	P-Tu-079, Th-C18	Cazorla-Amoro, Diego	P-Tu-098
Bronstein, Hugo	Th-A12	Ceballos, Gustavo	P-Mo-022, Th-A15, Th-A17
Brookes, Catherine	Mo-E11	Ceccato, Marcel	Th-E15
Brovko, Oleg	We-A02	Cechal, Jan	P-Mo-088, P-Th-083
Brown, Matthew	Tu-D11, P-Th-031	Celasco, Edvige	Th-A16
Brückner, Sebastian	P-Th-041	Celis Retana, Arlensiú E.	Tu-A23, P-Mo-006
Bruix, Albert	Tu-E08	Cepek, Cinzia	Th-A19
Brumboiu, Iulia Emilia	P-Mo-049	Cernicharo, Jose	Th-A01
Brun, Christophe	Mo-A14	César, Rodrigo	P-Mo-075
Buchholz, Maria	P-Mo-090	Cesura, Federico	Tu-C25+26
Büchner, Christin	We-D07, P-Th-087	Cháb, Vladimír	P-Mo-034
Buck, Manfred	Th-C16	Chabi, Thauanza	P-Mo-056
Budi, Akin	Mo-C11	Chacon, Cyril	Th-C22, P-Mo-035
Buga, Sergei	P-Th-057	Chahed, Larbi	P-Tu-003, P-Mo-044
Bugenhagen, Bernhard	Mo-C09		P-Tu-085
Bugnon, P.	Th-D23	Chalasanani, Rajesh	Tu-C25+26
Buhr, Sebastian	P-Mo-077	Champness, Neil	Th-C12
Burghard, Marko	Th-A05	Chanwattanakit, Jarussri	P-Th-004
Burson, Kristen	We-D07	Chapman, R. T.	P-Mo-008
Buske, Christian	P-Th-032	Chavadej, Sumaeth	P-Th-004
Buss, Felix	We-B01+02	Chekulaev, Dimitri	Tu-B04
Bussetti, Gianlorenzo	We-A09	Chellal, Khalida	P-Th-070
		Chen, Mingshu	Tu-E11
		Chen, Po-Hung	We-A03
		Chen, Ying	Th-A12
		Chen, Zongping	Tu-A06
		Cheng, Han-Te	Th-D06
		Chérioux, Frédéric	We-C10
		Cherkez, Vladimir	Mo-A14
		Chernov, S.	Th-D14
		Chettibi, Sabah	P-Tu-096, P-Th-073
		Chevallier, Virginie	Th-A06
		Cheynis, Fabien	Th-D05
		Chiechi, R.C.	P-Tu-065
		Chifiriuc, Mariana Carmen	P-Tu-059
		Chikyow, Toyohiro	P-Mo-061
		Chirolli, Luca	Mo-A15
		Chiter, Fatah	Th-E14
		Chitu, Adrian	P-Th-049
		Cho, Doo-Hee	Th-C06
		Cho, Il-Joo	We-E10
		Cho, Nam Sung	Th-C06
		Cho, Yasuo	Th-A21, P-Th-040
		Choi, Joong Il Jake	Mo-B18
		Choi, Juhee	Mo-B11
		Choi, Kyungho	P-Tu-048
		Choi, Sung-Wook	P-Tu-048
		Choi, Youngjin	P-Tu-048
		Chong, Michael	Mo-D14
Cabo, Antonija Grubisic	Tu-A24		
Cabrera-San Félix, Pepa	Tu-E16, P-Tu-092		
Cacho, C.	Th-D23		
Cacho, Cephise	P-Mo-008, P-Th-027		
Caciuleanu, Alexandru I.	P-Th-081		
Cai, Jinming	Tu-A06		
Cai, Pei-Yang	P-Th-062		
Callaghan, Stephen	P-Th-022		
Calleja, Fabian	Mo-A07, Tu-C01, Tu-A03		
Calloni, Alberto	We-A09		
Calò, Annalisa	P-Mo-093, Tu-B02, Tu-D23		
Camus, Yotam	Tu-C25+26		
Canadell, Enric	P-Th-023		
Candini, Andrea	Tu-A06		
Canfield, P. C	P-Th-001		
Cantoni, Claudia	Tu-B09+10		
Capdevila-Cortada, Marçal	Mo-B04		
Čaplovič, Ľubomír	P-Th-058		

Choueikani, Fadi	P-Tu-064	Datler, Martin	Mo-E10, P-Mo-077, P-Th-064
Chrissey, Douglas B.	P-Tu-059	Davies, Philip	P-Th-100
Christl, Maik	Tu-B13	Davis, Earl Matthew	Mo-B12
Chuang, Cheng-Hao	Tu-D10	de Andrés, Alicia	P-Mo-009
Chulkov, Evgueni	Tu-A03	de Heer, Walt	Th-A22, P-Mo-020, P-Mo-006
Chumakov, Ratibor	Th-C22	de la Figuera, Juan	Mo-A01+02, Mo-A03, P-Mo-082
Chuzel, Olivier	P-Tu-026	De Marchi, Fabrizio	P-Tu-071, Th-C14
Cibrev, Dejan	We-B05	de Miguel, Juan José	Tu-C03, P-Tu-017
Ciccacci, Franco	Mo-B01, P-Mo-084, Tu-D03, We-A09	de Oteyza, Dimas G.	Th-A09, Mo-C03+04
Cilento, F.	Th-D23	De Renzi, Valentina	Tu-A06, Tu-A07
Cirera, Borja	We-C07	de Simone, Monica	P-Tu-009, P-Tu-040
Claessen, Ralph	Mo-D16	Deák, László	Mo-B17
Clair, Sylvain	P-Tu-026, P-Tu-064, P-Tu-067, P-Tu-069	Debiossac, Maxime	Tu-D01, Tu-A17, P-Th-046
Clark, Philippa	We-B08	Debontridder, François	Mo-A14
Climent-Pascual, Esteban	P-Mo-009	Deilmann, Thorsten	Tu-C02
Clotet, Anna	P-Tu-027	del Cueto, Marcos	We-D01, P-Th-048
Cloutier, Martin	Th-D03	del Pennino, Umberto	Tu-A06, Tu-A07
Coati, Alessandro	P-Th-095	Delage, Sarah	Tu-E05, P-Tu-106
Cobian, Manuel	P-Tu-067	Delbos, Elise	P-Mo-051
Cohen, Hagai	Th-B06	Dementyev, Petr	Tu-E19, Th-E18
Colliex, Christian	Mo-B05	Demura, Masahiko	P-Th-099
Comelli, Giovanni	Th-A19	Demuth, Stephanie	Mo-D15
Condurache-Bota, Simona	P-Mo-091, P-Mo-092	Denk, Richard	Tu-A06
Conejeros, S.	P-Th-023	Derivaux, Frederic	Mo-B07
Conrad, Edward	Th-A22, P-Mo-006	Dethe, Ulhas	P-Tu-084
Constable, Edwin C.	We-C06	Dhanasekaran, Venkatesan	P-Th-095
Contini, Giorgio	Tu-C14, Tu-C19, P-Tu-033	Dhesi, S.	Th-D23
Coraux, Johann	Tu-B18, Th-A20	Dhesi, Sarnjeet	P-Tu-064
Cordero Edwards, Rohini K.	P-Tu-095, Th-B04	Di Capua, R.	P-Mo-085
Cordero, Kumara	P-Mo-093, Tu-B02	Di Giovannantonio, Marco	Tu-C14, Tu-C19, P-Tu-033
Corem, Gefen	Tu-D02	Di Santo, Giovanni	Mo-A09, Th-D20
Coreno, Marcello	P-Tu-009, P-Tu-040	Di Valentin, Cristiana	Th-A11
Cornish, Alix L.	Mo-E14	Díaz Arado, Óscar	Mo-B03
Coronado, Eugenio	Mo-A15	Díaz Arado, Óscar	Mo-A07, Tu-C01, We-D01, P-Th-048
Corradini, Valdis	Tu-A06, Tu-A07	Díaz, Cristina	Mo-C05
Correa, Alexander	Mo-D09, P-Th-026	Díaz-Tendero, Sergio	P-Tu-098
Corso, Martina	P-Mo-023, Tu-E16, Th-D11	Dib, Amel	Mo-B09, Mo-B16, Mo-B18, P-Mo-086, P-Mo-090, Th-E17, Th-E19
Cortés, Juan	P-Tu-074	Diebold, Ulrike	P-Tu-001
Cossaro, A.	We-D09	Diederich, Francois	P-Tu-005, Th-A10
Couraux, Johann	We-D04	Dienel, Thomas	Tu-E15
Cren, Tristan	Mo-A14	Diller, Katharina	Tu-E11
Crepaldi, A.	Th-D23	Ding, Ding	Tu-D25
Creuze, Jérôme	We-B10	Ding, Ren-Feng	P-Mo-075
Cristescu, Rodica	P-Tu-059	Diniz, José	P-Mo-011, P-Tu-077
Crivillers, Núria	Mo-D02, Th-E10, P-Mo-019	Diño, Wilson Agerico	Th-B05
Cui, Yi	Mo-B12, P-Mo-074, Tu-B11	Dionot, Jelle	P-Th-094
Curcio, D.	We-C11	Dirany, Nadine	P-Tu-062
Curcio, Davide	Tu-A20	Dirksen, Elena	P-Th-061
Curiotto, Stefano	Th-D05	Djadoun, Amar	P-Mo-053
Custance, Oscar	Tu-C11	Djemai, Ibtissem	P-Mo-012
Czajka, Ryszrad	P-Tu-036	Do, Van Lam	Tu-D19
		Dobberschütz, Søren	Mo-E15
		Dobrin, Sergey	P-Tu-096
		Doghmane, Malika	P-Mo-075
		Doi, Ioshiaki	Th-D07
		Domagala, Jaroslaw Z.	We-D09
		Domenichini, Bruno	Tu-B02, Th-B03, P-Tu-095
		Domingo Marimon, Neus	P-Mo-094
		Th-B04, P-Mo-093,	Mo-A04, Th-D15+16
		Dominguez Jimenez, M.A.	Tu-E09, P-Th-098
		Donath, Markus	
		Dong, Yi	

Dostert, Karl-Heinz
Drchal, Václav
Driss, Dergham
Drnec, J.
Drnec, Jakub
Dubal, Deepak P.
Dubey, Girjesh
Duchon, Tomáš
Ducke, Jacob
Duda, Radek
Duguet, Thomas
Dumur, Frédéric
Duncan, David A.
Duò, Lamberto

Dupont, Celine
Dürr, Michael
Dvořák, Filip
Dyniec, Paweł

E

Ebert, H.

Ebert, Hubert
Ebrahimi, Maryam

Echavarren, Antonio
Écija, David

Eddrief, Mahmoud
Edler, Frederik

Edmonds, Mark
Edström, Kristina
Ehara, Masahiro
Ehre, David
Ekthammathat, Nuengruethai
El Belghiti, Hanane
Elbakyan, Lusine
Eliseev, Andrey
Ellialtıoğlu, Şinasi
Ellis, John
Elmers, Hans-Joachim
El-Sayed, Afaf
Endrino, Jose
Engelund, Mads
Entani, Shiro
Eom, Daejin
Erbe, Andreas

Erdőhelyi, András
Ericsson, Leif
Eriksson, Olle
Eriksson, Susanna
Ermakov, Kirill Andrejevič
Ernst, Wolfgang E.
Esat, Taner
Escano, Mary Clare Sison
Escudero, Carlos

Espinosa, Francisco Miguel
Esplandiú, María José

Esser, Norbert
Esteve, Joan
Etcheberry, Arnaud

Tu-E14
P-Mo-034
P-Mo-040
P-Mo-085
We-D04
P-Mo-041
Th-A05
Tu-B15
Tu-E15, Tu-A18
P-Th-083
Th-C05
P-Tu-069
Tu-E15
Mo-B01, P-Mo-084,
Tu-D03, We-A09
We-D09
Tu-E12
P-Th-068
Tu-C23, P-Tu-013

Th-D14, Th-D23,
P-Th-016
Mo-A04, P-Th-027
Tu-C19, P-Tu-033,
P-Tu-071, Th-C14
Mo-C14
Mo-D13, Tu-E15,
We-C07
Tu-D01
Mo-D15, P-Mo-020,
P-Th-021
Tu-A19
Tu-D09
P-Th-085
Th-B06
P-Th-071
P-Mo-051
P-Mo-028
P-Mo-010
We-B03
Tu-D02, We-E04
Th-D14, P-Th-016
Mo-C03+04
P-Th-009, P-Th-011
Mo-C14
We-D05
Th-E23
P-Mo-073, P-Tu-062,
Th-E12, P-Th-010,
P-Th-029
P-Th-059
P-Mo-049
Mo-A08, P-Mo-049
Tu-D09
P-Tu-107
We-E03
Tu-C02
Th-E24
Mo-E05, Mo-E06,
Tu-B02, P-Mo-093,
P-Tu-095
Th-C04
Tu-B02, Tu-D23,
P-Mo-093
P-Tu-025
P-Tu-049, P-Tu-057
Th-E07, P-Mo-051,
P-Mo-079, P-Tu-011

Etgens, Victor
Etzkorn, Markus
Euaruksakul, Chanan
Evangelio, Laura
Evertsson, Jonas
Ewen, Pascal Raphael

F

Fabris, Stefano
Fadley, Charles
Fagot-Revurat, Yannick
Fairclough, Simon
Falsig, Hanne
Falta, Jens
Fang, Chung-Kai
Fariás, Daniel
Farinacci, Laëtitia
Farnesi Camellone, Matteo
Fasel, Roman

Fatayer, Shadi

Faungnawakij, Kajornsak
Feidenhans'l, Robert
Fekete, Ladislav
Felici, Roberto
Feng, Bingjie
Feng, Xinliang
Feringa, Ben L.
Fernández, Laura
Fernández-Garrido, S.
Fernández-Solis, Christian
Ferrando, Riccardo
Ferrer, Salvador
Ferretti, Andrea
Ferrighi, Lara
Ferstl, Pascal
Fester, Jakob
Feyer, Vitaliy
Fiala, Roman
Fiaschi, Giorgia
Fielding, Helen
Filali, Larbi
Filatova, Elena
Filimonov, Sergey
Finazzi, Marco

Finnocchi, Fabio
Fiordaliso, Elisabetta M.
Fischer, Christian
Fischer, Sybille
Flavell, Wendy
Flege, Jan Ingo
Fleszar, Andrzej
Floreano, L.
Floreano, Luca
Fobes, David
Foerster, M.
Foerster, Michael
Foglietti, Vittorio
Fokin, D.
Fonda, Emiliano
Fonin, Mikhail
Ford, I.
Förster, Stefan
Fortas, Ghania
Fortunelli, Alessandro
Foti, Giuseppe
Fouaz, Lakoui

Tu-D01
P-Tu-044
Mo-E14
Th-C03, Th-C04
Mo-B02, Th-E06
Mo-C06

P-Th-068
Mo-B05
Tu-C14, We-C10
We-B08
Mo-E12
Mo-E03, Mo-B08
Tu-D24
P-Mo-009
P-Tu-029
P-Th-068
Tu-A06, Tu-C15,
Th-A10, Th-A13+14
Tu-C16, We-C06,
Th-C10
P-Th-085
Tu-D16
P-Mo-034
We-D04, P-Mo-085
P-Mo-045, P-Mo-046
Tu-A06, Th-A10
P-Tu-065
Mo-A06
P-Th-035
Th-E12
P-Mo-078
Mo-E05, Th-B12
Tu-A06
Th-A11
Tu-B01, Tu-B16
Tu-B03
P-Mo-034
P-Mo-039
P-Th-049
P-Mo-083
P-Tu-003, P-Tu-085
Tu-B21
Tu-C05, P-Tu-103
Mo-B01, P-Mo-084,
Tu-D03, We-A09
Tu-D01
Mo-E04
P-Tu-054, P-Tu-058
Tu-E15
We-B08, We-B09
Mo-E03, Mo-B08
Mo-D16
We-D09
We-C08, P-Tu-023
Th-E17
P-Mo-082
Mo-A03, Th-B12
Tu-B09+10
Mo-A14
P-Mo-035
Tu-A25
We-C11
Tu-B13
P-Th-077
Tu-B17
P-Tu-004
P-Mo-040

Fouchet, Arnaud	P-Mo-079	Garnica Alonso, Manuela	Mo-A07, Tu-A03,
Franco, Carlos	Mo-D02		Tu-A18, Tu-C01,
Frankcombe, Terry J.	P-Th-048		Tu-E15
Franke, Katharina J.	Mo-A11+12, Mo-A10,	Garreau, Yves	P-Th-095
	Mo-A17, P-Tu-029	Gasperi, Gabriele	Mo-B08
Franssen, Maurice C.R.	Th-E11	Gastaldo, Michele	Th-A17
Frantzeskakis, E.	P-Th-023	Gauquelin, Nicolas	Tu-C24
Franz, Dirk	Tu-D06	Gautier, Sarah	Mo-E13
Franz�, Giorgia	P-Th-049	Gauvin, Raynald	P-Mo-062
Fratesi, Guido	Tu-D03	Gavarri, Jean Raymond	P-Th-094
Fraxedas, Jordi	Th-B18, Th-C04,	Gavrielides, Andreas	Th-C05
	P-Mo-072,	Gavrila, Raluca	P-Mo-091, P-Mo-092
Fredriksson, Hans	Mo-E08	Gawinkowski, Sylwester	Tu-C10
Frenken, Joost	Mo-E09	Geelhaar, L.	P-Th-035
Freund, Hans-Joachim	Mo-B12, Tu-B11,	Gelardi, Franco Mario	P-Tu-054
	Tu-E14, Tu-E19,	Genchev, Georgi	P-Mo-073
	Tu-E21, We-D07,	Generalov, Alexander	P-Th-022
	Th-E18, P-Mo-074,	Gengler, Regis Y. N.	P-Mo-012, P-Tu-065
	P-Tu-020, P-Th-087	Gerber, Iann	We-C10
Friend, Cynthia	Tu-E10	Gergieva, Bela	P-Tu-043
Fritz, Daniel Roman	P-Th-053	Gerhold, Stefan	Mo-B09
Fromm, Felix	Tu-A19	German, Estefania	P-Mo-042
Fr�chtli, Herbert	Th-C16	Gerstmann, U.	Th-E21
Fu, Chaoying	Mo-C13	Gerstmann, Uwe	We-B04
Fuchs, Harald	Mo-B03	Getzlaff, Mathias	P-Tu-083
F�chtbauer, Henrik G.	Tu-E08	Ghadami Yazdi, Milad	Mo-B02
Fuechsel, Gernot	We-D01	Ghalgaoui, Ahmed	Th-C21
Fuji, Jun	Th-D20	Ghanbari, Ebrahim	Tu-C18
Fujii, Shintaro	Tu-A04, P-Th-015	Gherbi, Naima	P-Tu-098
Fukaya, Yuki	We-D05, We-D08,	Giannotti, Dario	Mo-B01, P-Mo-084,
	Th-B21, Th-B22,		Tu-D03
	Th-B23	Gierz, I.	P-Mo-008
Fukidome, Hirokazu	Th-A21	Gies, Hermann	P-Tu-042
Fukuda, Tsuneo	We-B11	Giessibl, Franz Josef	Th-C11
Fukutani, Katsuyuki	Tu-B06, Tu-B20,	Gigmes, Didier	P-Tu-069
	P-Tu-012	Gim�nez, Xavier	P-Tu-088
Fukuzawa, Akihiro	P-Mo-064	Giordano, Livia	P-Mo-078
Funakubo, Kazutoshi	Th-A21	Giovanelli, Luca	P-Tu-064
Fusil, St�phane	Mo-B05	Girard, Yann	Th-C22, P-Mo-035
		Girardeaux, Christophe	Mo-B07
		Girovsky, Jan	Tu-C16, We-A04
		Glass, Stefan	Mo-D16
		Glatzel, Thilo	Tu-C15
		Gliemann, Bettina	Mo-C08, Th-C09
Gabouze, Noureddine	P-Th-077	Gloter, Alexandre	Mo-B05, P-Mo-006
Gade, Lutz H.	Tu-C16, Tu-C17,	Gluba, Lukasz	Th-D07
	Th-C10	Godlewski, Szymon	Mo-C10, Mo-C14
Gago, Raul	P-Th-009, P-Th-011	Godsi, Oded	Tu-D02
Gahl, Cornelius	P-Tu-079, Th-C18	Goel, Alok	P-Th-031
Galeotti, Gianluca	Tu-C14, Tu-C19,	Goiri, Elizabeth	Mo-C03+04
	P-Tu-033	Goldfarb, Ilan	Tu-C25+26
Gallagher, Mark	Mo-C13	Goldoni, Andrea	Mo-A09, Th-D20
Gallego, Jos� Mar�a	Mo-C05, Mo-D13,	Go�ek, Franciszek	P-Tu-016
	We-C07	Golshan Ebrahimi, Nadreh	P-Tu-050
Gamallo, Pablo	P-Tu-088, P-Th-090	G�mez, Roberto	We-B05
Gamba, Oscar	P-Mo-090	G�mez-Romero, Pedro	P-Mo-041
Gambardella, Pietro	Th-A15, Tu-C07+08,	Gomozov, Valeriy	P-Th-076
	Th-D22	Gon�alves, Anne-Marie	Th-E07
Ganduglia-Pirovano, M.V.	Mo-B13+14	Gonella, Grazia	Tu-D15
Gao, An	P-Mo-014	Goniakowski, Jacek	Tu-B22
Garc�a Michel, Enrique	Th-D13, P-Th-001,	Gonz�lez-Cuxart, Marc	P-Mo-021
	P-Th-002, P-Th-055	Gonzalez, Juliana	We-D04
Garc�a Salgado, Godofredo	P-Mo-094	Gonz�lez-Moreno, Rub�n	P-Tu-023, We-C08
Garc�a, Jaime	P-Tu-098	G�sweiner, Christian	We-E03
Garc�a, Ricardo	Th-C04	G�thelid, Mats	Mo-B02
Garc�a, Vincent	Mo-B05	Goto, T.	P-Mo-070
Garc�a-Lekue, Aran	Mo-C14, We-C08,	Gottardi, Stefano	P-Tu-031
	Th-A15, P-Tu-023	Gotterbarm, Karin	Tu-E13
Garc�a-Many�s, Sergi	Mo-C12	Gottwald, Alexander	Tu-C13
Gargallo-Caballero, Raquel	Mo-A03	G�tzinger, Alissa C.	P-Tu-062
Gargiani, Pierluigi	Tu-A09, Tu-A10,	Grachev, Evgeniy	P-Mo-065

G

Graghaniello, Luca	Tu-A25	Harnau, Ludger	Tu-Tu-045, P-Tu-074, Th-C20
Gramazio, Federico	P-Mo-072, Th-C04	Haršáni, Marián	P-Th-058
Granados, Cecilia	Mo-A03	Hasegawa, Yukio	Mo-A13, Mo-A16, Th-B20
Granados, Daniel	Mo-D13		P-Tu-018, P-Tu-022
Grånäs, Elin	Mo-B06, Mo-B10	Hasegawa, Yuri	P-Mo-040, P-Mo-053
Grazioli, Cesare	P-Tu-009, P-Tu-040	Hassani, Salim	Tu-D19, Tu-D20, Mo-D04
Greber, Thomas	Tu-C15	Hassenkam, Tue	P-Tu-029
Gregoratti, Luca	Mo-E07, Th-E04+05	Hatta, Shinichiro	Tu-D10
Grenèche, Jean Marc	P-Mo-056	Hatter, Nino	Th-D12
Grewal, Harpreet Singh	We-E10	Hävecker, Michael	P-Tu-091
Grigorkina, Galina	P-Tu-043	Hayashida, Takashi	P-Tu-064
Grill, Leonhard	Tu-C10	Hayashita, Hironori	Th-D12
Grioni, M.	Th-D23	Hayn, Roland	Tu-E15, Tu-A18
Grioni, Marco	P-Th-023	Hazama, Toru	Mo-B11
Groening, Oliver	P-Tu-005	He, Yuanqin	Th-D23
Grönbeck, Henrik	Mo-B11, Mo-E16, P-Th-067	Heard, Christopher J.	P-Th-027
Gröning, Oliver	Th-A10	Heckmann, O.	P-Mo-034
Groot, Irene	Mo-E09	Heckmann, Olivier	Tu-D02
Grumezescu, Alexandru M.	P-Tu-059	Heczko, Oleg	Tu-A19
Gruverman, Alexei	Th-B01+02	Hedgeland, Holly	Mo-A10, Mo-A17, P-Tu-029
Grządziel, Lucyna	P-Mo-073	Heidrich, Christian	Tu-B16
Gubo, Mathias	Tu-B16	Heinrich, Benjamin W.	Mo-E14
Gubó, Richárd	Tu-E23		Th-D23
Guesmi, Hazar	We-B10	Heinz, Klaus	Th-C02
Guillemot, Laurent	Th-C15	Held, Georg	Mo-B07
Guinea, Francisco	Mo-A15, Tu-A03	Held, K.	P-Tu-014
Gülseren, Oğuz	We-B03	Helmer, Dorothea	Th-B17
Gunceler, Deniz	We-B03	Hemeryck, Anne	We-A02
Güner, Sadık	P-Mo-059	Henry, Claude R.	P-Tu-025
Güney, Gülden	P-Tu-046	Heo, Jinhee	P-Mo-002
Guo, Donghui	Th-E09	Herden, Tobias	Tu-B12
Guo, Quanmin	Tu-C21, P-Tu-072	Hergenröder, Roland	P-Mo-094
Gupta, Ajay	We-E01	Hermann, Klaus	Mo-A08
Gürbüz, Osman	P-Mo-059	Hermansson, Kersti	P-Tu-065
Gurrath, Martin	Mo-C08, Th-C09	Hernández de la Luz, Álvaro	P-Tu-103
Gustafson, Johan	Mo-B11, Tu-B01, Tu-E07, Tu-E16, We-D03	Herper, Heike	We-D07, P-Th-087
	Tu-D09	Herpt, Jochem Van	We-E07, We-E08, We-E09
Gustafsson, Torbjörn	Th-B15	Hervieu, Yuri	P-Tu-041
Gutowski, Olof	Th-C20	Heyde, Markus	P-Th-099
Gutzler, Rico		Higuchi, Yuji	P-Tu-091
			Tu-B14
		Himmerlich, Marcel	Mo-D01
		Hirano, Toshiyuki	P-Tu-031
		Hiraya, Atsunari	P-Th-085
		Hirjibehedin, Cyrus	Th-C07
		Hirose, Kenji	Tu-B19
		Hirsch, Anna K. H.	Tu-D12+13
		Hirunsit, Pussana	Th-D09+10
		Hisamatsu, Yuri	Tu-E12
		Hitosugi, Taro	P-Tu-014
		Hodgson, Andrew	P-Mo-008
		Hoesch, Moritz	Tu-A21+22, Th-D11
		Höfer, Ulrich	Tu-A06
		Hoff, Brice	Mo-C16, P-Tu-072
		Hofmann, P.	P-Tu-090
		Hofmann, Philip	P-Mo-034
		Hohage, Michael	Tu-A24, Tu-A26, P-Tu-039
		Holmes, Scott	Th-E21
		Honda, Mitsunori	P-Tu-018
		Honolka, Jan	P-Tu-057
		Hornekær, Liv	We-C06
			Th-D23
		Horn-von Hoegen, M.	P-Th-027
		Hosokai, Takuya	Th-D20
		Hotsuki, Masaki	P-Th-062
		Housecroft, Catherine E.	
		Hricovini, K.	
		Hricovini, Karol	
		Hruban, Andrzej	
		Hsu, Po-Wei	

Hsu, Yao-Jane
Hu, Chunping
Hu, Xiao
Hu, Ya
Huber, Ferdinand
Hund, Zack M.
Hung, Ting-Chieh
Hurtado, Daniel
Hussain, Hadeel
Huttmann, Felix
Hwang, Ing-Shouh
Hyodo, Toshio

Hyun, Jung-Min

We-A03
Th-D04
Mo-A16
Th-A12, Th-C12
Th-C11
P-Th-048
P-Th-062
P-Tu-008
Th-E13
We-C09
Tu-D24, Tu-D25
We-D05, We-D08,
Th-B21, Th-B22,
Th-B23
P-Th-045

Johannsen, J.C.
Johansson, Lars
Jonsson, Niclas
Jonsson, Lars
Joo, Chul Woong
Jørgensen, Jakob

Juan, Alfredo
Jung, Jaehoon
Jung, Soon-Won
Jung, Thomas

Jupille, Jacques
Jurczyszyn, Leszek
Jürgensen, Astrid

P-Mo-008
Tu-C12
Mo-B06, Mo-B10
P-Th-024
Th-C06
Tu-A24, Tu-A26,
P-Tu-039
P-Mo-042
We-C05
P-Th-019
Tu-C15, Tu-C16,
Tu-C17, We-A04,
We-C06, Th-C10
We-D09
P-Tu-036, P-Th-037
P-Tu-025

I

Ibarra, Ricardo
Ichikawa, Akihide
Ichimiya, Ayahiko

Idriss, Hicham
Ienaga, Koichiro
Illas, Francesc
Ilyn, Maxim
Imada, Hiroshi
Inagaki, Kouji
Inoue, Tomoyasu
Ioffe, L.B.
Ishii, Hiroyuki
Ishikawa, Hirotaka
Island, Joshua
Itkis, Daniil
Ivanov, Vladimir
Ivars, Francisco

Ivas, Toni
Iwaya, Katsuya
Izumi, Akira

We-A01
Th-A02
We-D08, Th-B22,
Th-B23

Mo-E01+02
We-D10, P-Th-050
Th-B14, P-Th-090
Mo-A06
We-C05
Mo-C15
P-Mo-071
Mo-A14
Mo-D01
Th-D12
Mo-A15
Th-E04+05
P-Mo-065
Tu-E14, Tu-E19,
Th-E18
Th-C10
Tu-B19
P-Mo-070

K

Kaawar, Zeinab
Kabanov, Nikolay
Kaji, H.
Kajikawa, Jumpei
Kakitani, K.
Kaku, Masanori
Kalashnyk, Natalya
Kalinin, Sergei
Kalita, Golap
Kamiński, Wojciech
Kampen, Thorsten
Kanayama, Kaoru
Kaneko, Satoshi
Kang, Seung-Youl
Kantorovich, L.
Karasiewicz, Joanna
Karim, Altaf
Kasai, Hideaki
Kaser, Hendrik
Kasperski, Adam
Katano, Satoshi
Kato, Hiroki
Katto, Masahito
Kawahito, Yousuke
Kawai, Hiroyo
Kawai, Maki
Kawai, Shigeki
Kawakami, Takuto
Kawamoto, Erina
Kawamura, Norikazu
Kawamura, Ryutaro
Kawasuso, Atsuo

Kawauchi, Taizo
Kaya, Dogan
Kebab, Aissa

Kechouane, Mohamed
Keghouche, Nassira

Keller, Nico
Keller, Thomas F.
Kermadi, Salim
Kern, Klaus

Khajetoorians, Alexander A.
Khalaji, Saiede
Khalakhan, Ivan
Khalil, Kamal

P-Th-047
P-Th-039
P-Th-043
P-Tu-091
P-Th-043
P-Tu-086
Th-C15, P-Tu-069
Tu-B09+10
Tu-A13
Tu-D05
Th-B11
P-Mo-017
Mo-D03, P-Th-014
P-Mo-016
We-C11
P-Tu-021
P-Th-003
P-Mo-011
Tu-C13
P-Tu-073
P-Mo-057, Th-A03
Th-D04
P-Tu-086
P-Mo-011
Mo-C14
Mo-D12, Th-D17
Th-C10
Mo-A16
Th-D04
We-D10
Th-E08
Th-B21, Th-B22,
Th-B23
Tu-B20
Tu-C21
P-Mo-044, P-Tu-003,
P-Tu-085
P-Mo-050, P-Mo-053
P-Mo-052, P-Tu-096,
P-Th-073
Th-C02
Tu-D06
P-Mo-050
We-A02, Th-A05,
Th-C20, P-Tu-008,
P-Tu-044, P-Tu-045,
P-Tu-074,
Mo-C06
P-Tu-050
P-Mo-039
P-Mo-032

J

Jabeen, Naila
Jacobson, Peter
Jafari, Emad
Jałochowski, Mieczysław

Jang, Joon
Jany, Benedykt R.
Jardine, Andrew Peter
Jastrabik, Lubomir
Jean, Fabien
Jelínek, Pavel

Jenkins, Stephen J.
Jeong, Haguk
Jeong, Myung-Geun
Jesse, Stephen
Jiménez Divins, Núria
Jiménez-Villacorta, Félix
Jiricek, P.
Jiricek, Petr
Jnawali, G.
Joachim, Christian
Joco, Victor
Johánek, Viktor

Tu-A20
We-A02
P-Tu-050
Tu-C23, P-Tu-013,
P-Tu-015
Tu-B04
Tu-C24
Tu-D02
P-Tu-100
Th-A20
Tu-A12, Tu-C09,
P-Th-036
Th-E16
P-Mo-033
P-Tu-052, P-Th-092
Tu-B09+10
Mo-E05
P-Mo-009
P-Th-035
P-Mo-043
Th-E21
Mo-C14
Th-D13
P-Th-097

Khalil, Lama	Th-D20	Kongsfelt, Mikkel	Tu-A26
Khan, Adnan	Mo-E01+02	Kónya, Zoltán	Mo-B17, P-Mo-076, Tu-E23, P-Th-059
Khemliche, Hocine	Tu-D01, Tu-A17, P-Th-046	Konyushenko, Marina	Tu-B21
Khokonov, Azamat	P-Tu-078, P-Th-044	Koo, Jae Bon	P-Th-019
Khokonov, Murat	P-Th-044	Koo, Ja-Yong	Th-E23
Khubezhov, Soslan	P-Tu-043	Koo, Kyengmo	P-Mo-058
Kierren, Bertrand	Tu-C14, We-C10	Koo, Yoonbon	P-Mo-058
Kiguchi, Manabu	Mo-D03, Tu-A04, P-Th-014, P-Th-015	Kooda, Y.	P-Th-017
Kim, Bo Ra	P-Th-092, P-Tu-052	Koopmans, Bert	Tu-D04
Kim, Dae Han	P-Tu-052, P-Th-092	Kopciuszynski, Marek	Tu-C23
Kim, Do Hwan	P-Th-091	Kopeček, Jaromír	P-Mo-034
Kim, Hanchul	Th-E23, P-Th-045	Koshikawa, Takanori	Mo-A05
Kim, Howon	Mo-A13, Mo-A16, Th-B20	Koslowski, Sebastian	P-Tu-044
Kim, Il Hee	P-Tu-052, P-Th-092	Kotanigawa, Yuki	P-Tu-101
Kim, Jeong Won	P-Tu-019	Kotera, Masatoshi	P-Mo-062, P-Mo-063, P-Mo-064, P-Mo-066
Kim, Kangsoo	P-Mo-058	Koudia, Mathieu	P-Tu-064
Kim, Sehun	P-Tu-019	Koust, Stig	Tu-B05
Kim, Seon-Woo	P-Mo-058	Kovács, Imre	P-Tu-093
Kim, Soong Yeon	P-Tu-052, P-Th-092	Kovalev, Anatoly	P-Mo-010, P-Th-009, P-Th-011
Kim, Sunghun	P-Th-050	Kowalik, Iwona Agnieszka	Tu-C03, P-Tu-017
Kim, Yeonwoo	P-Th-060	Koyiloth Vayalil, Sarathlal	We-E01
Kim, Yongjin	P-Tu-048	Kralj, Marko	Tu-A08
Kim, Young Dok	P-Tu-052, P-Th-092	Krasovskii, E.E.	Th-D22
Kim, Yousoo	We-C05	Kraus, Patrick	We-E03
Kireche , Nora	P-Tu-056	Kravchuk, Tatayan	Tu-D02, We-D11
Kirschner, J.	Th-D14	Krawiec, Mariusz	Tu-C23, P-Tu-015
Kiryukhantsev-Korneev, Philipp	P-Th-042	Krejci, Ondrej	Tu-C09
Kiselev, Nikolay	P-Mo-010	Kret, Slawomir	Th-D07
Kiss, János	P-Mo-076, P-Tu-093, P-Th-059	Krischok, Stefan	P-Th-041
Kivala, Milan	Mo-C08, P-Tu-047, Th-C09	Krok, Franciszek	Tu-C24
Kivimäki, Antti	P-Tu-040	Krüger, Peter	Tu-C02, We-D09
Kizaki, Hidetoshi	Mo-C15	Krungchanuchat, Saowalak	P-Th-071
Klappenberger, Florian	Tu-E15	Krzywiecki, Maciej	P-Mo-073
Klavsyuk, Andrey	P-Th-038, P-Th-039	Kubo, Momoji	We-E07, We-E08, We-E09, P-Tu-081
Kleibert, Armin	Tu-C16, We-A04	Kubodera, Shoichi	P-Tu-086
Klein, C.	Th-E21	Kubyshkina, Elena	P-Th-024
Kleinschmidt, Peter	P-Th-041	Kucharczyk, Robert	We-B12
Klinbumrung, Arrak	P-Mo-087	Kuchuk, Kfir	P-Mo-067, Tu-D21, Th-B19
Klyatskaya, Svetlana	We-C07	Kudrnovský, Josef	P-Mo-034
Knop-Gericke, Axel	Tu-D10, Th-E04+05	Kuhlenbeck, Helmut	Mo-B12
Knospe, Alexander	P-Th-032	Kuhnness, David	Tu-B17
Knudsen, Jan	Mo-B06, Mo-B10, Tu-B01, Th-A07+08	Kukli, Kaupo	We-B05
Ko, Hsien-Chen	Tu-D24, Tu-D25	Kulbachinskii, Vladimir	P-Th-057
Kobayashi, Katsuyoshi	P-Th-056	Kumagai, Takashi	Tu-C10
Kobayashi, Nobuhiko	Mo-D01	Kumar, Sumit	P-Tu-065
Kocán, Pavel	P-Tu-028, P-Tu-034, P-Tu-068	Kumskov, Andrey	P-Mo-010
Koch, Norbert	Mo-D05+06	Kupka, Anna	P-Tu-042
Koch, Reinhold	We-A08	Kuptsov, Konstantin	P-Th-042
Koczorowski, Wojciech	Mo-C09, P-Tu-036, P-Th-037	Kurihara, Kazue	We-E07
Koga, Ryosuke	P-Tu-091	Kurnosikov, Oleg	Tu-D04
Kohn, Amit	Tu-C25+26	Kutluk, Galif	P-Th-017
Koleini, Mohammad	Th-D03	Kutnyakhov, D.	Th-D14
Koller, Georg	Tu-C13	Kutnyakhov, Dmytro	P-Th-016
Kolmer, Marek	Mo-C10, Mo-C14	Kuwahara, Takuya	We-E09
Koltsov, Alexey	Tu-B22	Kuznetsov, Mikhail	Th-D21
Komem, Yigal	P-Th-049	Kytin, Vladimir	P-Th-057
Komori, Fumio	We-D10, P-Th-050		
Komoto, Yuki	Mo-D03, P-Th-015		
Konashuk, Aleksei	Tu-B21		
Konczykowski, Marcin	Th-D20		
Kondo, Takahiro	Tu-E24, Th-E09		
Konečný, Martin	P-Mo-030		
		L	
		Laad, Rahul	P-Tu-084
		Labidi, Hatem	Th-D03
		Lacaze Dufaure, Corinne	Th-C05, Th-E14
		Lacovig, Paolo	Tu-A20
		Lagoute, Jérôme	Th-C22, P-Mo-035
		Lahav, Meir	Th-B06

Lahti, M.	P-Tu-006	Lisitsin, Elina	We-D11
Lai, Yu-Ling	We-A03	Lišková, Zuzana	P-Mo-029
Lalmi, Boubekeur	Tu-D01	Liu, Jia	Th-A10
Lam, Tu-Ngoc	We-A03	Liu, Junzhi	Th-A10
Lana-Villareal, Teresa	We-B05	Liu, Liwei	P-Tu-005
Lančok, Ján	P-Mo-034	Liu, Ning	Tu-C22
Lang, Philippe	Th-C19	Liu, Renjie	Mo-C13
Lang, Zhongling	P-Tu-027	Liu, Wei	Tu-E10
Langenkämper, Christian	Mo-A04	Liu, Y.	Th-D23
Langewisch, Gernot	Mo-B03	Livadaru, Lucian	Th-D03
Laskin, Gennadii	We-A02	Lizzit, D.	We-C11
Lauritsen, Jeppe V	Mo-E12, Tu-B03, Tu-B05, Tu-E08	Lizzit, Silvano	Tu-A20
	Tu-A08	Llorca, Jordi	Mo-E05, Mo-E06
Lazić, Predrag	Tu-C06	Lobo-Checa, Jorge	Tu-E16, Tu-C17, Th-A09, Th-D11, P-Mo-086
Le Bahers, Tanguy	Th-C20		Tu-A11, Th-A19
Le, Duy	Tu-B22	Locatelli, Andrea	Tu-A06, Tu-A07
Le, Ha-Linh Thi	Th-C22	Lodi Rizzini, Alberto	Tu-A25
Lebedev, Alexey	Tu-C02	Löfwander, Tomas	P-Tu-053
Lechtenberg, Benedikt	P-Th-051	Loh, Ih-Houng	Th-C19
Lee, C.J.	P-Mo-014, P-Tu-102	Lombana, Andrés	Tu-A03, Tu-C01
Lee, Chris	P-Th-045	López Vázquez de Parga, A.	Mo-B04
Lee, Geunseop	P-Tu-061, P-Th-060	López, N.	P-Tu-067
Lee, Hangil	P-Th-091	Loppacher, Christian	Tu-C06
Lee, Hye Jin	P-Tu-048	Lorente, Nicolas	Th-C03, Th-C04
Lee, Hyunsuk	Th-C06	Lorenzoni, Matteo	P-Tu-049, P-Tu-057
Lee, Jeong-Ik	P-Tu-048	Lousa, Arturo	P-Tu-023
Lee, Johnhwan	P-Mo-033	Lovat, Giacomo	P-Tu-009, P-Tu-040
Lee, Jong-beom	Th-C06	Lozzi, Luca	Th-C16
Lee, Jonghee	P-Tu-052, P-Th-092	Lu, Hao	P-Tu-053
Lee, Ju Ha	Th-C06	Lu, Pei-Lin	Tu-D24
Lee, Keunsoo	P-Mo-058	Lu, Yi-Hsien	Th-B06
Lee, Kyunghwan	P-Th-019	Lubomirsky, Igor	We-B06
Lee, Sang Seok	P-Mo-058	Lucas, Stéphane	P-Th-001
Lee, Sunsoo	Tu-B09+10	Luccas, R.F.	Mo-B08
Lee, Tien-Lin	P-Tu-053	Luches, Paola	Mo-D15
Lee, William	Tu-C14	Lücke, Andreas	Mo-A08, P-Tu-009, P-Tu-040
Lefevre, Patrick	We-B10	Lüder, Johann	Tu-C13
Legrand, Bernard	Tu-A25		P-Tu-089
Leicht, Philipp	P-Mo-053	Lüftner, Daniel	Th-E21
Lekoui, Fouaz	Tu-E09, P-Th-098	Luh, Dah-An	P-Mo-094
Lemay, Jean-Christian	Th-D05	Lükermann, D.	Tu-A17, P-Th-046
Leroy, Frédéric	We-B05	Luna López, José Alberto	Mo-B02, Mo-B11, Tu-B01, Tu-E07, Tu-E16, We-D03, Th-E06, P-Mo-055
Leskelä, Markku	P-Th-081	Lunca-Popa, Petru	P-Th-062
Lete, Cecilia	Tu-C25+26	Lundgren, Edvin	Th-A04
Levy, Rachel	Th-C12		Tu-C03, P-Tu-017
Lewis, William	Tu-A19		Th-A16
Ley, Lothar	Mo-D16		Tu-B04
Li, Gang	P-Mo-023		
Li, Jingcheng	P-Tu-031	Luo, Meng-Fan	
Li, Jun	P-Th-014	Luo, Wen	
Li, Yu	Mo-D02	Luque, Francisco Jesús	
Li, Yuan	P-Th-062	Lusuan, Angelique	
Liao, Ting-Wei	P-Th-062	Lydiatt, Francis	
Liao, Zhenhe	P-Th-076		
Liashok, Larisa	P-Tu-019		
Lim, Heeseon	Tu-D17+18		
Limmer, David	Tu-C06		
Limot, Laurent	Th-D06		
Lin, Cho-Ying	Th-D06		
Lin, Dongsung	We-A03		
Lin, Hong-Ji	We-A03		
Lin, Ming-Wei	Tu-B04, Th-E13		
Lindsay, Rob	P-Tu-008		
Lingenfelder, Magali	We-B04		
Lips, Klaus	Tu-C14, Tu-C19, P-Tu-033, P-Tu-071, Th-C14		
Lipton-Duffin, Josh	Mo-C14		
	Th-D20		
Lis, Jakub			
Lisi, Simone			

Magnano, Elena	We-B08, Th-A11	McGuinness, Cormac	P-Th-022
Mahdid, Khadidja	P-Mo-050	Mechehoud, Fayçal	P-Th-067
Maheshwari, Abha	P-Tu-084	Meddour-Boukhobza, Laaldja	P-Th-061
Mahiou, Linda	P-Mo-069	Medjanik, K.	Th-D14
Maibach, Julia	Tu-D09	Mehta, Bhoomi	P-Tu-084
Maier, Sabine	Mo-C08, P-Tu-047, Th-C09	Meinel, Klaus	Tu-B13
Maiolo, Luca	P-Th-049	Meinhardt, Ute	Mo-C08, Th-C09
Majer, Karel	P-Tu-028, P-Tu-034	Meirzadeh, Elena	Th-B06
Makasheva, K.	Tu-B23	Menard, Gerbold	Mo-A14
Malterre, Daniel	Tu-C14, We-C10, P-Mo-006	Meneghetti, Mário	P-Th-007
Malytskyi, Volodymyr	Th-C17	Meniai, A. Hassen	P-Tu-098
Malzner, Frederik J.	We-C06	Menshikov, Konstantin	Th-C22
Manassen, Yishai	P-Tu-060	Menteş, Tevfik Onur	Tu-A11, Th-A19
Mankad, Venu	Tu-B17	Merino, Pablo	Tu-A12
Mañas Valero, Samuel	Mo-A15	Merte, Lindsay R.	Mo-B06, Mo-B11, Tu-E16, We-D03
Mao, Zhiqiang	Th-E17	Merz, Klaus	P-Tu-042
March, Katia	Mo-B05	Mesquita, Vincent	P-Tu-026
Marchante, Elena	Th-E10	Mete, Ersen	P-Tu-046, We-B03
Marie, Jean Baptise	P-Mo-035	Meunier, Vincent	Tu-C14
Marinova, Maya	Mo-B05	Meyer, Bernd	Mo-C08, Th-C09
Mariot, Jean-Michel	P-Th-027	Meyer, Ernst	Tu-C15, Th-C10
Markovich, Gil	Tu-C25+26	Meziani, Samir	P-Mo-069
Marouani, Rania	P-Tu-098	Miccio, Alejandro	P-Mo-086
Marqués-González, Santiago	Tu-A04	Miccio, Luis Alejandro	Th-D11
Marsi, Marino	Th-D20	Miccoli, Ilio	Mo-D15, P-Th-021
Martín, Fernando	Tu-C01, We-C07	Michely, Thomas	We-C09
Martin, Jean-Michel	We-E08, We-E09	Migani, Annapaola	Mo-D10
Martín, Nazario	Mo-A07	Miglio, Leo	Tu-D07
Martín, Fernando	Mo-C05, Mo-A07, We-D01, P-Th-048	Mihaiescu, Dan	P-Tu-059
Martínez, José I.	Th-A01	Mikkelsen, Anders	Mo-B11, Th-E06
Martínez-Castro, José	Tu-B14	Minami, Ichiro	We-E11
Martínez-Velarte, M. Carmen	We-A01	Minamitani, Emi	Mo-D12, P-Mo-017, Tu-B19
Martín-Gago, José A.	Th-A01	Minár, Jan	Mo-A04, Th-D23, Th-D14, P-Th-016, P-Th-027
Martín-García, L.	P-Mo-082	Mirabella, Francesca	Tu-E19, Th-E18
Martín-García, Laura	Mo-A03	Mirabella, Salvo	P-Th-049
Martín-Jiménez, Alberto	Mo-C05, Mo-D13	Miranda, Rodolfo	Mo-C05, Mo-A07, Mo-D13, Tu-C01, Tu-A03, P-Tu-017, We-C07
Martinotti, Dominique	Th-B05	Mittendorfer, Florian	Mo-B16, Tu-B16, Th-E17, Th-E20
Martins, Maximiliano	P-Mo-022	Miyamachi, Toshio	We-D10, P-Th-050
Martins, Susanne	Tu-C16	Mizutani, Tsuyoshi	P-Th-063
Mascaraque, Arantzazu	P-Th-055	Mochizuki, Izumi	We-D05, We-D08, Th-B21, Th-B22, Th-B23
Mašek, Karel	Tu-B15, P-Th-097	Mohamed, Ouchaabane	P-Mo-040
Masse, François	Tu-E05	Mohd Tobi, Abdul Latif	Th-B16
Mas-Torrent, Marta	Mo-D02, Th-E10, P-Mo-019	Molinari, Elisa	Tu-A06
Mataigne, Jean-Michel	Tu-B22	Momeni, Anouchah	Tu-D01, Tu-A17, P-Th-046
Matencio, Sonia	Tu-C03, Th-C11	Mönig, Harry	Mo-B03
Mathevet, Fabrice	Mo-D14	Monjas, Leticia	P-Tu-031
Mathieu, Claire	Th-B05	Montalenti, Francesco	Tu-D07
Mathur, Shashank	Tu-B18	Moon, Jaehyun	P-Mo-016, Th-C06
Matolín, Vladimír	Tu-B15, P-Mo-039, P-Mo-081, P-Th-068, P-Th-097	Moons, Ellen	P-Mo-049
Matolínová, Iva	P-Mo-039, P-Th-068	Moradlou, Omer	We-B07
Matsumoto, Yoshiyasu	Tu-A08	Moreau, Luc	Tu-C14
Matsushita, S.Y.	Th-D04	Morellón, Luis	We-A01
Matsuyama, Haruyuki	Th-A02	Moreno, César	P-Mo-022, Tu-C11
Matthiesen, Jesper	Tu-D19, Tu-D20	Moreno López, Juan C.	P-Tu-031
Matvija, Peter	P-Tu-068	Morgenstern, Karina	Tu-D02, Tu-D05, P-Tu-036
Mayer, Alexander	P-Tu-076	Mori, Shigeyuki	We-E07
Mayne, Andrew	Tu-A17	Mori, Yutaro	P-Mo-017
Mayr-Schmölzer, Wernfried	Mo-B16, Th-E17, Th-E20	Morikawa, Yoshitada	Mo-C15
Mazej, Zoran	Tu-A19		
Mazzola, Federico	Th-D11		
Mbenkum, Beri	P-Th-095		
McBreen, Peter	Tu-E09, P-Th-098		
McDermott, Eamon	Th-E19		

Moro-Lagares, María
 Moses, Poul Georg
 Moshfegh, Alireza Z.
 Mottet, Christine
 Mouhat, Kawtar
 Moussi, Abderrahmane
 Mu, Zhao
 Mueller, Klaus
 Mueller, Patrick
 Muenks, Matthias
 Mugarza, Aitor

 Mugumaoderha, Mac
 Muhler, Martin
 Mulier, maxime
 Mullegger, Stefan
 Müllen, Klaus
 Müller, Kathrin
 Müller, Pierre
 Müller, Thomas J.J.
 Mund, Baibhav
 Muntwiler, Matthias
 Munuera, C.
 Muñoz Ramo, David
 Murabayashi, Hiroki
 Murai, Daigo
 Murn, Chris
 Mutombo, Pingo

 Muttaqien, Fahdzi
 Muzas, Alberto S.
 Mysliveček, Josef

We-A01
 Mo-E12
 We-B07
 We-B10
 P-Tu-069
 P-Mo-069
 Tu-A17
 Tu-A06
 Tu-D06
 We-A02
 Th-A17, Th-A15,
 Th-D22, P-Mo-022
 We-B06
 P-Mo-090
 Tu-D01
 We-A08
 Th-A10
 P-Tu-031
 Th-D05
 P-Tu-062
 P-Mo-014
 Tu-C15
 P-Mo-082
 Th-E16
 We-E08, We-E09
 Mo-D03
 Th-E13
 Tu-A12, P-Th-036,
 P-Th-041
 Mo-C15
 We-D01, P-Th-048
 P-Th-068

Nguyen, Thanh Hai
 Nguyen Dung, Tran
 Nicklin, Chris
 Nicklin, Richard E.J.
 Nicolás, Josep
 Nicolas, Louis
 Nicolet, Celia
 Nieckarz, Damian
 Niemantsverdriet, Hans
 Nihill, Kevin J.
 Nijhuis, Christian
 Nijs, Thomas

 Nikiel, Marek
 Nikitina, Larisa
 Nilius, Niklas
 Niño, Miguel Angel
 Nishimatsu, Takeshi

 Nishimura, Keisuke
 Nishino, Taiki
 Nishiyama, I.
 Nita, Pawel
 Niu, Fang
 Niu, Yuran
 Njel, Christian
 Noda, Taku
 Noei, Heshmat
 Noguera, Claudine
 Nonaka, Toshihiro
 Nony, Laurent
 Nowakowska, Sylwia

Nowakowski, Jan

 Nunes, Ábner

Th-A11
 P-Th-068
 Tu-B04
 Mo-E14
 Mo-E05, Th-B12
 Th-A09
 Th-C03
 We-C12
 Mo-E08, Tu-E06
 P-Th-048
 Mo-D02
 Tu-C16, We-C06,
 Th-C10
 Tu-C24
 Tu-C05
 Tu-B11, P-Tu-020
 Tu-C03, P-Tu-017
 P-Tu-081, We-E08,
 We-E09
 Th-C07
 P-Mo-066
 P-Mo-070
 P-Tu-013, P-Tu-015
 P-Th-029
 P-Mo-055
 Th-E07
 P-Mo-062
 P-Mo-090, Tu-D06
 Tu-B22
 P-Mo-080
 P-Tu-067
 Tu-C16, Tu-C17,
 We-C06, Th-C10
 Tu-C16, We-A04,
 Th-C10
 P-Th-007

N

Na, Bock Soon
 Nadeem, Amtiaz
 Nagai, Yuki
 Nagamori, Takashi
 Nagashio, Kosuke
 Nagatsuka, Naoki
 Nagayuk, Denis
 Nägelein, Andreas
 Nakagawa, Takeshi
 Nakamura, Jun
 Nakamura, Junji
 Nakamura, Shunya
 Nakanishi, Hiroshi
 Nakatake, M.
 Nakayama, Tomonobu
 Nakazawa, Takeo
 Nam, Jeonghoon
 Namatame, H.
 Nameki, Hirofumi
 Namiki, A.
 Nappini, Silvia
 Narayan, Roger J.
 Narayanan Nair, Maya

 Narita, Akimitsu
 Navarro, Christophe
 Navarro, Juan Jesús
 Navarro Moratalla, Efrén
 Navarro-Quezada, Andrea
 Naydenov, Anton
 Nemsak, Slavomir
 Neo, Darren
 Nepijko, S.A.
 Netzer, Falko P.
 Nevius, Meredith

P-Th-019
 Mo-E01+02
 Mo-A16
 P-Mo-018
 P-Mo-017
 Tu-B06
 P-Th-038
 P-Th-041
 Mo-A05
 P-Mo-013, Th-A02
 Tu-E24, Th-E09
 Tu-B19
 P-Mo-011, P-Tu-077
 P-Th-017
 Mo-A13, Mo-A16
 Th-D17
 P-Mo-058
 P-Th-017
 P-Th-063
 P-Mo-070
 We-B08, Th-A11
 P-Tu-059
 P-Mo-006, Tu-A23,
 P-Th-001
 Tu-A06
 Th-C03
 Tu-A03
 Mo-A15
 Tu-C18
 P-Th-072
 Mo-B05
 We-B08
 Th-D14
 Tu-B17
 P-Mo-006

O

O'Brien, Casey P.
 Ocal, Carmen

 Ochoa, Héctor
 Oda, Masato
 Oda, Yuichi
 Oelsner, A.
 Ofer, Oren
 Ogawa, Satoshi
 Ogawa, Shuichi
 Ogawa, Tetsuya
 Ogura, Shohei
 Oh, Ji-Young
 Ohno, Shinya
 Ohresser, Philippe
 Ohsawa, Takeo
 Ohtomo, Yudai
 Oizumi, H.
 Okuda, Taichi
 Okuyama, Hiroshi
 Olivieri, Giorgia
 Olle, Marc
 Olsson, Mats Henrik M.
 Olszowski, Piotr
 Omiciuolo, Luca
 Ondráček, Martin
 Oppen, Felix
 Oppeneer, Peter
 Orellana, Walter
 Ormazza, Maider

Tu-E14
 Tu-C03, We-B01+02,
 Th-C11
 Tu-A03
 P-Th-020
 Th-D12
 Th-D14
 We-D11
 P-Th-063
 Tu-E18, P-Tu-101
 Tu-E24
 Tu-B06
 P-Th-019
 P-Tu-010, P-Th-028
 P-Mo-035, P-Tu-064
 Tu-B19
 P-Tu-101
 P-Mo-070
 Mo-A04
 Mo-D04
 Tu-D11, P-Th-031
 Th-A15
 Tu-D19
 Mo-C10
 We-C11, Tu-A20
 Tu-A12, Tu-C09
 Mo-A17
 We-A04
 P-Mo-015
 Tu-C06

Ortega, Enrique	Mo-C03+04, Mo-A06, Tu-E16, Tu-C17, Th-A09, Th-D11, P-Mo-086 P-Th-081	Patera, Laerte Pathak, Hareesh Patrone, Lionel Paulus, Beate Pavelec, Jiri Payne, Daniel Pébère, Nadine Pecher, Josua Pedersen, Nina R. Pederson, Steen Pellegrin, Eric	Th-A19 P-Tu-084 P-Tu-026, Th-C17 P-Th-047 Th-E17 P-Mo-083 Th-E14 P-Tu-037 Tu-D19 Tu-A26 Mo-E05, P-Mo-021, Th-B12 Th-E17 Mo-A17 We-B08, We-B09 P-Mo-023 Th-A09 P-Tu-049, P-Tu-057 Mo-C13, Tu-C14, Tu-C19, P-Tu-033 Mo-B03, Tu-A05, Tu-A15+16 P-Mo-093 Tu-B02, P-Tu-095 Mo-E05, Mo-E06, Th-E04+05 Th-B18, Th-C03, Th-C04 P-Th-088 Tu-B14 Tu-A08 Tu-D10 Th-E21 Mo-D15, P-Th-021 P-Tu-001, P-Tu-031 P-Tu-084 P-Th-071 Tu-B14 P-Mo-029 Mo-B01, P-Mo-084, Tu-D03, We-A09 Tu-C05 Mo-A17 Th-A09, Th-A10 P-Tu-099 P-Mo-001 P-Th-007 Th-D22 P-Mo-086 Tu-C17, Th-D11 We-B06 We-B08, Th-A11 Tu-B15 Tu-C22 Th-D03 P-Mo-085 Th-D11 P-Tu-027 Tu-B18 P-Tu-076 P-Mo-004 P-Th-097 P-Mo-088 P-Th-083 P-Mo-003, P-Mo-005, P-Mo-024 Tu-A07 P-Mo-065 P-Mo-034 Tu-B17 Mo-A14, P-Th-023
Osiceanu, Petre Osiecki, Jacek	Mo-B10, We-B08, We-B09		
Ošťádal, Ivan	P-Tu-028, P-Tu-034, P-Tu-068		
Öström, Henrik Ostroverkh, Anna Oszkó, Albert Otero, Edwige Otero, Roberto	We-E05+06 P-Th-097 P-Th-059 P-Tu-064 Mo-C05, Mo-D13, P-Tu-013, P-Tu-015, We-C07 We-C08 Tu-A03 P-Th-055 P-Tu-009 P-Mo-052 P-Th-077 P-Mo-069 P-Mo-076 P-Tu-081, We-E08, We-E07, We-E09	Peng, Jin Peng, Yang Pengpad, Atip Peña, Diego Peña Gil, Diego Peralta, Jerson Perepichka, Dmitrii Pérez, Rubén Pérez, Victoria Pérez, Virginia Pérez-Dieste, Virginia Pérez-Murano, Francesc Perkins, Neil Persson, Mats Petrović, Marin Pfeifer, Verena Pfnür, H. Pfnür, Herbert Pham, Tuan Anh Phull, Gurlovleen Phuruangrat, Anukorn Piantek, Marten Piatek, Jakub Picone, Andrea Pidchenko, Mikhail Pientka, Falko Pignedoli, Carlo A. Pimpinelli, Alberto Pinakov, Dmitry Piovan, Leandro Piquerel, R. Piquero, Ignacio Piquero-Zulaica, Ignacio Pireaux, Jean-Jacques Pis, Igor Pistonesi, Carolina Pita, Isabel Pitters, Jason Plumb, N. Plumb, Nickolas C. Poblet, Josep M. Pochet, Pascal Pogorelko, Viktor Poikarpova, Natalia Polášek, Jan Polcak, Josef Polčák, Jan Polikarpova, Natalia Politano, Antonio Polonskiy, Boris Polyak, Yaroslav Pomp, Sascha Pons, Stéphane	
Otero-Irureta, Gonzalo Otrokov, Mikhail Otshubo, Yoshi Ottosson, Henrik Ouafek, Nora Ouir, Souad Outemzabet, Ratiba Óvári, László Ozawa, Nobuki			
P			
Pacchioni, Gianfranco Pachecka, Malgorzata Pacilè, Daniela Page, Robert Pagliara, Stefania Paik, Donghyun Pakes, Chris Pal, Jagriti Palacio, Irene	P-Mo-078, Tu-B07 P-Tu-102 Tu-A07 We-B09 Mo-C07 P-Tu-048 Tu-A19 P-Mo-078, Th-A16 P-Mo-006, P-Th-001, P-Th-055 Th-A15 Tu-C03 Mo-B05 P-Th-089 Mo-C16, P-Tu-072 We-C10 P-Mo-055, Th-E06 Mo-C16 P-Th-034 P-Mo-083, Tu-B12 P-Mo-022 Mo-A09, Th-D20 Tu-E15 Th-A11 Th-D20 P-Mo-076, Tu-E13 P-Th-019 P-Tu-052, P-Th-092 P-Tu-052, P-Th-092 P-Tu-048 Th-C06 P-Mo-090, Th-E19 Th-D23 P-Th-027 P-Tu-026 Th-A11 P-Mo-022 Mo-A10 P-Mo-023 P-Th-035 P-Th-041		
Palacios, Juan José Palacios, Rogger Pallson, Gunnar Karl Palma, Amedeo Palmer, Richard Palmino, Frank Pan, Jinshan Pan, Tianluo Pan, Jisheng Pang, Chi Lun Paniago, Roberto Panighel, Mirco Papageorgiou, Anthoula C. Papagni, Antonio Papalazarou, Evangelos Papp, Christian Park, Chan Woo Park, Eun Ji Park, Ki Jung Park, Sejun Park, Seung Koo Parkinson, Gareth Parmigiani, F. Parmigiani, Fulvio Parrain, Jean-Luc Parravicini, Matteo Parreiras, Sofia Pascual, José I. Pascual, Nacho Paskova, T. Paszuk, Agnieszka			

Ponzoni, Stefano Mo-C07
 Popova, Olha Tu-C16
 Posthuma de Boer, J We-C11
 Potter, Thomas Th-C16
 Pou, Pablo Tu-A05
 Pozzo, Monica Tu-A20
 Praisler, Mirela P-Mo-091, P-Mo-092
 Prats García, Héctor P-Th-090
 Prauzner-Bechcicki, Jakub S. Mo-C10
 Preda, Loredana P-Th-081
 Preobrajenski, Alexei P-Th-022
 Presel, Francesco Tu-A20
 Prezzi, Deborah Tu-A06
 Price, Rachel A. Mo-E14
 Prieto, Carlos P-Mo-009
 Procházka, Pavel P-Mo-029, P-Mo-030, P-Tu-107

Prodan, Gabriel Corneliu P-Mo-092
 Pronsato, María Estela Tu-B15
 Prosenc, Marc Heinrich Mo-C09
 Pruneda, Miguel Mo-D07+08
 Průša, Stanislav P-Th-083
 Przyrembel, Daniel Th-C18
 Puchalska, Agnieszka P-Th-037
 Pueyo Bellafont, Noelia Th-B14
 Puglia, Carla P-Tu-009, P-Tu-040
 Puschnig, Peter Tu-C13
 Pussi, K. P-Tu-006
 Pusttai, Péter P-Th-059

Q

Quan, Jiamei Tu-E24
 Quesada, A. P-Mo-082
 Quesada, Adrián Mo-A03
 Quirós, Carlos Tu-A09

R

Racis, Agnieszka P-Tu-036
 Rader, Oliver Th-D21
 Radkte, Hanna We-B09
 Radny, Marian Wojciech P-Tu-036, P-Th-037
 Radovic, M. P-Mo-085
 Radtke, Hanna We-B08
 Rahman, Talat Th-C20
 Raidel, Christian Tu-A19
 Raimundo, Jean-Manuel Th-C17
 Ramsey, Michael Tu-C13
 Rana, Nicola Angelo Tu-C19, P-Tu-033
 Rapp, Bastian E. Th-C02
 Rapp, Christin P-Th-032
 Raschke, Hannes P-Tu-025
 Rashid, Muhammad P-Th-003
 Rashidi, Mohammad Th-D03
 Rashkovskiy, Alexander P-Mo-010, P-Th-009, P-Th-011
 Rasmussen, Søren B. Mo-E12
 Rauls, Eva P-Tu-082, We-B04, Th-E22
 Rault, Julien Mo-B05
 Rauschenbach, Stephan P-Tu-044, P-Tu-045, P-Tu-074, Th-A05, Th-C20
 Ravani, Fotini We-A04
 Realpe, Henry P-Tu-060
 Rechmann, Julian P-Tu-062

Redinger, Josef Mo-B16, Tu-B16, Th-E17, Th-E20
 Rednyk, Andrii P-Mo-043
 Reecht, Gael Mo-D14
 Reinisch, Eva Maria Tu-C13
 Relat-Goberna, Josep Mo-C12
 Renaud, Gilles Th-A20
 Rensmo, Håkan Tu-D09
 Repain, Vincent Th-C22, P-Mo-035
 Resta, Andrea P-Th-095
 Reutzel, Marcel Tu-E12
 Rhyim, Youngmok Th-B17
 Ribeiro, Fabio P-Th-068
 Richter, C. Th-D23
 Richter, Christine P-Th-027
 Richter, Mathias Tu-C13
 Ridier, Karl P-Mo-079
 Riegel-Vidotti, Izabel P-Th-007
 Rimmen, Morten Tu-D20
 Rinke, Gordon P-Tu-045, Th-A05, Th-C20

Ristic, Z. P-Mo-085
 Ritala, Mikko We-B05
 Riva, Michele Mo-B01, Mo-B09, We-A09, P-Mo-084, Tu-D03
 Robledo, Maitreyi Mo-C05
 Robles, Roberto Tu-C06
 Rocca, Mario Agostino P-Mo-078, Th-A16
 Roche, Stephan Tu-A01+02
 Roditchev, Dimitri Mo-A14
 Rodrigo, Lucía Tu-A05
 Rodríguez, Laura P-Mo-093, Tu-B02, P-Tu-095

Rodríguez Hermoso, Diego Mo-B03
 Rodríguez-Fdez., Jonathan Mo-C05
 Rodríguez-Reyes, Juan C. Tu-E10
 Rogero, Celia Mo-C03+04, P-Mo-086, P-Tu-023, We-C08

Rohart, Stanislas P-Mo-036, We-A05+06
 Rohlfing, Michael Tu-C02
 Rohrmüller, Martin We-B04
 Rohwerder, Michael Th-E12
 Rokni Fard, Mahroo Tu-C21
 Romanyuk, O. P-Th-035
 Romanyuk, Oleksandr P-Th-041
 Roncin, Philippe Tu-D01, Tu-A17, P-Th-046

Roqueta, Jaume P-Mo-072
 Rosa, Andressa P-Mo-075
 Rosei, Federico Tu-C14, Th-C14, Tu-C19, P-Tu-033, P-Tu-071, P-Tu-083

Rosellen, Wolfgang P-Tu-044
 Rosenblatt, Daniel P. Tu-A13
 Rosmi, Mohamad Saufi We-E01
 Roth, Stephan V We-D04
 Rougemaille, Nicolas Th-C22, P-Mo-035
 Rousset, Sylvie Tu-D07
 Rovaris, Fabrizio Mo-D02, P-Mo-019, Th-E10

Rovira, Concepció P-Tu-008
 Ruano, Gustavo We-C07
 Rubén, Mario Mo-A17
 Ruby, Michael Mo-D02, P-Mo-019
 Rudnev, Alexander P-Mo-012, P-Tu-065
 Rudolf, Petra Mo-B05
 Rueff, Jean-Pascal Th-B15
 Ruett, Uta

Ruffieux, Pascal
Ruini, Alice
Rull Trinidad, Enrique
Rullik, Lisa

Rupprechter, Günther

Rutigliano, Maria
Ryan, Kevin

S

Sabatini, David A.
Sabba, Nassila
Sabik, Agata
Sabry, Diego Araujo
Sadi, Frida
Sadowski, Janusz
Saeys, Mark
Sahul, Martin
Saji, Shunsuke
Sakai, Seiji
Sakamoto, Kazuyuki
Sakhonenkov, Sergei
Sakurada, Ippei
Sakurai, Junya
Sala, Alessandro
Saletsky, Alexander
Sali, Samira
Salluzzo, M.
Salmeron, Miquel
Salomons, Mark
Salvalaglio, Marco
Sam, Sabrina
Samadi, Morasa
Sambi, Mauro
Šamořil, Tomáš
Sánchez de Armas, Rocío
Sánchez-Barriga, Jaime
Sánchez-Portal, Daniel

Sánchez-Sánchez, Carlos
Sander, Tim
Sanes, José
Sanna, Nico
Sanning, Jan
Santiso, José
Santoro, Gonzalo
Santos, Sergio
Sanyal, Biplab
Saraireh, Sherin
Sarasola, Ane

Sarraz, Adnan

Sarikhani, Navid
Sarpi, Brice
Sasaki, Masahiro
Sasaki, Wataru
Sasaki, Guilherme Lanzi
Sauer, Joachim
Sauerbrey, Marc
Saurín, Noelia
Sautet, Philippe
Sauthier, Guillome
Savio, Letizia

Savoyant, Adrien
Sawada, M
Sayós, Ramón

Tu-A06, Th-A10
Tu-A06
Th-B18
Mo-B02, Th-E06,
P-Mo-055,
Mo-E10, P-Mo-077,
P-Th-064
P-Th-089
Tu-C22

P-Th-004
P-Th-080
Tu-D05, P-Tu-016
P-Th-007
P-Th-070
Th-D07
Mo-C14
P-Th-058
Th-E09
We-D05
Th-D12
Tu-B21
P-Th-028
P-Th-099
Tu-A11, Th-A19
P-Th-038, P-Th-039
P-Mo-050
P-Mo-085
Tu-D10
Th-D03
Tu-D07
P-Th-077
We-B07
Mo-C07, Th-A09
P-Tu-107
Mo-A08
Th-D21
Mo-C14, Tu-E16,
Th-A15, P-Tu-092
Th-A10
Mo-C08, P-Tu-047
We-E11
P-Th-089
Mo-C06
Th-B03, P-Mo-072
We-E01
Tu-D23
Mo-A08
P-Tu-094
P-Tu-008, P-Tu-023,
We-C08
P-Mo-073, P-Tu-062,
P-Th-010
We-B07
Mo-B07
P-Tu-018, P-Tu-022
P-Tu-086
P-Th-007
P-Mo-074
Mo-B08
We-E11
Mo-E13
P-Mo-072
P-Mo-078, Th-A11,
Th-A16
P-Tu-064
P-Th-017
P-Tu-088, P-Th-090

Scamehorn, John F.
Schabel, Wilhelm
Schaefer, Joerg
Schaff, Oliver
Schauermann, Swetlana

Scheurer, Fabrice
Schiller, Frederik

Schirone, S.
Schleheck, Nicolas
Schlesinger, Itai

Schlexer, Philomena
Schlickum, Uta
Schlögl, Robert
Schlueter, Christoph
Schmeisser, Dieter
Schmid, Michael

Schmidt, Anke B.
Schmidt, Wolf Gero

Schmitt, Tobias
Schnadt, Joachim
Schnegg, Alexander
Schneider, Alexander

Schneider, M. Alexander
Schneider, Wolf-Dieter
Scholl, Andreas
Schön, Christian
Schönhense, G.
Schönung, Kerstin
Schubert, Sonja
Schüer, S.
Schull, Guillaume
Schulte, Karina

Schumann, Florian
Schwarz, Martin
Schweke, Danielle
Seber, Gonca
Sediva, Romana
Sedona, Francesco

Segovia, Pilar
Seifert, Jan
Seitz, Patrick
Selivanov, Andrey
Sementa, Luca
Şen, Şaduman
Şen, Uğur
Seo, Eonmi
Seo, Youngchae
Serebryanaya, Nadezhda
Seridi, Fatiha
Serrano, Giulia
Serrate, David
Sessi, Paolo
Setvin, Martin
Seufert, Knud
Seyller, Thomas
Sezen, Hikmet
Sforzini, Jessica
Shacham-Diamand, Yosi
Shaikh, Moin
Shaikhutdinov, Shamil

P-Th-004
We-B01+02
Mo-D16
Th-B11
Tu-E14, Tu-E19,
Th-E18
Mo-D14
Mo-A06, Tu-E16,
Th-D11P-Mo-086
Th-D22
We-C09
Tu-D21, Tu-D22,
Th-B19
Tu-B07, We-D07
P-Tu-044
Tu-D10
Tu-B09+10
We-B05
Mo-B09, Mo-B16,
Mo-B18, P-Mo-086,
Th-E17, Th-E19
Mo-A04
Mo-D15, We-B04,
Th-E21, Th-E22,
P-Tu-082
Th-C13
Mo-B06, Mo-B10
We-B04
Tu-B16, Th-A18,
Th-C13
Tu-B01
P-Tu-020
Tu-A09
P-Tu-074
Th-D14, P-Th-016
P-Th-013
P-Tu-029
Mo-B03
Mo-D14
Mo-B10, Tu-B01,
We-B08, We-B09
Tu-B13
Tu-A18
P-Tu-060
Mo-D02, P-Mo-019
Tu-B15
Mo-C07, Th-A09,
Th-A11
Th-D13, P-Th-002
Th-E18
P-Tu-047
Tu-B21
Tu-B17
P-Tu-105
P-Tu-105
Th-E23
P-Mo-058
P-Th-057
P-Tu-096, P-Th-073
We-A08
Tu-B14, We-A01
Th-D18+19
P-Mo-086
Tu-E15
Tu-A19
Mo-E07
Tu-A12
P-Th-049
P-Tu-084
Mo-B12, Tu-E21,
P-Mo-074

Shamoto, Shin-ichi	We-D05	Sort, Jordi	Th-B04
Shao-Horn, Yang	Th-E04+05	Spadafora, Evan	P-Th-036
Sharpe, Ryan	P-Th-093	Spataru, Nicolae	P-Th-081
Shayduk, Roman	Tu-D06	Spataru, Tanta	P-Th-081
Shchyrba, Aneliia	We-A04	Späth, Florian	Tu-E13
Sheveyko, Alexander	P-Th-042	Springate, E.	P-Mo-008, Th-D23
Shi, Lijuan	Tu-D19	Stania, Roland	Tu-C15
Shibuya, Riku	Th-E09	Stankevich, Vladimir	Th-C22
Shida, Shigenari	P-Mo-071	Staufer, Urs	Th-B18
Shidara, Tetsuo	We-D08, Th-B21, Th-B22, Th-B23	Stefanov, Plamen	P-Th-072
Shifeng, Liu	P-Mo-054	Steidl, Matthias	P-Th-041
Shim, Hyungjoon	P-Th-045	Steiner, Christian	Mo-C08, Th-C09
Shimizu, Koji	P-Tu-077	Steinrück, Hans-Peter	P-Mo-076, Tu-E13
Shimizu, Ryota	Tu-B19	Stepanyuk, Valeri	We-A02
Shimizu, Tomoko	Tu-C11, We-C05	Stephan, Odile	Mo-B05
Shimoyama, Iwao	P-Tu-090	Sterrer, Martin	Th-C21
Shin, Hyogeun	We-E10	Stetsovych, Oleksandr	Tu-C11
Shin, Jin-Wook	Th-C06	Stetsovych, Vitalii	Tu-B15
Shin, Ji-Young	Tu-A04	Stiehler, Christian	P-Tu-020
Shinde, Prashant	Th-A10	Stierle, Andreas	P-Mo-090, Tu-D06
Shinokubo, Hiroshi	Tu-A04	Stipp, Susan	Mo-C11, Tu-D16, Tu-D19, Tu-D20, Th-E15, P-Th-030
Shipilin, Mikhail	Mo-B11, We-D03	Stöger, Bernhard	Mo-B16, Th-E17
Shipway, Philip	Th-B16	Stöhr, Meike	Tu-C16, We-C03+04, Th-C10, P-Tu-001, P-Tu-031
Shirai, Kaito	Mo-A04		Mo-A07, Tu-A18, Tu-C01, P-Th-049
Shtansky, Dmitry	P-Th-042	Stradi, Daniele	Mo-C06
Shuichi, Ogawa	P-Tu-104	Strano, Vicky	Tu-B09+10
Shusuke, Kasamatsu	P-Mo-017	Strassert, Cristian A.	Tu-E17
Shuttleworth, Ian	P-Th-084	Strelcov, Evgheni	We-D07, P-Th-087
Siahahan, Timothy	Tu-D04	Strømsheim, Marie	P-Mo-014
Sib, Jamal Dine	P-Mo-044, P-Tu-003, P-Tu-085	Stuckenholz, Stefanie	P-Tu-102
Sibener, Steven J.	P-Th-048	Sturm, Jacobus	Tu-C13
Sicot, Muriel	P-Mo-006, Tu-C14, We-C10	Sturm, Marko	Mo-C14
Siegbahn, Hans	Tu-D09	Subach, Sergey	Mo-E10, P-Mo-077, P-Th-064
Sierda, Emil	Mo-C09	Such, Bartosz	Th-A21
Siewert, Dorota	We-A04	Suchorski, Yuri	P-Mo-070
Šikola, Tomáš	P-Mo-029, P-Mo-030, P-Mo-088, P-Tu-107, P-Th-083	Suemitsu, Maki	Tu-A08
Silaev, Ivan	P-Tu-043	Suga, O.	Th-C22
Siler, Cassandra	Tu-E10	Sugimoto, Toshiki	P-Th-017
Silien, Christophe	Tu-C22	Sukhanov, Leonid	Tu-E22
Silly, Mathieu	We-B08	Sumida, H.	Th-B16
Silvestri, Alessandro	P-Th-030	Sun, Qiang	P-Mo-056
Simon, Jean-Jacques	Th-C17	Sun, Wei	P-Th-041
Singh, Shalini	Tu-C22	Sunol, Joan Josep	Tu-B17
Sirotti, Fausto	We-B08	Supplie, Oliver	Th-D04
Siusys, Aloyzas	Th-D07	Surnev, Svetlozar	Th-E21
Sivan, Uri	P-Mo-067, Tu-D21, Tu-D22, Th-B19	Suto, Shozo	Th-B13
Skála, Tomáš	P-Mo-081, P-Th-068	Sutter, P.	Mo-A05
Skatkov, Leonid	P-Th-076	Suzer, Sefik	P-Th-040
Skov, Anders Lind	P-Tu-039	Suzuki, Masahiko	P-Mo-018
Slater, Anna	Th-C12	Suzuki, Masataka	P-Tu-090
Smerieri, Marco	Th-A11, Th-A16, P-Mo-078	Suzuki, Seiya	Th-C22
Smets, Yaou	Tu-A19	Svechnikov, Nikolai	Tu-A12, P-Th-036
Sobotík, Pavel	P-Tu-028, P-Tu-034, P-Tu-068	Švec, Martin	Tu-E17
Socol, Gabriel	P-Tu-059	Svenum, Ingeborg-Helene	Tu-D04
Sokolov, Andrey	Tu-B21	Swagten, Henk	P-Mo-075
Sokolova, Anastasia	Th-A18	Swart, Jacobus	P-Tu-073, We-C12
Soldemo, Markus	Mo-B02	Szabelski, Paweł	Tu-C24
Soler, Lluís	Mo-E06	Szajna, Konrad	Mo-B17
Solianyik, Leonid	P-Tu-031	Szenti, Imre	Th-D07
Solis, Brian	P-Mo-074	Szot, Michal	Mo-C10, Mo-C14
Solymosi, Frigyes	P-Tu-093, P-Th-069	Szymonski, Marek	
Song, Fei	P-Tu-001, P-Tu-031		
Sørensen, Henning	Tu-D16		

T

Tada, Tomofumi P-Th-015
 Tadich, Anton Tu-A19
 Taga, Yasunori Th-C07
 Tajiri, Hiroo P-Th-052
 Takagi, Kouta Mo-A05
 Takagi, Noriaki Mo-D12, Th-D17
 Takagi, Yasumasa Mo-A13
 Takahashi, Chisato Tu-A13
 Takahashi, Kazutoshi P-Tu-010
 Takahashi, Yukio We-D10, P-Th-050
 Takakuwa, Yuji Tu-E18, P-Tu-101
 Takeyasu, Kotaro Tu-B06
 Takikawa, Hirofumi P-Th-012
 Taleb, Ahmed P-Mo-053, P-Th-080
 Taleb-Ibrahimi, Amina Tu-A23, Th-A22,
 P-Mo-006, P-Th-001,
 P-Th-055

Talirz, Leopold Th-A10
 Tallarida, Massimo We-B05
 Tamm, Aile We-B05
 Tamtogl, Anton We-E04
 Tanaka, Hiroya P-Tu-010
 Tanaka, Kazuma P-Tu-010
 Tanaka, Masatoshi P-Tu-010, P-Th-028
 Tanemura, Masaki Tu-A13
 Tang, Jiayi Tu-E18
 Tang, Hao Th-E14
 Tarafder, Kartick We-A04
 Tarala, Vitali P-Th-044
 Tarasenko, Alexander P-Tu-100
 Tarelkin, Sergei P-Th-057
 Taucer, Marco Th-D03
 Tautz, Stefan Tu-C02, Tu-C13
 Taylor, Michael P-Tu-059
 Tebano, Antonello Tu-B09+10
 Tebi, Stefano We-A08
 Tegenkamp, C. Th-E21
 Tegenkamp, Christoph Mo-D15, P-Mo-020,
 P-Th-021
 Tejeda, A. P-Th-001
 Tejeda, Antonio Th-A22, P-Mo-006,
 P-Th-055

Tejeda Gala, Antonio Tu-A23
 Telychko, Mykola Tu-A12
 Temirov, Ruslan Tu-C02
 Teraoka, Yuden Tu-E18, P-Th-099
 Ternes, Markus We-A02, We-A07
 Tesch, Julia Tu-A25
 Tetlow, H. We-C11
 Teyssedre, G. Tu-B23
 Themlin, Jean-Marc P-Tu-064
 Thiagarajan, Balasubramanian Th-D13
 Thiaville, André P-Mo-036
 Thiede, Christian Mo-A04
 Thilgen, Carlo P-Tu-001
 Thissen, Andreas Th-B11
 Thomale, Ronny Mo-D16
 Thomas, Andrew Tu-B04
 Thongtem, Somchai P-Mo-087, P-Th-071
 Thongtem, Titipun P-Mo-087, P-Th-071
 Thornton, Geoff P-Mo-083, Tu-B04,
 Tu-B12

Tigau, Nicolae P-Mo-092
 Tikhonov, Dmitry P-Tu-076
 Tilocca, Antonio P-Th-075
 Timmer, Alexander Mo-B03
 Tkatchenko, Alexandre Tu-E10

Todoroki, Naoto Th-E08
 Todorovic, Milica Mo-B03
 Tognolini, Silvia Mo-C07
 Tokai, Masashi P-Mo-063
 Tokareva, Irina P-Th-076
 Tokumasu, Takashi Th-C01
 TOnkikh, Alexander P-Th-038
 Tonner, Ralf P-Tu-037
 Toparli, Cigdem P-Th-010
 Topolnicki, Rafal We-B12
 Topyla, Maciej P-Mo-023
 Torrelles, Xavier P-Mo-085, Tu-B04,
 P-Tu-042

Tosoni, Sergio P-Mo-078
 Totani, Roberta P-Tu-009, P-Tu-040
 Tovt, Andrii P-Th-068
 Townsend, Peter We-E04
 Treacy, Jon Tu-B04
 Tringides, M.C. Mo-A14
 Tripathi, Jitendra Tu-C25+26
 Tristant, Damien We-C10
 Trovarelli, Alessandro Mo-E06
 Trubitsyn, Andrey P-Mo-065
 Trützschler, Andreas Tu-B13
 Tsoncheva, Tanya P-Th-072
 Tsukagoshi, Kazuhito Mo-D03
 Tsukahara, Noriyuki Mo-D12
 Tsuruda, Takeshi We-E08, We-E09
 Tumbek, Levent P-Tu-099
 Turgeon, Pierre-Alexandre Tu-E05, Th-B24
 Tusche, C. Th-D14
 Tvauri, Inga P-Tu-043

U

Uchihashi, Takashi Mo-A13, Mo-A16
 Uehara, Yoichi P-Mo-057, Th-A03
 Ules, Thomas Tu-C13
 Ulstrup, S. P-Mo-008
 Ünal, Hatice We-B03
 Ünal, Uğur Tu-E25
 Uozumi, Yuki We-E02
 Urcuyo, Roberto Th-A05
 Urgel, Jose Ignacio We-C07

V

Václavů, Michal P-Mo-039
 Valbuena, Miguel Angel Th-D13, P-Th-023
 Valeri, Sergio Mo-B08
 Valvidares, Manuel Tu-A09, Tu-A10
 Van den Bossche, Maxime Mo-E16
 Van den Bos, R.A.J.M. P-Th-051
 Van der Hoeven, Jessica Th-E19
 Van der Zant, Herre Mo-A15
 Van Spronsen, Matthijs Mo-E09
 Varga, Erika P-Th-059
 Varga, Peter P-Mo-030, P-Th-083
 Vári, Gábor P-Mo-076
 Vasili, Hari Babu Tu-A10
 Vasseur, Guillaume Tu-C14, Th-A09
 Vattuone, Luca P-Mo-078, Th-A16
 Vaughan, David Tu-B04
 Vázquez, Héctor Tu-C04, P-Tu-004
 Vázquez de Parga, Amadeo Mo-A07
 Vázquez Valerdi, Diana E. P-Mo-094
 Veciana, Jaume Mo-D02, Th-E10,
 P-Mo-019,

[illegible]

Yang, Bo	Th-M10	Zamborini, Giovanni	Tu-A11, Th-A19
Yang, Chih-Wen	Tu-D24, Tu-D25	Zaporotskov, Pavel	P-Mo-003, P-Mo-004, P-Mo-005
Yang, Lixu	Th-C12		
Yang, Nan	Tu-B09+10	Zaporotskova, Irina	P-Mo-003, P-Mo-004, P-Mo-005, P-Mo-007, P-Mo-024, P-Mo-028
Yang, Sena	P-Tu-061		
Yang, Yaw-Wen	P-Tu-089		
Yang, Zechao	Mo-C08, P-Tu-047	Zapotoczny, Bartłomiej	Mo-C10
Yano, Masahiro	P-Tu-022	Zaum, Christopher	Tu-D05
Yaoita, Yuchi	Th-D12	Zavodny, Adam	Th-E19, P-Mo-088
Yashina, Lada	Th-E04+05, Th-D21	Zdyb, Ryszard	Tu-C23
Yassine, ADDI	P-Th-082	Zeininger, Johannes	Mo-E10, P-Mo-077
Yastrubchak, Oksana	Th-D07	Zeppenfeld, Peter	Tu-A06, Tu-C18, P-Th-053
Yasue, Tsuneo	Mo-A05		
Yasutomi, G.	P-Mo-070	Zerrouki, D.	P-Th-080
Yeh, Chiao-Yin	P-Tu-089	Zetterberg, Johan	Tu-E07
Yilmaz, Ayşen	P-Tu-046	Zeudmi Sahraoui, Fouzia	P-Mo-044
Yilmaz, Ceren	Tu-E25	Zhang, Chu	Mo-B11, We-D03
Yim, Chi Ming	Tu-B12	Zhang, Fan	Th-E06
Yokotani, Atushi	P-Tu-086	Zhang, Feng	Mo-B11
Yokoyama, Naoki	P-Tu-081	Zhang, Hanmin	Tu-C12
Yokoyama, Toshihiko	Mo-A05, Mo-A13	Zhang, Hao-Li	We-B07
Yoon, Eui-Sung	We-E10	Zhang, Jun	Tu-C15
Yoshida, Tomoko	P-Th-063	Zhang, Ke	Mo-B12, Tu-E21
Yoshigoe, Akitaka	Tu-E18, P-Th-099	Zhang, Peng	We-E01
Yoshikawa, Hideki	P-Mo-061	Zhang, Teng	P-Tu-009
Yoshimura, Masamichi	P-Mo-018	Zhang, Xiao Wei	Tu-B20
Yoshizawa, Shunsuke	Mo-A13, Mo-A16	Zhang, Yu	P-Mo-083
Youn, Young-Sang	P-Th-091	Zhao, Weihong	P-Th-041
Younal, Ksari	P-Tu-064	Zharnikov, Michael	Th-C16
Young, Anthony	Tu-A09	Zhou, Jianfeng	Tu-E07
Yu, Byoung-Gon	Th-C06	Zhu, Beien	We-B10
Yu, Hak Ki	P-Mo-009	Zhuravlev, Andrey	P-Tu-097
Yu, Tsai-Feng	P-Tu-089	Zielke, Kristof	P-Tu-079
Yugami, Hiroo	P-Tu-081	Zimmerleiter, Robert	P-Th-053
Yuji, Takakuwa	P-Tu-104	Zimmermann, Petr	P-Tu-028, P-Tu-034
Yuki, Kotanigawa	P-Tu-104	Zirak, Mohammad	We-B07
Yusop, Mohd Zamri Bin M.	Tu-A13	Zobelli, Alberto	P-Mo-006
		Zougar, Lyes	P-Mo-050
		Zoulíkha, K.	P-Th-080
		Zrig, Samia	Th-C19
		Zugarramurdi, Asier	Tu-A17, Tu-D01, P-Th-046
			Th-E11
			Mo-C10, Mo-C14
Zacchigna, M.	Th-D23	Zuilhof, Han	
Zafeiratos, Spiros	Th-A04	Zuzak, Rafal	
Zahl, P.	Th-E21		
Zakharov, Alexei	Th-D07, P-Mo-055		
Zakharov, Nikolai	P-Th-038		